

# LOAN DOCUMENT

	PHOTOGRAPH THIS SHEET	INVENTORY	<p><b>H A N D L E  W I T H  C A R E</b></p>																										
DTIC ACCESSION NUMBER	LEVEL																												
<p><b>AFRL-ML-TY-TR-1999-4556</b></p> <p>DOCUMENT IDENTIFICATION</p> <p>10 Nov 99</p>																													
<p><b>DISTRIBUTION STATEMENT A</b></p> <p>Approved for Public Release</p> <p>Distribution Unlimited</p>																													
DISTRIBUTION STATEMENT																													
<table border="1" style="width: 100%; border-collapse: collapse;"> <tr> <td colspan="2">ACCESSION ID</td> </tr> <tr> <td>NTIS</td> <td>GRAM <input checked="" type="checkbox"/></td> </tr> <tr> <td>DTIC</td> <td>TRAC <input type="checkbox"/></td> </tr> <tr> <td colspan="2">UNANNOUNCED JUSTIFICATION <input type="checkbox"/></td> </tr> <tr><td colspan="2"> </td></tr> <tr><td colspan="2"> </td></tr> <tr><td colspan="2"> </td></tr> <tr><td colspan="2"> </td></tr> <tr><td colspan="2">BY</td></tr> <tr><td colspan="2">DISTRIBUTION/</td></tr> <tr><td colspan="2">AVAILABILITY CODES</td></tr> <tr> <td>DISTRIBUTION</td> <td>AVAILABILITY AND/OR SPECIAL</td> </tr> <tr> <td style="height: 50px; vertical-align: bottom;">A-1</td> <td></td> </tr> </table>		ACCESSION ID		NTIS	GRAM <input checked="" type="checkbox"/>	DTIC	TRAC <input type="checkbox"/>	UNANNOUNCED JUSTIFICATION <input type="checkbox"/>										BY		DISTRIBUTION/		AVAILABILITY CODES		DISTRIBUTION	AVAILABILITY AND/OR SPECIAL	A-1			
ACCESSION ID																													
NTIS	GRAM <input checked="" type="checkbox"/>																												
DTIC	TRAC <input type="checkbox"/>																												
UNANNOUNCED JUSTIFICATION <input type="checkbox"/>																													
BY																													
DISTRIBUTION/																													
AVAILABILITY CODES																													
DISTRIBUTION	AVAILABILITY AND/OR SPECIAL																												
A-1																													
DISTRIBUTION STAMP		DATE ACCESSIONED																											
		DATE RETURNED																											
<p><b>20000627 102</b></p>																													
DATE RECEIVED IN DTIC		REGISTERED OR CERTIFIED NUMBER																											
PHOTOGRAPH THIS SHEET AND RETURN TO DTIC-FDAC																													

**AFRL-ML-TY-TR-1999-4556**



**MECHANISTIC INVESTIGATIONS OF  
ZERO-VALENT METAL REACTIONS WITH  
ORGANOHALIDES**

**A..L. ROBERTS, Ph.D.  
W.A. ARNOLD  
U. JANS  
L.A. TOTTEN  
J.P. FENNELLY**

**DEPARTMENT OF GEOGRAPHY AND ENVIRONMENTAL  
ENGINEERING  
THE JOHN HOPKINS UNIVERSITY  
313 AMES HALL  
3400 N. CHARLES STREET  
BALTIMORE MD 21218-2686**

**Approved for Public Release; Distribution Unlimited**

**AIR FORCE RESEARCH LABORATORY  
MATERIALS & MANUFACTURING DIRECTORATE  
AIRBASE & ENVIRONMENTAL TECHNOLOGY DIVISION  
TYNDALL AFB FL 32403-5323**

## NOTICES

USING GOVERNMENT DRAWINGS, SPECIFICATIONS, OR OTHER DATA INCLUDED IN THIS DOCUMENT FOR ANY PURPOSE OTHER THAN GOVERNMENT PROCUREMENT DOES NOT IN ANY WAY OBLIGATE THE US GOVERNMENT. THE FACT THAT THE GOVERNMENT FORMULATED OR SUPPLIED THE DRAWINGS, SPECIFICATIONS, OR OTHER DATA DOES NOT LICENSE THE HOLDER OR ANY OTHER PERSON OR CORPORATION; OR CONVEY ANY RIGHTS OR PERMISSION TO MANUFACTURE, USE, OR SELL ANY PATENTED INVENTION THAT MAY RELATE TO THEM.

THIS REPORT IS RELEASABLE TO THE NATIONAL TECHNICAL INFORMATION SERVICE (NTIS). AT NTIS, IT WILL BE AVAILABLE TO THE GENERAL PUBLIC, INCLUDING FOREIGN NATIONS.

THIS TECHNICAL REPORT HAS BEEN REVIEWED AND IS APPROVED FOR PUBLICATION.



**ALISON LIGHTNER**  
Program Manager



**CHRISTINE WAGENER-HULME, Lt Col, USAF, BSC**  
Chief, Environmental Technology Development Branch



**RANDY L. GROSS, Col, USAF, BSC**  
Chief, Airbase & Environmental Technology Division

<b>REPORT DOCUMENTATION PAGE</b>			Form Approved OMB No. 0704-0188	
Public reporting burden for this collection of information is estimated to average 1 hour per response, including the time for reviewing instructions, searching existing data sources, gathering and maintaining the data needed, and completing and reviewing the collection of information. Send comments regarding this burden estimate or any other aspect of this collection of information, including suggestions for reducing this burden, to Washington Headquarters Services, Directorate for Information Operations and Reports, 1215 Jefferson Davis Highway, Suite 1204, Arlington, VA 22202-4302, and to the Office of Management and Budget, Paperwork Reduction Project (0704-0188), Washington, DC 20503.				
1. AGENCY USE ONLY (Leave blank)		2. REPORT DATE 10 November 1999		3. REPORT TYPE AND DATES COVERED Final Report 9/19/95 - 3/18/98
4. TITLE AND SUBTITLE Mechanistic Investigations of Zero-Valent Metal Reaction with Organohalides			5. FUNDING NUMBERS F08637-95-C-6037	
6. AUTHORS A. Lynn Roberts, W.A. Arnold, U. Jans, L.A. Totten and J.P. Fennelly				
7. PERFORMING ORGANIZATION NAME(S) AND ADDRESS(ES) Department of Geography and Environmental Engineering The Johns Hopkins University, 313 Ames Hall 3400 N. Charles St., Baltimore MD 21218-2686			8. PERFORMING ORGANIZATION REPORT NUMBER	
9. SPONSORING/MONITORING AGENCY NAME(S) AND ADDRESS(ES) AFRL/MLQE 139 Barnes Drive, Ste 2 Tyndall AFB FL 32403-5323			10. SPONSORING/MONITORING AGENCY REPORT NUMBER  AFRL-ML-TY-TR-1999-4556	
11. SUPPLEMENTARY NOTES Technical Review conducted by Dr. David Burris				
12a. DISTRIBUTION/AVAILABILITY STATEMENT Approved for Public Release; Distribution Unlimited			12b. DISTRIBUTION CODE  A	
13. ABSTRACT (Maximum 200 words) Mechanisms of organohalide reactions with zero-valent metals in aqueous solution were examined in batch reactors. Of particular interest were questions of concertedness of electron transfer; reaction kinetics and pathways (especially the extent to which reductive $\alpha$ and $\beta$ elimination competed with stepwise hydrogenolysis); and correlations between reactivity and reduction potentials. Results with probe compounds (vicinal dibromide stereoisomers and alkyl monobromide free radical "clocks") suggested that reactions might be initiated by transfer of a single electron, but that transfer of a second electron was so fast that free alkyl radical intermediates were unlikely to undergo such characteristic reactions with dissolved species as dimerization and hydrogen atom abstraction. Chlorinated ethylenes react with both zinc and iron to a significant extent via reductive $\beta$ -elimination. For zinc, rate constants for chloroethylene reduction increase with one- or two-electron reduction potential, while for iron, the reverse situation occurs. Substantial intra- and interspecies competitive effects were observed for iron, requiring the use of a Langmuir-Hinshelwood model. 1,1,1-Trichloroethane also reacts with zinc and iron (and also with two bimetallic reductants, copper/iron and nickel/iron) to a significant extent via reductive $\alpha$ -elimination pathways. Evidence suggests in some cases reactions may proceed via organometallic intermediates.				
14. SUBJECT TERMS Permeable reactive barriers; zero-valent metals; chlorinated ethylenes; chlorinated organic solvents; remediation.			15. NUMBER OF PAGES 358	
			16. PRICE CODE	
17. SECURITY CLASSIFICATION OF REPORT UNCLASSIFIED	18. SECURITY CLASSIFICATION OF THIS PAGE UNCLASSIFIED	19. SECURITY CLASSIFICATION OF ABSTRACT UNCLASSIFIED	20. LIMITATION OF ABSTRACT  UL	



UNCLASSIFIED

SECURITY CLASSIFICATION OF THIS PAGE

CLASSIFIED BY:

DECLASSIFY ON:

## PREFACE

This report was prepared by Dr. A. Lynn Roberts (PI) of the Department of Geography and Environmental Engineering, at the Johns Hopkins University, 313 Ames Hall, 3400 N. Charles St., Baltimore, MD 21218-2686. W. A. Arnold, U. Jans, L. A. Totten, and J. P. Fennelly all assisted in acquisition of data and preparation of this report, which was completed as a part of the Department of the Air Force Contract Number FO8637 95 C6037 for the Air Force Research Laboratory Environics Directorate (AL/EQ), Suite 2, 139 Barnes Drive, Tyndall Air Force Base, Florida 32403-5319.

This final report describes investigations into the chemical pathways and reaction rates pertaining to reduction of organohalides by zero-valent metals (principally zinc and iron). Of particular interest were investigations into the free-radical character of the reaction; studies of the branching ratios (particularly between hydrogenolysis and reductive  $\alpha$  or  $\beta$ -elimination) that dictate reaction product distributions for reactions of chlorinated ethylenes and 1,1,1-trichloroethane; and investigations into intra- and interspecies competitive effects that influenced rates of reaction with Fe(0).

The authors wish to acknowledge the invaluable discussions held with Dr. David R. Burris of the Air Force Research Laboratory, Tyndall Air Force Base.

This work was performed between September 1995 and March 1998. The AL/EQS project officers were Captain Jeff Stinson, Lieutenant Dennis O'Sullivan, and Capt. Gus Fadel.

(The reverse of this page is blank)



# EXECUTIVE SUMMARY

## A. OBJECTIVES

This work reports on the results of investigations into the reactions of halogenated organic contaminants with zero-valent metals (primarily iron and zinc) in aqueous solution. Such reactions may be utilized *in situ* in so-called "permeable reactive barriers" to contain plumes of organic solvents in groundwater, or alternatively for *ex situ* (aboveground) treatment. Although the ultimate products of reaction of zero-valent metals with chlorinated solvents are relatively innocuous hydrocarbons plus chloride ion, partially halogenated intermediates do occur. Since these may be toxic and in some cases less reactive than the parent compounds, the dynamics of intermediate formation and decay influences the success of this approach. In many cases, an array of different products can be formed. A sound understanding of the pathways and kinetics encountered enables more efficient barrier design. Finally, a better understanding of the fundamental mechanisms through which reactions take place may provide insight into factors that dictate reactivity or branching ratios when more than one product can be generated. Ultimately such information may prove useful in designing a reductant with high reactivity and selectivity, resulting in improved barrier performance.

## B. BACKGROUND

Metal-promoted reductive dechlorination represents a corrosion process, with the zero-valent metal serving as the source of electrons. The two electrons provided by oxidation of the metal can be coupled to the reduction of organohalides. Two different reductive dehalogenation reactions have been recognized. The first (previously assumed to dominate reduction of organohalides) is referred to as **hydrogenolysis**. This involves replacement of a halogen by a hydrogen. The second is referred to as **reductive elimination**. In this reaction, transfer of two electrons results in loss of two halide ions. These may be vicinal halogens (*reductive  $\beta$ -elimination*), in which case reduction is accompanied by an increase in bond order; alternatively, the organohalide in question may be a geminal dihalide, in which case *reductive  $\alpha$ -elimination* generates a carbene or possibly a metal-stabilized carbenoid. A final reaction that may be of importance is **hydrogenation**, namely reduction of a triple bond to a double bond or of a double bond to a single bond.

These different reactions are therefore characterized by very different products, with greatly different toxicity and environmental persistence. Of the two reductive dehalogenation reactions, reductive elimination (either  $\alpha$  or  $\beta$ ) poses distinct advantages from a treatment perspective. Studies indicate that lesser-halogenated alkanes that might result from hydrogenolysis typically react with metals much more slowly than more highly-halogenated alkanes, to the extent that treatment of some contaminants (such as  $\text{CH}_2\text{Cl}_2$  and 1,2-dichloroethane) with  $\text{Fe}(0)$  is not deemed practical. In contrast, the products of reductive  $\beta$ -elimination (especially alkynes originating from reductive  $\beta$ -elimination of chlorinated ethylenes) react rapidly with metals. Pathways involving reductive  $\beta$ -elimination therefore lead to products that can be completely dehalogenated, while a sequence consisting solely of stepwise hydrolysis reactions might favor accumulation of lesser-halogenated products of regulatory concern.

The extent to which reductive  $\alpha$ -elimination may occur for geminal polyhalides will also

exert a major impact on barrier design and therefore the feasibility of treatment approaches based on zero-valent iron. For example, hydrogenolysis of 1,1-dichloroethylene would result in vinyl chloride, while reductive  $\alpha$ -elimination would generate an alkylidene carbenoid (which could then undergo reduction to ethylene or rearrangement to acetylene) might circumvent this monohaloolefin. Similarly, hydrogenolysis of 1,1,1-trichloroethane would result in 1,1-dichloroethane, while reductive  $\alpha$ -elimination could result in conversion to ethane via a sequence of reactions that need not involve 1,1-dichloroethane as an intermediate. Since 1,1-dichloroethane reaction with Fe(0) is slow enough that removal of this daughter product dictates the design of barriers intended for treatment of 1,1,1-trichloroethane and since vinyl chloride is a highly carcinogenic and environmentally undesirable species, reductive  $\alpha$ -elimination represents a desirable route. The branching ratio between reductive  $\alpha$ - or  $\beta$ -elimination and hydrogenolysis therefore emerges as an important parameter dictating the success of metal-based treatment methods, and considerable attention was paid in the present study to this parameter.

Whether reactions proceed via free radical pathways, or alternatively via an essentially concerted transfer of two electrons, may also affect the products formed and therefore the design of iron-based barriers. For example, it has been argued by others that a shift toward a two-electron mechanism in the reduction of  $\text{CCl}_4$  by iron induced by photoirradiation is responsible for a corresponding change in the product distribution favoring  $\alpha$ -elimination over hydrogenolysis. Other researchers have hypothesized that the  $\text{C}_4$  products resulting from reduction of chlorinated ethylenes by Fe(0) represent radical coupling products. Traditional methods for investigating free-radical reactions (namely, involving electron spin resonance (ESR) spectroscopy in conjunction with trapping agents to enhance sensitivity) cannot readily be applied to reactions with zero-valent metals, however, because of the instability of the trapping agents in the presence of such strong reductants. In the present study, alternative methods (involving examination of reactions of vicinal dibromide stereoisomers and alkyl bromide "free radical clocks") were therefore employed to assess the likelihood (and persistence) of radical intermediates.

### C. SCOPE

Specific questions for which answers were sought are:

- Do reactions proceed (at least in some cases) via free radical pathways? As noted above, previous studies have suggested that whether or not reactions proceed via single electron transfer (SET) pathways or alternatively via a more-or-less concerted transfer of two electrons will exert a significant influence on the identities of products that may be formed.
- When more than one product can be formed, are the branching ratios influenced by the identity of the metal? The answer may shed light on the processes involved. If the metal simply serves as a more-or-less passive source of electrons, with at best weak interactions between the organohalide and the metal surface, it might be anticipated that product ratios would be relatively insensitive to the nature of the metal. Conversely, if strong inner-sphere ionic complexes or organometallic species possessing some degree of covalent bonding were to form such that certain reactive intermediates could be preferentially stabilized, product ratios might show a dependence on the identity of the metal. The question of branching ratios is also of immediate practical significance: drinking water standards (and therefore design criteria) will be different for different reaction products.
- For multistep reaction sequences, what are the rate constants pertaining to individual steps? This information will enable development of "process models" which can be used to

- optimize the design of permeable reactive barriers.
- For reduction of chlorinated ethylenes (and their daughter products) with iron (the most important application to date of permeable barrier technology), can kinetic data be described by the commonly invoked pseudo-first order approach, in which pseudo-first order rate "constants" are assumed to be truly constant for a given electrolyte composition and metal loading? Or do substantial intra- and interspecies competitive effects occur that would obviate such an approach? This issue poses obvious practical ramifications to barrier design.
  - Do correlations exist between rate constants and one- or two-electron reduction potential? In addition to the mechanistic insight such correlations might provide, they might also prove useful in predicting rate constants or product distributions for untested compounds.

## D. METHODOLOGY

Most of the experiments described herein were conducted by monitoring parent compound disappearance and products in batch reactors containing a zero-valent metal plus a pH buffer and an electrolyte to poise ionic strength. Reactors were maintained at room temperature, and were rotated about their longitudinal axes to minimize the abrasion that might be encountered with stir bars. Liquid samples were periodically obtained, and were analyzed via gas chromatography (GC). Since analytes varied widely in their physical properties, a variety of GC methods were employed. In most cases, analyses were conducted via headspace injection GC with flame ionization detection. In some cases, samples were extracted with an organic solvent, followed by analysis of solvent extracts by GC with flame ionization or electron capture detection. In all cases, careful attention was paid to mass balances. Wherever possible, the identities of products were confirmed by combined gas chromatographic/mass spectrometric (GC/MS) analysis.

Several different parent compounds were introduced as starting material. These included:

- **vicinal dibromide stereoisomers:** *threo* and *erythro*-2,3-dibromopentanes, and ( $\pm$ )-1,2-dibromo-1,2-diphenylethane. The *E* to *Z* ratio of the olefin products which result from reductive  $\beta$ -elimination is a guide to the degree of concertedness of transfer of the two electrons. Metals investigated included iron, zinc, copper, and aluminum.
- **alkyl bromide "free radical clocks":** 6-bromo-1-hexene and bromomethylcyclopropane. The ratio of rearranged products to unrearranged products can be used to deduce a rate constant for the second electron transfer; product distributions therefore indicate the extent to which reactions proceed via free radical vs. concerted two-electron pathways. Metal reductants investigated included iron and zinc.
- **chlorinated ethylenes:** reactions of tetrachloroethylene (PCE), trichloroethylene (TCE), *cis*- and *trans*-1,2-dichloroethylene (*cis* and *trans*-DCE), 1,1-dichloroethylene (1,1-DCE), and vinyl chloride with iron and zinc were all investigated.
- **daughter products of chlorinated ethylenes:** chloroacetylene and dichloroacetylene were synthesized, and their reactions with iron and zinc examined. In addition, reactions of acetylene and ethylene with iron and zinc were examined.
- **1,1,1-trichloroethane and 1,1-dichloroethane:** reactions of 1,1,1-trichloroethane and its principal chlorinated daughter product, 1,1-dichloroethane, were examined with two metals (iron and zinc) and two bimetallic reductants (a copper/iron couple and a nickel/iron couple).

## E. RESULTS

Results of studies with probe compounds suggested that reactions of alkyl halides may proceed via transfer of a single electron rather than via so-called two-electron pathways. The rate of transfer of the second electron is, however, so fast ( $\sim 10^8$  to  $10^{10}$  s<sup>-1</sup>) that any *free* radical intermediates that might be formed are unlikely to persist long enough to escape the metal surface or to undergo such characteristic free-radical reactions as dimerization and hydrogen atom abstraction. This may indicate that the apparent coupling products sometimes encountered in metal promoted reactions may be formed by some means other than by coupling of two free radicals (e.g., by rearrangement of a dialkylorganometallic intermediate). An alternative explanation is that reactions may only occur at highly localized sites at metal surfaces, with coupling and hydrogen abstraction being facilitated by proximity effects.

Detailed kinetic and product studies confirmed our early report that both zinc and iron react with chlorinated ethylenes to a considerable extent via reductive  $\beta$ -elimination. For reaction with zinc, the importance of reductive  $\beta$ -elimination paralleled the thermodynamic favorability of this reaction relative to hydrogenolysis, increasing from 15% to 95% of the total as the degree of chlorination decreased. No such trend was observed for reactions of chlorinated ethylenes with iron; reductive elimination accounted for 87% to 99% of the total reaction. For 1,1-dichloroethylene, reductive  $\alpha$  elimination to ethylene appears to occur via a sequence that may involve  $\alpha$ -elimination and which circumvents vinyl chloride as an intermediate.

A substantial fraction (8%-82%, increasing with the degree of chlorination) of chlorinated acetylene reduction by Zn(0) occurs via hydrogenation of the double bond to generate chlorinated ethylenes rather than via hydrogenolysis to lesser-chlorinated acetylenes. In contrast, no measurable hydrogenation occurs in reaction of chloroacetylene with iron, and only 24% of dichloroacetylene reacts via hydrogenation. Reaction with iron is therefore better able to circumvent generation of partially chlorinated ethylenes such as vinyl chloride.

In the case of reaction of chlorinated ethylenes with zinc, a pseudo-first order model adequately describes reaction rates, and rate constants increase with one- and two-electron reduction potentials. In contrast, substantial intra- and interspecies inhibitory effects were observed for reaction of chlorinated ethylenes with iron, interpreted as evidence of competition for a limited number of reactive sites at the metal surface. Reactions could not therefore be modeled using a simple pseudo-first order approach. In most cases, a modified Langmuir-Hinshelwood-Hougen-Watson approach in which rates are limited by reaction at the metal surface adequately captured the major features of the observed timecourses. Kinetic constants for reactions of iron with chlorinated ethylenes displayed a decreasing trend with increasing halogenation. Thus, partially dechlorinated ethylenes reacted with iron faster than their more highly halogenated analogs, in sharp contrast to the behavior observed in reaction of chlorinated ethylenes with zinc.

Reaction rates, product distributions, and product branching ratios observed in the reduction of 1,1,1-trichloroethane with zero-valent metals and bimetallic reductants varied with the identity of the metal reductant. A substantial fraction of the reaction in each case occurred via reductive  $\alpha$ -elimination to ethane, a reaction in which 1,1-dichloroethane did not appear to serve a role as an intermediate. Apparent coupling products were observed for reaction with iron and bimetallic reductants, but not with zinc.

## F. CONCLUSIONS

These results are of immediate practical relevance to permeable barrier design. The important (in many cases, preeminent) role played by reductive  $\alpha$ - or  $\beta$ -elimination, as well as subsequent hydrogenation reactions for substituted acetylene daughter products, makes inclusion of such reactions important in process models used to optimize barrier design. In many cases, product branching ratios are such as to at least partially circumvent the generation of relatively stable partially dechlorinated products; this will reduce the hydraulic residence times required to meet drinking water standards in the effluent from permeable barriers. Modeling the results obtained in the Borden experiment suggests that reductive  $\beta$ -elimination may also play an important role in iron-promoted reactions of chlorinated ethylenes in the field, even when the iron type and electrolyte composition vary substantially from that employed in our laboratory experiments.

The substantial intra- and interspecies competitive effects observed in our batch experiments may also have important consequences to barrier design. Testing of granular media with single solutes or contaminants present at low concentrations may result in insufficiently conservative design parameters. Additional experiments are currently under way to confirm the existence of inter- and intraspecies competitive effects in steady-state column settings.

These studies also provided considerable insights into the mechanisms of the reactions of organohalides with zero-valent metals. It appears that the metal surface is much more than a "passive" source of electrons, and several indirect lines of evidence were consistent with the notion that organometallic intermediates could be formed. The decrease in rate constants with reduction potentials observed for reaction of chlorinated ethylenes with iron is at variance with previous suggestions that rates are limited by single electron (SET) transfer to the organohalide. Although this may reflect greater passivation of the iron surface by more highly oxidizing chloroethylenes, this reactivity pattern could also reflect a rate-limiting step involving chemical bonding between the chlorinated ethylene and the iron surface. Evidence in favor of the latter hypothesis is provided by  $^{12}\text{C}/^{13}\text{C}$  kinetic isotope effects reported for trichloroethylene reduction by iron. For the chlorinated ethylenes, the free radical "clocks", and 1,1,1-trichloroethane, the substantial differences in product branching ratios obtained with zinc vs. iron suggests the metal in some cases plays a direct role in the product-determining steps. Even though iron surfaces are much better than zinc at generating  $\text{H}_2$  and should therefore represent a better source of labile hydrogen atoms, much less hydrogenolysis was observed in reduction of chlorinated ethylenes with iron than with zinc, and much less hydrogenation was observed in reduction of chlorinated acetylenes by iron than with zinc. The substantial differences in the rate of the second electron transfer observed among the free radical "clocks" and the vicinal dibromide probes may also be indicative of organometallic intermediates; moreover, the complicated distribution of products obtained with one of these "clocks", 6-bromo-1-hexene, is consistent with what has been observed from reaction of organoiron intermediates. The apparent absence of hydrolytic trapping products or typical carbene rearrangement products such as acetaldehyde or vinyl chloride from the reductive  $\alpha$ -elimination of 1,1,1-trichloroethane, or of vinyl alcohol or acetylene from the reductive  $\alpha$ -elimination of 1,1-dichloroethylene, may indicate that intermediates occur as metal-bound carbenoids rather than as free carbenes. Recognition of the potential role played by organometallic species provides an important first step in understanding factors that control reactivity and selectivity in metal-promoted reduction reactions of organohalides.





## TABLE OF CONTENTS

Section	Title	Page
I	INTRODUCTION	
	A. INTRODUCTION .....	1
	B. BACKGROUND.....	3
	1. Background on Iron-Based Permeable Barriers .....	3
	2. Reactions of Organohalides with Zero-Valent Metals.....	5
	C. SCOPE .....	9
	D. REPORT ORGANIZATION .....	10
	E. SIGNIFICANT FINDINGS .....	12
	F. LITERATURE CITED.....	16
II	ALKYL BROMIDES AS MECHANISTIC PROBES OF REDUCTIVE DEHALOGENATION: REACTIONS OF VICINAL DIBROMIDE STEREOISOMERS WITH ZERO-VALENT METALS	
	A. ABSTRACT .....	23
	B. INTRODUCTION .....	23
	C. EXPERIMENTAL SECTION .....	28
	1. Reagents.....	28
	2. Preparation of Metals.....	29
	3. Goethite .....	30
	4. Cr(II) Solutions .....	30
	6. Iodide .....	31
	7. Reactions of DBP Isomers .....	31
	8. Reactions of ( $\pm$ )-SBr <sub>2</sub> .....	32
	9. Computational Estimates of Rotational Energy Barriers .....	32
	D. RESULTS .....	32
	1. MS and NMR Spectra of Synthesis Products .....	32

## TABLE OF CONTENTS (cont'd)

Section	Title	Page
	2. Hydrolysis of the Probe Compounds .....	41
	3. Reductive Dehalogenation of the Probe Compounds .....	43
	a. Reductions Promoted by Cr(II) .....	46
	b. Reductions Promoted by Iodide .....	48
	c. Reactions with Zero-Valent Metals .....	52
	d. Goethite Plus Fe(II) .....	55
	4. Rotational Barriers .....	58
E.	DISCUSSION .....	62
	1. Hydrolysis of Probe Compounds .....	62
	2. Reduction by Cr(II) .....	66
	3. Reduction by Iodide .....	67
	4. Reductions Promoted by Zero-Valent Metals .....	69
	5. Reductions Promoted by Fe(II) on Goethite .....	70
	6. Mechanistic Interpretation .....	71
	7. Implications for Zero-Valent Metal Based Remediation Technology .....	72
F.	LITERATURE CITED .....	73
III	ALKYL BROMIDES AS MECHANISTIC PROBES OF REDUCTIVE DEHALOGENATION: REACTIONS OF RADICAL CLOCKS WITH ZERO-VALENT METALS	
A.	ABSTRACT .....	77
B.	INTRODUCTION .....	77
C.	EXPERIMENTAL SECTION .....	81
	1. Reagents .....	81
	2. Preparation of Metals .....	81
	3. Reactions of 6-Bromo-1-hexene .....	84
	4. Reactions with BrMCP .....	88
	5. GC-MS Analysis .....	91
	6. Kinetic Modeling .....	91

## TABLE OF CONTENTS (cont'd)

Section	Title	Page
	D. RESULTS .....	92
	1. Hydrolysis of Radical Clocks .....	92
	2. Reaction of 6-Bromo-1-hexene with Zinc .....	96
	3. Reaction of BrMCP with Zn(0) .....	101
	4. Reactions of 6-Bromo-1-hexene with Iron .....	104
	5. Reduction of BrMCP by Iron .....	109
	E. DISCUSSION .....	110
	1. Radical Pathways .....	111
	2. Alternate Organometallic Reaction Pathways .....	113
	3. Role of Hydrogen Species .....	116
	4. Relative Importance of SET and Organometallic Reaction Pathways with Iron .....	117
	5. Relative Importance of SET and Organometallic Reaction Pathways with Zinc .....	118
	6. Alternate Methods of Detecting Radical Intermediates .....	119
	7. Implications for Remediation Schemes Involving Zero-Valent Metals .....	120
	F. LITERATURE CITED .....	121
IV	REDUCTIVE ELIMINATION OF CHLORINATED ETHYLENES BY ZERO-VALENT METALS	
	A. ABSTRACT .....	125
	B. INTRODUCTION .....	125
	C. EXPERIMENTAL SECTION .....	129
	1. Reduction of Dichloroethylenes by Fe(0) .....	129
	2. Reduction of Chlorinated Ethylenes by Zn(0) .....	129
	D. RESULTS AND DISCUSSION .....	130
	E. LITERATURE CITED .....	140

## TABLE OF CONTENTS (cont'd)

Section	Title	Page
<b>V</b>	<b>PATHWAYS OF CHLORINATED ETHYLENE AND CHLORINATED ACETYLENE REACTION WITH ZINC</b>	
	A. ABSTRACT .....	147
	B. BACKGROUND AND RATIONALE .....	147
	C. EXPERIMENTAL SECTION .....	150
	1. Chemicals .....	150
	2. Synthesis of Chlorinated Acetylenes .....	151
	3. Metal Preparation .....	151
	4. Experimental Systems .....	152
	5. Analytical Methods .....	153
	6. Kinetic Modeling .....	155
	D. RESULTS .....	156
	1. Effect of Metal Loading .....	158
	2. Vinyl Chloride and Acetylene .....	160
	3. Dichloroethylenes .....	160
	4. TCE and PCE .....	165
	5. Chlorinated Acetylene Reduction .....	169
	E. DISCUSSION .....	175
	1. Factors Influencing Reaction Products .....	175
	2. Quantitative Structure-Activity Relationships .....	177
	3. Environmental Significance of Reductive Elimination .....	180
	F. LITERATURE CITED .....	182
<b>VI</b>	<b>PATHWAYS AND KINETICS OF CHLORINATED ETHYLENE AND CHLORINATED ACETYLENE REACTION WITH IRON</b>	
	A. ABSTRACT .....	187
	B. BACKGROUND AND RATIONALE .....	187
	C. EXPERIMENTAL SECTION .....	194
	1. Chemicals .....	194

## TABLE OF CONTENTS (cont'd)

Section	Title	Page
	2. Synthesis of Chlorinated Acetylenes .....	194
	3. Metal Preparation .....	194
	4. Experimental Systems .....	195
	5. Analytical Methods .....	196
	6. Kinetic Modeling .....	196
D.	RESULTS .....	197
1.	Experimental Variables .....	197
a.	Effect of metal loading .....	197
b.	Effect of mixing rate and mass transfer .....	200
c.	Effect of initial oxidant concentration .....	202
2.	Kinetic Data .....	214
3.	Reaction Pathways .....	214
a.	Ethylene .....	214
b.	Acetylene .....	214
c.	Vinyl Chloride .....	219
d.	<i>cis</i> - and <i>trans</i> -DCE .....	219
e.	1,1-DCE .....	225
f.	Chlorinated Acetylenes .....	229
g.	TCE and PCE .....	236
4.	Competitive Experiments .....	241
5.	Comments on the Kinetic Model .....	246
E.	DISCUSSION .....	247
1.	Rate Constant and Initial Rate versus Initial Concentration ...	247
2.	Factors Affecting Product Distribution .....	247
3.	Comparison with Results of Others .....	248
4.	Quantitative Structure-Activity Relationships .....	255
5.	Model Simulations .....	260
6.	Mechanistic Insight .....	262
7.	Advantages of Fe(0) in Permeable Barriers .....	269
F.	LITERATURE CITED .....	270
VII	REACTION OF 1,1,1-TRICHLOROETHANE WITH ZERO- VALENT METALS AND BIMETALLIC REDUCTANTS	
A.	ABSTRACT .....	277
B.	INTRODUCTION .....	277

## TABLE OF CONTENTS (cont'd)

Section	Title	Page
C.	EXPERIMENTAL SECTION .....	279
1.	Reagents .....	279
2.	Metal Preparation .....	280
3.	Preparation of Bimetallic Reductants .....	280
4.	Reactions of 1,1,1-TCA and 2-Butyne .....	280
5.	Reactions of 1,1-DCA .....	281
6.	Reactions of Deuterated 1,1,1-TCA .....	282
7.	Sample Analysis .....	282
8.	Mass Spectral Modeling .....	284
D.	RESULTS .....	285
1.	Reaction of 1,1,1-TCA and 1,1-DCA with Zn .....	285
2.	Reaction of 1,1,1-TCA and 1,1-DCA with Fe .....	288
3.	Reaction of 1,1,1-TCA and 1,1-DCA with Bimetallic Reductants .....	288
4.	Reduction of 2-Butyne .....	291
E.	DISCUSSION .....	293
1.	Reaction Pathways .....	293
2.	Experiments with Trideuterated 1,1,1-TCA .....	297
3.	Relevance of Results .....	300
F.	LITERATURE CITED .....	303

## TABLE OF CONTENTS (cont'd)

Appendix	Title	Page
<b>A</b>	<b>HETEROGENEOUS KINETICS DERIVATION</b>	
	A.1 Definitions .....	A-1
	A.2 Case 1: $A \rightarrow B$ .....	A-1
	A.2.1 Steps in a Heterogeneous Reaction .....	A-2
	A.2.2 Adsorption as the Rate Limiting step .....	A-3
	A.2.3 Surface Reaction as the Rate Limiting Step .....	A-4
	A.2.4 Desorption as the Rate Limiting Step .....	A-5
	A.2.5 Determination of the Kinetic and Adsorption Parameters .....	A-6
	A.3 Coupling Reactions .....	A-7
	A.4 Case 2: Parallel and Sequential Reactions .....	A-7
	A.5 A Complete Model for PCE Reduction .....	A-8
	A.6 Effect of the Magnitude of $K$ .....	A-9
	A.7. Comments on the Heterogeneous Kinetic Model .....	A-9
	A.8 Literature Cited .....	A-12
 <b>B</b>	 <b>MODELING PROCEDURE</b>	
	B.1 Inhibition/Competition Term .....	B-1
	B.2 Equations .....	B-2
	B.3 Normalization Procedure .....	B-3
	B.4 Fitting Procedure .....	B-4



## LIST OF TABLES

Table	Title	Page
Table 1:	Ten most common organic contaminants found in ground water at Air Force installations, in order of decreasing frequency .....	2
Table 2:	Metals used in experiments with vicinal dibromides.....	30
Table 3:	Reactivity of <i>threo</i> -DBP and ( $\pm$ )-SBr <sub>2</sub> with zero-valent metals.....	46
Table 4:	Computed and experimental rotational energy barriers.....	60
Table 5:	Henry's law constants ( $K_h$ ) for the radical clocks and their products measured by the method of McAullife (1971).....	87
Table 6:	Estimates of rate constants for second electron transfer based on the methylcyclopentane/1-hexene product ratios observed in the reduction of 6-bromo-1-hexene.....	101
Table 7:	Calculated thermodynamic reduction potentials (relative to standard hydrogen electrode) for net two-electron reduction of chlorinated ethylenes to the corresponding hydrogenolysis products and $\beta$ -elimination products in aqueous solution at 25°C.....	128
Table 8:	Surface area normalized rate constants for the chlorinated ethylenes and their reaction products.....	157
Table 9:	Percentage of reaction occurring via reductive elimination.....	176
Table 10:	Model-derived kinetic parameters for chlorinated ethylenes and related species.....	213
Table 11:	Inhibition constants.....	241
Table 12:	Percentage of reaction occurring via reductive elimination.....	247
Table 13:	Fraction of chlorinated acetylene reaction occurring via hydrogenolysis.....	248
Table 14:	Kinetic parameters used in the simulations of the Borden field data.....	251
Table 15:	Summary of reaction rate data obtained for reactions of 1,1,1-TCA with zero-valent metals and bimetallic reductants .....	286
Table A-1:	Explanation of symbols used in heterogeneous kinetic model.....	A-1

## LIST OF FIGURES

Figure	Title	Page
Figure 1:	Idealized reaction schemes for the dibromide model compounds used in this study: a) single electron reduction pathway, and b) concerted nucleophilic pathway .....	26
Figure 2:	H-NMR spectra of <i>threo</i> -DBP determined on UNITYplus 400 MHz NMR in CDCl <sub>3</sub> (approximate concentration of DBP = 10 mg/mL).....	33
Figure 3:	H-NMR spectra of <i>erythro</i> -DBP determined on UNITYplus 400 MHz NMR in CDCl <sub>3</sub> (approximate concentration of DBP = 10 mg/mL).....	34
Figure 4:	H-NMR spectrum of (±)-SBr <sub>2</sub> determined on UNITYplus 400 MHz NMR in CDCl <sub>3</sub> (approximate concentration of (±)-SBr <sub>2</sub> = 10 mg/mL) .....	35
Figure 5:	Mass spectrum of <i>erythro</i> -DBP (parent ions at m/e = 228, 230, and 232) recorded under electron impact (EI) ionization on a Hewlett-Packard (HP) 5890 GC equipped with an HP 5970 mass spectrometer detector. ....	36
Figure 6:	Mass spectrum of <i>threo</i> -DBP (parent ions at m/e = 228, 230, and 232) recorded under electron impact (EI) ionization on a Hewlett-Packard (HP) 5890 GC equipped with an HP 5970 mass spectrometer detector. ....	37
Figure 7:	Mass spectrum of (±)-SBr <sub>2</sub> (parent ions at m/e = 338, 340, and 342) recorded under electron impact (EI) ionization on a VG instruments 70-S MS. ....	38
Figure 8:	Chromatographic analysis of 2,3-dibromopentanes and <i>E</i> - and <i>Z</i> -pentenes on a Carlo-Erba Mega 2 GC equipped with an FID and a PC-driven data acquisition system.....	39
Figure 9:	Chromatographic analysis of (±)-stilbene dibromide and <i>E</i> - and <i>Z</i> -stilbenes.....	40
Figure 10:	Hydrolysis of <i>threo</i> -DBP at pH 7.5 (5 mM Tris buffer, 0.1 M NaCl).....	41
Figure 11:	Hydrolysis of (±)-SBr <sub>2</sub> at pH 8 (5 mM borate buffer, 0.1 M NaCl). ....	42
Figure 12:	<i>E</i> - and <i>Z</i> -olefins (as a percent of total olefin) formed from the reaction of <i>threo</i> -DBP with various reductants. ....	44
Figure 13:	<i>E</i> - and <i>Z</i> -olefins (as a percent of total olefin) formed from the reaction of (±)-SBr <sub>2</sub> with various reductants.....	45
Figure 14:	Reaction of <i>threo</i> -DBP with 10 mM Cr(II) in 5 mM H <sub>2</sub> SO <sub>4</sub> (pH 2.0-2.1) at 25.0 (± 0.1)°C.....	47

Figure 15: Reaction of ( $\pm$ )-SBr <sub>2</sub> with 0.06 mM Cr(II) in 5 mM H <sub>2</sub> SO <sub>4</sub> (pH 2.0-2.1) at 25.0 ( $\pm$ 0.1)°C. ....	49
Figure 16: Reaction of <i>threo</i> -DBP with 1 M iodide in 0.1 M NaCl, 50 mM tetraborate buffer at pH 9.3, 25.0 ( $\pm$ 0.1)°C. ....	50
Figure 17: Reaction of ( $\pm$ )-SBr <sub>2</sub> with 1 M iodide in 0.1 M NaCl, 50 mM tetraborate buffer at pH 9.3, 25.0 ( $\pm$ 0.1)°C. ....	51
Figure 18: Reaction of <i>threo</i> -DBP with 5.0 g iron (3.26 m <sup>2</sup> /L) in 0.1 M NaCl (pH 6.5-8.5). ....	53
Figure 19: Reaction of <i>threo</i> -DBP with 1.0 g zinc (0.029 m <sup>2</sup> /L) in 0.1 M NaCl (pH 6-7.5). ....	54
Figure 20: Reaction of ( $\pm$ )-SBr <sub>2</sub> with 0.5 g iron (0.32 m <sup>2</sup> /L) in 0.1 M NaCl (pH 7.8-8.6). ....	56
Figure 21: Reaction of ( $\pm$ )-SBr <sub>2</sub> with 1 g zinc (0.028 m <sup>2</sup> /L) in 0.1 M NaCl (pH 7.7-7.9). ....	57
Figure 22: Relative energy of 3-bromopentyl radical rotational conformers.....	59
Figure 23: H-NMR spectrum of methylcyclopropane conducted on UNITYplus 400 MHz NMR in CDCl <sub>3</sub> . ....	82
Figure 24: GC-MS spectrum of methylcyclopropane [parent ion (M <sup>+</sup> ): 56] recorded under electron impact (EI) ionization on a Hewlett-Packard (HP) 5890 GC equipped with an HP 5970 mass spectrometer detector.....	83
Figure 25: Chromatogram of standards used to quantify products encountered in the reaction of 6-bromo-1-hexene with zero-valent metals.....	85
Figure 26: Chromatogram showing products 8 days after spiking 6-bromo-1-hexene into reactor (150 mL) containing 10 g Fe(0). ....	86
Figure 27: Chromatogram showing products 3 hours after spiking 6-bromo-1-hexene into reactor (150 mL) containing 2 g Zn(0).....	87
Figure 28: Chromatogram of reactor headspace showing products after 30 minutes of the reaction of BrMCP with 20 g Zn(0).....	89
Figure 29: Chromatogram of reactor headspace showing products after 30 minutes of the reaction of BrMCP with 20 g Fe(0). ....	90
Figure 30: Hydrolysis of 6-bromo-1-hexene at pH 8.5 in 50 mM Tris/0.1 M NaCl at 22°C. ....	93
Figure 31: GC-MS spectrum of the hydrolysis product of 6-bromo-1-hexene recorded under electron impact (EI) ionization on a Hewlett-Packard (HP) 5890 GC equipped with an HP 5970 mass spectrometer detector.....	94

Figure 32: GC-MS spectrum of authentic 5-hexen-1-ol recorded under electron impact (EI) ionization on a Hewlett-Packard (HP) 5890 GC equipped with an HP 5970 mass spectrometer detector. ....	95
Figure 33: Solvolysis of bromomethylcyclopropane at pH 8 in 50 mM Tris/0.1 M NaCl.....	97
Figure 34: Reaction of 6-bromo-1-hexene in 160 mL 0.1 M NaCl/50 mM Tris (pH 8) at 22°C (zero headspace) and 2 g zinc (0.47 m <sup>2</sup> /L). ....	98
Figure 35: Reaction of 6-bromo-1-hexene in 150 mL 0.1 M NaCl/50 mM Tris (pH 8) at 22°C (10 mL headspace) and 2 g zinc (0.47 m <sup>2</sup> /L).....	100
Figure 36: GC-MS of trace product (assumed to be cyclobutane) obtained in the reaction of BrMCP with 20 g of Zn(0).. ....	102
Figure 37: Reaction of 6-bromo-1-hexene in 150 mL 0.1 M NaCl/50 mM Tris (pH 8-8.5) at 22°C with 10 g Fe(0) (50.7 m <sup>2</sup> /L). ....	105
Figure 38: Pathways for the reaction of 6-bromo-1-hexene in the presence of iron metal.....	107
Figure 39: Reaction of <i>cis</i> - and <i>trans</i> -DCE in the presence of Fe(0) in high headspace system experiments.....	131
Figure 40: Proposed pathways for reduction of <i>trans</i> -dichloroethylene by zero-valent metals. ....	134
Figure 41: Reduction of PCE by Zn(0) in system containing 0.1 M deoxygenated NaCl solution with minimal headspace. ....	136
Figure 42: Hypothesized reaction sequence for reduction of chlorinated ethylenes and related compounds by Zn(0).....	149
Figure 43: Effect of zinc age on reactivity to PCE reduction. Experiments conducted in 0.1 M NaCl, 25 g Zn(0)/150 mL at 36 rpm. ....	152
Figure 44: <i>Scientist</i> model file containing the system of differential equations applied to the reduction of PCE and all daughter products.. ....	156
Figure 45: Effect of initial concentration on measured overall pseudo-first-order rate constant, $k_{obs}$ .....	159
Figure 46: Effect of zinc loading on the reduction rate constant for PCE, TCE, and acetylene.....	161
Figure 47: Reduction of acetylene by 25 g Zn(0) in 160 mL of 0.1 M NaCl/0.05 M Tris buffer (pH 7.2). ....	162
Figure 48: Reduction of <i>trans</i> -DCE by 25 g Zn(0) in 160 mL 0.1 M NaCl/0.05 M Tris buffer (pH 7.2).....	163
Figure 49: Reduction of <i>cis</i> -DCE by 25 g Zn(0) in 160 mL 0.1 M NaCl/0.05 M Tris buffer (pH 7.2).....	164

Figure 50: Reduction of 1,1-DCE by 25 g Zn(0) in 160 mL 0.1 M NaCl/0.05 M Tris buffer (pH 7.2).....	165
Figure 51: Reduction of TCE in 160 mL 0.1 M NaCl/0.05 M Tris buffer (pH 7.2) by 25 g Zn(0). ....	166
Figure 52: Reduction of PCE in 150 mL 0.1 M NaCl/0.05 M Tris buffer (pH 7.2) by 5 g Zn(0). ....	167
Figure 53: Mass spectra of a) chloroacetylene and b) dichloroacetylene compared to literature spectra .....	170
Figure 54: Reduction of chloroacetylene in 0.1 M NaCl/0.05 M Tris buffer (pH 7.2) by 1 g Zn(0). . ....	171
Figure 55: Model equations used to calculate the rate constants pertaining to the chloroacetylene data shown in Figure 54. ....	173
Figure 56: Reduction of dichloroacetylene in 0.1 M NaCl/0.05 M Tris buffer (pH 7.2) by 0.5 g Zn(0). . ....	174
Figure 57: Mass spectrum of the major contaminant peak observed from the synthesis of dichloroacetylene. ....	175
Figure 58: Correlation of surface area normalized rate constants ( $k_{SA}$ , Table 8) with one-electron reduction potentials.....	178
Figure 59: Correlation of surface area normalized rate constants ( $k_{SA}$ , Table 8) with two-electron reduction potentials for hydrogenolysis and reductive elimination.....	179
Figure 60: Hypothesized reaction pathways for the chlorinated ethylenes and other intermediates during reduction by Fe(0).....	189
Figure 61: Behavior of initial rate of reaction of parent compound A to single product B as a function of initial concentration ( $C_{A0}$ ) of compound A according to the LHHW heterogeneous kinetic model for a) an adsorption-limited reaction, b) a surface reaction-limited reaction, and c) a desorption-limited reaction.....	192
Figure 62: Effect of metal loading on initial pseudo-first order rate constant for <i>trans</i> -DCE reaction with Fe(0).....	199
Figure 63: Effect of rotation rate on the pseudo-first order rate constant for acetylene and <i>trans</i> -DCE .....	201
Figure 64: Effect of initial substrate concentration on initial pseudo-first order rate constant ( $k_{obs}$ ) and initial rate ( $k_{obs}C_0$ ) for reduction by Fe(0) of a) PCE, b) TCE, c) <i>trans</i> -DCE, d) <i>cis</i> -DCE, e) 1,1-DCE, f) vinyl chloride, g) ethylene, h) acetylene, i) chloroacetylene, and j) dichloroacetylene.....	203
Figure 65: Reduction of ethylene by 0.25 g Fe(0) in 160 mL of 0.1 M NaCl, 50 mM Tris buffer (pH 7.2).....	215

Figure 66: Reduction of acetylene by 0.10 Fe(0) in 160 mL of 0.1 M NaCl, 50 mM Tris buffer (pH 7.2) at a) low and b) high initial concentration.....	216
Figure 67: Reduction of vinyl chloride by 0.25 g Fe(0) in 160 mL of 0.1 M NaCl, 50 mM Tris buffer (pH 7.2). ....	220
Figure 68: Reduction of <i>cis</i> -DCE by 0.25 g Fe(0) in 160 mL of 0.1 M NaCl, 50 mM Tris buffer (pH 7.2) at a) low and b) high initial concentration....	221
Figure 69: Reduction of <i>trans</i> -DCE by 0.25 g Fe(0) in 160 mL of 0.1 M NaCl, 50 mM Tris buffer (pH 7.2) at a) low and b) high initial concentration.....	223
Figure 70: Reduction of 1,1-DCE by 0.25 g Fe(0) in 160 mL of 0.1 M NaCl, 50 mM Tris buffer (pH 7.2) at a) low and b) high initial concentration.....	226
Figure 71: Model predictions (dashed lines) for the reduction of 1,1-DCE using a sequence of hydrogenolysis reactions (1,1-DCE → VC → ethylene) compared to experimental data.....	228
Figure 72: Reduction of chloroacetylene by 0.10 g Fe(0) in 160 mL of 0.1 M NaCl, 50 mM Tris buffer (pH 7.2) at a) low; b) intermediate; and c) high initial concentrations.....	230
Figure 73: Reduction of dichloroacetylene by 0.10 g Fe(0) in 160 mL of 0.1 M NaCl, 50 mM Tris buffer (pH 7.2) at a) low; b) intermediate; and c) high initial concentrations.....	233
Figure 74: Reduction of TCE by 0.25 g Fe(0) in 160 mL of 0.1 M NaCl, 50 mM Tris buffer (pH 7.2) at a) low and b) high initial concentration. ....	237
Figure 75: Reduction of PCE by 0.25 g Fe(0) in 160 mL of 0.1 M NaCl, 50 mM Tris buffer (pH 7.2) at a) low and b) high initial concentration. ....	239
Figure 76: Reaction of <i>trans</i> -DCE in the absence and presence of competitors <i>cis</i> -DCE, 200 µM; and acetylene, 100 µM.....	242
Figure 77: Reaction of <i>cis</i> -DCE in the absence and presence of competitors acetylene, 100 µM; 1,1-DCE, 200 µM; and <i>trans</i> -DCE, 200 µM. ....	243
Figure 78: Reduction of chloroacetylene in the absence and presence of potential competitors: <i>trans</i> -DCE, 200 µM; <i>cis</i> -DCE, 200 µM and 1,1-DCE, 200 µM.....	245
Figure 79: Simulation (lines) of intermediates generated in the permeable iron barrier at the Borden test site using the parameters in Table 10. ....	252
Figure 80: Simulation (lines) of intermediates generated in the permeable iron barrier at the Borden test site assuming that reaction only occurs via hydrogenolysis. ....	254

Figure 81: Correlation of the kinetic parameter for chlorinated ethylene reduction with one-electron reduction potential ( $E_1$ ). .....	256
Figure 82: Correlation of the kinetic parameter for chlorinated ethylene reduction with two-electron reduction potential for a) reductive elimination and b) hydrogenolysis. ....	257
Figure 83: Model simulation of TCE degradation starting at saturation using pseudo-first order conditions, the LHHW model, and the LHHW model with PCE also beginning at saturation.....	262
Figure 84: Hypothesized mechanism for reaction of PCE with Fe(0).....	264
Figure 85: Plot of log $K$ values versus ionization potential for the chlorinated ethylenes.....	265
Figure 86: Correlation of ( $k^s S_i$ ) values for the chlorinated ethylenes (from Table 10) with second-order rate constants for reactions with ozone.....	267
Figure 87: Reduction of 1,1,1-TCA in 0.1 M NaCl/0.05 M Tris buffer (pH 7.5) by Zn(0).....	286
Figure 88: Reduction of 1,1,1-TCA in 0.1 M NaCl/0.05 M Tris buffer (pH 7.5) by Fe(0).....	289
Figure 89: Reduction of 1,1,1-TCA by bimetallic (Ni-plated Fe) reductant in 0.1 M NaCl/0.05 M Tris buffer (pH 7.5).....	290
Figure 90: Reaction of 1,1,1-TCA with bimetallic (Cu-plated Fe) reductant in 0.1 M NaCl/0.05 M Tris buffer (pH 7.5). ....	292
Figure 91: Proposed scheme for reaction of 1,1,1-TCA with Fe(0).....	294
Figure 92: Comparison of experimental with calculated GC/MS spectra for reaction of isotopically labeled 1,1,1-TCA-2,2,2- $d_3$ with iron: (a) experimental ethane mixture (solid bars); "best-fit" mass spectrum assuming a mixture of unlabeled, mono-, di-, and trideuterated ethane isotopomers (fit 1, patterned bars); and "best-fit" mass spectrum based on a mixture of unlabeled through tetradeuterated ethanes (fit 2, open bars); (b) experimental ethylene mixture (solid bars) and "best-fit" mass spectrum based on a mixture of unlabeled through trideuterated ethylene isotopomers (patterned bars).....	298
Figure 93: GC/MS spectra of (a) 1,1-dichloroethane-2,2,2- $d_3$ ; (b) 2-butyne-1,1,1,4,4,4- $d_6$ ; and (c) <i>cis</i> -2-butene- $d_6$ obtained in reaction of 1,1,1-TCA-2,2,2- $d_3$ with iron.....	301
Figure A-1: Effect of the adsorption parameter ( $K$ ) on the shape of the initial rate versus initial concentration curve for a surface reaction limited case.....	A-10

Figure B-1: <i>Scientist</i> model file for acetylene reaction with Fe(0).....	B-5
Figure B-2: <i>Scientist</i> model file for <i>cis</i> -dichloroethylene reaction with Fe(0).....	B-7
Figure B-3: <i>Scientist</i> model file for trichloroethylene reaction with Fe(0).....	B-9





# SECTION I

## INTRODUCTION

### A. INTRODUCTION

Remediation of groundwater contaminated by anthropogenic pollutants represents a particularly challenging endeavor. The magnitude of this problem at DOD sites is staggering, as detailed in a report by the EPA (U. S. EPA, 1993). As of 1991, 7,313 sites at current or former DOD installations had been identified as having soil or groundwater requiring remediation. Of those sites under Air Force control at which groundwater has been contaminated by hazardous waste, 20% contain chlorinated organic solvents. The ten most common organic compounds found in ground water during a 1990 study of over 7,000 sampling locations at 196 Air Force installations are shown in Table 1: half of these are chlorinated alkanes or olefins. It was estimated that remediation of contaminated groundwater at Air Force sites will cost \$61 million dollars over a 15-year period, with additional costs for long-term operations and maintenance at all Air Force sites (including contaminated soil and disposal facilities) on the order of \$1.1 billion dollars.

At present, the technique most commonly employed for remediation of groundwater contamination is a "pump and treat" approach in which a network of extraction wells is used to withdraw contaminated groundwater, which is subsequently treated in above-ground facilities. This technique is particularly ineffective whenever separate phases of organic liquids (referred to as NAPLs) are present (Mackay and Cherry, 1989). As summarized in a report of the National Research Council, application of conventional pump-and-treat strategies to sites containing typical volumes of subsurface NAPLs essentially requires a perpetual level of effort (NRC, 1994). More innovative technologies, which might include pulsed pump and treat remediation, soil vapor extraction techniques, air sparging, bioremediation, soil washing, thermal desorption,

**TABLE 1: TEN MOST COMMON ORGANIC CONTAMINANTS FOUND IN GROUND WATER AT AIR FORCE INSTALLATIONS, IN ORDER OF DECREASING FREQUENCY (SOURCE: U. S. EPA, 1993). COMPOUNDS THAT CAN POTENTIALLY BE REMEDIATED USING ZERO-VALENT METALS, AND WHOSE REACTIONS WERE INVESTIGATED IN THE PRESENT STUDY, ARE INDICATED IN BOLD FACE.**

<b>Contaminant</b>
<b>Trichloroethylene (TCE)</b>
Toluene
Benzene
Phenolics
<b>Tetrachloroethylene (PCE)</b>
Ethylbenzene
<b>1,1,1-Trichloroethane (1,1,1-TCA)</b>
<b><i>trans</i>-1,2-Dichloroethylene (<i>trans</i>-DCE)</b>
1,2-Dichlorobenzene
<b>1,1-Dichloroethane (1,1-DCA)</b>

solvent extraction, vitrification, and enhanced chemical transformation, are clearly required to enhance the economic viability of remediation. One such innovative treatment approach – involving reaction with zero-valent metals – represents the focus of the present report.

The greatest need is for those technologies that could be used to treat contaminants *in situ*, either through chemical or biological methods. Problems have previously been encountered in applying bioremediation to groundwater contaminated with chlorinated olefins or alkanes. Although trichloroethylene (TCE) can be transformed under aerobic conditions by methylotrophic bacteria, introduction of oxygen to the subsurface is made difficult by the low aqueous solubility of O<sub>2</sub>. Moreover, tetrachloroethylene (PCE) (being highly oxidized) does not appear to be degradable by aerobic bacteria. Even though all of the chlorinated olefins and alkanes in Table 1 are susceptible to biotransformation via reductive dechlorination, rates of reduction of such compounds by indigenous microorganisms in groundwater appear to be quite slow, with half-lives on the order of months or more (Bouwer, 1993). Furthermore, numerous investigators have observed the lesser-chlorinated products to undergo biological reduction much more slowly than parent compounds. As a result, partially dehalogenated products (such as vinyl chloride, a known human carcinogen) have often been reported to accumulate (Bouwer,

1993). Such issues represent the principal limitations to treatment of chlorinated organic solvents via intrinsic or enhanced bioremediation approaches. Chemical means through which contaminant removal could be rapidly effected – for example, via *in situ* treatment with zero-valent metals – would provide distinct advantages to bioremediation, provided that generation of harmful, persistent byproducts could be avoided.

## **B. BACKGROUND**

### **1. Background on Iron-Based Permeable Barriers**

An exciting alternative to bioremediation for attaining *in situ* containment of chlorinated organic solvents is to use zero-valent iron as a reducing agent (Senzaki and Kumagai, 1988; Senzaki and Kumagai, 1989; Gillham and O'Hannesin, 1994; Matheson and Tratnyek, 1994; Burris *et al.*, 1995; Cipollone *et al.*, 1995; Muftikian *et al.*, 1995; Mackenzie *et al.*, 1995; Vogan *et al.*, 1995; Yamane *et al.*, 1995; Orth and Gillham, 1996; Muftikian *et al.*, 1996; Roberts *et al.*, 1996; Johnson *et al.*, 1996; Allen-King *et al.*, 1997; Scherer *et al.*, 1997; Campbell *et al.*, 1997; Gottpagar *et al.*, 1997; Korte *et al.*, 1997; Liang *et al.*, 1997; Tratnyek *et al.*, 1997; Johnson *et al.*, 1998; Gottpagar *et al.*, 1998; O'Hannesin and Gillham, 1998; Balko and Tratnyek, 1998; Scherer *et al.*, 1998; Bonin *et al.*, 1998; Su and Puls, 1998). One of the attractive features of this reductant is that it can be readily incorporated into a passive "funnel and gate" treatment system in which plumes of contaminated groundwater are intercepted by or are diverted (using low-permeability "funnels") through a reaction zone or "gate", containing an immobilized reagent or a zone of augmented biological activity (Starr and Cherry, 1994; Bedient *et al.*, 1994; O'Hannesin and Gillham, 1998). As contaminated groundwater travels through the permeable reaction zone, contaminants are chemically or microbially transformed, allowing treated water to pass unimpeded. This approach avoids problems that might be encountered in achieving mixing of dissolved reagents or limiting nutrients with contaminated groundwater during injection in heterogeneous natural aquifers.

To date, 26 full-scale and pilot-scale systems employing zero-valent metals for treating chlorinated solvents are in place (U.S. EPA, 1998; RTDF, 1999), most of which meet or exceed design specifications. By far the most common chlorinated solvents treated are the chlorinated ethylenes, present at all of these sites. Other chlorinated solvents present as co-contaminants that are occasionally treated are 1,1,1-trichloroethane (three sites), Freon 113 (one site), and carbon

tetrachloride (one site). The longest-running field demonstration of this technology was conducted at Canadian Forces Base Borden (O'Hannesin and Gillham, 1998). This field trial demonstrated that such a system can effectively contain a mixed plume of trichloroethylene and tetrachloroethylene, with no deterioration in performance detected over the 5-year course of the experiment. Although the *in situ* field test was successful in removing 90% of the influent mass of trichloroethylene and tetrachloroethylene, removal was however still incomplete, with downgradient concentrations in excess of drinking water standards. Further, the observed products (which included 1,1-dichloroethylene, *cis*-1,2-dichloroethylene, and *trans*-1,2-dichloroethylene) are themselves of concern as drinking water contaminants.

Until now, the precise pathways through which zero-valent metals reduce halogenated organic solvents have not been fully elucidated, nor have in many cases reaction products or intermediates been completely characterized. Such information is essential to the optimization of permeable barrier system design, as well as to the assessment of potential hazards that may be posed by reaction products. Some products of chlorinated ethylene reaction with Fe(0), such as vinyl chloride (Gillham and O'Hannesin, 1994; Orth and Gillham, 1996; Vogan *et al.*, 1995; Liang *et al.*, 1997) are themselves of concern as drinking water contaminants, with very low maximum contaminant level (MCL) values imposed by the US EPA (Pontius, 1998). Others, including *cis*-1,2-dichloroethylene as well as vinyl chloride, have been reported by others to react relatively slowly in the presence of Fe(0) (Gillham and O'Hannesin, 1994; Johnson *et al.*, 1996). Claims have been made that the necessity of controlling levels of such undesirable by-products can dictate the overall design of metal-based remediation systems and thus the economic viability of this approach to aquifer remediation (Yamane *et al.*, 1995; Vogan *et al.*, 1995). The dynamics governing formation and subsequent removal of such undesirable intermediates would therefore be expected to play an important role in barrier design. Moreover, an improved understanding of the routes through which such products are formed, or of factors which might enable prediction of organohalide persistence or products of organohalide reaction, might prove useful in "engineering" reductants with improved catalytic abilities. This understanding would also aid in predicting rates and reaction products that could enable preliminary assessment of the feasibility of using this approach for treating new contaminants.

## 2. Reactions of Organohalides with Zero-Valent Metals

The ability of zero-valent metals to reduce halogenated alkanes has been recognized as far back as 1874 (as reviewed by Baciocchi, 1983). This reaction has received some attention by industrial chemists, since it is relevant to the corrosion of metals undergoing cleaning by halogenated organic solvents (Archer and Simpson, 1977) and also since it affects the stability of chlorofluorocarbons formerly used as refrigerants or as propellants in aerosol cans (Church and Mayer, 1961; Bower and Long, 1961; Sanders, 1965). At present, as with other corrosion reactions, we still have an imperfect understanding of the detailed chemical mechanism(s) through which reduction occurs.

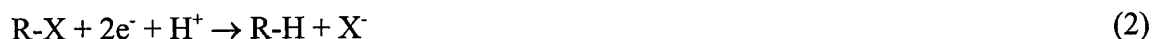
Although early studies of contaminant treatment with zero-valent metals were reported by Japanese researchers (Senzaki and Kumagai, 1988; Senzaki and Kumagai, 1989), the attention of the environmental community to metal-promoted reactions was stimulated by the work of Gillham and coworkers (Gillham and O'Hannesin, 1994). Their results indicated that a broad array of halogenated alkanes and olefins (including trichloroethylene, tetrachloroethylene, *trans*-1,2-dichloroethylene, 1,1-dichloroethylene, and 1,1,1-trichloroethane) react rapidly in aqueous solution at room temperature with zero-valent iron powder. CH<sub>2</sub>Cl<sub>2</sub> was the only compound tested which appeared inert.

As pointed out by Tratnyek and co-workers (Matheson and Tratnyek, 1994; Tratnyek, 1996), metal promoted reductive dechlorination essentially represents a corrosion process, with the zero-valent metal serving as the source of electrons:

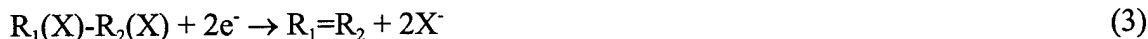


where M is a zero-valent metal such as iron or zinc.

This oxidation half-reaction can be coupled to the reduction of organohalides. Two different reductive dehalogenation reactions have been recognized. The first (and the reaction previously assumed to dominate reduction of organohalides; Gillham and O'Hannesin, 1994; Matheson and Tratnyek, 1994; Johnson *et al.*, 1996; Scherer *et al.*, 1998) is referred to as **hydrogenolysis**. This reaction involves replacement of a halogen X by a hydrogen:



The second is referred to as **reductive elimination**. In this reaction, transfer of two electrons is accompanied by loss of two halide ions. These may be vicinal halogens (*reductive  $\beta$  elimination*), in which case reduction is accompanied by an increase in bond order:



Alternatively, the organohalide in question may be a geminal dihalide, in which case *reductive  $\alpha$ -elimination* results in formation of a carbene or possibly a metal-stabilized carbenoid:



where Z can be a halogen, hydrogen, or alkyl. These reactions are therefore characterized by very different products, with different toxicity and greatly different environmental persistence.

Much of the thermodynamic driving force for these reactions is provided by solvation of the halide ions released. For example, for the hydrogenolysis reaction of 1,1,2,2-tetrachloroethane to 1,1,2-trichloroethane, we can compute the standard free energy change  $\Delta G^\circ_R$  of the reaction using thermodynamic data reviewed by Totten (1999) as:

$$\begin{aligned} \Delta G^\circ_R &= \Delta G^\circ_f(1,1,2\text{-trichloroethane, aq}) + \Delta G^\circ_f(\text{Cl}^-, \text{aq}) \\ &\quad - \Delta G^\circ_f(1,1,2,2\text{-tetrachloroethane, aq}) - \Delta G^\circ_f(\text{H}^+, \text{aq}) \\ &= (-81.15 \text{ kJ/mol}) + (-131.228 \text{ kJ/mol}) - (-84.19 \text{ kJ/mol}) - (0) = -128.19 \text{ kJ/mol} \end{aligned} \quad (5)$$

while for the reductive elimination of 1,1,2,2-tetrachloroethane to *cis*-1,2-dichloroethylene (the thermodynamically favored product), a similar calculation reveals:

$$\begin{aligned} \Delta G^\circ_R &= \Delta G^\circ_f(\text{cis-1,2-dichloroethylene, aq}) + 2\Delta G^\circ_f(\text{Cl}^-, \text{aq}) \\ &\quad - \Delta G^\circ_f(1,1,2,2\text{-tetrachloroethane, aq}) \\ &= (30.07 \text{ kJ/mol}) + 2(-131.228 \text{ kJ/mol}) - (-84.19 \text{ kJ/mol}) = -148.2 \text{ kJ/mol} \end{aligned} \quad (6)$$

Note in both cases the very large contribution to  $\Delta G^\circ_R$  made by solvation of the chloride ions. Even though the reductive elimination product, *cis*-1,2-dichloroethylene, is less stable than the hydrogenolysis product, 1,1,2-trichloroethane, the greater number of halide ions released during reductive elimination still makes this pathway more favorable in a thermodynamic sense than would be a hydrogenolysis reaction. Similar calculations (Section IV) comparing the thermodynamic favorability of hydrogenolysis to reductive elimination reactions for chlorinated ethylenes result in the same conclusion, *i.e.*, the reductive elimination pathway is always favored. If product branching ratios parallel thermodynamic trends, reductive  $\beta$ -elimination products should thus be favored over hydrogenolysis products. Although insufficient thermodynamic data are available for carbenes to enable similar generalizations for gem-dihalides concerning the favorability of hydrogenolysis relative to reductive  $\alpha$ -elimination reactions, the observation of products consistent with reductive  $\alpha$ -elimination pathways in a

variety of abiotic and biologically-mediated systems (Castro and Kray, 1966; Kennedy *et al.*, 1969; Ahr *et al.*, 1980; Dolbier and Burkholder, 1988, 1990; Krone *et al.*, 1991; Criddle and McCarty, 1991; Stromeyer *et al.*, 1992; Kriegman-King and Reinhard, 1992; Balko and Tratnyek, 1998) indicates that reductive  $\alpha$ -elimination reactions must also in some cases be a thermodynamically favorable process, despite the instability of carbene intermediates.

Of the two reductive dehalogenation reactions, reductive elimination (either  $\alpha$  or  $\beta$  elimination) poses distinct advantages from a treatment perspective. Studies conducted by other investigators and confirmed in our laboratory, for example, indicate that lesser-halogenated alkanes that might result from hydrogenolysis reactions typically react with metals much more slowly than more highly-halogenated alkanes (Scherer *et al.*, 1998; Arnold *et al.*, 1999). Some compounds, such as dichloromethane, chloromethane, chloroethane, and 1,2-dichloroethane, undergo reduction so slowly that treatment approaches based on Fe(0) are not even deemed practical (US EPA, 1998). In contrast, even monochloroethylene (vinyl chloride) reacts readily with Fe(0), as shown by the results of Section VI. Acetylenic compounds formed by the reductive  $\beta$ -elimination of polychlorinated ethylenes represent extremely reactive intermediates, as demonstrated by the results of Sections V and VI. Pathways involving reductive  $\beta$ -elimination therefore lead to products that can be readily and completely dehalogenated, while a sequence consisting solely of stepwise hydrolysis reactions would eventually result in transformation to (potentially persistent) partially halogenated products that would be expected to be regulated as drinking water contaminants.

The extent to which reductive  $\alpha$ -elimination may occur for geminal polyhalides lacking the  $\alpha$ ,  $\beta$  pair of halogens required for reductive  $\beta$ -elimination will also exert a major impact on barrier design and therefore the feasibility of treatment approaches based on zero-valent iron. For example, hydrogenolysis of 1,1-dichloroethylene would result in vinyl chloride, while reductive  $\alpha$ -elimination would generate an alkylidene carbenoid (Section VI) which could then undergo reduction to ethylene or rearrangement to acetylene in a manner that circumvents vinyl chloride formation. Alternatively, a free carbene would be expected to undergo very rapid reaction with the solvent via a process involving insertion into the H-O bond. In the case of carbenes generated from gem polyhaloalkanes, any  $\alpha$  halogen substituents remaining on the resulting alcohol hydrolytic trapping product would be rapidly eliminated, with the final product consisting of carbon monoxide or formate (from reduction of CCl<sub>4</sub>) or formaldehyde (from



reduction of  $\text{CHCl}_3$ ), both of which are readily degradable by microorganisms and which would therefore be considered as much more desirable products than the  $\text{CH}_2\text{Cl}_2$  which results from stepwise hydrogenolysis. Metal-stabilized carbenoids might persist long enough to undergo a succession of reduction steps; such a sequence of reactions was reported (Section VII) to be responsible for the facile conversion of 1,1,1-trichloroethane to ethane via a pathway that does not involve 1,1-dichloroethane as an intermediate. Since 1,1-dichloroethane reaction with  $\text{Fe}(0)$  is slow enough that removal of this daughter product dictates the design of barriers intended for treatment of 1,1,1-trichloroethane, reductive  $\alpha$ -elimination is also a more desirable route than hydrogenolysis. The branching ratio between reductive  $\alpha$ - or  $\beta$ -elimination and hydrogenolysis therefore emerges as an important parameter dictating the success of metal-based treatment methods.

This picture becomes complicated, because it is not only the branching ratio between hydrogenolysis and reductive  $\beta$ -elimination (or between hydrogenolysis and reductive  $\alpha$ -elimination) which dictates the distribution of intermediates and final reaction products. Olefins and acetylenes formed from reductive  $\beta$ -elimination can undergo either hydrogenolysis to lesser-halogenated homologs, or (at least in principle) can undergo reduction of the triple or the double bond (hydrogenation), accompanied by an increase in bond order. To the extent that this may generate partially dehalogenated and much more persistent products than the substituted acetylenes, a branching ratio favoring hydrogenation reactions would therefore be viewed as unfavorable from a treatment perspective. Our studies (Sections V and VI) demonstrate that for reduction of chlorinated ethylenes by  $\text{Zn}(0)$  and  $\text{Fe}(0)$ , reductive  $\beta$ -elimination and hydrogenolysis occur as competing reactions, just as hydrogenolysis and hydrogenation compete in the reduction of chlorinated acetylenes by these metals. The extent to which partially dechlorinated intermediates are generated therefore reflects the complex interplay between a large number of concurrent and consecutive reactions.

Whether reactions proceed via free radical pathways, or alternatively via an essentially concerted transfer of two electrons, may also exert an impact on the initial products formed during metal-promoted reductive dechlorination and therefore the design of iron-based barriers. For example, Balko and Tratnyek (1998) argue that a shift toward a two-electron mechanism in the reduction of  $\text{CCl}_4$  by iron induced by photoirradiation is responsible for a corresponding change in the product distribution favoring  $\alpha$ -elimination over hydrogenolysis. Moreover,

Sivavec (1995) has hypothesized that the  $C_4$  products resulting from reduction of chlorinated ethylenes by Fe(0) represent radical coupling products.

Unfortunately, many of the diagnostic criteria often used to differentiate between two-electron reaction pathways and free radical pathways cannot readily be applied to reduction by zero-valent metals or other strong reductants. The most common method of studying free radicals involves trapping them by reaction with nitroso compounds to form relatively stable nitroxide radicals, which can be subsequently examined via electron spin resonance spectroscopy. Zero-valent metals, however, are known to readily reduce both nitro groups and nitroso groups all the way to amines (in fact, reduction of nitro compounds by metals is an important route to the synthesis of amines; March, 1985), and nitroso spin traps are unlikely to persist long enough as stable species to make them useful as trapping agents under such strongly reducing conditions. Formation of radical coupling products, often used as a diagnostic indicator of free-radical processes, requires high concentrations of radical precursors and rapid rates of reaction, conditions that may not be met under environmentally relevant conditions owing to the limited solubility of halogenated alkanes and their relatively low reactivity. Moreover, rearrangement of organometallic species at the metal-solution interface can give rise to coupling products through processes that need not involve dimerization of two free radicals. It is for this reason that we have been exploring the utility of information derived from stereochemical studies of the reduction of vicinal dibromides and alkyl monobromide free radical "clocks" as a guide to reaction mechanism. In order to assess the likelihood that free radicals could accumulate to significantly elevated concentrations for self-coupling to occur, part of our studies (described in Sections II and III) focused on reduction of such probe compounds by zero-valent metals.

## C. SCOPE

Clearly, before technologies based on reactions of zero-valent metals with organohalides can be fully optimized for application to containment of chlorinated organic solvent contaminants in groundwater, a better understanding of the fundamental chemical mechanisms through which intermediates are generated is required. This study had several objectives:

- (a) to better characterize the mechanisms through which electron transfer occurs from the metal to the organohalide – specifically, to assess whether or not reactions of alkyl halides proceed via free radical pathways by examining product distributions obtained using "probe"

compounds;

- (b) to measure rates and products of chlorinated organic solvent reaction with two "model" zero-valent metals (zinc and iron) in aqueous solution under carefully-controlled batch conditions of essentially constant pH and ionic strength;
- (c) to use the resulting information from part (b) to develop kinetic models of chlorinated ethylene reaction with metals. As shown in Section VI, in the case of reaction of chlorinated ethylenes with Fe(0), the resulting kinetic models needed to incorporate both intra- and interspecies competitive effects. Such models in turn can be used to identify the sequence of reactions responsible for formation of specific halogenated intermediates, including the relative importance of hydrogenolysis, reductive  $\beta$ -elimination, and hydrogenation reactions. The kinetic models also provide the basis for development of "process models" through which design of permeable barriers can be optimized.
- (d) to attempt to utilize the kinetic information derived in part (c) to develop quantitative structure-activity relationships through which rates and products of reaction of new or untested compounds can be predicted.
- (e) to attempt to deduce from our results information pertaining to the mechanisms through which metal-promoted reduction reactions of organohalides take place.

## D. REPORT ORGANIZATION

Section II in this report, "Alkyl Bromides as Mechanistic Probes of Reductive Dehalogenation: Reactions of Vicinal Dibromide Stereoisomers with Zero-Valent Metals", reports on the stereoselectivity of reductive elimination reactions promoted by a variety of zero-valent metals. This work was initiated to shed light on the question of whether reactions of alkyl halides proceed via free radical pathways, or alternatively via an essentially concerted sequence of single-electron transfers. Investigation of these issues is continued in Section III, "Alkyl Bromides as Mechanistic Probes of Reductive Dehalogenation: Reactions of Radical Clocks with Zero-Valent Metals". Section IV, "Reductive Elimination of Chlorinated Ethylenes by Zero-Valent Metals", is the first of three sections which emphasize reactions of contaminants of concern to the Air Force (as opposed to the mechanistic probe compounds which were the focus of Sections II and III). This section reports on some of our initial findings concerning the pathways through which chlorinated ethylenes react with two metals, iron and zinc. The

experiments described in this section demonstrated that reductive dehalogenation of chlorinated ethylenes takes place at least in part via reductive  $\beta$ -elimination reactions. The existence of this pathway had not previously been documented in the environmental literature for this important class of contaminants. Section V, "Pathways of Chlorinated Ethylene and Chlorinated Acetylene Reaction with Zn(0)", focuses on reactions of chlorinated ethylenes and their daughter products with a model metal reductant, Zn(0). Section VI, "Pathways and Kinetics of Chlorinated Ethylene and Chlorinated Acetylene Reaction with Fe(0)", extends the efforts of the previous chapter to reactions with Fe(0) in batch systems. Finally, Section VII, "Reaction of 1,1,1-Trichloroethane with Zero-Valent Metals and Bimetallic Reductants", describes work we conducted to elucidate pathways through which this important chlorinated organic solvent reacts.

Some of the sections of this report represent somewhat expanded versions of papers that have been published in *Environmental Science and Technology* (Roberts *et al.*, 1996; Fennelly and Roberts, 1998b; Arnold and Roberts, 1998a). This study also formed part of the Ph.D. theses of two students (Totten, 1999; Arnold, 1999). Preliminary findings obtained in this study have been presented at a number of national meetings of professional societies and meetings of industry groups (Roberts *et al.*, 1995; Arnold *et al.*, 1996; Roberts and Burris, 1996; Arnold and Roberts, 1997; Fennelly and Roberts, 1998a; Roberts *et al.*, 1998; Totten and Roberts, 1998; Arnold and Roberts, 1998b; Arnold and Roberts, 1998c; Arnold and Roberts, 1999). Two graduate student paper awards from the Environmental Chemistry Division of the American Chemical Society (one to Totten in 1998, and a second to Arnold in 1999) resulted from this work; this represents the highest award conferred upon graduate students by the Environmental Chemistry Division of the American Chemical Society. In addition, a "Certificate of Merit" was conferred to Arnold by the Environmental Chemistry Division of the American Chemical Society for the presentation he made at the 1997 National Meeting (Arnold and Roberts, 1997).

## E. SIGNIFICANT FINDINGS

Results of studies with probe compounds (vicinal dibromide stereoisomers and free radical "clocks") suggested that for these compounds, reactions may proceed via transfer of a single electron rather than via so-called "two-electron" (nucleophilic) pathways. The rate of transfer of the second electron is, however, so fast ( $\sim 10^8$  to  $10^{10}$  s<sup>-1</sup>) that any *free* radical intermediates that might be formed are unlikely to persist long enough to escape the metal surface or to undergo such characteristic free-radical reactions with dissolved constituents as dimerization and hydrogen atom abstraction. This may indicate that the apparent coupling products sometimes encountered in metal-promoted reactions may be formed by some means other than by coupling of two free radicals (*e.g.*, by rearrangement of a dialkylorganometallic intermediate). An alternative explanation is that reactions may only occur at highly localized sites at metal surfaces, with coupling and hydrogen abstraction being facilitated by proximity effects.

Detailed kinetic and product studies confirmed the results presented in Section IV indicating that both zinc and iron react with chlorinated ethylenes to a considerable extent via reductive  $\beta$ -elimination. For reaction with zinc, the importance of reductive  $\beta$ -elimination paralleled the thermodynamic favorability of this reaction relative to hydrogenolysis, increasing from 15% to 95% of the total as the degree of chlorination decreased. No such trend was observed for reactions of chlorinated ethylenes with iron; reductive elimination accounted for 87% to 99% of the total reaction, and displayed no consistent trend with the degree of chlorination. For 1,1-dichloroethylene, reductive  $\alpha$ -elimination to ethylene appears to occur via a sequence that involves  $\alpha$ -elimination to an alkylidene carbenoid, which is subsequently reduced to ethylene; generation of vinyl chloride as an intermediate is thereby circumvented.

A substantial fraction (8%-82%, increasing with the degree of chlorination) of chlorinated acetylene reduction by Zn(0) occurs via hydrogenation of the double bond to generate chlorinated ethylenes rather than via hydrogenolysis to lesser-chlorinated acetylenes. In contrast, no measurable hydrogenation occurs in reaction of chloroacetylene with iron, and only 24% of dichloroacetylene reacts via hydrogenation. Reaction with iron is therefore better able to circumvent generation of partially chlorinated ethylenes such as vinyl chloride.

In the case of reaction of chlorinated ethylenes with zinc, a pseudo-first order model adequately describes reaction rates, and rate constants increase with one- and two-electron

reduction potentials. In contrast, substantial intra- and interspecies inhibitory effects were observed for reaction of chlorinated ethylenes with iron, interpreted as evidence of competition for a limited number of reactive sites at the metal surface. Such intraspecies competition has been previously reported in the reduction of  $\text{CCl}_4$  by  $\text{Fe}(0)$  (Johnson *et al.*, 1996; Scherer *et al.*, 1999). Reactions could not therefore be modeled using a simple pseudo-first order approach. In most cases, a modified Langmuir-Hinshelwood-Hougen-Watson approach in which rates are limited by reaction at the metal surface adequately captured the major features of the observed timecourses. For a few species (ethylene, vinyl chloride), rates of reaction were either limited by the rate of the adsorption step, or else were limited by the rate of the surface reaction while displaying small adsorption constants. Kinetic constants for reactions of iron with chlorinated ethylenes exhibited a distinct decreasing trend with increasing halogenation. Thus, partially dechlorinated ethylenes reacted with iron faster than their more highly halogenated analogs, in sharp contrast to the behavior observed in reaction of chlorinated ethylenes with zinc. This difference in behavior may be indicative of differences in mechanism between reaction of the two metals.

Reaction rates, product distributions, and product branching ratios observed in the reduction of 1,1,1-trichloroethane with zero-valent metals and bimetallic reductants varied with the identity of the metal reductant. Much more 1,1-dichloroethane was observed for reduction by Fe, Cu/Fe or Ni/Fe than with zinc. A substantial fraction of the reaction in each case occurred via reductive  $\alpha$ -elimination to ethane, a reaction in which 1,1-dichloroethane did not appear to serve a role as an intermediate. Apparent coupling products were observed for reaction with iron and the bimetallic reductants, but not with zinc.

These results are of immediate practical relevance to permeable barrier design. The important (in many cases, preeminent) role played by reductive  $\alpha$ - or  $\beta$ -elimination, as well as subsequent hydrogenation reactions for substituted acetylene daughter products, makes inclusion of such reactions important in process models used to optimize barrier design. In many cases, product branching ratios are such as to at least partially circumvent the generation of relatively stable partially dechlorinated products; this will reduce the hydraulic residence times required to meet drinking water standards in the effluent from permeable barriers. Part of the reason why iron is so useful in permeable barriers (aside from any questions of cost or toxicity of metal ions released) in fact stems from reactivity trends and product branching ratios. The high branching

ratio favoring reductive  $\beta$ - and  $\alpha$ -elimination reactions of chlorinated ethylenes, and the low branching ratios favoring hydrogenation of the substituted acetylenes, largely circumvents the generation of partially dechlorinated ethylenes. What partially dechlorinated ethylenes are generated tend to react more rapidly than the parent chloroolefins. The net effect of both of these factors is that partially dechlorinated intermediates do not tend to accumulate to high concentrations. Modeling the results obtained in the Borden experiment suggests that reductive  $\beta$ -elimination may also play an important role in iron-promoted reactions of chlorinated ethylenes in the field, even when the iron type and electrolyte composition vary substantially from that employed in our laboratory experiments.

The substantial intra- and interspecies competitive effects observed in our batch experiments may also have important consequences to barrier design. Pseudo-first order rate “constants” varied by more than an order of magnitude, depending on initial concentration of the parent compound or on the presence of inhibitory species. Testing of granular media with single solutes or contaminants present at lower concentrations than present in the field may therefore result in insufficiently conservative design parameters. Additional experiments are currently under way in our laboratory to confirm the existence of such inter- and intraspecies competitive effects in steady-state column settings.

These studies also provided considerable insights into the mechanisms of the reactions of organohalides with zero-valent metals. It appears that the metal surface is much more than a “passive” source of electrons, and several indirect lines of evidence were consistent with the notion that organometallic intermediates could be formed. The decrease in rate constants with reduction potentials observed with iron is at variance with previous suggestions (Scherer *et al.*, 1998) that reaction rates are limited by single electron (SET) transfer from the metal to a  $\pi^*$  or  $\sigma^*$  lowest unoccupied molecular orbital (LUMO) of the organohalide. This reactivity pattern is however consistent with a rate-limiting step involving carbon-iron bond formation at the particle/water interface. This notion is supported by  $^{12}\text{C}/^{13}\text{C}$  kinetic isotope effects for reduction of trichloroethylene by granular iron that can be inferred from the results of Slater *et al.* (1999), which are of the magnitude that might be anticipated for primary kinetic isotope effects.

For the chlorinated ethylenes, the free radical “clocks”, and 1,1,1-trichloroethane, the substantial differences in product branching ratios obtained with zinc vs. iron suggests the metal in some cases plays a direct role in the product-determining steps. Even though iron surfaces are

much better than zinc at generating  $H_2$  and should therefore represent a better source of labile hydrogen atoms, much less hydrogenolysis was observed in reduction of chlorinated ethylenes with iron than with zinc, and much less hydrogenation was observed in reduction of chlorinated acetylenes by iron than with zinc. The substantial differences in the rate of the second electron transfer observed among various "probe" molecules (free radical clocks and vicinal dibromide stereoisomers) may also be indicative of organometallic intermediates. Moreover, the complicated distribution of products obtained with one of these "clocks", 6-bromo-1-hexene, and especially the observation of the  $\beta$ -hydride elimination product 1,2-hexadiene as well as olefin isomerization products, is consistent with what has been observed from reaction of organoiron intermediates. The apparent absence of significant amounts of hydrolytic trapping products or typical carbene rearrangement products such as acetaldehyde or vinyl chloride from the reductive  $\alpha$ -elimination of 1,1,1-trichloroethane, or of vinyl alcohol or acetylene from the reductive  $\alpha$ -elimination of 1,1-dichloroethylene, may indicate that intermediates occur as metal-bound carbenoids rather than as free carbenes. Recognition of the potential role played by organometallic species provides an important first step in understanding factors that control reactivity and selectivity in metal-promoted reduction reactions of organohalides.



## F. LITERATURE CITED

- Ahr, H. J.; King, L. J.; Nastainczyk, W.; Ullrich, V. The mechanism of chloroform and carbon monoxide formation from carbon tetrachloride by microsomal cytochrome P-450. *Biochem. Pharmacol.* **1980**, *29*, 2855-2861.
- Allen-King, R. M., R. M. Halket, and D. R. Burris. Reductive transformation and sorption of *cis*- and *trans*-1,2-dichloroethene in a metallic iron-water system. *Environ. Toxicol. Chem.* **1997**, *16*, 424-429.
- Archer, W. L.; Simpson, E. L. Chemical profile of polychloroethanes and polychloroalkenes. *Ind. Eng. Chem., Prod. Res. Dev.* **1977**, *16*, 158-162.
- Arnold, W. A. *Kinetics and Pathways of Chlorinated Ethylene and Chlorinated Ethane Reaction with Zero-Valent Metals*. PhD dissertation, **1999**, The Johns Hopkins University.
- Arnold, W. A.; A. L. Roberts. Development of a quantitative model for chlorinated ethylene reduction by zero-valent metals. *Natl. Meet. - Am. Chem. Soc., Div. Environ. Chem.* **1997**, *37(1)*, 76-77 (Abstr.).
- Arnold, W. A.; A. L. Roberts. Pathways of chlorinated ethylene and chlorinated acetylene reaction with Zn(0). *Environ. Sci. Technol.* **1998a**, *32*, 3017-3025.
- Arnold, W. A.; A. L. Roberts. Pathways and kinetics of chlorinated ethylene reaction with Fe(0). Poster presented at the Remediation Technologies Development Forum (RTDF) Permeable Reactive Barriers Action Team Meeting, Oak Ridge, TN, Nov. 17, **1998b**.
- Arnold, W. A.; A. L. Roberts. Advantages of zero-valent iron for use in permeable barriers: kinetics and reaction pathways. Paper presented in "Physical and Chemical Remediation of Contaminated Aquifers", Hydrology Section, Amer. Geophys. Union National Meeting, San Francisco, CA, December 10, **1998c**.
- Arnold, W. A.; A. L. Roberts. Pathways and kinetics of chlorinated ethylene and chlorinated acetylene reaction with Fe(0). *Natl. Meet. - Am. Chem. Soc., Div. Environ. Chem.* **1999**, *39(2)*, 158-160, (Abst.).
- Arnold, W. A.; Roberts, A. L.; Burris, D. R.; Campbell, T. J. Quantitative evaluation of pathways involved in trichloroethylene reduction by zero-valent metals: iron and zinc.

Society of Environmental Toxicology and Chemistry 17<sup>th</sup> Ann. Mtg., Washington, D. C., November 18, **1996**.

Arnold, W. A.; W. P. Ball, and A. L. Roberts. Polychlorinated ethane reaction with zero-valent zinc: pathways and rate control. *J. Contam. Hydrol.* **1999**, *40*(2), 183-200.

Bacocchi, E. "1,2-Dehalogenations and related reactions". In S. Patai and Z. Rappoport, Eds., *The Chemistry of Functional Groups*, Supplement D: The Chemistry of Halides, Pseudo-Halides, and Azides, Part 1, John Wiley and Sons, **1983**, 161-201.

Balko, B. A., and P. G. Tratnyek. Photoeffects on the reduction of carbon tetrachloride by zero-valent iron. *J. Phys. Chem. B.* **1998**, *102*, 1459-1465.

Bedient, P. B.; Rifai, H. S.; Newell, C. J. *Ground Water Contamination: Transport and Remediation*. Prentice Hall, Englewood Cliffs, New Jersey **1994**, 541 pp.

Bonin, P. M. L., M. S. Odziemkowski, and R. W. Gillham. Influence of chlorinated solvents on polarization and corrosion behavior of iron in borate buffer. *Corrosion Science* **1998**, *40*, 1391-1409.

Bouwer, E. J.. Bioremediation of chlorinated solvents using alternate electron acceptors. In R. D. Norris, *et al.*, *Handbook of Bioremediation*, Lewis Publishers, **1993**, 257 pp.

Bower, F. A.; Long, L. J.. How to formulate stable alcohol-based aerosols. *Soap Chem. Spec.* **1961**, *37*, 127-137.

Burris, D. R., T. J. Campbell, and V. S. Manoranjan. Sorption of trichloroethylene and tetrachloroethylene in a batch reactive metallic iron-water system. *Environ. Sci. Technol.* **1995**, *29*, 2850-2855.

Campbell, T. J., Burris, D. R., A. L. Roberts, and J. R. Wells. Trichloroethylene and tetrachloroethylene reduction in a metallic iron-water-vapor batch system. *Environ. Toxicol. Chem.* **1997**, *16*, 625-630.

Castro, C. E.; Kray, W. C. Carbenoid intermediates from polyhalomethanes and chromium (II). The homogeneous reduction of geminal halides by chromous sulfate. *J. Amer. Chem. Soc.* **1966**, *88*, 4447-4455.

Church, J. M.; Mayer, J. H. Stability of trichlorofluoromethane in the presence of moisture and certain metals. *J. Chem. Eng. Data* **1961**, *6*, 449-453.

- Cipollone, M. G., N. L. Wolfe, and S. M. Hassan. Kinetic studies on the use of metallic iron to reduce organic compounds in water under environmental conditions. *Natl. Meet.-Am. Chem. Soc., Div. Environ. Chem.* **1995**, *35*, 812-814 (Abstr.).
- Criddle, C. S.; McCarty, P. L. Electrolytic model system for reductive dehalogenation in aqueous environments. *Environ. Sci. Technol.* **1991**, *25*, 973-978.
- Dolbier, W. R.; Burkholder, C. R. Generation of chlorofluorocarbene by dehalogenation of fluorotrichloromethane with reduced titanium. A new synthesis of 1-chloro-1-fluorocyclopropanes. *Tet. Lett.* **1988**, *29*, 6749-6752.
- Dolbier, W. R.; Burkholder, C. R. Chlorofluorocarbene from reaction of fluorotrichloromethane with reduced titanium. Synthesis of 1-chloro-1-fluorocyclopropanes. *J. Amer. Chem. Soc.* **1990**, *55*, 589-594.
- Fennelly, J. P.; A. L. Roberts. Reaction of 1,1,1-trichloroethane with zero-valent metals and bimetallic reductants. Paper presented at the First International Conference on Remediation of Chlorinated and Recalcitrant Compounds, Monterey, CA, May 18, **1998a**.
- Fennelly, J. P.; A. L. Roberts. Reaction of 1,1,1-trichloroethane with zero-valent metals and bimetallic reductants. *Environ. Sci. Technol.* **1998b**, *32*, 1980-1988.
- Gillham, R. W.; O'Hannesin, S. F.. Enhanced degradation of halogenated aliphatics by zero-valent iron. *Ground Water* **1994**, *32*, 958-967.
- Gotpagar, J., E. Grulke, T. Tsang, and D. Bhattacharyya. Reductive dehalogenation of trichloroethylene using zero-valent iron. *Environ. Prog.* **1997**, *16*, 137-143.
- Gotpagar, J. K., E. A. Grulke, and D. Bhattacharayya. Reductive dehalogenation of trichloroethylene: kinetic models and experimental verification. *Jour. Haz. Mater.* **1998**, *62*, 243-264.
- Johnson, T. L., M. M. Scherer, and P. G. Tratnyek. Kinetics of halogenated organic compound degradation by iron metal. *Environ. Sci. Technol.* **1996**, *30*, 2634-2640.
- Johnson, T. L., W. Fish, Y. A. Gorby, and P. G. Tratnyek. Degradation of carbon tetrachloride by iron metal: complexation effects on the oxide surface. *Jour. Contam. Hydrol* **1998**, *29*, 377-396.

- Kennedy, F. S.; Buckman, T.; Wood, J. M. Carbenoid intermediates from the photolysis of haloalkylcobalamins. *Biochim. Biophys. Acta* **1969**, *177*, 661-663.
- Korte, N., L. Liang, R. Muftikian, C. Grittini, and Q. Fernando. The dechlorination of hydrocarbons: palladised iron utilized for ground water purification. *Platinum Metals Rev.* **1997**, *41*, 2-7.
- Kriegman-King, M. R.; Reinhard, M. Transformation of carbon tetrachloride in the presence of sulfide, biotite, and vermiculite. *Environ. Sci. Technol.* **1992**, *26*, 2198-2206.
- Krone, U. E.; Thauer, R. K.; Hogenkamp, H. P. C.; Steinbach, K. Reductive formation of carbon monoxide from CCl<sub>4</sub> and FREONs 11, 12, and 13 catalyzed by corrinoids. *Biochemistry* **1991**, *30*, 2713-2719.
- Liang, L., N. Korte, J. D. Goodlaxson, J. Clausen, Q. Fernando, and R. Muftikian. Byproduct formation during the reduction of TCE by zero-valence iron and palladized iron. *Ground Water Monit. Remed.* **1997**, *Winter*, 122-127.
- Mackay, D. M.; Cherry, J. A. Groundwater contamination: pump-and-treat remediation. *Environ. Sci. Technol.* **1989**, *15*, 1475-1481.
- Mackenzie, P. D.; S. S. Baghel, G. R. Eykholt, D. P. Horney, J. J. Salvo, and T. M. Sivavec. Pilot-scale demonstration of reductive dechlorination of chlorinated ethenes by iron metal. *Natl. Meet.-Am. Chem. Soc., Div. Environ. Chem.* **1995**, *35*, 796-799 (Abstr.).
- March, J. *Advanced Organic Chemistry: Reactions, Mechanisms, and Structure*. John Wiley and Sons, N.Y., **1985**.
- Matheson, L. J.; Tratnyek, P. G. Reductive dehalogenation of chlorinated methanes by iron metal. *Environ. Sci. Technol.* **1994**, *28*, 2045-2053.
- Muftikian, R., Q. Fernando, and N. Korte. A method for the rapid dechlorination of low molecular weight chlorinated hydrocarbons in water. *Water Res.* **1995**, *29*, 2434-2439.
- Muftikian, R., K. Nebesny, Q. Fernando, and N. Korte. X-ray photoelectron spectra of the palladium-iron bimetallic surface used for the rapid dechlorination of chlorinated organic environmental contaminants. *Environ. Sci. Technol.* **1996**, *30*, 3593-3596.
- National Research Council. *Alternatives for Ground Water Cleanup*. National Academy Press: Washington, DC, **1994**.

- O'Hannesin, S. F., and Gillham, R. W. Long-term performance of an in situ "iron wall" for remediation of VOCs. *Ground Water* **1998**, *36*, 164-170.
- Orth, S. W., and R. W. Gillham. Dechlorination of trichloroethene in aqueous solution using Fe(0). *Environ. Sci. Technol.* **1996**, *30*, 66-71.
- Pontius, F.W. New horizons in federal regulations. *Journal AWWA* **1998**, *90*(3), 38-46.
- Remediation Technologies Development Forum (RTDF). Permeable reactive barrier installation profiles. [Online]. Available: <http://www.rtdf.org/public/permbarr/barrdocs.htm> [April 19, 1999].
- Roberts, A. L.; Burris, D. R.. Reductive elimination reactions of chlorinated ethenes: a comparison of chemical and biomimetic systems. *Emerging Technologies in Hazardous Waste Management VIII -- American Chemical Society, Indust. & Eng. Chem. Div.* **1996**, 182-185, (Abst).
- Roberts, A. L.; Burris, D. R.; Campbell, T. J. Influence of electron transfer pathway on products resulting from metal-promoted reduction of chlorinated ethenes. Paper presented at IBC's International Symposium on Biological Dehalogenation, Annapolis, MD, October 19, **1995**.
- Roberts, A. L., L. A. Totten, W. A. Arnold, D. R. Burris, and T. J. Campbell. Reductive elimination of chlorinated ethylenes by zero-valent metals. *Environ. Sci. Technol.* **1996**, *30*, 2654-2659.
- Roberts, A. L.; Arnold, W. A.; Eykholt, G. R. Role of environmental chemistry in designing permeable barriers for containment of chlorinated organic solvents in groundwater. *Natl. Meet. - Am. Chem. Soc., Div. Environ. Chem.* **1998**, *38*(2), 289 (Abstr.).
- Sanders, P. A. Reaction of propellant 11 with water. *Soap Chem. Spec.* **1965**, *41*, 117-158.
- Scherer, M. M.; J. C. Westall, M. Ziomek-Moroz, and P. G. Tratnyek. Kinetics of carbon tetrachloride reduction at an oxide-free iron electrode. *Environ. Sci. Technol.* **1997**, *31*, 2385-2391.
- Scherer, M. M.; Balko, B. A.; Gallagher, D. A.; Tratnyek, P. G. Correlation analysis of rate constants for dechlorination by zero-valent iron. *Environ. Sci. Technol.* **1998**, *32*, 3026-3033.

- Senzaki, T., and Y. Kumagai. Removal of organochloro compounds in wastewater by reductive treatment. I. Reductive degradation of 1,1,2,2-tetrachloroethane with iron powder. *Kogyo Yosui* **1988**, 357, 2-7.
- Senzaki, T., and Y. Kumagai. Removal of organic chlorine compounds by use of some reduction processes: processing trichloroethylene with iron powder. *Kogyo Yosui* **1989**, 369, 19-25.
- Sivavec, T. M., and D. P. Horney. Reductive dechlorination of chlorinated ethenes by iron metal. *Natl. Meet.-Am. Chem. Soc., Div. Environ. Chem.* **1995**, 35, 695-698 (Abstr.).
- Slater, G. F.; Dempster, H.D.; Sherwood-Lollar, B.; Spivack, J.; Brennan, M.; Mackenzie, P. "Isotopic tracers of degradation of dissolved chlorinated solvents." In *Natural Attenuation: Chlorinated and Recalcitrant Compounds*. Wickramanayake, G.B. and Hincee, R.E. Eds. Battelle Press: Columbus, OH, May 18-21, **1998**, 133-138.
- Starr, R. C.; Cherry, J. A.. *In situ* remediation of contaminated ground water: the funnel-and-gate system. *Ground Water* **1994**, 32, 465-476.
- Stromeyer, S. A.; Stumpf, K.; Cook, A. M.; Leisinger, T. M. Anaerobic degradation of tetrachloromethane by *Acetobacterium woodii*: separation of dechlorinative activities in cell extracts and roles for vitamins B<sub>12</sub> and other factors. *Biodegradation* **1992**, 3, 113-123.
- Su, C., and R. W. Puls. Kinetics of trichloroethene reduction by zero-valent iron and tin: pretreatment effect, apparent activation energy, and intermediate products. *Environ. Sci. Technol.* **1999**, 33, 163-168.
- Totten, L. A. R. *The Use of Model and Probe Compounds to Investigate the Mechanisms of Reductive Dehalogenation Reactions*. PhD dissertation, **1999**, The Johns Hopkins University.
- Totten, L. A.; A. L. Roberts. Alkyl bromides as probes of reductive dehalogenation: 1) Reactions with zero-valent metals. *Natl. Meet. - Am. Chem. Soc., Div. Environ. Chem.* **1998**, 38(2), 256-257 (Abst.).
- Tratnyek, P. G. Putting corrosion to use: remediation of contaminated groundwater with zero-valent metals. *Chem. & Ind.* **1996**, 13, 499-503.
- Tratnyek, P. G., T. L. Johnson, M. M. Scherer, and G. R. Eykholt. Remediating groundwater with zero-valent metals: kinetic considerations in barrier design. *Ground Water Monit. Remed.* **1997**, 17(4), 108-114.

U. S. EPA and Emergency Response. *Cleaning Up the Nation's Waste Sites: Markets and Technology Trends*. Office of Solid Waste, **1993**, EPA 542-R-92-012.

U. S. EPA. *Permeable Reactive Barrier Technologies for Contaminant Remediation*. Office of Solid Waste and Emergency Response, **1998**, EPA/600/R-98/125.

Vogan, J. L., R. W. Gillham, S. F. O'Hannesin, and W. H. Matulewicz. Site specific degradation of VOCs in groundwater using zero valent iron. *Natl. Meet.-Am. Chem. Soc., Div. Environ. Chem.* **1995**, 35, 800-804 (Abstr.).

Yamane, C. L.; S. D. Warner, J. D. Gallinatti, F. S. Szerdy, T. A. Delfino, D. A. Hankins, and J. L. Vogan. Installation of a subsurface groundwater treatment wall composed of granular zero-valent iron. *Natl. Meet.-Am. Chem. Soc., Div. Environ. Chem.* **1995**, 35, 792-795 (Abstr.).

## SECTION II

# ALKYL BROMIDES AS MECHANISTIC PROBES OF REDUCTIVE DEHALOGENATION: REACTIONS OF VICINAL DIBROMIDE STEREOISOMERS WITH ZERO- VALENT METALS

### A. ABSTRACT

The mechanism through which zero-valent metals (most notably iron and zinc) reduce alkyl polyhalides in aqueous solution at room temperature was investigated using several stereoisomers of vicinal dibromides as mechanistic probes: *threo*- and *erythro*-2,3-dibromopentanes (DBPs) and *D,L*-1,2-dibromo-1,2-diphenylethane [(±)-SBr<sub>2</sub>]. Examination of the *E* to *Z* ratio of the olefin products is often taken to indicate whether the reduction takes place by a single electron transfer (SET) mechanism or by an inner-sphere nucleophilic reduction pathway. Most prior work has, however, been restricted to organic solvents or to reduction in mixed organic:aqueous solution at high temperatures. Although both Zn(0) and Fe(0) reduce vicinal DBPs to >95% stereospecific products, they also produce both *E*- and *Z*-stilbene from (±)-SBr<sub>2</sub> in approximately a 70/30 ratio. The *E*-stilbene yield and distribution of pentene products are similar to those observed in reduction of the probes by iodide ion, a reaction normally attributed to a nucleophilic pathway. In contrast, reduction of the probe compounds by the one-electron donor Cr(II) yields large proportions of both *E*- and *Z*-2-pentenes from DBPs and virtually 100% *E*-stilbene from (±)-SBr<sub>2</sub>. While the product distribution arising from reduction of the probes by both iron and zinc is consistent with a nucleophilic mechanism, the heterogeneous nature of the reaction complicates interpretation of the results. The products may equally well be explained by a mechanism in which initial SET creates a radical which is reduced by a second electron to a stable product at a rate that is fast relative to C-C bond rotation.

### B. INTRODUCTION

Zero-valent metals have been the focus of much recent attention in the environmental community because they offer great promise in treating contaminated groundwater through their ability to promote abiotic reductive dehalogenation (Gillham and O'Hannesin, 1994; Matheson and Tratnyek, 1994; Lipczynska-Kochany *et al.*, 1994; Boronina and Klabunde, 1995; Helland *et al.*, 1995; Warren *et al.*, 1995; Burris *et al.*, 1995; Roberts *et al.*, 1996; Johnson *et al.*, 1998; Balko and Tratnyek, 1998). Nevertheless, many basic questions about the mechanism of these



reactions remain unanswered. Reduction reactions promoted by zero-valent metals include hydrogenolysis (replacement of halogen by hydrogen), reductive  $\beta$ -elimination (removal of two vicinal halogens, accompanied by an increase in bond order), reductive  $\alpha$ -elimination (*e.g.*, reduction of carbon tetrachloride to dichlorocarbene) and other reductions, including those of double or triple bonds. Each of these reductions involves a net transfer of two electrons. The principal goal of this research is to investigate the degree of concertedness of transfer of the two electrons.

Theoretically, electron transfer may occur either via single electron transfer (SET) (which may occur via outer-sphere or inner-sphere pathways) or via inner-sphere two-electron pathways (Eberson, 1987). If reduction occurs via SET, the resulting radicals might persist long enough to undergo characteristic free-radical reactions, such as coupling and hydrogen atom abstraction. Such reactions can affect the ultimate distribution of products, which in turn may exert a major influence on the success of treatment approaches based on zero-valent metals.

For example, Balko and Tratnyek (1998) argue that a shift toward a two-electron mechanism in the reduction of carbon tetrachloride by iron metal caused by photoirradiation (which increases the production of conduction band electrons in the oxide which coats the metal) is responsible for a corresponding change in the product distribution. Photoirradiation favors the production of CO (a product of dichlorocarbene hydrolysis) at the expense of chloroform. This change is desirable from a remediation perspective, because CO is readily oxidized to CO<sub>2</sub> even by anaerobic bacteria (Krone *et al.*, 1991). Chloroform, however, is a regulated pollutant (Pontius, 1998) which reacts only slowly with iron to form predominantly dichloromethane, which in turn is largely unreactive in the presence of Fe(0) (Matheson and Tratnyek, 1994).

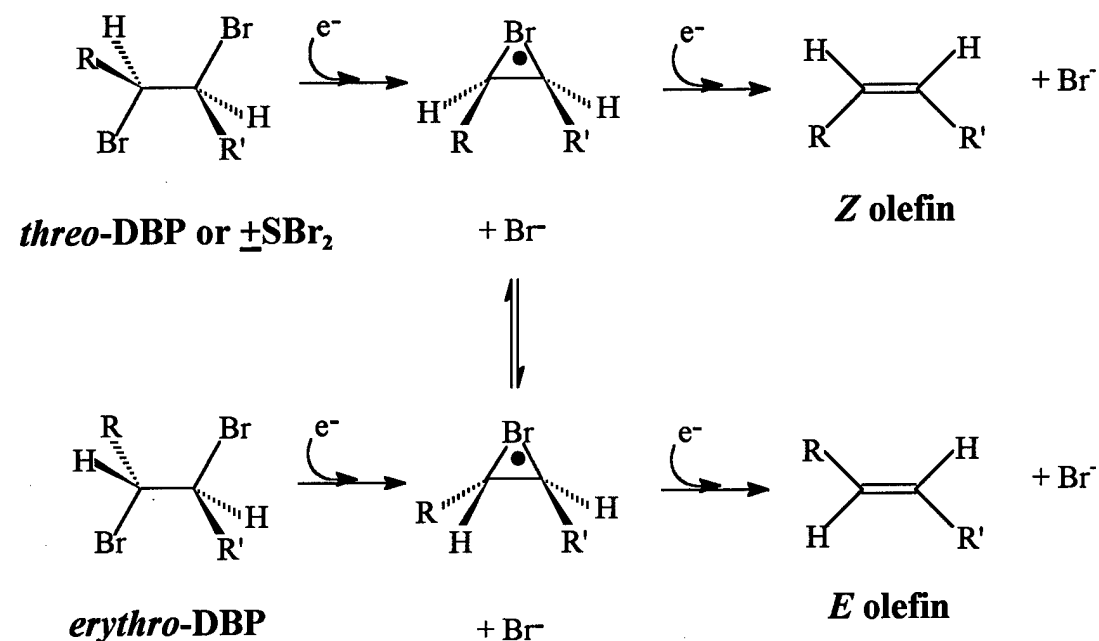
A better understanding of the mechanism through which zero-valent metals reduce organohalides may also help explain the results of recent investigations (Fennelly and Roberts, 1998) of the reduction of 1,1,1-trichloroethane by iron metal, which have revealed that a significant portion (up to 9%) of the carbon mass balance may be found in the form of C<sub>4</sub> hydrocarbons, which apparently arise via the coupling of reactive intermediates. In contrast, no coupling products were observed when zinc served as the reducing agent. This shift in product distribution may reflect a difference in the mechanism of reduction.

Sivavec (1995) has hypothesized that C<sub>4</sub> products resulting from chlorinated ethylene reduction by iron arise from the coupling of intermediate radicals. To date, however, techniques designed to confirm the existence of free radicals have not been successfully applied to the study of reaction of organohalides with zero-valent metals in aqueous solution. Although electron spin resonance (ESR) spectroscopy is commonly employed (in conjunction with free radical trapping agents to enhance sensitivity) to investigate radical intermediates, its applicability to reductions promoted by zero-valent metals is potentially problematic because of the likelihood that trapping agents will react with these strong reductants.

In order to explore the mechanism by which zero-valent metals reduce alkyl halides, the distribution of products arising from reduction of a series of stereochemical probe compounds (Figure 1) has been examined. These probe compounds include 2*R*-3*S*-2,3-dibromopentane (DBP) and its stereoisomeric enantiomer, 2*S*-3*R*-2,3-dibromopentane (the mixture of the two stereoisomers is hereafter referred to as *erythro*-DBP) as well as the 2*R*-3*R*-2,3-dibromopentane and its stereoisomeric enantiomer, 2*S*-3*S*-2,3-dibromopentane (hereafter referred to as *threo*-DBP). The other stereochemical probe employed was 1*R*-2*R*-1,2-dibromo-1,2-diphenylethane [and its enantiomeric isomer, abbreviated as *D,L*-stilbene dibromide or (±)-SBr<sub>2</sub>].

If these vicinal dihalides undergo reduction via an SET process, the first one-electron reduction would yield a radical (Figure 1a), which is partially stabilized by delocalization of the unpaired electron over the remaining bromine. This "bridged" bromine radical could experience rotation around the C-C bond before being further reduced, resulting in a mixture of *E*- and *Z*-product.

**a) reduction via single electron pathway**



**b) reduction via concerted nucleophilic pathway**

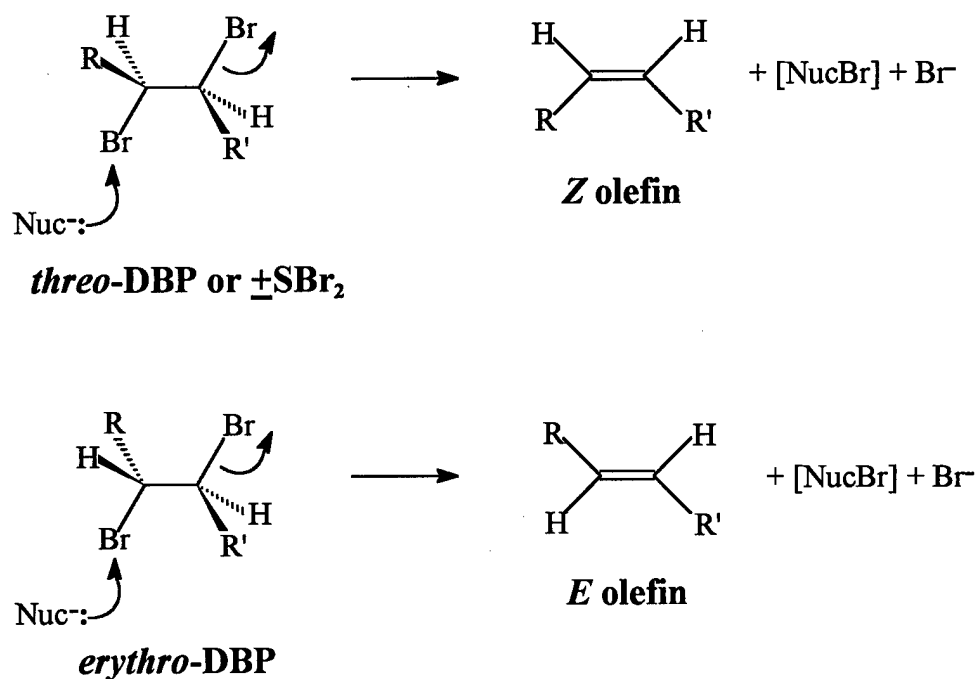


**Figure 1:** Idealized reaction schemes for the model dibromide compounds used in this study: a) single electron reduction pathway, and b) concerted nucleophilic pathway ( $Nuc^-$  = nucleophile). For DBPs, R = methyl, R' = ethyl (or vice versa). For  $(\pm)$ - $SBr_2$ , R = R' = phenyl.

The *E/Z* ratio of olefins formed from the reduction of vicinal dihalides through an SET mechanism is largely a function of the rate at which the second electron is transferred to the intermediate radical relative to the rate of C-C bond rotation, the latter in turn being related to the energy barrier for rotation. Although rates of C-C bond rotation for the different radicals which may be generated by these probes have not been determined experimentally, they can be estimated via computational techniques.

If electron transfer to the radical intermediate is very slow relative to C-C bond rotation, then the final distribution of *E*- and *Z*-olefin products is likely to be determined by the relative proportions of the different rotamers of the radical intermediate that are present at rotational equilibrium. In the case of the DBPs, the relatively small steric hindrance posed by the methyl and ethyl substituents is likely to result in the formation of significant quantities of both *E*- and *Z*-2-pentenenes from an SET pathway. Steric interactions between the bulky phenyl substituents are likely to cause much greater proportions of *E*-stilbene to be formed from an SET reduction of ( $\pm$ )-SBr<sub>2</sub>.

In contrast to the SET mechanism, if vicinal dihalides were to undergo reduction via a more-or-less concerted transfer of two electrons (Figure 1b), the reaction typically demonstrates a strong preference for an *anti* stereochemistry, and should therefore result in a marked predominance of one olefin isomer over the other (Baclocchi, 1983). *Threo*-DBP would react to form primarily *Z*-2-pentene, and *erythro*-DBP to primarily *E*-2-pentene. Numerous exceptions to this *anti* stereoselectivity have, however, been observed for  $\alpha$ ,  $\beta$ -disubstituted *threo*- and ( $\pm$ )-dibromides where R and (or) R' are phenyl groups, such as ( $\pm$ )-SBr<sub>2</sub>. These exceptions have been most commonly attributed to a halonium ion mechanism (Baclocchi, 1983), as discussed subsequently.

The phrase "two-electron reduction" is somewhat misleading because electrons can only be transferred one at a time (Pross, 1985). Products characteristic of a two-electron reduction may arise either from an SET mechanism (either inner-sphere or outer-sphere) in which the transfer of the second electron is much faster than C-C bond rotation, or from an inner-sphere attack of the reductant on the dihalide. The latter mechanism may be envisioned as a nucleophilic attack of the reductant on one of the bromines, rather than on carbon as in a typical S<sub>N</sub>2 reaction.

Reductive elimination of vicinal dihalides by the strong nucleophile iodide has commonly been attributed to just such a concerted nucleophilic mechanism (Bacocchi, 1983; Winstein *et al.*, 1939; Mathai *et al.*, 1970).

Vicinal dibromides have been extensively used in the past to investigate a variety of reduction reactions; Bacocchi (1983) provides an excellent review. The mechanism through which elimination occurs is a function not only of the reductant, but also of the structure of the dihalide probe, the solvent, and the temperature. Thus, although the reactions of zero-valent metals with vicinal dihalides have in some cases already been investigated, these experiments were generally conducted in organic solvents or at high temperatures (Mathai *et al.*, 1970; Sicher *et al.*, 1968). The goal of this research was to investigate the mechanism of the reactions of a variety of zero-valent metals [Fe(0), Zn(0), Al(0) and Cu(0)] under environmentally relevant conditions (*i.e.*, at room temperature, in water). These metals were selected because all have been demonstrated to degrade 1,1,1-trichloroethane (Gillham *et al.*, 1993), and thus represent potential candidates for *in situ* treatment approaches.

A further goal of this research is to assess the overall feasibility of applying vicinal dihalide probes to the investigation of a broad range of environmentally relevant reduction reactions. Reactions promoted by reductants other than zero-valent metals were therefore also investigated, including a model one-electron reductant [Cr(II) (aq)], and a model nucleophilic reductant (iodide). Some researchers have suggested that Fe(II) species adsorbed to oxides coating iron surfaces may represent important reductants in the Fe(0) system (Matheson and Tratnyek, 1994; Johnson *et al.*, 1998; Balko and Tratnyek, 1998; Sivavec, 1995). Reductions promoted by Fe(II) species adsorbed to a Fe(III) mineral surface (goethite) were thus also studied. The hydrolysis of the vicinal dihalide probe compounds was also briefly examined, because it may occur sufficiently rapidly to compete with dehalogenation. Such competition could thus represent a major limitation to the use of these compounds as probes under environmentally relevant conditions.

## C. EXPERIMENTAL SECTION

### 1. Reagents

All chemicals were obtained from commercial sources and used as received, except as

noted. *Threo*- and *erythro*-DBPs and ( $\pm$ )-SBr<sub>2</sub> were synthesized from the *Z*- and *E*-2-pentenenes and *Z*-stilbene, respectively, by stereospecifically brominating the olefins with pyridinium tribromide according to the method of Fieser and Williamson (1979). The olefin was reacted with a stoichiometric excess of pyridinium tribromide in glacial acetic acid on a steam bath. The reaction mixture was extracted into ether, which was then evaporated to yield the final product. ( $\pm$ )-SBr<sub>2</sub> was purified by recrystallization in methanol and was found to be essentially 100% pure by gas chromatographic (GC) analysis employing a flame ionization detector (FID). Analysis of the *threo*- and *erythro*-2,3-DBPs by GC with FID revealed that each contained less than 0.5% impurity of the undesired isomer. The identities of the products were verified by mass spectrometric (MS) and proton nuclear magnetic resonance (H-NMR) analysis. Mass spectra were typically recorded under electron impact (EI) ionization on a Hewlett-Packard (HP) 5890 GC equipped with an HP 5970 mass spectrometer detector by injecting samples dissolved in hexane (residue-analyzed 95% *n*-hexane, JT Baker). The chromatographic column, injector configuration, and temperature program for GC-MS analysis were the same as those used for GC-FID sample analysis (described below). Some additional mass spectra of neat synthesis products were collected courtesy of the Johns Hopkins University Chemistry Department on a VG instruments 70-S mass spectrometer.

## **2. Preparation of Metals**

Important characteristics of each metal are listed in Table 2. Each metal was cleaned to remove surface oxides by soaking for 2-20 minutes in a cleaning solution (Table 2) recommended by Wood (1982), and was then rinsed with deoxygenated water and dried at 100°C under argon, which was purified using an in-line molecular sieve and oxygen traps. In order to avoid reoxidation of the metal surfaces, all cleaning procedures were conducted in an anaerobic glove box (90% N<sub>2</sub>, 10% H<sub>2</sub> atmosphere). Surface area analyses were conducted via Kr or N<sub>2</sub> BET adsorption using a Micromeritics Flowsorb II 2300 device.

**TABLE 2: METALS USED IN EXPERIMENTS WITH VICINAL  
DIBROMIDES.**

<b>Metal</b>	<b>Mesh Size</b>	<b>Purity</b>	<b>Source</b>	<b>Surface Area (m<sup>2</sup>/g)</b>	<b>Cleaning Solution</b>
Al	40	>99%	Baker	ND <sup>a</sup>	chromic <sup>b</sup>
Cu	40	99.5%	Aldrich	0.13 <sup>c</sup>	0.4% sulfuric
Fe	100	95.3%	Fisher	0.76 <sup>c</sup>	1N HCl
Zn	30	100.5%	Baker	0.035 <sup>d</sup>	0.4% sulfuric

<sup>a</sup> not determined. <sup>b</sup> 2 g chromic acid + 4 mL sulfuric acid (66° Be) in 100

mL distilled water. <sup>c</sup> by nitrogen BET. <sup>d</sup> by krypton BET.

### 3. Goethite

Goethite slurry (44.2 g goethite/L) was synthesized by Barbara Coughlin and was provided by Alan T. Stone. The goethite had a specific surface area of 47.5 m<sup>2</sup>/g and adsorption isotherms demonstrated that it is able to adsorb a maximum of 2.8 atoms of Fe(II) per nm<sup>2</sup> (Coughlin and Stone, 1995). Experiments were conducted with 1.4 mmoles Fe(II) and 10 g of goethite slurry (0.442 g goethite). The Fe(II) was present at 5 times molar excess to the number of available sites. Some experiments were conducted at pH 7.5 using 5 mM tris(hydroxymethyl)aminomethane (Tris) buffer. Others were conducted at pH 10.5 using 5 mM 2-amino-2-methyl-1-propanol (AMP) buffer. At pH above 6, all of the surface sites on the goethite should be occupied by Fe(II) (Coughlin and Stone, 1995).

### 4. Cr(II) Solutions

Cr(II) solutions were synthesized in the glove box by the method of Castro (1961) in which aqueous Cr(III) sulfate is reduced using 40 mesh granular zinc metal. The resulting bright blue solution was centrifuged at 2500 RPM for 10 min in 50-mL glass centrifuge tubes and was then filtered through a 0.2 µm syringe filter. An aliquot of the Cr(II) stock solution (~0.5 M) was pipetted into each reaction flask to achieve the desired Cr(II) concentration. Initial Cr(II) concentrations were determined independently by reaction with Fe(III), with quantitation of the resulting Fe(II) by a bathophenanthroline disulfonic acid (BPDS) colorimetric assay (Diehl, 1980). Control experiments demonstrated that possible Zn(II) contamination from the synthesis method did not interfere with quantitation of Cr(II) by this method. Cr(II) reactions were carried out in 5

mM H<sub>2</sub>SO<sub>4</sub> (pH 2.0-2.1) in a constant temperature water bath at 25.0 (± 0.1)°C. A low pH was employed to avoid precipitation of Cr(II) or Cr(III) species and to ensure that essentially all of the Cr(II) was in the form Cr(H<sub>2</sub>O)<sub>6</sub><sup>2+</sup> (Kelsall *et al.*, 1988).

## 6. Iodide

Reactions with iodide were conducted in 1 M KI, 0.1 M NaCl, 50 mM tetraborate buffer (pH 9.3) in a constant temperature water bath at 25.0 (± 0.1)°C. This pH value was employed to provide consistency with other experiments involving strong nucleophiles (Jans and Roberts, 1998).

## 7. Reactions of DBP Isomers

Reaction flasks were prepared in a glove box to minimize contamination with oxygen. Reactions with metals were carried out in 1-L flasks (nominal volume). Reactions with goethite, Cr(II), iodide, and hydrolysis experiments were carried out in 125-mL flasks (nominal volume). Each flask was equipped with a stopcock adapter which was plugged with an NMR-type septum. The stopcock served to protect the flask contents from potential sorption onto the NMR septum, except during brief sampling intervals. The reaction solution (typically 0.1 M NaCl) was deoxygenated via sparging with purified argon. The reductant was weighed or pipetted into each flask, which was then filled completely with aqueous solution. For reactions with zero-valent metals, an aliquot of the solution was removed for pH measurement after equilibrating with the metal overnight. The flask was then filled completely with aqueous solution, leaving no headspace. Flasks were spiked with either *threo*- or *erythro*-DBP in methanol solution to achieve an initial dibromide concentration of about 0.2 mM and a resulting methanol concentration of 0.025 M. Flasks were then placed on a roller table at 40 RPM for mixing at room temperature. Samples (1 mL) were taken without introducing headspace by periodically injecting an aliquot of deoxygenated solution through the septum, which forced the sample into a second sampling syringe. Aqueous samples (1mL) were extracted into 1 mL hexane and were analyzed on a Carlo-Erba Mega 2 GC equipped with an FID and a PC-driven data acquisition system. Hexane extracts were injected via an AS 800 autosampler by a direct cold on-column technique onto a capillary guard column connected to a 30 m, 0.32 mm ID, 5 µm film thickness Rtx-1 capillary column



(Restek).

## 8. Reactions of ( $\pm$ )-SBr<sub>2</sub>

Experimental procedures were the same as those for the DBPs except that all reactions were conducted in 1-L (nominal volume) bottles. Each bottle was spiked with a methanolic solution of ( $\pm$ )-SBr<sub>2</sub> to give an initial aqueous concentration of dibromide of about 4  $\mu$ M (and a resulting methanol concentration of 0.025 M). The lower starting concentration of ( $\pm$ )-SBr<sub>2</sub> was necessitated by its lower aqueous solubility relative to the DBPs. No attempt was made to keep these systems headspace free, because the estimated Henry's law constants of the stilbene reaction products and ( $\pm$ )-SBr<sub>2</sub> are low enough that no appreciable losses caused by partitioning into the headspace were anticipated. Aqueous samples (10 mL) were taken from each bottle, with the volume being displaced by purified nitrogen instead of deoxygenated aqueous solution. The aqueous samples were extracted with 1 mL of hexane, and 1  $\mu$ L hexane samples were injected onto a 15 m, 0.25 mm ID, 0.25  $\mu$ m film thickness EC-5 capillary column (Alltech) with an FID for GC analysis.

## 9. Computational Estimates of Rotational Energy Barriers

The heights of the barriers to C-C bond rotation for the 2-bromopentyl, 3-bromopentyl, and bromostilbene radicals were estimated via computational chemistry techniques using *Spartan* v. 5.0 (Wavefunction Inc., Irvine, CA) on a Silicon Graphics Indigo workstation. Note that in these radicals, the stereochemical distinction between *erythro* and *threo*, or *meso* and ( $\pm$ ) is lost. The dihedral angle centered on the radical carbon and the carbon containing the remaining bromine was rotated through 360° in 30 steps, with the geometry of the radical optimized at each step using the AM1 semi-empirical basis set. The energy of each rotational conformer was then calculated by density functional theory using the perturbative Becke-Perdew (pBP) method with the DN\*\* basis set.

# D. RESULTS

## 1. MS and NMR Spectra of Synthesis Products

The H-NMR and mass spectra of the synthesis products are displayed in Figures 2 through 7. Typical gas chromatograms are displayed in Figures 8 and 9.

PULSE SEQUENCE

Relax. delay arrayed

1<sup>st</sup> pulse arrayed

2<sup>nd</sup> pulse 31.5 degrees

Acq. time 3.744 sec

Width 5000.0 Hz

Arrayed repetitions

OBSERVE H1, 399.68 Hz

DATA PROCESSING

FT size 65536

Total time 1 minute

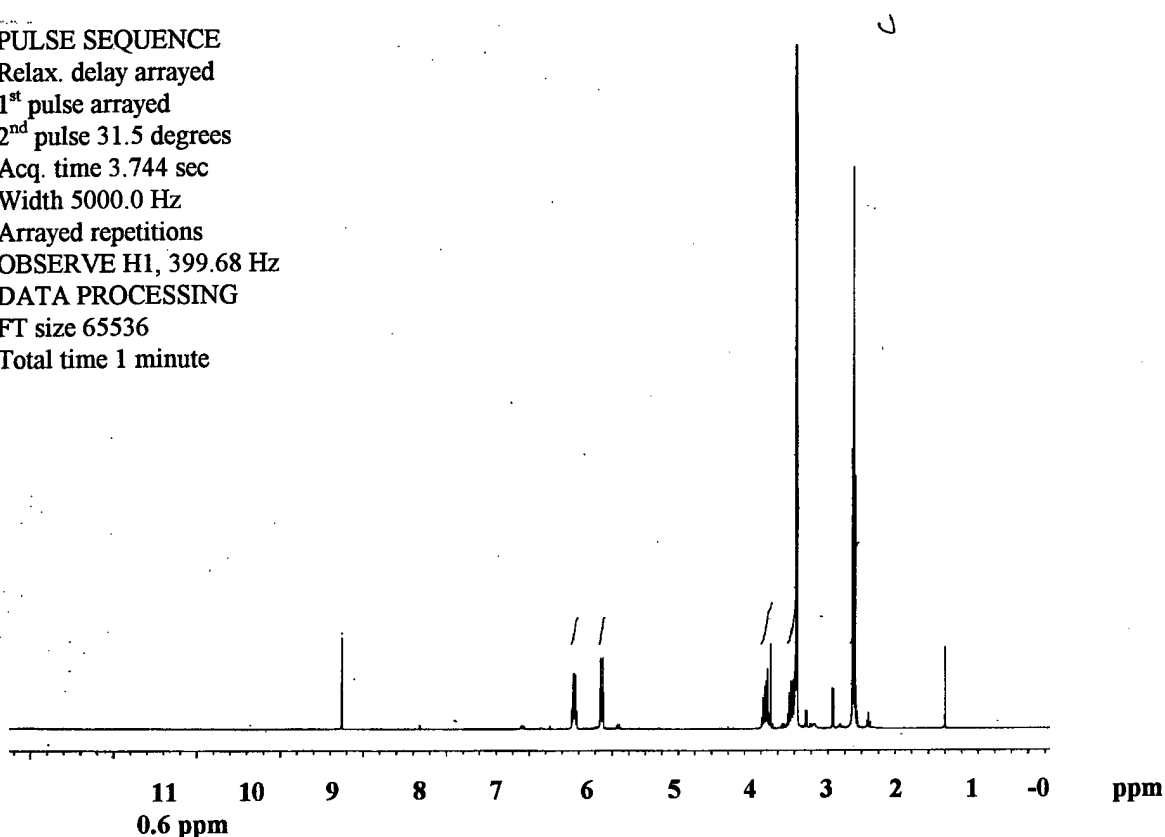


**Figure 2:** H-NMR spectra of *threo*-DBP determined on UNITYplus 400 MHz NMR in  $\text{CDCl}_3$  (approximate concentration of DBP = 10 mg/mL). Peak shifts: 7.260, 4.466, 4.458, 4.449, 4.441, 4.134, 4.108, 2.137, 2.129, 2.118, 2.080, 1.811, 1.793, 1.782, 1.775, 1.765, 1.107, 1.089, and 1.071 ppm. Peak at 0 ppm represents tetramethylsilane used as an internal standard.

PULSE SEQUENCE  
Relax. delay arrayed  
1<sup>st</sup> pulse arrayed  
2<sup>nd</sup> pulse 31.5 degrees  
Acq. time 3.744 sec  
Width 5000.0 Hz  
Arrayed repetitions  
OBSERVE H1, 399.68 Hz  
DATA PROCESSING  
FT size 65536  
total time 1 minute

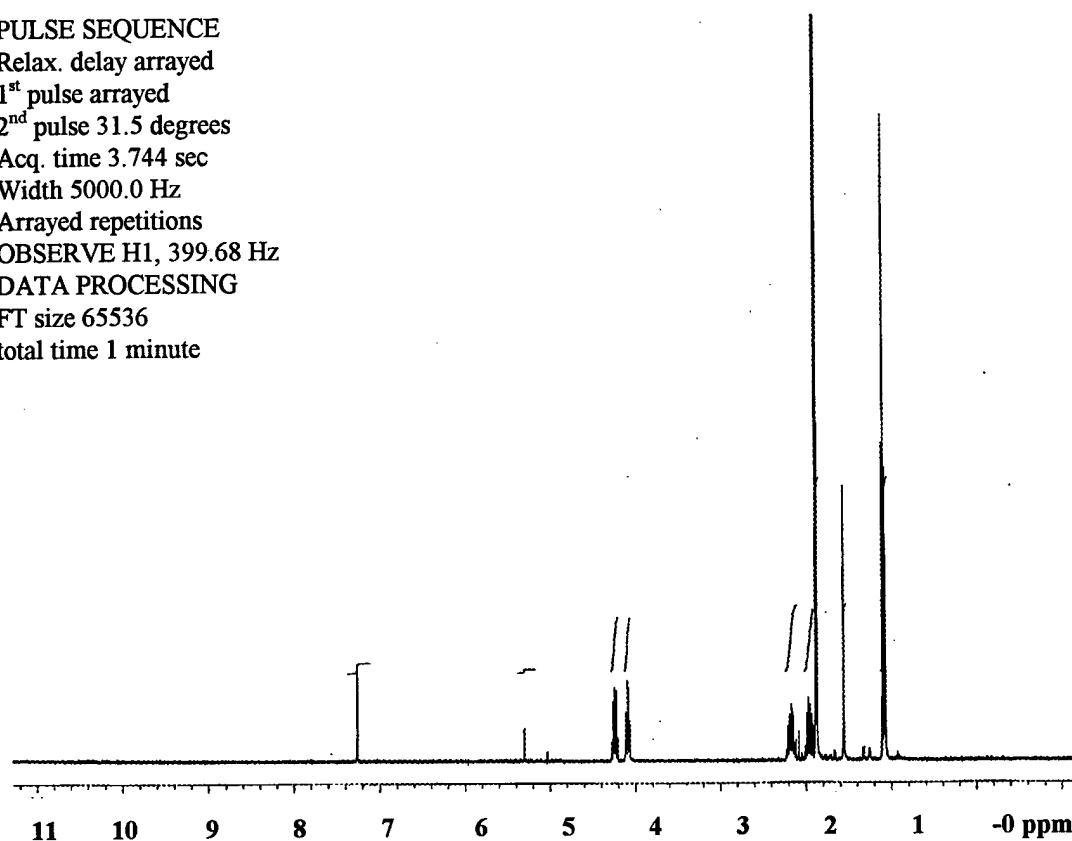


**Figure 3:** <sup>1</sup>H-NMR spectra of *erythro*-DBP determined on UNITYplus 400 MHz NMR in CDCl<sub>3</sub> (approximate concentration of DBP = 10 mg/mL).

PULSE SEQUENCE

Relax. delay arrayed

1<sup>st</sup> pulse arrayed

2<sup>nd</sup> pulse 31.5 degrees

Acq. time 3.744 sec

Width 5000.0 Hz

Arrayed repetitions

OBSERVE H1, 399.68 Hz

DATA PROCESSING

FT size 65536

total time 1 minute

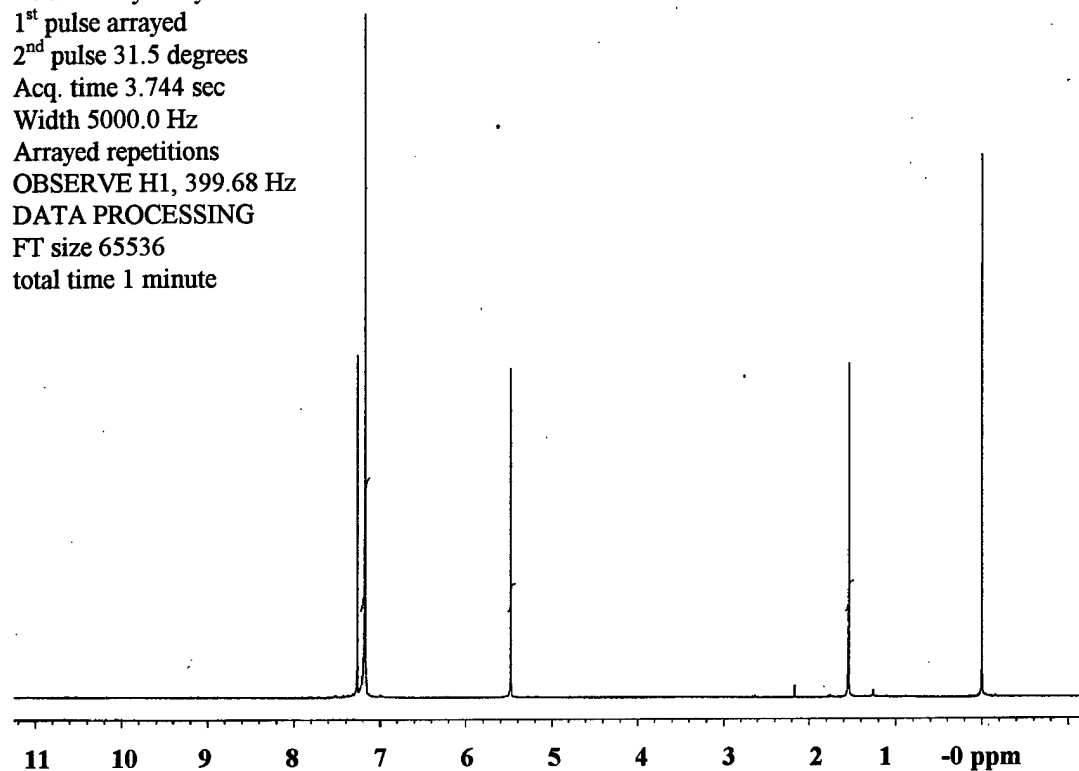


**Figure 4:**  $^1\text{H}$ -NMR spectrum of  $(\pm)\text{-SBr}_2$  determined on UNITYplus 400 MHz NMR in  $\text{CDCl}_3$  (approximate concentration of  $(\pm)\text{-SBr}_2 = 10 \text{ mg/mL}$ ). Major peaks occur at 7.260, 7.174, 5.477, and 1.543 ppm. Peak at 0 ppm represents tetramethylsilane used as an internal standard.

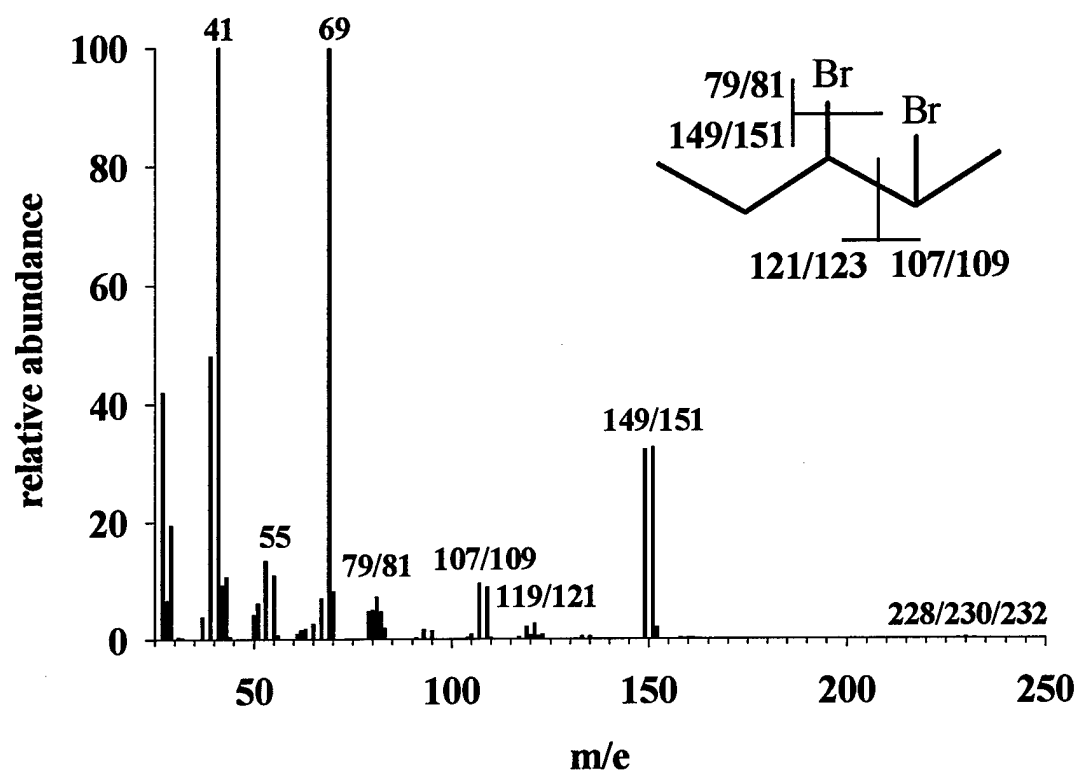


**Figure 5:** Mass spectrum of *erythro*-DBP (parent ions at  $m/e = 228, 230,$  and  $232$ ) recorded under electron impact (EI) ionization on a Hewlett-Packard (HP) 5890 GC equipped with an HP 5970 mass spectrometer detector. Scans recorded across a mass range of 25-250 atomic mass units. Note the 1:1 abundance ratio of ions at  $m/e = 107/109, 119/121,$  and  $149/151$  due to a 1:1  $^{79}\text{Br}$  and  $^{81}\text{Br}$  isotope abundance. Peaks at  $m/e = 69$  and  $41$  represent  $\text{C}_5\text{H}_9$  and  $\text{C}_3\text{H}_5$  fragments.

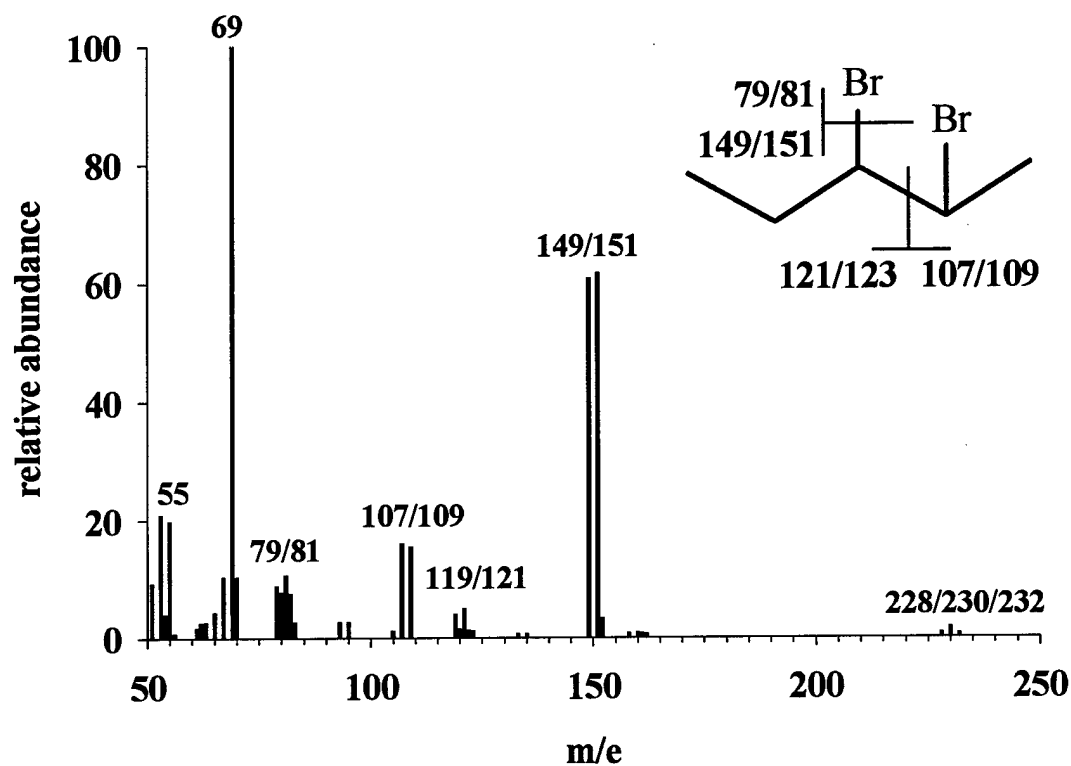


**Figure 6:** Mass spectrum of *threo*-DBP (parent ions at  $m/e = 228, 230$ , and  $232$ ) recorded under electron impact (EI) ionization on a Hewlett-Packard (HP) 5890 GC equipped with an HP 5970 mass spectrometer detector. Scans recorded across a mass range of 50-250 atomic mass units. Note the 1:1 abundance ratio of ions at  $m/e = 107/109$ ,  $119/121$ , and  $149/151$  due to a 1:1  $^{79}\text{Br}$  and  $^{81}\text{Br}$  isotope abundance. Peak at  $m/e = 69$  represents a  $\text{C}_5\text{H}_9$  fragment.

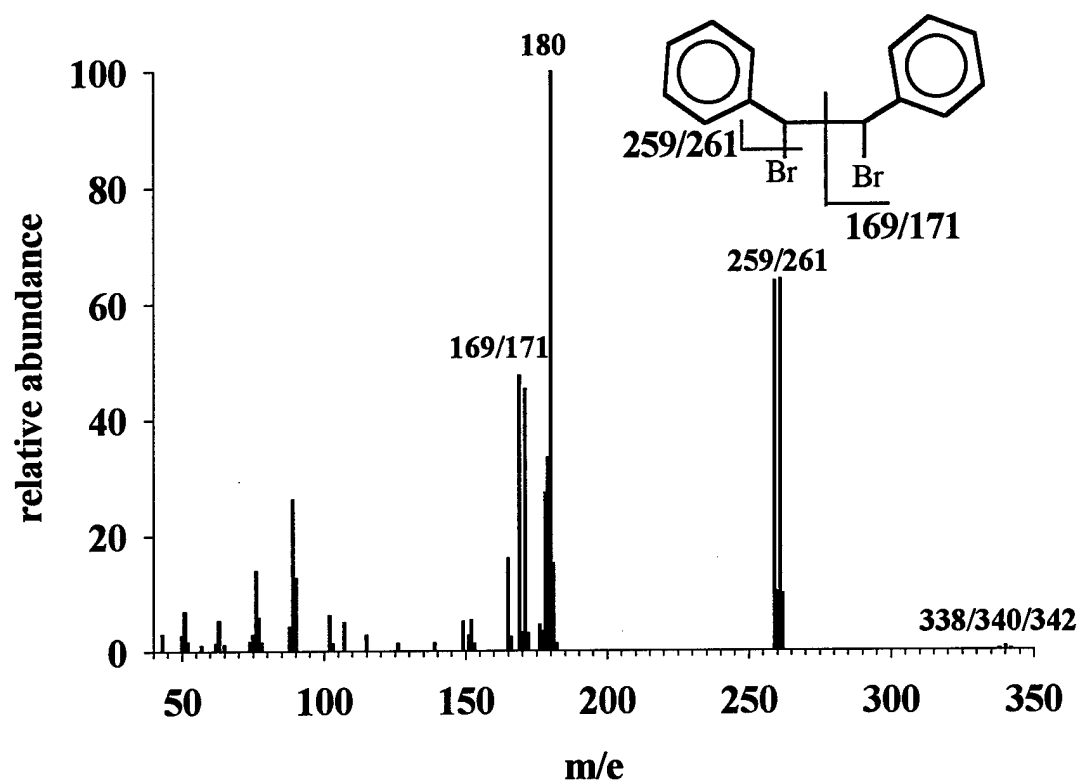


**Figure 7:** Mass spectrum of (±)-SBr<sub>2</sub> (parent ions at m/e = 338, 340, and 342) recorded under electron impact (EI) ionization on a VG instruments 70-S MS. Scans recorded across a mass range of 40-350 atomic mass units. Note the 1:1 abundance ratio of ions at m/e = 169/171, and 259/261 due to a 1:1 <sup>79</sup>Br and <sup>81</sup>Br isotope abundance. Peak at m/e = 180 represents elimination of Br<sub>2</sub> from the parent to form stilbene.

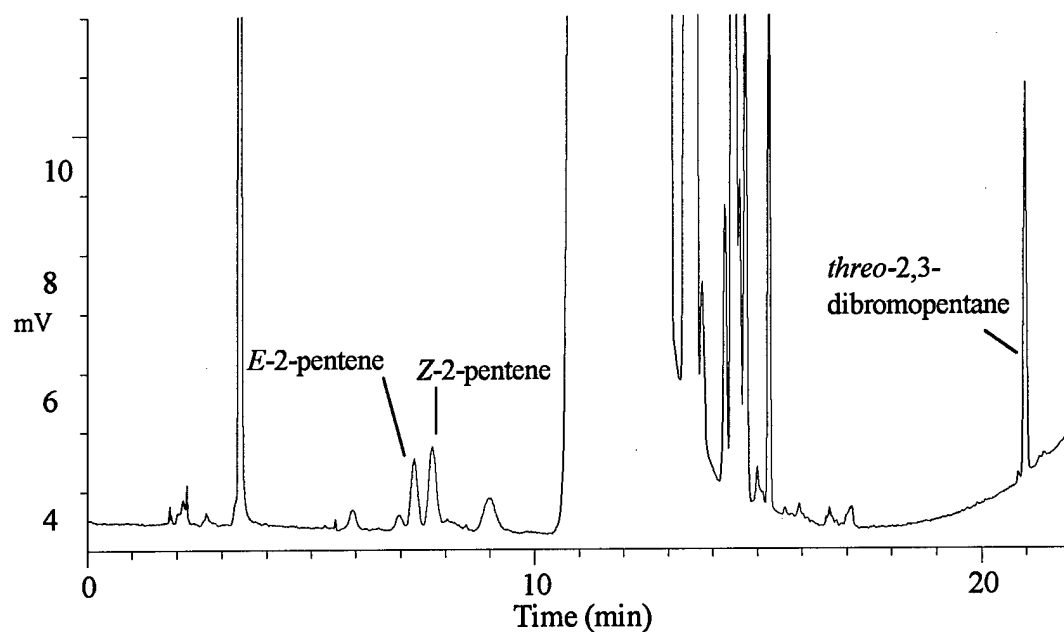


**Figure 8:** Chromatographic analysis of 2,3-dibromopentanes and E- and Z-2-pentenenes on a Carlo-Erba Mega 2 GC equipped with an FID and a PC-driven data acquisition system. Hexane extracts (1  $\mu$ L) were injected via an AS 800 autosampler by a direct cold on-column technique onto a capillary guard column connected to a 30 m, 0.32 mm ID, 5  $\mu$ m film thickness Rtx-1 capillary column (Restek). Temperature program: inject at 40°C hold 10 minutes, ramp 20°C/minute to 200°C. Unlabeled peaks were also present in hexane solvent blanks.



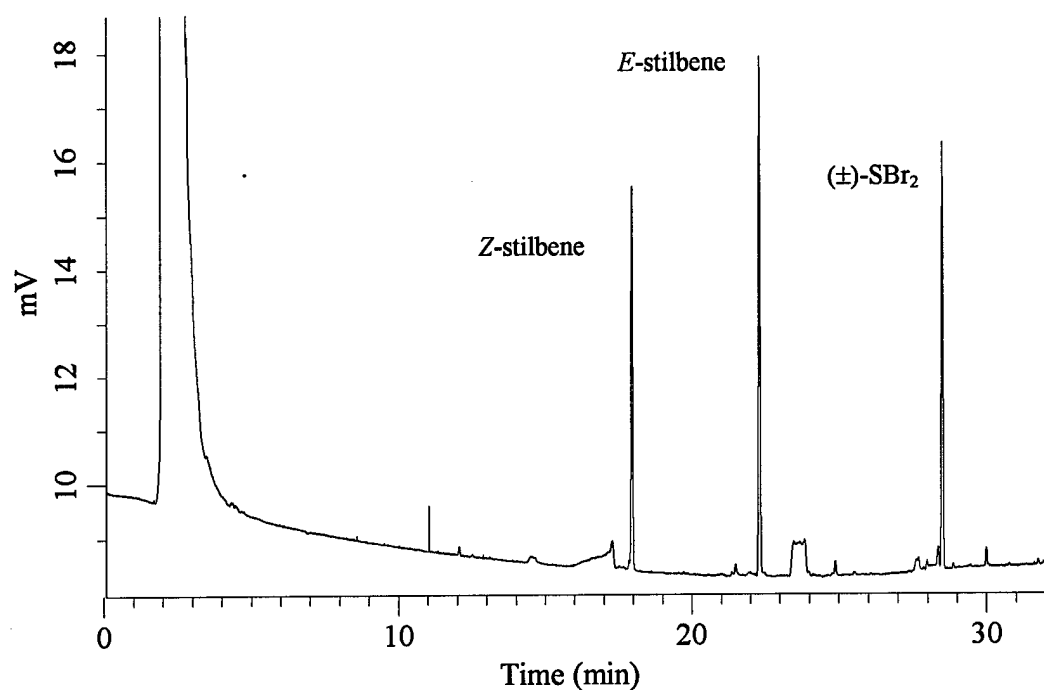


**Figure 9:** Chromatographic analysis of (±)-stilbene dibromide and *E*- and *Z*-stilbenes. Hexane samples (1 mL) were injected via cold on-column technique onto a 15 m, 0.25 mm ID, 0.25  $\mu$ m film thickness EC-5 capillary column (Alltech) with an FID for GC analysis. Temperature program: inject at 65°C, hold 1 minute. Ramp 5°C/minute to 165°C, then ramp 6°C/minute to 205°C, then ramp 10°C/minute to 285°C, hold 5 minutes. Unlabeled peaks were present in hexane solvent blanks. Meso-SBr<sub>2</sub> elutes slightly after (±)-SBr<sub>2</sub> and can be fully resolved from it via this temperature program.

## 2. Hydrolysis of the Probe Compounds

All of the dibromide probe compounds hydrolyzed relatively rapidly (Figures 10 and 11) at a rate essentially independent of pH between 7 and 9.3. Hydrolysis rate constants for the DBPs were  $0.02 \text{ hr}^{-1}$  (*erythro*) and  $0.006 \text{ hr}^{-1}$  (*threo*) at pH 7.5 (5 mM Tris buffer), corresponding to half-lives of 1 and 5 days, respectively. The hydrolysis products were tentatively identified by GC-MS after extraction into hexane as 2-bromo-pentan-3-ol and 3-bromo-pentan-2-ol. Because authentic standards of these products were not commercially available, no attempt was made to quantitate them.

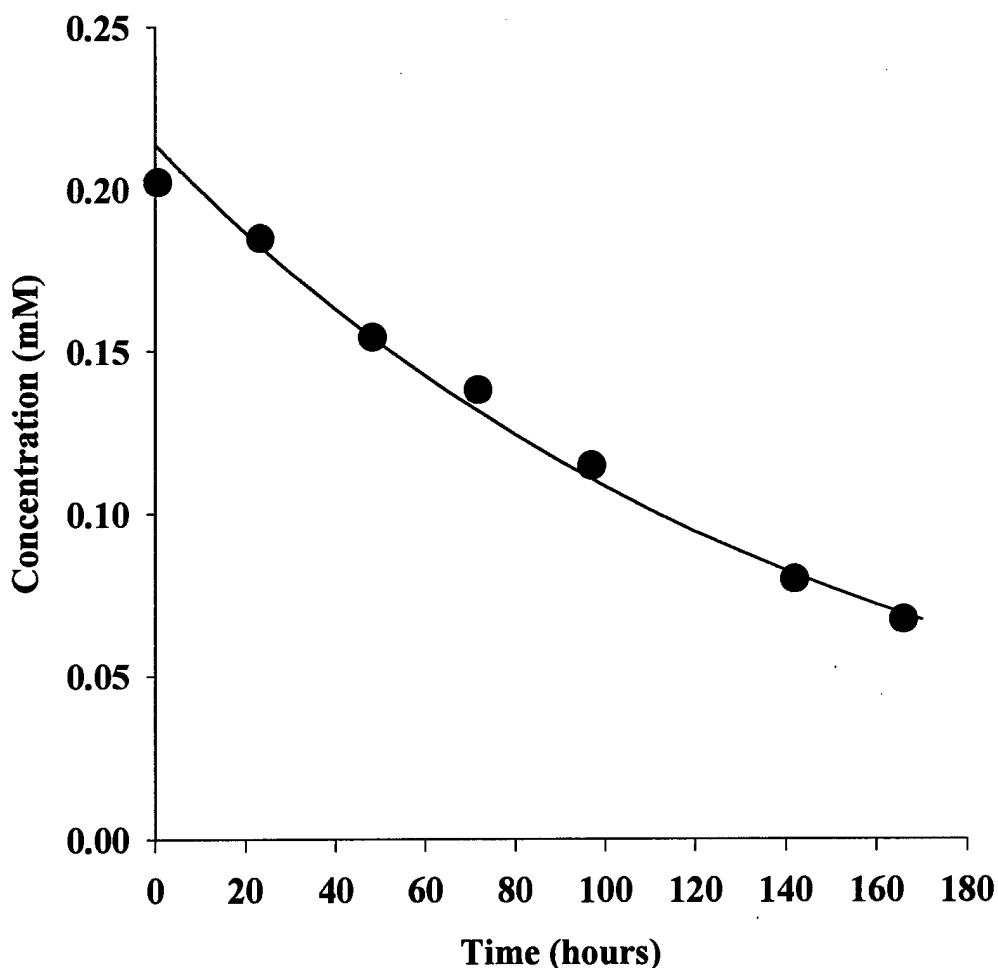


**Figure 10:** Hydrolysis of *threo*-DBP (●) at pH 7.5 (5 mM Tris buffer, 0.1 M NaCl). Line represents fit to data assuming pseudo-first order decay.

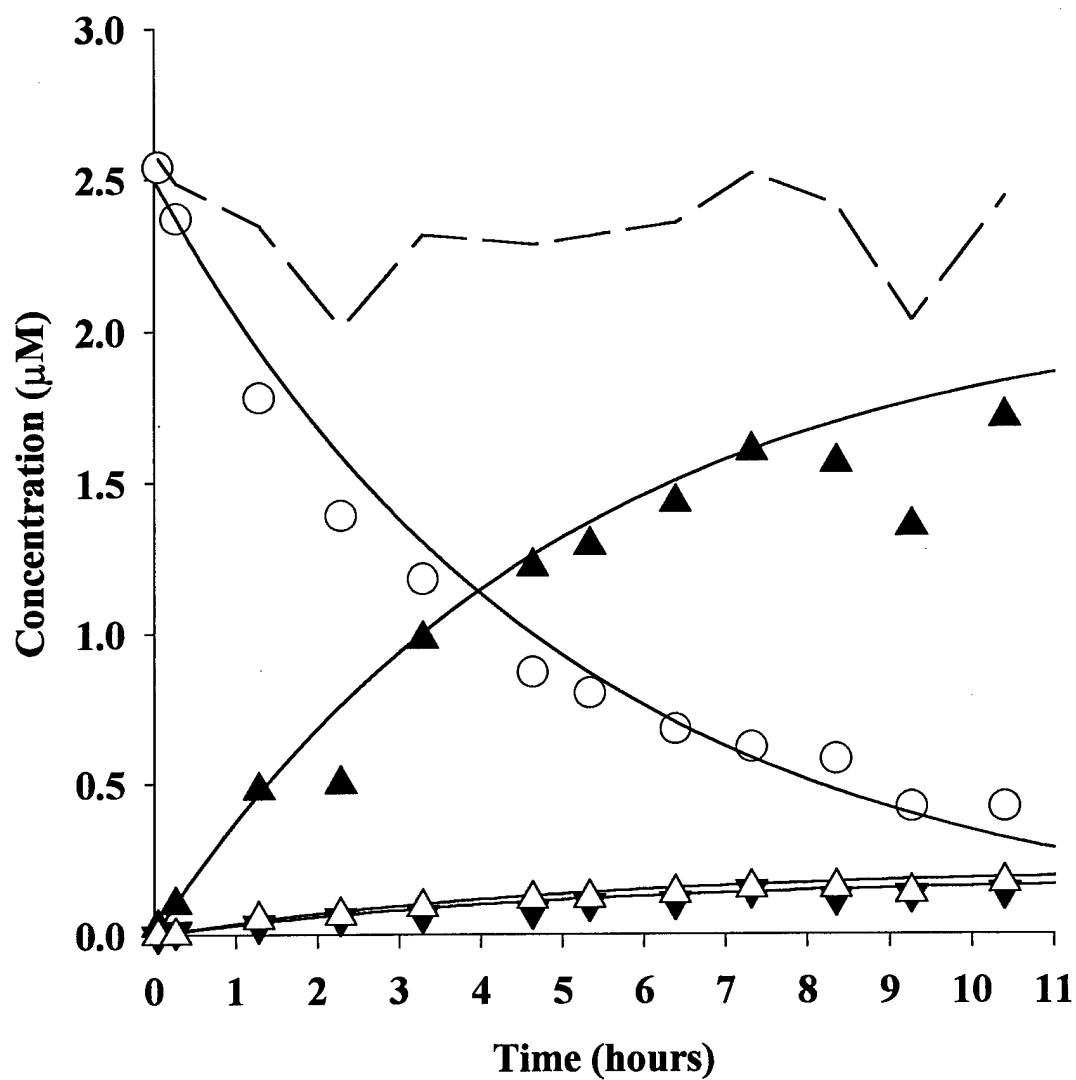


**Figure 11:** Hydrolysis of (±)-SBr<sub>2</sub> (O) at pH 8 (5 mM borate buffer, 0.1 M NaCl). Products are *E*-stilbene oxide (▲), *Z*-stilbene oxide (Δ), and *E*-stilbene (▼). Solid lines represent fits to data assuming pseudo-first order decay to the observed products. Dashed line represents calculated mass balance.

The hydrolysis rate constant for ( $\pm$ )-SBr<sub>2</sub> was 0.17 hr<sup>-1</sup> at pH 8-9. The major hydrolysis product was the epoxide, *E*-stilbene oxide (95%). Traces of *Z*-stilbene oxide (less than 10% of the total oxide yield) were also formed, along with minor amounts of the reduction product *E*-stilbene. *Z*-stilbene was not detected as a hydrolysis product. Both the *E*- and *Z*-stilbene oxide were found to be stable in buffered aqueous solutions at pH 7.5. For example, no isomerization of *Z*-stilbene oxide to the *E*-isomer was observed after 24 hours in buffered solutions at pH 7.5.

### 3. Reductive Dehalogenation of the Probe Compounds

The stereochemistry of the reductive elimination reactions is expressed as the percent *E* olefin present in the total olefin yield. The results for the dehalogenation of *threo*-DBP and ( $\pm$ )-SBr<sub>2</sub> promoted by a variety of reductants are summarized in Figures 12 and 13. Some of the reactivity parameters for *threo*-DBP and ( $\pm$ )-SBr<sub>2</sub> are listed in Table 3. Reactivity is normalized to metal surface area and expressed as  $k_{SA}$ , calculated by dividing the observed pseudo-first order rate constant for reduction of the dibromide (in s<sup>-1</sup>) by the metal loading (in m<sup>2</sup> per L of solution). The *threo*-DBP isomer was used instead of the *erythro*-DBP isomer in most of these experiments, because the steric strain in the less stable "Z-like" configuration of the intermediate radical should foster more rapid C-C bond rotation (Figure 1).

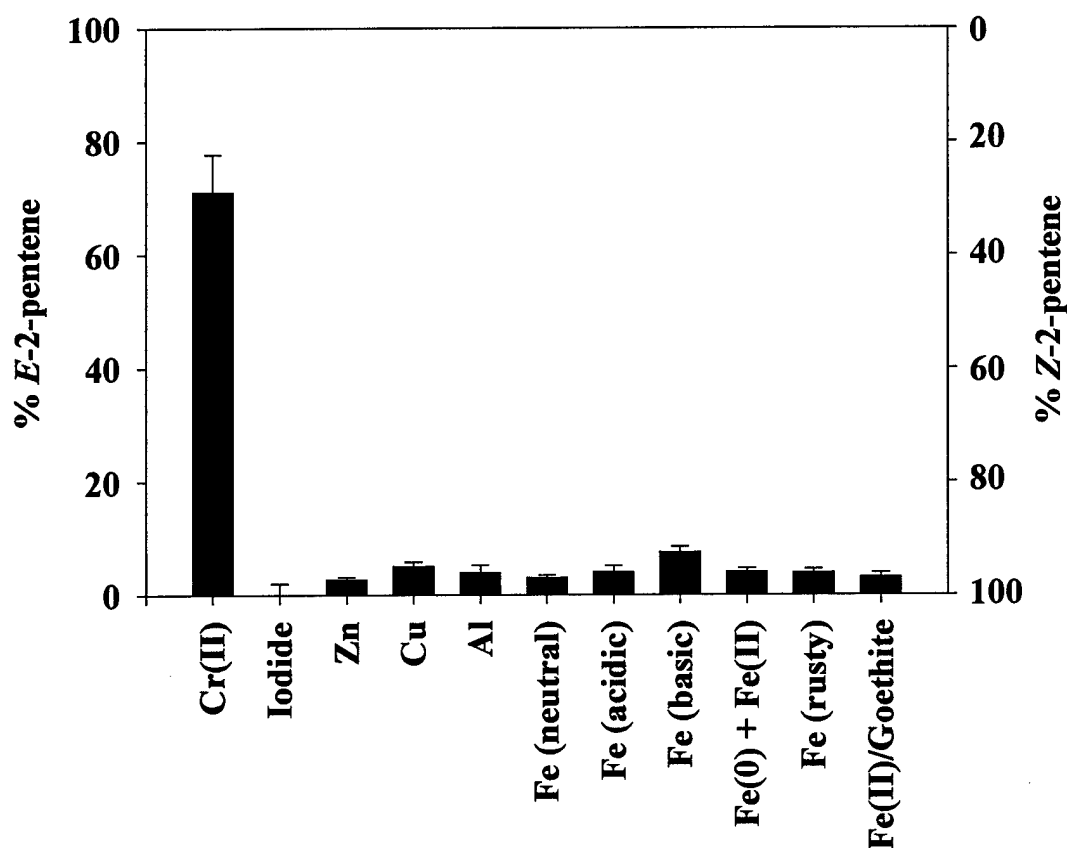


**Figure 12:** *E*- and *Z*-olefins (as a percent of total olefin) formed from the reaction of *threo*-DBP with various reductants. Fe(0) (neutral) refers to the reduction carried out in 0.1 M NaCl without pH adjustment (see Table 2-2 for pH data). Fe(0) (acidic) refers to the reduction carried out in 0.1 M NaCl solution initially adjusted to pH 4 with HCl. Fe(0) (basic) refers to the reduction carried out in 0.1 M NaCl solution initially adjusted to pH 10 with NaOH. Fe(II)/goethite experiments were conducted at pH 10.5. See text for other reaction conditions. Error bars represent 95% confidence limits.

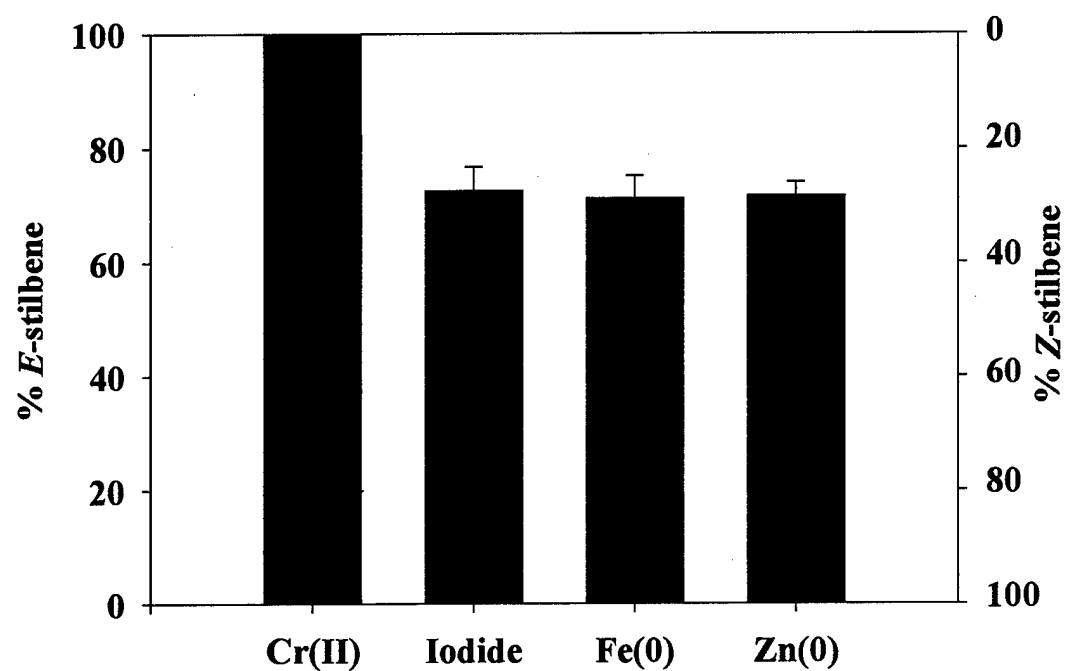


**Figure 13:** *E*- and *Z*-olefins (as a percent of total olefin) formed from the reaction of ( $\pm$ )-SBr<sub>2</sub> by various reductants. All reactions were conducted in 0.1 M NaCl at room temperature. See text for other conditions.

**TABLE 3: REACTIVITY OF *THREO*-DBP AND ( $\pm$ )-SBR<sub>2</sub> WITH ZERO-VALENT METALS.**

<i>threo</i> -DBP				( $\pm$ )-SBr <sub>2</sub>		
	metal	pH	$k_{SA}$	metal	pH	$k_{SA}$
Metal	(g/1.2 L)	trend <sup>a</sup>	(L·s <sup>-1</sup> ·m <sup>-2</sup> )	(g/1.2 L)	trend <sup>a</sup>	(L·s <sup>-1</sup> ·m <sup>-2</sup> )
Al	5.0	8.5, 8.5				
Cu	50	6.5, 6	$3 \times 10^{-6}$			
Fe	1.0	6.5, 8.5	$1 \times 10^{-4}$	0.5	7.8, 8.6	$1 \times 10^{-3}$
	2.4	6.5, 8.5	$1 \times 10^{-4}$			
	5.0	6.5, 8.5	$7 \times 10^{-5}$			
Zn	1.0	6, 7.5	$6 \times 10^{-3}$	1	7.7, 7.9	$7 \times 10^{-3}$
	2.5	6, 7.5	$3 \times 10^{-3}$			
	5.0	6, 7.5	$3 \times 10^{-3}$			

<sup>a</sup> Initial, final. Values are approximate

#### a. Reductions Promoted by Cr(II)

Cr(II) was used as a model reducing agent because it has been demonstrated to act as a one-electron reductant of vicinal dibromides, at least in mixed dimethylsulfoxide/water solution (Kochi and Singleton, 1968). Reduction of 0.2 mM 2,3-DBPs by dissolved Cr(II) is not stereospecific; a Cr(II) concentration of 10 mM resulted in 68% *E*-2-pentene from the *threo* isomer (Figure 14) and 73% from the *erythro* isomer. Disappearance of the DBPs followed good pseudo-first order kinetics, based on the linearity of log of concentration vs time plots. Dividing the pseudo-first order rate constant by the Cr(II) concentration yields an estimate of the second-order rate constants for reaction of Cr(II) with *threo*- and *erythro*-DBP of 0.012 M<sup>-1</sup>s<sup>-1</sup> and 0.018 M<sup>-1</sup>s<sup>-1</sup>, respectively. Because the rate of reduction by Cr(II) was fast relative to hydrolysis, no corrections for concurrent hydrolysis were required. *E*- and *Z*-2-pentene were found to be stable under the reaction conditions.

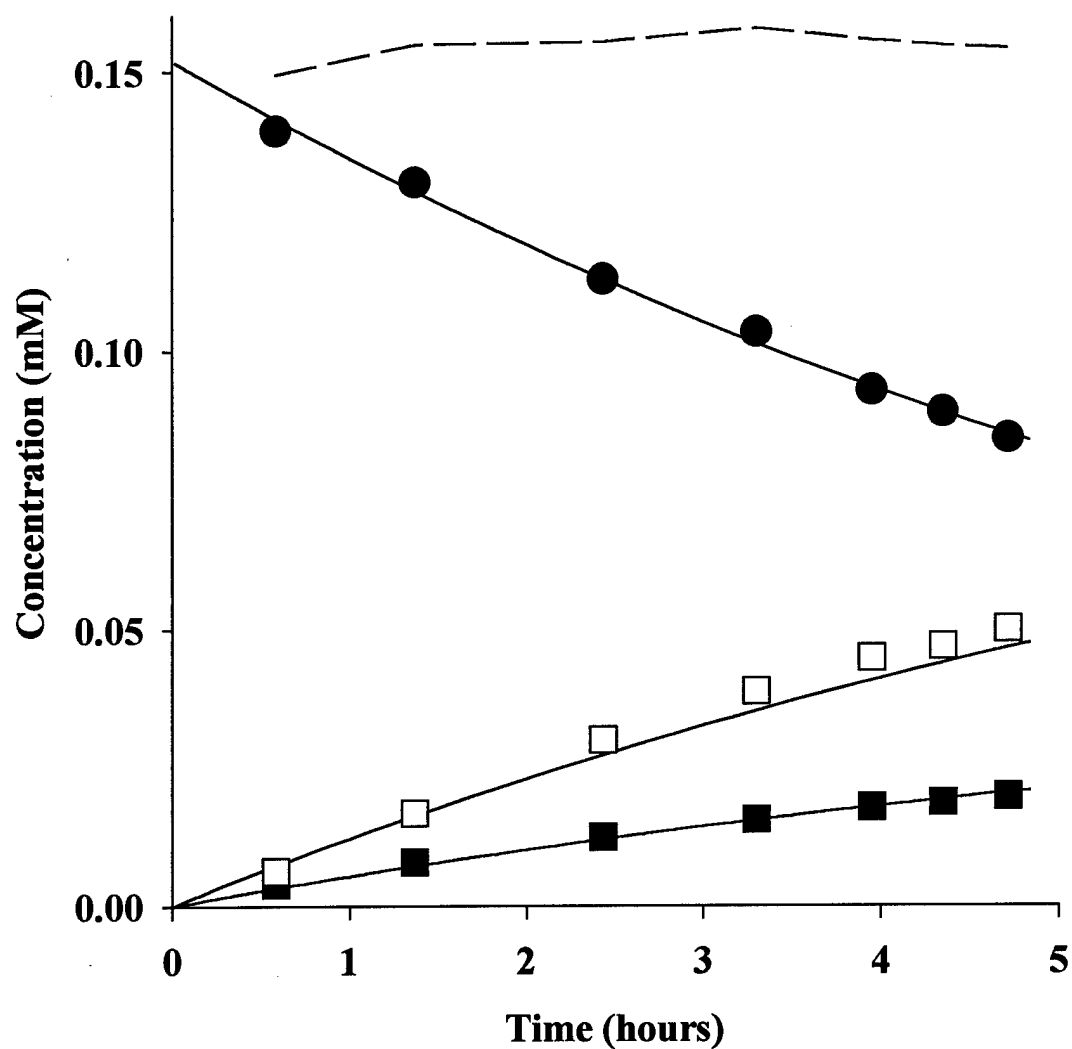


**Figure 14:** Reaction of *threo*-DBP (●) with 10 mM Cr(II) in 5 mM H<sub>2</sub>SO<sub>4</sub> (pH 2.0-2.1) at 25.0 (± 0.1)°C. Products are *E*-2-pentene (□) and *Z*-2-pentene (■). Solid lines represent fits to data assuming pseudo-first order decay to observed products. Dashed line represents calculated mass balance.



( $\pm$ )-SBr<sub>2</sub> reacted with 0.06 mM Cr(II) to give *E*-stilbene as the sole observed product (Figure 15). The pseudo-first order rate constant for reaction of ( $\pm$ )-SBr<sub>2</sub> with Cr(II) was approximated by dividing the observed first-order rate constant for disappearance of ( $\pm$ )-SBr<sub>2</sub> by the Cr(II) concentration. The resulting second-order rate constant for reaction of ( $\pm$ )-SBr<sub>2</sub> with Cr(II) was 3.7 M<sup>-1</sup>s<sup>-1</sup>. Again, the rate of reduction of ( $\pm$ )-SBr<sub>2</sub> by Cr(II) was fast relative to hydrolysis. Control experiments demonstrated that *E*- and *Z*-stilbene were stable under the reaction conditions.

#### **b. Reductions Promoted by Iodide**

The stereospecificity encountered in reduction of the dibromide probe molecules by iodide was explored because prior work has shown that this species serves as a nucleophilic (two-electron) reductant, at least in organic solvent (Winstein *et al.*, 1939; Mathai *et al.*, 1970; Sicher *et al.*, 1968; Schubert *et al.*, 1955). *Threo*-DBP was reduced by iodide (Figure 16) to form exclusively *Z*-2-pentene, and *erythro*-DBP was reduced by iodide to form exclusively *E*-2-pentene. Mass balances were essentially complete (100%). Reactions of ( $\pm$ )-SBr<sub>2</sub> with 1 M iodide were sufficiently slow that hydrolysis competed with reductive elimination. ( $\pm$ )-SBr<sub>2</sub> was reduced by iodide (Figure 17) to form both *Z*- and *E*-stilbene. Stilbenes comprised 58% of the total products, of which 74% was *E*-stilbene. Mass balances were good (100-110%).

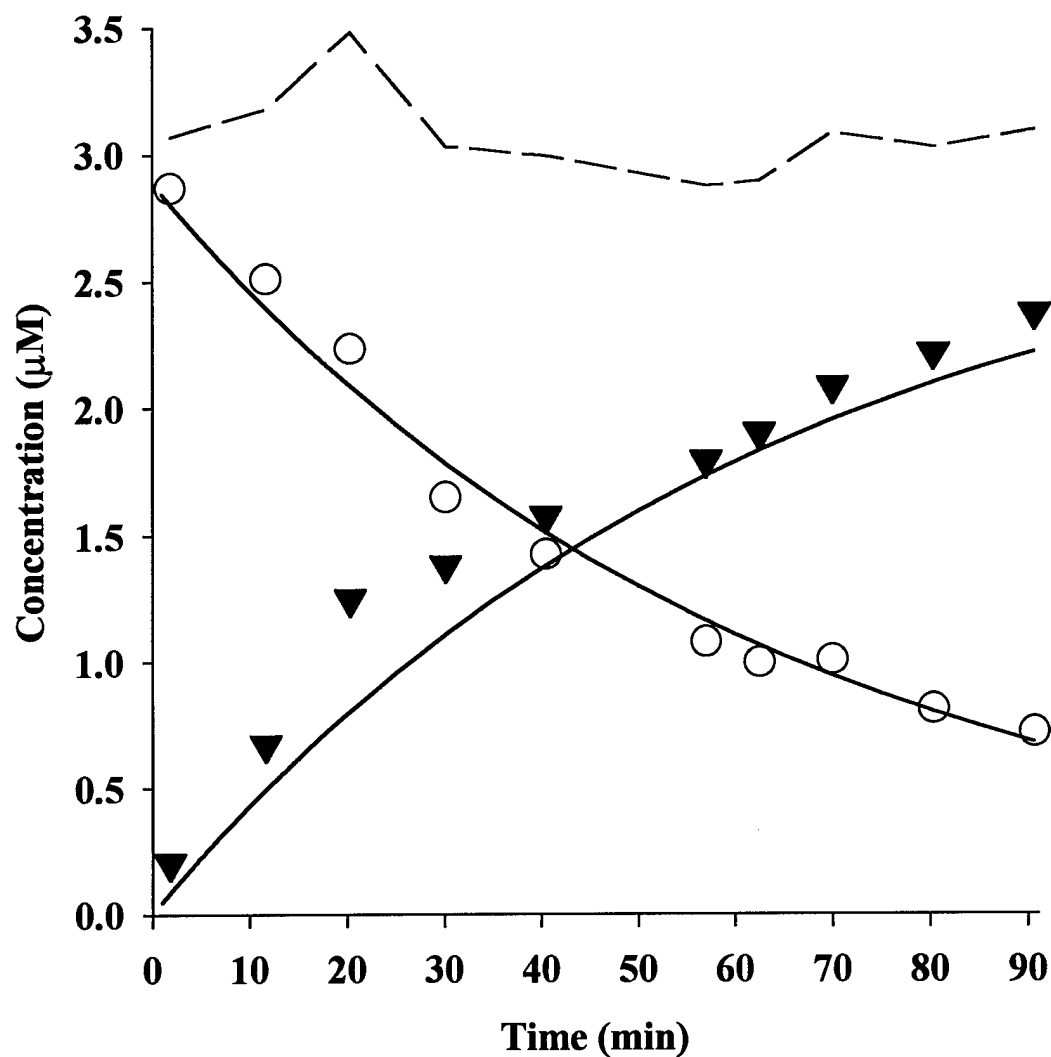


**Figure 15:** Reaction of (±)-SBr<sub>2</sub> (O) with 0.06 mM Cr(II) in 5 mM H<sub>2</sub>SO<sub>4</sub> (pH 2.0-2.1) at 25.0 (± 0.1)°C. Product is *E*-stilbene (▼). Solid lines represent fits to data assuming pseudo-first order decay to observed product. Dashed line represents calculated mass balance.

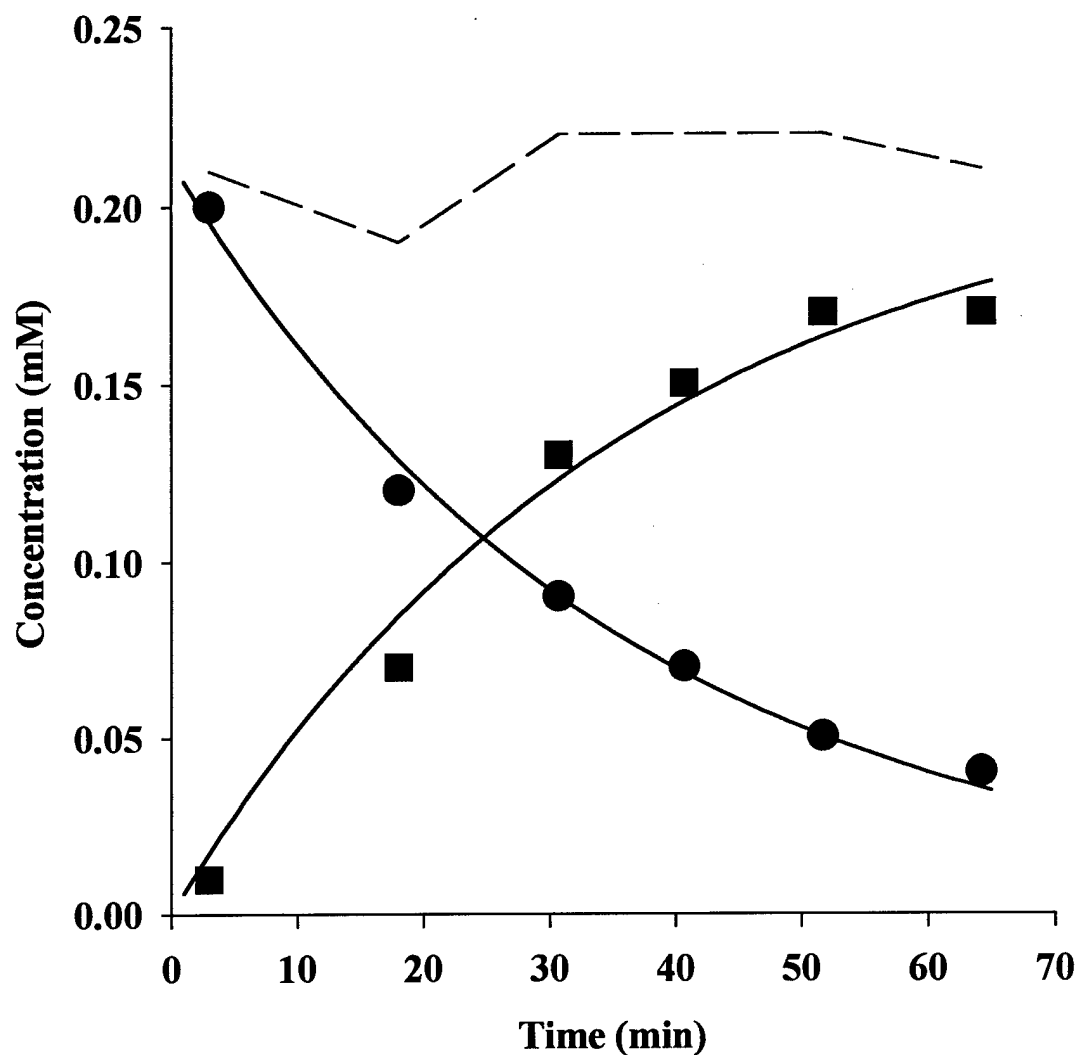


**Figure 16:** Reaction of *threo*-DBP (●) with 1 M iodide in 0.1 M NaCl, 50 mM tetraborate buffer at pH 9.3, 25.0 ( $\pm 0.1$ )°C. Sole observed product is *Z*-2-pentene (■). Solid lines represent fits to data assuming pseudo-first order decay to observed product. Dashed line represents calculated mass balance.

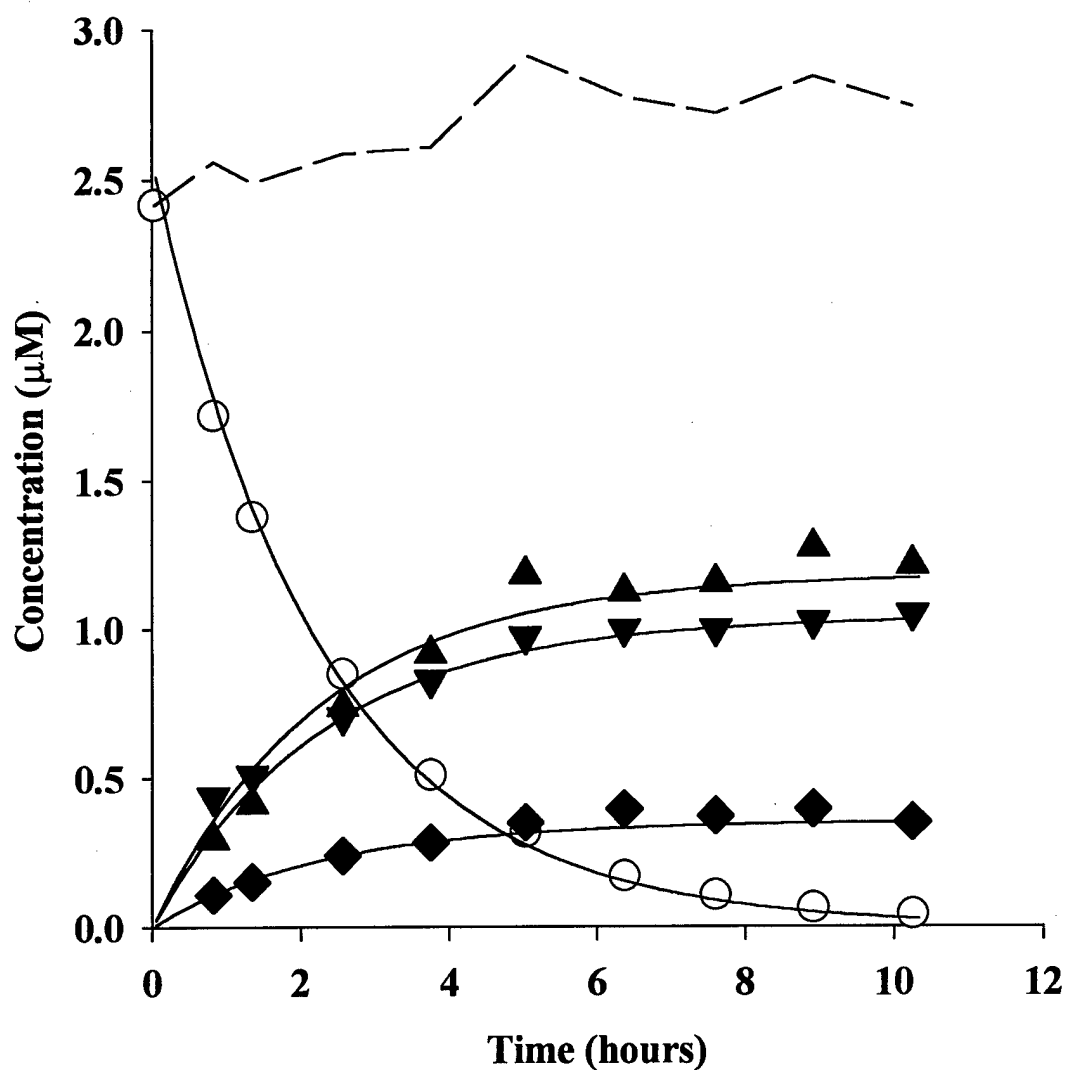


**Figure 17:** Reaction of (±)-SBr<sub>2</sub> (O) with 1 M iodide in 0.1 M NaCl, 50 mM tetraborate buffer at pH 9.3, 25.0 (± 0.1)°C. Products are *E*-stilbene oxide (▲), *Z*-stilbene (◆), and *E*-stilbene (▼). Solid lines represent fits to data assuming pseudo-first order decay to observed products. Dashed line represents calculated mass balance.

### c. Reactions with Zero-Valent Metals

Reduction of the DBPs followed good pseudo-first order kinetics with Fe, Zn, Cu, and Al. Reaction rate constants normalized to metal surface area ( $k_{SA}$ ) generally followed the order Zn>Fe>>Cu (Table 3), although absolute values of  $k_{SA}$  varied somewhat with metal loading and with mixing speed. The surface area of the Al could not be measured due to the static charge that accumulated on the particles, which made it impossible to introduce the particles into the narrow tubes used for BET analysis. The pseudo-first order rate constant for reaction of *threo*-DBP with 5.0 g of Al was 0.05 hr<sup>-1</sup> (after accounting for hydrolysis).

Each of the zero-valent metals reduced both *threo*- and *erythro*-2,3-DBP in a highly stereospecific manner, resulting in >95% of the *anti* elimination product. Representative timecourses illustrating the reaction of *threo*-2,3-DBP with iron and zinc are shown in Figures 18 and 19. Mass balances were close to 100% for all metals except aluminum, which evolved large amounts of hydrogen gas, into which the volatile pentenes tended to partition. The *Z* and *E* pentene products were stable under the reaction conditions with all metals. No hydrogenolysis products (2- or 3-bromopentanes) were detected.

The pH dependence of the stereospecificity of reaction with iron was investigated by adjusting the initial pH of the reaction solution with either NaOH or HCl. Although the initial pH was not maintained, the rate of reaction was affected. The reaction was roughly 2 times faster at both high and low pH than at neutral pH. The stereoselectivity changed at best only slightly with pH (Figure 12).

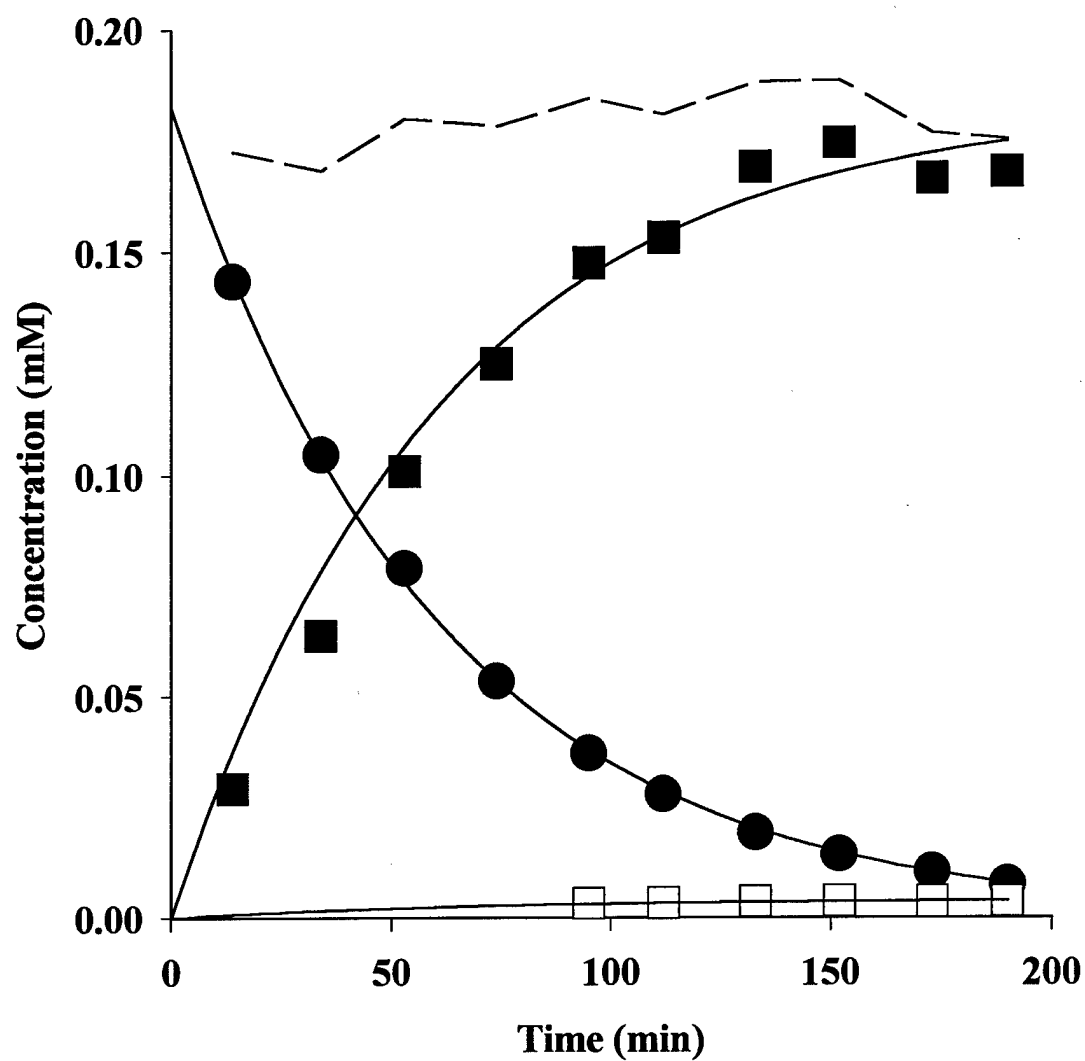


**Figure 18:** Reaction of *threo*-DBP (●) with 5.0 g iron (3.26 m<sup>2</sup>/L) in 0.1 M NaCl (pH 6.5-8.5). Products are *E*-2-pentene (□) and *Z*-2-pentene (■). Solid lines represent fits to data assuming pseudo-first order decay to observed products. Dashed line represents calculated mass balance.

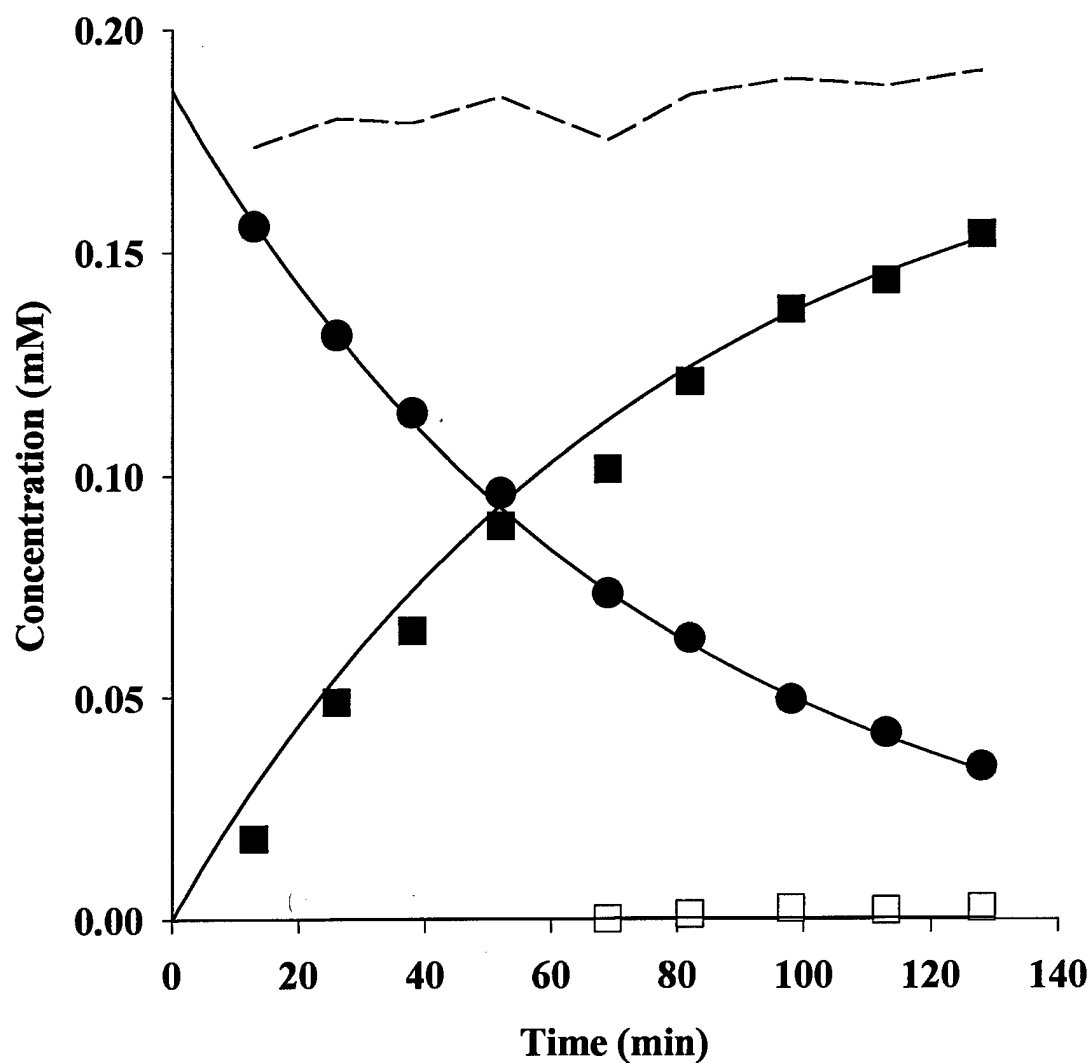


**Figure 19:** Reaction of *threo*-DBP (●) with 1.0 g zinc (0.029 m<sup>2</sup>/L) in 0.1 M NaCl (pH 6-7.5). Products are *E*-2-pentene (□) and *Z*-2-pentene (■). Solid lines represent fits to data assuming pseudo-first order decay to observed products. Dashed line represents calculated mass balance.

( $\pm$ )-SBr<sub>2</sub> was rapidly reduced by zinc and iron to a mixture of *Z*- and *E*-stilbenes (Figures 20 and 21). The percentage of *E*-stilbene in the olefin mixture was 71% for iron and 70% for zinc. The disappearance of ( $\pm$ )-SBr<sub>2</sub> displayed good pseudo-first order behavior. These reactions were sufficiently rapid that hydrolysis did not contribute significantly to the loss of ( $\pm$ )-SBr<sub>2</sub>. Mass balances were essentially 100%.

#### **d. Goethite Plus Fe(II)**

Because reduction of DBPs in the presence of goethite plus Fe(II) was slow, hydrolysis of the probe compounds consumed most of the spiked mass. At pH 7.5, the yield of pentenes was less than 10%, but only the stereospecific isomer (*Z*-2-pentene from *threo*-DBP and *E*-2-pentene from *erythro*-DBP) was detected. Control experiments demonstrated that the DBPs were not dehalogenated in goethite suspensions which did not contain Fe(II), or in Fe(II) solutions which did not contain goethite (*i.e.*, pentenes and bromopentanes were not detected as products in these systems). Disappearance of DBPs in these control experiments apparently resulted only from hydrolysis.



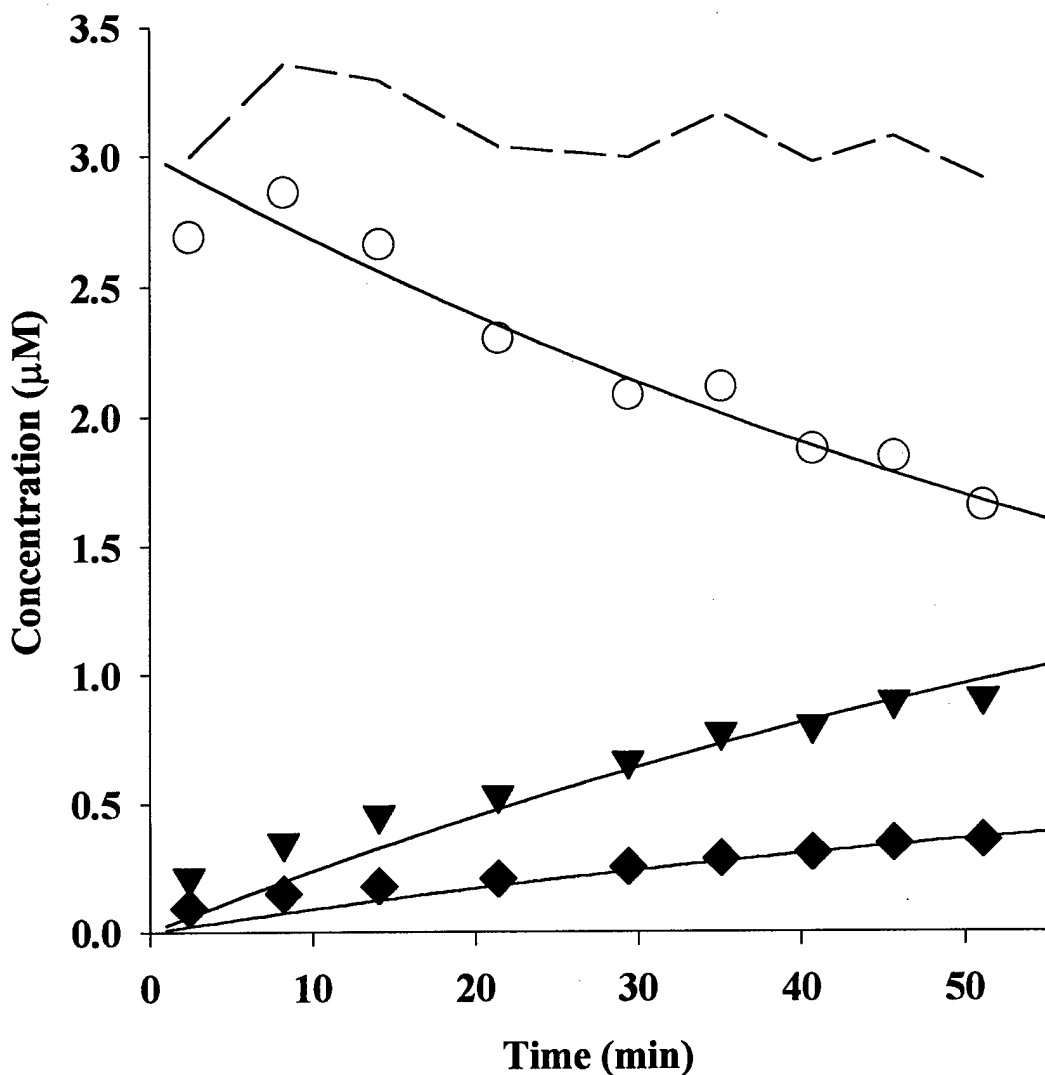


**Figure 20:** Reaction of (±)-SBr<sub>2</sub> (O) with 0.5 g iron (0.32 m<sup>2</sup>/L) in 0.1 M NaCl (pH 7.8-8.6). Products are *E*-stilbene (▼) and *Z*-stilbene (◆). Solid lines represent fits to data assuming pseudo-first order decay to observed products. Dashed line represents calculated mass balance.

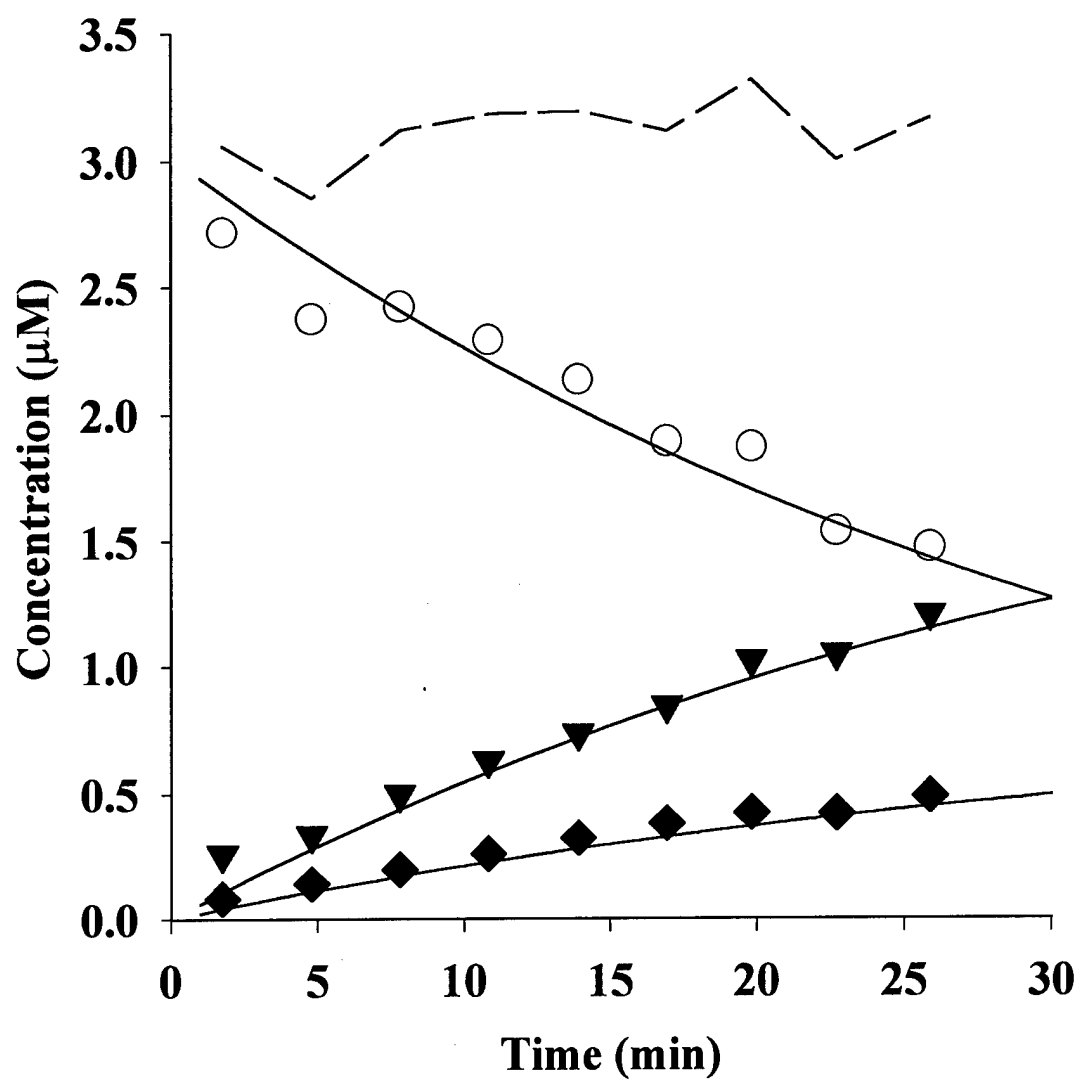


**Figure 21:** Reaction of (±)-SBr<sub>2</sub> (O) with 1 g zinc (0.028 m<sup>2</sup>/L) in 0.1 M NaCl (pH 7.7-7.9). Products are *E*-stilbene (▼) and *Z*-stilbene (◆). Solid lines represent fits to data assuming pseudo-first order decay to observed products. Dashed line represents calculated mass balance.

In order to speed up the reaction between the Fe(II)/goethite and the DBPs, some experiments were conducted at pH 10.5 using 5 mM AMP buffer. Modest (17%) conversion of *threo*-DBP to 2-pentenes was achieved in 8 hours. *E*-2-pentene represented 3% of the 2-pentene products. The mass balance was 95% (consisting mostly of unreacted *threo*-DBP). At this high pH, however, Fe(II) is expected to precipitate as Fe(OH)<sub>2</sub> (s). Control experiments in which a solution of Fe(II) at pH 10.5 was spiked with *threo*-DBP showed no production of pentenes despite the formation of a cloudy gray-green precipitate [presumably Fe(OH)<sub>2</sub> (s)].

(±)-SBr<sub>2</sub> displayed no apparent reaction with Fe(II)/goethite. Disappearance of (±)-SBr<sub>2</sub> in goethite/Fe(II) systems as well as in goethite and Fe(II) controls was no faster than could be accounted for by hydrolysis.

#### 4. Rotational Barriers

Barriers for rotation about the central C-C bond in the intermediate bromopentyl and bromostilbene radicals were estimated via computational techniques. The C-C bond must rotate through one of two eclipsed conformations to achieve the “*E*-like” conformation (Figure 22). The rotational energy barrier ( $\Delta H_{\text{rot}}$ ) was calculated by subtracting the energy of the stable “*Z*-like” rotamer from the energy of the more stable of the two eclipsed conformations (*i.e.*, the lower of the two possible energy barriers). The rate constant for C-C bond rotation ( $k_{\text{rot}}$ ) was then calculated by assuming  $\Delta H_{\text{rot}}$  is equal to the enthalpy of activation for the reaction ( $\Delta H^\ddagger$ ), and that  $\Delta S^\ddagger$  is equal to zero (Ebersson and Senning, 1983):

$$k_{\text{rot}} = \frac{\kappa T}{h} \exp\left(\frac{\Delta S^\ddagger}{R} - \frac{\Delta H^\ddagger}{RT}\right) \quad (7)$$

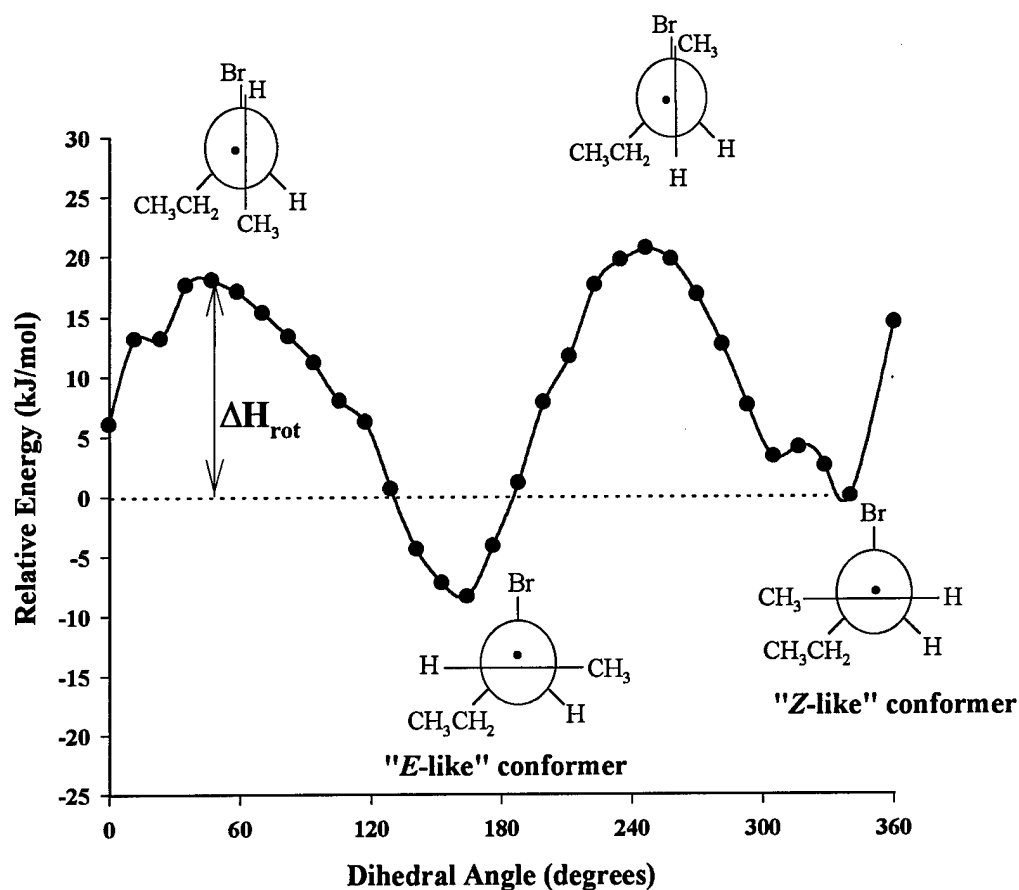


**Figure 22:** Relative energy of 3-bromopentyl radical rotational conformers. Similar plots were generated for the 2-bromopentyl and bromostilbene radicals. The energy of each conformer is calculated relative to the energy of the most stable "Z-like" conformer.

where  $R$  is the gas constant,  $T$  is the temperature in Kelvin,  $\kappa$  is the Boltzmann constant, and  $h$  is Planck's constant.

As with any computational technique, it is essential that the output of the model be checked against experimentally measured values (taken from Schubert *et al.*, 1955). For this purpose, the rotational barriers for a series of substituted ethanes were also calculated by the same method. The results were generally in reasonable agreement with the experimental values (Table 4).

**TABLE 4: COMPUTED AND EXPERIMENTAL ROTATIONAL ENERGY BARRIERS.**

Compound <sup>a</sup>	Computed (kJ/mol)	Experimental (kJ/mol) <sup>b</sup>
CH <sub>3</sub> -CH <sub>3</sub>	12.8	12
CH <sub>3</sub> -CH <sub>2</sub> CH <sub>3</sub>	14.2	14
CH <sub>3</sub> -CH(CH <sub>3</sub> ) <sub>2</sub>	15.1	16
CH <sub>3</sub> -C(CH <sub>3</sub> ) <sub>3</sub>	16.4	20
CH <sub>3</sub> CH <sub>2</sub> -CH <sub>2</sub> CH <sub>3</sub>	23.3	25
CH <sub>3</sub> -CH <sub>2</sub> F	14.0	14
CH <sub>3</sub> -CH <sub>2</sub> Cl	16.2	16
CH <sub>3</sub> -CH <sub>2</sub> Br	16.3	16
CH <sub>3</sub> -CH <sub>2</sub> I	16.2	13
CH <sub>3</sub> CHBr- <sup>•</sup> CHCH <sub>2</sub> CH <sub>3</sub> (2-bromopentyl radical)	21.1	
CH <sub>3</sub> CH <sup>•</sup> -CHBrCH <sub>2</sub> CH <sub>3</sub> (3-bromopentyl radical)	18.1	
PhCH <sup>•</sup> -CHBrPh (bromostilbene radical)	27.1	

<sup>a</sup> Barriers are those for rotation about the bond indicated in the formula.

<sup>b</sup> From Schubert *et al.* (1955).

A few caveats apply to the estimated rotational barriers for the radicals, however. First, although the estimation method gives reasonable results for closed-shell species and should be suitable for calculations involving radical species, experimental data on radicals which might be used to check this assumption are not available. One major difference between the closed-shell and radical species is the ability of the remaining bromine to "bridge" the C-C bond and stabilize the radical. This bridging orbital overlap is destroyed when the partially  $sp^2$  hybridized orbital containing the unpaired electron is rotated out of the plane containing the remaining bromine (*i.e.*, the loss of this stabilization energy represents part of the energy barrier to rotation).

Second, both the estimated values and the experimental values for the height of the rotational barriers apply only to the gas phase. Because none of these species is ionic in character, any changes in the height of the rotational energy barriers introduced by solvation effects are expected to be small.

The estimated rotational energy barriers can be used to calculate rate constants for C-C bond rotation of about  $10^9 \text{ s}^{-1}$  for the bromopentyl radicals and  $10^8 \text{ s}^{-1}$  for the bromostilbene radical. These results are in good agreement with those of Lund *et al.* (1993), who assumed a rotational barrier of 25 kJ/mol for the bromostilbene radical based on the measured value for butane. These researchers used this barrier height to estimate that an intermediate bromoalkyl rotational conformer would have a lifetime of at least  $10^{-8} \text{ s}$  before undergoing C-C bond rotation.

The computational calculations of the relative energies of rotamers can also be used to estimate their equilibrium distribution at equilibrium. The computational calculations suggest that the energy difference between the most stable *E*- and *Z*-like rotamers is about 8.3 kJ/mol for the dibromopentyl radicals, and about 31 kJ/mol for the bromostilbene radical. Thus while the *E*-like rotamer of the bromopentyl radical is expected to outnumber the *Z*-like rotamer by only about 30 to 1 at equilibrium, the *E*-like bromostilbene radical should outnumber the *Z*-like rotamer by nearly 300,000 to 1.

## E. DISCUSSION

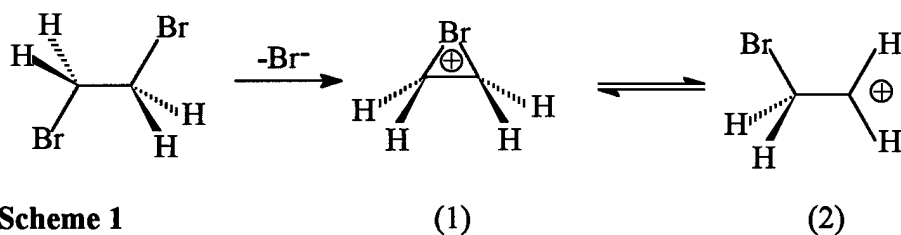
### 1. Hydrolysis of Probe Compounds

The relatively rapid hydrolysis of ( $\pm$ )-SBr<sub>2</sub> (half life = 4 hours) complicates its use as a probe in long-term experiments. *Threo*-DBP, with a hydrolysis half-life of 4.8 days, may be used to study reactions on a somewhat longer time scale.

Hydrolysis of ( $\pm$ )-SBr<sub>2</sub> results predominantly in *E*-stilbene oxide. Because *Z*-stilbene oxide does not isomerize to the *E* isomer under the conditions employed in the experiments involving ( $\pm$ )-SBr<sub>2</sub>, the mechanism of hydrolysis of this compound must account for the irreversible formation of one dominant epoxide stereoisomer. This mechanism may have important implications for interpreting the stereochemistry of nucleophilic reduction of ( $\pm$ )-SBr<sub>2</sub>. It will therefore be discussed in some detail.

The independence of hydrolysis rate on hydroxide concentration over the pH range studied, which was observed for all of the vicinal dibromide probe compounds, is consistent with either an S<sub>N</sub>2 mechanism in which the neutral species (H<sub>2</sub>O) serves as the nucleophile, or with an S<sub>N</sub>1 mechanism in which the rate-limiting step is the elimination of bromide to form a carbocation. The relatively rapid rate of hydrolysis of both the DBPs and ( $\pm$ )-SBr<sub>2</sub> may suggest that reactions proceed primarily via an S<sub>N</sub>1 pathway. For example, the neutral hydrolysis of 1,2-dibromoethane occurs with a rate constant almost three orders of magnitude smaller (Jeffers and Wolfe, 1996) than the rate constant observed for hydrolysis of *threo*-DBP. The faster reaction of the more sterically hindered substrates is consistent with an S<sub>N</sub>1 mechanism but is counter to the trend anticipated for an S<sub>N</sub>2 reaction.

An alternative explanation for the high reactivity of the probe molecules involves an intramolecular S<sub>N</sub>2 reaction. Jungclaus and Cohen (1986) have hypothesized that hydrolysis of 1,2-dibromoethane occurs via a mechanism involving intramolecular displacement of bromide via such anchimeric assistance, resulting in a bridged halonium ion (1) (Scheme 1).

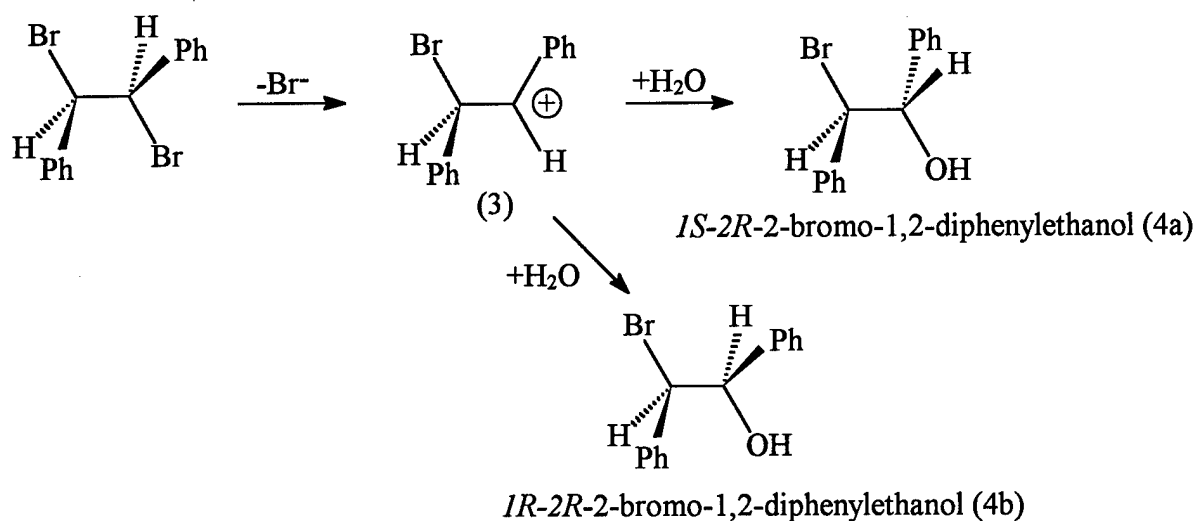


**Scheme 1**

The halonium ion (1) is thought to be slightly more stable than the open primary carbocation (2), but may undergo ring opening, resulting in an equilibrium between (1) and (2) (March, 1992). A bridged cation such as (1) is not expected to be capable of C-C bond rotation (March, 1992), which may be an important issue in determining the stereochemistry of the epoxide formed from hydrolysis of  $(\pm)$ -SBr<sub>2</sub>. March (1992) suggests that bromonium ions such as (1) are not formed where the open carbocations (2) are stabilized in other ways, such as by resonance interactions with the adjacent phenyl ring. Hydrolysis of  $(\pm)$ -SBr<sub>2</sub> is likely to proceed via an open carbocation, regardless of whether it results from an initial S<sub>N</sub>1 step or alternatively from the opening of a bromonium ion formed by a reaction analogous to Scheme 1, for reasons discussed below.

A further argument against an initial internal S<sub>N</sub>2 reaction in the hydrolysis of  $(\pm)$ -SBr<sub>2</sub> concerns the relative rates of hydrolysis of structurally similar bromides. Anchimeric assistance would be expected to increase the rate of hydrolysis relative to reaction of a molecule which lacks a neighboring bromide (March, 1992). The half-life of  $(\pm)$ -SBr<sub>2</sub> with respect to hydrolysis is actually somewhat longer than the half-life of benzyl bromide (1.32 hr at 298 K, pH 7; Mabey and Mill, 1978). In the absence of substantial acceleration introduced by the presence of the neighboring bromine, invoking a reaction involving anchimeric assistance would seem questionable. It appears more likely that  $(\pm)$ -SBr<sub>2</sub> hydrolysis occurs via an S<sub>N</sub>1 mechanism which involves an open benzylic carbocation (3), which should be capable of free C-C bond rotation (March, 1992) (Scheme 2).

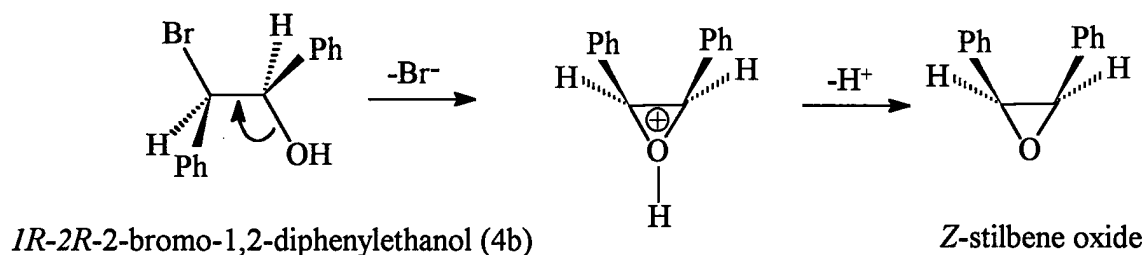
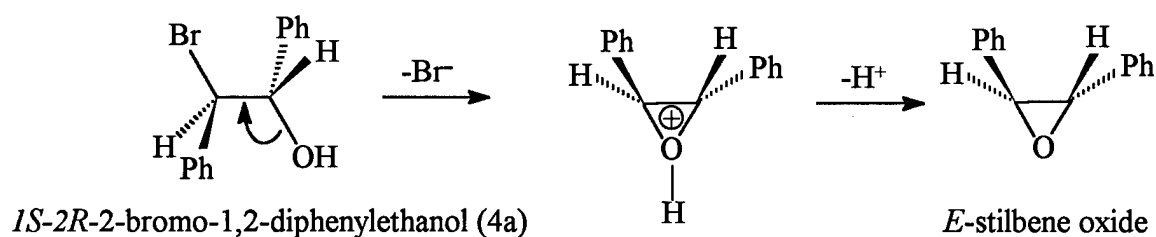




## Scheme 2

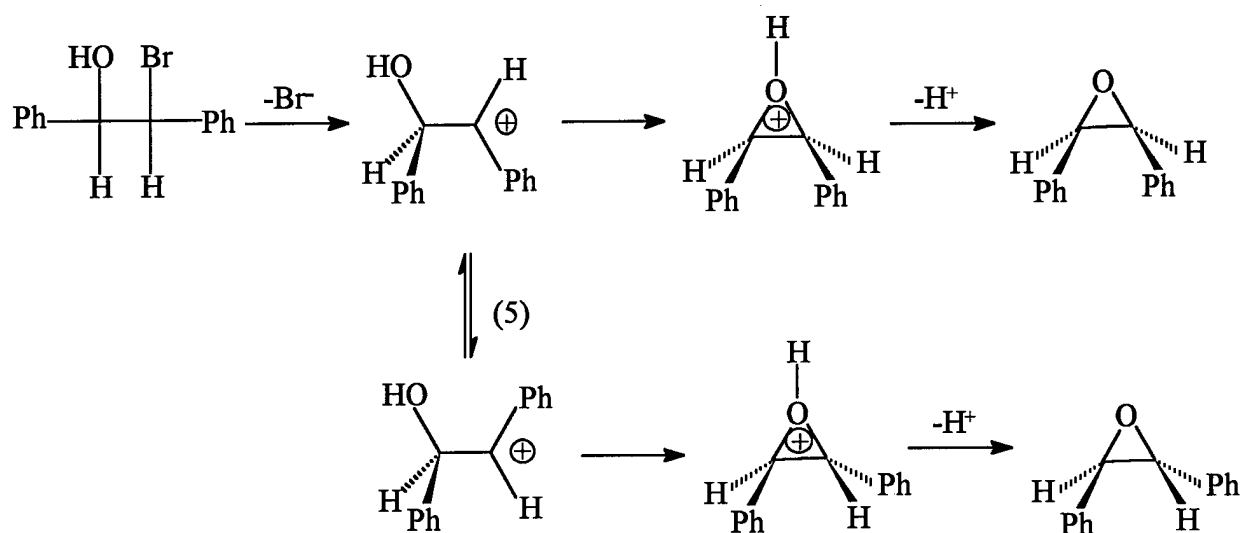
Attack of  $\text{H}_2\text{O}$  at either face of the carbocation (3) is likely to yield a pair of  $\beta$ -bromo alcohol diastereomers.  $\beta$ -Bromo alcohols were inferred to be products of DBP hydrolysis, but were not observed in  $(\pm)\text{-SBr}_2$  hydrolysis. That the alcohols (4) are not observed as products of  $(\pm)\text{-SBr}_2$  hydrolysis suggests that they rapidly undergo further reaction and therefore do not achieve a detectable steady-state concentration.

Elimination of bromide from (4) might also occur either via a mechanism involving anchimeric assistance or via an  $\text{S}_{\text{N}}1$  mechanism involving another open carbocation intermediate. An intramolecular  $\text{S}_{\text{N}}2$  (anchimeric assistance) mechanism would require an antiperiplanar arrangement of the bromine and the hydroxyl group. A mixture of diastereomers of (4) would result in both *E*- and *Z*-stilbene oxides by this mechanism (Scheme 3).



### Scheme 3

Because both the *E* and *Z* oxides were observed, and they do not interconvert under the conditions investigated, formation of the epoxides probably does not occur via two successive intramolecular steps, each involving anchimeric assistance, unless an open  $\alpha$ -bromocarbenium ion also exists as an intermediate. We feel it is more likely that the first step involves an  $\text{S}_{\text{N}}1$  reaction to an open  $\beta$ -bromocarbenium ion, which then reacts to a  $\beta$ -bromoalcohol. We cannot rule out the possibility of anchimeric assistance in the second step involving reaction of the  $\beta$ -bromoalcohol to the epoxide; alternatively, the second bromide may depart via an  $\text{S}_{\text{N}}1$  mechanism (Scheme 4).



**Scheme 4**

The closing of the epoxide ring is thought to be irreversible because *Z*-stilbene oxide does not appear to isomerize to the *E* isomer under the reaction conditions. Thus in order for hydrolysis of  $(\pm)$ -SBr<sub>2</sub> to yield only traces of *Z*-stilbene oxide, the carbocations (5) or (3) must persist for a sufficient length of time to come to a rotational equilibrium in which the phenyl groups are *trans* to one another in about 95% of the molecules before the epoxide ring closes.

Hydrolysis of  $(\pm)$ -SBr<sub>2</sub> therefore appears to involve the formation of relatively stable benzylic cations which have an open structure. These cations are thought to be capable of extensive C-C bond rotation (March, 1992). They presumably persist for a sufficient length of time for this rotation to come to an equilibrium in which the phenyl groups are likely to be located *trans* to one another for a large proportion of the molecules.

## 2. Reduction by Cr(II)

Cr(II) was employed as a model one-electron reductant to assess the stereochemistry of reductive elimination via a radical pathway. Reaction of  $(\pm)$ -SBr<sub>2</sub> with Cr(II) resulted in essentially 100% *E*-stilbene. Mathai *et al.* (1970) also observed that one-electron reductants, including Cu<sup>+</sup>, Fe<sup>2+</sup>, Cr<sup>2+</sup>, Ti<sup>3+</sup>, and Co<sup>2+</sup>, all reduce  $(\pm)$ -SBr<sub>2</sub> in a variety of organic solvents to essentially 100% *E*-stilbene with only traces of *Z*-stilbene formed. The high percentage of *E*-stilbene produced from  $(\pm)$ -SBr<sub>2</sub> results from the steric strain in the *Z*-configuration of the

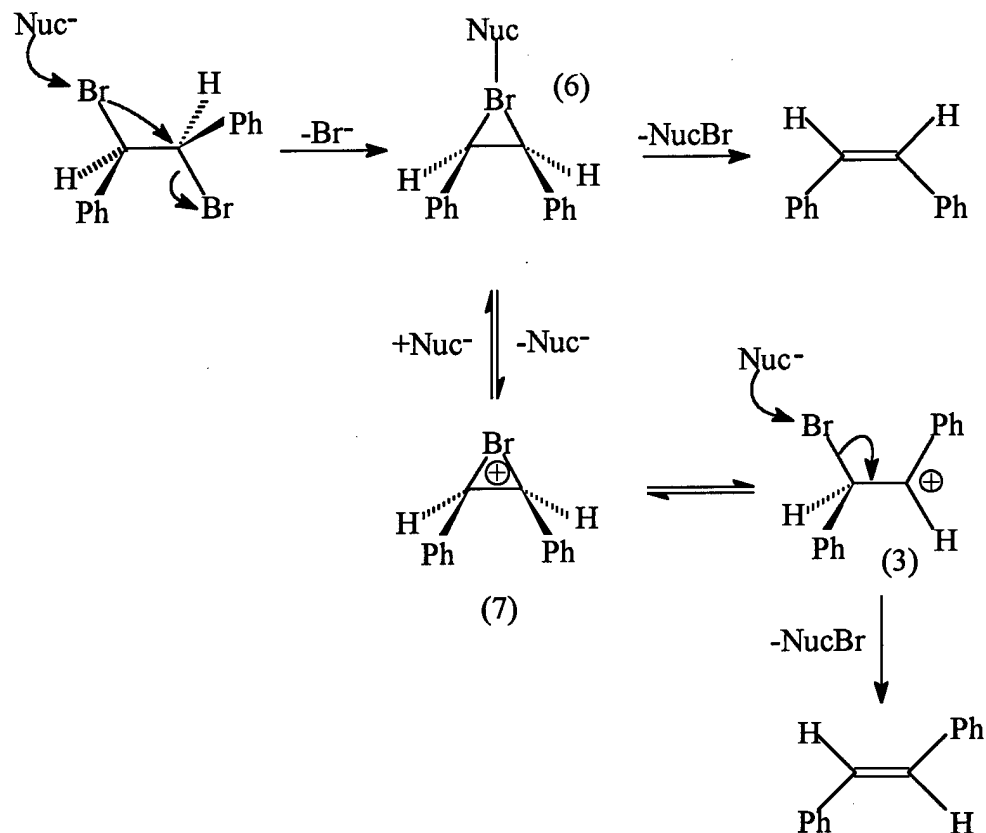
intermediate radical, which drives bond rotation (see Fig. 1). These radicals apparently persist long enough to come to rotational equilibrium, in which essentially 100% of the radicals are in the *E*-like configuration.

Likewise, the formation of *Z*- and *E*-2-pentenenes (68% *E* isomer) during the reduction of *threo*-DBP by 10 mM Cr(II) indicates that the radical formed from the first one-electron reduction of this probe can, at least under some circumstances, persist long enough to undergo C-C bond rotation. These results are in good agreement with those of Kochi and Singleton (1968) who observed a similar ratio of *E*- and *Z*-olefins from the reduction of ( $\pm$ )-2,3-dibromobutane by 0.068 M Cr(II) in (30/10) acetonitrile/water. These researchers also observed that proportionately more *Z*-olefin was produced as Cr(II) concentrations increased. Unlike ( $\pm$ )-SBr<sub>2</sub>, aliphatic vicinal dibromides are reduced to a mixture of *E* and *Z* olefin because the *E*-like and *Z*-like rotational conformers of the bromopentyl radicals are closer in energy and therefore significant amounts of each exist at equilibrium.

### 3. Reduction by Iodide

Reduction of ( $\pm$ )-SBr<sub>2</sub> by iodide resulted in both *E*- and *Z*-stilbene, with the *E* isomer representing 74% of the total stilbene yield. Understanding the mechanism of hydrolysis for ( $\pm$ )-SBr<sub>2</sub> helps to explain the formation of both *E* and *Z* stilbenes during these reactions. This result is problematic because a concerted, two-electron elimination mechanism, as depicted in Fig. 1b, might be expected to yield only *Z*-stilbene, and a one-electron reduction pathway [by analogy with the results obtained for Cr(II)] should yield only the *E* isomer.

Elimination of the two halogens need not be concerted for the reaction to represent a two-electron process. Baciocchi (1983) concludes that nucleophilic dehalogenations of ( $\pm$ )-SBr<sub>2</sub> in organic solvents most likely occurs via a halonium ion mechanism (Scheme 5).



**Scheme 5**

Note that the cationic intermediate (7) has a bridged structure. Because hydrolysis of (±)-SBr<sub>2</sub> is thought to occur via the open carbocation (3), nucleophilic reduction of (±)-SBr<sub>2</sub> in a polar solvent such as water might be expected to occur via such an open intermediate as well.

Rotation about the C-C bond of (3) is hypothesized to occur freely (March, 1992); such rotation could account for the formation of large amounts of *E*-stilbene during the reduction of (±)-SBr<sub>2</sub> by nucleophilic reductants such as iodide in aqueous systems without invoking a *syn*-elimination pathway (Fawell *et al.*, 1990; Inesi and Rampasso, 1974). Steric interactions between the phenyl groups would be expected to cause the *E*-like rotamer to dominate the rotational equilibrium of (3). Reduction of (3) might therefore be expected to produce very little *Z*-stilbene (by analogy with the hydrolysis results) if C-C bond rotation comes to equilibrium.

Reduction of (±)-SBr<sub>2</sub> by iodide in water results in a mixture of *E*- and *Z*-stilbenes, however, with the *Z* isomer accounting for some 30% of the stilbene products. The *Z*-stilbene might be produced via rearrangement of (6) to the final product via the upper pathway shown in

Scheme 5, while the *E*-isomer arises from nucleophilic reduction of (3). Alternatively, the product distribution could reflect a concerted nucleophilic reduction (Figure 1b) operating concurrently with nucleophilic reduction via a halonium ion intermediate.

Other researchers have noted smaller proportions of *E*-stilbene in the total stilbene yield resulting from reduction of ( $\pm$ )-SBr<sub>2</sub> by iodide in organic solvents, with *E*-stilbene (as a percent of total stilbene) ranging from 4% to 35% (Mathai *et al.*, 1970). Although the relatively small *E*-stilbene yields observed by other researchers may seem at odds with the larger proportions of *E*-stilbene produced in the aqueous systems employed in this work, close scrutiny of the published data reveals that the % *E*-stilbene increases as the solvent becomes more polar. This most likely reflects increasing stabilization of a cationic intermediate in more polar solvents, and thus a greater propensity for the reaction to proceed via such an intermediate. The increase in *E*-stilbene yield may, however, reflect at least in part a temperature effect, since reactions in most of the prior work were conducted at the boiling point of the solvent and more polar solvents tend to have higher boiling points.

In contrast to ( $\pm$ )-SBr<sub>2</sub>, the DBPs were reduced by iodide to essentially 100% of the stereospecific *anti* elimination product (*i.e.*, *threo*-DBP was reduced to *Z*-2-pentene, and *erythro*-DBP was reduced to *E*-2-pentene). This result is in agreement with previous studies which demonstrated that aliphatic bromides react with iodide primarily via concerted nucleophilic reductive elimination pathways (Figure 1b), rather than via a halonium ion mechanism (Baclocchi, 1983). For example, reduction of ( $\pm$ )-2,3-dibromobutane by iodide yields 95-100% *Z*-2-butene in 90/10 methanol/water (59°C) (Schubert *et al.*, 1955). The greater tendency to react via a concerted nucleophilic mechanism probably reflects lesser stabilization of a charged intermediate by the alkyl substituents of the DBPs vs. the phenyl substituents of ( $\pm$ )-SBr<sub>2</sub>.

#### **4. Reductions Promoted by Zero-Valent Metals**

Reduction of *threo*-DBP by the zero-valent metals investigated resulted almost exclusively in *Z*-2-pentene, similar to the results obtained for reaction with iodide. Earlier studies conducted in various organic solvents also demonstrate that aliphatic vicinal dibromides are reduced to characteristic *anti* elimination products by zero-valent metals. For example, ( $\pm$ )-5,6-dibromodecane is reduced to 95% *Z*-5-decene by Zn(0) (methanol, room temperature) and 72%

Z-5-decene by Li(0) (tetrahydrofuran, room temperature) (Sicher *et al.*, 1968).

Likewise, the *E/Z* ratios obtained in this study from reduction of ( $\pm$ )-SBr<sub>2</sub> by zinc and iron were similar to those resulting from reduction by iodide. These results are consistent with the previous studies of Mathai *et al.* (1970) in which ( $\pm$ )-SBr<sub>2</sub> was reduced to a mixture of *E*- and *Z*-stilbenes by a variety of zero-valent metals, including Zn(0), Cu(0), Mg(0), Al(0), Cd(0), and Pb(0). Results from reductions by Zn(0) were typical of the other metals. *E*-stilbene represented between 75% and 97% of the total stilbene yield in a variety of solvents for reactions conducted under reflux conditions. In water (100°C), the *E*-stilbene constituted 88% of the stilbene products. The proportion of *E*-stilbene formed displayed no apparent trend with solvent polarity.

The similarity in the product distribution resulting from reduction of ( $\pm$ )-SBr<sub>2</sub> by metals and by iodide is striking: the percent of the *E* isomer in the total stilbene yield is the same (within experimental error) for reductions promoted by iodide, Fe(0), and Zn(0), as demonstrated by the error bars in Figure 13. Furthermore, reduction of ( $\pm$ )-SBr<sub>2</sub> in water by a variety of other strong nucleophiles (including bisulfide and polysulfides) at varying concentrations has been observed to result in a similar percentage of *Z*-stilbene (about 30-40% of total stilbene yield) (Jans and Roberts, 1998). It is possible that the mechanism of the reaction is different for these various reductants but that exactly the same product distribution nevertheless results. It may be more plausible, however, to assume that the similarity in product distribution reflects a common (or at least a very similar) intermediate.

## 5. Reductions Promoted by Fe(II) on Goethite

The reduction of the DBPs via stereospecific *anti* elimination by Fe(II) adsorbed to goethite might initially seem somewhat surprising, since Fe(II) would presumably serve as a one-electron reductant. Reduction of the vicinal dibromides by Fe(II) adsorbed to goethite may be comparable to reduction of these compounds by Li(0), for which elimination is highly stereospecific (in tetrahydrofuran) despite the fact that Li(0) is presumably oxidized by a single electron to Li<sup>+</sup> (Sicher *et al.*, 1968). In both cases, reduction occurs at a surface which contains an excess of available reductant. Given the site density on goethite (7.0 sites/nm<sup>2</sup>), a simple calculation shows that the sorbed Fe(II) atoms are only about 0.2 nm apart. The C-C bond of the dibromopentane is roughly 0.15 nm in length, so a second Fe(II) atom should be available within a

reasonable bonding distance to donate the second electron, assuming that all of the sorbed Fe(II) is reactive. Thus the rate of C-C bond rotation may be sufficiently slow relative to the transfer of the second electron that the intermediate bromopentyl radicals are reduced to alkenes before undergoing C-C bond rotation.

## 6. Mechanistic Interpretation

For both the DBPs and ( $\pm$ )-SBr<sub>2</sub>, the products observed from reduction by iron and zinc have essentially the same *E/Z* ratio as those encountered with the classic nucleophilic reductant, iodide. It cannot be definitively concluded, however, that these probe compounds are reduced by zero-valent metals via a nucleophilic two-electron mechanism, because the reactions are heterogeneous in nature and occur at a surface which possesses an excess of reductant. For the DBPs, a similar product distribution was obtained when Fe(II) adsorbed to goethite served as the reductant, suggesting that the reactions with zero-valent metals could equally well occur via a mechanism in which initial SET yields a radical which is rapidly reduced by a second electron to the alkene at a rate that is rapid relative to C-C bond rotation.

The computational estimates of the energy barriers for C-C bond rotation in the intermediate radicals allow approximate limits to be placed on the pseudo-first order rate constants corresponding to transfer of a second electron to the radical. If C-C bond rotation occurs with an estimated rate constant of  $10^9 \text{ s}^{-1}$  for the bromopentyl radicals, then the second electron would have to be transferred to the radical with a pseudo-first order rate constant on the order of  $10^{10} \text{ s}^{-1}$  in order to produce 95% *Z*-2-pentene from *threo*-DBP. Similarly, if C-C bond rotation occurs with an estimated rate constant of  $10^8 \text{ s}^{-1}$  for the bromostilbene radical, the second electron transfer would have to occur with a pseudo-first order rate constant on the order of  $10^8 \text{ s}^{-1}$  in order to produce 70% *E*-stilbene via an SET pathway.

In order for other bimolecular reactions to compete with transfer of the second electron, they would have to be extremely fast. Even a diffusion-limited reaction, such as self-coupling of free radicals (which occurs with a bimolecular rate constant on the order of  $10^{10} \text{ M}^{-1}\text{s}^{-1}$ ) could only begin to compete with the second one-electron transfer if the concentration of the radical species was greater than  $10^{-2}$  to  $10^{-3} \text{ M}$ . Such a high concentration of reactive transients is extremely unlikely in zero-valent metal systems. Hydrogen atoms might be generated at the metal



surface in high concentrations, but because bromopentane and bromostilbene products were not observed from the reactions of the probe compounds with iron and zinc, the coupling of organic radicals with nascent hydrogen atoms apparently did not occur to any significant extent in these systems.

The stereochemistry of the products suggests, then, that if radical intermediates are in fact generated during reduction of vicinal dibromides by zero-valent metals, they do not escape the surface before undergoing rapid further reduction.

### **7. Implications for Zero-Valent Metal Based Remediation Technology**

Because zero-valent metals (as well as Fe(II) adsorbed to iron (hydr)oxide surfaces) reduce vicinal dibromides via a very rapid transfer of two electrons, any intermediate radical that is formed is short-lived and is unlikely to escape from the metal [or (hydr)oxide] surface before being reduced to a relatively stable closed-shell species. In general, then, characteristic free-radical reactions such as hydrogen atom abstraction and intermolecular dimerization of free radicals should be rare events in zero-valent metal based remediation schemes. Radical coupling (including the coupling of organic radicals with hydrogen atoms) is likely to occur only if radicals are generated very close to one other at the metal-water interface. In order for the coupling products observed during the reduction of 1,1,1-TCA by iron (Fennelly and Roberts, 1998) to originate from the coupling of free radicals, a large number of radicals would have to be produced at specific highly reactive areas on the iron surface. Alternatively, coupling may take place via a process other than the collision of two free radicals, perhaps by an intramolecular mechanism involving rearrangement of a dialkyl organometallic intermediate. This possibility will be explored further in Chapter 3.

Because DBP's and ( $\pm$ )-SBr<sub>2</sub> give similar products during reduction by both iron and zinc, these probes cannot discern any difference in the mechanism of reduction by these two metals, and therefore cannot directly explain the production of coupling products by iron but not by zinc. For this reason, further research has focused on elucidating the mechanism of electron transfer promoted by these metals using a different kind of mechanistic probe which, in theory, should allow a more accurate determination of the rate at which a second electron is transferred to the intermediate radical. The results of these investigations will be presented in the next section.

## F. LITERATURE CITED

- Baclocchi, E. "1,2-Dehalogenations and related reactions." In *The Chemistry of Halides, Pseudo-halides and Azides*, Supplement D; Patai, S.G., Rappoport, Z., Eds.; Wiley and Sons: New York, 1983; Vol. 1, 161-201.
- Balko, B. A.; Tratnyek, P. G. Photoeffects on the reduction of carbon tetrachloride by zero-valent iron. *J. Phys. Chem. B* **1998**, *102*, 1459-1465.
- Boronina, T.; Klabunde, K. J.; Sergeev, G. Destruction of organohalides in water using metal particles: carbon tetrachloride/water reactions with magnesium, tin, and zinc. *Environ. Sci. Technol.* **1995**, *29*, 1511-1517.
- Burris, D. R.; Campbell, T. J.; Manoranjan, V. S. Sorption of trichloroethylene and tetrachloroethylene in a batch reactive metallic iron-water system. *Environ. Sci. Technol.* **1995**, *29*, 2850-2855.
- Castro, C. E. The role of halide in the reduction of carbonium ions by chromium(II). *J. Am. Chem. Soc.* **1961**, *83*, 3262-3264.
- Coughlin, B. R.; Stone, A. T. Nonreversible adsorption of divalent metal ions ( $\text{Mn}^{\text{II}}$ ,  $\text{Co}^{\text{II}}$ ,  $\text{Ni}^{\text{II}}$ ,  $\text{Cu}^{\text{II}}$ ,  $\text{Pb}^{\text{II}}$ ) onto goethite: effects of acidification,  $\text{Fe}^{\text{II}}$  addition, and picolinic acid addition. *Environ. Sci. Technol.* **1995**, *29*, 2445-2455.
- Diehl, H. *The Iron Reagents*; 3rd ed.; G. Frederick Smith Chemical Company: Columbus, Ohio, 1980.
- Ebersson, L.; Senning, A. *Organische Chemie I*; 2nd ed.; Verlag Chemie: Weinheim, 1983.
- Ebersson, L. *Electron Transfer Reactions in Organic Chemistry*; Springer-Verlag: New York, 1987.
- Fawell, P.; Avraamides, J.; Hefter, G. Reduction of vicinal dihalides. I. The electrochemical reduction of *meso*- and ( $\pm$ )-1,2-dibromo-1,2-diphenylethane. *Aust. J. Chem.* **1990**, *43*, 1421-1430.
- Fennelly, J. P.; Roberts, A. L. Reaction of 1,1,1-trichloroethane with zero-valent metals and bimetallic reductants. *Environ. Sci. Technol.* **1998**, *32*, 1980-1988.

- Fieser, L. F.; Williamson, K. L. *Organic Experiments*; 4th ed.; DC Heath and Co.: Lexington, MA, 1979.
- Gillham, R. W.; O'Hannesin, S. F.; Orth, W. S. Metal enhanced abiotic degradation of halogenated aliphatics: laboratory tests and field trials. In *HazMat Central Conference*, Chicago, IL; 1993.
- Gillham, R. W.; O'Hannesin, S. F. Enhanced degradation of halogenated aliphatics by zero-valent iron. *Ground Water* **1994**, *32*, 958-967.
- Helland, B. R.; Alvarez, P. J. J.; Schnoor, J. L. Reductive dechlorination of carbon tetrachloride with elemental iron. *J. Haz. Mat.* **1995**, *41*, 205-216.
- Inesi, A.; Rampasso, L. Stereoselective reduction of *meso* and *dl*-1,2-dibromo-1,2-diphenylethane at the mercury electrode. *J. Electroanal. Chem.* **1974**, *54*, 289.
- Jans, U.; Roberts, A. L. 1,2-Dibromo-1,2-diphenylethane ( $\pm$ SBr<sub>2</sub>): A mechanistic probe of reductive dehalogenation by reduced sulfur species in the presence of electron transfer mediators. *Natl. Meet.-Am. Chem. Soc., Div. Environ. Chem.*, **1998**, *38*(2), 123-124 (Abstr.).
- Jeffers, P. M.; Wolfe, N. L. Homogeneous hydrolysis rate constants-Part II: Additions, corrections, and halogen effects. *Environ. Toxicol. Chem.* **1996**, *15*, 1066-1070.
- Johnson, T. L.; Fish, W.; Gorby, Y. A.; Tratnyek, P. G. Degradation of carbon tetrachloride by iron metal: Complexation effects on the oxide surface. *J. Contam. Hydrol.* **1998**, *29*, 379-398.
- Jungclaus, G. A.; Cohen, S. Z. Hydrolysis of ethylene dibromide. *Division of Environmental Chemistry, Extended Abstracts* **1986**, *26*, 12-16.
- Kelsall, G. H.; House, C. I.; Gudyanga, F. P. Chemical and electrochemical equilibria and kinetics in aqueous Cr(III)/Cr(II) chloride solutions. *Journal of Electroanalytical Chemistry* **1988**, *244*, 179-201.
- Kochi, J. K.; Singleton, D. M. Stereochemistry of reductive elimination by chromium (II) complexes. *J. Am. Chem. Soc.* **1968**, *90*, 1582-1589.

- Krone, U. E.; Thauer, R. K.; Hogenkamp, H. P. C.; Steinbach, K. Reductive formation of carbon monoxide from  $\text{CCl}_4$  and FREONs 11, 12, and 13 catalyzed by corrinoids. *Biochem.*, **1991**, *30*, 2713-2719.
- Lipczynska-Kochany, E.; Harms, S.; Milburn, R.; Sprah, G.; Nadarajah, N. Degradation of carbon tetrachloride in the presence of iron and sulphur containing compounds. *Chemosphere* **1994**, *29*, 1477-1489.
- Lowe, J. P. Barriers to internal rotation about single bonds. *Prog. Phys. Org. Chem.* **1968**, *6*, 1-80.
- Lund, T.; Bjorn, C.; Hansen, H. S.; Jensen, A. K.; Thorsen, T. K. Debromination of *meso* and ( $\pm$ )-1,2-dibromo-1,2-diphenylethane by 9-substituted fluorenyl anions. Correlation between stereochemical results and redox potentials. *Acta Chemica Scandinavica* **1993**, *47*, 877-884.
- Mabey, W.; Mill, T. Critical review of hydrolysis of organic compounds in water under environmental conditions. *J. Phys. Chem. Ref. Data* **1978**, *7*, 383-415.
- March, J. *Advanced Organic Chemistry: Reactions, Mechanisms and Structure*; 4th ed.; Wiley-Interscience: New York, 1992.
- Mathai, I. M.; Schug, K.; Miller, S. I. Stereoselectivity in the debromination of the stilbene dibromides by several metals and inorganic reductants in several solvents. *J. Org. Chem.* **1970**, *35*, 1733-1736.
- Matheson, L. J.; Tratnyek, P. G. Reductive dehalogenation of chlorinated methanes by iron metal. *Environ. Sci. Technol.* **1994**, *28*, 2045-2053.
- Pontius, F.W. New horizons in federal regulations. *J. AWWA*, **1998**, *90*(3), 38-46.
- Pross, A. The single electron shift as a fundamental process in organic chemistry: The relationship between polar and electron-transfer pathways. *Acc. Chem. Res.* **1985**, *18*, 212-219.
- Roberts, A. L.; Totten, L. A.; Arnold, W. A.; Burris, D. R.; Campbell, T. J. Reductive elimination of chlorinated ethylenes by zero-valent metals. *Environ. Sci. Technol.* **1996**, *30*, 2654-2659.
- Schubert, W. M.; Steadly, H.; Rabinovitch, B. S. The stereochemistry of the debromination of *meso*-1,2-dibromo-1,2-dideuteroethane by iodide ion. *J. Am. Chem. Soc.* **1955**, *77*, 5755.

- Sicher, J.; Havel, M.; Svoboda, M. Preferred overall *syn*-elimination in metal promoted cycloalkene formation of vicinal dibromides. *Tetrahedron Letters* **1968**, *40*, 4269-4272.
- Sivavec, T. M. Reductive dechlorination of chlorinated solvents by iron metal and iron sulfide minerals. In *IBC International Symposium on Biological Dehalogenation*, Annapolis, MD; 1995.
- Warren, K. D.; Arnold, R. G.; Bishop, T. L.; Lindholm, L. C.; Betterton, E. A. Kinetics and mechanism of reductive dehalogenation of carbon tetrachloride using zero-valence metals. *J. Haz. Mat.* **1995**, *41*, 217-227.
- Winstein, S.; Pressman, D.; Young, W. G. Investigations on the stereoisomerism of unsaturated compounds. V. A mechanism for the formation of butenes from 2,3-dibromobutanes by the action of iodide ion. *J. Am. Chem. Soc.* **1939**, *61*, 1645-1647.
- Wood, W.G., Ed. Surface cleaning, finishing and coating. In *Metals Handbook*, American Society for Metals: Metals Park, OH, 1982; Vol. 5.

## SECTION III

# ALKYL BROMIDES AS MECHANISTIC PROBES OF REDUCTIVE DEHALOGENATION: REACTIONS OF RADICAL CLOCKS WITH ZERO-VALENT METALS

### A. ABSTRACT

Understanding the extent to which free radicals are involved in reactions between zero-valent metals and organohalides may help environmental chemists predict reaction rates and likely products in zero-valent metal-based treatment systems. This issue was investigated using radical clocks (6-bromo-1-hexene and bromomethylcyclopropane), which yield characteristic products if reactions proceed via single electron transfer (SET) pathways. Measurement of the product distribution can shed light on the one- or two-electron character of the reduction and can in some cases allow an estimate of the pseudo-first order rate constant ( $k_2$ ) associated with reduction of the intermediate radicals. Both Zn(0) and Fe(0) produce detectable amounts of rearranged products from 6-bromo-1-hexene and bromomethylcyclopropane, which could be interpreted as evidence that radical intermediates are involved. The observed rearrangement products could, however, also arise from organometallic intermediates. Reaction of both radical clocks with Fe(0) gives rise to several byproducts which are characteristic of the decomposition of organoiron species. Such species are apparently crucial in determining the product distribution and may be responsible for the formation of coupling and alkene isomerization products. A "pure" SET mechanism cannot account for formation of many of these observed products; SET appears therefore to occur either as the first step in the formation of organoiron species, or as a minor side reaction.

### B. INTRODUCTION

Despite the current research into reactions of zero-valent metals with alkyl and vinyl polyhalides (Gillham and O'Hannesin, 1994; Matheson and Tratnyek, 1994; Lipczynsa-Kochany *et al.*, 1994; Boronina and Klabunde, 1995; Powell *et al.*, 1995; Helland *et al.*, 1995; Warren *et al.*, 1995; Burris *et al.*, 1995; Agrawal and Tratnyek, 1996; Roberts *et al.*, 1996; Johnson *et al.*, 1998; Balko and Tratnyek, 1998), many basic questions about the mechanism of these reduction reactions remain unanswered. Understanding the mechanisms of these reactions is essential in order to predict rates at which polyhalogenated contaminants might react with zero-valent metals, as well as the products which may result.

The previous section described efforts to elucidate the mechanism through which zero-valent metals reduce organohalides by examining the stereochemistry of products arising from reduction of vicinal dibromide stereochemical probes. These studies suggested that zero-valent metals reduce dibromopentanes either via a series of very rapid single electron transfer (SET) steps, or via a "two-electron" nucleophilic reduction pathway. The results of the vicinal dibromide probe studies did not, however, allow a conclusive discrimination between these two possibilities. Only a very small fraction of the products resulting from reduction of dibromopentanes by iron was consistent with an intermediate radical that could have persisted long enough to have undergone C-C bond rotation. Any intermediate radical formed was therefore likely to have undergone reduction to a relatively stable closed-shell species before it could diffuse away from the metal surface. Such characteristic free-radical reactions as hydrogen atom abstraction and radical-radical coupling should thus be rare events in zero-valent metal based remediation schemes.

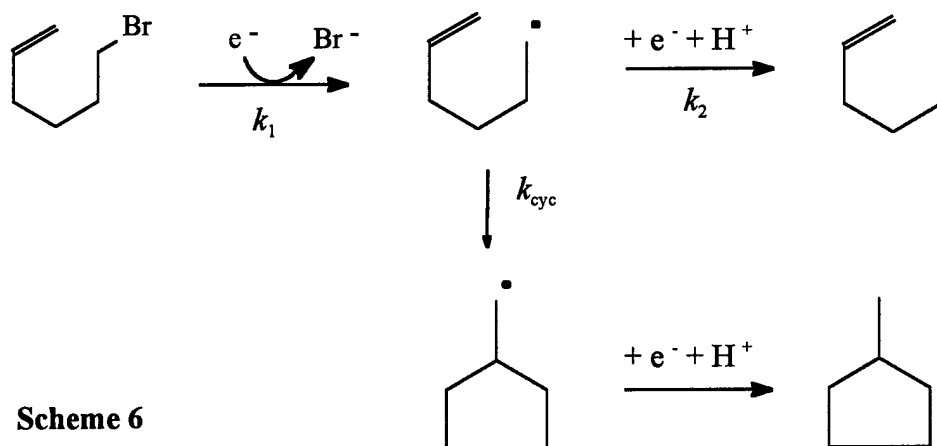
These conclusions, however, cannot explain the coupling products that are observed during the reduction of 1,1,1-trichloroethane (1,1,1-TCA) by iron but not by zinc (Fennelly and Roberts, 1998). Coupling of radicals might only be anticipated if a large number of radicals were produced at localized highly reactive regions of the iron surface. Alternatively, coupling may take place via some process other than the collision of two free radicals, such as through an intramolecular rearrangement of a dialkyl organometallic species, as has been suggested by Boronina *et al.* (1998).

In order to further elucidate the mechanism through which zero-valent metals reduce alkyl halides, the reduction of an additional class of mechanistic probes has been investigated, one which (in theory) should allow an accurate determination of the lifetimes of radical intermediates. The probe compounds employed in the present work are 6-bromo-1-hexene and bromomethylcyclopropane (BrMCP). They are referred to as a "radical clocks" because the distribution of their reaction products may be used to calculate the rate constant associated with the second electron transfer.

Griller and Ingold (1980) and Newcomb and Curran (1988) provide good overviews of the use of radical clocks. In addition to their utility in measuring rate constants for electron transfer reactions, radical clocks have also been used to investigate whether reactions follow

single electron transfer (SET) or two-electron pathways. They have been used, for example, to investigate the mechanism of reduction of alkyl halides by many reductants, including magnesium metal in organic solvents (*i.e.*, formation of Grignard reagents; Ashby and Oswald, 1988), zinc metal in acetic acid/ether (Brace and Elswyk, 1976), and macrocyclic nickel complexes in alkaline aqueous solution (pH 12 and above) (Bakac and Espenson, 1986). In all of these cases, the radical clock is an alkyl halide, and the radical is generated via dissociative electron transfer which cleaves the C-X bond. Hydrocarbon radical clocks have also been employed in the study of oxidation reactions, in which the radical is typically generated via hydrogen atom abstraction. For example, the mechanism through which methane monooxygenase enzymes catalyze the hydroxylation of hydrocarbons has been investigated by this approach (Fu *et al.*, 1991; Liu *et al.*, 1993).

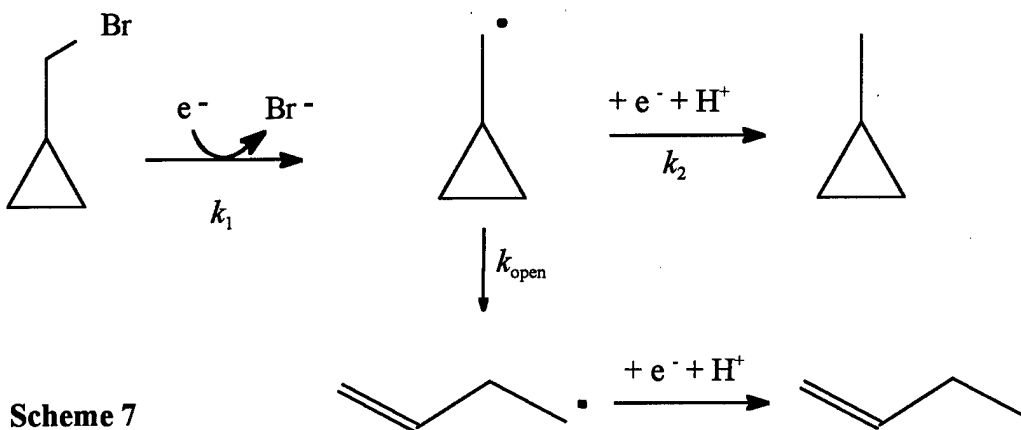
Outer- or inner-sphere SET to 6-bromo-1-hexene would yield the 5-hexenyl radical (Scheme 6), which may cyclize irreversibly ( $k_{cyc} = 2.2 \times 10^5 \text{ s}^{-1}$  at 25°C in water; Bakac and Espenson, 1986; Chatgililoglu *et al.*, 1981) before being further reduced to methylcyclopentane. This cyclization competes with reduction to 1-hexene.



In essence, the double bond acts as a radical trap. Because this trapping is an intramolecular process, it does not rely on the collision of the radical with another species and occurs with extremely high efficiency.

Likewise, SET to BrMCP would yield the cyclopropylmethyl radical, which may be reduced directly to methylcyclopropane, or which may undergo an extremely fast ring-opening isomerization ( $k_{open} \sim 2 \times 10^8 \text{ s}^{-1}$  at 25°C; Maillard *et al.*, 1976) to form the 3-butenyl radical, which may then be reduced to 1-butene (Scheme 7).

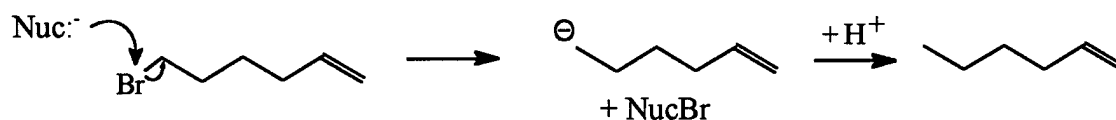




**Scheme 7**

The ratio of rearranged to unrearranged products in these reactions depends in theory only on the ratio of  $k_2$  to  $k_{cyc}$  or to  $k_{open}$ . Since the rate constants for these ring closing and ring opening reactions are well known,  $k_2$  can in principle be readily calculated from the product ratio.

In contrast, the reduction of alkyl halides such as these radical clocks may occur via “two-electron transfer”. This phrase is somewhat misleading, however, because electrons can only be transferred one at a time (Pross, 1985). Products characteristic of a two-electron transfer may arise either from an SET mechanism in which the transfer of the second electron is much faster than rearrangement of the radical, or from an inner-sphere (nucleophilic) attack of the reductant on the dihalide. Thus while SET may occur via either an inner- or outer-sphere mechanism, “two-electron transfer” is necessarily an inner-sphere process. Nucleophilic reduction of 6-bromo-1-hexene might yield a carbanion, which would be quickly protonated in aqueous solution (Scheme 8).



**Scheme 8**

In this mechanism, no rearrangement of the intermediate would be expected and thus no methylcyclopentane should be formed during the reaction of 6-bromo-1-hexene. Unfortunately, the cyclopropyl ring is so unstable that it can open rapidly via several mechanisms which involve carbanions and intermediates other than free radicals (Alnajjar *et al.*, 1984). For this reason, experiments with BrMCP were conducted primarily to qualitatively corroborate the results obtained from the 6-bromo-1-hexene experiments.

The purpose of these experiments was thus to employ radical clocks to attempt to determine whether free radicals are formed during the reduction of alkyl halides by zero-valent metals in aqueous solution at circum-neutral pH. If evidence of the intermediacy of radicals were found, these experiments would also allow an estimate of their lifetime and the rate at which they are reduced to final products. The lifetime of the radicals can suggest whether they are likely to build up to a sufficient steady-state concentration that free radical reactions are likely to be important in determining the product distribution in zero-valent metal-based remediation schemes. These experiments may also reveal differences in the mechanisms of the reduction of alkyl halides promoted by iron and by zinc metal which may help to explain why coupling products are frequently detected from the reduction of alkyl halides by iron but are less frequently encountered in reductions promoted by zinc.

## C. EXPERIMENTAL SECTION

### 1. Reagents

All chemicals were obtained from commercial sources and were used as received (98% pure or better), except methylcyclopropane, which was synthesized by reaction of 1,3-dibromobutane with zinc dust in boiling isopropanol (Demjanoff, 1895). Methylcyclopropane was collected as a gas in a syringe which pierced the septum sealing the reactor. The identity of the product was verified by proton nuclear magnetic resonance (H-NMR) analysis (Renk *et al.*, 1961) (Figure 23). A portion of the gas was bubbled through a milliliter of  $\text{CDCl}_3$  in a sealed autosampler vial, and the  $\text{CDCl}_3$  sample was then used to collect the H-NMR spectrum, which was recorded on a 400 MHz UNITYplus instrument. Product identity was also confirmed by combined gas chromatographic (GC)-mass spectral (MS) analysis (Figure 24), using the same column and temperature program used for analysis of headspace samples in the BrMCP reactions (described below).

### 2. Preparation of Metals

Both iron and zinc were cleaned prior to use as described in the previous chapter. Iron (Fisher electrolytic, 100 mesh, 95.3%) was washed with 1 N HCl for 2 minutes. Zinc (Baker, 30 mesh, 100.5%) was washed with 0.4%  $\text{H}_2\text{SO}_4$  for 10 minutes. Both metals were then rinsed with

OBSERVE H1  
FREQUENCY 399.958 Hz  
SPECTRAL WIDTH 3.744 sec  
Acq. time 3.744 sec  
Relaxation Delay 8.550 sec  
Pulse Width 7.0 sec  
No. Repetitions 64  
Double Precision Acquisition  
DATA PROCESSING  
FT size 65536  
total acquisition time 4 minutes

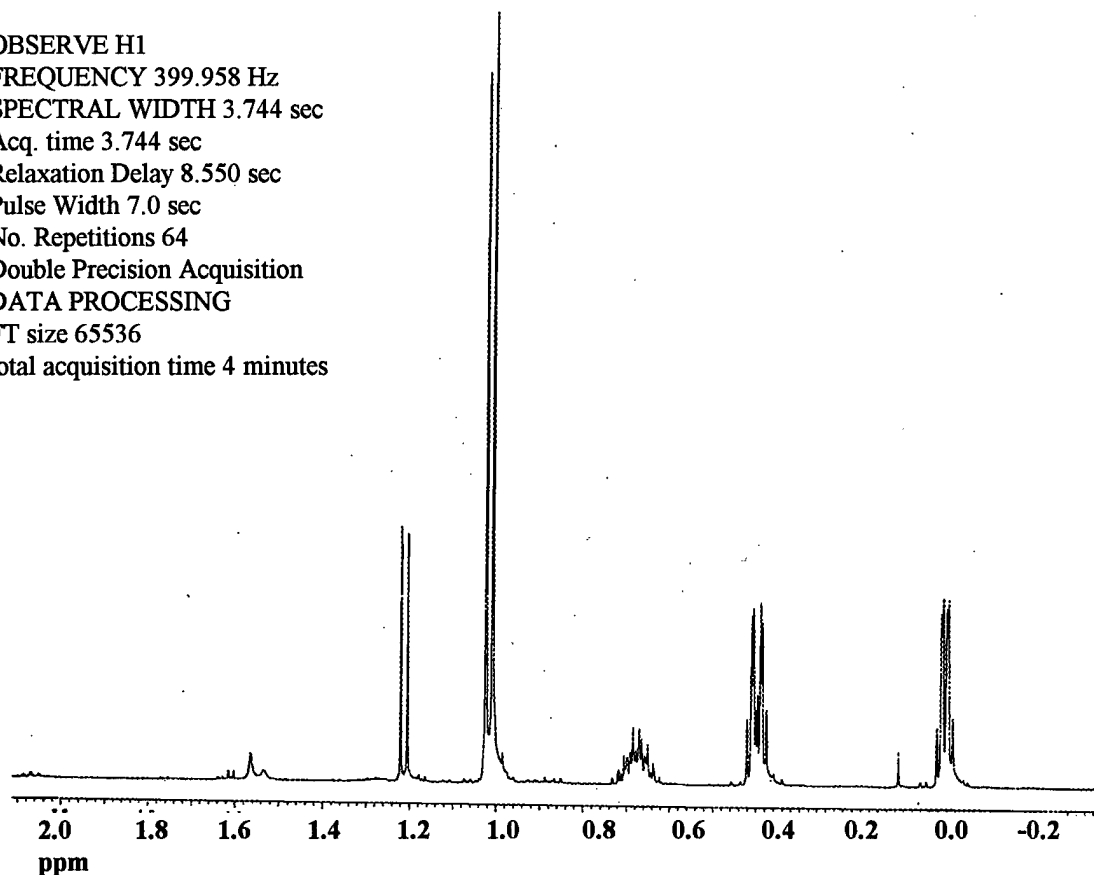


**Figure 23:**  $^1\text{H}$ -NMR spectrum of methylcyclopropane conducted on UNITYplus 400 MHz NMR in  $\text{CDCl}_3$ . Major peak shifts: 1.024, 1.009, 0.421, 0.411, 0.407, 0.401, 0.397, 0.391, 0.386, 0.376, -0.017, -0.027, -0.031, -0.039, -0.042, and -0.053 ppm. Peaks appearing near 1.2 ppm are attributed to isopropanol contamination.

deoxygenated water and acetone and dried at  $100^\circ\text{C}$  under argon. In order to minimize reoxidation of the metal surfaces, all cleaning procedures were conducted in an anaerobic glove box (90%  $\text{N}_2$ , 10%  $\text{H}_2$ ). Surface area analyses were conducted via Kr or  $\text{N}_2$  BET adsorption using a Micromeritics Flowsorb II 2300 device. The specific surface area of the iron was  $0.76 \text{ m}^2 \text{ g}^{-1}$  ( $\text{N}_2$ ) and that of the zinc was  $0.035 \text{ m}^2 \text{ g}^{-1}$  (Kr).

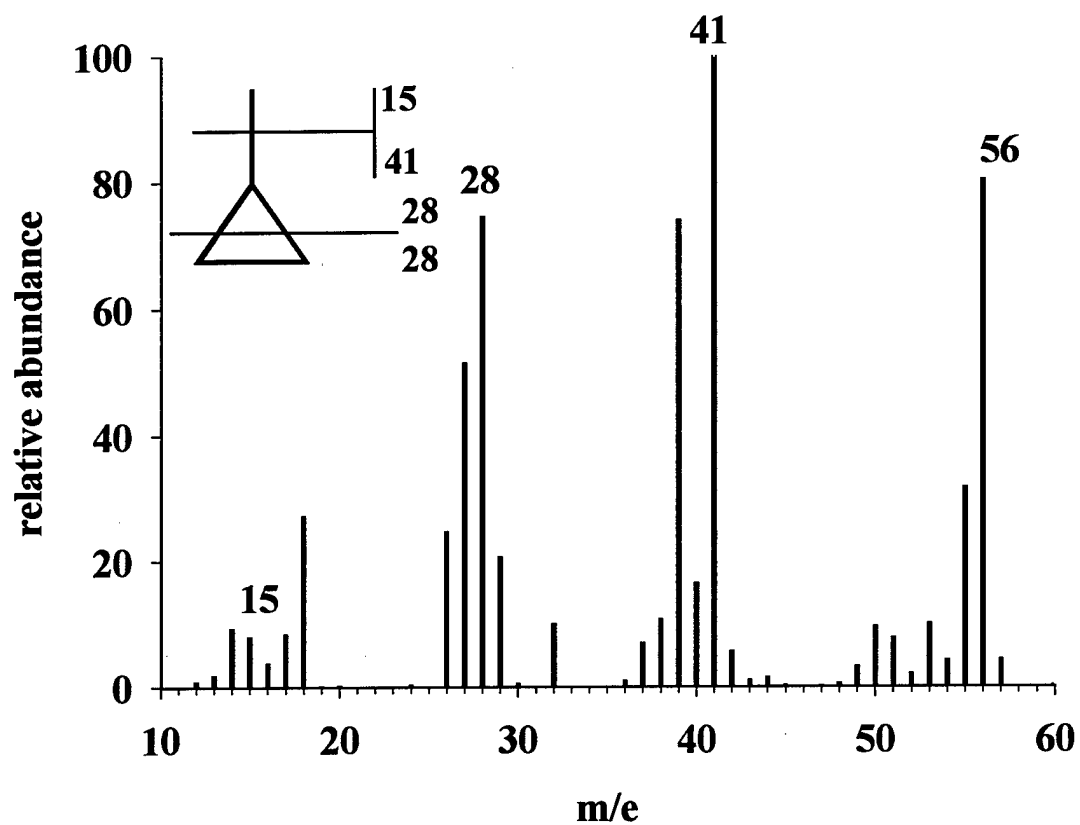


**Figure 24:** GC-MS spectrum of methylcyclopropane [parent ion ( $M^+$ ): 56] recorded under electron impact (EI) ionization on a Hewlett-Packard (HP) 5890 GC equipped with an HP 5970 mass spectrometer detector. Scans recorded across a mass range of 10-60 atomic mass units.

### 3. Reactions of 6-Bromo-1-hexene

Reactions were conducted in 150-mL serum bottles. Reactors were prepared and sampled in the glove box. Bottles were filled with deoxygenated 0.1 M NaCl/50 mM tris(hydroxymethyl)aminomethane (Tris) buffer (pH 8.0 unless otherwise noted), and were sealed with Teflon-faced butyl-rubber septa. Each bottle was spiked with a methanolic solution of 6-bromo-1-hexene to give an initial aqueous concentration of about 0.1 mM (experiments conducted without headspace) or 0.25 mM (experiments conducted in the presence of headspace). Reactors were mixed at 80 RPM on a roller table in a 22°C constant temperature room. Metal loading varied from 1 to 20 g.

For zero-headspace experiments, samples (1 mL) were taken without introducing headspace by simultaneously injecting deoxygenated reaction medium. Samples were expelled into 2.6 mL autosampler vials, which were immediately crimped and stored inverted until analysis. To aid in the detection of trace products, some experiments were conducted in the presence of 1.0 mL of headspace, which was introduced into each bottle via a gas-tight syringe. Atmosphere from the glove box was used as headspace to minimize introduction of oxygen into the system. Gas samples (200  $\mu$ L) were removed directly from this headspace at each sampling point. Fe(0) evolved enough H<sub>2</sub>(g) to compensate for the loss of gas due to sampling. Zn(0) evolved less hydrogen, so gas samples were withdrawn in the glove box and then the system was vented with a needle to equalize the pressure inside the bottle with the glove box atmosphere.

Headspace samples (200  $\mu$ L) were injected manually via a gas-tight syringe into a splitless injector (150°C) on a Carlo-Erba Series 8000 gas chromatograph (GC) equipped with a 30 m, 0.32 mm i.d., 3  $\mu$ m film thickness Rtx-1 (Restek Corp.) column and a flame ionization detector (FID). The temperature program was: 40°C isothermal for 10 minutes, ramp 20°C per minute to 240°C. Typical standard and sample chromatograms for reactions of 6-bromo-1-hexene are shown in Figures 25, 26, and 27. The Henry's law constant ( $K_H$ ) for each compound was measured (McAullife, 1971) and was used to calculate aqueous concentrations (Table 5).

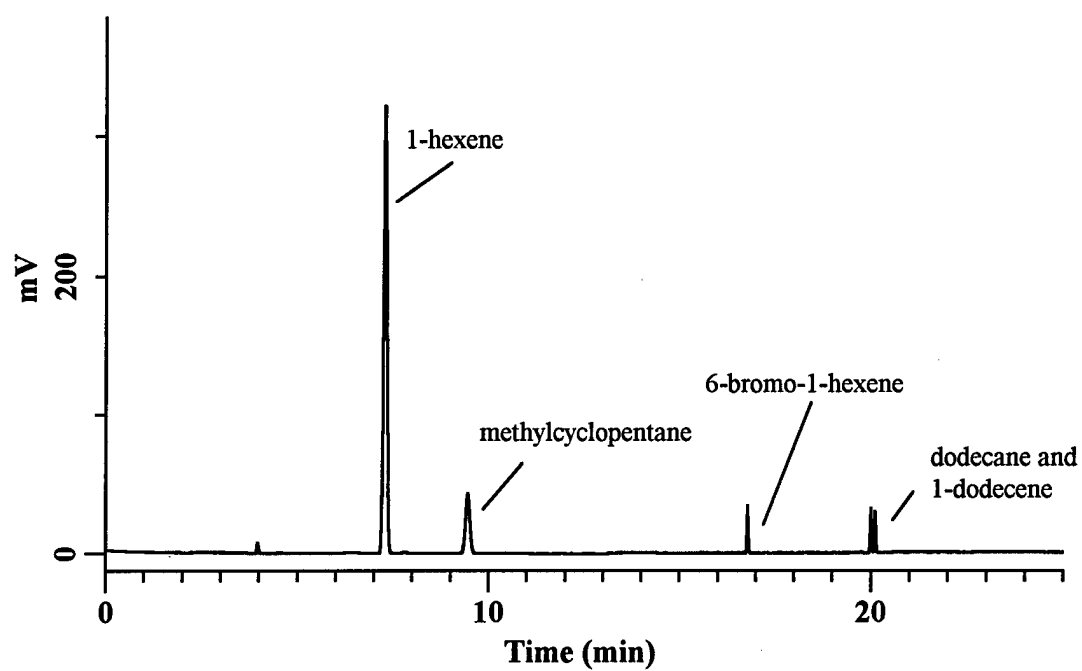


**Figure 25:** Chromatogram of standards used to quantify products encountered in the reaction of 6-bromo-1-hexene with zero-valent metals.

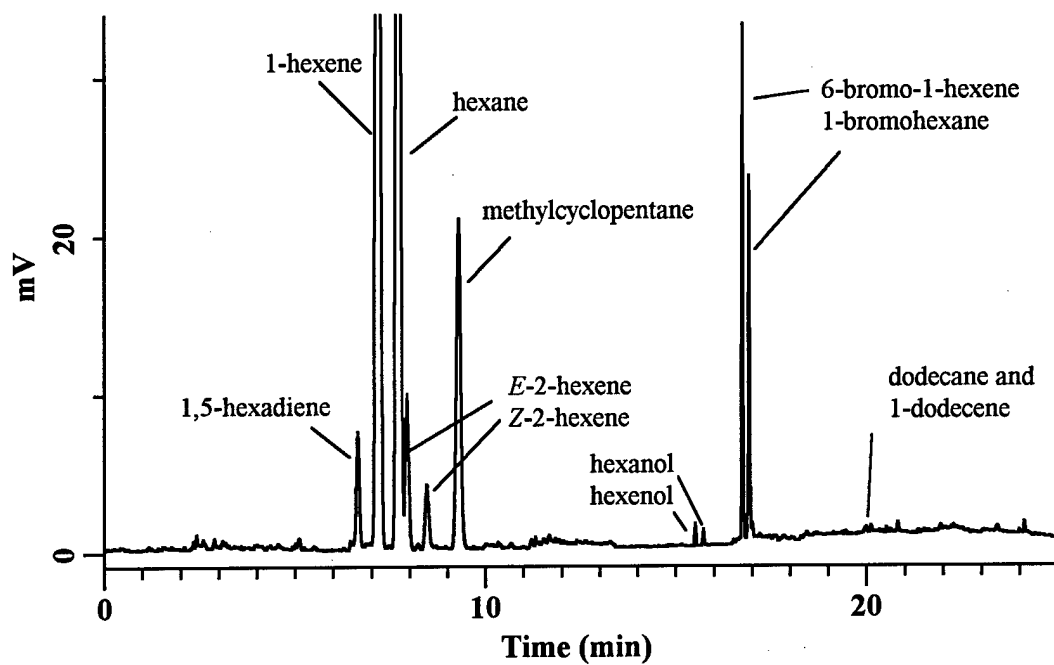


**Figure 26:** Chromatogram showing products 8 days after spiking 6-bromo-1-hexene into reactor (150 mL) containing 10 g Fe(0).

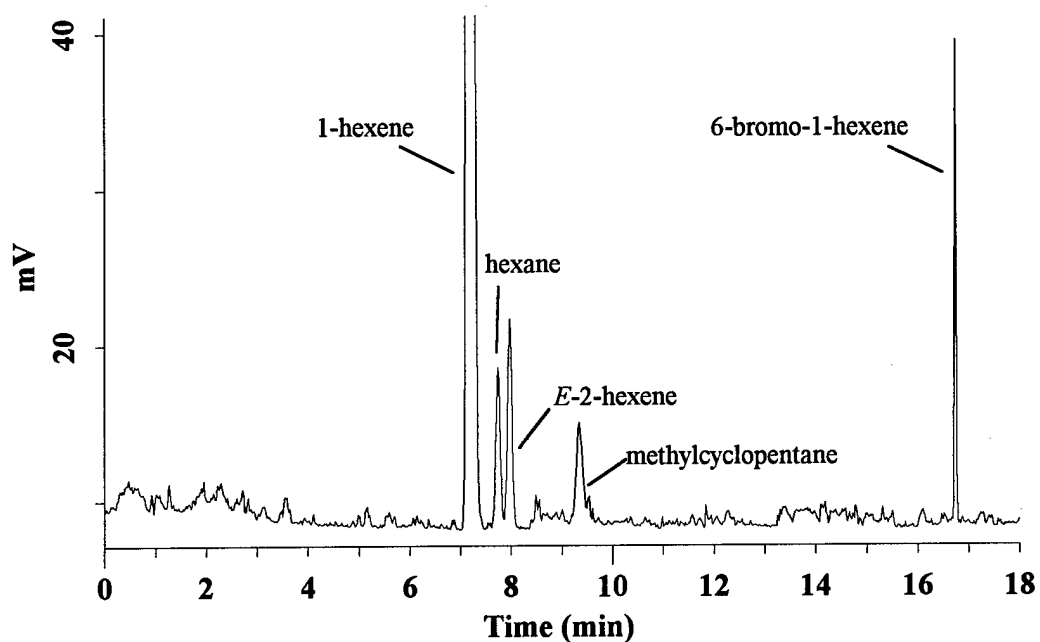


**Figure 27:** Chromatogram showing products 3 hours after spiking 6-bromo-1-hexene into reactor (150 mL) containing 2 g Zn(0).

**TABLE 5: HENRY'S LAW CONSTANTS ( $K_H$ ) FOR THE RADICAL CLOCKS AND THEIR PRODUCTS MEASURED BY THE METHOD OF MCAULLIFE (1971).**

Compound	$K_H \left( \frac{\text{mol/L}_{\text{air}}}{\text{mol/L}_{\text{water}}} \right)$
6-bromo-1-hexene	0.416
1-bromohexane	0.657
methylcyclopentane	10.5
1-hexene	13.1
hexane	56.4
1,5-hexadiene	5.66
E-2-hexene	9.45
Z-2-hexene	12.8
methylcyclopropane	8.45
1-butene	11.1
C <sub>4</sub> H <sub>8</sub> product (cyclobutane?)	7.21



#### 4. Reactions with BrMCP

BrMCP rapidly solvolyzes in polar solvents such as water and methanol, reacting to form several alcohols and the rearrangement product, 4-bromo-1-butene (Caserio *et al.*, 1960). This instability severely limited the quality of the information to be gained from these experiments, and necessitated new experimental methods. Experiments were performed in 150-mL serum bottles containing 20 g of zinc or iron in 50 mM Tris/0.1 M NaCl solution (pH 8). The bottles were spiked with 150  $\mu$ L of a solution of BrMCP in tetrahydrofuran (THF). To determine the kinetics of the disappearance of BrMCP, zero-headspace experiments were conducted. Aqueous samples (1 mL) were taken without introducing headspace as described above, and were extracted into 1 mL of hexane. This treatment quenched the reactions of BrMCP with both water and metal.

Hexane extracts (1  $\mu$ L) were injected on the same GC system used for bromohexene analysis. The temperature program was 40°C isothermal for 3 minutes, ramp 20°C per minute to 200°C. Quantitation of BrMCP was accomplished with external standards.

Because of the difficulty associated with preparing accurate standards of gaseous products in hexane and the rapidity of the reaction of BrMCP (relative to the duration of GC runs), changes in product yield over time could not be investigated. The final product distribution was quantified in a separate analysis in which 1 mL of headspace was introduced into each bottle before spiking with BrMCP. The bottles were then mixed on a shaker table for 30 minutes (long enough for the BrMCP to have reacted completely) and a single 50  $\mu$ L headspace sample was taken from each bottle and injected on the GC system previously described using the same temperature program. Typical chromatograms are shown in Figures 28 and 29.

Quantitation was accomplished by using a 1-butene gas standard (Scott Specialty Gases). The FID response factor of methylcyclopropane was assumed to be the same as that of 1-butene. In order to convert peak areas to aqueous concentration, the Henry's law constants for 1-butene and methylcyclopropane were measured via a multiple equilibration procedure that relies only on measuring changes in peak area (McAullife, 1971) (Table 5).

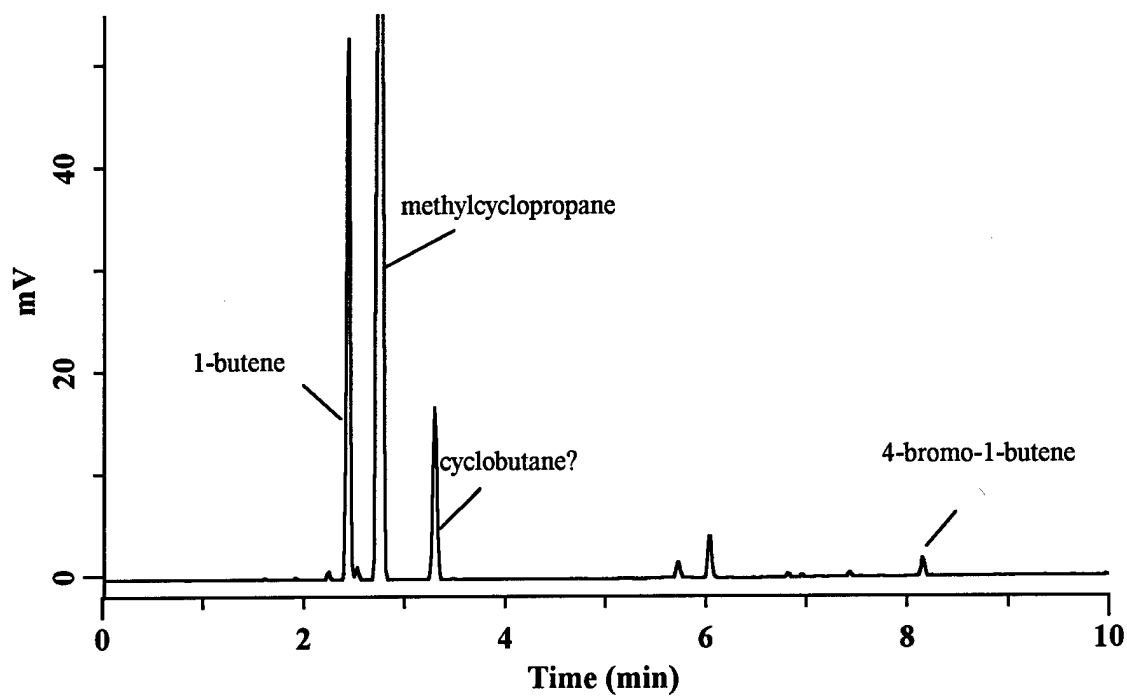


**Figure 28:** Chromatogram of reactor headspace showing products after 30 minutes of the reaction of BrMCP with 20 g Zn(0). Unidentified peaks represent unknown products of the reaction.

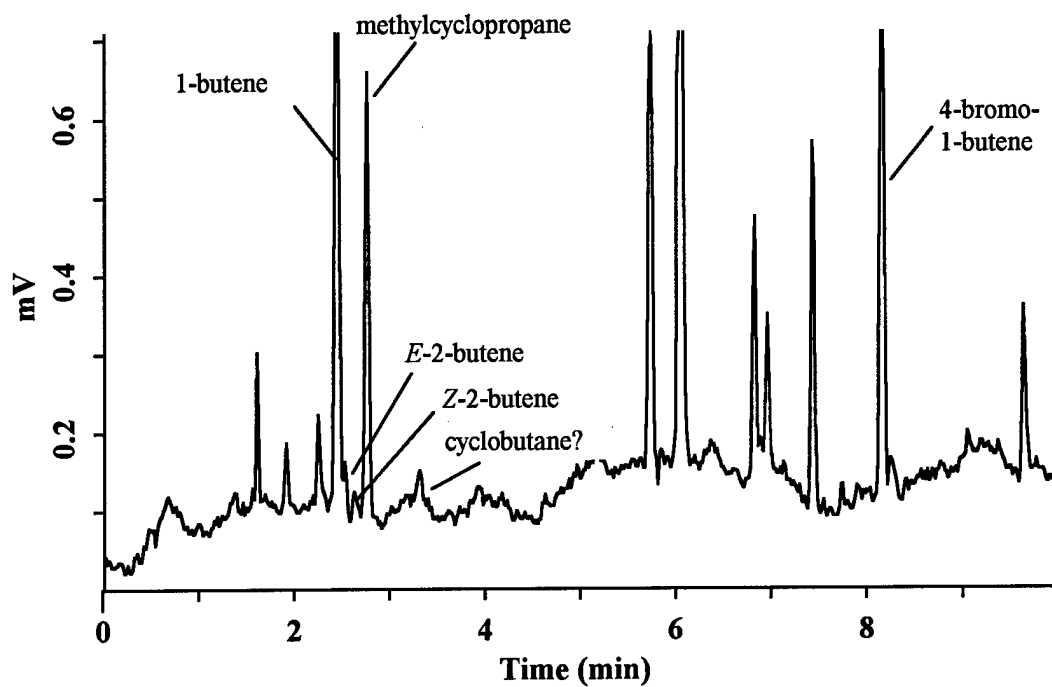


**Figure 29:** Chromatogram of reactor headspace showing products after 30 minutes of the reaction of BrMCP with 20 g Fe(0). Unidentified peaks represent unknown products of the reaction.

## 5. GC-MS Analysis

Combined gas chromatographic/mass spectral (GC-MS) analysis was conducted for both headspace samples and hexane extracts under electron impact (EI) ionization on a Hewlett-Packard (HP) 5890 GC equipped with an HP 5970 mass spectrometer detector. The GC column and injector configuration for GC-MS analysis were the same as those used for GC analysis with flame ionization detection.

## 6. Kinetic Modeling

Due to the complexity of reactions of 6-bromo-1-hexene with iron, selected timecourses for these reactions were modeled using the software package *Scientist for Windows* (v. 2.01, Micromath, Salt Lake City, UT). This program calculates the pseudo-first order rate constants based on a system of differential equations:

$$\frac{dC_i}{dt} = -\left(\sum_{j=1}^{N_j} k_{ij}\right)C_i = -k_{obs}C_i \quad (8)$$

$$\frac{dC_j}{dt} = \left(\sum_{i=1}^{N_i} k_{ij}\right)C_i - \left(\sum_{m=1}^{N_m} k_{jm}\right)C_j \quad (\text{for all } j) \quad (9)$$

where  $C$  represents aqueous concentrations and  $k$  values are pseudo-first order rate constants. Equation 8 pertains to the reaction of the parent species,  $i$ , forming all possible daughter products,  $j$ . In equation 9, the daughter product,  $j$ , may be produced by multiple parents,  $i$ , and can itself react to other species,  $m$ , according to rate constants  $k_{jm}$ .

Given the experimental data, differential rate expressions, and initial conditions, *Scientist* calculates the selected parameters (in this case,  $k_{ij}$  and the initial concentration of the parent compound) via a least squares fit of the data to numerically integrated solutions of the system of rate expressions. By computing each  $k_{ij}$  value according to the distribution of products, the model apportions the overall rate constant for parent compound disappearance into the contributions for the competing reactions. When calculating the  $k_{ij}$  values for a given species, the rate constants ( $k_{jm}$ ) for reactions of daughter products that were detected in a given experiment were constrained to be equal to those determined in independent experiments in which the daughter products were introduced as the starting material.

## D. RESULTS

### 1. Hydrolysis of Radical Clocks

As with the stereochemical probes used in the previous section, hydrolysis represents a primary limitation associated with the use of radical clocks in aqueous solution. Reactions with zinc were sufficiently fast that hydrolysis was negligible. In contrast, reaction with iron was slow enough that hydrolysis accounted for a major portion of the overall disappearance of 6-bromo-1-hexene. Reduction of this compound by less reactive metals, such as copper, was simply too slow to compete with hydrolysis.

The hydrolysis half-life of 6-bromo-1-hexene was 16 days ( $k = 0.0018 \text{ hr}^{-1}$ ) in Tris buffer at pH 8.5 (Figure 30). Hydrolysis of the vicinal dibromide probe compounds was substantially faster; the half-lives of *threo*-2,3-dibromopentane and ( $\pm$ )-stilbene dibromide with respect to hydrolysis were 5 days and 4 hours, respectively. The hydrolysis experiments were conducted at pH 8.5 because this was roughly the pH attained by the iron systems over the course of each experiment. Because 1-bromohexane was produced during the reaction of 6-bromo-1-hexene with iron, its rate of hydrolysis was also measured and found to be essentially the same as that of 6-bromo-1-hexene ( $k = 0.0018 \text{ hr}^{-1}$ ). The resulting alcohol products could not be adequately quantified by the headspace methods employed because their Henry's law constants were very low.

Bromohexane hydrolyzed to 1-hexanol, but the hydrolysis product of 6-bromo-1-hexene was difficult to identify. Although its retention time (15.5 min.) was similar to that of authentic 5-hexen-1-ol (15.7 min.), its mass spectrum (Figure 31) was sufficiently different from that of 5-hexen-1-ol (Figure 32) to suggest these two are different compounds. Many other hexenol and cyclopentanol isomers were eliminated as possible hydrolysis products based on mass spectrum and retention time. No dehydrobromination of 1-bromohexane or 6-bromo-1-hexene (to form 1-hexene or 1,5-hexadiene) was observed during hydrolysis in the absence of metals.

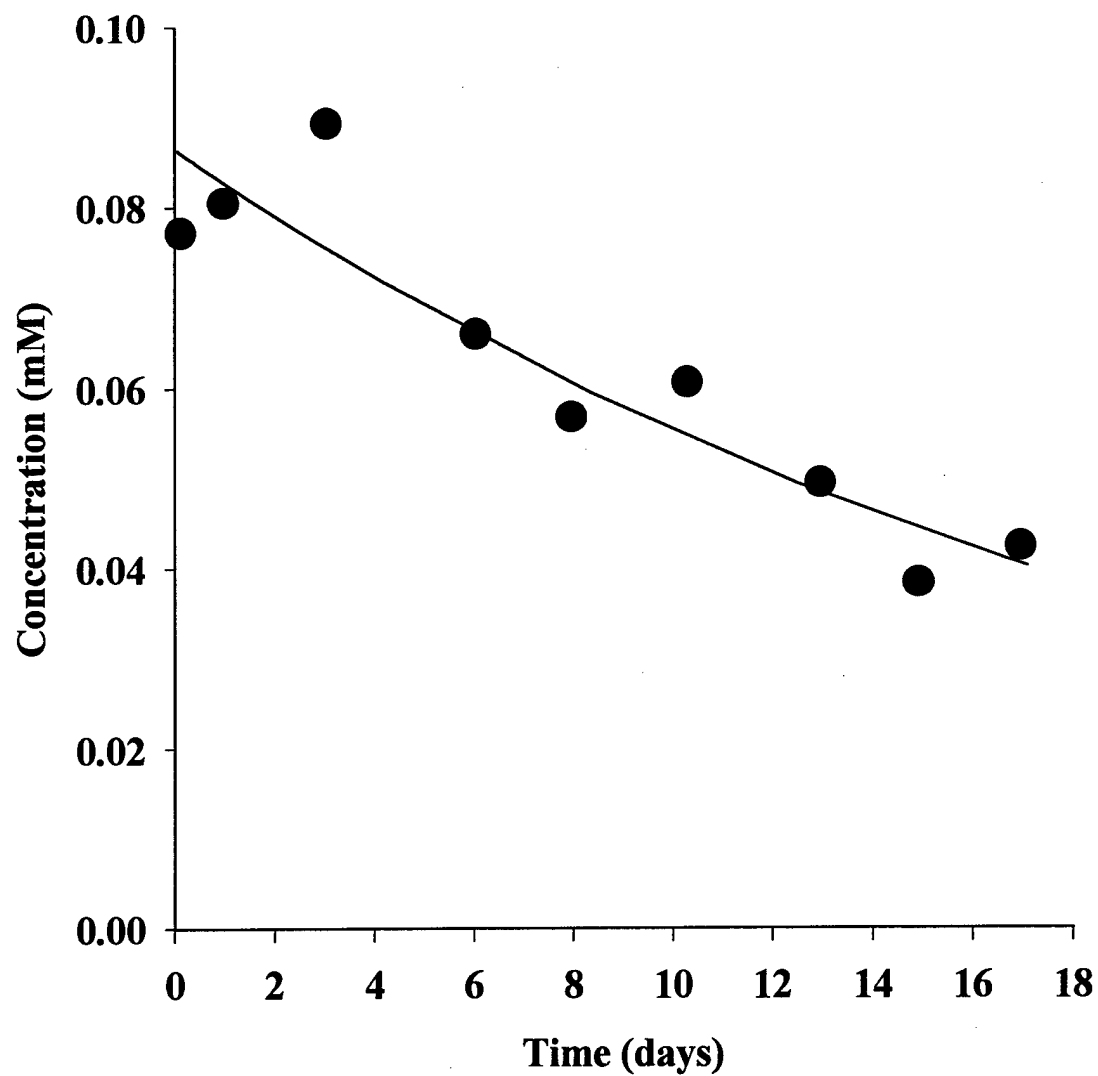


**Figure 30:** Hydrolysis of 6-bromo-1-hexene (●) at pH 8.5 in 50 mM Tris/0.1 M NaCl at 22°C.

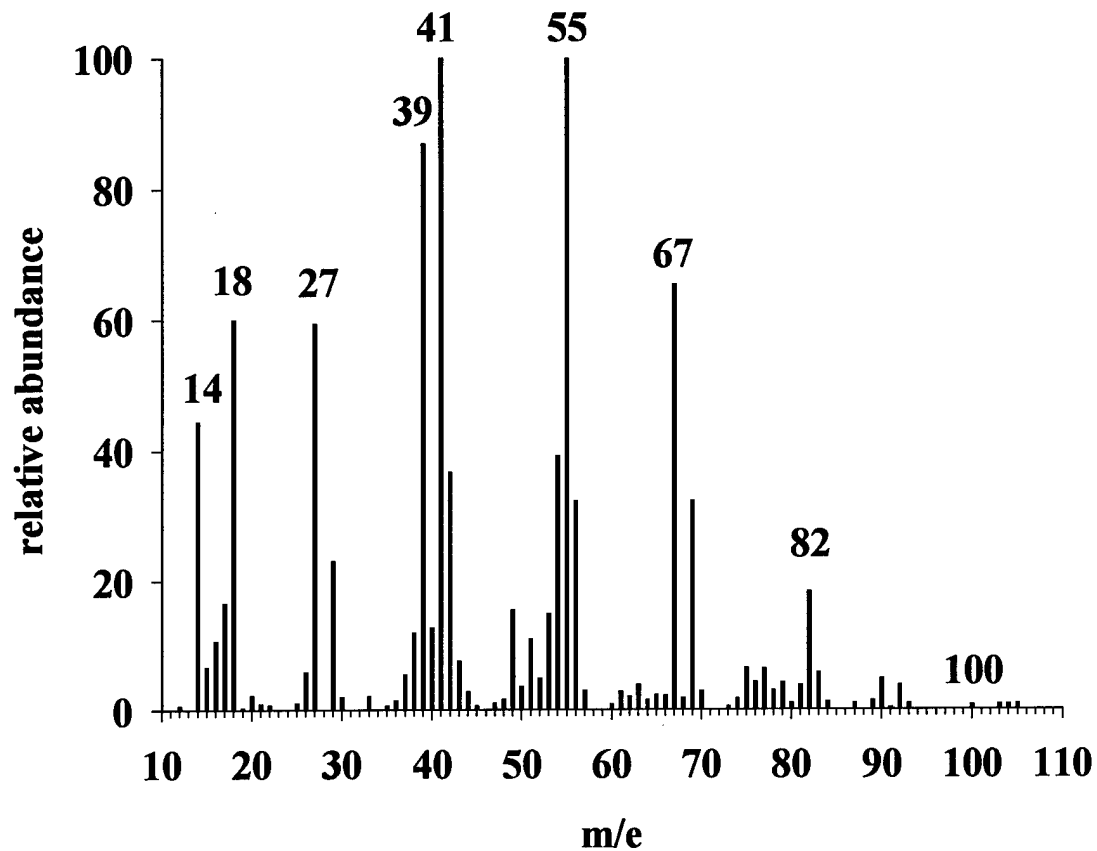


**Figure 31:** GC-MS spectrum of the hydrolysis product of 6-bromo-1-hexene recorded under electron impact (EI) ionization on a Hewlett-Packard (HP) 5890 GC equipped with an HP 5970 mass spectrometer detector. Scans recorded across a mass range of 10-110 atomic mass units.

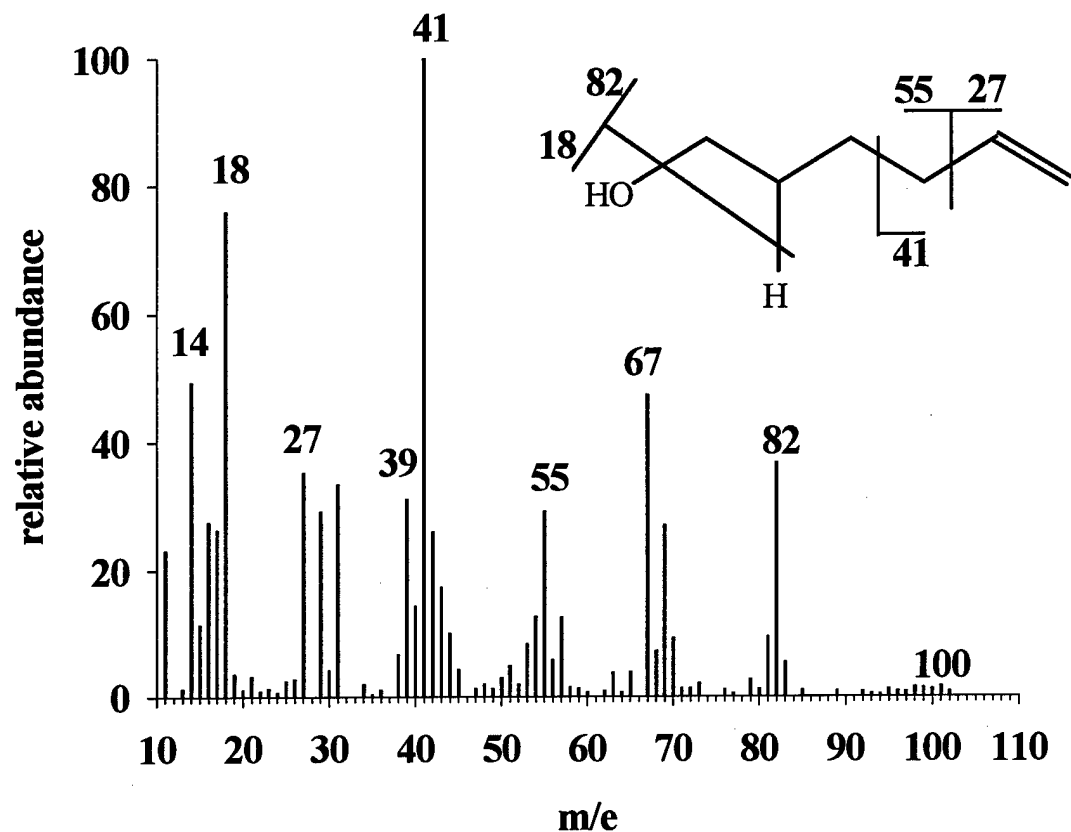


**Figure 32:** GC-MS spectrum of authentic 5-hexen-1-ol recorded under electron impact (EI) ionization on a Hewlett-Packard (HP) 5890 GC equipped with an HP 5970 mass spectrometer detector. Scans recorded across a mass range of 10-110 atomic mass units. Major differences in the relative abundances of peaks at  $m/e = 27, 39, 55, 67,$  and  $82$  suggest that this compound is not the product of the hydrolysis of 6-bromo-1-hexene (see Figure 31).



Solvolysis is especially problematic for BrMCP ( $k = 0.0032 \text{ s}^{-1}$ , corresponding to a half life of about 4 minutes at pH 8 in Tris buffer, Figure 33). In addition, solvolysis of BrMCP involves not only displacement of bromide by the solvent, but also rearrangement of the parent compound to form 4-bromo-1-butene (Caserio *et al.*, 1960). About 25% of the BrMCP rearranged via this pathway.

## **2. Reaction of 6-Bromo-1-hexene with Zinc**

Reduction of 6-bromo-1-hexene by zinc was rapid relative to hydrolysis, with a half-life in the presence of 2 g of zinc of about 5 hours. The pH of the buffer solution remained stable at 8.0. The distribution of hydrocarbon products was quite simple (Figure 34), and mass balances were close to 100%. Methylcyclopentane and 1-hexene were the major products and were found to be stable under the reaction conditions. No  $\text{C}_{12}$  products were detected. Two other products (<0.5% mass balance) were detected. The retention times of these products match those of authentic standards of hexane and 2-hexene, but the sensitivity of the GC-MS instrument used to analyze the samples was insufficient to provide confirmation of their identity.

The 6-bromo-1-hexene as received from Aldrich contained two impurity peaks (comprising about 1% each based on GC peak areas) which exhibited mass spectra consistent with  $\text{C}_6\text{H}_{11}\text{Br}$  and  $\text{C}_6\text{H}_{13}\text{Br}$  isomers. Thus it is possible that the trace products arose from reduction of these impurities and not from 6-bromo-1-hexene.

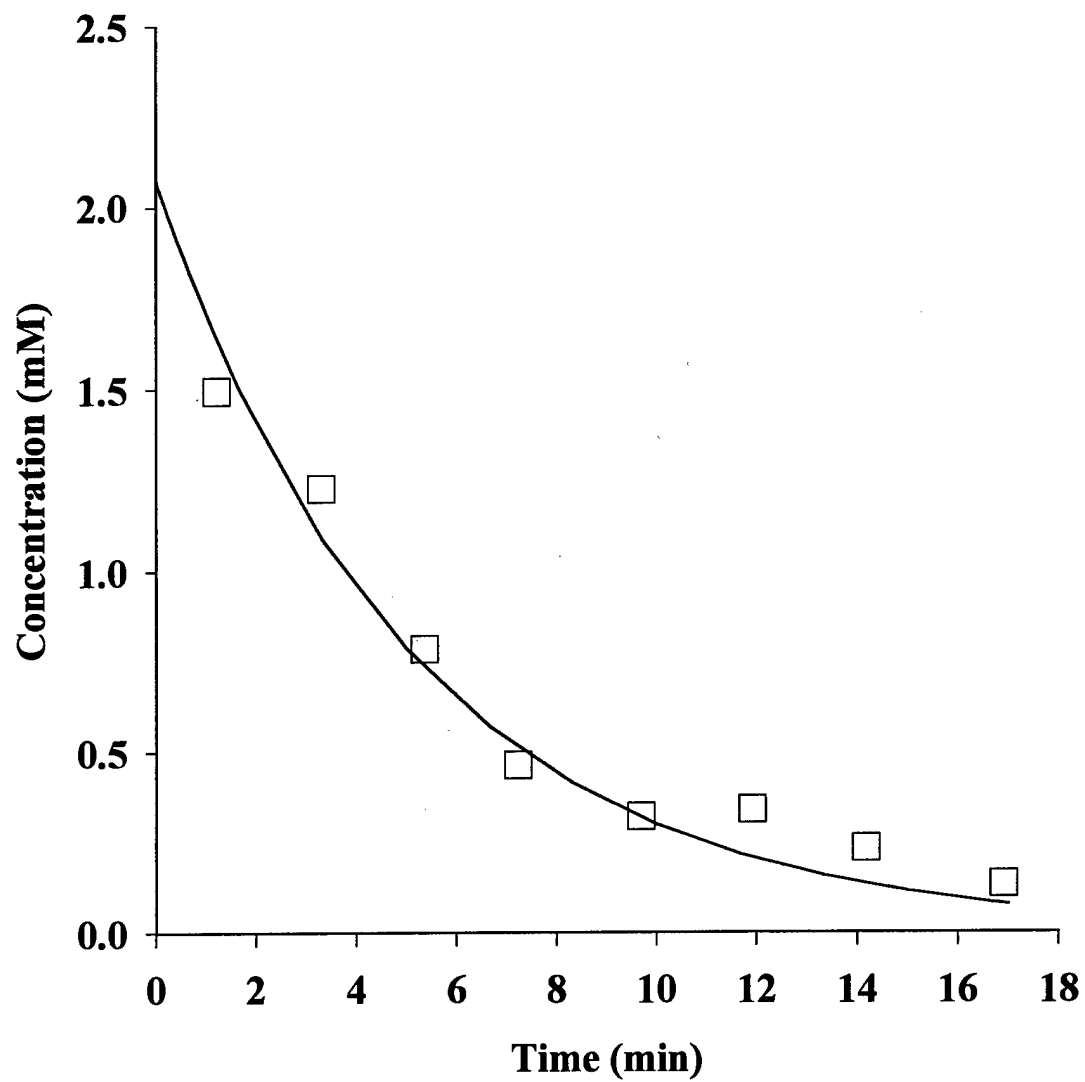


**Figure 33:** Solvolysis of bromomethylcyclopropane (□) at pH 8 in 50 mM Tris/0.1 M NaCl.

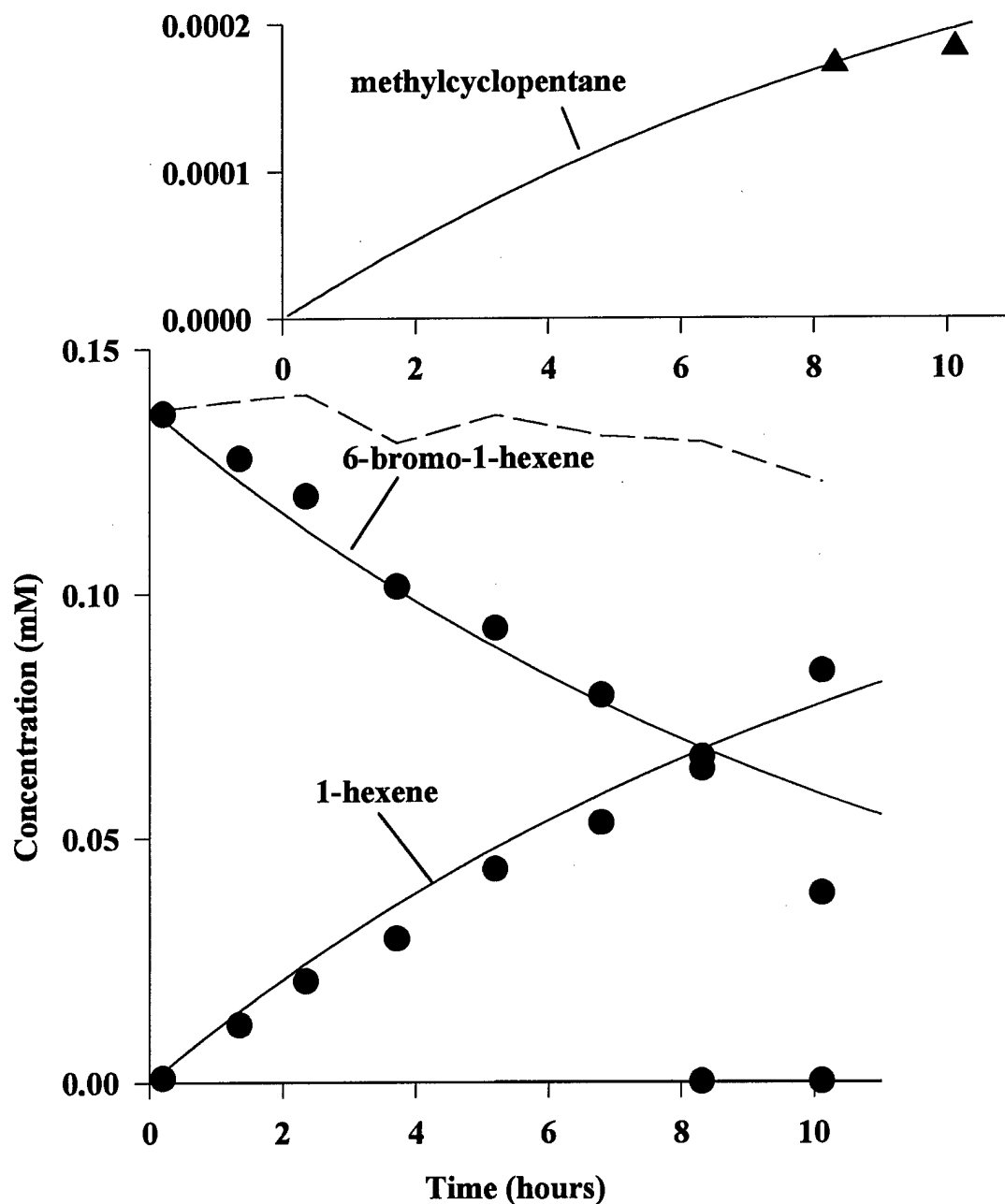


**Figure 34:** Reaction of 6-bromo-1-hexene (●) in 160 mL 0.1 M NaCl/50 mM Tris (pH 8) at 22°C (zero headspace) and 2 g zinc (0.47 m<sup>2</sup>/L). Symbols represent measured concentrations of all species. Solid lines represent model simulations of the data; dashed line represents calculated mass balance. Products are 1-hexene (■) and methylcyclopentane (▲). Detection limit for methylcyclopentane was about 0.00015 mM by this (zero headspace) method.

In order to ensure that methylcyclopentane did not arise from a possible bromomethylcyclopentane impurity in the starting material, a sample of the 6-bromo-1-hexene as received was reacted with an excess of pyridinium bromide perbromide, which should brominate any compounds containing double bonds. Gas chromatography revealed only one peak remaining in the window of retention time expected for  $C_6H_{11}Br$  and  $C_6H_{13}Br$  isomers. This peak exhibited a mass spectrum and retention time consistent with authentic 1-bromohexane. If bromomethylcyclopentane were one of the impurities, it should continue to appear in the chromatograms after this treatment, just as bromohexane did. Analysis of the brominated sample by GC-MS in selective ion monitoring mode did not detect any peaks with a major ion at  $m/e = 162$  (1-bromohexane displays molecular ion peaks at  $m/e = 164$  and  $166$ , while bromomethylcyclopentane should display molecular ion peaks at  $162$  and  $164$ ). Thus the methylcyclopentane obtained in the  $Zn(0)$  reaction appears to have originated from reduction of 6-bromo-1-hexene and not from reaction of some impurity in the starting material.

The ratio of methylcyclopentane and 1-hexene can be used to estimate  $k_2$  by equation 10, if it is assumed that methylcyclopentane arises from the cyclization of the 5-hexenyl radical and that the 5-hexenyl and methylcyclopentyl radicals are quantitatively reduced only to 1-hexene and methylcyclopentane (Newcomb and Curran, 1988).

$$\frac{k_2}{k_{cyc}} = \frac{[1\text{-hexene}]}{[\text{methylcyclopentane}]} \quad (10)$$

These assumptions may be reasonable for reactions of 6-bromo-1-hexene with zinc, since only two major products were obtained. Because the amount of methylcyclopentane produced was very close to the detection limit in the zero-headspace experiments, the ratio was calculated at each time point from the experiments conducted in the presence of headspace (Figure 35), for which the detection limit for methylcyclopentane was lower. This ratio yields an estimate of  $k_2$  for zinc of  $1.9 (\pm 0.3) \times 10^7 \text{ s}^{-1}$  at pH 8 (Table 6). A limited number of experiments suggests that  $k_2$  is faster at pH 7 and slower at pH 9, with the total increase in  $k_2$  being less than an order of magnitude. The rate of reduction of 6-bromo-1-hexene was also fastest at pH 7 and slowest at pH 9.

In order to assess whether the small amount of methylcyclopentane observed in these reactions might be an artifact of the sampling method, an experiment was performed in which

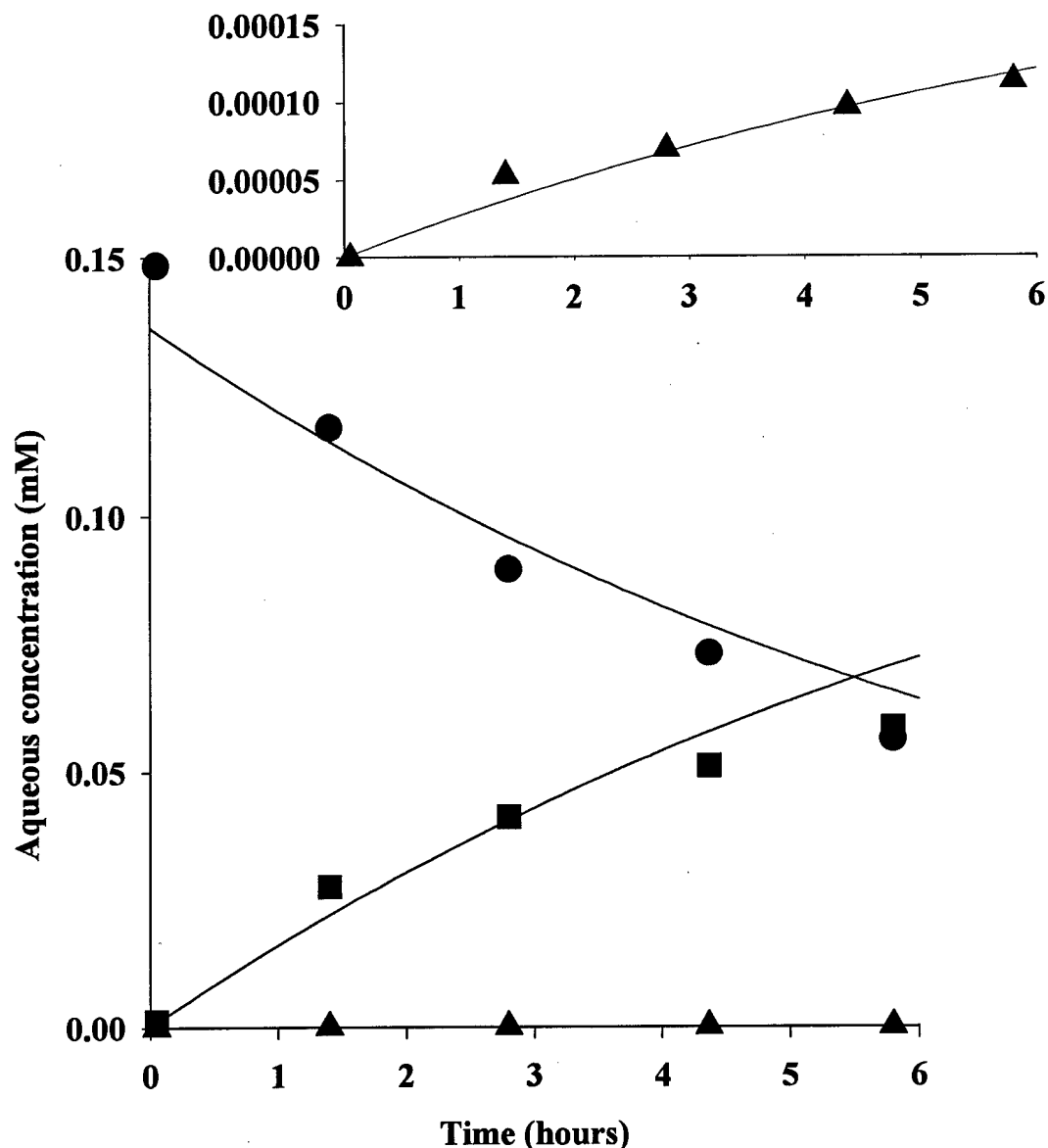


**Figure 35:** Reaction of 6-bromo-1-hexene (●) in 150 mL 0.1 M NaCl/50 mM Tris (pH 8) at 22°C (10 mL headspace) and 2 g zinc (0.47 m<sup>2</sup>/L). Symbols represent calculated aqueous concentrations (based on measured headspace concentration) of all species. Lines represent model simulations of the data. Products are 1-hexene (■) and methylcyclopentane (▲).

oxygen was deliberately introduced to the system, because it was hypothesized that oxygen might potentially initiate a free-radical process eventually resulting in a cyclized product. In this experiment, the 1.0 mL of headspace was introduced as regular air, and sampling was done outside of the glove box. The methylcyclopentane to 1-hexene ratio was not affected (Table 6).

**TABLE 6: ESTIMATES OF RATE CONSTANTS FOR SECOND ELECTRON TRANSFER BASED ON THE METHYLCYCLOPENTANE/1-HEXENE PRODUCT RATIOS OBSERVED IN THE REDUCTION OF 6-BROMO-1-HEXENE.**

Reductant <sup>a</sup>	$k_2$ (s <sup>-1</sup> ) <sup>b</sup>	n <sup>c</sup>
2 g zinc	$1.9 (\pm 0.3) \times 10^7$	1
2 g zinc (O <sub>2</sub> added) <sup>d</sup>	$1.6 (\pm 0.4) \times 10^7$	1
1 g iron, pH 8	$2.3 (\pm 0.4) \times 10^6$	1
0.5 g iron, pH 8	$1.7 (\pm 0.2) \times 10^6$	1
10 g iron, pH 7	$3.5 (\pm 0.2) \times 10^6$	1
10 g iron, pH 8	$1.7 (\pm 0.4) \times 10^6$	6
10 g iron, pH 8 <sup>e</sup>	$1.9 (\pm 0.3) \times 10^6$	5
10 g iron, pH 9	$4.0 (\pm 2.0) \times 10^6$	1
10 g iron, pH 8 (uncleaned)	$1.5 (\pm 0.1) \times 10^6$	1
10 g iron, pH 8 (O <sub>2</sub> added) <sup>d</sup>	$2.3 (\pm 0.8) \times 10^6$	1
10 g iron, pH 7 (Fe(II) added)	$3.7 (\pm 0.2) \times 10^6$	1

<sup>a</sup>In 160 mL of solution. <sup>b</sup>All uncertainties represent 95% confidence limits on replicate determinations. When only one experiment was performed, replicate determinations were performed by calculating  $k_2$  at each time point. <sup>c</sup>Number of experiments used to calculate  $k_2$ . <sup>d</sup>1.0 mL of air added to each bottle during reaction. <sup>e</sup>Calculated from *Scientist* model.

### 3. Reaction of BrMCP with Zn(0)

The pseudo-first order rate constant for disappearance of BrMCP in the presence of 20 g of zinc at pH 8 was 0.0059 s<sup>-1</sup>. Hydrolysis thus represented some 54% of the overall reaction. Methylcyclopropane was the primary product observed (24%), with much smaller amounts of 1-butene (3%) and one other C<sub>4</sub> hydrocarbon (2%) produced. The mass spectrum (Figure 36) of this latter product suggests that it has the molecular formula C<sub>4</sub>H<sub>8</sub>. Its retention time (3.3 minutes) did not match that of *Z*- or *E*-2-butene (2.5 and 2.6 minutes, respectively), or methylpropene (2.3 minutes), suggesting that it may be cyclobutane, which has a higher boiling point than these other C<sub>4</sub>H<sub>8</sub> isomers (Lide, 1991). Its K<sub>H</sub> value was measured (Table 5) and it was quantified by the same technique as methylcyclopropane. The C<sub>4</sub> products represented roughly 29% of the spiked mass of BrMCP, which suggests an overall mass balance of about 83% in these reactions, after correcting for hydrolysis.

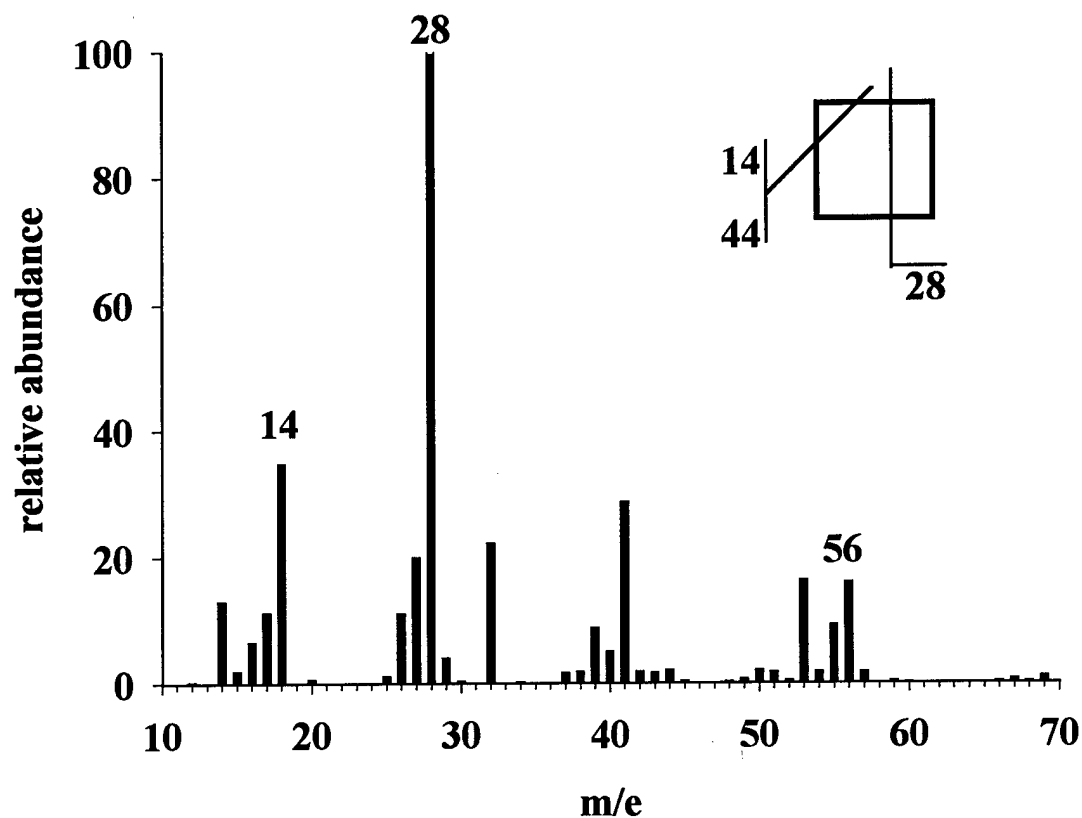


**Figure 36:** GC-MS of trace product (assumed to be cyclobutane) obtained in the reaction of BrMCP with 20 g of Zn(0). GC analysis was via injection of a headspace sample taken one hour after spiking BrMCP into the reactor. The spectrum was recorded under electron impact (EI) ionization on a Hewlett-Packard (HP) 5890 GC equipped with an HP 5970 mass spectrometer detector. Scans were recorded across a mass range of 10-70 atomic mass units.

Experiments at other zinc loadings demonstrated that as zinc loading increased from 1 to 20 g, the ratio of methylcyclopropane to 1-butene also increased from 3 to 8. Such increases might be anticipated, because at lower zinc loadings, BrMCP persists long enough to isomerize to 4-bromo-1-butene, which might undergo reduction to 1-butene. Control experiments employing 4-bromo-1-butene as the reactant demonstrate, however, that its reaction with zinc is about 10 times slower than that of BrMCP with zinc. Modeling of the data suggests that, given the slow rate of reaction of 4-bromo-1-butene with zinc, this pathway can account for no more than about 10% of the 1-butene formed, even at the lowest zinc loading of 1 g. Thus the increase in the methylcyclopropane/1-butene ratio with increasing zinc loading cannot be explained by the formation of 1-butene via the reaction of 4-bromo-1-butene with zinc.

If it is assumed that essentially all of the 1-butene formed arises from the opening of the methylcyclopropyl radical, an approximate estimate of the rate constant for the second electron transfer ( $k_2$ ) can again be based on the product ratio (Newcomb and Curran, 1988):

$$\frac{k_2}{k_{open}} = \frac{[\text{methylcyclopropane}]}{[1\text{-butene}]} \quad (11)$$

Zinc reduces BrMCP to methylcyclopropane and 1-butene in a ratio of about 8:1, which corresponds to a  $k_2$  of about  $10^9 \text{ s}^{-1}$ . This value is about 50 times faster than the value for  $k_2$  obtained in the 6-bromo-1-hexene experiments with Zn(0).



#### 4. Reactions of 6-Bromo-1-hexene with Iron

Reaction of 6-bromo-1-hexene with iron was generally slower than the reaction with zinc and displayed a much more complicated distribution of products (Figure 37). The half-life of 6-bromo-1-hexene in the presence of 10 g of iron was about 4 days. Hydrolysis of 6-bromo-1-hexene and 1-bromohexane (a reaction product) on this time scale was significant, and hydrogen evolution from the reduction of protons by the metal produced several milliliters of headspace in each bottle. Separating reaction with iron from volatilization into the hydrogen headspace was therefore difficult, especially for the more volatile reaction products. Despite the presence of 50 mM Tris buffer, the pH in these experiments typically drifted from 8 at the beginning to about 8.5 after several days of reaction.

In addition to the 1-hexene and methylcyclopentane products which were also observed during reduction by zinc, reaction of 6-bromo-1-hexene with iron produced 2-hexenes (*E* and *Z*), 1,5-hexadiene, hexane, 1-bromohexane, 1-dodecene, *n*-dodecane, and other  $C_{12}H_{24}$  and  $C_{12}H_{26}$  products. A few experiments conducted at pH 7 and 9 demonstrated that the yield of 1-bromohexane increased as pH decreased. In addition, significant amounts of hydrolysis products (the unidentified hexenol isomer and 1-hexanol) were formed. Most of the trace products (1-hexanol, *E*- and *Z*- 2-hexenes, 1,5-hexadiene, hexane, 1-bromohexane, 1-dodecene, and *n*-dodecane) were identified by comparison of retention time and mass spectra with those of authentic standards. Hexane co-eluted with 3-hexene isomers on the column employed. Therefore traces of 3-hexenes might also have been produced without being detected in this system.

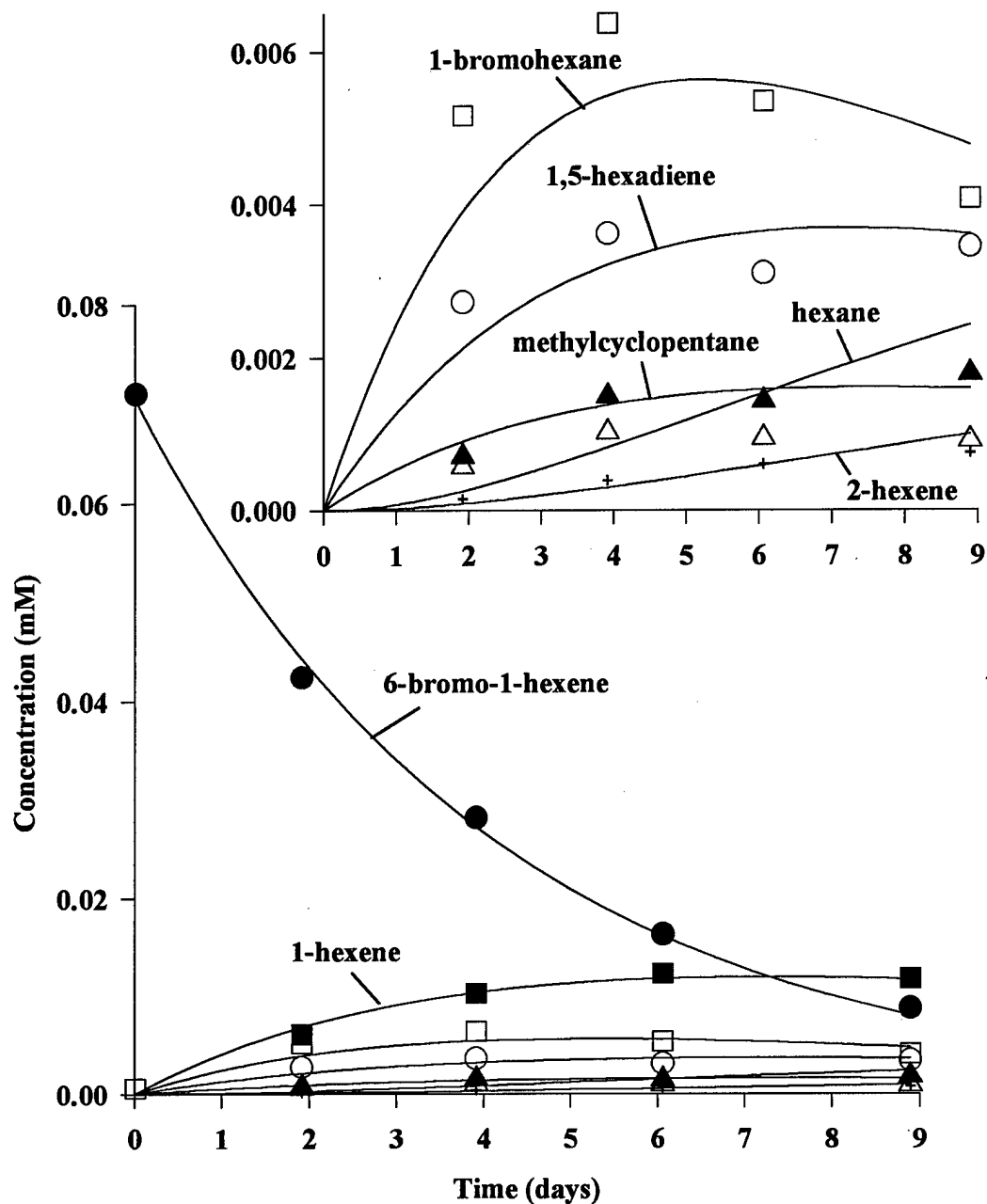


**Figure 37:** Reaction of 6-bromo-1-hexene in 150 mL 0.1 M NaCl/50 mM Tris (pH 8-8.5) at 22°C with 10 g Fe(0) (50.7 m<sup>2</sup>/L). Symbols represent measured concentrations of all quantified species. Lines represent model simulations of the data using experimentally determined rate constants (see text). Products are: 1-hexene (■); methylcyclopentane (▲); 1-bromohexane (□); 1,5-hexadiene (○); hexane (Δ); and 2-hexene (+).

The estimated amount of impurities in the starting material was insufficient to account for the mass of the additional C<sub>6</sub> products. The yield of methylcyclopentane in the iron system was roughly ten times greater than in the zinc system.

It should be noted that the aqueous solubility of *n*-dodecane and 1-dodecene are about 10<sup>-8</sup> and 10<sup>-6</sup> M, respectively (Mackay *et al.*, 1993). If these coupling products were to represent more than 0.01% (*n*-dodecane) to 1% (1-dodecene) of the total C<sub>6</sub> mass balance, they would be present above saturation and could begin to condense. Quantitation based on headspace analyses would underestimate product yields in such a case. In order to better quantify the yield of coupling products, a set of experiments was performed in which the entire reactor was extracted into 2 mL of hexane after the final timepoint and the hexane fraction was analyzed for C<sub>12</sub> products. These experiments demonstrated that coupling products accounted for only about 5% of the mass balance.

Despite efforts that were made to separately quantify all of these products, mass balances were incomplete for reactions of 6-bromo-1-hexene with iron. Although mass balances were typically 100% at the start of each timecourse, they decayed to as low as 40% after about 10 days of reaction. The discrepancy in the mass balance may have arisen in part from the difficulties encountered in quantifying the alcohol hydrolysis products. Such alcohols are difficult to quantify by the headspace analysis method employed because of their low Henry's law constants. Although every attempt was made to minimize volatilization losses, the significant amounts of hydrogen gas produced in these systems undoubtedly also contributed to the low mass balances by allowing volatile products to partition into the hydrogen headspace. At the final timepoint of these experiments, a maximum of about 8 mL of headspace may have been present in each reactor, which would then contain approximately 150 mL of aqueous solution. The K<sub>H</sub> values listed in Table 5 can be used to calculate that at this headspace/solution ratio, 41% of the total 1-hexene mass would be in the headspace, versus 36% of the methylcyclopentane mass, and 75% of the hexane mass. Such volatilization losses could thus potentially account for the entire mass balance discrepancy arising for reactions of 6-bromo-1-hexene with iron.

A scheme that could account for the observed products of 6-bromo-1-hexene reduction by iron is shown in Figure 38. These pathways were verified by control experiments in which 1,5-hexadiene, 1-hexene, methylcyclopentane, and 1-bromohexane were reacted with Fe(0) under the

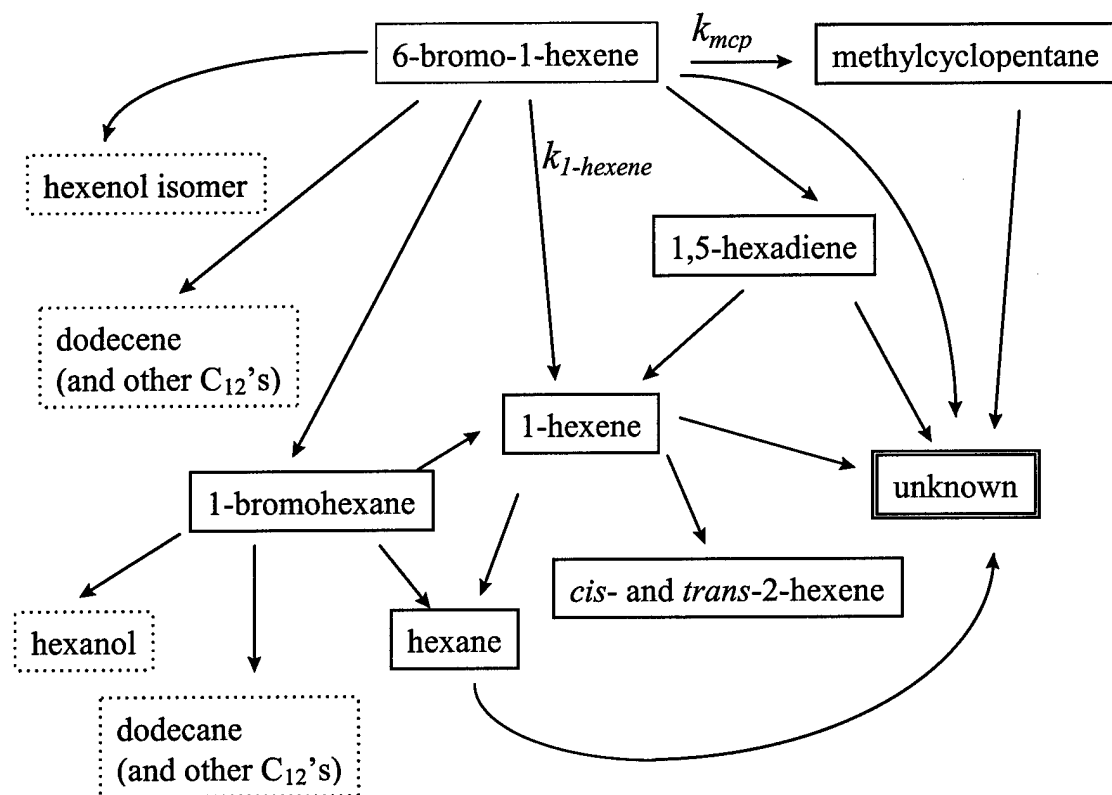


**Figure 38:** Pathways for the reaction of 6-bromo-1-hexene in the presence of iron metal. Species in solid boxes were detected and quantified. Species in dashed boxes were detected but not quantified. Species in double boxes were not detected, but their existence was inferred from modeling of data.

same conditions as employed with 6-bromo-1-hexene. Reactions were generally conducted at the same starting concentrations of reactants (0.1 mM), but the reactions of 1-hexene and methylcyclopentane were also investigated at starting concentrations which were similar to those produced during reduction of 6-bromo-1-hexene in order to assess whether the pseudo-first order rate constants were dependent on initial concentration ( $C_0$ ), as has been observed for reactions of  $CCl_4$  and chlorinated ethylenes with iron (Johnson *et al.*, 1998; Section VI). No significant effect of  $C_0$  on rate constants was observed.

Although the control experiments confirmed the major features of the pathways depicted in Figure 38, this diagram cannot be assumed to represent all of the possible reactions occurring in the Fe(0) system. Because the mass balances were incomplete in nearly all of these reactions, the generation of unknown products was assumed as part of the kinetic model. Thus, additional reactions may have been occurring in the iron system which were not revealed by the control experiments.

Estimating  $k_2$  for the 6-bromo-1-hexene probe in the iron system is complicated by the presence of unexpected products and the poor mass balances derived from these reactions. The variety of products observed suggests that the assumptions inherent in the calculation of  $k_2$  from the ratio of methylcyclopentane and 1-hexene (equation 10) might not be reasonable for reactions of 6-bromo-1-hexene with iron. Even if these assumptions are made, a simple product ratio gives only an approximate value of  $k_2$  in the iron system (Table 6), because 1-hexene can be produced via three different pathways and because both methylcyclopentane and 1-hexene may continue to react with iron and to volatilize into the headspace. Volatilization has a relatively small impact on the calculated *ratio* of 1-hexene to methylcyclopentane in these systems, however, because the  $K_H$  values for these compounds are similar. Even at the maximum headspace/solution ratios likely to be encountered in these experiments, volatilization of 1-hexene and methylcyclopentane into the headspace of the reactor affects the calculated product ratio by less than 10%.

An alternate method of estimating  $k_2$  in the iron system was developed which attempted to account for the low mass balances and unexpected products encountered. A kinetic model was developed based on the pathways outlined in Figure 38. The rate constants from the control experiments were used in the kinetic model, and  $k_{1\text{-hexene}}$  and  $k_{mcp}$  (Figure 38) were then obtained from fitting the concentration versus time data for experiments involving 6-bromo-1-hexene. The rate constant for transfer of the second electron to the 5-hexenyl radical,  $k_2$ , was then estimated from the ratio of  $k_{mcp}$  to  $k_{1\text{-hexene}}$ :

$$\frac{k_2}{k_{cyc}} = \frac{k_{1\text{-hexene}}}{k_{mcp}} \quad (12)$$

The resulting  $k_2$  values are shown in Table 6.

This method of estimating  $k_2$  was a crude attempt to account for the three pathways for production of 1-hexene and the different rates at which methylcyclopentane and 1-hexene

disappear from the aqueous phase due either to reaction with iron or to volatilization into the headspace. The kinetic model assumes that the reaction rates of all species obeyed pseudo-first order kinetics. Volatilization cannot, however, necessarily be assumed to represent a pseudo first-order process in this system (although the concentration versus time data for the control experiments involving 1-hexene and methylcyclopentane appeared to be adequately described by a pseudo-first order decay model).

Only the data from experiments using 10 g of clean iron at pH 8 could be modeled, because the control experiments were only conducted under these conditions. The error limits on  $k_2$  were calculated from the model results for replicate experiments. They do not incorporate the error inherent in this system due to incomplete mass balances. For this limited set of experiments, the product ratio and model results give very similar values of  $k_2$  ( $10^6 \text{ s}^{-1}$ ) largely because methylcyclopentane and 1-hexene disappear in the presence of iron at similar rates (perhaps because their  $K_H$  values differ little) and also because the contribution of dehydrobromination of bromohexane and hydrogenation of 1,5-hexadiene to the 1-hexene concentration is minor.

Although product ratios can only give an approximate value,  $k_2$  was calculated by this method for all other reaction conditions (Table 6). The  $k_2$  values remained remarkably constant over a range of reaction conditions. Variations in  $k_2$  were less than a factor of three despite changes in metal loading, surface cleaning, and pH. Addition of 5 mmol  $\text{FeCl}_2$  and 1 mL of air (containing  $\text{O}_2$ ) also failed to significantly affect  $k_2$ . Thus  $k_2$  appears not to be first-order with respect to protons or metal loading.

## **5. Reduction of BrMCP by Iron**

The rate constant for disappearance of BrMCP in aqueous solution in the presence of 20 g of iron ( $k = 0.0030 \text{ sec}^{-1}$ ) was not significantly different from the overall disappearance rate constant obtained in the absence of iron. Only about 1% of the spiked mass of BrMCP was recovered as  $\text{C}_4$  products in these systems, because the rate of reduction was simply too slow to effectively compete with rapid rearrangement and hydrolysis of BrMCP. BrMCP was reduced to a mixture of  $\text{C}_4$  isomers including 1-butene (~ 40% of recovered mass), methylcyclopropane (~ 40%), and traces of *Z*- and *E*-2-butenes and the same unidentified  $\text{C}_4\text{H}_8$  product observed in the  $\text{Zn(0)}$  system. All products (except the unidentified  $\text{C}_4\text{H}_8$  isomer) were identified by comparison

of retention time and mass spectra with authentic standards. Based solely on the 1-butene/methylcyclopropane ratio,  $k_2$  is calculated to be  $2 \times 10^8 \text{ s}^{-1}$ , about 100 times faster than the value obtained in the 6-bromo-1-hexene experiments with iron. Control experiments demonstrated that reaction of 4-bromo-1-butene with iron did not generate detectable amounts of 1-butene on the time scale of the BrMCP experiments.

## E. DISCUSSION

These experiments were designed to determine whether radical intermediates are involved in the reduction of alkyl halides by zero-valent metals. Because detectable amounts of methylcyclopentane were produced during reduction of 6-bromo-1-hexene by both iron and zinc, it is tempting to conclude that the reduction occurs via an SET pathway. Newcomb and Curran (1988) warn, however, that detection of rearranged products in a radical clock reaction is not sufficient proof that the reaction occurs via SET, because side reactions can sometimes result in substantial amounts of rearranged products. The variety of products detected during reaction of 6-bromo-1-hexene with iron clearly indicates that processes other than SET must be operating, since a simple SET mechanism cannot account for all the products observed. The product distribution arising from these reactions is in fact completely consistent with a pathway in which organometallic intermediates are formed. These species could also account for the production of methylcyclopentane. Thus the appearance of methylcyclopentane is not necessarily proof that there is a free-radical component to the reaction.

The product distribution suggests that organometallic intermediates are formed in the iron system. An SET pathway may also be operating in this system. These two mechanistic possibilities are not mutually exclusive; in fact it is quite possible (and perhaps likely) that both pathways are operating with organometallic intermediates forming subsequent to an initial SET step. The kinetics of reactions of organohalides with metals are likely to be determined by the initial step in their transformation (possibly SET), while the products of such reactions may be determined largely by the relative importance of organometallic intermediates. Potential implications of the radical and organometallic pathways are discussed below.

## 1. Radical Pathways

Assuming for heuristic purposes that the reaction of 6-bromo-1-hexene with both iron and zinc proceeds primarily via the formation of 5-hexenyl radicals, and assuming that these radicals are able to escape from the surface of the metal, they will have a finite lifetime before being destroyed by coupling, hydrogen atom abstraction, or diffusion back to the metal surface and subsequent reduction. During this time they are virtually certain to undergo the one most facile reaction available to them: cyclization.

The fastest bimolecular reactions, such as radical-radical coupling (with a diffusion-limited rate constant,  $k_{\text{couple}}$ , on the order of  $10^{10} \text{ M}^{-1}\text{s}^{-1}$ ) can only begin to compete with cyclization to the methylcyclopentyl radical ( $k_{\text{cyc}} = 2.2 \times 10^5 \text{ s}^{-1}$ ) if the reactants are present at concentrations greater than  $10^{-6} \text{ M}$ . Newcomb (1990) calculates, for example, that the 5-hexenyl radical will cyclize with 99.6% efficiency when it is generated in ether at  $25^\circ\text{C}$ . Hydrogen atom abstraction from the solvent only captures 0.4% of the radicals, even when ether is present at 9.5 M. Water, in fact, is such a weak hydrogen atom donor that radicals would be much more likely to abstract a hydrogen atom from an alternate source, most likely from metal hydrides being produced at the surface of the metal during production of  $\text{H}_2$  (g).

The small amount of methylcyclopentane detected in these systems therefore suggests that if radicals are formed, they only possess a fleeting existence as transient intermediates. The  $k_2$  estimates obtained for the 5-hexenyl radicals suggest that subsequent reactions proceed so rapidly that most of the radicals do not persist for a sufficient length of time to enable them to diffuse away from the surface of the metal before undergoing further reactions.

If radicals are formed, the larger amounts of methylcyclopentane produced by iron would suggest that radicals persist longer in iron systems ( $k_2 \sim 2 \times 10^6 \text{ s}^{-1}$ ) than with zinc ( $k_2 \sim 2 \times 10^7 \text{ s}^{-1}$ ). Radical coupling is a second-order process and is therefore highly dependent on radical concentration. The steady-state concentration of the 5-hexenyl radical,  $([\text{R}^\bullet]_{\text{ss}})$ , can be estimated by the equation:

$$[\text{R}^\bullet]_{\text{ss}} = \frac{k_1[\text{6-bromo-1-hexene}]}{k_2 + k_{\text{couple}}[\text{R}^\bullet]_{\text{ss}} + k_{\text{cyc}}} \quad (13)$$

where  $k_1$  is a pseudo-first-order rate constant for the reduction of 6-bromo-1-hexene to the 5-hexenyl radical,  $k_2$  is the rate constant for reduction of the 5-hexenyl radical to 1-hexene, and



$k_{couple}$  is the rate constant for coupling of two 5-hexenyl radicals. The coupling process is expected to be diffusion limited, but the concentration of radicals is certainly orders of magnitude less than  $10^{-4}$  M (the starting concentration of 6-bromo-1-hexene). Therefore,  $k_2$  is much greater than the product of  $k_{couple}$  and  $[R^*]_{ss}$ , and the second term of the denominator of equation (13) can be safely neglected. Also, for both iron and zinc,  $k_2$  is much greater than  $k_{cyc}$ . Thus the equation for  $[R^*]_{ss}$  becomes:

$$[R^*]_{ss} \cong \frac{k_1}{k_2} [6 - \text{bromo} - 1 - \text{hexene}] \quad (14)$$

For zinc,  $k_1$  can be assumed to equal the overall rate constant for disappearance of 6-bromo-1-hexene ( $7 \times 10^{-5} \text{ s}^{-1}$ ). For iron,  $k_1$  is less than the overall rate constant for disappearance of 6-bromo-1-hexene but is greater than or equal to the rate constant pertaining to 1-hexene formation (*i.e.*,  $k_1$  is between  $8 \times 10^{-7}$  and  $2 \times 10^{-6} \text{ s}^{-1}$ ). Using  $[6\text{-bromo-1-hexene}] = 10^{-4} \text{ M}$ ,  $[R^*]_{ss}$  is approximately equal to  $4 \times 10^{-16} \text{ M}$  for zinc and is between  $4 \times 10^{-18}$  and  $9 \times 10^{-17} \text{ M}$  for iron, suggesting that if anything, coupling of radicals would be more likely in the zinc system, even though coupling products were only observed in the iron system.

This analysis assumes that the putative radicals are uniformly distributed throughout the bulk solution. Computing the average steady-state radical concentration per unit surface area by dividing the radical concentration computed above by the amount of metal surface area ( $\text{m}^2\text{L}^{-1}$ ) in each system also results in a lower abundance of radicals in the Fe(0) system ( $7 \times 10^{-20}$  to  $2 \times 10^{-18} \text{ mol/m}^2$ ) than in the Zn(0) system ( $7 \times 10^{-16} \text{ mol/m}^2$ ). A greater likelihood of radical-radical coupling in the iron system can only be rationalized if radical production is limited to highly localized areas of the metal surface (such as in corrosion pits). Alternatively, coupling may occur via a mechanism other than intermolecular dimerization of two free radicals, such as through reactions involving organometallic intermediates (as discussed in more detail below).

The BrMCP experiments result in estimates of  $k_2$  of about  $10^8 \text{ M}^{-1}\text{s}^{-1}$  for iron and  $10^9 \text{ M}^{-1}\text{s}^{-1}$  for zinc. Both of these values are about 50-100 times faster than the  $k_2$  values derived from the 6-bromo-1-hexene experiments for the same metals. Because of the solvolysis of BrMCP, the data probably do not provide accurate estimates of  $k_2$ , but a fifty- to hundred-fold discrepancy is sufficiently large as to raise questions concerning the accuracy of one of these sets of results. That any methylcyclopropane is produced in these systems at all suggests either that

electron transfer is extremely rapid (*i.e.*, that radicals have an extremely short lifetime), or that inner-sphere two-electron transfer is occurring. From the experiments with vicinal dibromide stereochemical probes (Section II),  $k_2$  was estimated for both iron and zinc to be about  $10^8 \text{ s}^{-1}$  (based on experiments conducted with ( $\pm$ )-stilbene dibromide) to about  $10^{10} \text{ s}^{-1}$  (based on experiments conducted with *threo*-2,3-dibromopentane). These  $k_2$  values are in reasonable agreement with the values derived from the BrMCP experiments. The stereochemical experiments suggested, however, that the  $k_2$  values for iron and zinc were roughly equal, while both the experiments with BrMCP and with 6-bromo-1-hexene suggest that the  $k_2$  values are quite different for these two metals.

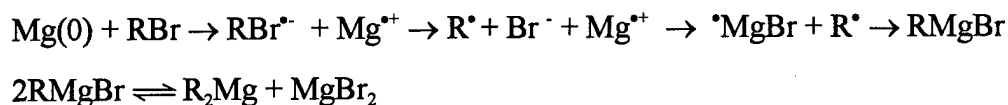
Newcomb and Curran (1988) note: "As a minimum requirement of evidence for SET, a series of probes should be studied to demonstrate that the product ratios correlate with the rates of rearrangement of the series." In the radical clock experiments with 6-bromo-1-hexene and BrMCP, and in the vicinal dibromide probe experiments with stilbene dibromide and 2,3-dibromopentane, a series of probes have failed to demonstrate a correlation between product ratios and rates of rearrangement. Although it is possible that the four different probe compounds are reacting at different types of reactive sites on the metal surface, it seems more plausible to assume that they react at the same types of sites, but via a mechanism other than one involving pure SET.

It appears that pathways involving only SET reactions cannot describe all the features of the reactions of the probe compounds with iron. The very complicated product distribution; the discrepancy in  $k_2$  values calculated from several different probe compounds; and the lack of coupling products observed in experiments with zinc (which simple calculations suggest should produce a higher concentration of radicals and thus a greater likelihood of radical dimerization) all suggest that another process may be operating.

## **2. Alternate Organometallic Reaction Pathways**

The distribution of products arising from reaction of 6-bromo-1-hexene with Fe(0) is entirely consistent with a mechanism in which organometallic intermediates are formed. This observation is based largely on evidence in the chemical literature from experiments which have yielded similar results. Ashby and Oswald (1988), for example, studied the formation of Grignard reagents in organic solvent using 6-bromo-1-hexene as a mechanistic probe. The Grignard

reaction is thought to occur via an initial SET from Mg(0) to the alkyl bromide, followed by a fast coupling of the metal bromide and the radical to form a  $\sigma$ -bonded organometallic complex. Once formed, the Grignard reagent (RMgBr) rapidly disproportionates to form a dialkyl magnesium species (March, 1992) (Scheme 9).



#### Scheme 9

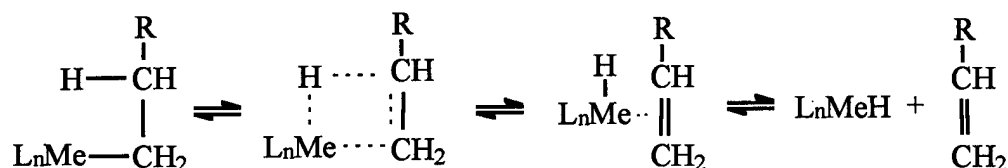
Because the radicals ( $\text{R}^{\cdot}$ ) are generated so close to the surface  ${}^{\cdot}\text{MgBr}$  species, coupling to form RMgBr occurs much more rapidly than cyclization of the 5-hexenyl radical. Thus direct reaction of 6-bromo-1-hexene with Mg(0) (22°C in THF) produces roughly 90% 1-hexene, 5% methylcyclopentane, and traces of coupling products. (Final product distribution is determined after workup, in which the Grignard reagent is destroyed by reaction with protons in water, which attack the nucleophilic carbon bonded to magnesium). This reaction mechanism is a good example of how SET and the formation of organometallic intermediates are not mutually exclusive pathways.

When Ashby and Oswald (1988) added a catalytic amount (2%) of  $\text{FeCl}_3$  to the system used to generate the Grignard reagent, a black Fe(0) precipitate was formed, and the product distribution changed dramatically. More dimers (6.7% of products), more methylcyclopentane (22.5%), and substantial amounts of 1,5-hexadiene (25.9%) were formed. 1,5-Hexadiene also formed when the Grignard reagent ( $\text{CH}_2=\text{CH}(\text{CH}_2)_3\text{CH}_2\text{MgBr}$ ) was reacted with  $\text{FeCl}_3$  in the absence of Mg(0). Because of its position in the electromotive series, Fe should exchange with Mg in the Grignard reagent (March, 1992). Iron thus catalyzes coupling of the alkyl chains and facilitates  $\beta$ -hydride elimination (which produces 1,5-hexadiene).

Kauffmann (1996) used 6-bromo-1-hexene as a probe to study reactions of alkyl halides with organoiron complexes. These complexes are formed from the reaction of  $\text{FeCl}_2$  or  $\text{Fe}(\text{CN})_2$  with alkyllithium or Grignard reagents in organic solvents. They are used in organic synthesis to couple alkyl groups. These organoiron species are relatively stable; for example,  $(\text{CH}_3)_4\text{FeLi}_2$  is stable at room temperature in organic solvent.

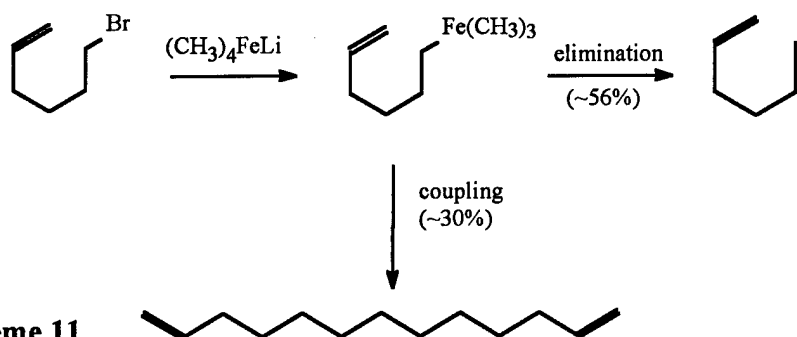
Alkyliron complexes react with 6-bromo-1-hexene to give a new organometallic complex in which one of the alkyl groups is replaced by the 5-hexenyl group. This complex may undergo

$\beta$ -hydride elimination (Scheme 10) (Elschenbroich and Salzer, 1989):



**Scheme 10**

where L represents any ligand and Me is a metal atom. Alternatively, the complex may react with another molecule of 6-bromo-1-hexene to give 1,11-dodecadiene (Scheme 11) (Kaufmann, 1996).

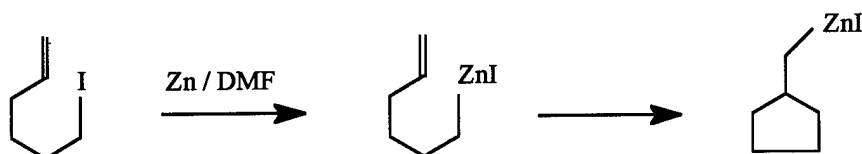


**Scheme 11**

Kauffman found that no methylcyclopentane is formed in this reaction, which he interpreted to signify that this reaction is not a radical process in organic solvent. In water, these organometallic species are typically destroyed via electrophilic attack by protons, which in the above example would yield 1-hexene. In addition, reactions of 1-bromoalkanes with these alkyliron complexes reportedly results not only in the  $\alpha$ -alkene (1-hexene from 1-bromohexane, for example) but also in the  $\beta$ -alkene (2-hexene from 1-bromohexane, for example) (Kaufmann, 1996).

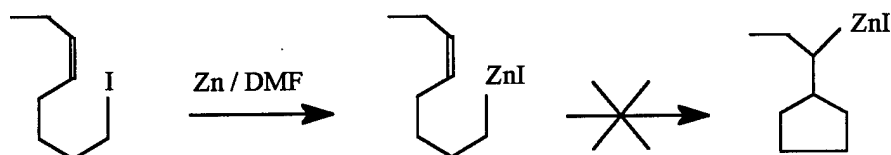
Thus the product distribution observed from the reaction of 6-bromo-1-hexene with iron in aqueous solution is not without precedent. Other researchers have observed similar product distributions arising from the reactions of 6-bromo-1-hexene in the presence of iron in organic solvents. In both cases, many of the products, including coupling products, 1,5-hexadiene, and 2-hexenes, are thought to arise from an organoiron intermediate.

Zinc metal is also known to form stable alkylzinc species; zinc metal reacts with 6-iodo-1-hexene in dimethylformamide (DMF) directly to form an alkylidozinc complex which can undergo a cyclization reaction which forms the methylcyclopentyl zinc complex (Meyer and Marek, 1993) (Scheme 12).



**Scheme 12**

These alkylzinc species may then be attacked by protons to yield the observed products, 1-hexene and methylcyclopentane. The radical cyclization of 5-hexenyl to methylcyclopentyl radical is largely immune to steric effects, but the anionic cyclization mechanism in scheme 12 is sensitive to the steric environment of the double bond. This same isomerization reaction does not occur with *Z*-5-octen-1-yl zinc (Scheme 13). Because the steric hindrance of the ethyl group prevents cyclization, the mechanism apparently does not involve radical intermediates (Meyer and Marek, 1993).



**Scheme 13**

A pathway such as the one depicted in scheme 12 could account for the formation of some or all of the methylcyclopentane produced in the reactions of 6-bromo-1-hexene with iron and zinc. If a portion of the methylcyclopentane produced in these systems comes from this pathway, the overall ratio of methylcyclopentane to 1-hexene arising from a radical process would be lower, and the true value of  $k_2$  would be higher, bringing it into closer agreement with the  $k_2$  values estimated from the BrMCP and vicinal dibromide reactions. Thus it is possible that both iron and zinc react directly with 6-bromo-1-hexene to give an alkylmetal intermediate that decomposes in various ways to produce most of the observed reaction products, and that the formation of methylcyclopentane is not conclusive evidence of the existence of free radical intermediates.

### 3. Role of Hydrogen Species

Although  $\sigma$ -bonded organometallic intermediates may explain the formation of most of the products observed in the Fe(0) system, at least one other mechanism is apparently operating. Fe(0) is clearly capable of hydrogenating double bonds, as evidenced by the reduction of 6-bromo-1-hexene to 1-bromohexane and of 1-hexene to hexane, *etc.* Such hydrogenation reactions were not apparent when zinc served as the reductant. Hydrogenation is thought to occur via an

interaction between metal hydride species and olefins in which a  $\pi$ -bonded organometallic intermediate is formed (Ponec and Bond, 1995).

During hydrogen evolution reactions, metal-hydrogen bonds are formed. The Fe-H bond is stronger than the Zn-H bond, and the hydrogen possesses more hydride character when bonded to iron (Barclay, 1973). This is part of the reason why hydrogen evolution is much faster (*i.e.*, has a higher exchange current density) for iron than for zinc (Jones, 1992). It also partly explains why organoiron complexes are more prone to decomposition via  $\beta$ -hydride elimination (Scheme 10).

The formation of 2-hexene from 1-hexene in this system is another manifestation of the Fe-H interaction. A similar isomerization has been observed in the gas-phase reaction of 1-butene to *cis*- and *trans*-2-butene on iron films in the presence of  $H_2$  (g). Such isomerization reactions are much more rapid for  $\alpha$ -olefins than for  $\beta$ -olefins (Rouroude and Gault, 1974). Isomerizations of this type are characteristic of metal hydride complexes, and are thought to occur via either  $\pi$ -bonding between a transition metal and the double bond (as depicted in Scheme 10), allowing 1,3 hydride migrations (Casey and Cyr, 1973), or via 1,2 hydride addition/elimination (Cramer, 1966). Iron carbonyl complexes are thought to mediate olefin isomerization via a  $\pi$ -allyl metal hydride intermediate (Casey and Cyr, 1973; Manuel, 1962).

Thus  $\pi$ -bonded transition metal complexes may represent another kind of organometallic intermediate which mediates important reactions in the zero-valent iron system. Zinc metal is much less likely to form hydrides (Barclay, 1973), which may explain why no 2-hexenes are formed from the reaction of 6-bromo-1-hexene with zinc.

#### **4. Relative Importance of SET and Organometallic Reaction Pathways with Iron**

In the iron system, the pathways which form organometallic intermediates appear to dominate the overall product distribution. "Pure" SET is at best a minor reaction pathway, as evidenced by the small amounts of methylcyclopentane formed from 6-bromo-1-hexene. Although it is plausible that *all* of the methylcyclopentane observed in this system arises from the anionic cyclization of the alkyl iron intermediate, that Kauffmann did not observe this type of isomerization suggests that methylcyclopentane may truly represent the product of a radical mechanism. A certain extent of SET is probably occurring in the iron system, either as a first step in the pathway which produces the organoiron species, or as a separate, concurrent reaction

pathway.

### **5. Relative Importance of SET and Organometallic Reaction Pathways with Zinc**

It is more difficult to judge which pathway dominates in the zinc system. A simple SET mechanism could account for all of the products observed to arise from reactions of 6-bromo-1-hexene with zinc. If SET were the only mechanism operating, the small amounts of methylcyclopentane observed in the product distribution would suggest that radicals do not persist long in the presence of the metal before being reduced to hydrocarbon products. Thus characteristic radical reactions such as hydrogen atom abstraction and radical-radical coupling are not likely to occur to a significant extent. An initial SET step is also consistent with the observed correlation between surface area-normalized rate constants and reduction potentials for reaction of zinc with chlorinated ethylenes (Arnold and Roberts, 1998) and some chlorinated ethanes (Arnold *et al.*, 1999). This explanation cannot, however, account for the discrepancies in  $k_2$  values obtained from experiments with different probe compounds.

Alternatively, organometallic intermediates could also account for the 1-hexene and some or all of the methylcyclopentane formed during reactions of 6-bromo-1-hexene with zinc. The many other products which are observed during reactions of 6-bromo-1-hexene with iron would not necessarily be expected from an organozinc intermediate. Because Zn-H bonds are much weaker than Fe-H bonds, alkylzinc species are less prone to  $\beta$ -hydride elimination, and olefins are less prone to isomerization and hydrogenation reactions in the presence of zinc.

Alkylzinc species are commonly used reagents in organic synthesis. These reagents are readily generated via a process analogous to the formation of classic Grignard reagents in which zinc metal reacts with a primary alkyl bromide, typically in ether (March, 1992). Such alkylzinc species are involved in both the Reformatsky reaction and the Wurtz reaction. Similarly, the Simmons-Smith procedure involves formation of a zinc carbenoid from the reaction of  $\text{CH}_2\text{I}_2$  with  $\text{Zn}(0)$  in ether (March, 1992; Simmons and Smith, 1959). The only significant difference between these organic synthesis reactions and the reduction of 6-bromo-1-hexene by zinc investigated herein lies in the solvent.

Other researchers have argued that reactions of zinc metal with chlorinated methanes and ethanes in water involve organometallic zinc carbenoid species (Fennelly and Roberts, 1998;

Boronina *et al.*, 1998). These arguments are based in part on the fact that zinc mediates total dechlorination of carbon tetrachloride and 1,1,1-trichloroethane to methane and ethane, respectively, but the lesser-chlorinated species (dichloromethane and 1,1-dichloroethane) are not intermediates in these reactions. In addition, Boronina *et al.* (1998) detected coupling products in reactions between zinc metal and  $\text{CCl}_4$ ,  $\text{CHCl}_3$  and  $\text{CH}_2\text{Cl}_2$ , which they hypothesized to arise from the coupling of surface-bound carbenoid species.

Thus the possibility that organozinc compounds are formed in the reactions of alkyl halides with this metal in water cannot be ignored. Carbenoid organozinc intermediates may be important in determining the product distribution arising from the reactions of aliphatic chlorides, and  $\sigma$ -bonded organozinc compounds might explain the formation of some or all of the methylcyclopentane produced from reactions of 6-bromo-1-hexene with zinc. Because little or no hydrogenation or isomerization of olefins was observed in the zinc system,  $\pi$ -bonded organozinc compounds would appear to be less important than with iron. In general, though, the relative importance of the organometallic and SET pathways cannot be assessed from the limited amount of experimental data available for reactions of zinc with alkyl halides in water.

## **6. Alternate Methods of Detecting Radical Intermediates**

The difficulty in discerning between the SET and organometallic pathways is due in large part to the heterogeneous nature of these reactions. As discussed earlier, if 5-hexenyl radicals were generated in bulk solution, they might be expected to persist much longer before encountering a second reducing equivalent. During this time they would be virtually certain to undergo cyclization, and large amounts of methylcyclopentane would be formed. Because radicals are produced at the surface of the metal, in close proximity to an excess of reducing equivalents, a second reduction step may occur so rapidly that little methylcyclopentane is formed. In this regard, reactions of iron and zinc with organohalides in water are similar to reactions of magnesium with alkyl bromides in organic solvent to form Grignard reagents. The radical nature of the Grignard reaction remained a matter of debate for many years until Bodewitz *et al.* (1972, 1973) used chemically induced dynamic nuclear polarization (CIDNP) to demonstrate the intermediacy of free radicals. Even ESR spectroscopy had failed to detect free radicals in the Grignard reaction because of their extremely low steady-state concentration. Similar CIDNP studies may thus be necessary to definitively establish whether radicals are involved in the



reactions of alkyl halides with zero-valent metals in water.

## ***7. Implications for Remediation Schemes Involving Zero-Valent Metals***

Environmental engineers are primarily interested in predicting the possible products and the kinetics of reactions of halogenated contaminants with zero-valent metals. These experiments have demonstrated that the distribution of products arising from the reduction of a simple alkyl halide substrate can be very complicated, and that iron tends to produce a greater variety of products than zinc. Hydrogenation of double bonds is substantially more important in the iron system than in the zinc system. Coupling products are also more likely to form in Fe(0) systems. Recognition of the possibility that organometallic species may be formed during these reactions can help environmental chemists better predict the products likely to occur.

## F. LITERATURE CITED

- Agrawal, A.; Tratnyek, P. G. Reduction of nitroaromatic compounds by zero-valent iron metal. *Environ. Sci. Technol.* **1996**, *30*, 153-160.
- Alnajjar, M. S.; Smith, G. F.; Kuivila, H. G. Reactions of cyclopropylcarbinyl halides with (trimethylstannyl)alkalis. Evidence that kinetically free intermediates need not be involved in cyclopropylcarbinyl to 3-butenyl rearrangements. *J. Org. Chem.* **1984**, *49*, 1271-1276.
- Arnold, W. A.; Roberts, A. L. Pathways of chlorinated ethylene and chlorinated acetylene reaction with Zn(0). *Environ. Sci. Technol.* **1998**, *32*, 3017-3025.
- Arnold, W. A.; Ball, W. P.; Roberts, A. L. Polychlorinated ethane reaction with zero-valent zinc: pathways and rate control. *J. Contam. Hydrol.* **1999**, *40*(2), 183-200.
- Ashby, E. C.; Oswald, J. Concerning the mechanism of Grignard reagent formation. Evidence for radical escape and return to the surface of magnesium. *J. Org. Chem.* **1988**, *53*, 6068-6076.
- Bakac, A.; Espenson, J. H. Kinetics and mechanism of alkylnickel formation in one-electron reductions of alkyl halides and hydroperoxides by a macrocyclic nickel(I) complex. *J. Am. Chem. Soc.* **1986**, *108*, 713-719.
- Balko, B. A.; Tratnyek, P. G. Photoeffects on the reduction of carbon tetrachloride by zero-valent iron. *J. Phys. Chem. B* **1998**, *102*, 1459-1465.
- Barclay, D. J. The possible hydridic nature of adsorbed hydrogen in the hydrogen evolution reaction. *Electroanal. Chem.* **1973**, *44*, 47-51.
- Bodewitz, H. W. H. J.; Blomberg, C.; Bickelhaupt, F. The formation of Grignard compounds--I. *Tetrahedron Letters* **1972**, 251.
- Bodewitz, H. W. H. J.; Blomberg, C.; Bickelhaupt, F. The formation of Grignard compounds--II. *Tetrahedron* **1973**, *29*, 719-726.
- Boronina, T.; Klabunde, K. J. Destruction of organohalides in water using metal particles: Carbon tetrachloride/water reactions with magnesium, tin, and zinc. *Environ. Sci. Technol.* **1995**, *29*, 1511-1517.
- Boronina, T. N.; Lagadic, I.; Sergeev, G. B.; Klabunde, K. J. Activated and nonactivated forms of zinc powder: Reactivity toward chlorocarbons in water and AFM studies of surface

- morphologies. *Environ. Sci. Technol.* **1998**, *32*, 2614-2622.
- Brace, N. O.; Elswyk, J. E. V. Evidence for free-radical reductive dehalogenation in the reaction of zinc and acid with 1-perfluoroalkyl-2-iodoalkanes and with 1-perfluoroalkyl-2-iodoalkenes. *J. Org. Chem.* **1976**, *41*, 766-771.
- Burris, D. R.; Campbell, T. J.; Manoranjan, V. S. Sorption of trichloroethylene and tetrachloroethylene in a batch reactive metallic iron-water system. *Environ. Sci. Technol.* **1995**, *29*, 2850-2855.
- Caserio, M. C.; Graham, W. H.; Roberts, J. D. Small-ring compounds-XXIX A reinvestigation of the solvolysis of cyclopropylcarbinyl chloride in aqueous ethanol. Isomerization of cyclopropylcarbinol. *Tetrahedron* **1960**, *11*, 171-182.
- Casey, C. P.; Cyr, C., R. Iron carbonyl catalyzed isomerization of 3-ethyl-1-pentene. Multiple olefin isomerizations *via* a  $\pi$ -allyl metal hydride intermediate. *J. Am. Chem. Soc.* **1973**, *95*, 2248-2253.
- Chatgililoglu, C.; Ingold, K. U.; Scaiano, J. C. Rate constants and Arrhenius parameters for the reactions of primary, secondary, and tertiary alkyl radicals with tri-*n*-butyltin hydride. *J. Am. Chem. Soc.* **1981**, *103*, 7739-7742.
- Cramer, R. Olefin coordination compounds of rhodium. III. The mechanism of olefin isomerization. *J. Am. Chem. Soc.* **1966**, *88*, 2272-2282.
- Demjanoff, N. Ueber das Methyltrimethylen. *Chem. Ber.* **1895**, *23*, 21-25.
- Elschenbroich, C.; Salzer, A. *Organometallics: A Concise Introduction*; VCH: New York, 1989.
- Fennelly, J. P.; Roberts, A. L. Reaction of 1,1,1-trichloroethane with zero-valent metals and bimetallic reductants. *Environ. Sci. Technol.* **1998**, *32*, 1980-1988.
- Fu, H.; Newcomb, M.; Wong, C.-H. *Pseudomonas oleovorans* monooxygenase catalyzed asymmetric epoxidation of allyl alcohol derivatives and hydroxylation of a hypersensitive radical probe with the radical ring opening rate exceeding the oxygen rebound rate. *J. Am. Chem. Soc.* **1991**, *113*, 5878-5880.
- Gillham, R. W.; O'Hannesin, S. F. Enhanced degradation of halogenated aliphatics by zero-valent iron. *Ground Water* **1994**, *32*, 958-967.
- Griller, D.; Ingold, K. U. Free-radical clocks. *Acc. Chem. Res.* **1980**, *13*, 317-323.

- Helland, B. R.; Alvarez, P. J. J.; Schnoor, J. L. Reductive dechlorination of carbon tetrachloride with elemental iron. *J. Haz. Mat.* **1995**, *41*, 205-216.
- Johnson, T. L.; Fish, W.; Gorby, Y. A.; Tratnyek, P. G. Degradation of carbon tetrachloride by iron metal: Complexation effects on the oxide surface. *J. Contam. Hydrol.* **1998**, *29*, 379-398.
- Jones, D. A. *Principles and Prevention of Corrosion*; Macmillan: New York, 1992.
- Kauffmann, T. Nonstabilized alkyl complexes and alkyl-cyano-ate complexes of iron(II) and cobalt(II) as new reagents in organic synthesis. *Angew. Chem. Int. Ed. Engl.* **1996**, *35*, 386-403.
- Lide, D. R. *CRC Handbook of Chemistry and Physics, 72nd edition*; CRC Press: Boca Raton, 1991.
- Lipczynska-Kochany, E.; Harms, S.; Milburn, R.; Sprah, G.; Nadarajah, N. Degradation of carbon tetrachloride in the presence of iron and sulphur containing compounds. *Chemosphere* **1994**, *29*, 1477-1489.
- Liu, K. E.; Johnson, C. C.; Newcomb, M.; Lippard, S. J. Radical clock substrate probes and kinetic isotope effect studies of the hydroxylation of hydrocarbons by methane monooxygenase. *J. Am. Chem. Soc.* **1993**, *115*, 939-947.
- Mackay, D.; Shiu, W. Y.; Ma, K. C. *Illustrated Handbook of Physical-Chemical Properties of and Environmental Fate for Organic Chemicals*; Lewis: Ann Arbor, MI, 1993; Vol. 3.
- Maillard, B.; Forrest, D.; Ingold, K. U. Kinetic applications of electron paramagnetic resonance spectroscopy. 27. Isomerization of cyclopropylcarbinyl to allylcarbinyl. *J. Am. Chem. Soc.* **1976**, *98*, 7024-7026.
- Manuel, T. A. Some reactions of monoolefins with iron carbonyls. *J. Org. Chem.* **1962**, *27*, 3941-3945.
- March, J. *Advanced Organic Chemistry: Reactions, Mechanisms and Structure*; 4th ed.; Wiley-Interscience: New York, 1992.
- Matheson, L. J.; Tratnyek, P. G. Reductive dehalogenation of chlorinated methanes by iron metal. *Environ. Sci. Technol.* **1994**, *28*, 2045-2053.
- McAulliffe, C. GC determination of solutes by multiple phase equilibration. *Chem. Tech.* **1971**, *1*, 46-51.

- Meyer, C.; Marek, I.; Courtemanche, G.; Normant, J.-F. Carbocyclization of functionalized zinc organometallics. *Synlett* **1993**, 4, 266-268.
- Newcomb, M.; Curran, D. P. A critical evaluation of studies employing alkenyl halide "mechanistic probes" as indicators of single-electron-transfer processes. *Acc. Chem. Res.* **1988**, 21, 206-214.
- Newcomb, M. Radical kinetics and the quantitation of alkyl halide mechanistic probe studies. *Acta Chemica Scandinavica* **1990**, 44, 299-310.
- Ponec, V.; Bond, G. C. *Catalysis by Metals and Alloys*; Elsevier: New York, 1995; Vol. 95.
- Powell, R. M.; Puls, R. W.; Hightower, S. K.; Sabatini, D. A. Coupled iron corrosion and chromate reduction: Mechanisms for subsurface remediation. *Environ. Sci. Technol.* **1995**, 29, 1913-1922.
- Pross, A. The single electron shift as a fundamental process in organic chemistry: The relationship between polar and electron-transfer pathways. *Acc. Chem. Res.* **1985**, 18, 212-219.
- Renk, E.; Shafer, P. R.; Graham, W. H.; Mazur, R. H.; Roberts, J. D. Small-ring compounds. XXXIII. A study by nuclear magnetic resonance of the extent of isotope-position rearrangement in the vapor-phase photochlorination of methyl-<sup>13</sup>C-cyclopropane. *J. Am. Chem. Soc.* **1961**, 83, 1987-1989.
- Roberts, A. L.; Totten, L. A.; Arnold, W. A.; Burris, D. R.; Campbell, T. J. Reductive elimination of chlorinated ethylenes by zero-valent metals. *Environ. Sci. Technol.* **1996**, 30, 2654-2659.
- Simmons, H. E.; Smith, R. D. A new synthesis of cyclopropanes. *J. Am. Chem. Soc.* **1959**, 81, 4256-4264.
- Touroude, R.; Gault, F. G. The mechanisms of isomerization and exchange of olefins over metal catalysts II. Exchange of olefins in the presence of perdeuteropropene on iron films. *J. Catal.* **1974**, 32, 288-293.
- Warren, K. D.; Arnold, R. G.; Bishop, T. L.; Lindholm, L. C.; Betterton, E. A. Kinetics and mechanism of reductive dehalogenation of carbon tetrachloride using zero-valence metals. *J. Haz. Mat.* **1995**, 41, 217-227.

## SECTION IV

# REDUCTIVE ELIMINATION OF CHLORINATED ETHYLENES BY ZERO-VALENT METALS

### A. ABSTRACT

Zero-valent metals currently offer a promising approach for groundwater remediation. The precise pathways through which such species reduce chloroethylenes have not been fully elucidated, nor have reaction products been completely characterized. Although reductive elimination reactions have been observed for polyhaloalkanes, they have not previously been proposed for vinyl polyhalides under environmental conditions. Thermodynamic calculations indicate reductive  $\beta$ -elimination is comparable energetically to hydrogenolysis for chloroethylenes. Batch experiments with Fe(0) suspended in water demonstrate that *cis*- and *trans*-1,2-dichloroethylene react in part via reductive  $\beta$ -elimination to acetylene. Indirect experimental evidence suggests  $\beta$ -elimination to dichloroacetylene could also occur in tetrachloroethylene reduction by Zn(0); furthermore, GC/MS analyses tentatively identify chloroacetylene as a minor product in trichloroethylene reaction with Fe(0). Such reactions may be of concern because chlorinated acetylenes are toxic. Limited information indicates chloroacetylenes may react by hydrogenolysis (to yield acetylene), hydrolysis (resulting in either acetylene or carboxylic acids), and reduction to olefins (1,2-dichloroethylenes and vinyl chloride). Some of these (especially vinyl chloride and *cis*-1,2-dichloroethylene) are only slowly degraded by zero-valent metals, and their production may dictate reactive barrier design. On the other hand, other products of reductive elimination reactions (such as acetylene and acetate) may be viewed as relatively innocuous from a remediation perspective.

### B. INTRODUCTION

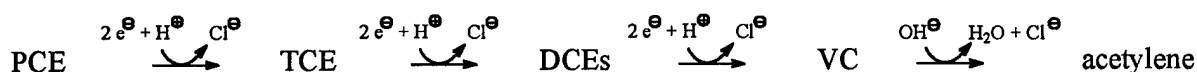
Reductive dehalogenation reactions are generally divided into two categories (Macalady *et al.*, 1986; Schwarzenbach *et al.*, 1993; Larson and Weber, 1994): hydrogenolysis (replacement of a halogen by a hydrogen); and reductive elimination (in which two halide ions are released). Both are accompanied by a net transfer of two electrons. Numerous examples of hydrogenolysis have been cited, including reduction of 1,1,1-trichloro-2,2-bis(*p*-chlorophenyl)ethane (DDT) to 1,1-dichloro-2,2-bis(*p*-chlorophenyl)ethane (DDD) (*e.g.*, Kallman and Andrews, 1963; Castro, 1964; Barker *et al.*, 1965; Guenzi and Beard, 1967; Zoro *et al.*, 1974), CCl<sub>4</sub> to CHCl<sub>3</sub> (*e.g.*, Ahr *et al.*,

1980; Bouwer and McCarty, 1983; Castro *et al.*, 1985; Galli and McCarty, 1989), and  $\text{Cl}_2\text{C}=\text{CCl}_2$  to  $\text{Cl}_2\text{C}=\text{CHCl}$  (*e.g.*, Parsons *et al.*, 1984; Vogel and McCarty, 1985; Fathepure and Boyd, 1988; Bagley and Gossett, 1990; Gantzer and Wackett, 1991). An example of reductive elimination is  $\text{Cl}_3\text{C}-\text{CCl}_3$  reaction to  $\text{Cl}_2\text{C}=\text{CCl}_2$  (*e.g.*, Kray and Castro, 1964; Criddle and McCarty, 1986; Schanke and Wackett, 1992; Roberts and Gschwend, 1994; Curtis and Reinhard, 1994). Although  $\text{CCl}_4$  reduction to CO and formate (Ahr *et al.*, 1980; Castro and Kray, 1966; Wolf *et al.*, 1977; Criddle and McCarty, 1991; Krone *et al.*, 1991; Stromeyer *et al.*, 1992) is occasionally cited as a third category, "hydrolytic reduction", this term is misleading since hydrolysis is incidental to the actual reduction. In fact, this is another example of reductive elimination, albeit one in which the halogens are released from the same carbon (reductive  $\alpha$ -elimination) to form a carbene, which subsequently reacts with the solvent. To date, however, it does not appear to have been demonstrated in the literature that halogenated ethylenes can undergo reductive  $\beta$ -elimination to alkynes under environmental conditions. The purpose of this section is to provide experimental evidence that such pathways may be involved in the reaction of chloroethylenes with zero-valent metals, as well as to speculate on the significance of the products that may result.

The use of zero-valent metals to degrade contaminants represents an active research area (Gillham and O'Hannesin, 1994; Matheson and Tratnyek, 1994; Lipczynska-Kochany *et al.*, 1994; Schreier and Reinhard, 1994; Boronina *et al.*, 1995; Powell *et al.*, 1995; Helland *et al.*, 1995; Warren *et al.*, 1995; Burris *et al.*, 1995; Orth and Gillham, 1996; Agrawal and Tratnyek, 1996). In large part this was sparked by the suggestion of Gillham and coworkers that Fe(0) could be utilized as an immobilized reagent in a passive approach to groundwater remediation. Iron's utility in subsurface treatment walls for removing organohalides has been confirmed by controlled field experiments by this group of researchers (Gillham *et al.*, 1993; Gillham, 1995). Several test installations have been completed at contaminated sites, and more are planned (Gillham *et al.*, 1993; Gillham, 1995; Puls *et al.*, 1995; Yamane *et al.*, 1995; Wilson, 1995; Roush, 1995). To date, the precise pathways through which metals reduce chloroethylenes have not been fully elucidated, nor have reaction products or intermediates been completely characterized. Such information is essential to the optimal design of remediation systems. Some of the observed products, such as vinyl chloride (Gillham and O'Hannesin, 1994; Orth and Gillham, 1996; Vogan *et al.*, 1995) are themselves of concern as drinking water contaminants, with very low maximum

contaminant level values imposed by the US EPA (Pontius, 1995). Others, including *cis*-1,2-dichloroethylene as well as vinyl chloride, react relatively slowly in the presence of Fe(0) (Gillham and O'Hannesin, 1994). The necessity of controlling levels of such undesirable by-products may dictate the overall design of metal-based remediation systems and thus the economic viability of this approach (Yamane *et al.*, 1995; Vogan *et al.*, 1995). Any efforts to identify the routes through which such products are formed, or which can account for their persistence, would clarify the potential limitations of this promising technique, or might even enable improved approaches to contaminant remediation.

One product reported in tetrachloroethylene and trichloroethylene reaction with Fe(0) is acetylene. Cipollone *et al.* (1995) have speculated this arises through the sequential hydrogenolysis of tetrachloroethylene (PCE) to trichloroethylene (TCE), dichloroethylenes (DCEs), and then vinyl chloride (VC), followed by VC dehydrohalogenation to acetylene (Scheme 14):



**Scheme 14**

Although dehydrohalogenation does occur for haloethylenes (Houser *et al.*, 1955; Miller and Lee, 1959; Kwok *et al.*, 1969), it requires extreme conditions in homogeneous solution. Thus, the second-order rate constant for OH<sup>-</sup> reaction with TCE in water at 25°C is  $1.8 \times 10^{-7} \text{ M}^{-1}\text{s}^{-1}$  (Jeffers *et al.*, 1989), yielding a half-life at pH 7 of  $10^6$  years. Even at the higher pH typical of Fe(0)-promoted reactions, reaction should still be slow, with a calculated half-life of  $10^3$  years at pH 10. Since base-promoted dehydrohalogenation reactions (which are likely to dominate over the pH-independent reaction for such substrates) are sensitive to inductive effects (Roberts *et al.*, 1993), they will undoubtedly proceed much more slowly for VC than for TCE. Such a pathway would therefore seem unlikely unless these reactions are somehow catalyzed by metal surfaces.

Calculations (shown in Table 7) indicate that reductive β-elimination reactions of chloroethylenes are in fact comparable energetically to hydrogenolysis at neutral pH. Experiments were therefore initiated to assess whether β-elimination reactions of chlorinated ethylenes could occur in the presence of two zero-valent metals, Fe and Zn.

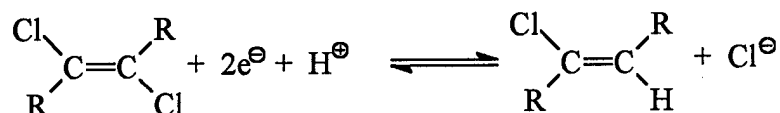


**TABLE 7. CALCULATED THERMODYNAMIC REDUCTION POTENTIALS  
(RELATIVE TO STANDARD HYDROGEN ELECTRODE) FOR NET TWO-  
ELECTRON REDUCTION OF CHLORINATED ETHYLENES TO THE  
CORRESPONDING HYDROGENOLYSIS PRODUCTS AND  $\beta$ -ELIMINATION  
PRODUCTS IN AQUEOUS SOLUTION AT 25°C.**

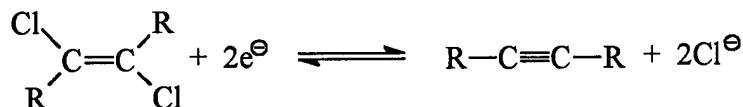
Parent Compound	Product	$E_H^\circ(W)$ (V) <sup>b</sup>	Product	$E_H^\circ(W)$ (V) <sup>c</sup>
tetrachloroethylene	trichloroethylene	0.592	dichloroacetylene	0.631
trichloroethylene	cis-1,2-dichloroethylene	0.530	chloroacetylene	0.599
trichloroethylene	1,1-dichloroethylene	0.513		
trichloroethylene	trans-1,2-dichloroethylene	0.509		
1,1-dichloroethylene	vinyl chloride	0.423	NA <sup>d</sup>	
cis-1,2-dichloroethylene	vinyl chloride	0.407	acetylene	0.568
trans-1,2-dichloroethylene	vinyl chloride	0.428	acetylene	0.589
vinyl chloride	ethylene	0.481	NA <sup>d</sup>	

<sup>a</sup>Calculations assume that radical species have the same Henry's law constant as the hydrogenated parent (Eberson, 1982) and  $\{H^+\} = 10^{-7}$  m,  $\{Cl^-\} = 10^{-3}$  M, all other species at unit activity. Gas-phase thermodynamic data from Wagman *et al.* (1982); Dean (1987); Taylor (1991); and Wang (1994), corrected for air-water partitioning using Henry's law constants recommended by Mackay *et al.* (1993), reported by Hine and Mookerjee (1975), or estimated according to the method of Hine and Mookerjee (1975).

<sup>b</sup>Reduction potential corresponding to overall hydrogenolysis reaction:



<sup>c</sup>Reduction potential corresponding to overall reductive  $\beta$ -elimination reaction:



<sup>d</sup>NA = not applicable; reductive  $\beta$ -elimination pathway does not exist for this compound

## C. EXPERIMENTAL SECTION

### 1. Reduction of Dichloroethylenes by Fe(0)

Experiments were conducted in 25-mL serum bottles capped with Teflon septa. Each bottle contained 1.7 g of Fe(0) (Fisher, 40 mesh) and 34 mg of finely ground Fe pyrite (Ward's Natural Science Est, Inc.), suspended in 1.7 mL of deoxygenated (Ar-sparged) deionized water (Milli-Q Plus UV, Millipore). Pyrite was included for consistency with studies reported elsewhere (Burris *et al.*, 1995; Allen-King *et al.*, 1997). The iron was cleaned by washing in Ar-sparged 1 N HCl. Surface area analyses conducted via Kr BET adsorption using a Micromeritics Flowsorb II 2300 device indicated a surface area of  $0.7 \text{ m}^2/\text{g}$ . Reaction mixtures were prepared in an anaerobic chamber (Coy Laboratory products) containing an atmosphere of 10%  $\text{H}_2$  in  $\text{N}_2$ . Bottles were spiked with either 6.7  $\mu\text{L}$  of a solution of *trans*-DCE, 4.4  $\mu\text{L}$  of *cis*-DCE, 10  $\mu\text{L}$  of 1,1-DCE, or 30  $\mu\text{L}$  of VC in methanol (containing hexane as an internal standard), and were mixed on a rotator (Cole-Parmer) at 4 RPM. At selected intervals, 100  $\mu\text{L}$  headspace aliquots were removed (accompanied by injection of an equivalent volume of purified argon), and were injected in splitless mode onto a Fisons 8000 Series Gas Chromatograph (GC) equipped with a GS-Q PLOT column (J & W Scientific) and a flame ionization detector (FID). The possibility of mass transfer-limited air-water exchange of parent compounds and reaction products into the headspace in these systems forestalls a detailed kinetic analysis of the resulting data. Nevertheless, the high ratio of headspace to solution volume in these experiments provides an advantage in identifying reaction pathways, in that more highly volatile reaction products and intermediates will partition into the headspace rather than remaining in solution or sorbing to the metal surface (Burris *et al.*, 1995), thereby slowing their further reaction, enhancing their accumulation, and facilitating their detection.

### 2. Reduction of Chlorinated Ethylenes by Zn(0)

Reactions were carried out in 1-L flasks equipped with a glass stopcock adapter, filled with 0.1 M deoxygenated NaCl solution to which 200 g of 30 mesh Zn(0) (100.5%, J. T. Baker) was added. Although a pH buffer was not employed, the pH remained relatively stable, diminishing at most from  $\text{pH } 7.1 \pm 0.1$  to  $6.7 \pm 0.1$ . The zinc was cleaned by washing with 400 mL 0.4%  $\text{H}_2\text{SO}_4$ . Krypton BET analyses indicated a surface area of  $0.035 \text{ m}^2/\text{g}$ . Note that in these

experiments, essentially no headspace was initially present (to facilitate kinetic modeling of reaction pathways), although minor amounts ( $< 20$  mL) were eventually produced, presumably through  $H_2$  evolution from reaction of Zn with water. Flasks were spiked with 0.5 mL of a methanol solution of the target compound (either PCE, TCE, or *trans*-DCE), and were mixed by rotating about their long axes at 20-30 RPM. One-mL aliquots were periodically removed using 2-mL glass syringes (equipped with 3-way metal stopcock adapters, one end of which was plugged with an airtight septum), accompanied by introduction of an equivalent volume of deoxygenated water. One mL of air was then injected through the septum into the syringe, as was 1  $\mu$ L of a methanol solution of hexane (as an internal standard). Syringes were shaken vigorously by hand, and 100  $\mu$ L headspace samples were analyzed by GC-FID as previously described. Results were modeled using the kinetic package *Scientist for Windows* v. 2.01 (Micromath Scientific Software, Inc., Salt Lake City, UT). This software package determines reaction rate constants and associated parameters by fitting experimental data to numerically integrated solutions of systems of differential rate expressions.

## D. RESULTS AND DISCUSSION

Results for *trans*- and *cis*-DCE transformation are shown in Figure 39. Both react primarily to acetylene and ethylene, with acetylene exhibiting accumulation and decay typical of a reaction intermediate. Lesser amounts of ethane and VC were also observed, as were trace quantities of methane, propane, propene, butane, and 1-butene. In the absence of headspace, *trans*-DCE reacts with  $Fe(0) \sim 10 \times$  faster than *cis*-DCE (Allen-King *et al.*, 1997); this reactivity contrast is however muted in the presence of appreciable headspace, owing to the higher Henry's law constant of *trans*-DCE.

a) *trans*-DCE

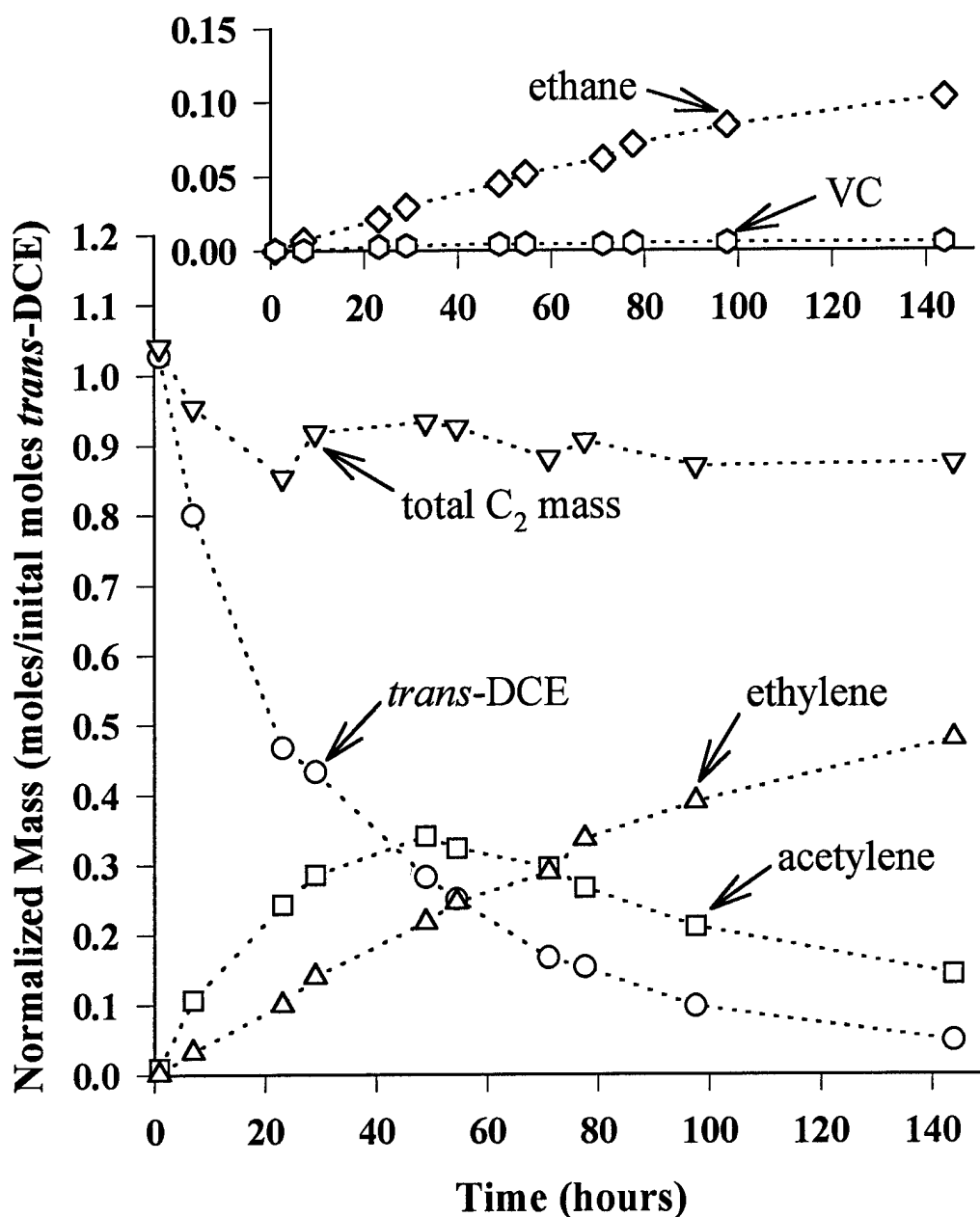


**Figure 39:** Reaction of *cis*- and *trans*-DCE in the presence of Fe(0) in high headspace system experiments. Results not corrected for sorption of dichloroethylenes onto Fe(0) (Allen-King *et al.*, 1997) (a) results for *trans*-DCE; (b) results for *cis*-DCE. Initial DCE concentrations obtained by fitting DCE data to an exponential decay expression.

**b) *cis*-DCE**

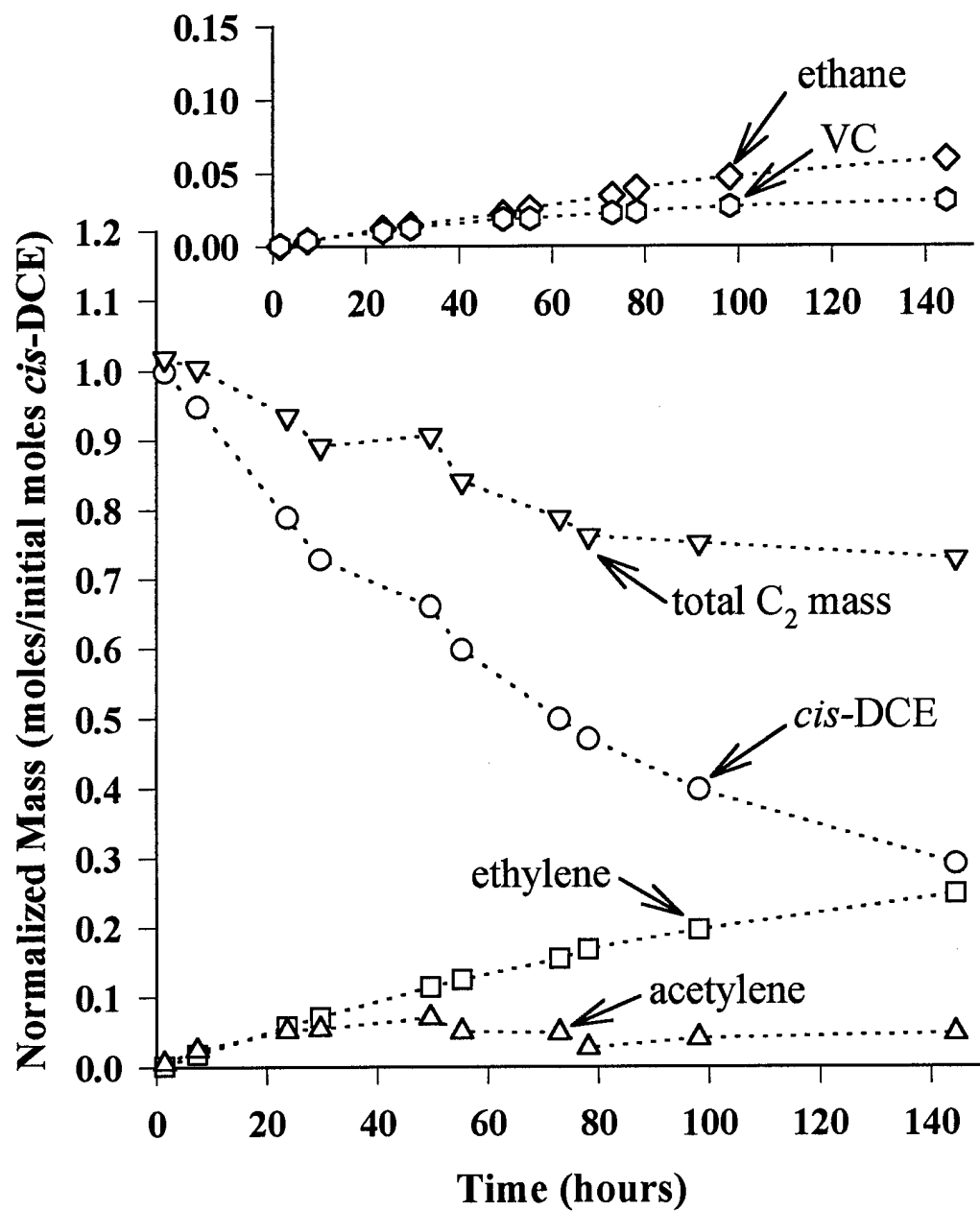


Figure 39 (continued)

The results indicate a VC yield from *cis*-DCE approximately 7 times as great as from *trans*-DCE. Parallel experiments failed to evince any acetylene production in the reduction of VC or 1,1-DCE over the course of 10 days (during which 25% of the VC and 10% of the 1,1-DCE underwent transformation); rather, both reacted to ethylene and ethane as principal products. Nor was any acetylene observed in the absence of added organohalide.

A scheme that could account for these products is shown in Figure 40 for reduction of *trans*-DCE. In principle, reaction could proceed through transfer of a single electron to form a free radical. This could either undergo a second one-electron reduction to a vinyl carbanion, or else abstract a hydrogen atom from a suitable donor to yield VC. Alternatively, reaction could occur by transfer of two electrons essentially in a single step. This two electron transfer could yield a vinyl carbanion, or it could proceed in a concerted manner to produce acetylene directly.

It is known from experiments in homogeneous solution that vinyl carbanions are reversibly formed in haloethylene dehydrohalogenation. For example, the hydrogen of TCE can be exchanged with that of water (Houser *et al.*, 1955; Leitch *et al.*, 1950). Such vinyl carbanions are more stable than are alkyl carbanions owing to the higher degree of *s* character in the  $sp^2$  hybrid orbital (March, 1985). Although the deprotonation step in dehydrohalogenation is slow, Miller and Lee (1959) found that the free vinyl carbanion resulting from deprotonation of *cis*-1,2-dibromoethylene- $d_2$  underwent reprotonation  $\sim 25$  times more rapidly than elimination. Thus, if reaction of chlorinated ethylenes were to proceed either via a free vinyl carbanion or a free radical intermediate, some of the corresponding hydrogenolysis product might be anticipated.

On the other hand, the vinyl carbanion could also undergo  $\beta$ -elimination to an alkyne. A characteristic of such reactions is that elimination of *trans* substituents is much more favorable than is *cis* elimination. In the absence of isomerization of the vinyl carbanion, dehalogenation should therefore proceed more readily for substrates bearing a  $\beta$ -halogen *trans* to the lone pair on the  $\alpha$  carbon than for substrates possessing a  $\beta$ -halogen only in the *cis* position. Such isomerization has previously been shown to be negligible for  $\text{:CCl=CHCl}$  carbanions (Miller and Lee, 1959).

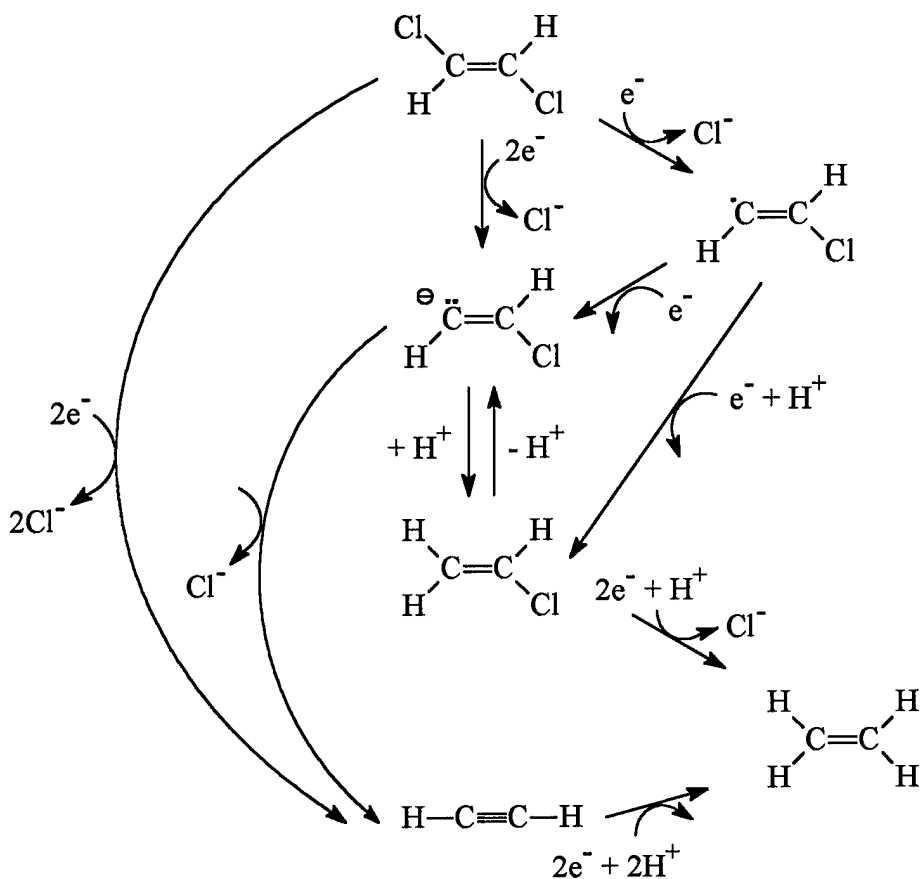


**Figure 40:** Proposed pathways for reduction of *trans*-dichloroethylene by zero-valent metals.

Acetylenes could also originate from the concerted elimination of an  $\alpha$ ,  $\beta$ -dihaloolefin, especially if the halogens were *trans* to one another. The unavailability of a concerted reductive *trans*  $\beta$ -elimination pathway and the greater likelihood of carbanion protonation relative to *cis* elimination should together dictate that a higher yield of a hydrogenolysis product should result from reduction of a *cis*- $\alpha$ ,  $\beta$ -dihaloolefin, compared to a *trans*-dihaloalkene. This prediction is in accordance with the results obtained with *cis*- and *trans*-DCE. In addition to geometric factors, whether or not a given compound might undergo reduction to a vinyl carbanion (part of which could protonate to the hydrogenolysis product) or alternatively undergo a concerted reaction to an alkyne, may depend in part on factors that serve to stabilize the vinyl carbanion. These might include the presence of electron-withdrawing substituents such as halogens (March 1985) or coordination by metal ions (possibly adsorbed at the metal surface).

A pathway analogous to Figure 40 would imply that PCE could be reduced to dichloroacetylene, and TCE to chloroacetylene, reactions potentially of environmental significance. Both dichloroacetylene and chloroacetylene are reported to be toxic (Piganiol, 1950; Rutledge, 1968). The amounts that might accumulate would depend on rates of their production and subsequent transformation.

Limited evidence suggests that chlorinated acetylenes are unstable. Both are spontaneously flammable in air (Piganiol, 1950), and calculations (Table 7) indicate that their hydrogenolysis to form lesser-halogenated acetylenes is plausible under appropriate conditions, as is their reduction to substituted ethylenes. An additional process chloroacetylenes might undergo is hydrolysis. Although the  $sp^2$ -hybridized carbon of chloroethylenes is resistant to hydrolysis, the C-Cl bond of  $sp$ -hybridized carbon of chlorinated acetylenes possesses unique features that render it susceptible to such reactions. Nucleophilic solvents can attack at Cl (rather than C) to yield the same lesser-halogenated acetylene derivatives that result from hydrogenolysis (Rutledge, 1968; Delavarenne and Viehe, 1969) plus HOCl (in the case of attack by OH<sup>-</sup>). Alternatively, the solvent can react with the halogenated acetylene derivative *via* an addition pathway to ultimately form carboxylic acids (Piganiol, 1950; Delavarenne and Viehe, 1969). Thus, some acetate might be produced from chloroacetylene hydrolysis in aqueous solution; similarly, chloroacetate might be expected to result from dichloroacetylene hydrolysis.

Reduction of PCE by Zn(0) (Figure 41) provides indirect evidence that dichloroacetylene may represent an unstable intermediate. TCE represents the principal product, although lesser amounts of both *trans*-DCE and acetylene were also observed, as well as traces of ethylene and *cis*-DCE. Parallel experiments confirmed that TCE and *trans*-DCE reacted at least an order of magnitude more slowly than PCE under these conditions. Attempts to model the *trans*-DCE and acetylene data by invoking sequential reduction of PCE → TCE → *trans*-DCE → acetylene were unsuccessful (see inset in Figure 41); TCE and *trans*-DCE react insufficiently rapidly to account for the rate of accumulation of their respective products. Modeling the data by invoking parallel reactions of PCE to TCE, *trans*-DCE, and acetylene, however, captures most of the features of the observed *trans*-DCE and acetylene data. This is consistent with the possibility that acetylene could be formed from the reduction of a transitory dichloroacetylene intermediate which



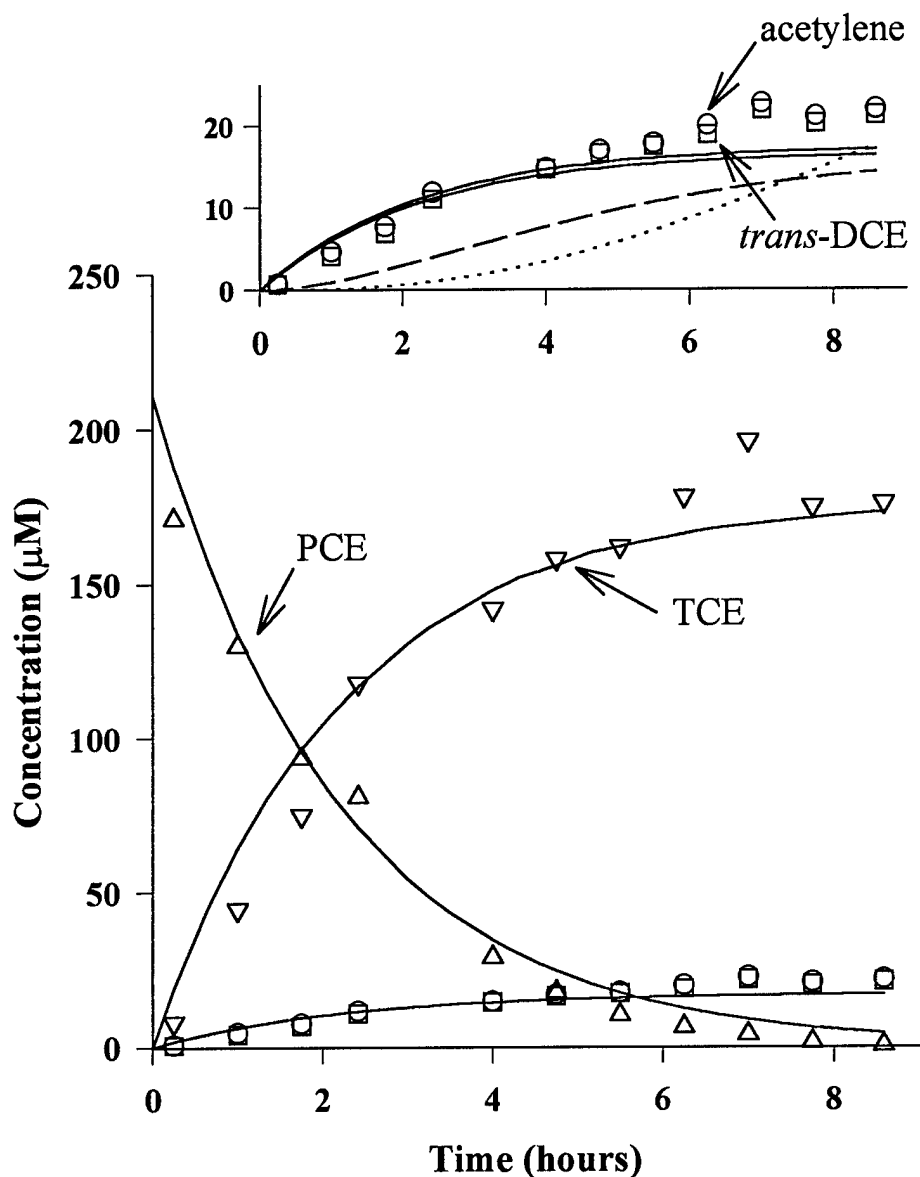


**Figure 41:** Reduction of PCE by Zn(0) in system containing 0.1 M deoxygenated NaCl solution with minimal headspace. Solid lines represent model fits assuming parallel reactions of PCE to TCE, *trans*-DCE, and acetylene, assuming all reaction products to be stable during the time frame of this experiment. Dashed line and dotted line in inset represent model fit to *trans*-DCE and acetylene data, respectively, assuming sequential reduction of PCE → TCE → *trans*-DCE → acetylene.

undergoes rapid reduction to *trans*-DCE and chloroacetylene, the latter rapidly reacting further to acetylene. The true situation is likely to represent some combination of parallel and sequential reactions; more extensive studies will be required to assess the relative contributions of each.

There is some precedent for invoking chloroacetylenes as products of more highly chlorinated ethylene reduction. For example, one pathway to chloroacetylene synthesis involves the reduction of vicinal polyhaloalkanes or alkenes by zero-valent metals in organic solvents (Nieuwland and Vogt, 1945). Delavarenne and Viehe (1969) note that a similar reduction in protic solvents is of limited practical value, since the products often react further. One group of researchers (Tezuka and Yajima, 1991) claims to have measured chloroacetylene (but not dichloroacetylene) in the electrochemical reduction of PCE in aqueous hexamethylphosphoramide solution. Interestingly, although reaction of substituted acetylenes with H<sub>2</sub> (hydrogenation) to the corresponding substituted olefins should preferentially follow a *cis* addition pathway, these researchers proposed that dichloroacetylene underwent reduction to *trans*-DCE. Castro and Stephens (1964) have found that the reduction of substituted acetylenes by Cr<sup>2+</sup> in aqueous solution results exclusively in *trans* rather than *cis*-olefins. This supports the possibility that the *trans*-DCE observed in PCE reduction by Zn(0) could have arisen from a dichloroacetylene intermediate. If chlorinated acetylenes were to be formed during PCE or TCE reduction by zero-valent metals, such reactions could thus at least partially account for the production of VC and 1,2-DCE isomers. Sivavek (1995) has also identified chloroacetylene in the reduction of TCE by Fe(0) in aqueous solution. We have also tentatively identified chloroacetylene as a trace product of TCE reduction by Fe(0), based on GC/MS analyses of headspace samples.

At present, insufficient information exists to prove whether electron transfer to chlorinated ethylenes is a one- or a two-electron process for reduction by zero-valent metals. Spin-trapping agents that might be useful in ESR analyses react readily with metals, possibly accounting for the lack of success reported to date (Sivavec and Horney, 1995). A comparison of the calculated one- and two-electron reduction potentials of chloroethylenes (Table 7) demonstrates that two-electron pathways (either hydrogenolysis or reductive  $\beta$ -elimination reactions) are favored over single-electron pathways, reflecting the relative instability of free radical intermediates in aqueous solution. We have found that the reductive elimination of probe compounds (*erythro* and *threo* isomers of 2,3-dibromopentane) by Zn(0), Fe(0), Al(0) and Cu(0) in aqueous solution at room

temperature proceeds with virtually complete stereospecificity (Totten and Roberts, 1995). This indicates that electron transfer from these metals to the substrates proceeds rapidly compared to the rate of rotation about the carbon-carbon bond, suggesting that at least some metal-promoted reductive  $\beta$ -elimination reactions can be viewed as an essentially concerted transfer of two electrons.

Further indirect evidence that tends to support a two-electron pathway comes from attempted linear free-energy relationships between reactivity in the Fe(0)-promoted reduction of chloroethylenes and thermodynamic reduction potentials. If regressions are conducted for reaction rate constants reported by Gillham and O'Hannesin (1994) against the one- and two-electron reduction potentials shown in Table 7, the results indicate that the relationship between reactivity and one-electron reduction potential is very weak [ $R^2(\text{adj}) = -0.0754$ ]. In contrast, significantly better correlations are obtained by regressing reaction rate constants against 2-electron reduction potentials, either for hydrogenolysis reactions [ $R^2(\text{adj}) = 0.749$ ] or  $\beta$ -elimination reactions [ $R^2(\text{adj}) = 0.808$ ]. Further proof of the one- versus the two-electron character of the reaction must await more detailed investigations.

If reduction of halogenated ethylenes with zero-valent metals does show a strong preference for a concerted two-electron  $\beta$ -elimination pathway, this might account for the sluggish rates of reaction of chloroethylenes lacking the requisite *trans*  $\alpha$ ,  $\beta$  pair of halogens, such as VC, 1,1-DCE, and *cis*-DCE, potentially accounting for their persistence in zero-valent metal-based remediation schemes. Although the reduction of PCE by Zn(0) does result in TCE as a major product, an observation inconsistent with a concerted reductive  $\beta$ -elimination pathway, this may simply reflect the greater degree of stabilization of a vinyl carbanion by the additional halogen substituents, and may not signify a similar minor role for the concerted  $\beta$ -elimination of lesser-halogenated ethylenes.

Reductive  $\beta$ -elimination may be mediated by species other than zero-valent metals. For example, Burris *et al.* (1996) have found the reduction of PCE and TCE by vitamin B<sub>12</sub> yields a significant amount of acetylene. It may be noteworthy that in these experiments, vitamin B<sub>12</sub> was reduced with Ti(III) citrate, which spectroscopic evidence has shown to reduce the metal center to the Co(I) oxidation state (Chiu and Reinhard, 1995). This raises the possibility that fully reduced vitamin B<sub>12</sub> could serve as a two-electron reductant. Strongly nucleophilic species are

known to promote reductive elimination of vicinal dihaloalkanes through a process (involving nucleophilic attack on a halogen) that can be viewed as a two-electron reduction (Schrauzer and Deutsch, 1969); in this respect, it may be worth noting that Co(I) corrinoids have been referred to as “supernucleophiles” (Schrauzer and Deutsch, 1969). Belay and Daniels (1987) have also reported acetylene production from 1,2-dibromoethylene (isomer unspecified) in pure cultures of methanogenic bacteria. These workers did not speculate as to the pathway involved. In light of the foregoing evidence, we consider reductive  $\beta$ -elimination to be a plausible explanation. Future investigations should consider the possibility of reductive  $\beta$ -elimination reactions of vicinal dihaloalkenes, as well as the potential environmental significance of some of the intermediates of these reactions.

## E. LITERATURE CITED

- Agrawal, A.; Tratnyek, P. G., 1995. Reduction of nitroaromatic compounds by zero-valent iron metal. *Environ. Sci. Technol.* **1996**, *30*, 153-160.
- Ahr, H. J.; King, L. J.; Nastainczyk, W.; Ullrich, V. The mechanism of chloroform and carbon monoxide formation from carbon tetrachloride by microsomal cytochrome P-450. *Biochem. Pharmacol.* **1980**, *29*, 2855-2861.
- Allen-King, R. M.; Halket, R. M.; Burris, D. R. Reductive transformation and sorption of *cis*- and *trans*-1,2-dichloroethylene in a metallic iron-water system. *Environ. Toxicol. Chem.*, **1997**, *16*, 424-429.
- Bacocchi, E. "1,2-Dehalogenations and related reactions." In *The Chemistry of Halides, Pseudo-Halides, and Azides, Supplement D*; Patai, S. G.; Rappoport, Z., Eds.; Wiley and Sons: New York, 1983; Vol.1, 161-201.
- Bagley, D. M.; Gossett, J. M. Tetrachloroethene transformation to trichloroethene and *cis*-1,2-dichloroethene by sulfate-reducing enrichment cultures. *Appl. Environ. Microbiol.* **1990**, *56*, 2511-2516.
- Barker, P. S.; Morrison, F. O.; Whitaker, R. S. Conversion of DDT to DDD by *Proteus vulgaris*, a bacterium isolated from the intestinal flora of a mouse. *Nature* **1965**, *205*, 621-654.
- Belay, N.; Daniels, L. Production of ethane, ethylene and acetylene from halogenated hydrocarbons by methanogenic bacteria. *Appl. Environ. Microbiol.* **1987**, *53*, 1604-1610.
- Boronina, T.; Klabunde, K. J.; Sergeev, G. Destruction of organohalides in water using metal particles: carbon tetrachloride/water reactions with magnesium, tin, and zinc. *Environ. Sci. Technol.* **1995**, *29*, 1511-1517.
- Bouwer, E. J.; McCarty, P. L. Transformations of halogenated organic compounds under denitrification conditions. *Appl. Environ. Microbiol.* **1983**, *45*, 1295-1299.
- Burris, D. R.; Campbell, T. J.; Manoranjan, V. S. Sorption of trichloroethylene and tetrachloroethylene in a batch reactive metallic iron-water system. *Environ. Sci. Technol.* **1995**, *29*, 2850-2855.

- Burris, D. R.; Delcomyn, C. A.; Smith, M. H.; Roberts, A. L.. Reductive dechlorination of tetrachloroethene and trichloroethene catalyzed by vitamin B<sub>12</sub> in homogeneous and heterogeneous systems. *Environ. Sci. Technol.*, **1996**, *30*, 3047-3052.
- Castro, C. E. The rapid oxidation of iron (II) porphyrins by alkyl halides. A possible mode of intoxication of organisms by alkyl halides. *J. Amer. Chem. Soc.* **1964**, *86*, 2310-2311.
- Castro, C. E.; Stephens, R. D. The reduction of multiple bonds by low-valent transition metal ions. The homogeneous reduction of acetylenes by chromous sulfate. *J. Amer. Chem. Soc.* **1964**, *86*, 4358-4363.
- Castro, C. E.; Kray, W. C. Carbenoid intermediates from polyhalomethanes and chromium (II). The homogeneous reduction of geminal halides by chromous sulfate. *J. Amer. Chem. Soc.* **1966**, *88*, 4447-4455.
- Castro, C. E.; Wade, R. S.; Belser, N. O. Biodehalogenation: reactions of cytochrome P-450 with polyhalomethanes. *Biochem.* **1985**, *24*, 204-210.
- Chiu, P.-C.; Reinhard, M. Metallocoenzyme-mediated reductive transformation of carbon tetrachloride in titanium (III) citrate aqueous solution. *Environ. Sci. Technol.* **1995**, *29*, 595-603.
- Cipollone, M. G.; Wolfe, N. L.; Hassan, S. M. Kinetic studies on the use of metallic iron to reduce organic compounds in water under environmental conditions. *Natl. Meet. - Am. Chem. Soc., Div. Environ. Chem.* **1995**, *35*, 812-814 (Abstr.).
- Criddle, C. S.; McCarty, P. L.; Elliott, M.C.; Barker, J. F. Reduction of hexachloroethane to tetrachloroethylene in groundwater. *J. Contam. Hydrol.* **1986**, *1*, 133-142.
- Criddle, C. S.; McCarty, P. L. Electrolytic model system for reductive dehalogenation in aqueous environments. *Environ. Sci. Technol.* **1991**, *25*, 973-978.
- Curtis, G. P.; Reinhard, M. Reductive dehalogenation of hexachloroethane, carbon tetrachloride, and bromoform by anthraquinone disulfonate and humic acid. *Environ. Sci. Technol.* **1994**, *28*, 2393-2401.
- Dean, J. A. *Handbook of Organic Chemistry*; McGraw-Hill: New York, 1987.

- Delavarenne, S. Y.; Viehe, H. G. In *Chemistry of Acetylenes*; Viehe, H. G., Ed.; Marcel Dekker: New York, 1969; pp. 651-750.
- Eberson, L. Electron transfer reactions in organic chemistry. II. An analysis of alkyl halide reduction by electron transfer reagents on the basis of Marcus theory. *Acta Chem. Scand. B* **1982**, *36*, 533-543.
- Fathpure, B. Z.; Boyd, S. A. Dependence of tetrachloroethylene dechlorination of methanogenic substrate consumption by *Methanosacina* sp. strain DCM. *Appl. Environ. Microbiol.* **1988**, *54*, 2976-2980.
- Galli, R.; McCarty, P. L. Biotransformation of 1,1,1-trichloroethane, trichloromethane, and tetrachloromethane by a *Clostridium* sp. *Appl. Environ. Microbiol.* **1989**, *55*, 837-844.
- Gantzer, C. J.; Wackett, L. P. Reductive dechlorination catalyzed by bacterial transition-metal coenzymes. *Environ. Sci. Technol.* **1991**, *25*, 715-722.
- Gillham, R. W.; O'Hannesin, S. F.; Orth, W. S. Metal enhanced abiotic degradation of halogenated aliphatics: laboratory tests and field trials. Paper presented at the 1993 HazMat Central Conference, Chicago, Illinois, March 9-11, 1993.
- Gillham, R. W.; O'Hannesin, S. F. Enhanced degradation of halogenated aliphatics by zero-valent iron. *Ground Water* **1994**, *32*, 958-967.
- Gillham, R. W. Resurgence of research concerning organic transformations enhanced by zero-valent metals and potential application in remediation of contaminated groundwater. *Natl. Meet. - Am. Chem. Soc., Div. Environ. Chem.* **1995**, *35*, 691-694 (Abstr.).
- Guenzi, W. D.; Beard, W. E. Anaerobic biodegradation of DDT to DDD in soil. *Science* **1967**, *156*, 1116-1117.
- Helland, B. R.; Alvarez, P. J. J.; Schnoor, J. L. Reductive dechlorination of carbon tetrachloride with elemental iron. *J. Haz. Mater.* **1995**, *41*, 205-216.
- Hine, J.; Mookerjee, P. K. The intrinsic hydrophilic character of organic compounds. Correlations in terms of structural contributions. *J. Org. Chem.* **1975**, *40*, 292-298.

- Houser, T. J.; Bernstein, R. B.; Miekka, R. G.; Angus, J. C. Deuterium exchange between trichloroethylene and water. Infrared spectral data for trichloroethylene-*d*. *J. Amer. Chem. Soc.* **1955**, *77*, 6201-6203.
- Jeffers, P. M.; Ward, L. M.; Woytowitch, L. M.; Wolfe, N. L. Homogeneous hydrolysis rate constants for selected methanes, ethanes, ethenes, and propanes. *Environ. Sci. Technol.* **1989**, *23*, 965-969.
- Kallman, B. J.; Andrews, A. K. Reductive dechlorination of DDT to TDE by yeast. *Science* **1963**, *141*, 1050-1051.
- Kray, W. C.; Castro, C. E. The cleavage of bonds by low-valent transition metal ions. The homogeneous dehalogenation of vicinal dihalides by chromous sulfate. *J. Amer. Chem. Soc.* **1964**, *86*, 4603-4608.
- Krone, U. E.; Thauer, R. K.; Hogenkamp, H. P. C.; Steinbach, K. Reductive formation of carbon monoxide from CCl<sub>4</sub> and FREONS 11, 12, and 13 catalyzed by corrinoids. *Biochem.* **1991**, *30*, 2713-2719.
- Kwok, W. K.; Lee, W. G.; Miller, S. I. The kinetics, isotope rate effect, and mechanism of dehydrobromination of *cis*-1,2-dibromoethylene with triethylamine in dimethylformamide. *J. Amer. Chem. Soc.* **1969**, *91*, 468-476.
- Larson, R. A.; Weber, E. J. *Reaction Mechanisms in Environmental Organic Chemistry*; Lewis Publishers: Boca Raton, 1994.
- Leitch, L. C.; Bernstein, H. J. Deuterium exchange in trichloroethylene. *Can. J. Research* **1950**, *28B*, 35-36.
- Lipczynska-Kochany, E.; Harms, S.; Milburn, R.; Sprah, G.; Nadarajah, N. Degradation of carbon tetrachloride in the presence of iron and sulfur containing compounds. *Chemosphere* **1994**, *29*, 1477-1489.
- Macalady, D. L.; Tratnyek, P. G.; Grundl, T. J., 1986. Abiotic reduction reactions of anthropogenic organic chemicals in anaerobic systems: a critical review. *J. Contam. Hydrol.* **1986**, *1*, pp. 1-28.



- Mackay, D.; Shiu, W. Y.; Ma, K. C. *Illustrated Handbook of Physical-Chemical Properties and Environmental Fate for Organic Chemicals*, Vol. 3; Lewis Publishers: Boca Raton, FL, 1993.
- March, J. *Advanced Organic Chemistry: Reactions, Mechanisms, and Structure*; 3rd ed.; John Wiley and Sons: New York, 1985.
- Matheson, L.; Tratnyek, P. G. Reductive dehalogenation of chlorinated methanes by iron metal. *Environ. Sci. Technol.* **1994**, *28*, 2045-2053.
- Miller, S. I.; Lee, W. G. The vinyl carbanion. *J. Amer. Chem. Soc.* **1959**, *81*, 6313-6319.
- Nieuwland, J. A.; Vogt, R. R. *The Chemistry of Acetylene*; Reinhold Publishing: New York, 1945.
- Orth, W. S.; Gillham, R. W. Dechlorination of trichloroethene in aqueous solution using  $\text{Fe}^0$ . *Environ. Sci. Technol.* **1996**, *30*, 66-71.
- Parsons, F.; Wood, P. R.; DeMarco, J. Transformations of tetrachloroethene and trichloroethene in microcosms and groundwater. *J. Am. Water Works Assoc.* **1984**, *76*, 56-59.
- Piganiol, P. *Acetylene Homologs and Derivatives*; Mapleton House: New York, 1950.
- Pontius, F. W. An update of the federal drinking water regulations. *Jour. AWWA* **1995**, *87*, 48-58.
- Powell, R. M.; Puls, R. W.; Hightower, S. K.; Sabatini, D. A. Coupled iron corrosion and chromate reduction: mechanisms for subsurface remediation. *Environ. Sci. Technol.* **1995**, *29*, 1913-1922.
- Puls, R. W.; Powell, R. M.; Paul, C. J. In situ remediation of ground water contaminated with chromate and chlorinated solvents using zero-valent iron: a field study. *Natl. Meet. - Am. Chem. Soc., Div. Environ. Chem.* **1995**, *35*, 788-791 (Abstr.).
- Roberts, A. L.; Jeffers, P. M.; Wolfe, N. L.; Gschwend, P. M. Structure-reactivity relationships in dehydrohalogenation reactions of polychlorinated and polybrominated alkanes. *Critical Reviews in Environmental Science and Technology* **1993**, *23*, 1-39.
- Roberts, A. L.; Gschwend, P. M. Interaction of abiotic and microbial processes in hexachloroethane transformation in groundwater. *J. Contam. Hydrol.* **1994**, *16*, 157-174.
- Roush, W. Building a wall against toxic waste. *Science* **1995**, *269*, 473.

- Rutledge, T. F. *Acetylenic Compounds: Preparation and Substitution Reactions*; Reinhold: New York, 1968.
- Schanke, C. A.; Wackett, L. P. Environmental reductive elimination reactions of polychlorinated ethanes mimicked by transition-metal coenzymes. *Environ. Sci. Technol.* **1992**, *26*, 830-833.
- Schrauzer, G. N.; Deutsch, E. Reactions of cobalt (I) supernucleophiles. The alkylation of vitamin B<sub>12</sub>s, cobaloximes (I), and related compounds. *J. Amer. Chem. Soc.* **1969**, *91*, 3341-3350.
- Schreier, C. G.; Reinhard, M. Transformation of chlorinated organic compounds by iron and manganese powders in buffered water and in landfill leachate. *Chemosphere* **1994**, *29*, 1743-1753.
- Schwarzenbach, R. P.; Gschwend, P. M.; Imboden, D. M. *Environmental Organic Chemistry*. Wiley-Interscience: New York, 1993.
- Sivavec, T. M. Reductive dechlorination of chlorinated solvents by iron metal and iron sulfide minerals. IBC International Symposium on Biological Dehalogenation, Annapolis, MD, Oct. 19, 1995 (Abstr.).
- Sivavec, T. M.; Horney, D. P. Reductive dechlorination of chlorinated ethenes by iron metal. *Natl. Meet. - Am. Chem. Soc., Div. Environ. Chem.* **1995**, *35*, 695-698 (Abstr.).
- Stromeyer, S. A.; Stumpf, K.; Cook, A. M.; Leisinger, T. Anaerobic degradation of tetrachloromethane by *Acetobacterium woodii*: separation of dechlorinative activities in cell extracts and roles for vitamin B<sub>12</sub> and other factors. *Biodegradation* **1992**, *3*, 113-123.
- Taylor, P. H.; Dellinger, B.; Tirey, D. A. Oxidative pyrolysis of CH<sub>2</sub>Cl<sub>2</sub>, CHCl<sub>3</sub>, and CCl<sub>4</sub> - I: Incineration implications. *Int. J. Chem. Kinetics* **1991**, *23*, 1051-1074.
- Tezuka, M.; Yajima, T. Electroreductive dechlorination of chloroethylenes. *Denki Kagaku oyobi Kogyo Butsuri Kagaku* **1991**, *59*, 517-518.
- Totten, L. A.; Roberts, A. L. Investigating electron transfer pathways during reductive dehalogenation reactions promoted by zero-valent metals. *Natl. Meet. - Am. Chem. Soc., Div. Environ. Chem.* **1995**, *35*, 706-710 (Abstr.).

- Vogan, J. L.; Gillham, R. W.; O'Hannesin, S. F.; Matulewicz, W. H.; Rhodes, J. E., 1995. Site specific degradation of VOCs in groundwater using zero valent iron. *Natl. Meet. - Am. Chem. Soc., Div. Environ. Chem.* **1995**, *35*, 800-804 (Abstr.).
- Vogel, T. M.; McCarty, P. L. Biotransformation of tetrachloroethylene to trichloroethylene, dichloroethylene, vinyl chloride and carbon dioxide under methanogenic conditions. *Appl. Environ. Microbiol.* **1985**, *49*, 1080-1083.
- Wagman, D. D.; Evans, W. H.; Parker, V. B.; Schumm, R. H.; Halow, I.; Bailey, S. M.; Churney, K. L.; Nuttall, R. L. The NBS tables of chemical thermodynamic properties. Selected values for inorganic and C<sub>1</sub> and C<sub>2</sub> organic substances in SI units. *J. Phys. Chem. Ref. Data*, *II*, **1982**, 1-103.
- Wang, H.; Frenklach, M. Calculations of rate coefficients for the chemically activated reactions of acetylene with vinylic and aromatic radicals. *J. Phys. Chem.* **1994**, *98*, 11465-11489.
- Warren, K. D.; Arnold, R. G.; Bishop, T. L.; Lindholm, L. C.; Betterton, E. A. Kinetics and mechanism of reductive dehalogenation of carbon tetrachloride using zero-valence metals. *J. Haz. Mater.* **1995**, *41*, 217-227.
- Wilson, E. K. Zero-valent metals provide possible solution to groundwater problems. *C&E News* **1995**, *73* (27), 19-22.
- Wolf, C. R.; Mansuy, D.; Nastainczyk, W.; Deutschmann, G.; Ullrich, V. The reduction of polyhalogenated methanes by liver microsomal cytochrome P-450. *Molec. Pharmacol.* **1977**, *13*, 698-705.
- Yamane, C. L.; Gallinatti, J. D.; Szerdy, F. S.; Delfino, T. A.; Hankins, D. A.; Vogan, J. L. Installation of a subsurface groundwater treatment wall composed of granular zero-valent iron. *Natl. Meet. - Am. Chem. Soc., Div. Environ. Chem.* **1995**, *35*, 792-795 (Abstr.).
- Zoro, J. A.; Hunter, J. M.; Eglinton, G.; Ware, G. C. Degradation of p,p'-DDT in reducing environments. *Nature* **1974**, *247*, 235-237.

## SECTION V

# PATHWAYS OF CHLORINATED ETHYLENE AND CHLORINATED ACETYLENE REACTION WITH ZINC

### A. ABSTRACT

In order to successfully design treatment systems relying on reactions of chlorocarbons with zero-valent metals, information is needed concerning the kinetics and pathways through which transformations occur. In this study, pathways of chlorinated ethylene reaction with Zn(0) have been elucidated through batch experiments. Data for parent compound disappearance and product appearance were fit to pseudo-first order rate expressions in order to develop a complete kinetic model. Results indicate that reductive  $\beta$ -elimination plays an important role, accounting for 15% of tetrachloroethylene (PCE), 30% of trichloroethylene (TCE), 85% of *cis*-dichloroethylene (*cis*-DCE), and 95% of *trans*-dichloroethylene (*trans*-DCE) reaction. The fraction of PCE, TCE, *trans*-DCE, and *cis*-DCE transformation that occurs via reductive elimination increases as the two-electron reduction potential ( $E_2$ ) for this reaction becomes more favorable relative to hydrogenolysis. In the case of PCE and TCE, reductive elimination gives rise to chlorinated acetylenes. Chloroacetylene and dichloroacetylene were synthesized and found to react rapidly with zinc, displaying products consistent with both hydrogenolysis and reduction of the triple bond. Surface area normalized rate constants ( $k_{SA}$ ) for chlorinated ethylene disappearance correlate well with both one-electron ( $E_1$ ) and two-electron ( $E_2$ ) reduction potentials for the appropriate reactions. Correlation with  $E_2$  allows prediction of the distribution of reaction products as well as the rate of disappearance of the parent compound.

### B. BACKGROUND AND RATIONALE

The use of zero-valent metals as reductants of chloroalkanes and chloroethylenes represents a promising new approach for treating groundwater contaminated with such solvents. Removal of the parent compound, however, may not be sufficient to attain drinking water standards, as partially dechlorinated reaction products or intermediates may also pose human health risks. For example, some moderately persistent species, such as *cis*-dichloroethylene (*cis*-DCE) and vinyl chloride (VC), which have been detected as products of tetrachloroethylene (PCE) (Campbell *et al.*, 1997) and trichloroethylene (TCE) (Orth and Gillham, 1996; Liang *et al.*,

1997; O'Hannesin and Gillham, 1998) reduction by iron, are themselves of concern as contaminants. The necessity of controlling effluent levels of such species may dictate the overall design of metal-based treatment systems (Vogan *et al.*, 1995; Yamane *et al.*, 1995; Tratnyek *et al.*, 1997). In order to develop process models which could be used to optimize the design of *in situ* or *ex situ* treatment systems, information is needed concerning the rates and pathways through which chlorinated intermediates are formed and subsequently degrade.

Zinc was selected in the present study in order to gain insight into pathways through which one possible candidate metal reacts with chlorinated ethylenes. Zinc has previously been studied for use as a reductant of carbon tetrachloride (Boronina *et al.*, 1995; Warren *et al.*, 1995), as well as lindane ( $\gamma$ -hexachlorocyclohexane), 1,1,1-trichloroethane, and chloroform (Schlimm and Heitz, 1996). Methyl parathion has also been found to undergo reduction when contaminated soil is mixed with zinc metal (Butler *et al.*, 1981). Although oxidation of zinc metal might be anticipated to release Zn(II) species, which might be of concern in drinking water, Carraway and co-workers (Song *et al.*, 1999) have recently demonstrated that dissolved  $\text{Zn}^{2+}$  concentrations generated in the reaction of PCE with Zn(0) can be minimized by adding hydroxyapatite, onto which the Zn(II) is presumably removed via adsorption (Xu *et al.*, 1994; Chen *et al.*, 1997; Song *et al.*, 1999).

Our previous work (Roberts *et al.*, 1996; Campbell *et al.*, 1997) has shown that chlorinated ethylene reduction by zero-valent metals, such as iron and zinc, proceeds via two parallel pathways: hydrogenolysis and reductive  $\beta$ -elimination. In the case of ethylenes bearing an  $\alpha,\beta$  pair of chlorines, reductive elimination gives rise to substituted acetylenes. A third reaction that may occur in these systems is the reduction of multiple bonds. This creates the possibility that a particular intermediate may arise from multiple pathways. For example, vinyl chloride may be produced via hydrogenolysis of the dichloroethylenes or alternatively by reduction of the triple bond of chloroacetylene. The existence of such competing reactions greatly complicates the modeling of transformation pathways. A scheme that accounts for reactions of chlorinated ethylenes and other possible intermediates with zinc is detailed in Figure 42 (Roberts *et al.*, 1996; Campbell *et al.*, 1997). Although our prior work established the overall plausibility of this scheme, the data reported by us (Roberts *et al.*, 1996; Campbell *et al.*, 1997) and others (Gillham and

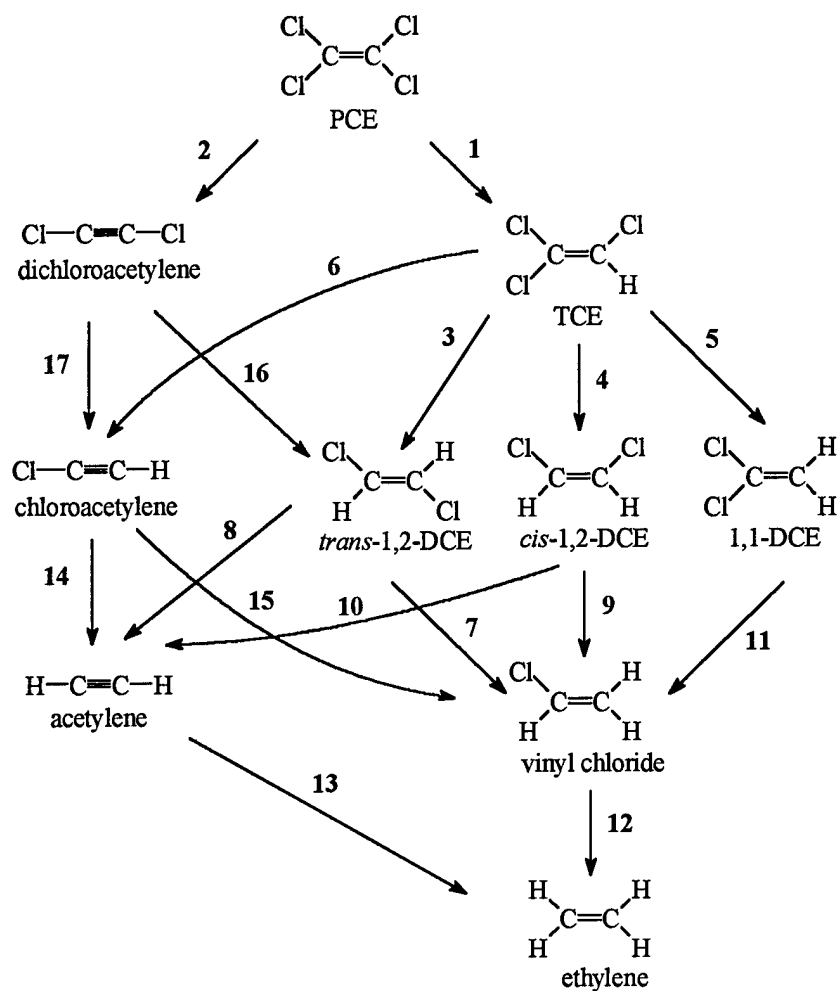


**Figure 42.** Hypothesized reaction sequence (Roberts *et al.*, 1996; Campbell *et al.*, 1997) for reduction of chlorinated ethylenes and related compounds by Zn(0). Reaction numbers correspond to those given in Table 8.

O'Hannesin, 1994; Schreier and Reinhard, 1994; Muftikian *et al.*, 1995; Orth and Gillham, 1996; Liang *et al.*, 1997; O'Hannesin and Gillham, 1998) have not been sufficiently detailed as to determine the rate constants associated with each of these reactions. The principal objective of this work was to determine the kinetics of chlorinated ethylene reaction with Zn(0) through detailed measurements in batch systems.

A second question relates to our ability to develop quantitative structure-activity relationships (QSARs) through which rates and products might be predicted for the reaction of

other organohalides with metals. Johnson *et al.* (1996) proposed that surface area normalized rate constants ( $k_{SA}$  values) could be correlated with two-electron reduction potentials for hydrogenolysis, even though many of the species employed in their correlation could potentially react to a significant extent via competing reductive  $\beta$ -elimination.

Without detailed knowledge of the product distributions in the experiments compiled by Johnson *et al.* (1996), it has not been possible to properly account for the contributions of such competing reactions. Reduction potentials for hydrogenolysis and reductive elimination can be quite different (Roberts *et al.*, 1996); failure to correctly account for the pathways by which different species react may influence the success of such attempted correlations. In undertaking this study, we also sought to assess whether QSARs could be improved through separate correlations of the two types of reductive dehalogenation, as well as through correlation of reaction rate constants with one-electron reduction potentials.

## C. EXPERIMENTAL SECTION

### 1. Chemicals

The following chemicals were used as received: tetrachloroethylene (99.9%, HPLC grade, Aldrich); trichloroethylene (99.5+%, Aldrich); *cis*-dichloroethylene (97+%, Aldrich); *trans*-dichloroethylene (*trans*-DCE, Supelco); 1,1-dichloroethylene (1,1-DCE, 99%, Aldrich); vinyl chloride in methanol (Chem Service, 2000  $\mu\text{g/mL}$ ); 10% ethylene in helium (Scott Specialty gas); and 1% acetylene in helium (Scott Specialty gas). Methanolic (HPLC grade, J.T. Baker) spiking solutions were prepared for PCE, TCE, and the DCE isomers.

Acid solutions for cleaning metals were prepared using deoxygenated, deionized water (Milli-Q Plus UV, Millipore). Solutions were deoxygenated by sparging (1 h/L) with argon, which was purified using an in-line molecular sieve and oxygen traps. Reaction bottles were filled with deoxygenated solutions containing 0.1 M NaCl (99%; J.T. Baker) and 50 mM Tris buffer (tris[hydroxymethyl]aminomethane, reagent grade; Sigma), pH 7.2. The high (relative to typical groundwater) NaCl concentration was employed to poise the chloride content in the system, as chloride ion is released during reductive dechlorination. Chloride is known to accelerate corrosion by weakening the passive oxide film on metals (Jones, 1992), and its presence has been shown to

increase the rate of carbon tetrachloride reduction by iron (Johnson *et al.*, 1998).

## **2. Synthesis of Chlorinated Acetylenes**

Chloroacetylene and dichloroacetylene were synthesized from *cis*-DCE and TCE, respectively. Potassium hydride (35% in mineral oil, Aldrich) was rinsed twice with pentane (J.T. Baker) and once with freshly-distilled dry tetrahydrofuran (THF). Dehydrohalogenation of *cis*-DCE or TCE was induced by potassium hydride and a catalytic amount of methanol in dry THF as described by Denis *et al.* (1987). Verification of the identities of the synthesis products was conducted via gas chromatography/mass spectrometry (GC/MS). The resulting solutions of the chlorinated acetylenes in THF were used as spiking solutions. No purification of these reportedly explosive (Piganiol, 1950; Rutledge, 1968; Denis *et al.*, 1987) gases was attempted.

## **3. Metal Preparation**

The zinc metal (J.T. Baker, 30 mesh) was cleaned with 0.4% H<sub>2</sub>SO<sub>4</sub> to remove surface oxides (Wood, 1982). Within the anaerobic chamber, the zinc metal and acid were placed in an 250 mL Erlenmeyer flask (2 mL acid per gram of metal) and shaken by hand for 10 minutes. The acid was decanted and the metal was rinsed three times with deoxygenated water and once with acetone. The flask was then stoppered and removed from the anaerobic chamber, so that the metal could be oven dried (100°C) under argon. The cleaned metal was used within 24 hours, for it was found that the reactivity of the metal steadily decreased by a factor of three over a period of three weeks, even when stored in an anaerobic chamber (Figure 43). The surface area was 0.035 m<sup>2</sup>/g as measured via Kr adsorption using a Micromeritics Flowsorb II 2300.



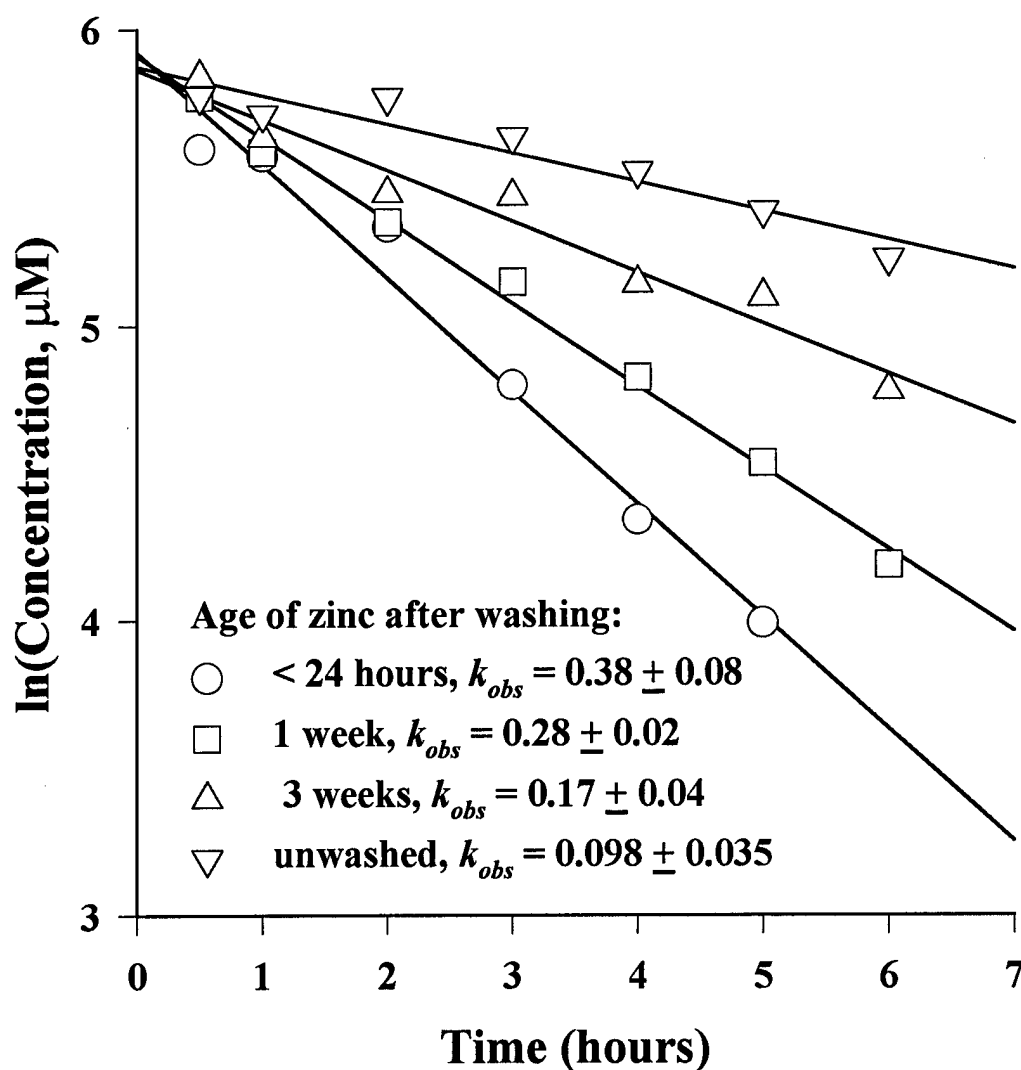


**Figure 43:** Effect of zinc age on reactivity to PCE reduction. Experiments conducted in 0.1 M NaCl, 25 g Zn(0)/150 mL at 36 rpm.

#### 4. Experimental Systems

Reaction bottles were filled with deoxygenated 0.1 M NaCl, 50 mM Tris buffer within an anaerobic chamber. Depending on the reactivity of the compound being studied, varying quantities of metal were added to the flask, with higher zinc loadings being used to increase the reaction rate of less reactive compounds. Reactions of PCE were studied using 5 g of zinc in 125 mL (nominal volume) glass bottles with glass stopcock adapters. The stopcock outlets were fitted with an NMR septum (Aldrich) to facilitate sampling while excluding oxygen. The glass stopcocks isolated the flask contents from the potentially sorptive NMR septum except during the

brief sampling intervals. The bottles were mixed by rotating about their longitudinal axes on a rotator (Cole-Parmer) at 56 rpm; incubations were conducted at room temperature ( $23 \pm 1^\circ\text{C}$ ).

Reactions of all other species were carried out in 160 mL serum bottles sealed with Teflon<sup>®</sup> faced butyl rubber septa (Wheaton). Serum bottles were used in preference to the 125 mL bottles used for PCE because the pressure buildup caused by hydrogen gas evolution at high metal loadings or over long reaction times causes the glass stopcock adapters on the 125 mL reactors to leak. For the remaining chlorinated ethylenes, acetylene, and ethylene, 25 g of zinc was used and bottles were rotated at 36 rpm. Reaction bottles used for chloroacetylene and dichloroacetylene contained 1 g and 0.5 g of zinc, respectively, and were rotated at 56 rpm. The chlorinated acetylenes and PCE were substantially more reactive than any of the other species. Although calculations using a mass transfer correlation (described more fully in Arnold *et al.*, 1999) did not indicate the presence of mass transfer limitations, experiments conducted with PCE suggested that a possible mass transfer limitation existed at lower mixing speeds for this species; experiments with the most highly reactive species were thus conducted at a high mixing rate in an attempt to overcome this problem. Reaction rate was independent of mixing speed between 15 and 45 rpm for the less reactive species.

Chlorinated ethylenes were introduced to the reactors via a methanolic spike (resulting in 0.003 to 0.06% methanol by weight) and the chlorinated acetylenes via the THF solution in which they were synthesized (resulting in 0.03% THF by weight). Spiking solutions of acetylene or ethylene were made by equilibrating the appropriate gas/helium mixture with deoxygenated buffer in a 1 liter syringe (Hamilton). The syringe was then transferred to an anaerobic chamber where aliquots of the equilibrated solution were introduced to the reaction flasks to achieve the desired starting concentration. Reactions were performed at various initial concentrations ranging from 3-80  $\mu\text{M}$  for acetylene, 3-30  $\mu\text{M}$  for vinyl chloride, and 15-350  $\mu\text{M}$  for the dichloroethylenes, TCE and PCE. At specified intervals, 1 mL samples were withdrawn from the reactors while simultaneously injecting 1 mL of deoxygenated buffer. This made it possible to avoid introducing headspace to the bottle during sampling, allowing anoxic conditions to be maintained.

## **5. Analytical Methods**

Aqueous samples were transferred to 2.5 mL (nominal volume) autosampler vials. Headspace samples (200  $\mu\text{L}$ ) were analyzed by gas chromatography (Fisons GC 8000) with flame

ionization detection (FID) using a 30 m × 0.53 mm ID GS-Q PLOT column (J&W Scientific). Before injection, samples were equilibrated by shaking at 60°C for 30 minutes in the oven of an Fisons HS 850 headspace autosampler. Data were collected using a PC driven data acquisition system (*Xchrom* v. 2.1, LabSystems). The THF solutions containing the chlorinated acetylenes were analyzed via cold on-column injection onto a GC equipped with an Rtx-1 column (30 m × 0.32 mm ID, 3 µm film thickness, Restek) and an FID detector.

Calibration curves were generated using aqueous standards (0.1 M NaCl, 50 mM Tris, pH 7.2) of PCE, TCE, and the DCE isomers prepared in 20 mL glass syringes. These standards were analyzed using the same method as samples. Acetylene, ethylene and vinyl chloride were calibrated using gas standards (Scott Specialty Gas). The gas standards were mixed in a 2 mL syringe (with a wetted barrel) equipped with a 3-way stopcock, one end of which was fitted with a septum. Gas samples (200 µL) were withdrawn and injected manually. Aqueous concentrations were calculated using the "dimensionless" Henry's Law constants  $\left( \frac{\text{mol} / L_{\text{air}}}{\text{mol} / L_{\text{water}}} \right)$  determined via a modified EPICS method (Gosset, 1987) at 60°C (the temperature of the autosampler oven) in the buffer solution. The values obtained were 1.1 for acetylene, 1.1 for vinyl chloride and 8.7 for ethylene. Due to the lack of commercial availability of the chlorinated acetylenes and uncertainty as to the exact yield obtained in the syntheses, calibrations for these species could not be conducted directly.

Bottles were initially filled without headspace. As much as 6 mL of headspace evolved during the longer incubations, presumably attributable to the reduction of protons by the metal to form hydrogen gas. For most species observed in these experiments, less than 4% of the mass would have been lost via partitioning to the headspace at 25°C. Ethylene, however, has a substantially higher Henry's Law constant than the other species and losses of over 25% of the mass of this species into the headspace could be incurred for the reactions of long duration. Reported aqueous ethylene concentrations, therefore, include the calculated fraction that partitioned into the headspace. As ethylene is stable under the conditions employed, its partitioning into the headspace does not affect its subsequent behavior. Partitioning of all other species into the headspace was minimal, so reported aqueous concentrations were not corrected.

The identities of all reaction products detected were confirmed by GC/MS analysis.

Samples were placed in 2.5 mL autosampler vials and shaken by hand for 3 minutes. A 50-200  $\mu\text{L}$  headspace sample was then withdrawn and manually injected (via splitless injector) on a Hewlett-Packard (HP) 5890 GC equipped with an HP 5970 mass spectrometer detector and a GS-Q PLOT column (30 m  $\times$  0.32 mm ID; J&W Scientific). The THF solutions containing the chlorinated acetylenes were analyzed on the same GC/MS using the Rtx-1 column previously described.

The pH of the aqueous medium was measured before and after the reaction, using a Ross<sup>®</sup> combination electrode (Orion). The pH during the reduction of PCE (which reacted completely in  $\sim 8$  hours) was stable at pH 7.3. The solution pH did rise slightly during the longer incubations required for other species, however, starting at pH 7.3 and ending at 7.6.

## 6. Kinetic Modeling

Pseudo-first order rate constants were calculated using the software package *Scientist for Windows* (v. 2.01, Micromath, Salt Lake City, UT). The relevant system of differential equations is given by:

$$\frac{dC_i}{dt} = - \left( \sum_{j=1}^{N_j} k_{ij} \right) C_i = -k_{obs} C_i \quad (15)$$

$$\frac{dC_j}{dt} = \left( \sum_{i=1}^{N_i} k_{ij} \right) C_i - \left( \sum_{m=1}^{N_m} k_{jm} \right) C_j \quad (\text{for all } j) \quad (16)$$

where  $C$  represents aqueous concentrations and  $k$  values are pseudo-first order rate constants. Equation 1 pertains to the reaction of the parent species,  $i$ , forming all possible daughter products,  $j$ . In equation 2, the daughter product,  $j$ , may be produced by multiple parents,  $i$ , and can itself react to other species,  $m$ , according to rate constants  $k_{jm}$ . The model equations for PCE reduction are given in Figure 44.

Given experimental data, differential rate expressions, and initial conditions, *Scientist* calculates the selected parameters (in this case,  $k_{ij}$  and the initial concentration of the parent compound) via a least squares fit of the data to numerically integrated solutions of the system of rate expressions. By computing each  $k_{ij}$  value according to the distribution of products, the model apportions the overall rate constant for parent compound disappearance into the contributions for the competing reactions. When calculating the  $k_{ij}$  values for a given species, the rate constants ( $k_{jm}$ ) for reactions of daughter products that were detected in a given experiment were constrained

```

// MicroMath Scientist Model File
IndVars: T
DepVars: pce, dcace, tce, cace, tdce, cdce, 11dce, vc, ace, eth
Params: k1, k2, k3, k4, k5, k6, k7, k8, k9, k10, k11, k12, k13, k14, k15, k16, k17, Co
pce' = -(k1+k2)*pce
dcace' = k2*pce - (k16+k17)*dcace
tce' = k1*pce - (k3+k4+k5+k6)*tce
cace' = k17*dcace + k6*tce - (k14+k15)*cace
tdce' = k16*dcace + k3*tce - (k7+k8)*tdce
cdce' = k4*tce - (k9+k10)*cdce
11dce' = k5*tce - k11*11dce
vc' = k7*tdce + k9*cdce + k15*cace + k11*11dce - k12*vc
ace' = k14*cace + k8*tdce + k10*cdce - k13*ace
eth' = k12*vc + k13*ace
//IC
T=0
pce=Co
dcace=0
tce=0
cace=0
tdce=0
cdce=0
11dce=0
vc=0
ace=0
eth=0

```

**Figure 44:** Scientist model file containing the system of differential equations applied to the reduction of PCE and all daughter products. Rate constants correspond to those depicted in Figure 42 and listed in Table 8. Abbreviations are as follows: pce = tetrachloroethylene, dcace = dichloroacetylene, tce = trichloroethylene, cace = chloroacetylene, tdce = trans-dichloroethylene, cdce = cis-dichloroethylene, 11dce = 1,1-dichloroethylene, vc = vinyl chloride, ace = acetylene, eth = ethylene.

to be equal to those determined in independent experiments in which the daughter products were introduced as the starting material.

## D. RESULTS

Pseudo-first order rate constants for each reaction shown in Figure 42 were divided by the metal surface area per liter of solution to obtain  $k_{SA}$  values. These  $k_{SA}$  values are given in Table 8

**TABLE 8. SURFACE AREA NORMALIZED RATE CONSTANTS FOR THE CHLORINATED ETHYLENES AND THEIR REACTION PRODUCTS. REACTION NUMBERS PERTAIN TO THOSE ILLUSTRATED IN FIGURE 42.**

Reaction	$k_{SA}$ (L m <sup>-2</sup> hr <sup>-1</sup> ) <sup>a</sup>	n <sup>b</sup>	E <sub>1</sub> (V) <sup>c,d</sup>	E <sub>2</sub> (V) <sup>c</sup>
1 PCE→TCE	0.3(±0.01)	9	-0.358	0.582
2 PCE→dichloroacetylene	4.5(±0.7)×10 <sup>-2</sup>	9	-0.358	0.631
3 TCE→ <i>trans</i> -DCE	1.5(±0.1)×10 <sup>-3</sup>	5	-0.597	0.534
4 TCE→ <i>cis</i> -DCE	6.0(±1.0)×10 <sup>-4</sup>	5	-0.578	0.543
5 TCE→1,1-DCE	6.8(±9.1)×10 <sup>-5</sup>	5	-0.840	0.523
6 TCE→chloroacetylene	9.4(±1.2)×10 <sup>-4</sup>	5	-0.578	0.609
7 <i>trans</i> -DCE→VC	6.4(±8.2)×10 <sup>-7</sup>	2	-0.880	0.488
8 <i>trans</i> -DCE→acetylene	1.3(±0.1)×10 <sup>-5</sup>	2	-0.880	0.573
9 <i>cis</i> -DCE→VC	5.2(±1.5)×10 <sup>-7</sup>	2	-0.898	0.478
10 <i>cis</i> -DCE→acetylene	3.0(±0.2)×10 <sup>-6</sup>	2	-0.898	0.564
11 1,1-DCE→VC	4.1(±0.3)×10 <sup>-5</sup>	3	-0.773	0.498
12 VC→ethylene	1.0(±0.5)×10 <sup>-4</sup>	3	-1.013	0.375
13 acetylene→ethylene	5.0(±1.4)×10 <sup>-4</sup>	5		
14 chloroacetylene→acetylene	6.5(±0.7)	1		
15 chloroacetylene→VC	0.50(±0.3)	1		
16 dichloroacetylene→ <i>trans</i> -DCE	20.6(±0.9)	4		
17 dichloroacetylene→chloroacetylene	4.4(±0.3)	4		

<sup>a</sup>Uncertainties represent 95% confidence limits.

<sup>b</sup>Number of replicate experiments used to determine rate constants.

<sup>c</sup>Calculations assume the Henry's Law constant for a radical species is the same as that of the hydrogenated parent (Eberson, 1982), {H<sup>+</sup>} = 10<sup>-7</sup> M, {Cl<sup>-</sup>} = 1 mM, and that all other species are present at unit activity. Gas-phase thermodynamic data are from Wagman *et al.* (1982); Taylor *et al.* (1991); Ho *et al.* (1992), corrected for air-water partitioning using Henry's Law constants recommended by Hine and Mookerjee (1975) or Mackay *et al.* (1993). The small changes in the E<sub>1</sub> and E<sub>2</sub> values compared to those previously reported (Roberts *et al.*, 1996) result from differences in the source of thermodynamic data.

<sup>d</sup>E<sub>1</sub> values are for the formation of the appropriate radical species. Reactions shown with identical one-electron reduction potentials produce the same radical intermediates.

along with the corresponding one- and two-electron reduction potentials.

Different initial concentrations of organohalide did not have a significant effect on the observed rate constants (Figure 45); thus, the values in Table 8 represent averages of the rate constants determined at each initial concentration. Confidence limits were calculated by propagating the errors associated with the model-calculated uncertainties obtained from several different timecourses. For the majority of the reactions listed in Table 8, the rate constants could be determined with a fair degree of precision ( $\pm 15\%$ , based on the 95% confidence limits). Substantially greater uncertainty arose, however, for some of the minor reactions that result in only trace product accumulation (*e.g.*, reactions 5, 7, and 9).

Preliminary experiments conducted at lower mixing speeds with PCE had suggested a dependence of reaction rate on initial concentration (Arnold and Roberts, 1997). This effect, however, was not observed at the higher mixing rates employed in the present study. Competitive inhibition effects were systematically investigated for the two most reactive species, PCE and TCE. For example, 15  $\mu\text{M}$  PCE was added to each of six reaction bottles. One bottle contained no competitor and each of the others contained 200  $\mu\text{M}$  of one of the other chlorinated ethylenes (TCE, *cis*-, *trans*-, or 1,1-DCE, VC). Similar experiments were performed with TCE. No significant decrease in the rate of reaction of PCE or TCE was observed under these conditions, indicating that competitive effects, if present, were too small to detect. Carbon mass balances at the end of the experiments were  $>90\%$  of the regressed initial parent compound concentration. No losses were observed in zinc-free blanks, suggesting that sorption to the Teflon<sup>®</sup> faced septa and losses through needle punctures were minimal. Further experimental results and modeling details are discussed in the following sections.

### **1. Effect of Metal Loading**

Normalization of rate constants by metal surface area assumes that a linear relationship exists between observed rate constant and metal loading. Results of some investigations with iron (Scherer and Tratnyek, 1995; Gotpagar *et al.*, 1997) have, however, suggested that reaction rate might not be directly proportional to metal loading. Scherer and Tratnyek (1995), for example, found that the rate of carbon tetrachloride reaction reached a plateau as iron loading was increased. A similar relationship between TCE reduction rate and iron loading was observed by Gotpagar *et al.* (1997). Such a nonlinear dependence on metal loading was not encountered in the

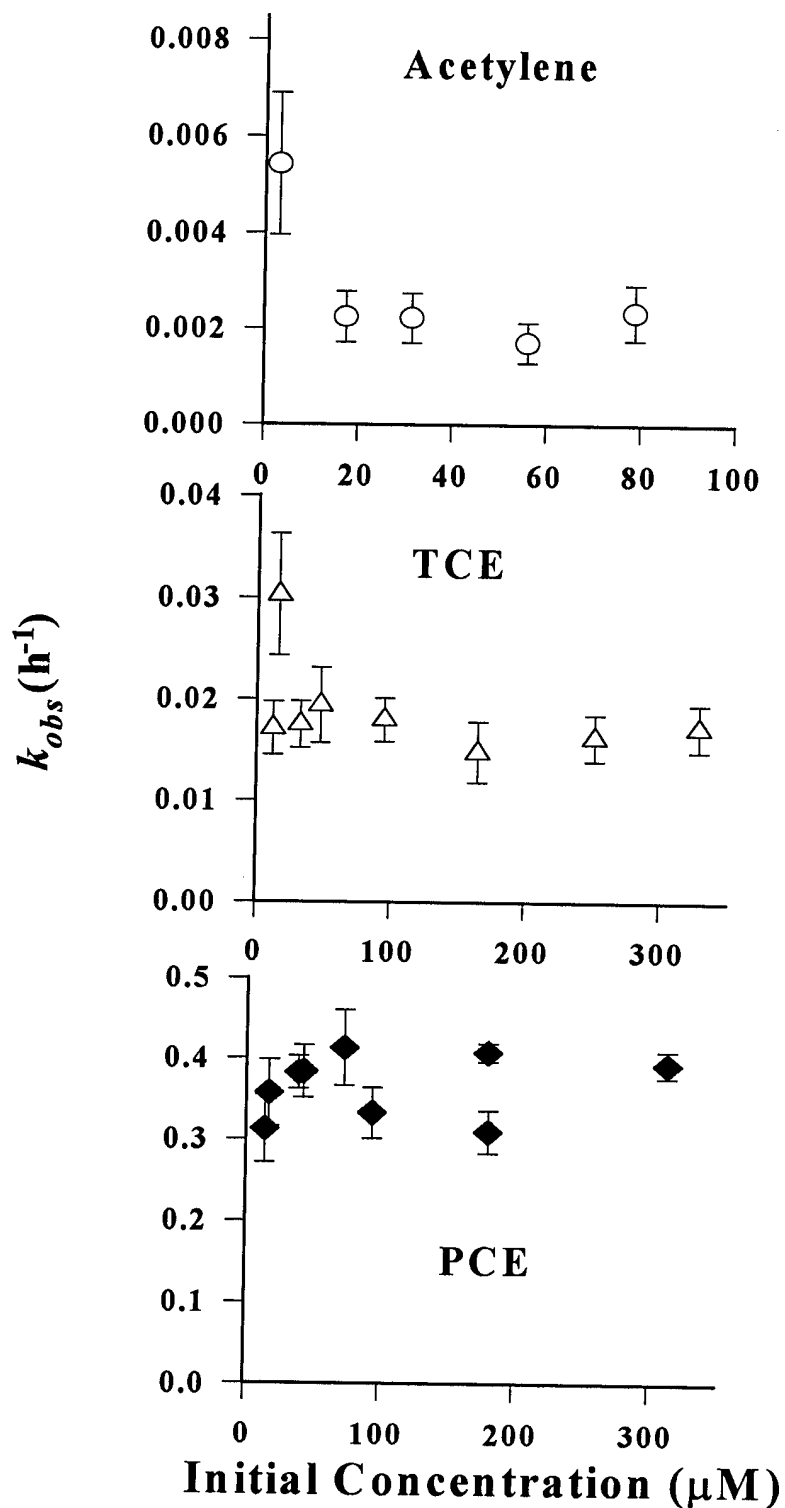


**Figure 45.** Effect of initial concentration on measured overall pseudo-first-order rate constant,  $k_{obs}$ . All experiments were conducted in 0.1 M NaCl/0.05 M Tris (pH 7.2) buffer. Reaction with acetylene and TCE used 25 g Zn(0)/160 mL buffer and those with PCE 5 g Zn(0)/150 mL buffer.



present study; rather, the pseudo-first order rate constant for parent compound disappearance was found to increase linearly with metal loading as shown in Figure 46, giving  $r^2$  values of 0.983 for PCE (at zinc loadings from 6-56 g/L), 0.993 for TCE, and 0.994 for acetylene (the latter two over a range of 65-240 g/L of zinc).

## **2. Vinyl Chloride and Acetylene**

Both of these species reacted to form ethylene. A representative plot of concentration versus time for acetylene is shown in Figure 47. No subsequent reduction of ethylene to ethane was observed. Pseudo-first order rate constants were calculated by simultaneously fitting the disappearance of the parent compound and the production of ethylene. It should be noted that no acetylene was observed in the reduction of vinyl chloride. From the measured rates of disappearance of vinyl chloride and acetylene, substantial accumulation of acetylene would be anticipated if it were an intermediate in the reduction of vinyl chloride to ethylene.

## **3. Dichloroethylenes**

Reaction of *cis*- and *trans*-DCE with Zn(0) produced acetylene, vinyl chloride, and ethylene. Only the latter two products were observed from the reaction of 1,1-DCE. For the DCE isomers, reaction proceeded so slowly (with a  $t_{1/2} > 125$  days) at a zinc loading of 25 g/160 mL that accurate determination of the rate of disappearance of the parent compounds was not feasible. Rate constants reported in Table 8 were, therefore, based on the rate of appearance of the reaction products under pseudo-zero-order conditions, assuming the concentration of the parent compounds to be invariant at very low conversions.

Representative plots of experimental results obtained for the DCE isomers are given in Figures 48-50. The solid lines are the model fits with rate constants for vinyl chloride and acetylene reaction constrained to equal values determined in independent experiments.

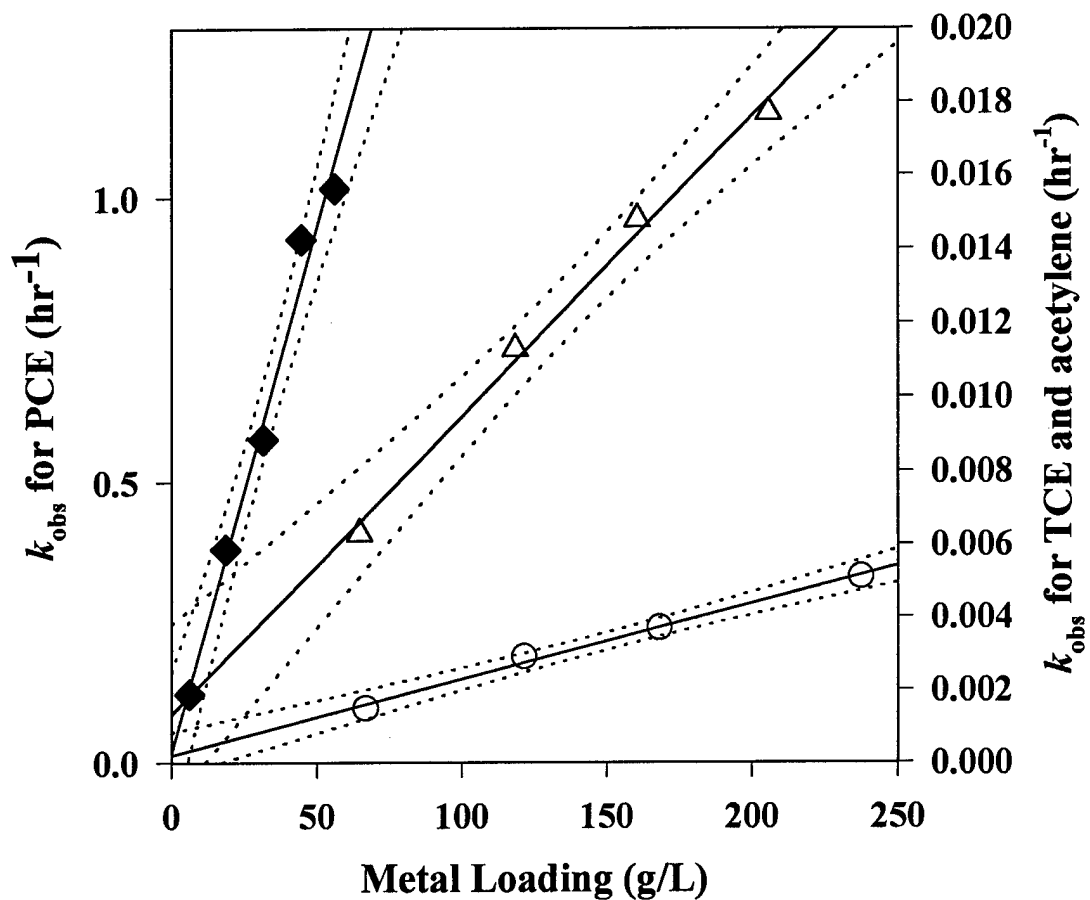


**Figure 46.** Effect of zinc loading on the reduction rate constant for PCE (◆), TCE (Δ), and acetylene (○). All experiments were conducted in 0.1 M NaCl/0.05 M Tris buffer (pH 7.2).

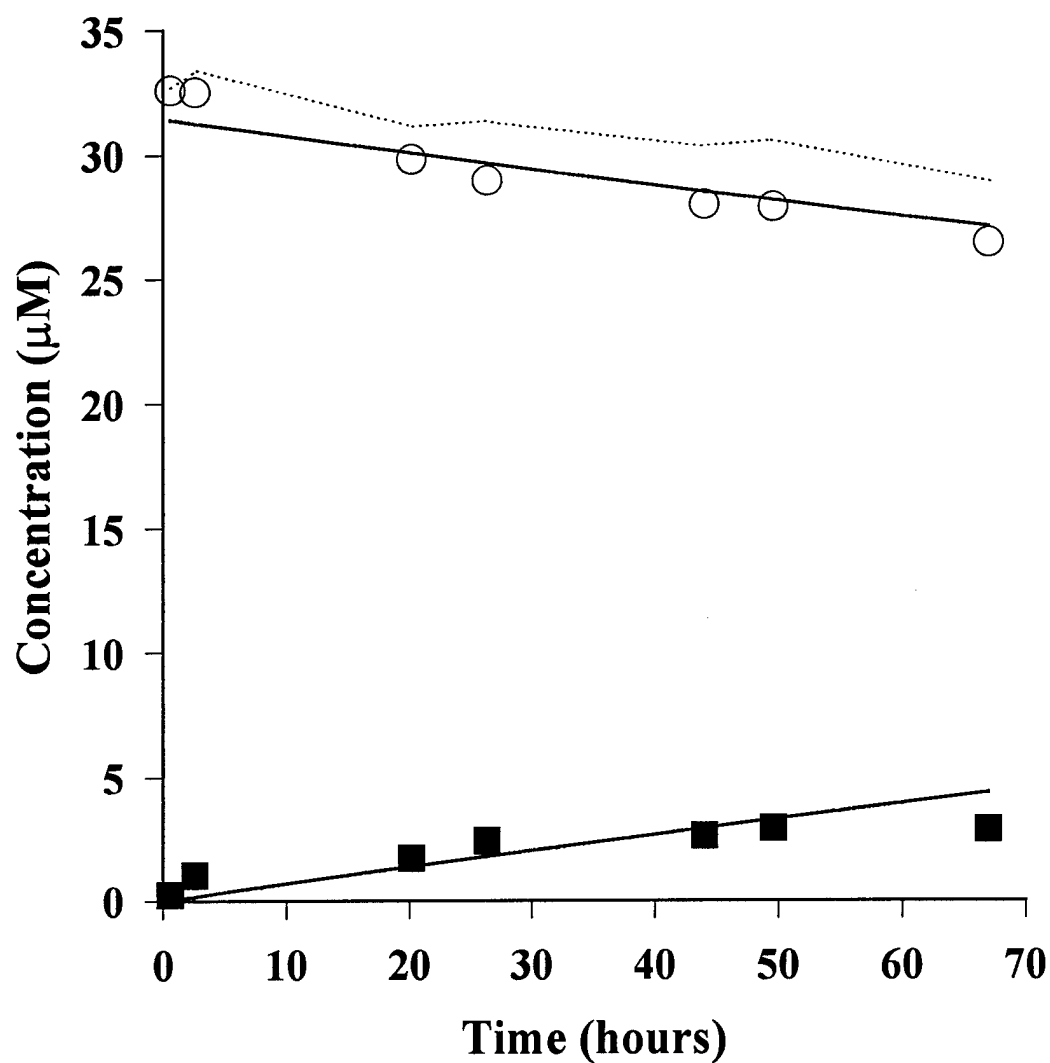


**Figure 47.** Reduction of acetylene (O) by 25 g Zn(0) in 160 mL of 0.1 M NaCl/0.05 M Tris buffer (pH 7.2). The only observed product was ethylene (■). Solid lines represent model fits.

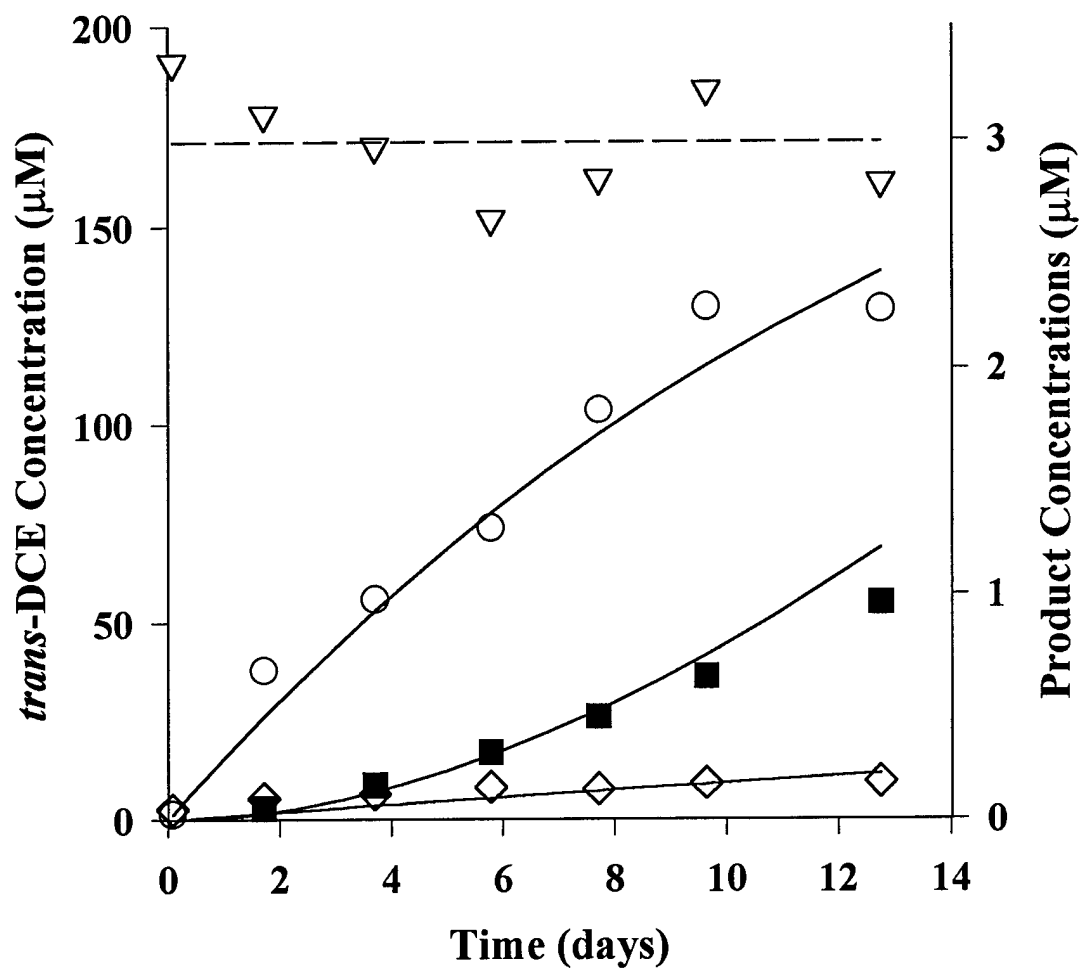


**Figure 48.** Reduction of *trans*-DCE (▽) by 25 g Zn(0) in 160 mL 0.1 M NaCl/0.05 M Tris buffer (pH 7.2). Solid lines are model fits to reaction products acetylene (○), ethylene (■), and vinyl chloride (◇). The dashed line represents the mean concentration of *trans*-DCE determined by averaging the data points shown.

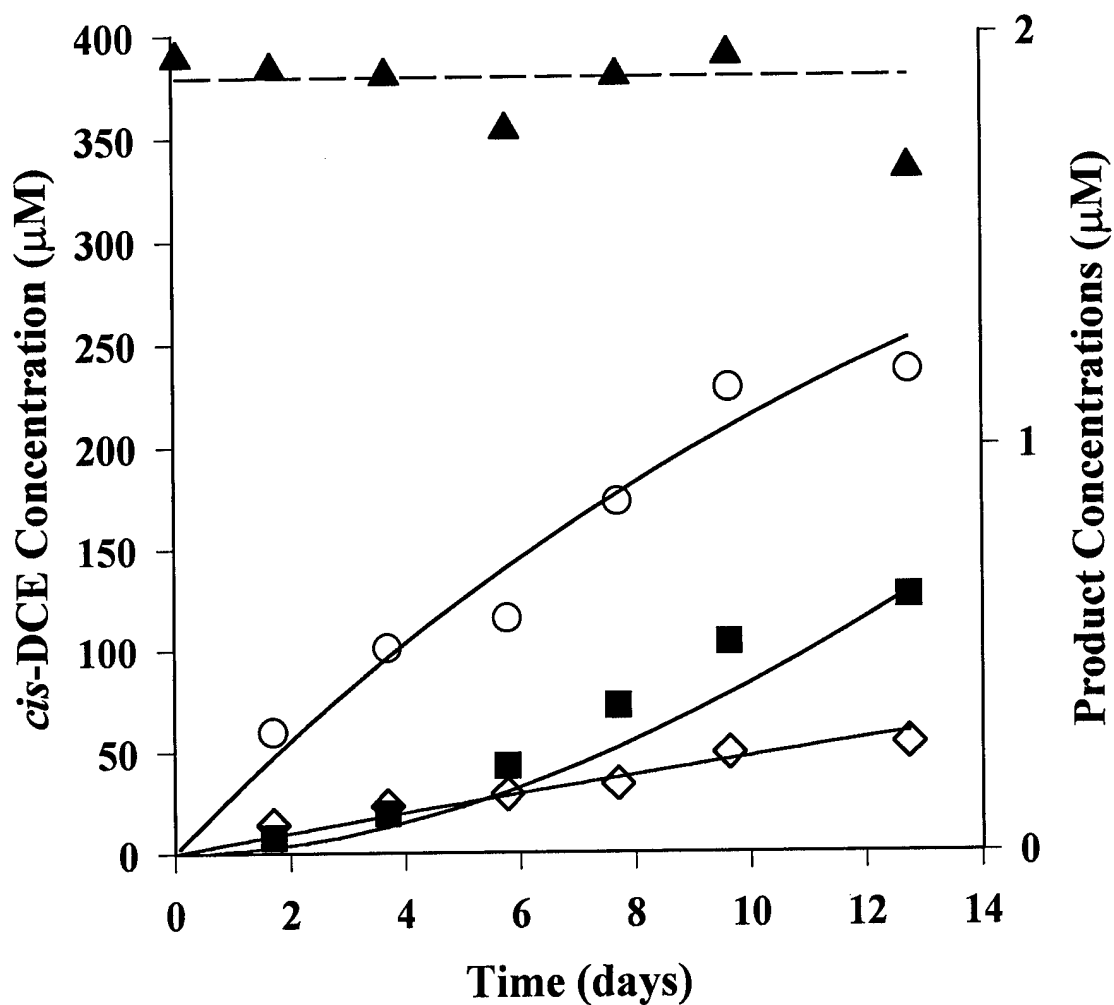


**Figure 49.** Reduction of *cis*-DCE (▲) by 25 g Zn(0) in 160 mL 0.1 M NaCl/0.05 M Tris buffer (pH 7.2). Solid lines are model fits to reaction products acetylene (○), ethylene (■), and vinyl chloride (◇). The dashed line represents the mean concentration of *cis*-DCE determined by averaging the data points shown.

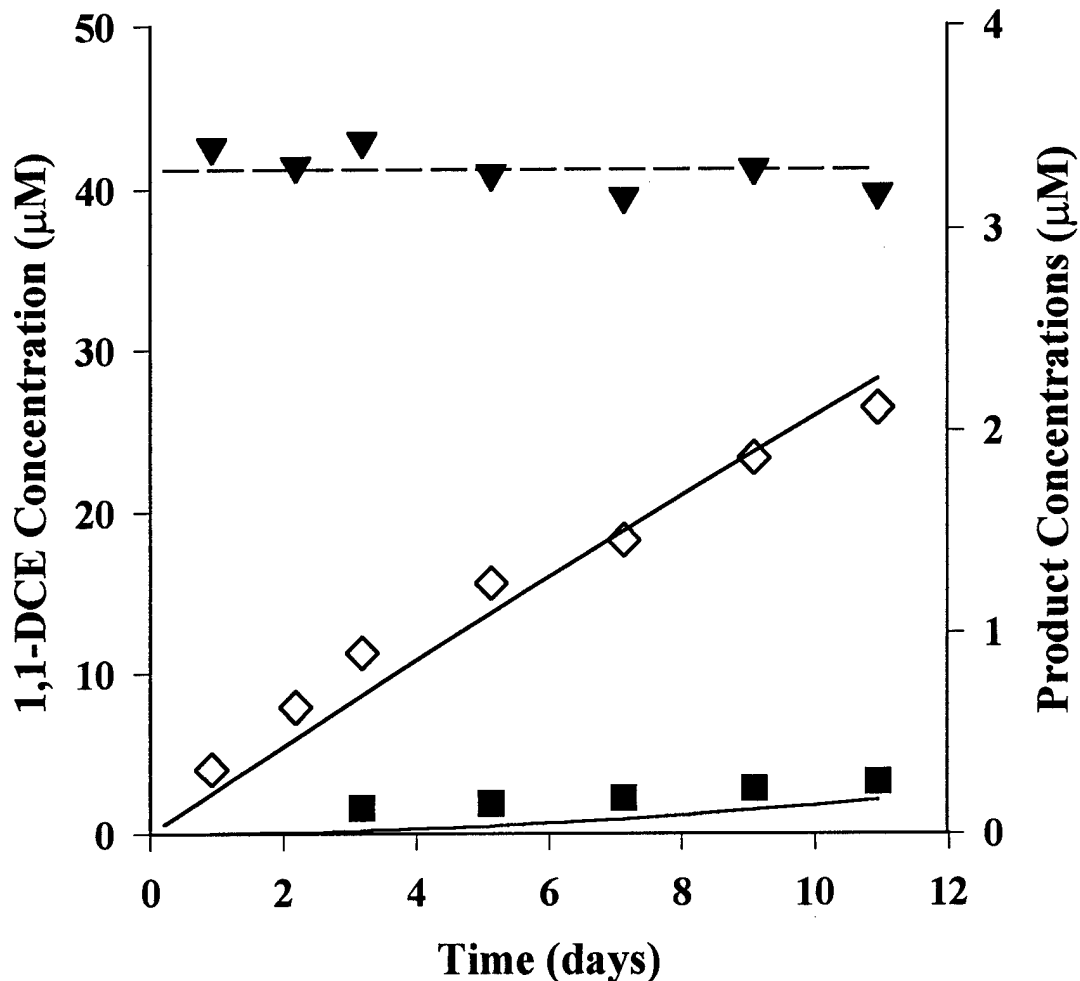


**Figure 50.** Reduction of 1,1-DCE (▼) by 25 g Zn(0) in 160 mL 0.1 M NaCl/0.05 M Tris buffer (pH 7.2). Solid lines are model fits to reaction products ethylene (■) and vinyl chloride (◇). The dashed line represents the mean concentration of 1,1-DCE determined by averaging the data points shown.

#### 4. TCE and PCE

Example timecourses obtained for TCE and PCE along with the corresponding model fits are shown in Figures 51 and 52, respectively. The pseudo-first order rate constants were calculated by simultaneously fitting the disappearance of the parent compound and the appearance of the daughter species, constraining subsequent reactions of daughter species as previously described. Reaction of TCE with zinc gave rise to the three dichloroethylene isomers, vinyl chloride,

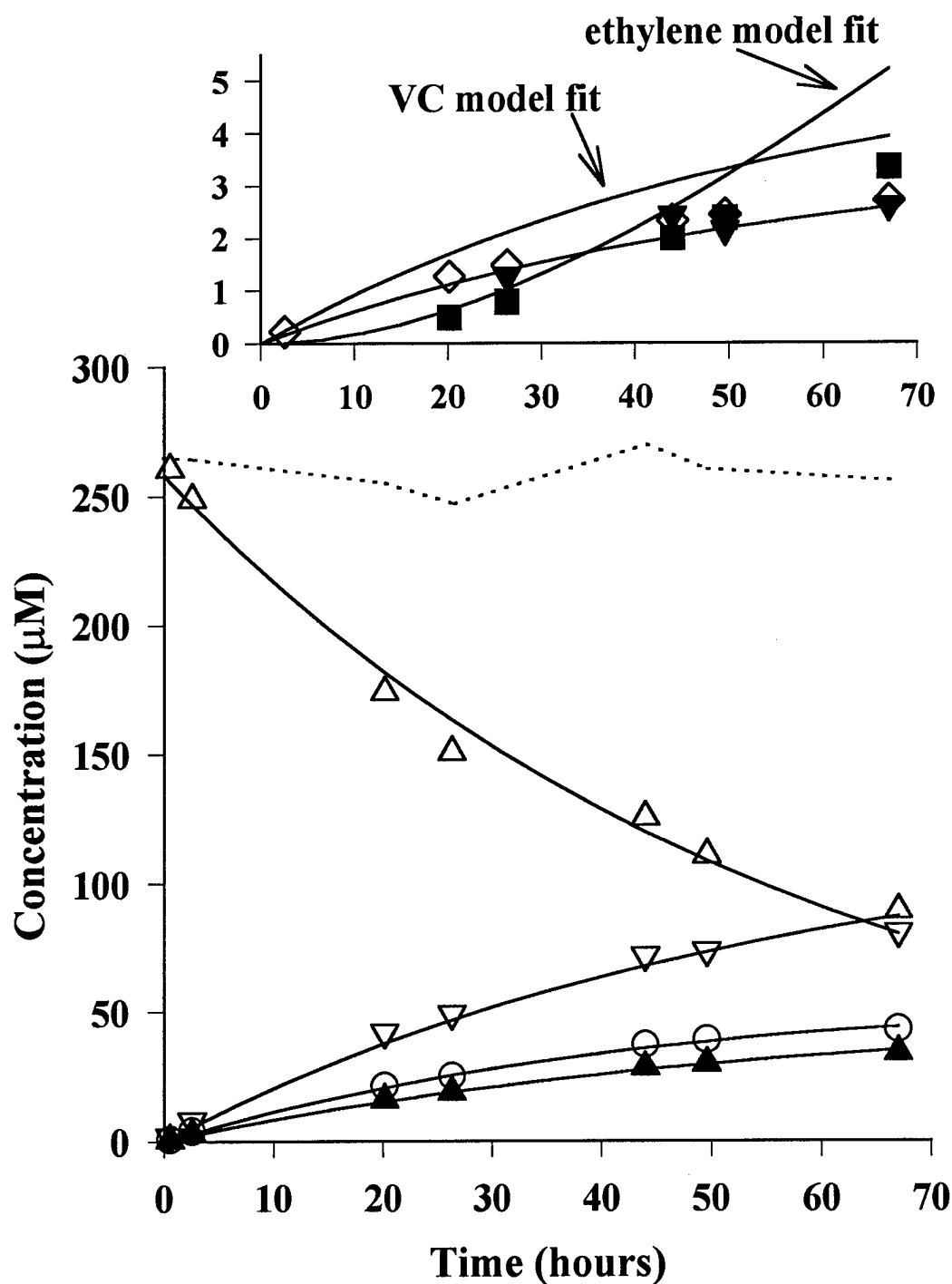


**Figure 51.** Reduction of TCE ( $\Delta$ ) in 160 mL 0.1 M NaCl/0.05 M Tris buffer (pH 7.2) by 25 g Zn(0). Major products are *trans*-DCE ( $\nabla$ ), acetylene ( $\circ$ ), and *cis*-DCE ( $\blacktriangle$ ). Inset shows trace products 1,1-DCE ( $\blacktriangledown$ ), ethylene ( $\blacksquare$ ), and vinyl chloride ( $\diamond$ ). The dotted line represents the observed C<sub>2</sub> mass balance, while solid lines are model fits.

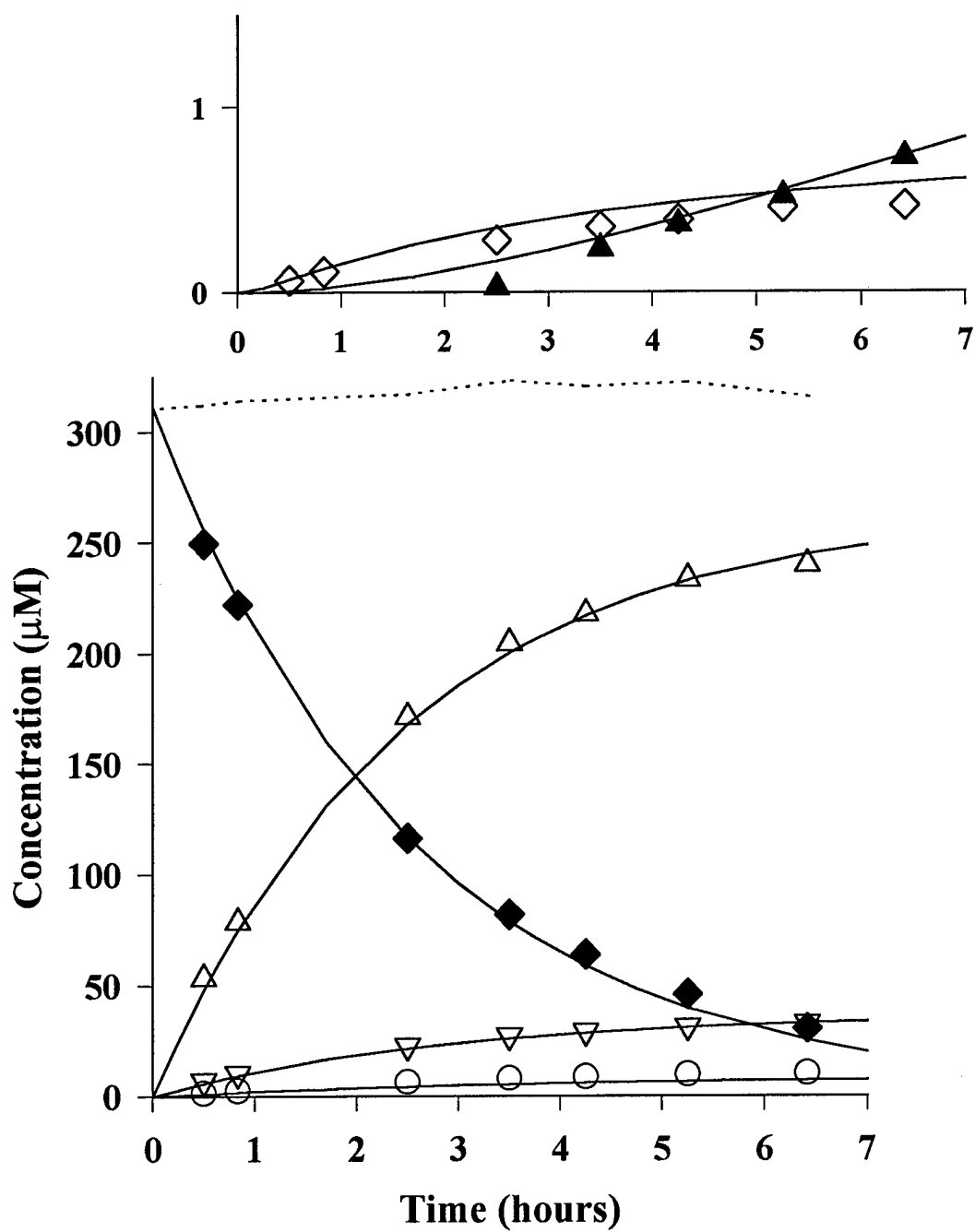


**Figure 52.** Reduction of PCE ( $\blacklozenge$ ) in 150 mL 0.1 M NaCl/0.05 M Tris buffer (pH 7.2) by 5 g Zn(0). Major products are TCE ( $\triangle$ ), *trans*-DCE ( $\nabla$ ), and acetylene ( $\circ$ ). Inset shows trace products *cis*-DCE ( $\blacktriangle$ ) and vinyl chloride ( $\diamond$ ). The dotted line represents the observed  $\text{C}_2$  mass balance, while solid lines are model fits.



acetylene and ethylene. It is interesting to note that even though *cis*-DCE is the thermodynamically favored species (Table 8) and is often the preferred product of microbial TCE reduction (Mohn and Tiedje, 1992), *trans*-DCE was the predominant DCE isomer formed from TCE reduction by zinc. Modeling the results of TCE reduction (Figure 51) again results in overprediction of the ethylene concentration, most likely due to the venting that occurred towards the end of the experiment (to which we attribute the 4% loss in mass balance observed for this experiment). The predicted concentrations of vinyl chloride are also higher than the observed values. This is a reflection of the high degree of uncertainty associated with the rate constant for formation of vinyl chloride from chloroacetylene (reaction 15; see below).

The major products of PCE reduction are TCE, *trans*-DCE, and acetylene (Figure 52). Trace amounts of *cis*-DCE, vinyl chloride, and chloroacetylene (not shown) were also observed. Experiments with PCE were relatively short in duration; as a result, no headspace evolved.

The acetylene observed in the experiments with both PCE and TCE appeared too rapidly to originate from the reductive elimination of the *cis*- or *trans*-DCE observed as daughter products in these systems. Attempts to model the data via a sequence such as  $\text{PCE} \rightarrow \text{TCE} \rightarrow \text{DCEs} \rightarrow \text{acetylene}$  proved unsuccessful, as previously demonstrated by (Roberts *et al.*, 1996). Such a sequence would predict curves for acetylene that were concave upwards, in sharp contrast to the observed results. In a similar manner, the rate of appearance of vinyl chloride from TCE reduction (Figure 51), as well as that of *trans*-DCE formation from PCE reduction (Figure 52), were too rapid to be attributable to a sequence of hydrogenolysis reactions of the sort  $\text{TCE} \rightarrow \text{trans-DCE} \rightarrow \text{VC}$  or  $\text{PCE} \rightarrow \text{TCE} \rightarrow \text{trans-DCE}$ .

Further evidence that the acetylene and vinyl chloride observed in TCE reduction did not arise from reactions of dichloroethylenes was provided by computing product yields as a function of time. For example, when TCE is the starting material, *cis*- and *trans*-DCE (as well as 1,1-DCE) are formed. If the observed acetylene and vinyl chloride were secondary products derived from these DCE isomers, their yields relative to the DCEs would increase over time. During the reduction of TCE (Figure 51), however, the yields of acetylene and vinyl chloride relative to *cis*- and *trans*-DCE were constant. The yield of vinyl chloride was also constant relative to 1,1-DCE. This suggests that the vinyl chloride and acetylene observed during TCE reduction are produced via a highly reactive intermediate through a pathway that operates concurrently to hydrogenolysis

of TCE to DCEs (and their subsequent reactions). Yields of acetylene and *trans*-DCE (relative to TCE) were also constant during PCE reduction (Figure 52), again consistent with their formation through a highly reactive intermediate or intermediates.

### 5. Chlorinated Acetylene Reduction

As the chlorinated acetylenes do not make up a significant portion of the mass balance in the reduction of PCE or TCE, reductive elimination to such species could only be a significant pathway if these react too rapidly to enable their accumulation. Independent confirmation was therefore sought by synthesizing dichloro- and chloroacetylene and measuring their rates and products of reaction. Based on our attempts to model the reduction of TCE, we anticipated chloroacetylene would react to form acetylene and vinyl chloride via reactions 14 and 15 (see Figure 42) if it were the intermediate responsible for the generation of these species.

Dichloroacetylene could give these same products after first being reduced to chloroacetylene via reaction 17; alternatively, reduction of the triple bond could result in *trans*-DCE via reaction 16 or (in principle) could produce *cis*-DCE.

The identities of the synthesized chloro- and dichloroacetylene were verified via GC/MS. As shown in Figure 53, the spectra closely match those found in the literature. Analysis of the chloroacetylene solution via GC/MS revealed no contaminant peaks other than those expected (unreacted *cis*-DCE and residual pentane from washing of the potassium hydride).

Results obtained for chloroacetylene reaction with zinc are shown in Figure 54. Measured rates of chloroacetylene reaction were sufficiently rapid that no detectable accumulation would be predicted to result from TCE reduction. The sole observed products of chloroacetylene reaction were acetylene and vinyl chloride, as anticipated. Note that at this zinc loading (1 g/160 mL compared to the 25 g/160 mL used for the experiments with the DCE isomers), reaction of the *cis*-DCE present to these products is extremely slow.

In principle, water may add to the triple bond of chloroacetylene to form an  $\alpha$ -halo vinyl alcohol (Piganiol, 1950). This species is an enol, which can rearrange to give acetyl chloride or form acetate after addition of a second water molecule (Scheme 15):

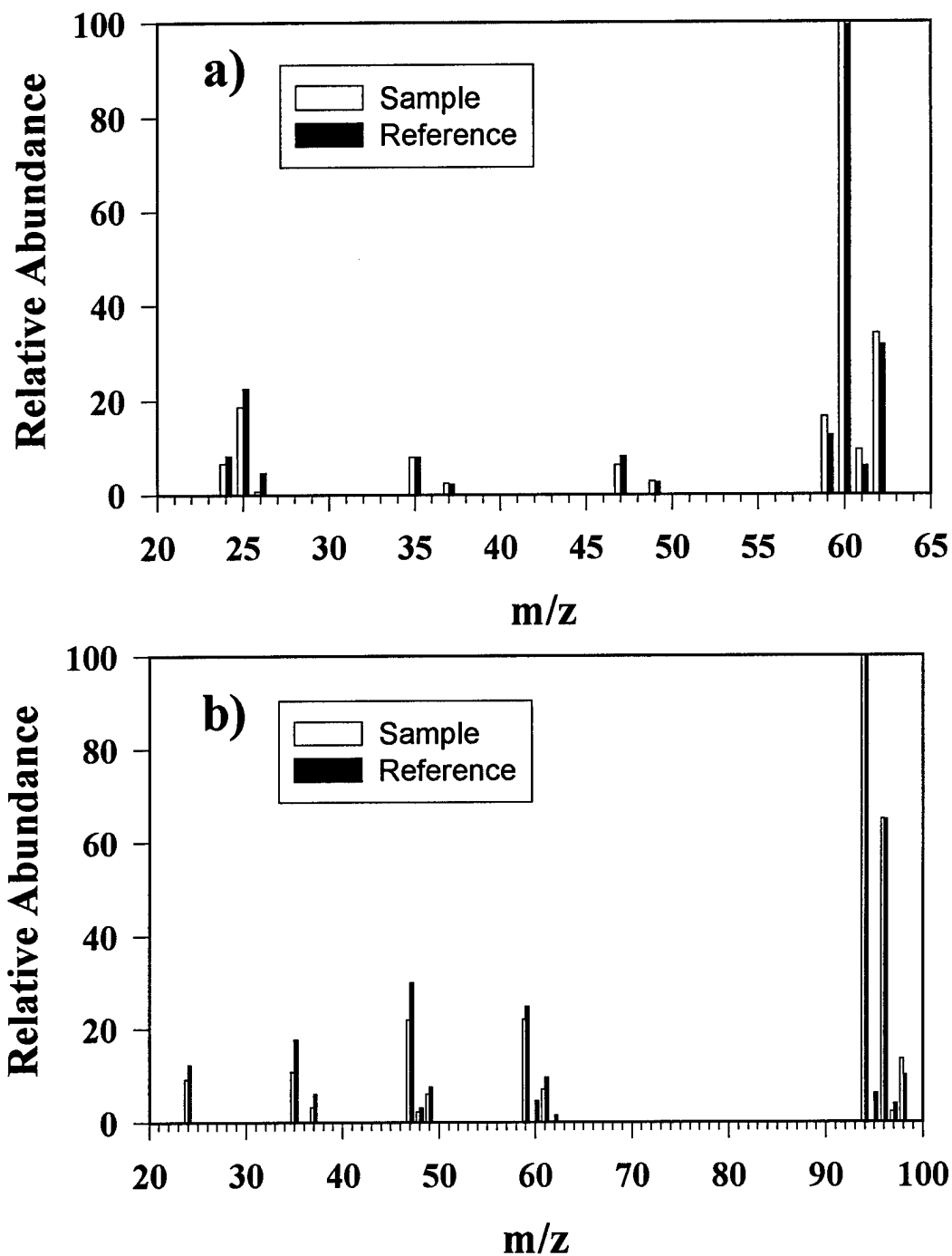


**Figure 53.** Mass spectra of a) chloroacetylene and b) dichloroacetylene compared to literature spectra (NIST Mass Spectral Data Center, March 1998). Retention times (relative to ethane) were 4.0 minutes for chloroacetylene and 11.7 minutes for dichloroacetylene using the temperature program: hold at 60°C for 1 min, ramp 5°C/min to 120°C, ramp 10°C/min to 240°C, and hold at 240°C for 6 min.

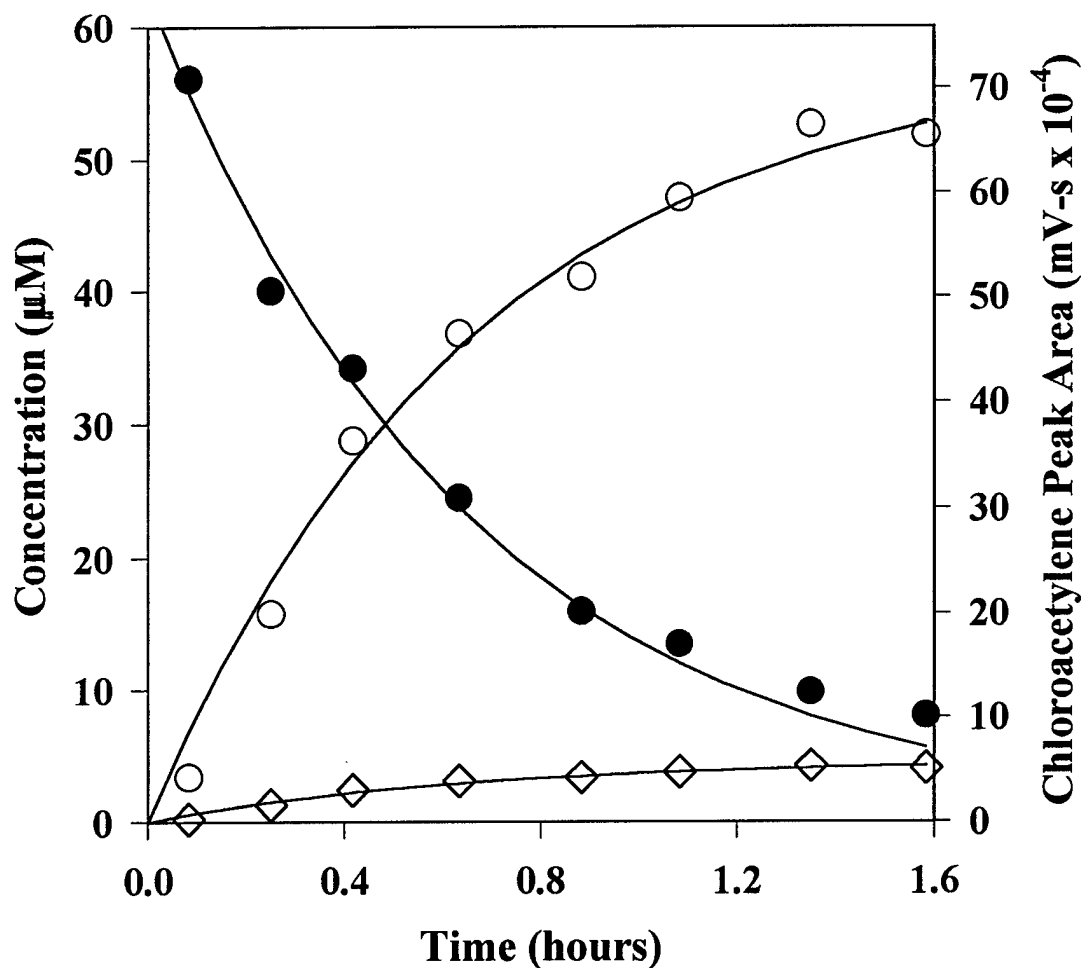
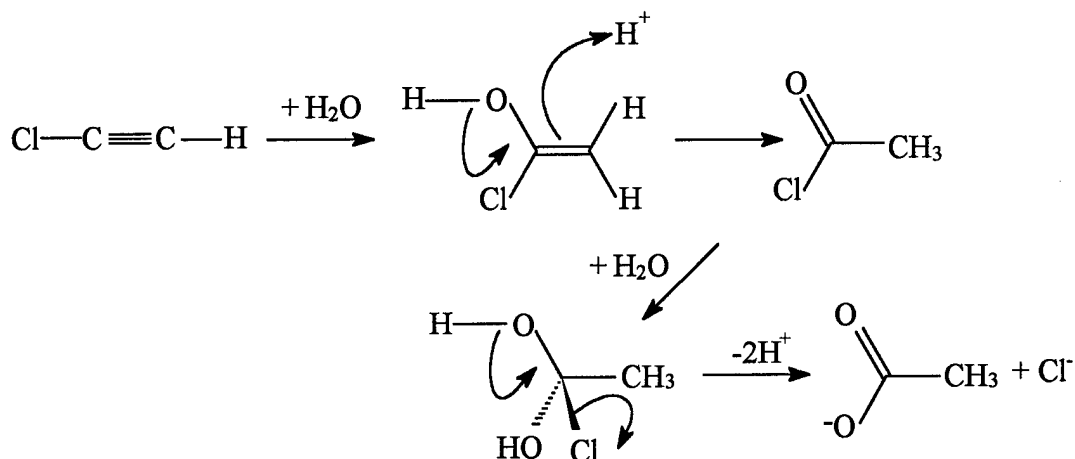


**Figure 54.** Reduction of chloroacetylene in 0.1 M NaCl/0.05 M Tris buffer (pH 7.2) by 1 g Zn(0). Solid symbols (●) represent chloroacetylene peak areas, while open symbols for acetylene (○) and vinyl chloride (◇) reflect measured concentrations. The model fit for the chloroacetylene data represents model-calculated concentrations.



### Scheme 15

Experiments in the absence of zinc, however, failed to reveal any significant loss of chloroacetylene that might be attributed to hydrolysis over a 24 hour period.

Owing to a lack of quantitative standards, concentrations of chloroacetylene could not be directly determined. A rate constant for chloroacetylene reaction was therefore computed by simultaneously fitting the chloroacetylene peak area and the concentrations of the reaction products as a function of time. This was accomplished by expressing the differential equation for the disappearance of chloroacetylene (see equation 15) in terms of peak area. An additional equation was included, in which a linear coefficient relating peak area to concentration was treated as a fitting parameter. The equations used are given in Figure 55. The model fit through the chloroacetylene peak areas shown in Figure 54 therefore represents the aqueous chloroacetylene concentration values calculated by the model.

Justification for this approach is provided by computing molar response factors from the results. Using the modified EPICS method (Gosset, 1987), dimensionless Henry's Law constants at 60°C in the 50 mM Tris, 0.1 M NaCl solution were found to be 2.4 for chloroacetylene and 3.5 for dichloroacetylene (see below). The value for chloroacetylene is within a factor of two of the value reported by Semadeni *et al.* (1998). From these Henry's Law constants, the model-derived aqueous concentrations, and the known air:water ratio in the vials, the total mass of chlorinated acetylene injected onto the GC, and thus the molar FID response factor ( $\mu\text{V}\cdot\text{s}/\text{nmol}$  injected), could be calculated at each time point. For chloroacetylene and dichloroacetylene, the FID molar response factors (relative to acetylene) were estimated as 1.07 and 1.12, respectively.

```

// MicroMath Scientist Model File
IndVars: T
DepVars: ace, vc, area, cace
Params: k1, k2, Co, alpha
cace=area/alpha
area'=- (k1+k2)*area
cace'=- (k1+k2)*cace
ace'=k1*(cace)
vc'=k2*(cace)
//Initial Cond.
T=0
area=Co
cace=Co/alpha
ace=0
vc=0

```

**Figure 55.** Model equations used to calculate the rate constants pertaining to the chloroacetylene data shown in Figure 54. The term “area” is the chloroacetylene peak area and “alpha” is the coefficient relating peak area to concentration.

The similarity of these response factors to that of acetylene gives independent confirmation of the validity of the model-derived concentrations. We note that FID molar response factors for the chlorinated ethylenes display a similar trend with increasing chlorination. The response factors relative to ethylene on our instrument are 1.02 for vinyl chloride, 0.90 for 1,1-DCE, 1.02 for *trans*-DCE, 1.06 for *cis*-DCE, 1.11 for TCE, and 1.22 for PCE.

Results obtained for the reaction of dichloroacetylene with zinc are displayed in Figure 56. No hydrolysis of dichloroacetylene was observed in the absence of zinc over a period of 24 hours. Dichloroacetylene reaction rates in the presence of zinc were sufficiently rapid that no detectable accumulation of dichloroacetylene, and only traces of chloroacetylene, would be anticipated from PCE reduction, consistent with our observations. Dichloroacetylene reacted to form *trans*-DCE, chloroacetylene, acetylene and vinyl chloride as the only observed reaction products. Reaction of residual TCE was not a significant source of these products at this metal loading. The observed acetylene concentration, however, was much too high to arise from the sequential reaction of dichloroacetylene→chloroacetylene→acetylene or from the other known acetylene precursors (*trans*-DCE, TCE) present. Modeling the data suggested that acetylene was also being produced by reaction of another species. The concentration of this hypothesized contaminant(s), as

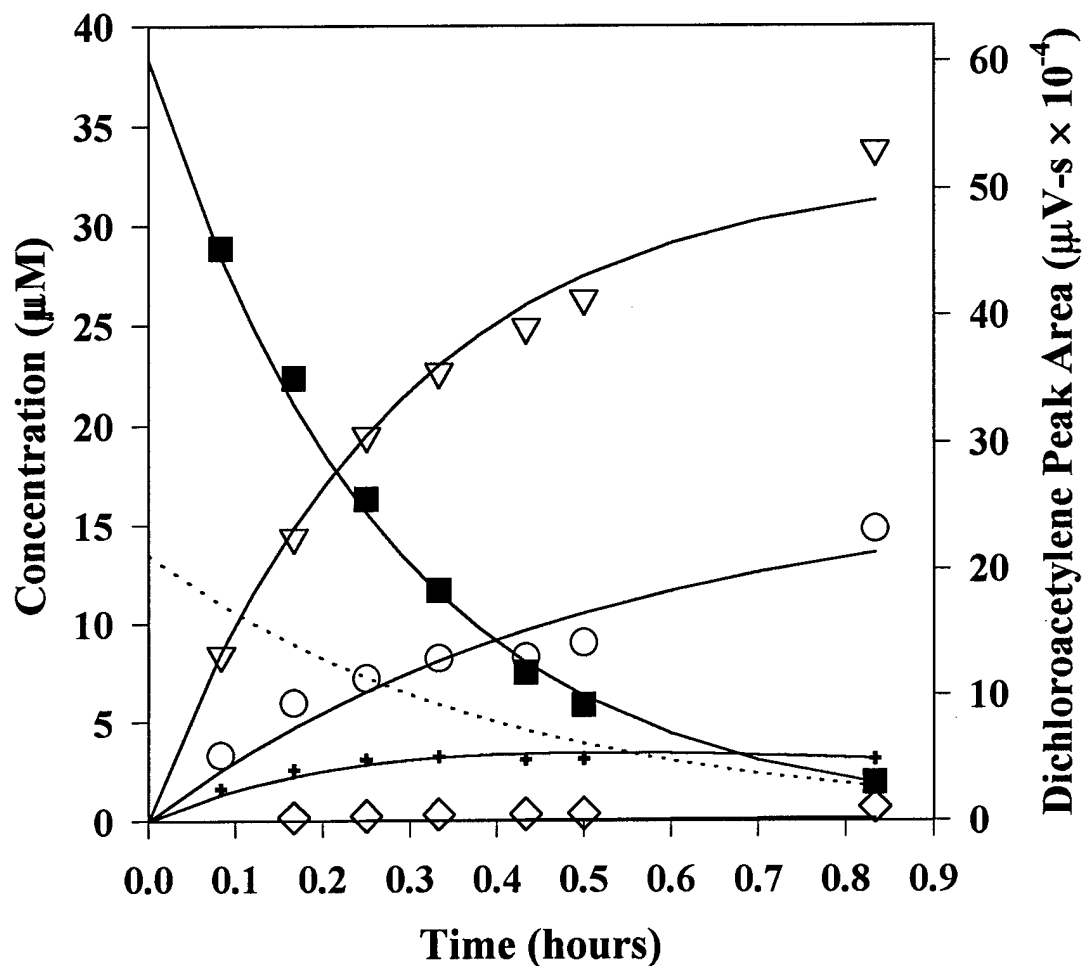


**Figure 56.** Reduction of dichloroacetylene in 0.1 M NaCl/0.05 M Tris buffer (pH 7.2) by 0.5 g Zn(0). Solid symbols (■) represent dichloroacetylene peak areas. The model fit for the dichloroacetylene data represents model-calculated concentrations. Open symbols for *trans*-DCE (▽), acetylene (○), and vinyl chloride (◇) are measured concentrations. The chloroacetylene concentration (+) was calculated using the relationship between peak area and aqueous concentration developed in Figure 54. The dashed line represents the calculated concentration of a hypothesized contaminant assumed to react to form acetylene.

calculated by the model, is given by the dotted line in Figure 56. Direct analysis of the THF solution via GC/MS and GC/FID revealed several contaminant peaks besides the expected TCE and pentane, most likely arising from side reactions during the synthesis. These compounds were not detectable via the headspace analysis method employed in monitoring the reaction kinetics. The largest of these peaks has a mass spectrum consistent with that given for 1,2-dichloro-1-methoxyethylene (Shainyan and Vereshchagin, 1993), as shown in Figure 57.

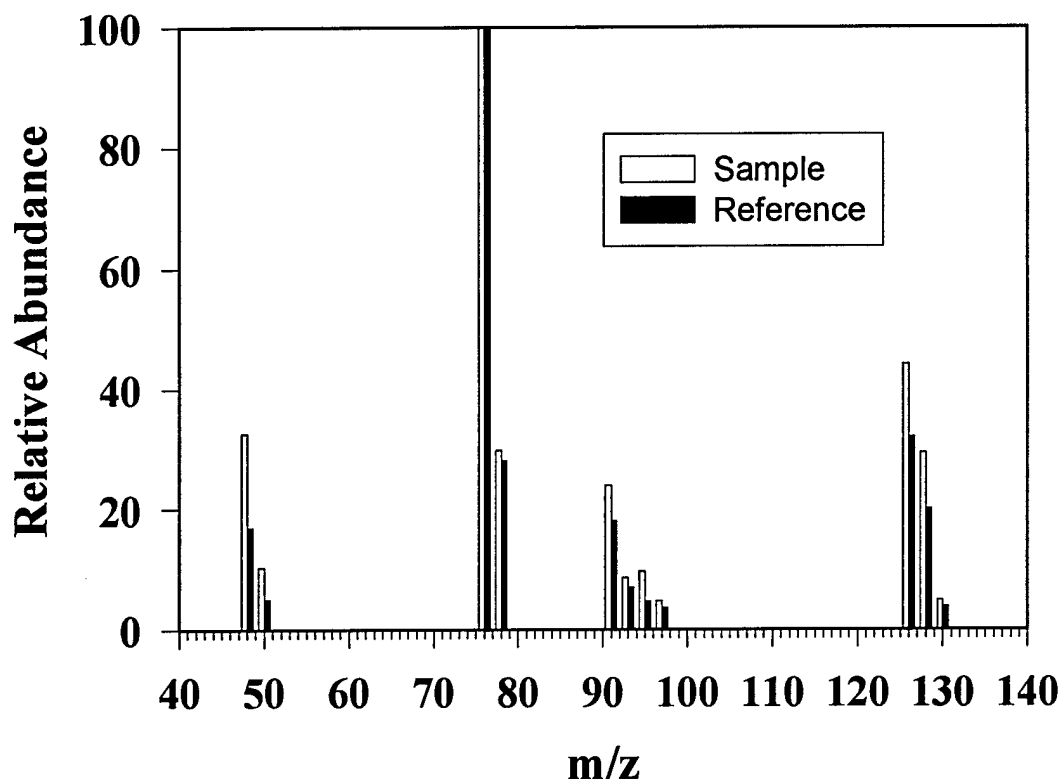


**Figure 57.** Mass spectrum of the major contaminant peak observed from the synthesis of dichloroacetylene. The reference spectrum is 1,2-dichloro-1-methoxyethylene (Shainyan and Vereshchagin, 1993). The reference spectrum is 1,2-dichloro-1-methoxyethylene (39). The retention time of the peak (relative to ethane) was 13.1 minutes using the temperature program: hold at 60°C for 1 min, ramp 5°C/min to 120°C, ramp 10°C/min to 240°C, and hold at 240°C for 6 min.

## E. DISCUSSION

### 1. Factors Influencing Reaction Products

Based on the rate constants given in Table 8, the fraction of the overall reaction that occurs via reductive  $\beta$ -elimination may be calculated for each chlorinated ethylene possessing an  $\alpha,\beta$  pair of chlorine atoms. This percentage was calculated by comparing the rate constant for reductive elimination to that for overall parent compound disappearance (reductive elimination + hydrogenolysis). Error limits were obtained by propagating the errors associated with the different rate constants. As the results summarized in Table 9 reveal, reductive elimination is an important contributor and cannot be ignored in pathway modeling under the conditions employed in the



**TABLE 9. PERCENTAGE OF REACTION OCCURRING VIA REDUCTIVE ELIMINATION.**

Species	% Reductive Elimination	$\Delta E_2 = (E_{\text{red. elim}} - E_{\text{hydrogenolysis}})$
PCE	15( $\pm 2$ ) <sup>a</sup>	0.049
TCE	30( $\pm 4$ )	0.075 <sup>b</sup>
<i>cis</i> -DCE	85( $\pm 8$ )	0.086
<i>trans</i> -DCE	95( $\pm 2$ )	0.085

<sup>a</sup>Uncertainties represent 95% confidence limits.

<sup>b</sup>Using the value for the reduction of TCE to *trans*-DCE (the principal observed DCE isomer).

present experiments. Additional studies (beyond the scope of the present investigation) will be required to address the impact of reaction conditions (*e.g.*, electrolyte composition and concentration; pH; concentration of potential hydrogen atom donors such as methanol, THF, and natural organic matter; temperature; metal cleaning or aging of the metal surface) on product branching ratios.

Note that as the reductive elimination reaction becomes more thermodynamically favorable relative to hydrogenolysis, the percentage of reaction occurring through reductive elimination increases. If we assume that the thermodynamic data for the reductive elimination and hydrogenolysis reactions are of comparable accuracy, it does not appear that the reaction products are purely under thermodynamic control. If the  $E_2$  values for hydrogenolysis and reductive elimination were identical, a 50:50 split of reaction products would be expected, while it is clear that even with reductive elimination favored thermodynamically (*e.g.*, for PCE and TCE), only 15-30% of the reaction proceeds via this route.

Product distributions are not only affected by the competition between the reductive elimination and hydrogenolysis pathways for the chlorinated ethylenes, but also by the branching ratio between hydrogenolysis and reduction of the triple bond for the chlorinated acetylenes. Only 8% of chloroacetylene is reduced to form vinyl chloride. With dichloroacetylene, however, 82% of the reaction proceeds via reduction of the triple bond to form *trans*-DCE.

Hydrogenation (reduction of triple bonds to double bonds by  $H_2$ ) is usually thought to occur via *cis*-addition, giving rise to *cis*-olefins. For example, we have found in our laboratory that 2-butyne is reduced to *cis*-2-butene by iron (Fennelly and Roberts, 1998). Zinc has also been shown to promote the stereospecific reduction of substituted alkynes to *cis*-alkenes in ethanol (Aerssens and Brandsma, 1984; Aerssens *et al.*, 1990) or THF/MeOH/ $H_2O$  (Chou *et al.*, 1991); a

strong preference for *cis*- reduction has also been observed for the zinc-copper couple in ethanol (Clarke and Crombie, 1957). Our results with zinc, however, indicate that the reduction of the dichloroacetylene triple bond forms *trans*-DCE rather than the *cis*- isomer. There are precedents for reduction of substituted acetylenes to *trans*- olefins by certain dissolving metal reductants. For example, reaction of sodium metal in ammonia produces *trans*-olefins from substituted acetylenes (Smith, 1968; Evans, 1970; Kemp and Vellachio, 1980). Zinc has also been cited for use in the semireduction of alkynes to *trans*-alkenes (Hudlicky, 1984).

When PCE or TCE react with zinc, several of the products, namely *trans*-DCE, vinyl chloride, and acetylene, may arise through more than one route. For example, vinyl chloride may be produced via hydrogenolysis (reaction 7, 9, or 11) or via reduction of chloroacetylene (reaction 15). Based on the rate constants given in Table 8, we can determine the percentage of the *trans*-DCE, vinyl chloride, and acetylene that originates from an initial reductive elimination of PCE or TCE via reactions 2 or 6. At relatively low conversions (<25%) of TCE, greater than 99.7% of the vinyl chloride and acetylene observed arise from an initial reductive elimination reaction of TCE to form chloroacetylene via reaction 6. At longer times (92% TCE conversion), the DCE daughter products have begun to react to form acetylene and vinyl chloride, but >97% of vinyl chloride and acetylene present still results from an initial reductive elimination to chloroacetylene. Similar results are obtained for PCE. For 92% conversion of PCE, 95% of the *trans*-DCE observed is produced via a dichloroacetylene intermediate. At shorter times, the percentage is higher, for hydrogenolysis of TCE has not yet contributed appreciably to the observed *trans*-DCE accumulation. Virtually all of the acetylene and vinyl chloride observed during PCE reduction arise either from the reductive elimination of PCE to dichloroacetylene or else from the subsequent reductive elimination of the initial daughter product (TCE) to chloroacetylene.

## 2. Quantitative Structure-Activity Relationships

If reaction were to occur via an outer-sphere single electron transfer pathway, a good correlation between one-electron reduction potential ( $E_1$ ) and the relevant rate constant might be anticipated (Eberson, 1987). Our results indicate that rate constants do correlate well with one-electron reduction potentials, as shown in Figure 58. The calculated regression equation is  $\log(k_{SA}) = 8.23 (\pm 1.79) \times E_1 + 2.21 (\pm 1.30)$ , where stated errors represent 95% confidence

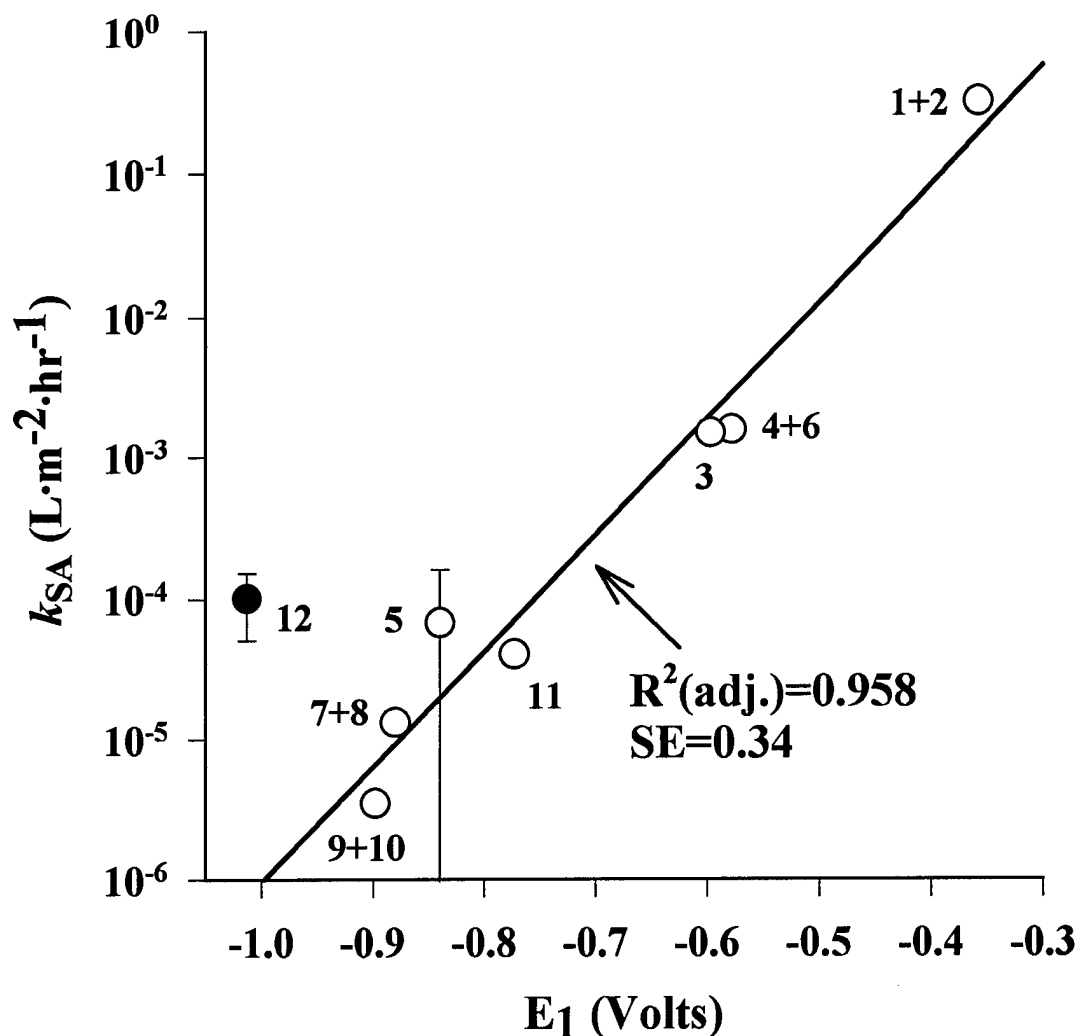


**Figure 58.** Correlation of surface area normalized rate constants ( $k_{SA}$ , Table 8) with one-electron reduction potentials. Numbering corresponds to the reactions indicated in Table 8. Regression line excludes the data point for vinyl chloride (filled circle, reaction 12). If no error bar is shown, it is smaller than the symbol.

limits. The regression reported excludes the data point for vinyl chloride (as with regressions against  $E_2$ , see below).

Although one-electron reduction potentials could be used to predict the overall rate constant pertaining to disappearance of a particular species, this descriptor does not provide any insight as to the distribution of reaction products that will result. Separate correlation of hydrogenolysis rate constants and rate constants for reductive elimination against two-electron reduction potentials furnishes a means of predicting reaction products as well as rates. Figure 59 displays correlations of  $k_{SA}$  versus two-electron reduction potential ( $E_2$ ) values for the

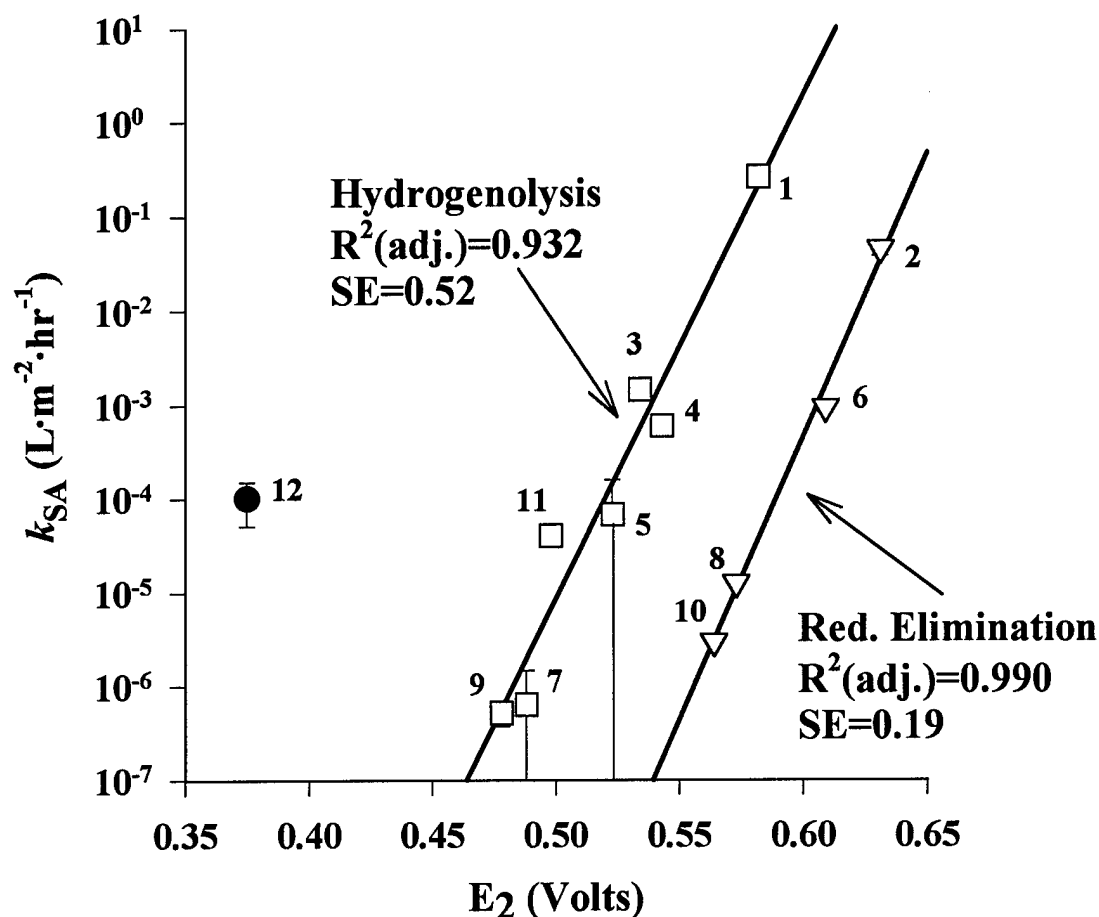


**Figure 59.** Correlation of surface area normalized rate constants ( $k_{SA}$ , Table 8) with two-electron reduction potentials for hydrogenolysis and reductive elimination. Numbering corresponds to the reactions indicated in Table 8. Regression lines exclude the data point for vinyl chloride (filled circle, reaction 12). If no error bar is shown, it is smaller than the symbol.

hydrogenolysis component of the reaction ( $\log(k_{SA}) = 53.56 (\pm 15.06) \times E_2 - 31.85 (\pm 7.86)$ ) and the reductive elimination component ( $\log(k_{SA}) = 60.39 (\pm 15.09) \times E_2 - 39.58 (\pm 8.97)$ ), where stated errors again represent 95% confidence limits. The high rate constant for vinyl chloride reaction to ethylene seems to be anomalous and was excluded from the relevant regression.

An overall favorable thermodynamic driving force exists if the two-electron reactions for zinc oxidation (to  $Zn^{2+}$ ) and chloroethylene reduction (either to hydrogenolysis or to reductive elimination products) are coupled. The correlations in Figures 58 or 59 represent a first step in deducing the mechanism through which chloroethylenes react with zinc. The trend observed, however, could be consistent with either adsorption (assuming chloroethylenes adsorb via a  $\pi$ -

bonding interaction; see Section VI) or electron transfer as the rate-limiting step. The pseudo-first order kinetic model used in this study is consistent with adsorption limitation (see Section VI). Further work will be needed to determine the molecular processes controlling the rate of organohalide reaction with zero-valent zinc.

The correlations of rate constants with both  $E_1$  and  $E_2$  are statistically significant, but the mechanistic implications of the relationships are unclear. They are also based on results obtained for a relatively small number of substrates. Despite their potential utility for predicting reactivity or product distributions, they should be applied with caution to untested compounds.

### **3. Environmental Significance of Reductive Elimination**

At first glance, reductive elimination of PCE or TCE may not seem overly beneficial. For example, the subsequent reduction of dichloroacetylene produces *trans*-DCE, a relatively persistent by-product compared to the parent species, PCE. This reaction pathway, however, partially circumvents TCE formation, a product that undergoes reduction in part to 1,1-DCE (a species that reacts only to vinyl chloride) and to *cis*-DCE (which produces approximately three times more vinyl chloride per mole as does *trans*-DCE). Mathematical simulations of the reactions of saturated PCE and TCE solutions with zinc reveal that *cis*-DCE, by virtue of being the least reactive species in the system, represents a bottleneck to attaining the drinking water limit for vinyl chloride. Reductive elimination of PCE reduces the amount of TCE formed, decreasing the amounts of *cis*-DCE, 1,1-DCE, and finally vinyl chloride produced.

Recent work has investigated the uncertainty associated with barrier design based on variations in rate constants, flow rates, and other transport processes (Eykholt, 1995; Eykholt, 1997; Tratnyek *et al.*, 1997). In these studies, however, the branching ratio between hydrogenolysis and reductive elimination was not explicitly known, making it difficult to quantitatively assess the importance of reductive elimination reactions. The results of the present study should facilitate more definitive investigations. We can further demonstrate the environmental significance of reductive elimination by comparing model predictions using the rate constants determined in this work with those obtained from a model that assumes the disappearance of any given species can be described by the same overall rate constant, but with reaction only occurring through hydrogenolysis. In other words, PCE is assumed to react solely to TCE via a rate constant obtained by summing reactions 1 and 2, TCE is assumed to react solely to

a mixture of the three DCE isomers (68.7% *trans*-DCE, 28.1% *cis*-DCE, and 3.2% 1,1-DCE) with an overall rate constant equal to the sum of reactions 3 through 6, and *cis*- and *trans*-DCE react only to vinyl chloride, via a sum of the rate constants for reactions 9 plus 10 or 7 plus 8, respectively. For a saturated solution of PCE, the model that constrains all transformations to a sequence of stepwise hydrogenolysis reactions requires hydraulic residence times (for a well-mixed reactor) to reach the drinking water limit for vinyl chloride (2 µg/L; Pontius, 1998) that are 76% greater than if reductive elimination reactions are incorporated. Similar calculations indicate hydraulic residence times that are 41% greater to attain the vinyl chloride drinking water limit from a saturated TCE solution when reductive elimination reactions are routed into the hydrogenolysis pathway.

Despite the production of undesirable species from subsequent reactions of chlorinated acetylenes, we note that if reductive elimination did not occur, all PCE or TCE initially present would be converted to vinyl chloride. Even though chlorinated acetylenes are toxic (Piganiol, 1950; Rutledge, 1968; Denis *et al.*, 1987), their rapid rate of reaction with zinc does not allow accumulation to high concentrations, decreasing the likelihood that these species will be of toxicological concern in the effluent from a metal-based treatment scheme. This suggests reductive elimination, by partially circumventing the formation of persistent, undesirable products, should be viewed as an environmentally desirable reaction.

## F. LITERATURE CITED

- Aerssens, M.H.P.J.; Brandsma, L. Regio- and stero-specific reduction of conjugated and non-conjugated triple bonds by activated zinc powder. *J. Chem. Soc., Chem. Commun.* **1984**, 735-736.
- Aerssens, M.H.P.J.; Heiden, R.v.d.; Heus, M.; Brandsma, L. A quick procedure for the partial reduction of triple bonds. *Synth. Commun.* **1990**, 20, 3421-3425.
- Arnold, W.A.; Roberts, A.L. Development of a quantitative model for chlorinated ethylene reduction by zero-valent metals. *Natl. Meet.-Am. Chem. Soc., Div. Environ. Chem.* **1997**, 37, 76-77 (Abstr.).
- Arnold, W. A.; Ball, W. P.; Roberts, A. L. Polychlorinated ethane reaction with zero-valent zinc: pathways and rate control. *J. Contam. Hydrol.*, **1999**, 40(2), 183-200.
- Boronina, T.; Klabunde, K.J.; Sergeev, G. Destruction of organohalides in water using metal particles: carbon tetrachloride/water reactions with magnesium, tin, and zinc. *Environ. Sci. Technol* **1995**, 29, 1511-1517.
- Butler, L.C.; Staiff, D.C.; Sovocool, W.; Davis, J.E. Field disposal of methyl parathion using acidified powdered zinc. *J. Environ. Sci. Health*, **1981**, B16, 49-58.
- Campbell, T.J.; Burris, D.R.; Roberts, A.L.; Wells, J.R. Trichloroethylene and tetrachloroethylene reduction in a batch metallic iron/water/vapor system. *Environ. Toxicol. Chem.* **1997**, 16, 625-630.
- Chen, X.; Wright, J.V.; Conca, J.L.; Peurung, L.M. Effects of pH on heavy metal sorption on mineral apatite. *Environ. Sci. Technol.* **1997**, 31, 624-631.
- Chou, W.N.; Clark, D.L.; White, J.B. The use of Rieke zinc metal in the selective reduction of alkynes. *Tetrahed. Lett.* **1991**, 32, 299-302.
- Clarke, A.J.; Crombie, L. Selective and stereospecific *cis*-reduction of acetylenes with copper-zinc couple. *Chem. Ind.* **1957**, 143.
- Denis, J.N.; Moyano, A.; Greene, A.E. Practical synthesis of dichloroacetylene. *J. Org. Chem.* **1987**, 52, 3461-3462.

- Eberson, L. Electron transfer reactions in organic chemistry. II. An analysis of alkyl halide reduction by electron transfer reagents on the basis of Marcus theory. *Acta Chem. Scand. B* **1982**, *36*, 533-543.
- Eberson, L., *Electron Transfer Reactions in Organic Chemistry*. Springer-Verlag: New York, 1987.
- Evans, R.F., *Modern Reactions in Organic Synthesis*. Van Nostrand Reinhold: London, 1970.
- Eykholt, G.R., Contaminant transport issues for reactive-permeable barriers, in *Geoenvironment 2000, Vol. 2, Characterization, Containment, Remediation, and Performance in Environmental Geotechnics*, Y.B. Acar and D.E. Daniel, Editors. 1995, American Society of Civil Engineers: New York. p. 1608-1621.
- Eykholt, G.R., Uncertainty-based scaling of iron reactive barriers, in *In Situ Remediation of the Geoenvironment*, J. Evenas and L. Reddi, Editors. 1997, American Society of Civil Engineers: New York. p. 41-55.
- Fennelly, J.P.; Roberts, A.L. Reaction of 1,1,1-trichloroethane with zero-valent metals and bimetallic reductants. *Environ. Sci. Technol.* **1998**, *32*, 1980-88.
- Gillham, R.W.; O'Hannesin, S.F. Enhanced degradation of halogenated aliphatics by zero-valent iron. *Ground Water* **1994**, *32*, 958-967.
- Gosset, J.M. Measurement of Henry's law constants for C<sub>1</sub> and C<sub>2</sub> chlorinated hydrocarbons. *Environ. Sci. Technol.* **1987**, *21*, 202-208.
- Gotpagar, J.; Grulke, E.; Tsang, T.; Bhattacharyya, D. Reductive dehalogenation of trichloroethylene using zero-valent iron. *Environ. Progr.* **1997**, *16*, 137-143.
- Hine, J.; Mookerjee, P.K. The intrinsic hydrophilic character of organic compounds. Correlations in terms of structural contributions. *J. Org. Chem.* **1975**, *40*, 292-297.
- Ho, W.; Yu, Q.; Bozzelli, J.W. Kinetic study on pyrolysis and oxidation of CH<sub>3</sub>Cl in Ar/H<sub>2</sub>/O<sub>2</sub> mixtures. *Combust. Sci. and Tech.* **1992**, *85*, 22-63.
- Hudlicky, M., *Reductions in Organic Chemistry*. John Wiley & Sons: New York, 1984.
- Johnson, T.L.; Fish, W.; Gorby, Y.A.; Tratnyek, P.G. Degradation of carbon tetrachloride by iron metal: complexation effects on the oxide surface. *J. Contam. Hydrol.* **1998**, *29*, 379-398.



- Johnson, T.L.; Scherer, M.M.; Tratnyek, P.G. Kinetics of halogenated organic compound degradation by iron metal. *Environ. Sci. Technol.* **1996**, *30*, 2634-3640.
- Jones, D., *Principles and Prevention of Corrosion*. Macmillan Publishing Company: New York, 1992.
- Kemp, D.S.; Vellachio, F., *Organic Chemistry*. Worth Publishers, Inc.: New York, 1980.
- Liang, L.; Korte, N.; Goodlaxson, J.D.; Clausen, J.; Fernando, Q.; Muftikian, R. Byproduct formation during the reduction of TCE by zero-valence iron and palladized iron. *Ground Water Monit. Rem.* **1997**, 122-127.
- Mackay, D.; Shiu, W.Y.; Ma, K.C., *Illustrated Handbook of Physical-Chemical Properties and Environmental Fate for Organic Chemicals*, Vol. 3; Lewis Publishers: Boca Raton, FL, 1993.
- Mohn, W.W.; Tiedje, J.M. Microbial reductive dehalogenation. *Microbiol. Rev.* **1992**, *56*, 482-507.
- Muftikian, R.; Fernando, Q.; Korte, N. A method for the rapid dechlorination of low molecular weight chlorinated hydrocarbons in water. *Water Res.* **1995**, *29*, 2434-2439.
- NIST Mass Spectral Data Center, **1999**. IR and Mass Spectra, in *NIST Chemistry WebBook*, *NIST Standard Reference Database Number 69*, W.G. Mallard and P.J. Linstrom, Editors. National Institute of Standards and Technology: Gaithersburg, MD. [Online] Available: <http://webbook.nist.gov> [June 10, 1999].
- O'Hannesin, S.F.; Gillham, R.W. Long-term performance of an in situ "iron wall" for remediation of VOCs. *Ground Water* **1998**, *36*, 164-170.
- Orth, W.S.; Gillham, R.W. Dechlorination of trichloroethene in aqueous solution using  $\text{Fe}^0$ . *Environ. Sci. Technol.* **1996**, *30*, 66-71.
- Piganiol, P., *Acetylene Homologs and Derivatives*. Mapleton House: New York, 1950.
- Pontius, F.W. New horizons in Federal regulation. *J. Am. Water Works Assoc.* **1998**, *90*, 38-46.
- Roberts, A.L.; Totten, L.A.; Arnold, W.A.; Burris, D.R.; Campbell, T.J. Reductive elimination of chlorinated ethylenes by zero-valent metals. *Environ. Sci. Technol.* **1996**, *30*, 2654-2659.
- Rutledge, T.F., *Acetylenic Compounds: Preparation and Substitution Reactions*. Reinhold: New York, 1968.

- Scherer, M.M.; Tratnyek, P.G. Dechlorination of carbon tetrachloride by iron metal: effect of reactant concentrations. *Natl. Meet.-Am. Chem. Soc., Div. Environ. Chem.* **1995**, *35*, 805-806 (Abstr.).
- Schlimm, C.; Heitz, H. Development of a wastewater treatment process: reductive dehalogenation of chlorinated hydrocarbons by metals. *Environ. Progr.* **1996**, *15*, 38-47.
- Schreier, C.G.; Reinhard, M. Transformation of chlorinated organic compounds by iron and manganese powders in buffered water and in landfill leachate. *Chemosphere* **1994**, *29*, 1743-1753.
- Semadeni, M.; Chiu, P.; Reinhard, M. Reductive transformation of trichloroethene by cobalamin: reactivities of the intermediates acetylene, chloroacetylene, and the DCE isomers. *Environ. Sci. Technol.* **1998**, *32*, 1207-1213.
- Shainyan, B.A.; Vereshchagin, A.L. Nucleophilic reactions at a vinylic center - XXVIII. Fluorochloroethenes and fluorobromoethenes in reactions with sodium alcoholates and arenethiolates. *Russ. J. Org. Chem. Transl. of Zh. Org. Khim.* **1993**, *29*, 1981-1989.
- Smith, M., "Dissolving Metal Reductions", in *Reduction: Techniques and Applications in Organic Synthesis*, Augustine R.L., Ed., Marcel Dekker, Inc.: New York, 1968; p. 95-170.
- Song, H.; Kim, Y.-H.; Carraway, E.R.; Batchelor, B. Effects of hydroxyapatite on PCE degradation by zero valent zinc. *Natl. Mtg. Am. Chem. Soc., Div. Environ. Chem.* **1999**, *39*, 359-361 (Abstr.).
- Taylor, P.H.; Dellinger, B.; Tirey, D.A. Oxidative pyrolysis of  $\text{CH}_2\text{Cl}_2$ ,  $\text{CHCl}_3$ , and  $\text{CCl}_4$  - I: incineration implications. *Int. J. Chem. Kinetics* **1991**, *23*, 1051-1074.
- Tratnyek, P.G.; Johnson, T.L.; Scherer, M.M.; Eykholt, G.R. Remediating ground water with zero-valent metals: chemical considerations in barrier design. *Ground Water Monit. Rem.* **1997**, 108-114.
- Vogan, J.L.; Gillham, R.W.; O'Hannesin, S.F.; Matulewicz, W.H.; Rhodes, J.E. Site specific degradation of VOCs in groundwater using zero valent iron. *Natl. Meet.-Am. Chem. Soc., Div. Environ. Chem.* **1995**, *35*, 800-804 (Abstr.).

- Wagman, D. D.; Evans, W. H.; Parker, V. B.; Schumm, R. H.; Halow, I.; Bailey, S. M.; Churney, K. L.; Nuttall, R. L. The NBS tables of chemical thermodynamic properties. Selected values for inorganic and C<sub>1</sub> and C<sub>2</sub> organic substances in SI units. *J. Phys. Chem. Ref. Data*, **II**, **1982**, 1-103.
- Warren, K.D.; Arnold, R.G.; Bishop, T.L.; Lindholm, L.C.; Betterton, E.A. Kinetics and mechanism of reductive dehalogenation of carbon tetrachloride using zero-valence metals. *J. Haz. Mat.* **1995**, *41*, 217-227.
- Wood, W.G., Ed. Surface cleaning, finishing and coating. In *Metals Handbook*; American Society for Metals: Metals Park, OH, 1982; Vol. 5.
- Xu, Y.; Schwartz, F.W.; Traina, S.J. Sorption of Zn<sup>2+</sup> and Cd<sup>2+</sup> on hydroxyapatite surfaces. *Environ. Sci. Technol.* **1994**, *28*, 1472-1480.
- Yamane, C.L.; Warner, S.D.; Gallinatti, J.D.; Szerdy, F.S.; Delfino, T.A. Installation of a subsurface groundwater treatment wall composed of granular zero-valent iron. *Natl. Meet.-Am. Chem. Soc., Div. Environ. Chem.* **1995**, *35*, 792-795 (Abstr.).

## SECTION VI

# PATHWAYS OF CHLORINATED ETHYLENE AND CHLORINATED ACETYLENE REACTION WITH IRON

### A. ABSTRACT

Pathways and kinetics through which chlorinated ethylenes and their daughter products react with Fe(0) were investigated through batch experiments. Substantial intra- and interspecies inhibitory effects were observed, requiring the use of a modified Langmuir-Hinshelwood-Hougen-Watson (LHHW) kinetic model in which species compete for a limited number of reactive sites at the metal surface. Results indicate that reductive  $\beta$ -elimination accounts for 87% of tetrachloroethylene (PCE), 97% of trichloroethylene (TCE), 94% of *cis*-dichloroethylene (*cis*-DCE), and 99% of *trans*-dichloroethylene (*trans*-DCE) reaction. For the highly reactive chloro- and dichloroacetylene intermediates produced from the reductive elimination of TCE and PCE, 100% and 76% of reaction, respectively, occurs via hydrogenolysis to lesser chlorinated acetylenes. The branching ratios for reactions of PCE or TCE (and their daughter products) with Fe(0) are such that production of vinyl chloride (a known human carcinogen) is largely circumvented. The reactivity trends and pathways observed in this work explain why lesser-chlorinated ethylenes have only been reported as minor products in prior laboratory and field studies of PCE and TCE reaction with Fe(0).

### B. BACKGROUND AND RATIONALE

Zero-valent iron permeable "barriers" represent a promising new treatment approach for sites contaminated with chlorinated solvents. Several iron walls have been installed around the world at sites polluted with organohalides or oxidized metal ions (RTDF, 1999). Preliminary data suggest that such walls may function for many years before replacement is required (O'Hannesin and Gillham, 1998), and that the containment they provide is an economical alternative to traditional remediation strategies such as "pump-and-treat". Even though demonstration sites have proven successful, data pertaining to the detailed kinetics and pathways for reactions of chlorinated solvents with Fe(0) are limited. Such data are needed for developing process models that might be used to optimize the design of *in situ* permeable barriers.

Over the past few years, considerable research has focused on the reduction of chlorinated ethylenes by Fe(0) (Senzaki and Kumagai, 1988; Senzaki and Kumagai, 1989; Gillham and

O'Hannesin, 1994; Burris *et al.*, 1995; Cipollone *et al.*, 1995; Mackenzie *et al.*, 1995; Vogan *et al.*, 1995; Yamane *et al.*, 1995; Orth and Gillham, 1996; Roberts *et al.*, 1996; Allen-King *et al.*, 1997; Campbell *et al.*, 1997; Gotpagar *et al.*, 1997; Liang *et al.*, 1997; Gotpagar *et al.*, 1998; O'Hannesin and Gillham, 1998; Su and Puls, 1999). No investigations exist, however, in which the rates and products of reactions of all the chlorinated ethylenes were measured under a uniform set of conditions. Most studies have focused on the decay of the parent species, with only a few including information on reaction products.

Observed products of PCE and TCE reduction include *cis*-DCE and vinyl chloride (Orth and Gillham, 1996; Campbell *et al.*, 1997; Liang *et al.*, 1997; O'Hannesin and Gillham, 1998), species which are regulated as contaminants in drinking water. Even though these represent minor products of PCE and TCE reaction, their presence has been reported to dictate the overall design and thus the economic viability of metal-based treatment systems (Vogan *et al.*, 1995; Yamane *et al.*, 1995; Tratnyek *et al.*, 1997). Also, as the lesser chlorinated ethylenes (especially *cis*-DCE) may occur in "weathered" plumes, it is important to recognize the extent to which these species may react to form vinyl chloride.

To improve our understanding of the production and persistence of different reaction products, additional information is needed concerning the mechanisms through which they are formed and subsequently degrade. Determination of reaction rate constants for a suite of related compounds may also provide insight into the mechanisms through which reactions occur.

Several different reactions of chlorinated ethylenes and their daughter products can in principal occur: hydrogenolysis (replacement of a halogen by hydrogen), reductive  $\beta$ - or  $\alpha$ -elimination (dihalo-elimination), and hydrogenation (reduction of multiple bonds). A plausible scheme for the reduction of the chlorinated ethylenes by Fe(0) can thus be represented by Figure 60. Note that for many compounds, competing reactions may exist; partially dehalogenated products may form by more than one route, and branching ratios between competing reactions will thus play an important role in product distributions. Prior studies (Roberts *et al.*, 1996; Campbell *et al.*, 1997) have provided both direct and indirect evidence that reductive  $\beta$ -elimination occurs for reactions of Fe(0) with chlorinated ethylenes possessing an  $\alpha$ ,  $\beta$  pair of chlorine atoms. One goal of the present study was to obtain rate constants for each of the reactions shown in Figure 60 and thereby determine the relative importance of the different

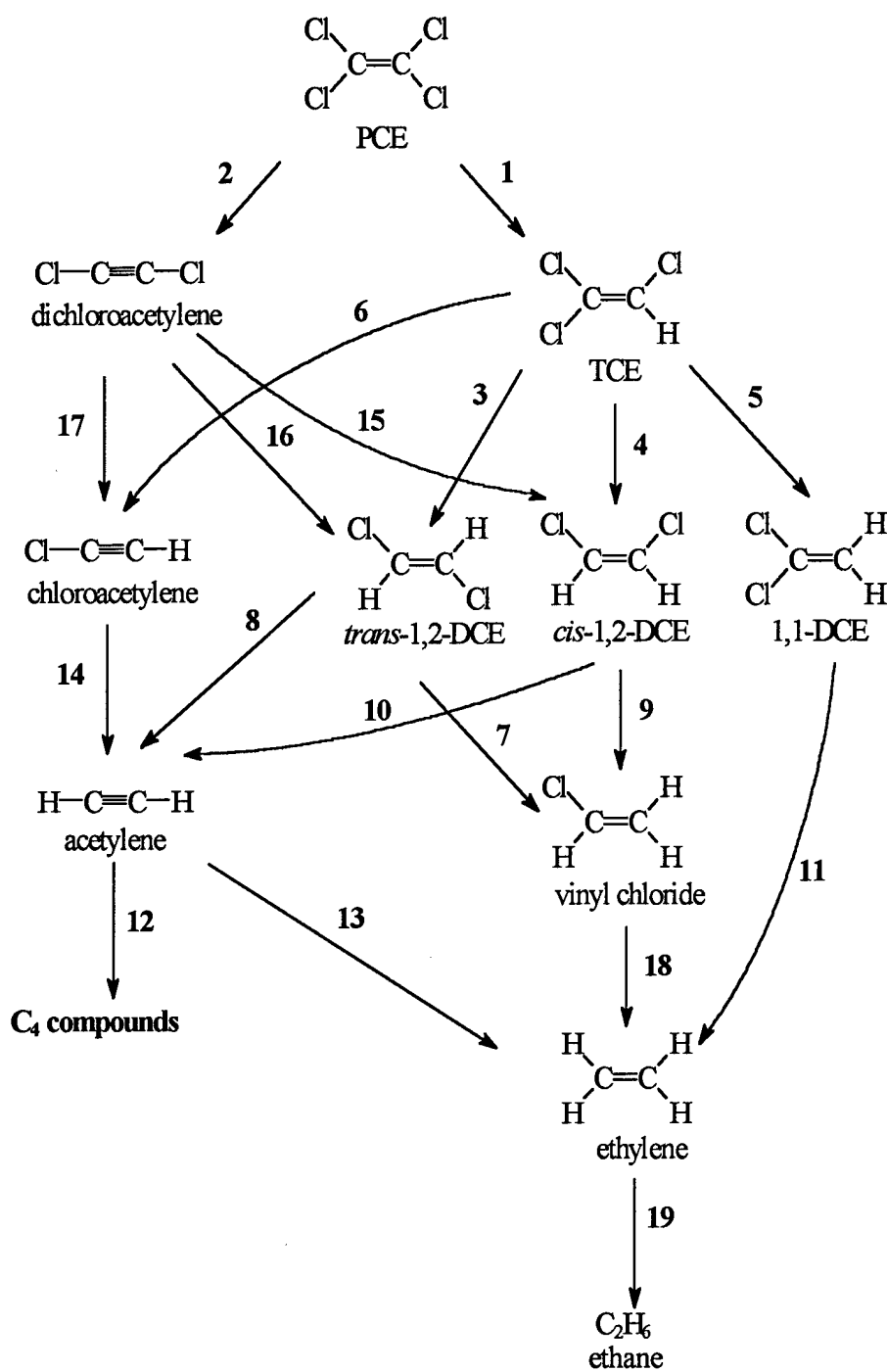


**Figure 60.** Hypothesized reaction pathways for the chlorinated ethylenes and other intermediates during reduction by  $\text{Fe}(0)$ . Numbering corresponds to Table 10. Reactions 1, 3, 4, 5, 7, 9, 14, 17, and 18 correspond to hydrogenolysis reactions, while reactions 2, 6, 8, and 10 are reductive  $\beta$ -elimination reactions, reaction 11 results from reductive  $\alpha$ -elimination, and reactions 13, 15, 16, and 19 are hydrogenation reactions.

reactions taking place.

In order to establish the pathways through which chlorinated ethylenes react with Fe(0), a kinetic model must first be developed. Previous investigations have generally invoked a pseudo-first order approach to explain the disappearance of the parent species. In general, an expression such as:

$$\frac{dC}{dt} = -k_{obs}C \quad (17)$$

is used, where  $C$  is concentration and  $k_{obs}$  ( $=k_{SA} \cdot \rho_{SA}$ ) is the pseudo-first-order rate constant. This rate constant  $k_{obs}$  is thought to be composed of the product of the metal loading of the system,  $\rho_{SA}$  ( $\text{m}^2/\text{L}$ ), and an intrinsic (or surface area normalized) rate constant,  $k_{SA}$  (with units of  $\text{L} \cdot \text{m}^{-2} \cdot \text{h}^{-1}$ ).

Numerous examples suggest that such a pseudo-first order model may, however, be inadequate. The pseudo-first order rate "constant" for reaction of carbon tetrachloride with iron (Scherer and Tratnyek, 1995; Johnson *et al.*, 1996; Johnson *et al.*, 1998) has been shown to be dependent upon the initial concentration of carbon tetrachloride. Similar results were observed for the reduction of nitrobenzenes by Fe(II) adsorbed to magnetite (Klausen *et al.*, 1995) and by Fe(0) (Devlin *et al.*, 1998). These observations suggest that iron particles may contain a limited number of reactive sites. Although some studies suggest that  $k_{SA}$  may be influenced by solution conditions (pH, chloride ion, *etc.*; Johnson *et al.*, 1998) the impact of a finite number of reactive sites on  $k_{SA}$  has received only limited attention (Scherer *et al.*, 1999). Modeling the kinetics of reactions displaying such behavior requires an alternative to a simple pseudo-first-order approach. Such effects can be incorporated into a kinetic model by recognizing that reactions at surfaces involve several steps: (a) adsorption of substrates to reactive sites at the surface; (b) reaction of the substrate; (c) desorption of the products. The model discussed here is based on an adaptation of Langmuir-Hinshelwood-Hougen-Watson (LHHW) kinetics (Carberry, 1976; Froment and Bischoff, 1990; Fogler, 1992). This model is often invoked to describe surface-mediated catalytic reactions.

Assuming that mass transfer limitations are either unimportant or can be overcome by efficient mixing (Arnold *et al.*, 1999), the rate at which a reaction occurs at a surface can be controlled by any of the three steps listed above. The rate controlling step may be identified by examining the influence of initial substrate concentration on initial rate, as demonstrated in

Figure 61. The rate expressions in the case of reaction of a parent compound A to a single product B for each case are given in Figure 61 and below, where  $k$  values are kinetic constants,  $S_t$  is the concentration of reactive sites, and  $K$  values are adsorption parameters.

For an adsorption-limited case in the absence of species that compete for reactive sites (Figure 61a), it can be demonstrated (see Appendix A) that the initial rate can be expressed as:

$$-r_{A0} = (k^a S_t) C_{A0} \quad (18)$$

This is equivalent to the pseudo-first order expression given in Equation (17).

A hyperbolic relationship between initial rate and initial concentration is observed for the surface reaction-limited case (Figure 61b).

$$-r_{A0} = \frac{(k^s S_t) K_A C_{A0}}{1 + K_A C_{A0} + K_B C_{B0}} \quad (19)$$

Note that if the adsorption parameters  $K$  (as well as the concentration  $C_{B0}$  of the product) are very small (such that  $\sum K_m \cdot C_m \ll 1$ ), the surface-reaction limited case cannot be distinguished experimentally from an adsorption-limited or pseudo-first order reaction.

Finally, the rate of disappearance of the parent compound for the desorption limited case (Figure 61c) is expressed as (see Appendix A):

$$-r_A = r_d = (k^d S_t) \quad (20)$$

where  $k^d$  ( $\text{h}^{-1}$ ) is the kinetic constant for a given desorption-limited reaction. For this case, the rate of reaction is independent of concentration (*i.e.*, pseudo-zero order).

The simple equations given above need to be extended for a multi-step process involving parallel and sequential reactions such as those shown in Figure 60. It can be shown (Appendix A) that for a surface reaction-limited process the relevant expressions are:

$$\frac{dC_i}{dt} = - \frac{\left( \sum_{j=1}^{N_j} k_{ij}^s S_t \right) K_i C_i}{1 + \sum_{m=1}^{N_m} K_m C_m} = -k_{obs} C_i \quad (21)$$

$$\frac{dC_j}{dt} = \frac{\left( \sum_{i=1}^{N_j} k_{ij}^s S_t \right) K_i C_i}{1 + \sum_{m=1}^{N_m} K_m C_m} - \frac{\left( \sum_{p=1}^{N_p} k_{jp}^s S_t \right) K_j C_j}{1 + \sum_{m=1}^{N_m} K_m C_m} \quad (\text{for all } j) \quad (22)$$



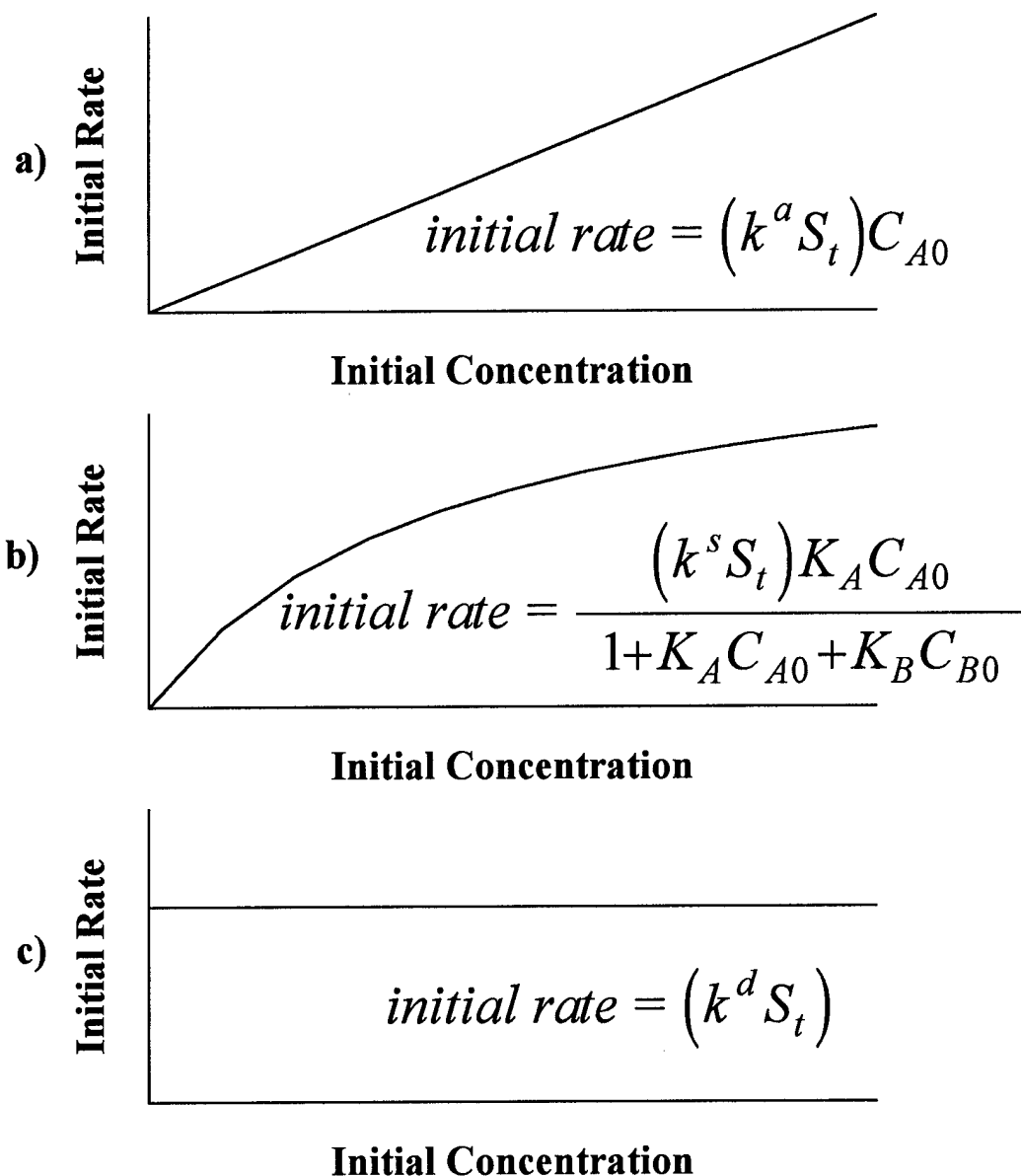


**Figure 61.** Behavior of initial rate of reaction of parent compound A to single product B as a function of initial concentration ( $C_{A0}$ ) of compound A according to the LHHW heterogeneous kinetic model for a) an adsorption-limited reaction, b) a surface reaction-limited reaction, and c) a desorption-limited reaction. Note that only for an adsorption-limited reaction (case a) would a measured pseudo-first order rate “constant” be truly constant.

where  $C$  is aqueous concentration,  $k_{ij}^s$  ( $\text{h}^{-1}$ ) is the kinetic constant for a given surface-limited reaction,  $S_t$  ( $\mu\text{M}$ ) is the abundance of reactive sites per L of solution, and  $K$  is an adsorption parameter (with units of  $\mu\text{M}^{-1}$ ). In our experiments, the kinetic constant for a given reaction and the site concentration cannot be determined independently, and are lumped together as  $(k^s S_t)$  with units of  $\mu\text{M}/\text{h}$ . The subscript  $i$  identifies the parent species;  $N_j$  is the total number of primary products formed directly from the parent;  $N_p$  is the total number of secondary products formed from the reaction of a primary daughter product; and  $N_m$  is the total number of species that inhibit the reaction of the parent and/or daughter species. Note in Equation (21) that  $k_{obs}$ , the pseudo-first order rate "constant", is not in fact constant but rather varies with the concentration of the parent compound and other species which compete for reactive sites.

Equation (22) assumes that the rate of reaction of the product is also surface-reaction limited. If reaction of the daughter product is adsorption-limited, the decay term is replaced as follows:

$$\frac{dC_j}{dt} = \frac{\left( \sum_{j=1}^{N_j} k_{ij}^s S_t \right) K_i C_i}{1 + \sum_{m=1}^{N_m} K_m C_m} - \frac{\left( \sum_{p=1}^{N_p} k_{jp}^a S_t \right) C_j}{1 + \sum_{m \neq j}^{N_m} K_m C_m} \quad (23)$$

For this case, the lumped kinetic parameter  $(k^a S_t)$  has units of  $\text{h}^{-1}$ .

In this study, the rates and products of chlorinated ethylene and chlorinated acetylene reaction with Fe(0) were examined in batch systems under a consistent set of solution conditions. Data were interpreted in the context of the LHHW model to account for intra- and interspecies competitive effects. The results were then used to calculate the relative contributions of competing reductive elimination and hydrogenolysis reactions (in the case of chlorinated ethylenes) or competing hydrogenolysis and hydrogenation reactions (in the case of substituted acetylenes). As with our earlier studies with zinc, a further objective of our investigations was to assess the possibility of developing quantitative structure-activity relationships (QSARs) for the reduction of the chlorinated ethylenes by iron. The final goal of this work was to interpret all of the available evidence so as to propose a mechanism for the surface-mediated reaction.

## C. EXPERIMENTAL SECTION

### 1. Chemicals

The following chemicals were used without further purification: tetrachloroethylene (99.9%, HPLC grade, Aldrich); trichloroethylene (99.5+%, Aldrich); *cis*-dichloroethylene (97+%, Aldrich); *trans*-dichloroethylene (Supelco); vinylidene chloride (1,1-dichloroethylene, 99%, Aldrich); vinyl chloride in methanol (Chem Service, 2000 µg/mL); 10% ethylene in helium and 1% acetylene in nitrogen (Scott Specialty gas). Spiking solutions were prepared for PCE, TCE, and the DCE isomers in methanol (HPLC grade, J.T. Baker).

The 1 N HCl acid solution for cleaning the iron was prepared using deoxygenated (argon-sparged), deionized water (Milli-Q Plus UV, Millipore). The argon stream was purified using an in-line molecular sieve and oxygen traps. Reaction bottles were filled with deoxygenated solutions of 0.1 M NaCl (99%; J.T. Baker) and 50 mM Tris buffer (tris[hydroxymethyl]aminomethane, reagent grade; Sigma), pH 7.2. Solutions were deoxygenated by sparging (1 h/L) with the purified argon. The high (relative to typical groundwater) NaCl concentration was employed to poise the chloride content in the system, as chloride ion is released during reductive dechlorination.

### 2. Synthesis of Chlorinated Acetylenes

Chloroacetylene and dichloroacetylene were synthesized from *cis*-dichloroethylene and trichloroethylene, respectively. Potassium hydride (35% in mineral oil, Aldrich) was rinsed three times with freshly-distilled dry tetrahydrofuran (THF). The dehydrohalogenation of the *cis*-DCE or TCE was induced by potassium hydride and a catalytic amount of methanol in dry tetrahydrofuran as described by Denis *et al.* (1987). Verification of the identities of the synthesis products was conducted via gas chromatography/mass spectrometry (GC/MS). The resulting solutions of the chlorinated acetylenes in tetrahydrofuran were used as spiking solutions. Although no purification of these reportedly explosive (Piganiol, 1950; Rutledge, 1968; Denis *et al.*, 1987) gases was attempted, the progress of the reaction was monitored by GC and the supernatant was not removed until *cis*-DCE and TCE could no longer be detected.

### 3. Metal Preparation

The iron metal (Fisher, 100 mesh electrolytic) was cleaned with 1 M HCl to remove surface oxides (Wood, 1982). Within the anaerobic chamber, the iron metal and acid were placed

in a 250 mL Erlenmeyer flask and shaken by hand for 3 minutes. The acid was decanted and the metal was rinsed three times with deoxygenated water and once with acetone. The flask was then closed and removed from the anaerobic chamber so that the metal could be oven dried (100°C) under argon. The cleaned metal was returned to the anaerobic chamber after drying, and was used within 24 hours. The surface area was 0.16 m<sup>2</sup>/g as measured via Kr adsorption using a Micromeritics Flowsorb II 2300 (Fennelly and Roberts, 1998).

#### **4. Experimental Systems**

Reaction bottles were filled with the deoxygenated 0.1 M NaCl, 50 mM Tris solution within an anaerobic chamber. All experiments were carried out in 160 mL serum bottles sealed with Teflon<sup>®</sup> faced butyl rubber septa (Wheaton). Experiments were performed with 0.25 g iron for all species. Additional reactions with the acetylenes were conducted at an iron loading of 0.10 g. The bottles containing the deoxygenated buffer solution and iron were aged overnight prior to spiking with the species of interest the following morning to allow the pH to stabilize. The bottles were mixed around their longitudinal axes at 45 rpm on a rotator (Cole-Parmer) both during the aging and during the subsequent incubations with the organohalides.

Chlorinated ethylenes were introduced to the reactors via a methanolic spike (resulting in 0.003 to 0.06% methanol by weight), and the chlorinated acetylenes via the tetrahydrofuran solution in which they were synthesized (resulting in 0.006-0.06% THF by weight). Experiments were conducted to verify that methanol concentration did not affect reaction rates. Nonetheless, additional methanol was added to the bottles such that all contained 0.06% by weight in order to maintain a consistent set of experimental conditions. Spiking solutions of acetylene or ethylene were prepared by equilibrating the buffer solution with the target gas mixture in a 1 L polycarbonate syringe (Hamilton). Reactors were spiked with aliquots of the equilibrated solution to achieve the desired starting concentration. Experiments were performed over a range of initial concentrations (3-300 µM). At specified intervals, 1 mL samples were withdrawn from the reactors while simultaneously injecting 1 mL of deoxygenated buffer solution. This made it possible to avoid introducing headspace during sampling, allowing anoxic conditions to be maintained.

Additional studies of the reactions of *cis*-DCE, vinyl chloride, and ethylene with Fe(0) were conducted in deuterated water (Aldrich, 99.9 atom % D). The procedures were identical to

those described above except for the substitution of H<sub>2</sub>O by D<sub>2</sub>O. H/D exchange for ethylene and acetylene in 0.1 M NaCl/50 mM Tris/D<sub>2</sub>O was also examined in the absence of iron.

The pH was reasonably stable over the course of the experiments. The initial buffer solution had a pH of 7.3. After being equilibrated with the iron metal overnight, the pH was 7.4-7.5. The maximum pH measured at the end of an experiment was 7.7. This reading was for the PCE experiments which had the longest duration (11 days).

## **5. Analytical Methods**

The analytical methods employed were essentially identical to those described in Section V. The only exception is that aqueous chlorinated acetylene concentrations were quantitated directly using the acetylene calibration curve, the FID response factors (relative to acetylene) and Henry's Law constants determined in Section V.

Samples from experiments conducted in deuterated water were analyzed on a Trace GC 2000 (Thermo-Quest) equipped with a Voyager quadrupole mass spectrometer detector (Thermo-Quest) and a GS-GasPro column (60 m × 0.32 mm ID; J&W Scientific). The mass spectra were recorded in electron impact (EI) mode by scanning in the range of  $m/e$  12-200. Samples were injected in split mode using an HS 2000 headspace autosampler (Thermo-Quest). The distributions of isotopomers were estimated using the approach described in Section VII.

## **6. Kinetic Modeling**

The kinetic modeling was performed using the software package *Scientist for Windows* (v. 2.01, Micromath, Salt Lake City, UT). When calculating the necessary parameters for a given species, the kinetic and adsorption constants for reactions of intermediates that were detected in a given experiment were constrained to be equal to those determined in independent experiments in which the intermediates were introduced as the starting material. The rate of parent compound disappearance and the product distribution data were then used to determine the relative magnitudes of the competing reactions for the parent compound. The kinetic model is described more thoroughly in Appendix A.

For each species, the entire suite of experiments conducted at different initial concentrations was modeled simultaneously. In this manner, both the kinetic and adsorption parameters could be obtained in a single fitting exercise. This approach also enabled the contributions of the competing reactions to be determined directly. If the results obtained from

each individual timecourse were modeled separately, statistically useful values for the kinetic and adsorption parameters could not be calculated.

It was quickly discovered that if *Scientist* were used to simultaneously model the results of experiments conducted over a two order-of-magnitude range in initial concentration, a higher priority was placed on fitting the results from the experiments conducted at high initial concentrations. The kinetic and adsorption constants obtained successfully described experimental results at high initial concentrations, but fits proved much poorer for experiments conducted at low initial concentrations. To avoid such problems, all data (for parent and product species alike) pertaining to transformation of a particular test compound were normalized by the initial concentration of the parent species added to the reactor. The initial concentrations were calculated by fitting the data for the parent compound to an exponential decay expression. As all data were normalized by an initial concentration that was calculated prior to the fitting using the heterogeneous model, these initial concentration values were held fixed during the subsequent data fitting.

The model equations used for each species and further details concerning the modeling procedure are given in Appendix B. Example *Scientist* model files used for the normalized data are also given in Appendix B, along with explanations of the changes to the equations necessitated by the normalization procedure. As the parent compounds and reaction products may compete with one another for reactive sites, competitive behavior was also included in the model whenever it was encountered (or in some cases, was assumed to occur).

## D. RESULTS

### 1. *Experimental Variables*

Investigations published in the literature thus far have suggested that several variables may play a role in the measured rates of reduction of chlorinated ethylenes in zero-valent iron systems. Among these are metal loading, mixing rate, and initial organohalide concentration. As all of these factors may substantially influence the accuracy and type of descriptive values derived from the model, the investigation initially focused on these variables.

#### a. *Effect of metal loading*

Although some researchers have found a linear relationship between iron loading and reaction rate (Su and Puls, 1999), other investigations have suggested that reaction rate may not

be directly proportional to metal loading (Scherer and Tratnyek, 1995; Gotpagar *et al.*, 1997). Normalization of rate constants by metal loading, without testing if such a procedure is in fact valid, could bias the results of kinetic models or attempted LFERs. In investigating the effect of metal loading on reaction rate, only one initial concentration was employed (4  $\mu\text{M}$ ) to prevent possible confounding effects caused by differences in initial organohalide concentration. The results for *trans*-DCE are shown in Figure 62.

As Figure 62 reveals, the pseudo-first order rate constant is only directly proportional to metal loading over a limited range (0-0.5 g per 160 mL). It might be tempting to assume that a shift from kinetic to mass transfer control has occurred, an explanation that has been advanced by others (Gotpagar *et al.*, 1997). This answer is not wholly satisfying, however, for a mass transfer rate coefficient, as well as the surface reaction coefficient, should be directly proportional to metal loading, as shown in the expression for the overall rate coefficient,  $k_{\text{overall}}$  (Arnold *et al.*, 1999):

$$\frac{1}{k_{\text{overall}}} = \frac{1}{a} \left( \frac{1}{k_{\text{mt}}} + \frac{1}{k_{\text{SA}}} \right) \quad (24)$$

where  $a$  is the metal surface area per liter of solution and  $k_{\text{mt}}$  is the mass transfer rate coefficient. An explanation more consistent with the data shown in Figure 62 is that mixing is inefficient at the higher metal loadings (Poniec and Bond, 1995). The mixing system employed may not adequately expose all of the added metal surface area to the surrounding solution.

Further screening studies were performed with other species to verify that pseudo-first order rate constants displayed a linear response to metal loading (for a given initial concentration) over the same iron loading range (0-0.5 g per 160 mL). The initial pseudo-first order rate constants for all the chlorinated ethylenes were found to be linearly proportional to iron loading over this range. To avoid possible difficulties introduced by a nonlinear relationship between rate constant and metal loading, all experiments were conducted in the linear range of metal loading, with most being performed at 0.25 g iron per serum bottle (160 mL).

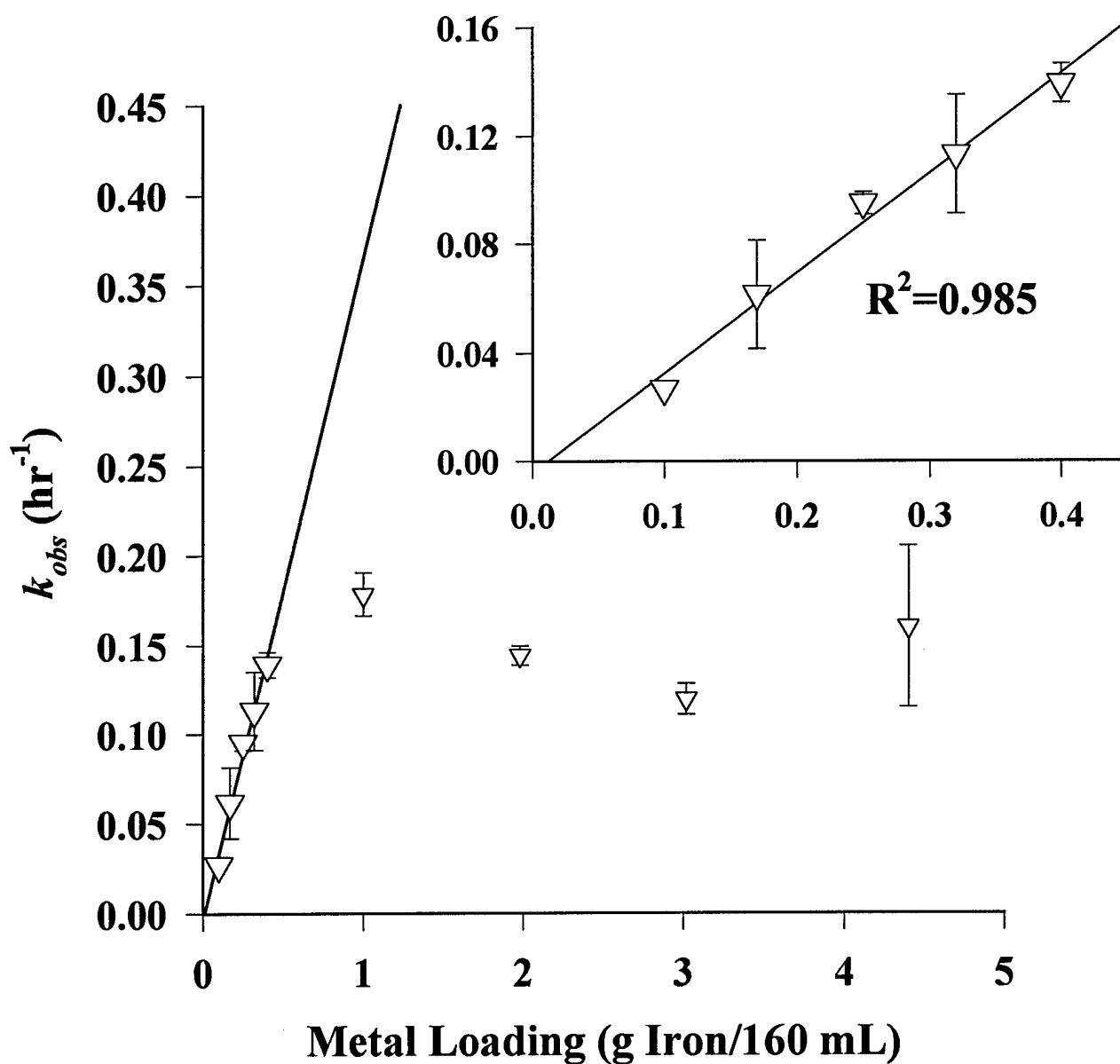


**Figure 62.** Effect of metal loading on initial pseudo-first order rate constant for *trans*-DCE reaction with Fe(0). Initial concentration of *trans*-DCE was 4  $\mu$ M. Experiments were conducted in 160 mL of 0.1 M NaCl, 50 mM Tris buffer (pH 7.2) and rotated at 45 rpm.



### **b. Effect of mixing rate and mass transfer**

As a check that mixing rate was not introducing mass transfer limitations, experiments were performed at various mixing speeds. Again, to prevent intraspecies competition for reactive sites from affecting the results, all experiments were carried out at one initial concentration. Two of the species found to be most reactive, *trans*-DCE and acetylene, were chosen for detailed study, as more highly reactive species are those most likely to encounter mass transfer limitations. As shown in Figure 63, there was little effect of mixing speed on reaction rate between 30 and 60 rpm. A mixing speed of 45 rpm was therefore chosen for the remainder of the experiments.

The potential existence of a mass transfer limitation was also examined via a mass transfer correlation. As the iron particles seemed to be suspended in solution by our mixing apparatus, a correlation for mass transfer to suspended particles (Harriott, 1962) was used to calculate a mass transfer coefficient, assuming that the iron particles were spherical. This approach has worked well for quantifying mass transfer limitations in the reduction of polychlorinated ethanes by zinc particles (Arnold *et al.*, 1999) under very similar experimental conditions. Calculations suggested that mass transfer limitations were unlikely for the chlorinated ethylenes, but that experiments conducted at low concentrations with the highly reactive acetylenic species may have been partially mass transfer limited, as the values of  $k_{mt} \cdot a$  for the acetylenes were around  $2 \text{ h}^{-1}$ .

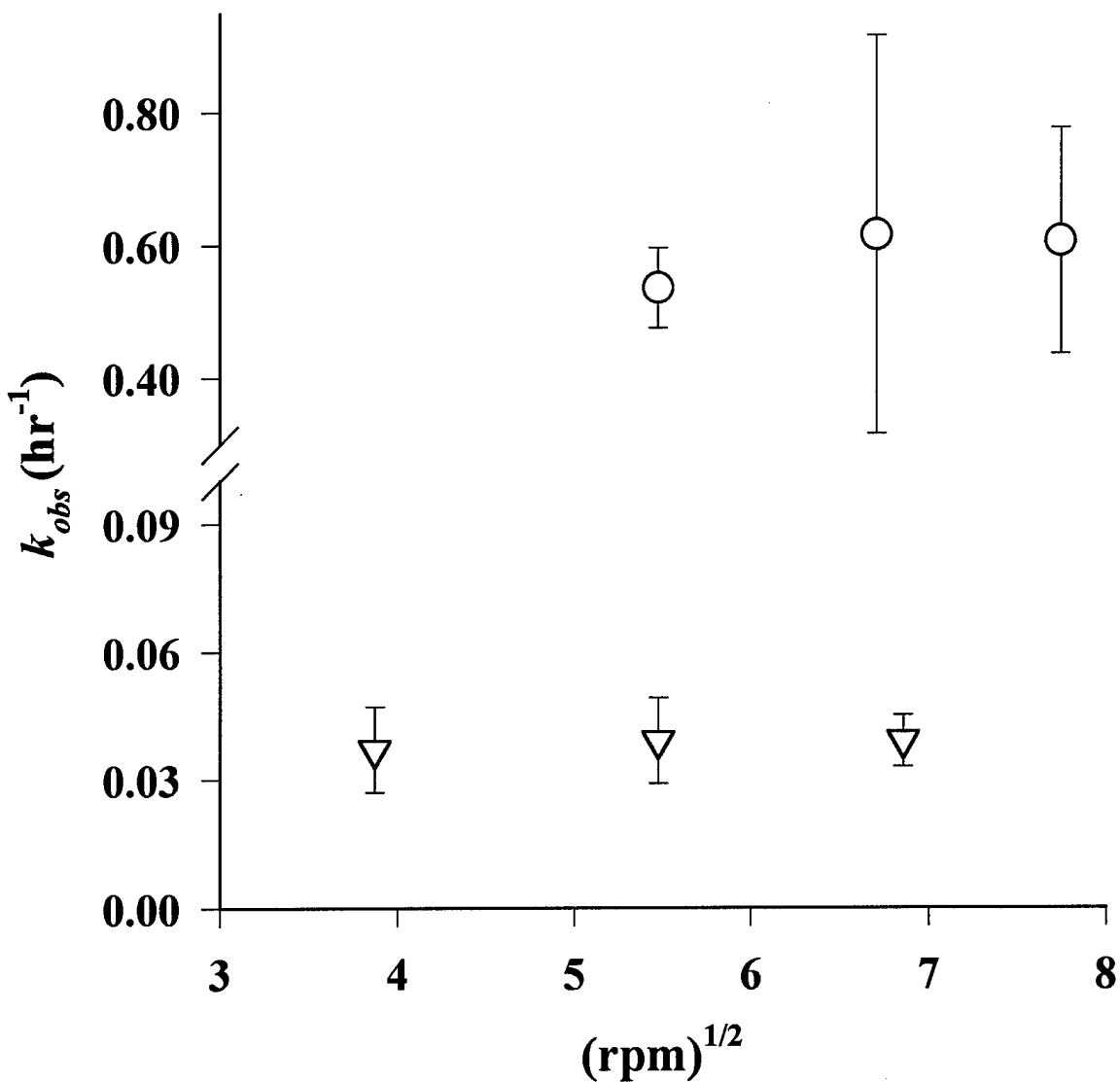


**Figure 63.** Effect of rotation rate on the pseudo-first order rate constant for acetylene (O) and *trans*-DCE ( $\nabla$ ). Initial concentration of acetylene was 3  $\mu\text{M}$  and *trans*-DCE was 4  $\mu\text{M}$ . Experiments were conducted in 160 mL of 0.1 M NaCl, 50 mM Tris buffer (pH 7.2) with 0.25 g Fe(0).

### c. Effect of initial oxidant concentration

The effect of initial oxidant concentration on the measured initial pseudo-first order rate constant ( $k_{obs}$ ) and on the calculated initial rate ( $k_{obs} \cdot C_0$ ) is shown for the chlorinated ethylenes, chlorinated acetylenes, acetylene and ethylene in Figure 64. PCE did not undergo sufficient transformation to allow the direct determination of initial pseudo-first order rate constants from parent compound disappearance at high concentrations, so a pseudo-zero order approach was employed. Most species displayed a hyperbolic dependence of initial rate on initial concentration, consistent with surface-reaction limitation (eqn. 19; Figure 61b). This suggests that species compete for a limited number of reactive sites at the particle surface.

Results for vinyl chloride and ethylene were the exception; behavior of these compounds was consistent with adsorption limitation (or surface reaction with small adsorption constants). Adsorption parameters ( $K_i$ ) for each species are provided in Table 10. With few exceptions,  $K$  values follow the trend acetylenes > TCE or PCE > dichloroethylenes. That vinyl chloride and ethylene appear to demonstrate adsorption limitation rather than surface reaction limitation may just represent a continuation of this trend, with  $K$  values too small to determine. As the mass transfer calculations suggest that reactions of the acetylenes are only partially mass transfer limited (at low concentrations), the overall rate constant may still display a concentration dependence if the appropriate expression (based on an normalized rate "constant" obtained from Equation 21) is inserted for  $k_{SA}$  in Equation (24).

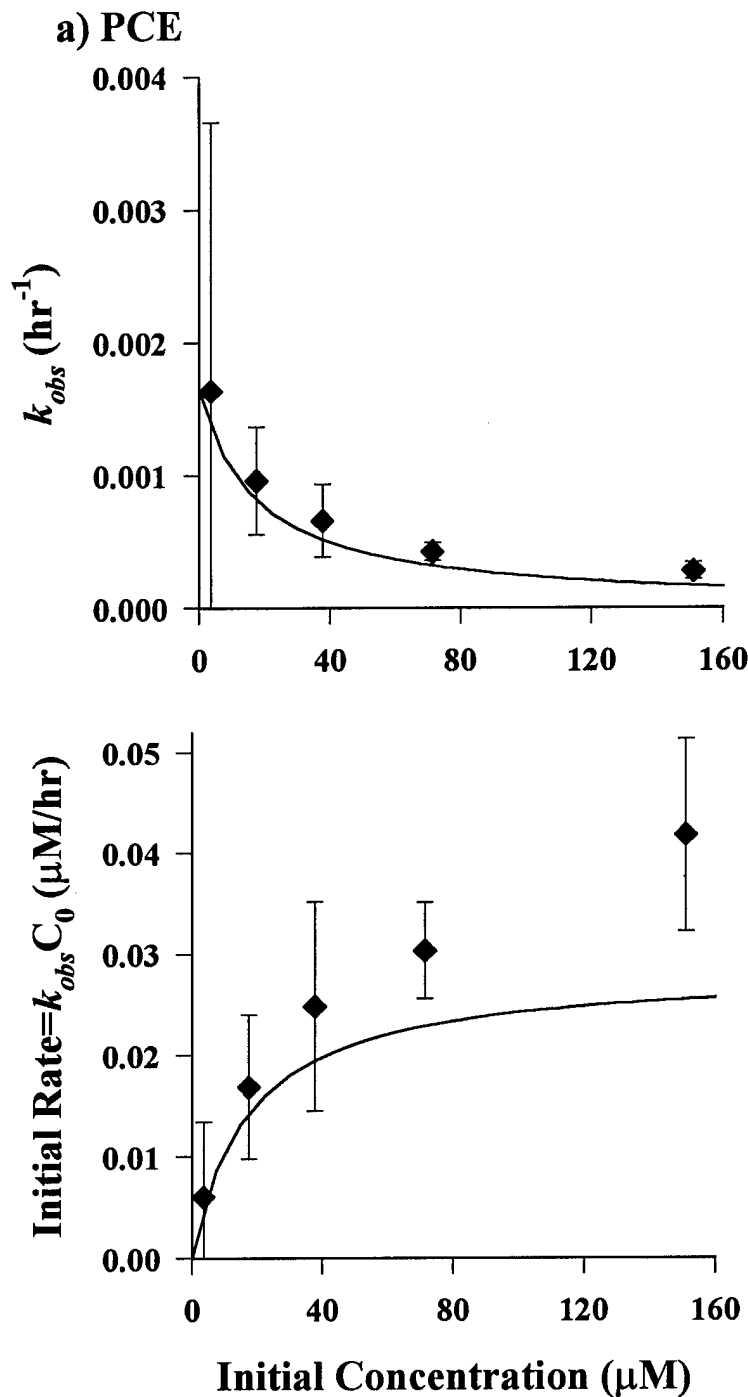


**Figure 64.** Effect of initial substrate concentration on initial pseudo-first order rate constant ( $k_{obs}$ ) and initial rate ( $k_{obs}C_0$ ) for reduction by Fe(0) of a) PCE (◆), b) TCE (Δ), c) *trans*-DCE (∇), d) *cis*-DCE (▲), e) 1,1-DCE (▼), f) vinyl chloride (◇), g) ethylene (■), h) acetylene (○), i) chloroacetylene (+), and j) dichloroacetylene (●). Experiments were performed in reactors containing 160 mL of 0.1 M NaCl, 50 mM Tris buffer (pH 7.2) rotated at 45 rpm. A mass of 0.25 g Fe(0) was used for the ethylene species and 0.10 g for the acetylene compounds. Lines represent model predictions based on the parameters in Table 10 and are not fits to the data shown.

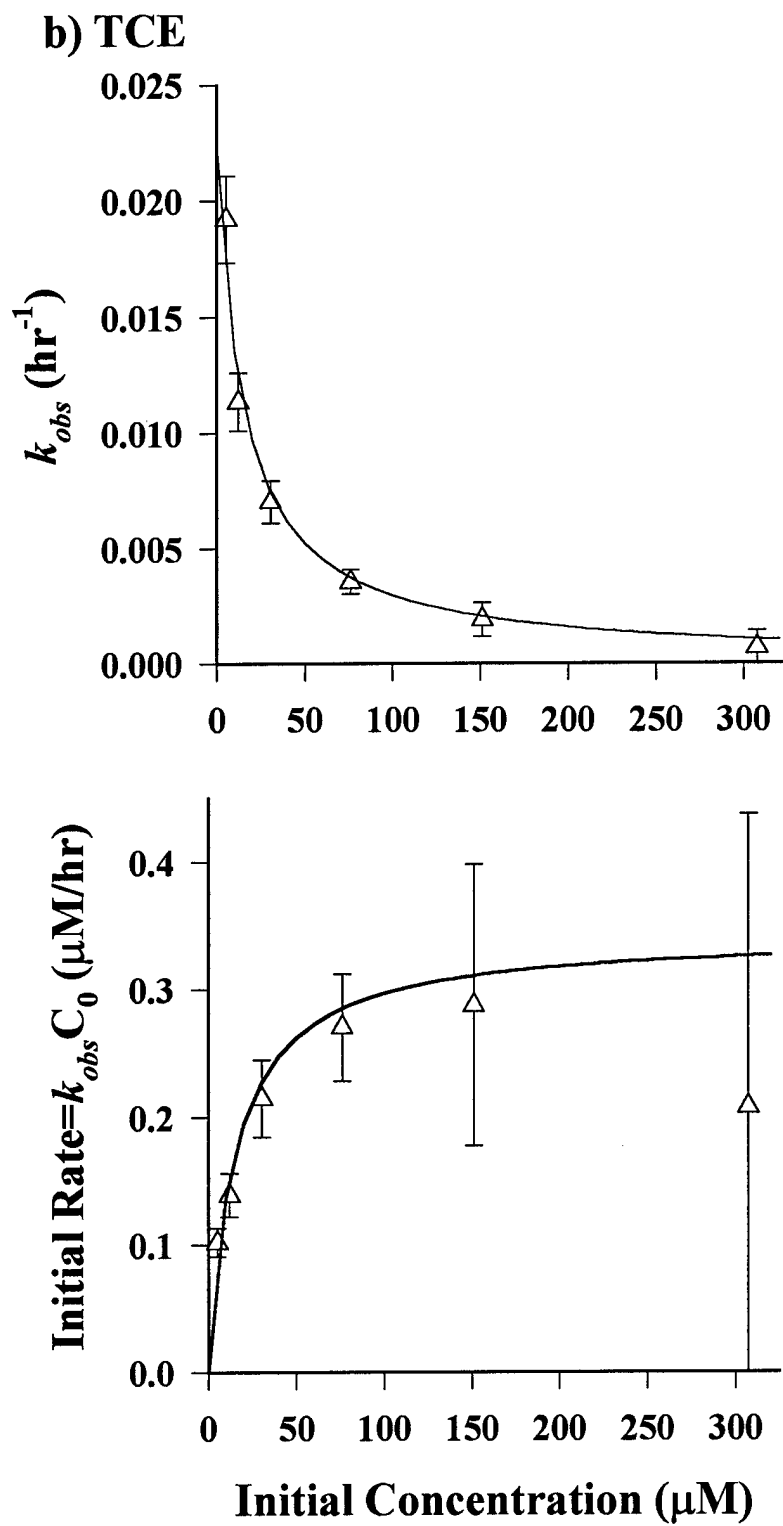


Figure 64 (continued).

c) *trans*-DCE

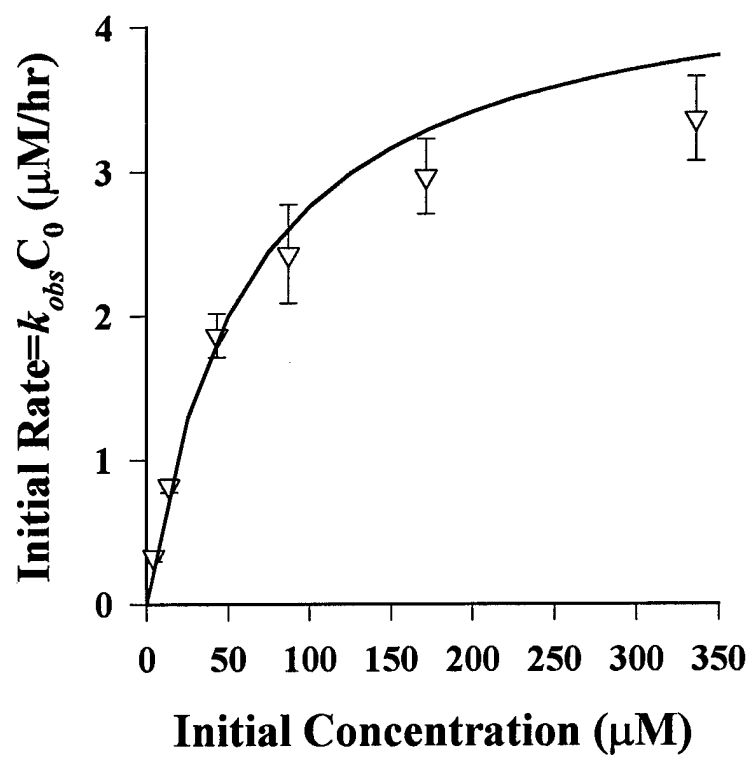
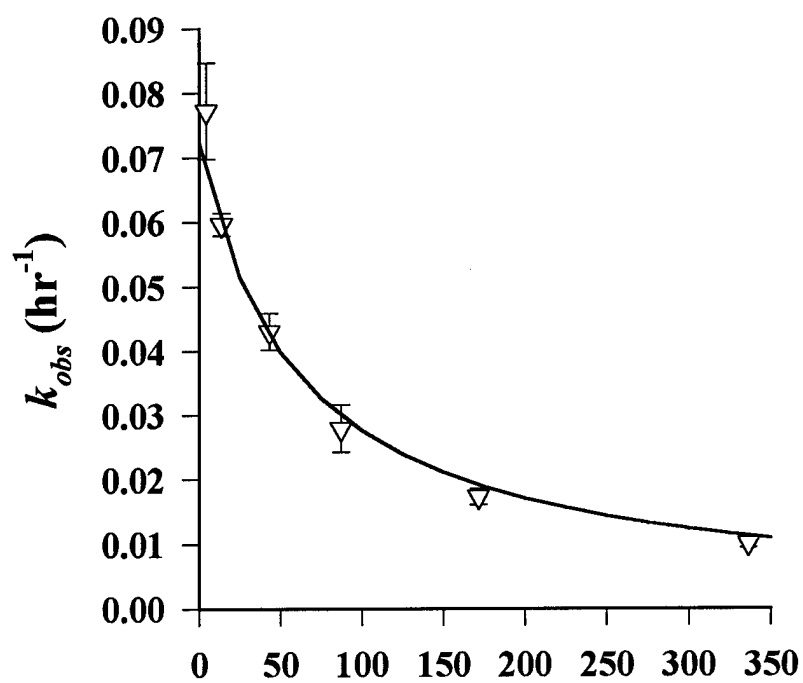


Figure 64 (continued).

d) *cis*-DCE

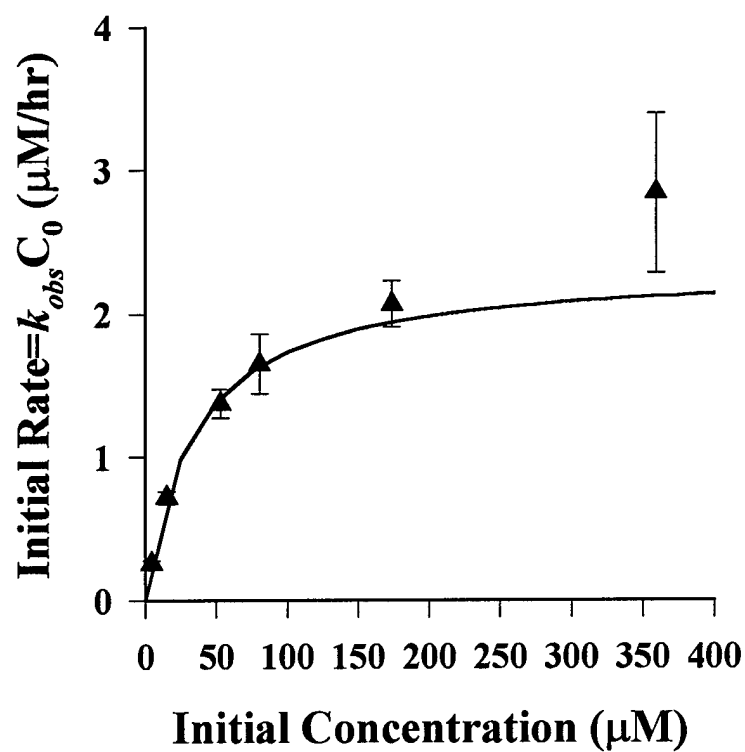
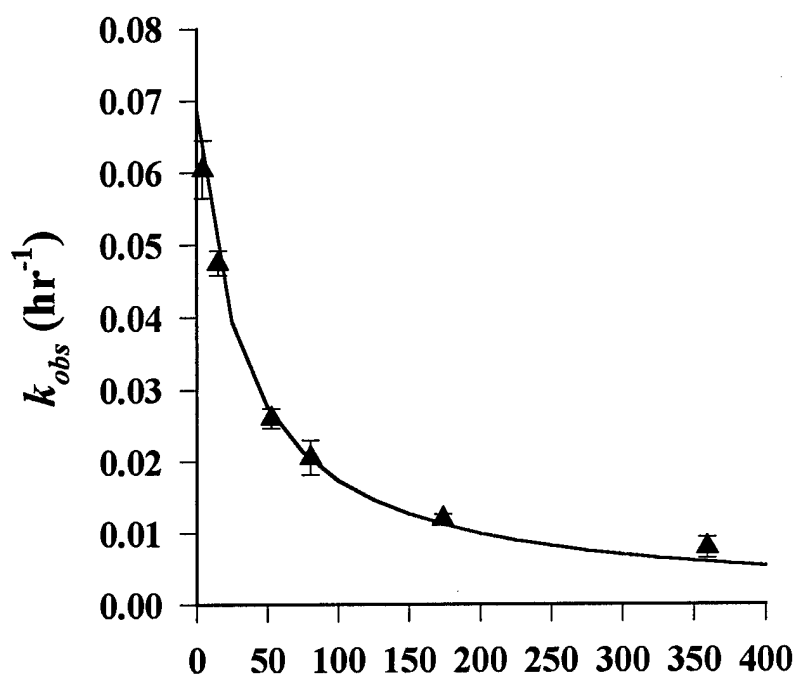


Figure 64 (continued).

**e) 1,1-DCE**

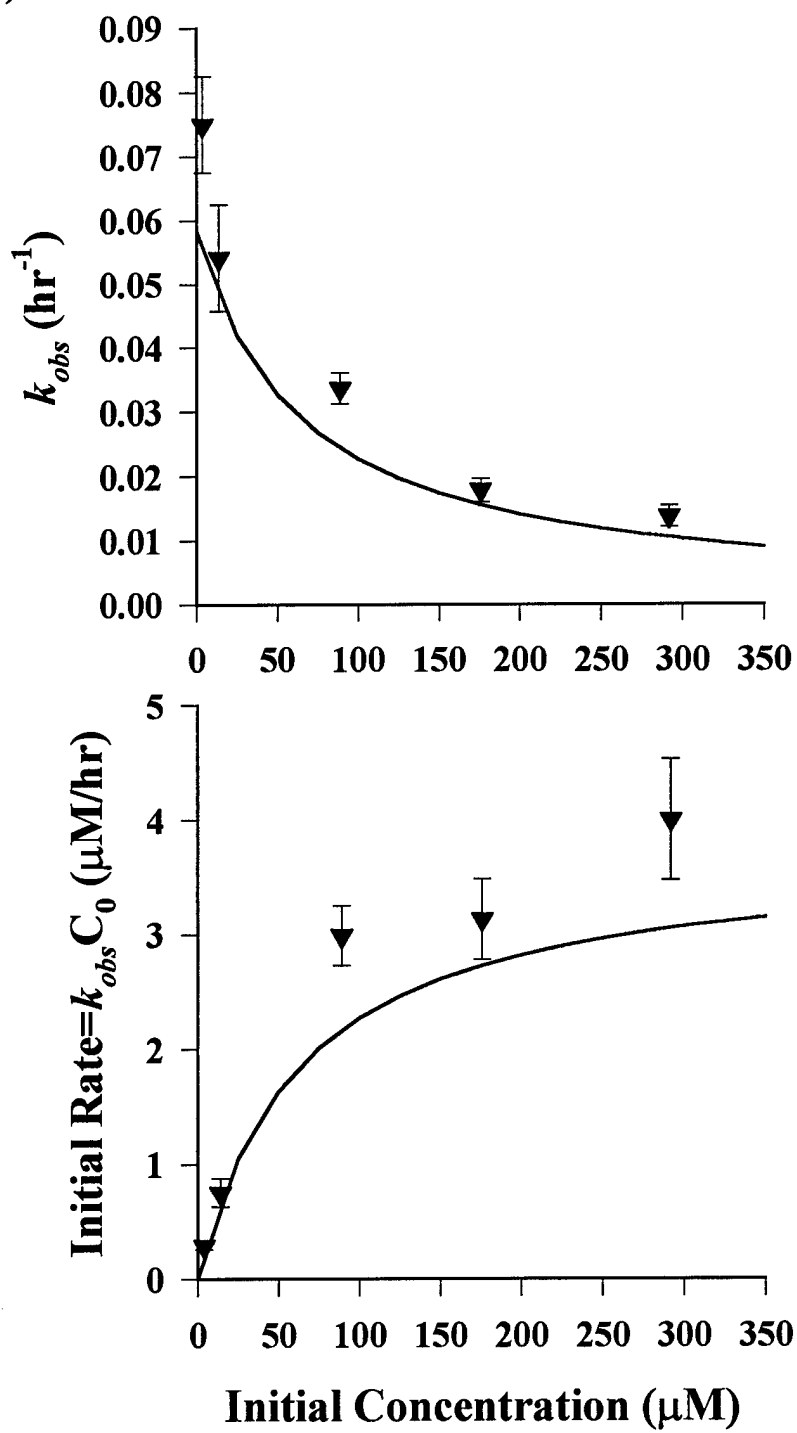


Figure 64 (continued).



**f) vinyl chloride**

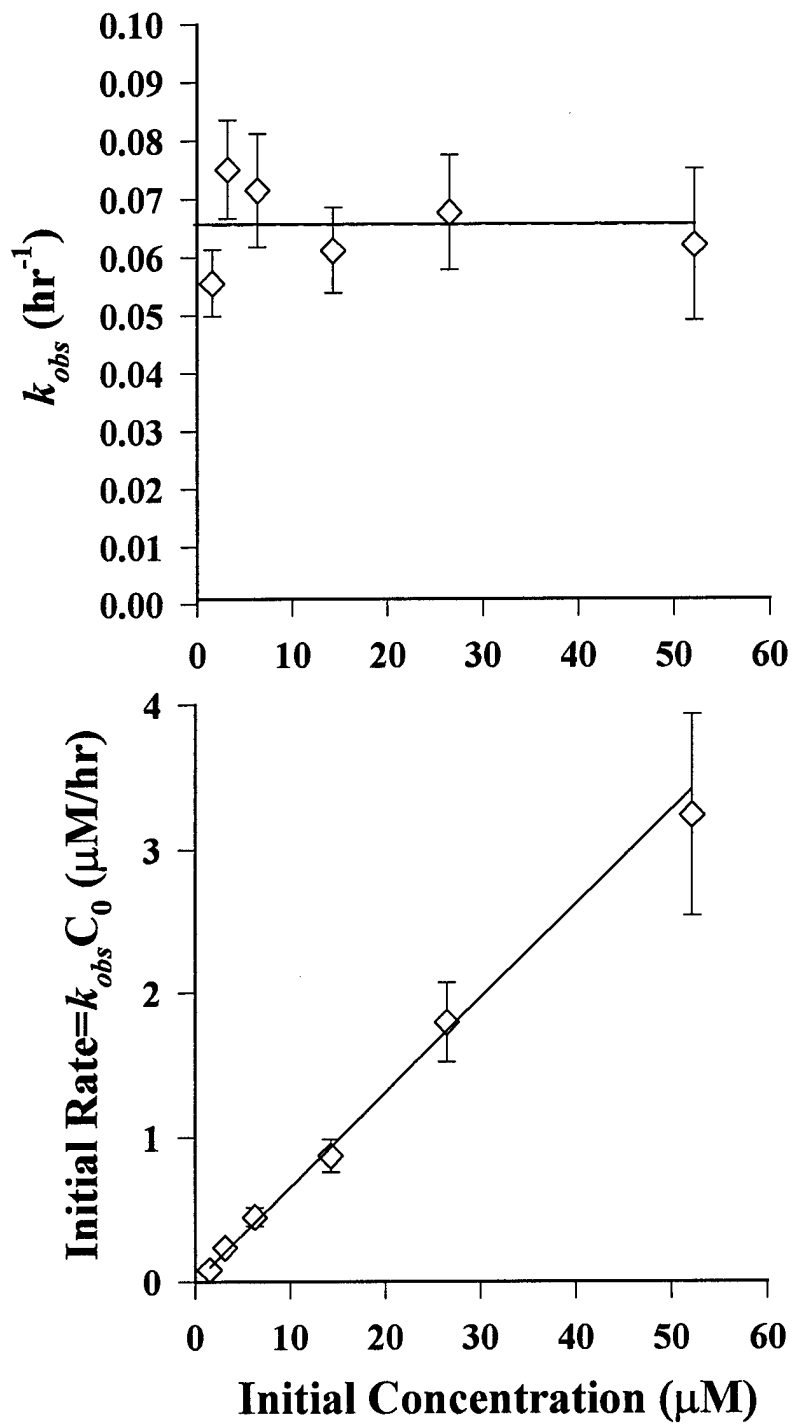
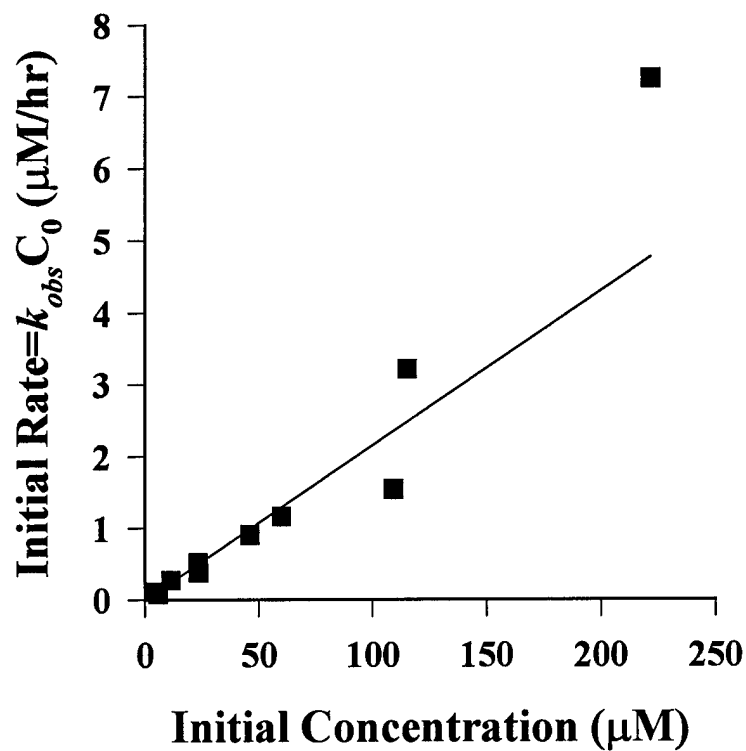
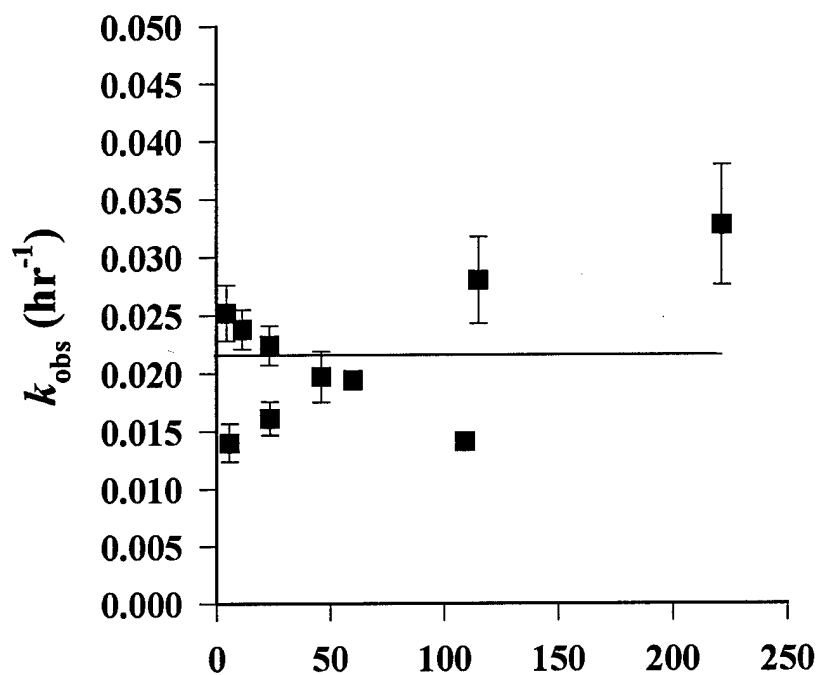


Figure 64 (continued).

**g) ethylene**



**Figure 64 (continued).**

**h) acetylene**

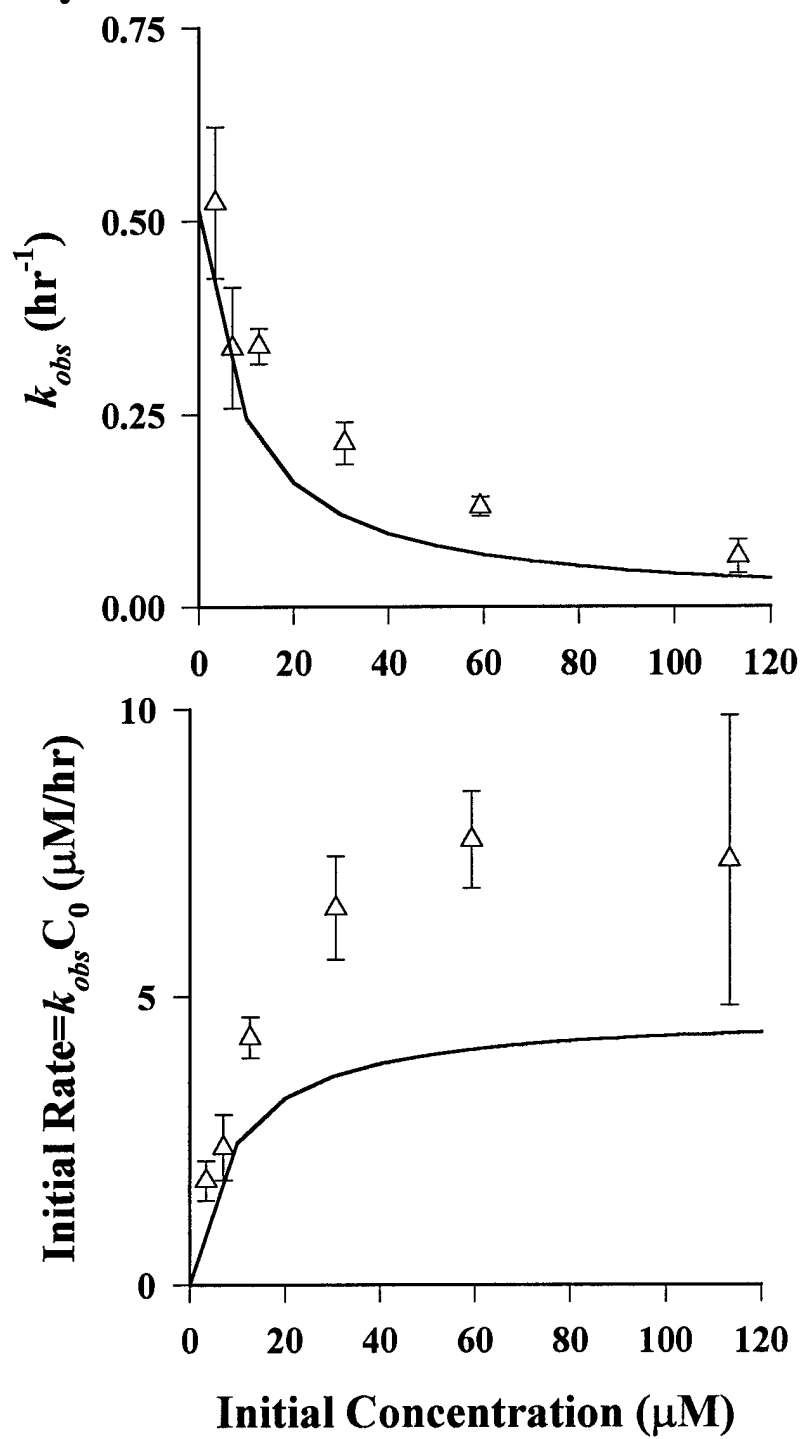


Figure 64 (continued).

**i) chloroacetylene**

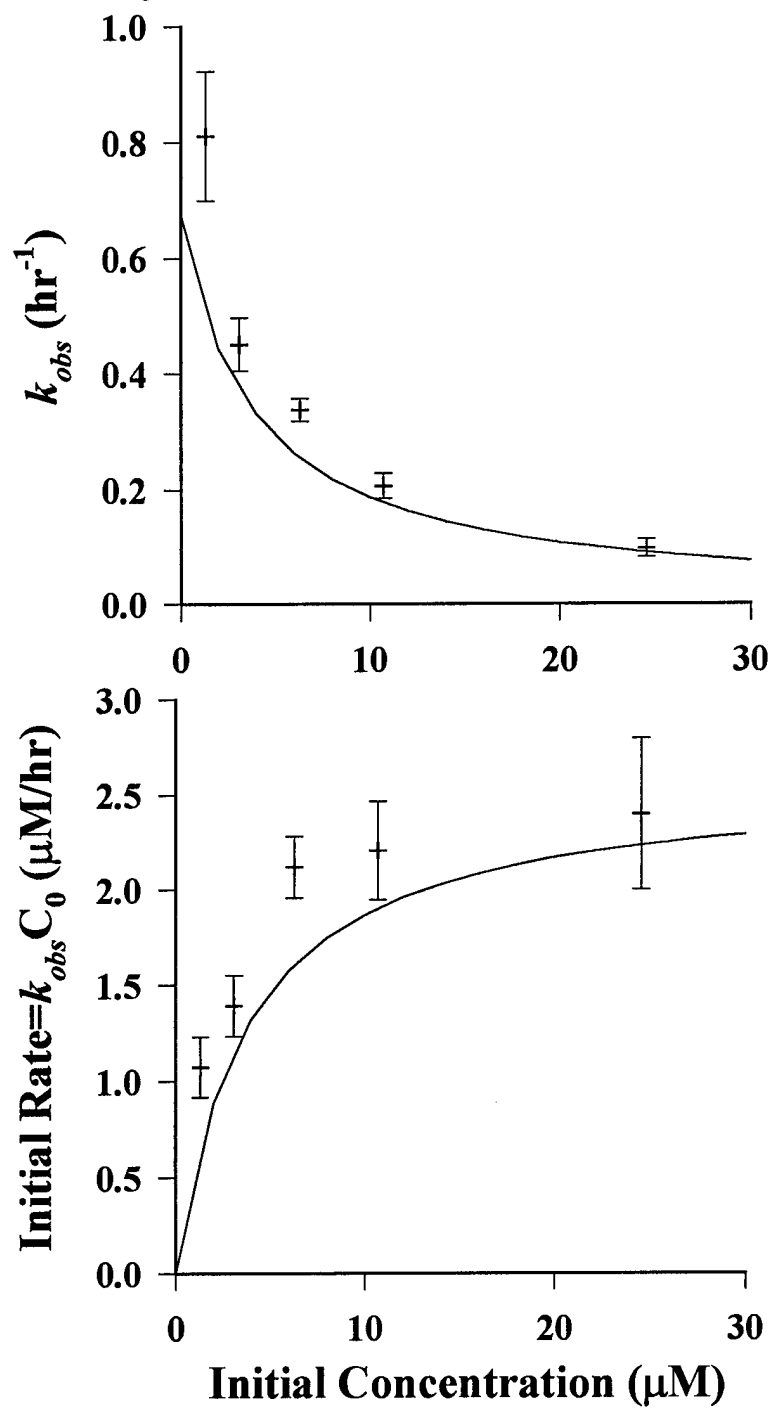


Figure 64 (continued).

j) dichloroacetylene

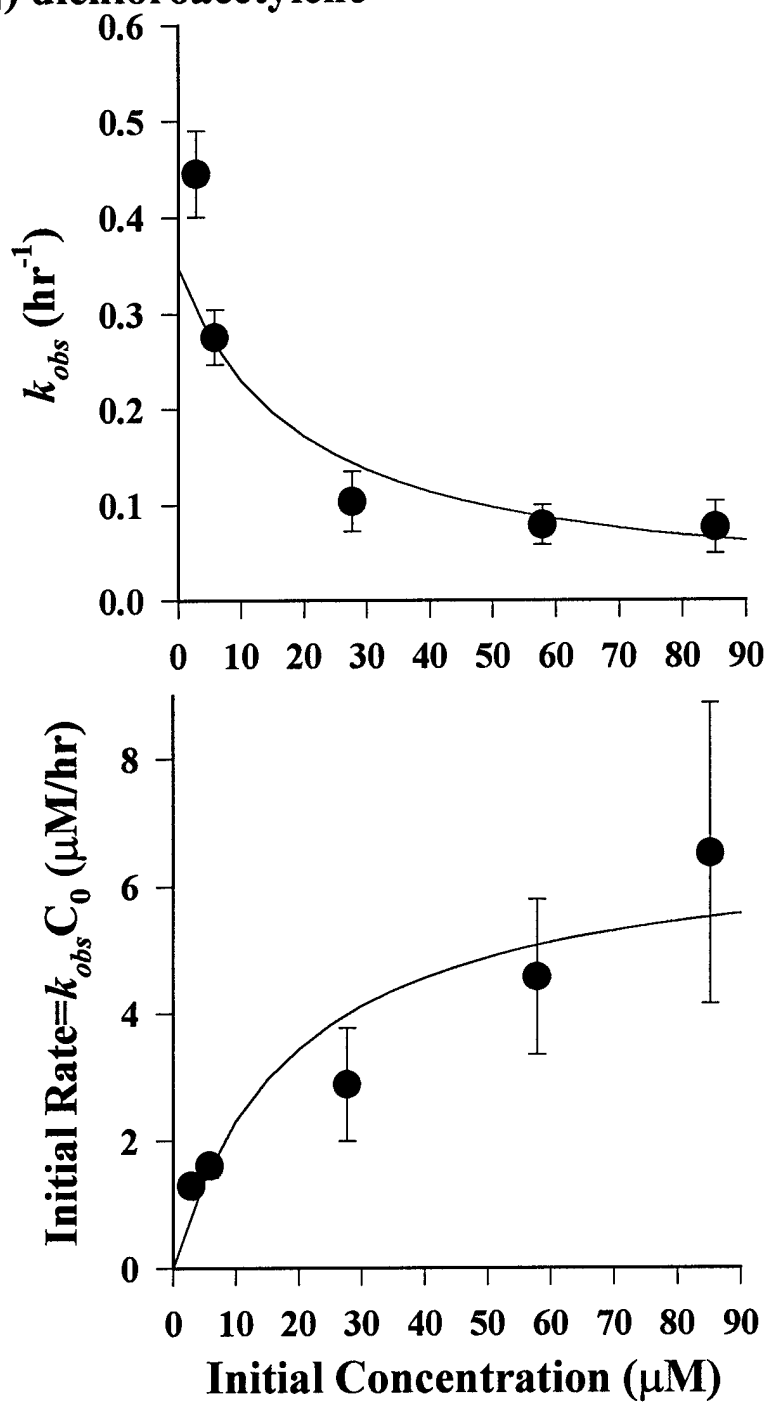


Figure 64 (continued).

**TABLE 10: MODEL-DERIVED KINETIC PARAMETERS FOR CHLORINATED ETHYLENES AND RELATED SPECIES<sup>a</sup>**

	Parent	Product	$(k^{\circ}S_i)$ ( $\mu\text{M}\cdot\text{h}^{-1}$ ) <sup>b</sup>	$K$ ( $\mu\text{M}^{-1}$ )	$n^c$	$E_1(\text{V})^{\text{d,e}}$	$E_2(\text{V})^{\text{d}}$
1	PCE	TCE	$3.63(\pm 0.52) \times 10^{-3}$	$0.058(\pm 0.014)$	5	-0.358	0.582
2	PCE	dichloroacetylene	$2.48(\pm 0.46) \times 10^{-2}$	$0.058(\pm 0.014)$	5	-0.358	0.631
3	TCE	<i>trans</i> -DCE	$7.72(\pm 9.68) \times 10^{-4}$	$0.065(\pm 0.009)$	6	-0.597	0.534
4	TCE	<i>cis</i> -DCE	$5.91(\pm 0.53) \times 10^{-3}$	$0.065(\pm 0.009)$	6	-0.578	0.543
5	TCE	1,1-DCE	$4.42(\pm 0.49) \times 10^{-3}$	$0.065(\pm 0.009)$	6	-0.840	0.523
6	TCE	chloroacetylene	$0.33(\pm 0.03)$	$0.065(\pm 0.009)$	6	-0.578	0.609
7	<i>trans</i> -DCE	VC	$5.32(\pm 15.1) \times 10^{-2}$	$0.016(\pm 0.002)$	6	-0.880	0.488
8	<i>trans</i> -DCE	acetylene	$4.42(\pm 0.45)$	$0.016(\pm 0.002)$	6	-0.880	0.573
9	<i>cis</i> -DCE	VC	$0.14(\pm 0.06)$	$0.029(\pm 0.003)$	6	-0.898	0.478
10	<i>cis</i> -DCE	acetylene	$2.18(\pm 0.15)$	$0.029(\pm 0.003)$	6	-0.898	0.564
11	1,1-DCE	ethylene	$3.72(\pm 0.25)$	$0.016(\pm 0.002)$	5	-0.773	
12	acetylene	C <sub>4</sub> 's	$9.15(\pm 5.95) \times 10^{-2\text{f}}$	$0.109(\pm 0.022)$	6		
13	acetylene	ethylene	$11.51(\pm 1.24)$	$0.109(\pm 0.022)$	6		
14	chloroacetylene	acetylene	$6.46(\pm 0.94)$	$0.261(\pm 0.086)$	5		
15	dichloroacetylene	<i>cis</i> -DCE	$1.02(\pm 1.34)$	$0.051(\pm 0.014)$	5		
16	dichloroacetylene	<i>trans</i> -DCE	$2.96(\pm 1.27)$	$0.051(\pm 0.014)$	5		
17	dichloroacetylene	chloroacetylene	$12.97(\pm 2.46)$	$0.051(\pm 0.014)$	5		

	Parent	Product	$(k^{\circ}S_i)$ ( $\text{h}^{-1}$ ) <sup>g</sup>	$n^c$
18	VC	ethylene	$6.55(\pm 0.93) \times 10^{-2}$	6
19	ethylene	ethane	$2.15(\pm 0.25) \times 10^{-2}$	10

<sup>a</sup>Numbering corresponds to reactions designated in Figure 60. Uncertainties represent 95% confidence limits.

<sup>b</sup>All  $(k^{\circ}S_i)$  values are for 0.25 g Fe(0)/160 mL buffer solution.

<sup>c</sup>Number of experiments used to determine the kinetic and adsorption parameters.

<sup>d</sup>Calculations assume the Henry's Law constant for a radical species is the same as that of the hydrogenated parent (Eberson, 1982),  $\{\text{H}^+\}=10^{-7}\text{M}$ ,  $\{\text{Cl}^-\}=1\text{mM}$ , and that all other species are present at unit activity. Gas-phase thermodynamic data are from Wagman *et al.* (1982); Taylor *et al.* (1991); Ho *et al.* (1992), corrected for air-water partitioning using Henry's Law constants recommended by Hine and Mookerjee (1975) or Mackay *et al.* (1993).

<sup>e</sup> $E_1$  values are for the formation of the appropriate radical species. Reactions shown with identical one-electron reduction potentials produce the same radical intermediates.

<sup>f</sup>Reaction 12 is a surface mediated coupling reaction, where  $(k^{\circ}S_i)$  has units of  $\text{h}^{-1}$ .

<sup>g</sup>Reactions 18 and 19 were modeled as adsorption limited reactions. The  $(k^{\circ}S_i)$  values reported are for 0.25 g Fe(0)/160 mL buffer solution. Stated uncertainties represent 95% confidence limits.

## 2. Kinetic Data

Table 10 presents the kinetic parameters [ $(k^f S_i)$  or  $(k^a S_i)$ ] determined for each species. In most cases, uncertainty in these kinetic constants is quite modest ( $\pm 7$ -15%). For minor reactions to trace products (*e.g.*, reactions 3 and 7), substantially greater uncertainty arose.

Reactions of vinyl chloride and the DCEs were monitored for 1 to 3 half-lives, and the reaction progress of the acetylenes was followed for 0.5 to 2 half-lives. For the less reactive TCE and PCE, observed conversions ranged from 6-50% for TCE to 3-17% for PCE.

For most species,  $C_2$  mass balances were essentially 100%. The  $C_2$  mass balances for acetylene and ethylene were between 85 and 95%. Evolution of headspace in the reaction bottles (attributed to reduction of protons to form hydrogen gas) was not significant even for experiments of long duration, as the metal loadings used were quite small. Controls (without iron) showed no losses over the time scale at which the experiments were conducted, suggesting that sorption to the septa and losses through the needle punctures were minimal.

Results for each individual species are presented below. Although interspecies competitive experiments are discussed subsequently, they were included in the modeling efforts throughout.

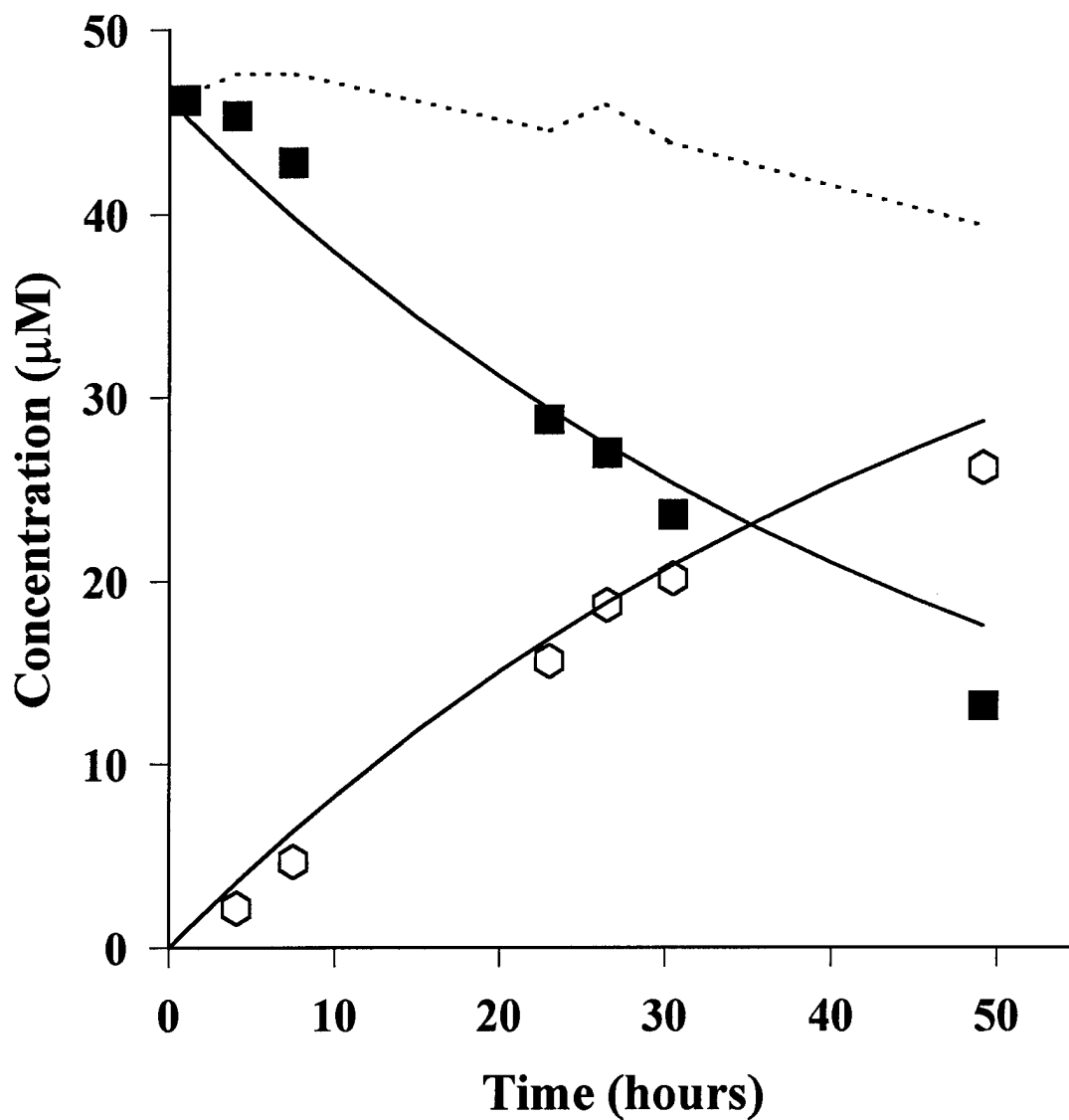
## 3. Reaction Pathways

### a. Ethylene

The only product observed from the reduction of ethylene was ethane. No coupling to form longer-chain hydrocarbons was observed. Inhibition of ethylene by ethane was assumed to be negligible. A representative timecourse is given in Figure 65.

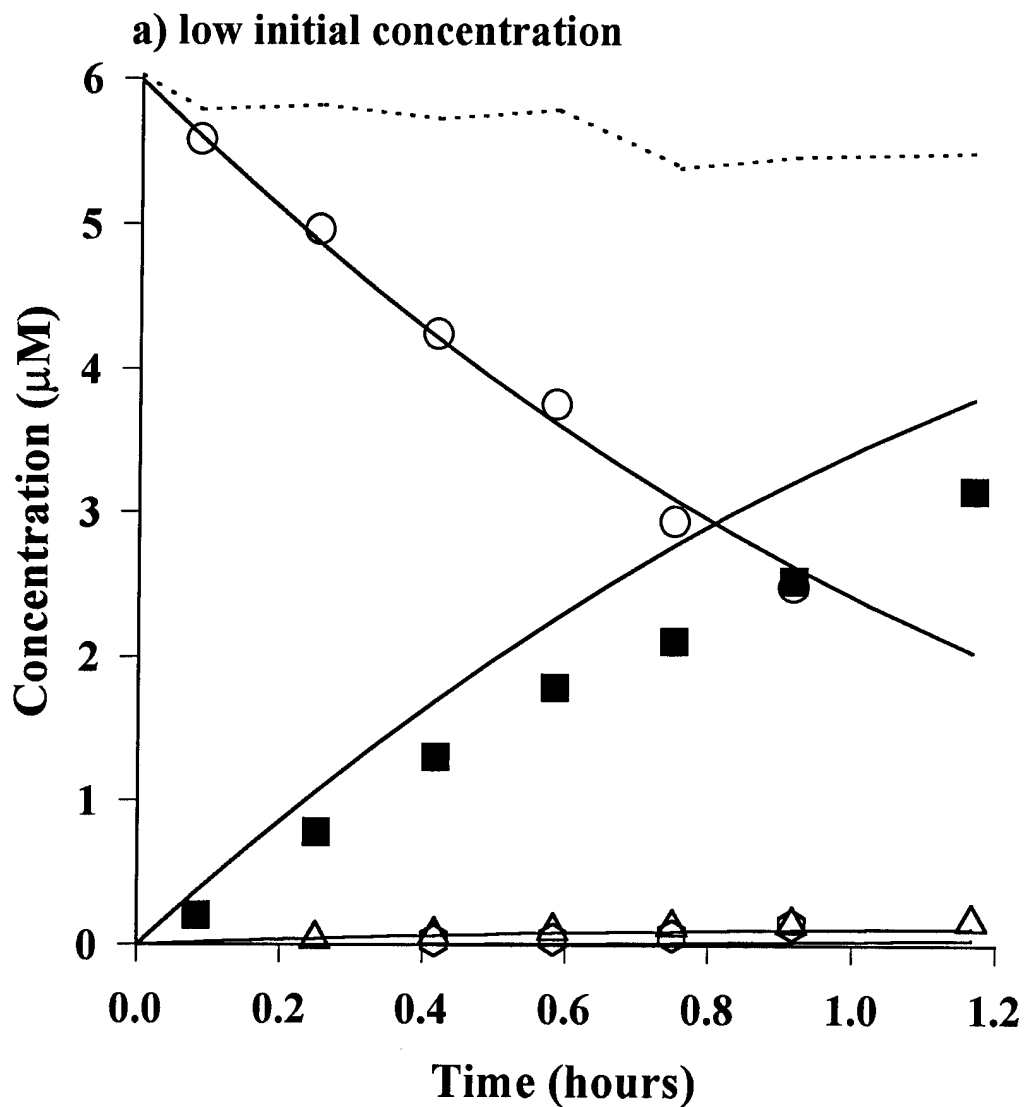
### b. Acetylene

Figure 66 reveals that the reduction of acetylene was extremely rapid and resulted primarily in the formation of ethylene (which subsequently reacted to ethane). The concentration of ethylene was systematically overpredicted. This is attributable to the implicit assumption of mass balance by the model, whereas the observed mass balance was only 85-95%. Acetylene is known to couple upon reaction on metal surfaces in the gas phase (Ponec and Bond, 1995); products consistent with such a process were observed in this system. The major coupling products formed were  $C_4$  hydrocarbons [1-butene (10-20% of total  $C_4$ ), n-butane (<1%), 1, 3-butadiene (65-85%), *cis*-2-butene (3-7%) and *trans*-2-butene (4-8%)], comprising up to 15% of



**Figure 65.** Reduction of ethylene (■) by 0.25 g Fe(0) in 160 mL of 0.1 M NaCl, 50 mM Tris buffer (pH 7.2). The only observed product is ethane (⬡). Lines represent model predictions based on the parameters presented in Table 10. The dotted line represents the  $C_2$  mass balance.





**Figure 66.** Reduction of acetylene (○) by 0.10 Fe(0) in 160 mL of 0.1 M NaCl, 50 mM Tris buffer (pH 7.2) at a) low and b) high initial concentration. Observed products include ethylene (■), ethane, (◊), and C<sub>4</sub> compounds (Δ). Lines represent model predictions based on the parameters presented in Table 10. The dotted lines represent the C<sub>2</sub> mass balance.

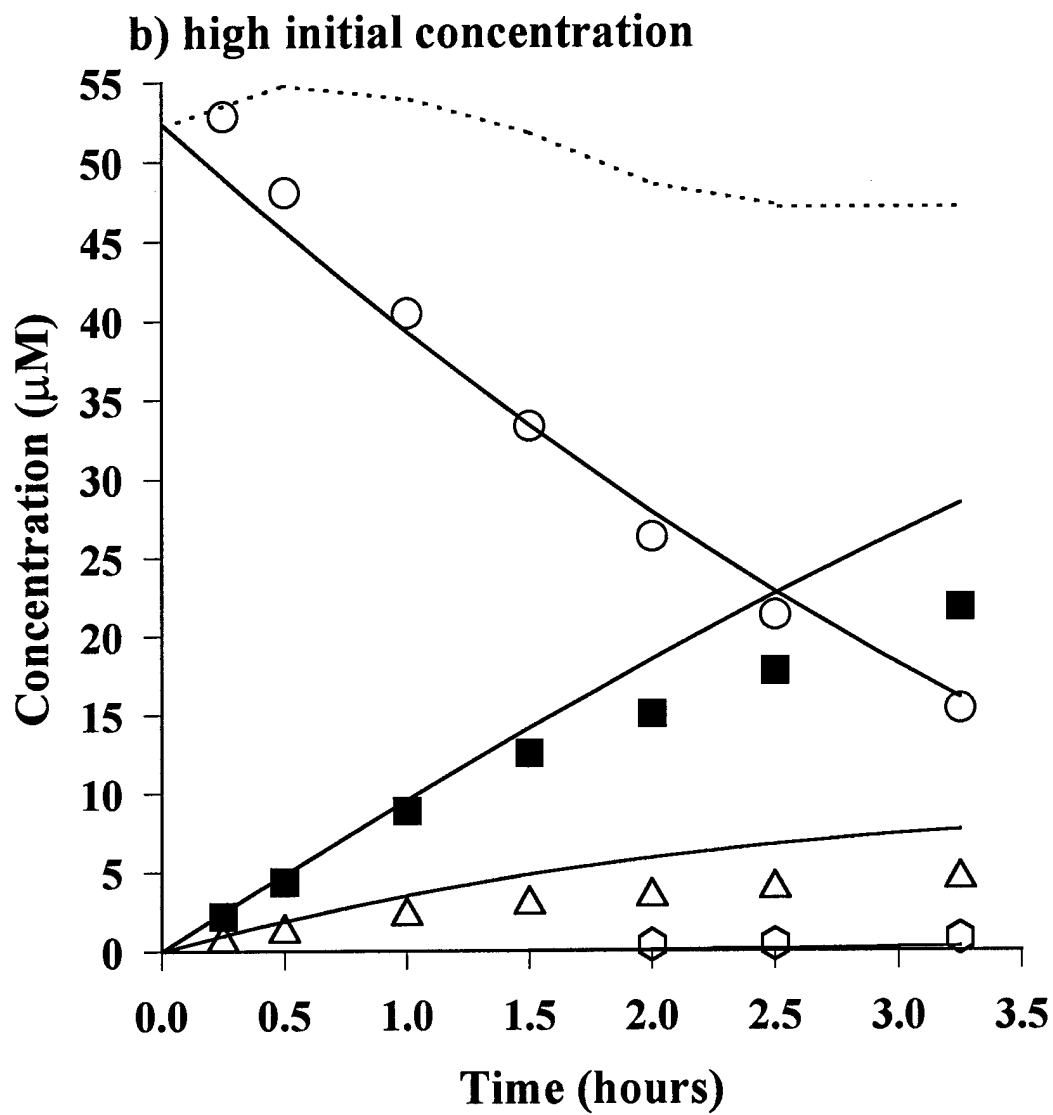


Figure 66 (continued).

the C<sub>2</sub> mass balance. Traces of other longer chain hydrocarbons (C<sub>3</sub>, C<sub>5</sub>, C<sub>6</sub>) were also detected, as previously observed during the reduction of <sup>13</sup>C labeled TCE (Campbell *et al.*, 1997). The total concentration of C<sub>3</sub>, C<sub>5</sub>, and C<sub>6</sub> products was sufficiently low (< 0.5% of initial C<sub>2</sub>) that they were ignored in the modeling efforts.

As shown in Figure 66, the yield of C<sub>4</sub> products increased with increasing initial acetylene concentration. To account for the formation of the C<sub>4</sub> species, a second-order reaction was included. The concentrations of the individual C<sub>4</sub> species were summed, and subsequent interconversions through isomerization (*e.g.*, 1-butene → 2-butene) and reduction reactions (*e.g.*, 1-butene → n-butane) were ignored. As the yield of C<sub>4</sub> compounds remained reasonably constant throughout the course of each experiment, these simplifications would appear reasonable.

Comparing results from experiments conducted at 0.25 g Fe(0)/160 mL with those at 0.10 g Fe(0)/160 mL indicated the dependence of the coupling reaction on metal loading (*i.e.*, site concentration) was first order, suggesting only one surface-bound species was involved in the coupling. According to LHHW kinetics, a surface-limited reaction involving two surface sites would have a second-order dependence on metal loading/site concentration (see Appendix A). The coupling reaction was therefore modeled as a reaction of one surface-adsorbed and one aqueous species, similar to an Eley-Rideal mechanism (Fogler, 1992).

### c. Vinyl Chloride

Vinyl chloride underwent reduction to ethylene, which subsequently reacted to ethane. Neither acetylene nor the coupling products associated with the subsequent reduction of acetylene were observed, suggesting acetylene is not an intermediate in vinyl chloride reduction. A representative plot of concentration vs. time is given in Figure 67.

### d. *cis*- and *trans*-DCE

Ethylene and ethane were the major products of the reduction of *cis*- and *trans*-DCE by Fe(0), as shown in Figures 68 and 69, respectively. For *cis*-DCE, vinyl chloride was produced with a maximum yield of 7% and the C<sub>4</sub> hydrocarbons at ~2% yield. With *trans*-DCE, the C<sub>4</sub> hydrocarbons were produced at ~4% yield and vinyl chloride at a maximum 1% yield. Acetylene was observed in trace amounts for both *cis*- and *trans*-DCE. As displayed in these figures, the LHHW model captures the major features of the data at different initial concentrations where the pseudo-first order rate constants differed considerably. The vinyl chloride concentration does seem to be slightly underpredicted for the high initial concentration of *cis*-DCE.

In modeling the transformation of *trans*-DCE, the measured vinyl chloride yield was very low, and the model consistently would set the rate constant for this reaction to zero. Thus, an initial modeling attempt was performed, in which only the *trans*-DCE and vinyl chloride data were provided to the model. The model calculated a kinetic parameter for the degradation of *trans*-DCE and apportioned it into a parameter for the formation of vinyl chloride and an “unknown sink”. In this manner, the decay of *trans*-DCE and production of vinyl chloride could be estimated. A second fit was then performed in which all the data were used, but the kinetic constant for the rate of vinyl chloride formation was constrained to be equal to the value found in the preliminary fit. In this manner, the production of vinyl chloride could be more accurately predicted for *trans*-DCE.

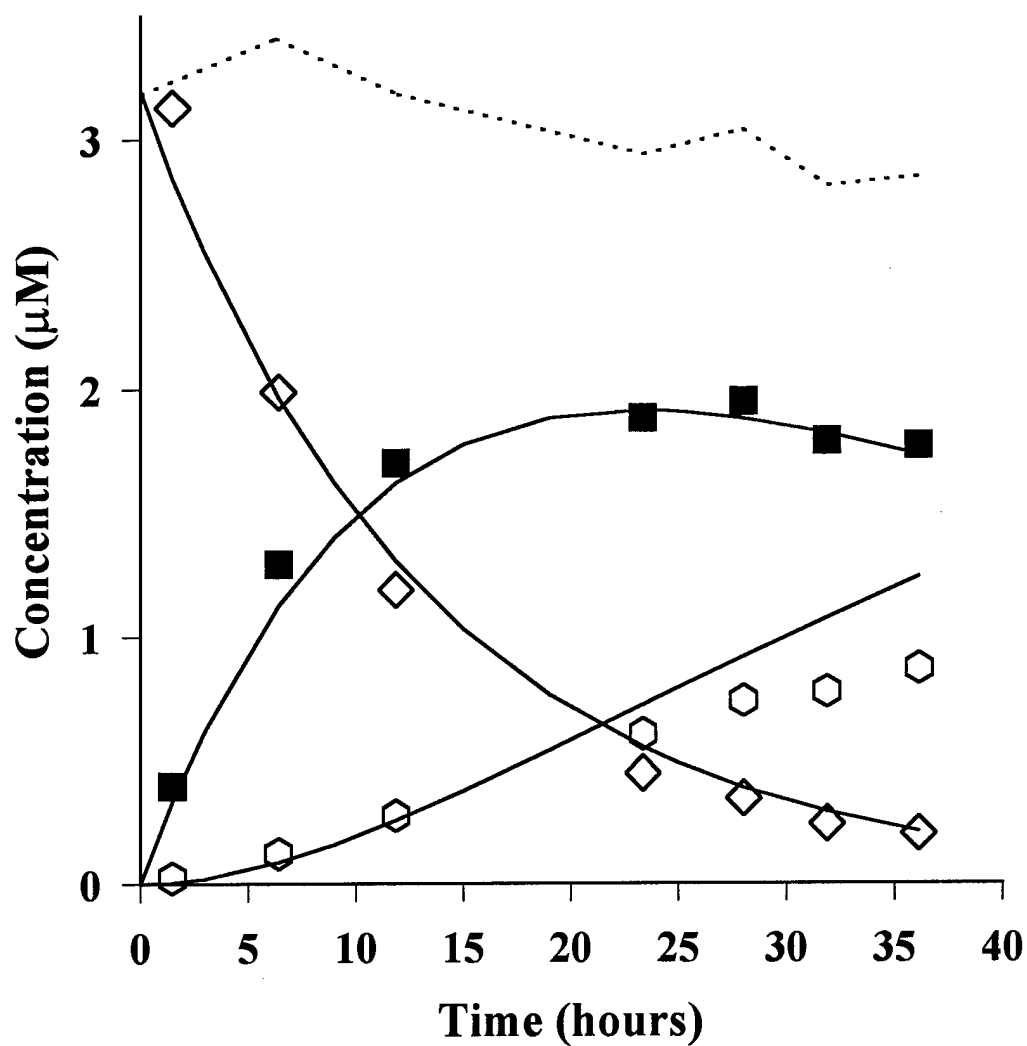


**Figure 67.** Reduction of vinyl chloride (◇) by 0.25 g Fe(0) in 160 mL of 0.1 M NaCl, 50 mM Tris buffer (pH 7.2). Observed products include ethylene (■) and ethane (◻). Lines represent model predictions based on the parameters presented in Table 10. The dotted line represents the C<sub>2</sub> mass balance.

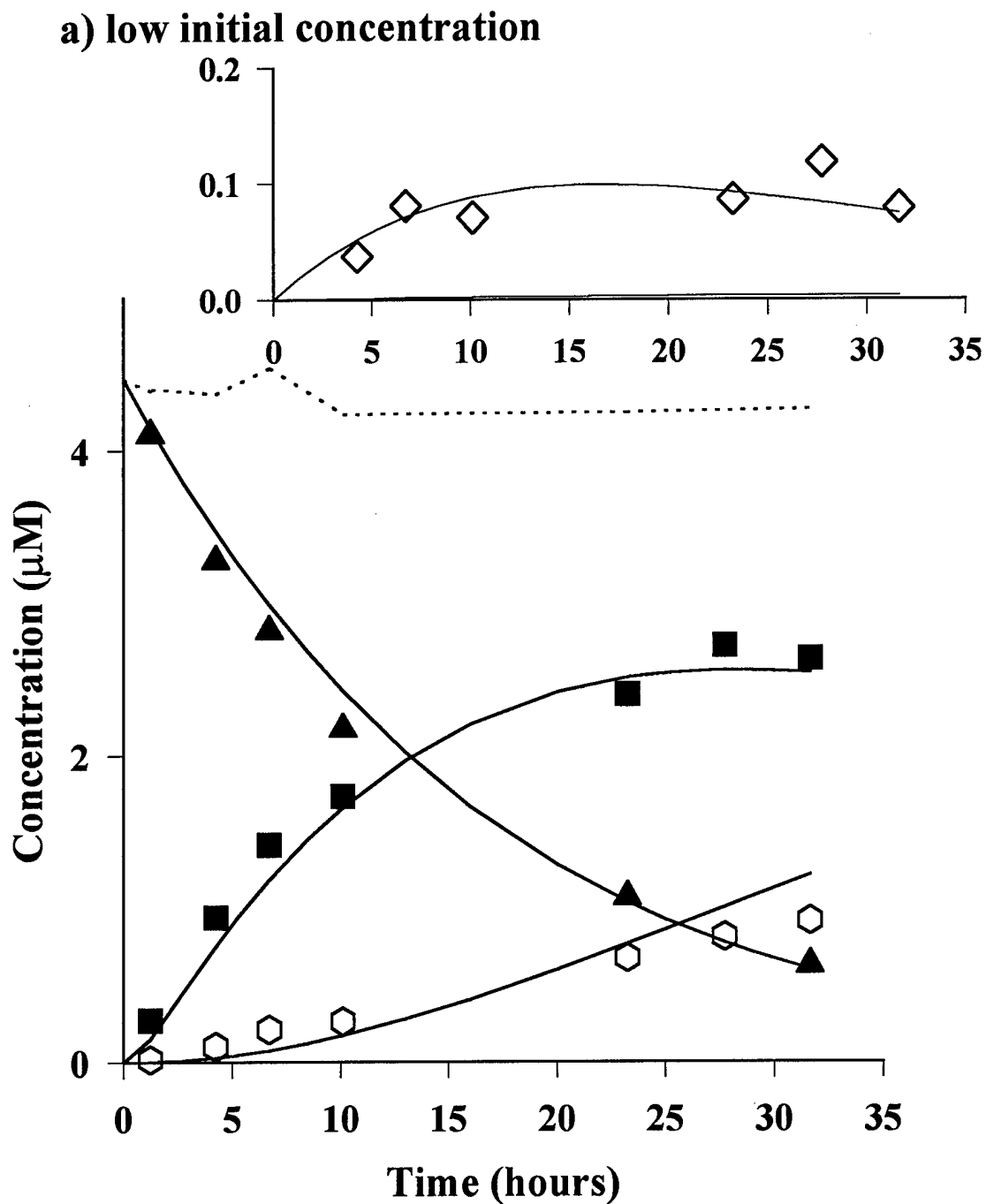


**Figure 68.** Reduction of *cis*-DCE (▲) by 0.25 g Fe(0) in 160 mL of 0.1 M NaCl, 50 mM Tris buffer (pH 7.2) at a) low and b) high initial concentration. Major observed products are ethylene (■) and ethane (◻). Insets show the trace products vinyl chloride (◊) and C<sub>4</sub> hydrocarbons (Δ). Lines represent model predictions based on the parameters presented in Table 10. The dotted lines represent the C<sub>2</sub> mass balance.

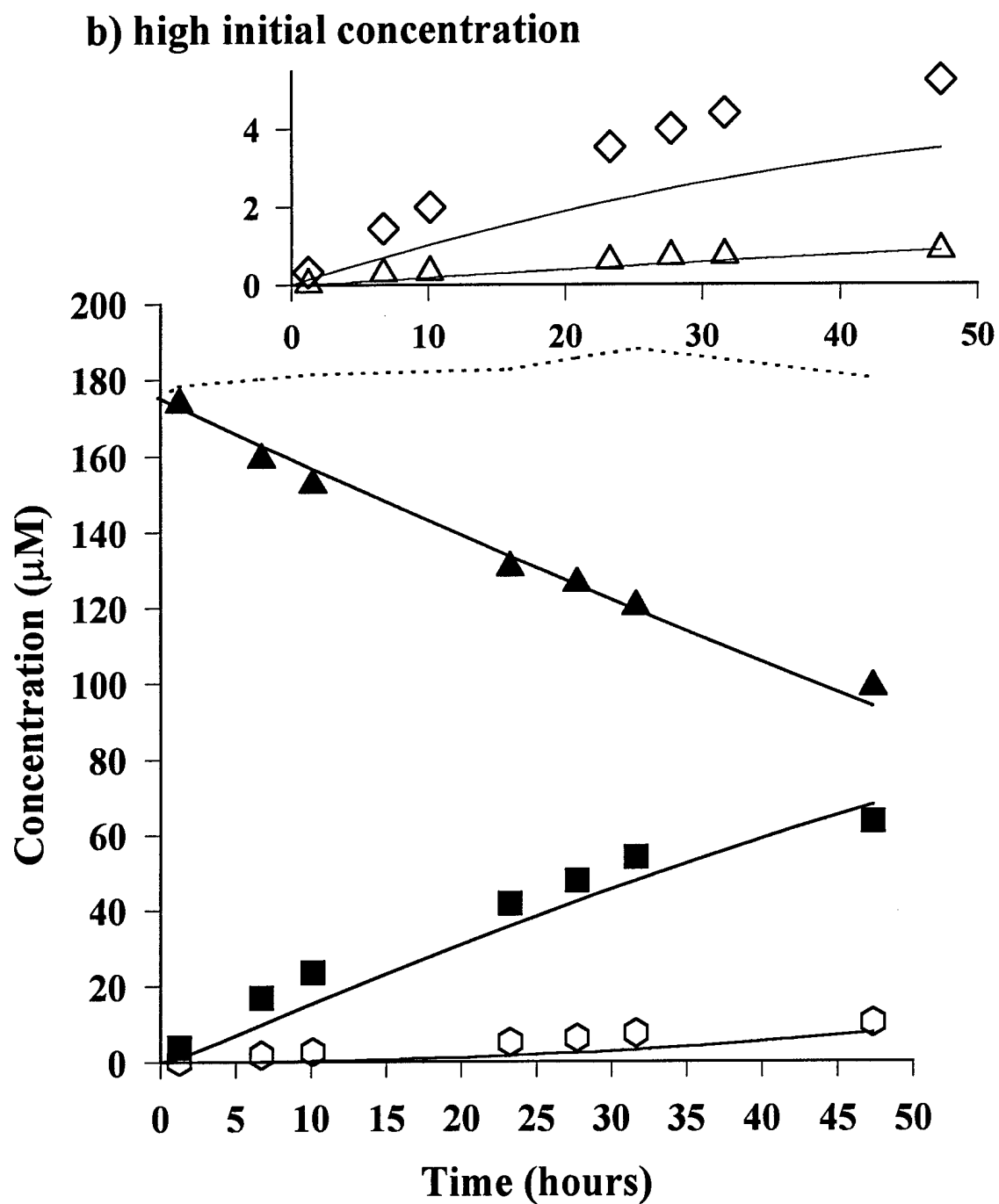
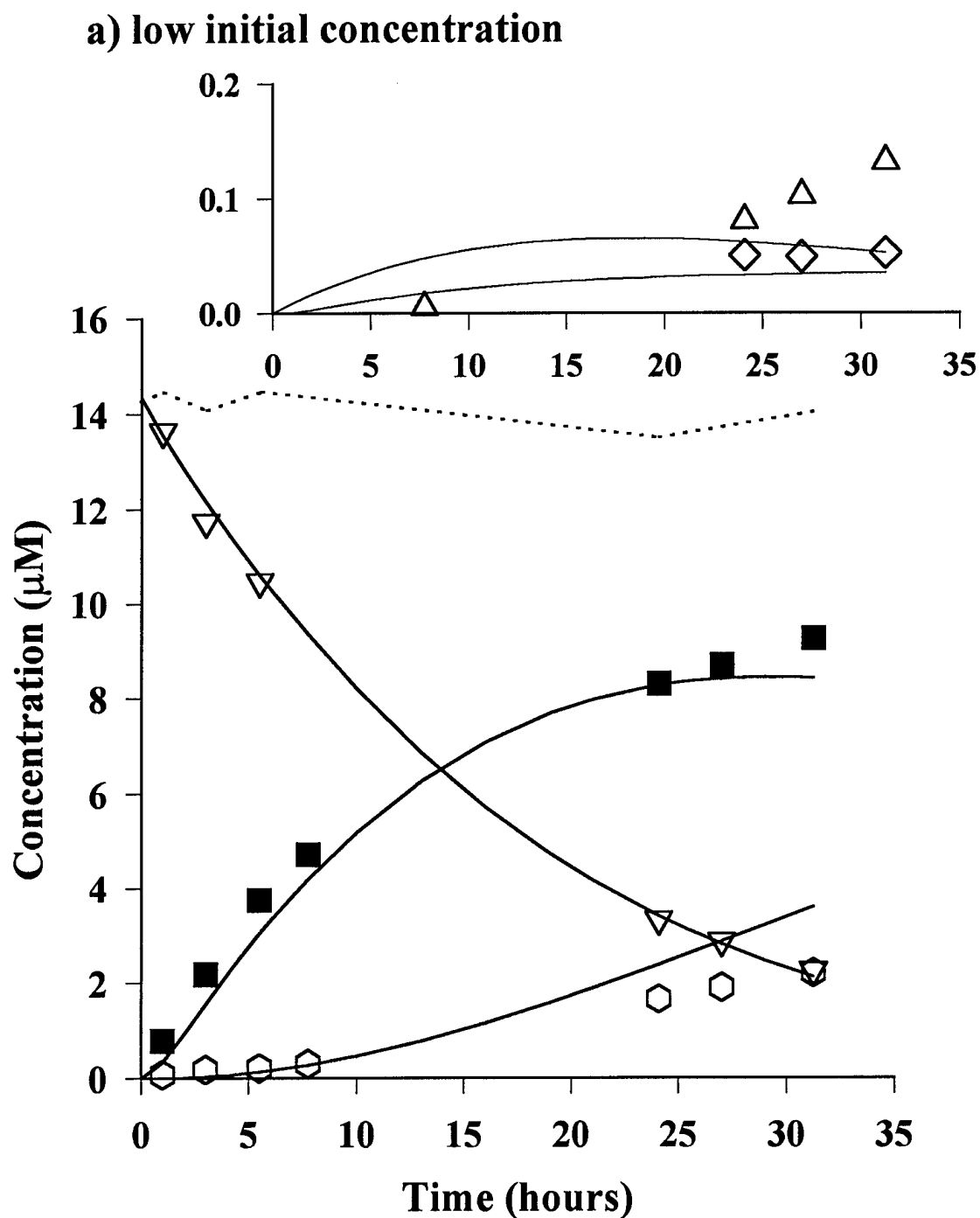


Figure 68 (continued).



**Figure 69.** Reduction of *trans*-DCE ( $\nabla$ ) by 0.25 g Fe(0) in 160 mL of 0.1 M NaCl, 50 mM Tris buffer (pH 7.2) at a) low and b) high initial concentration. Major observed products are ethylene ( $\blacksquare$ ) and ethane ( $\hexagon$ ). Insets show the trace products vinyl chloride ( $\diamond$ ) and C<sub>4</sub> hydrocarbons ( $\Delta$ ). Lines represent model predictions based on the parameters presented in Table 10. The dotted lines represent the C<sub>2</sub> mass balance.



**b) high initial concentration**

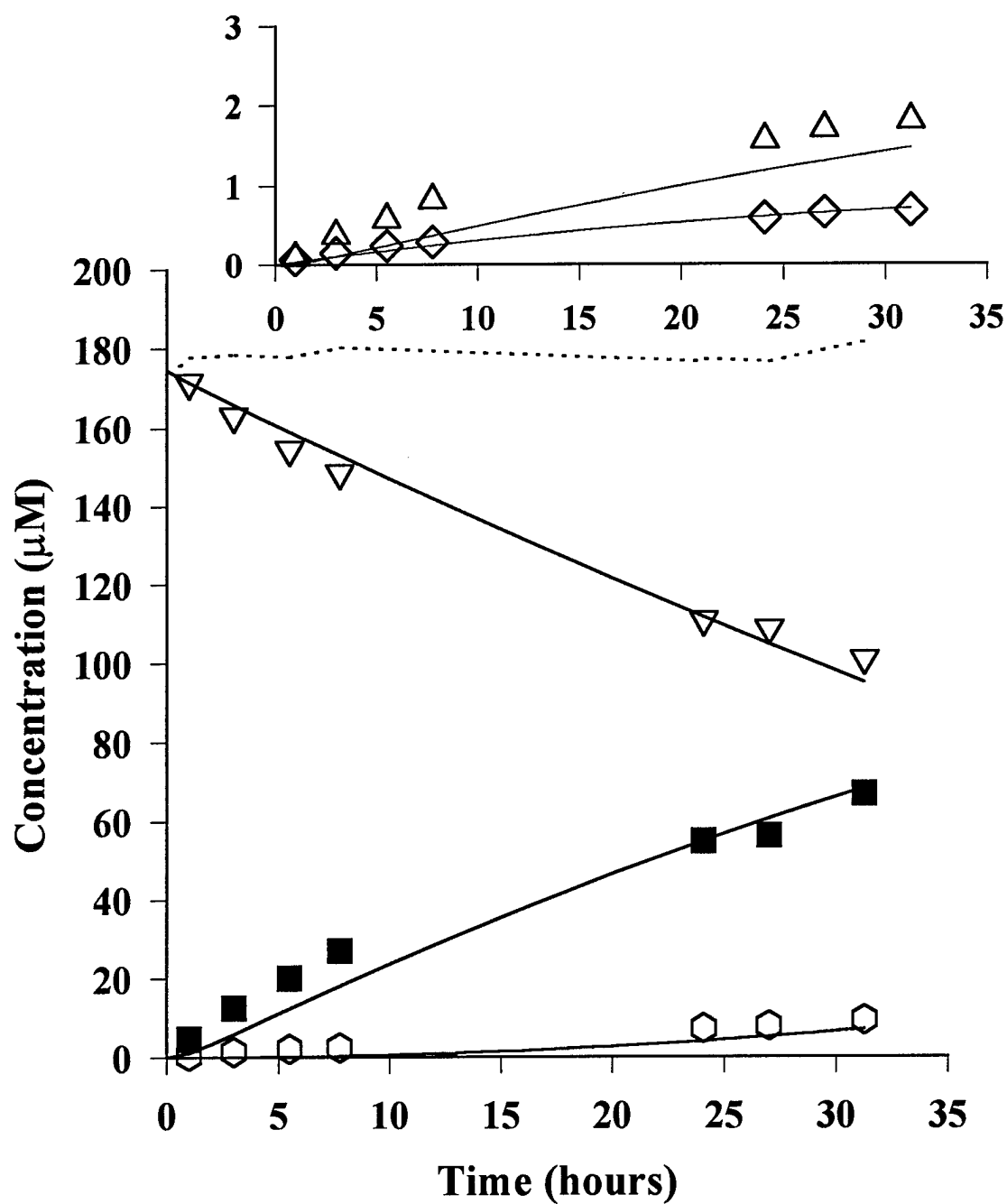
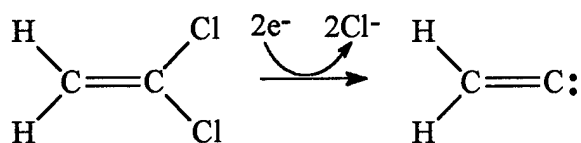


**Figure 69 (continued).**

### e. 1,1-DCE

Example timecourses for the reduction of 1,1-DCE are displayed in Figure 70. The major products observed were ethylene and ethane. At high concentrations and at long times, traces of vinyl chloride (<0.2 % yield) were observed. Modeling the reaction of 1,1-DCE as a sequence of hydrogenolysis reactions ( $1,1\text{-DCE} \rightarrow \text{vinyl chloride} \rightarrow \text{ethylene}$ ) and constraining the rate of vinyl chloride reaction to that determined in independent experiments proved unsuccessful. As Figure 71 demonstrates, such a sequence would result in substantial accumulation of vinyl chloride. The possibility of formation of acetylene or chloroacetylene was also discounted, for a mixture of  $C_4$  coupling products would have resulted had acetylene been present in the system as an intermediate. Traces of *cis*-2-butene were detected, but none of the other  $C_4$  species, suggesting that acetylene was not an intermediate.

As shown in Figure 70, the distribution of products observed to result from the reduction of 1,1-DCE was best described by a reaction of 1,1-DCE to the four-electron reduction product, ethylene, which was subsequently assumed to react to ethane. The ethylene formed was subsequently assumed to react to ethane. There is precedent for such a pathway; both experimental (Semadeni *et al.*, 1998) and spectroscopic (Lesage *et al.*, 1998) evidence suggest that reduction of 1,1-DCE to ethylene by cob(I)alamin (vitamin  $B_{12a}$ ) may proceed without vinyl chloride as an intermediate. A possible mechanism for such a pathway would involve the formation of an alkylidene carbene ( $H_2C=C:$ ) or metal-stabilized carbenoid via a reductive  $\alpha$ -elimination of the 1,1-DCE:



Formation of such a carbene has been shown to result from  $\alpha$ -elimination of 1-haloolefins during reaction with strong base (Stang, 1978). The subsequent stepwise or concerted transfer of two electrons and two protons would give rise to ethylene; alternatively, the carbenoid could undergo rearrangement to acetylene (Stang, 1978). As  $C_4$  coupling products were not observed during the reduction of 1,1-DCE by  $\text{Fe}(0)$ , acetylene does not appear to be an intermediate in this system. Acetylene has been observed, however, in the reduction of 1,1-DCE by cob(I)alamin (Glod *et al.*, 1997b).

**a) low initial concentration**

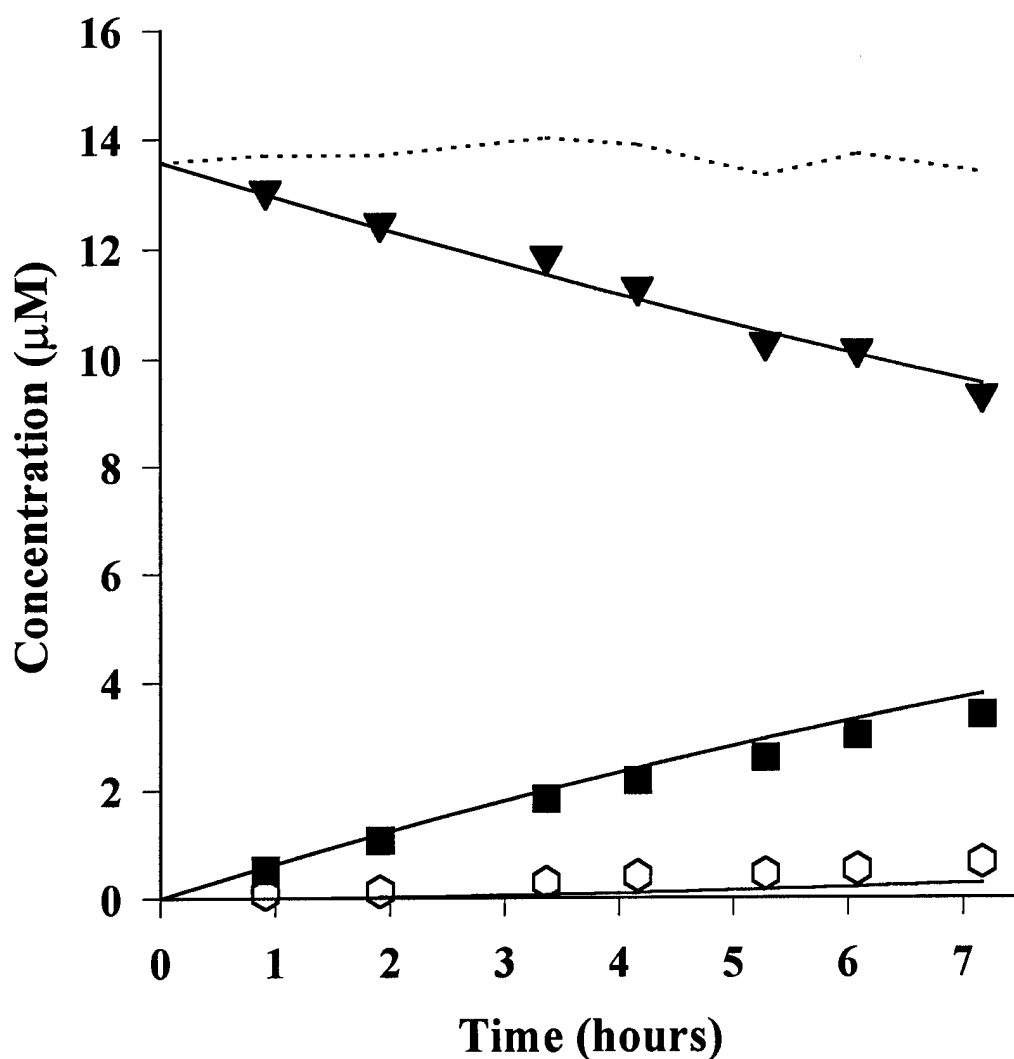


**Figure 70.** Reduction of 1,1-DCE (▼) by 0.25 g Fe(0) in 160 mL of 0.1 M NaCl, 50 mM Tris buffer (pH 7.2) at a) low and b) high initial concentration. The observed products are ethylene (■) and ethane (◻). Lines represent model predictions based on the parameters presented in Table 10. The dotted lines represent the  $\text{C}_2$  mass balance.

**b) high initial concentration**

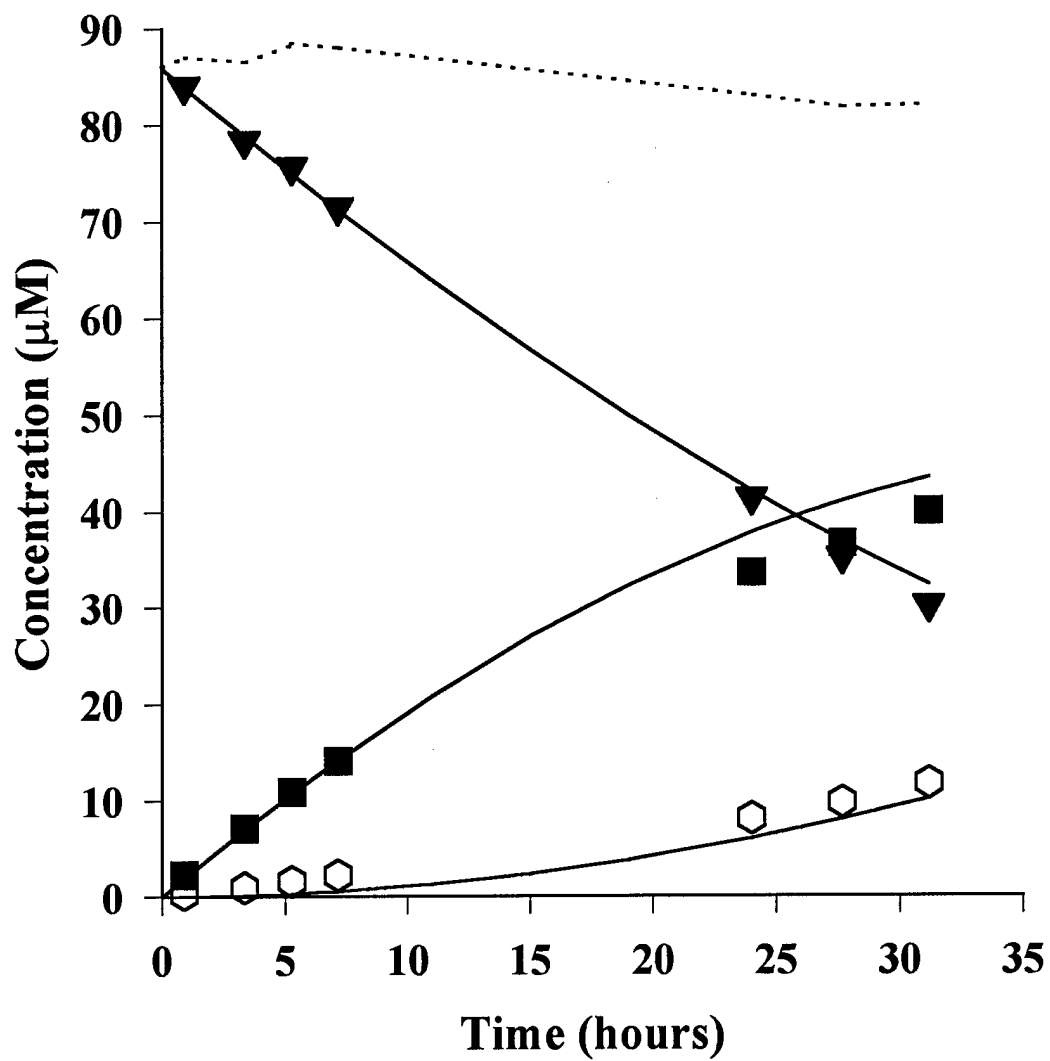


**Figure 70 (continued).**

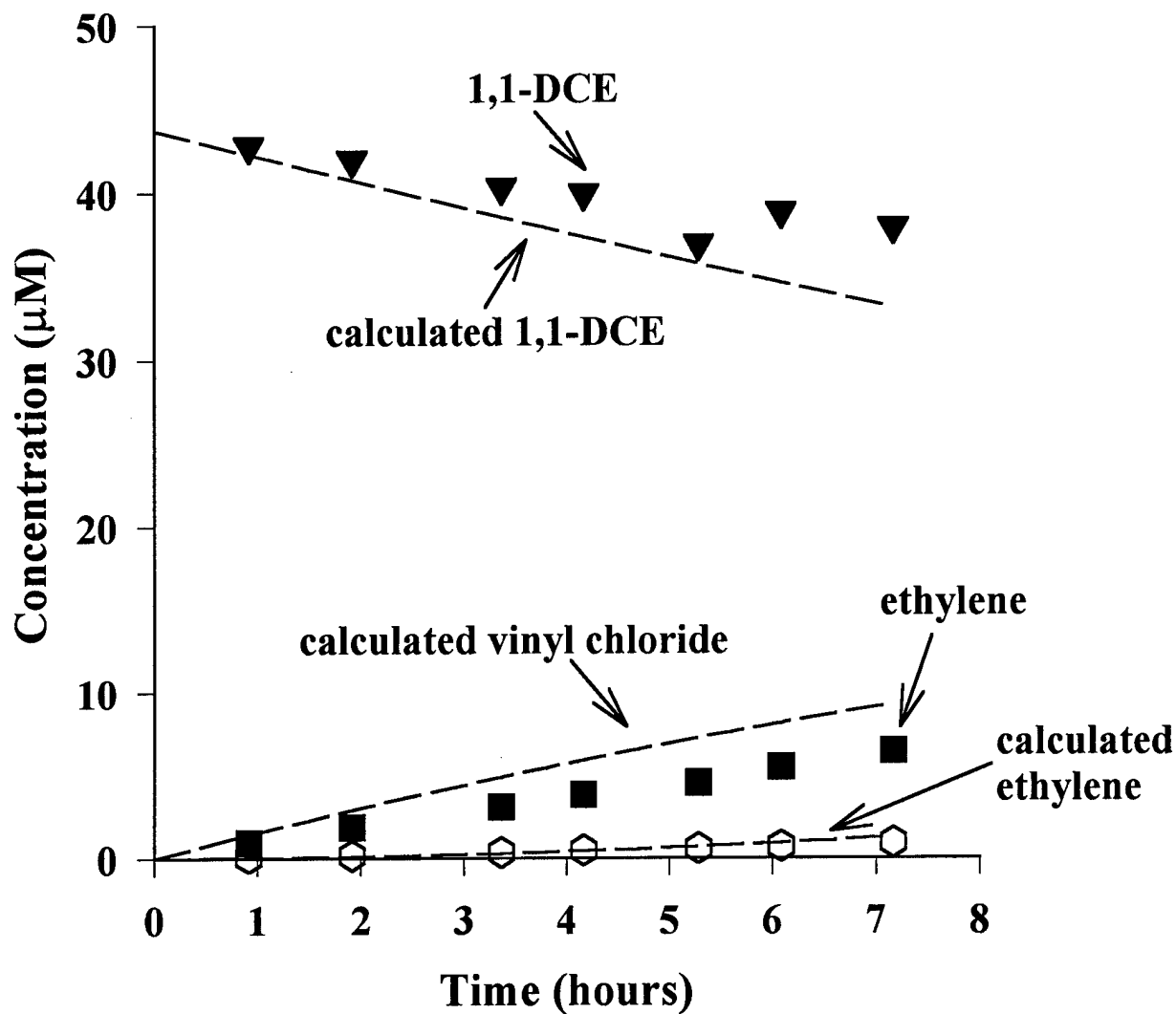


**Figure 71.** Model predictions (dashed lines) for the reduction of 1,1-DCE using a sequence of hydrogenolysis reactions ( $1,1\text{-DCE} \rightarrow \text{VC} \rightarrow \text{ethylene}$ ) compared to experimental data for 1,1-DCE ( $\blacktriangledown$ ), ethylene ( $\blacksquare$ ) and ethane ( $\bigcirc$ ). Vinyl chloride did not accumulate to detectable levels ( $\geq 0.19 \mu\text{M}$ ; Section VII) in this experiment.

## f. Chlorinated Acetylenes

Prior work with Fe(0) (Campbell *et al.*, 1997) and the results from Section V with Zn(0) suggest that the chlorinated acetylenes represent highly reactive, transient intermediates in zero-valent metal systems. Reactions of chloroacetylene and dichloroacetylene with Fe(0) were therefore investigated.

Both chlorinated acetylenes reacted very rapidly with iron, as the calculated parameters in Table 10 reveal. Chloroacetylene reacted to form acetylene (Figure 72); all other products observed could be accounted for as daughter products of acetylene (or its subsequent transformation products). In particular, no vinyl chloride was observed, even though this represents a significant (8%) pathway for reduction of chloroacetylene by Zn(0).

The measured concentrations of ethane and the C<sub>4</sub> hydrocarbons were substantially higher than those predicted by the model. This may result from the inaccuracies introduced in the acetylene rate constants due to the incomplete mass balance in experiments with this species. It is also possible that the chlorinated acetylenes undergo additional reactions (*e.g.*, coupling).

The reaction of dichloroacetylene with iron gave rise to chloroacetylene and its subsequent daughter products, as well as *trans*- (and to a lesser extent) *cis*-dichloroethylene (Figure 73). As shown in Table 10, the rate constant for the formation of *trans*-DCE is approximately three times greater than that for *cis*-DCE.

Fitting the data collected from the experiments conducted with the dichloroacetylene proved difficult. The model apportioned the reaction correctly between hydrogenolysis and hydrogenation, and accurately predicted the concentrations of the products resulting from hydrogenation. Concentrations of chloroacetylene and acetylene produced via the hydrogenolysis pathway from dichloroacetylene were, however, in some cases inaccurate. As the reactions of these species (chloroacetylene → acetylene and acetylene → ethylene) are rapid relative to reduction of the chlorinated ethylenes, the alkynes do not accumulate to high concentrations. Since the branching ratios are correctly represented by the model, inaccuracies in the calculated intermediate chloroacetylene and acetylene concentrations should have a negligible effect on modeling of chlorinated ethylenes.

**a) low initial concentration**

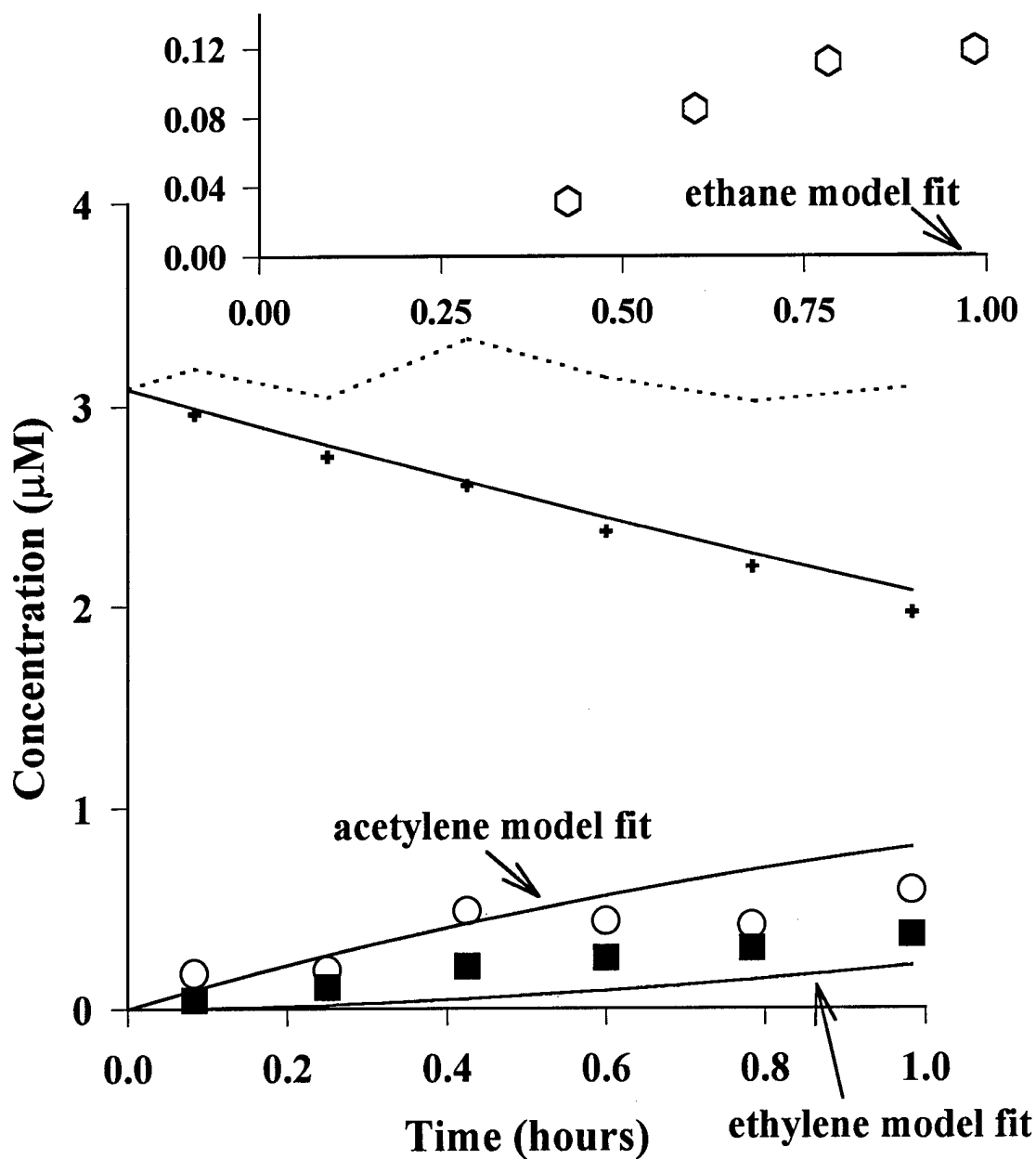


**Figure 72.** Reduction of chloroacetylene (+) by 0.10 g Fe(0) in 160 mL of 0.1 M NaCl, 50 mM Tris buffer (pH 7.2) at a) low; b) intermediate; and c) high initial concentrations. Major products include acetylene (O) and ethylene (■). Insets show the trace products ethane (⬡) and C<sub>4</sub> hydrocarbons (Δ). Lines represent model predictions based on the parameters presented in Table 10. The dotted lines represent the C<sub>2</sub> mass balance.

**b) intermediate initial concentration**

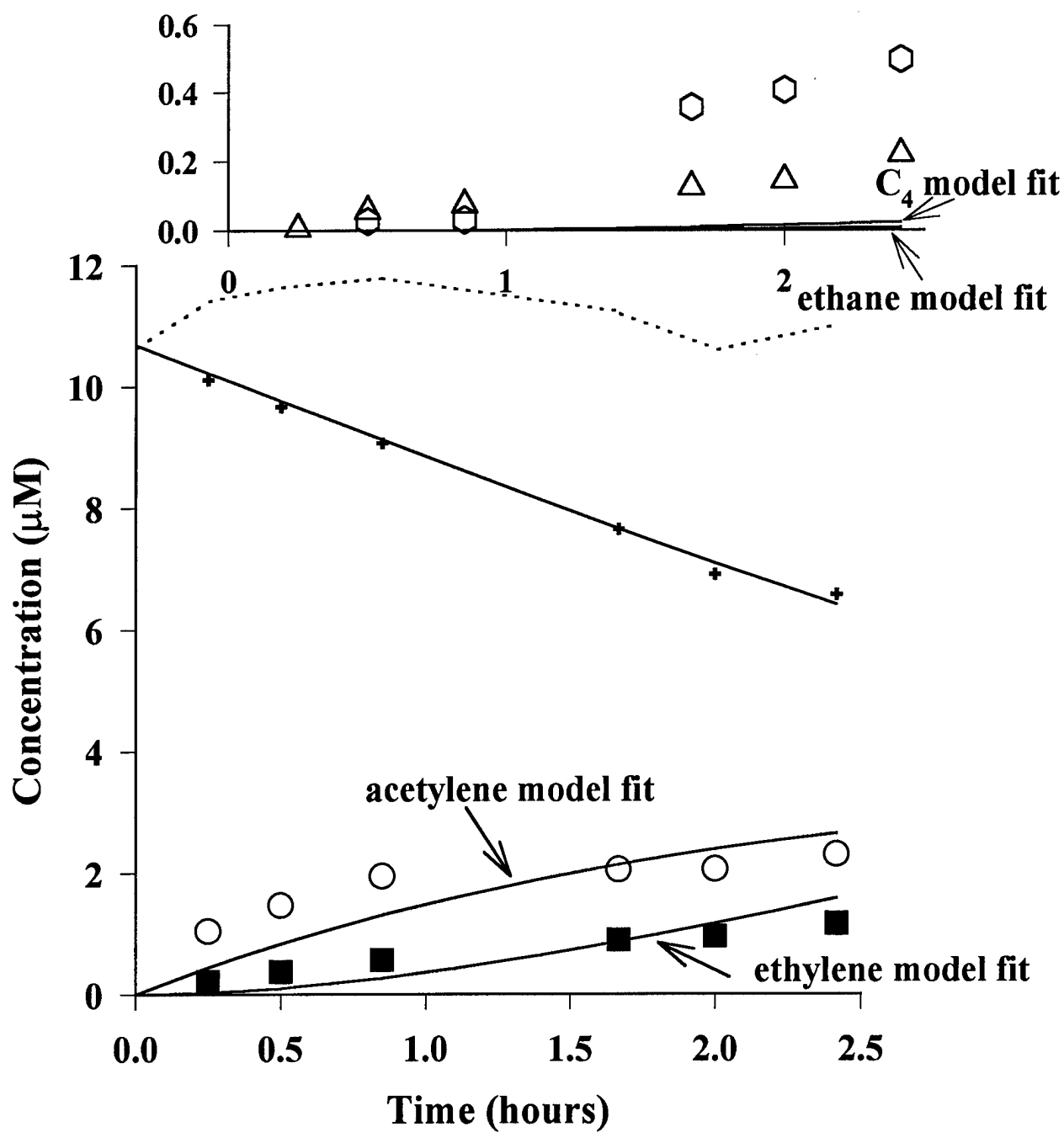


Figure 72 (continued).



c) high initial concentration

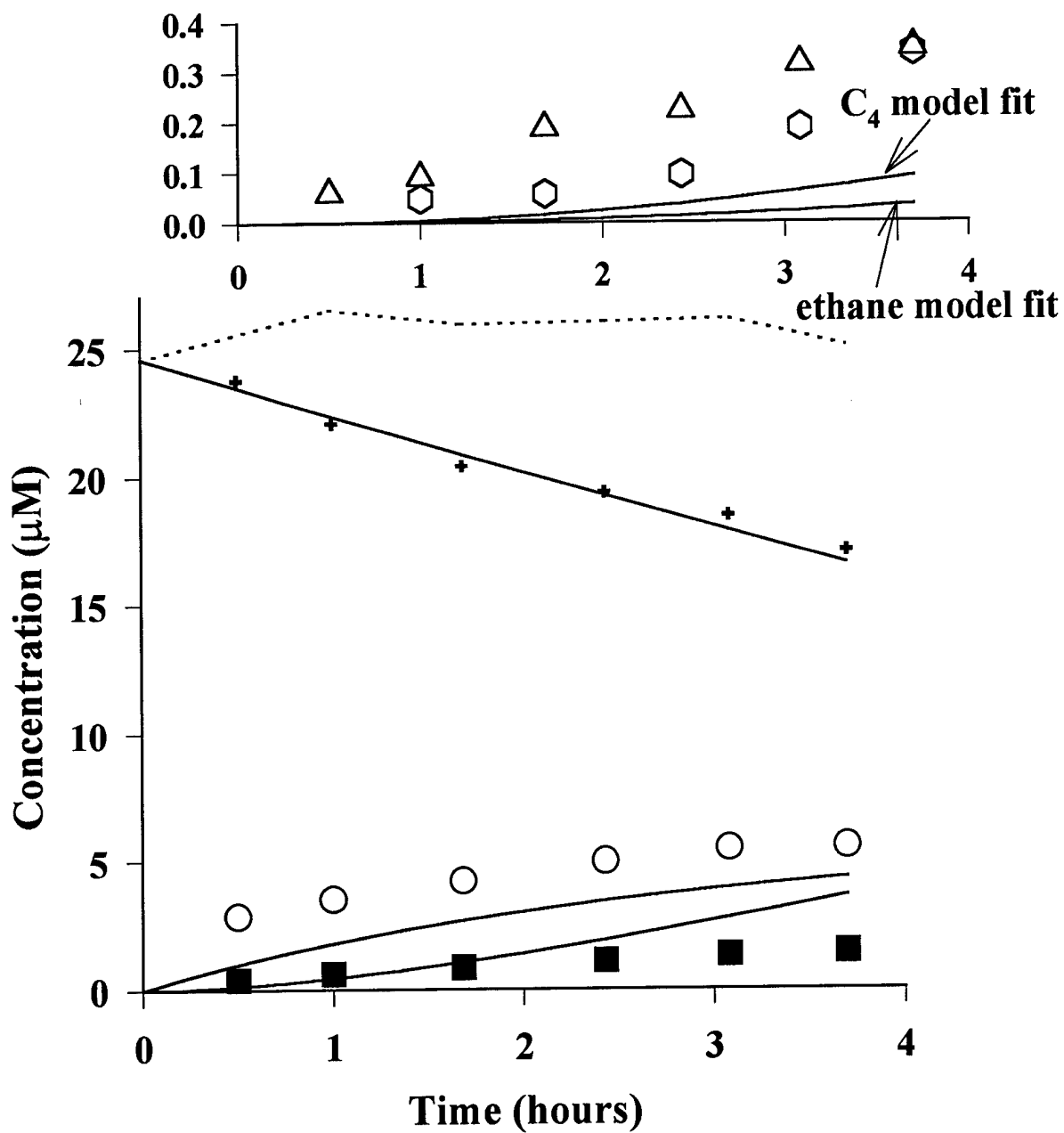
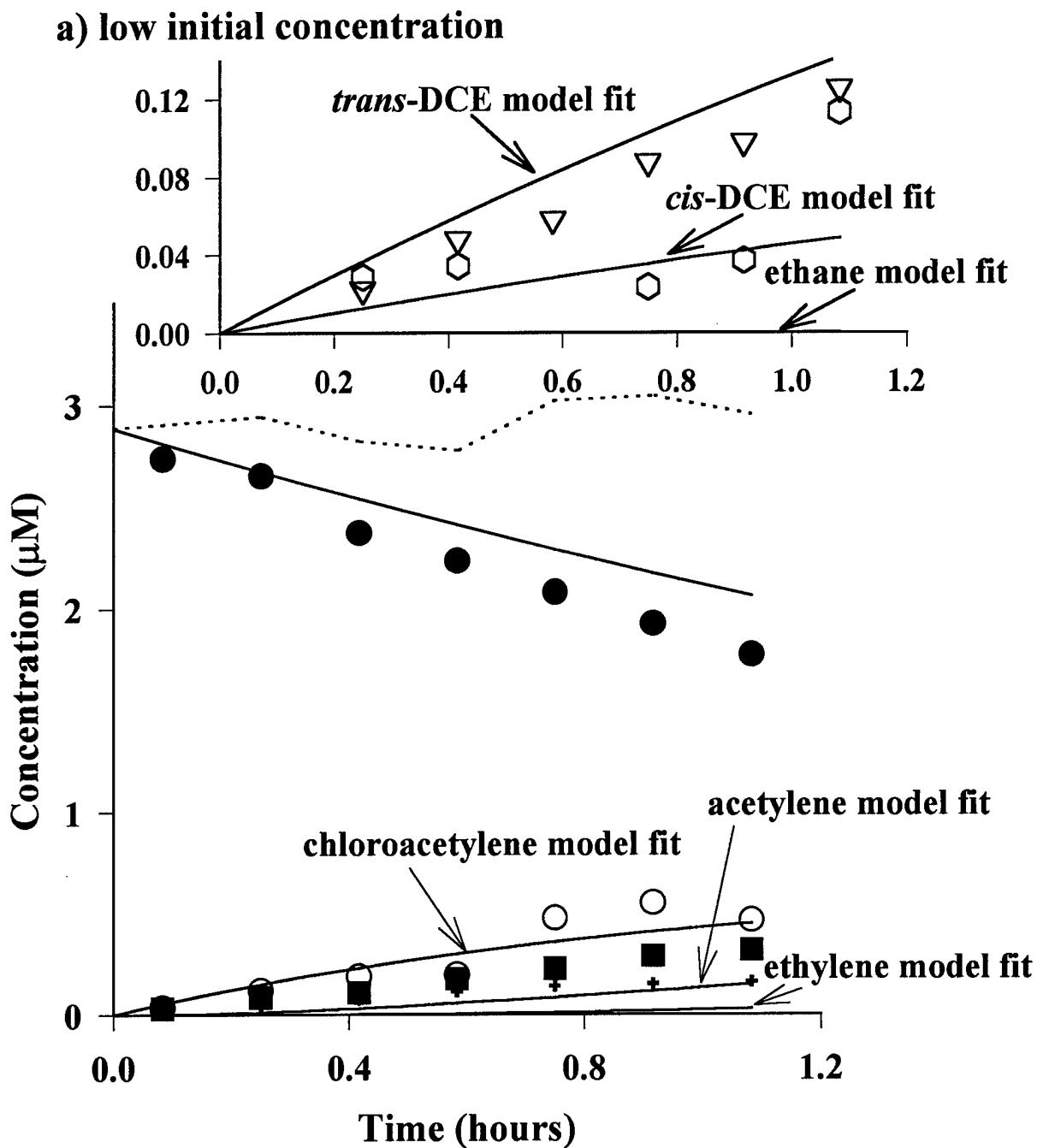


Figure 72 (continued).



**Figure 73.** Reduction of dichloroacetylene (●) by 0.10 g Fe(0) in 160 mL of 0.1 M NaCl, 50 mM Tris buffer (pH 7.2) at a) low; b) intermediate; and c) high initial concentrations. Major products include chloroacetylene (+), acetylene (O) and ethylene (■). Insets show the trace products *trans*-DCE (▽), *cis*-DCE (▲) and ethane (◊). Data for the C<sub>4</sub> hydrocarbons are not shown. Lines represent model predictions based on the parameters in Table 10. The dotted lines represent the C<sub>2</sub> mass balance.

b) intermediate initial concentration

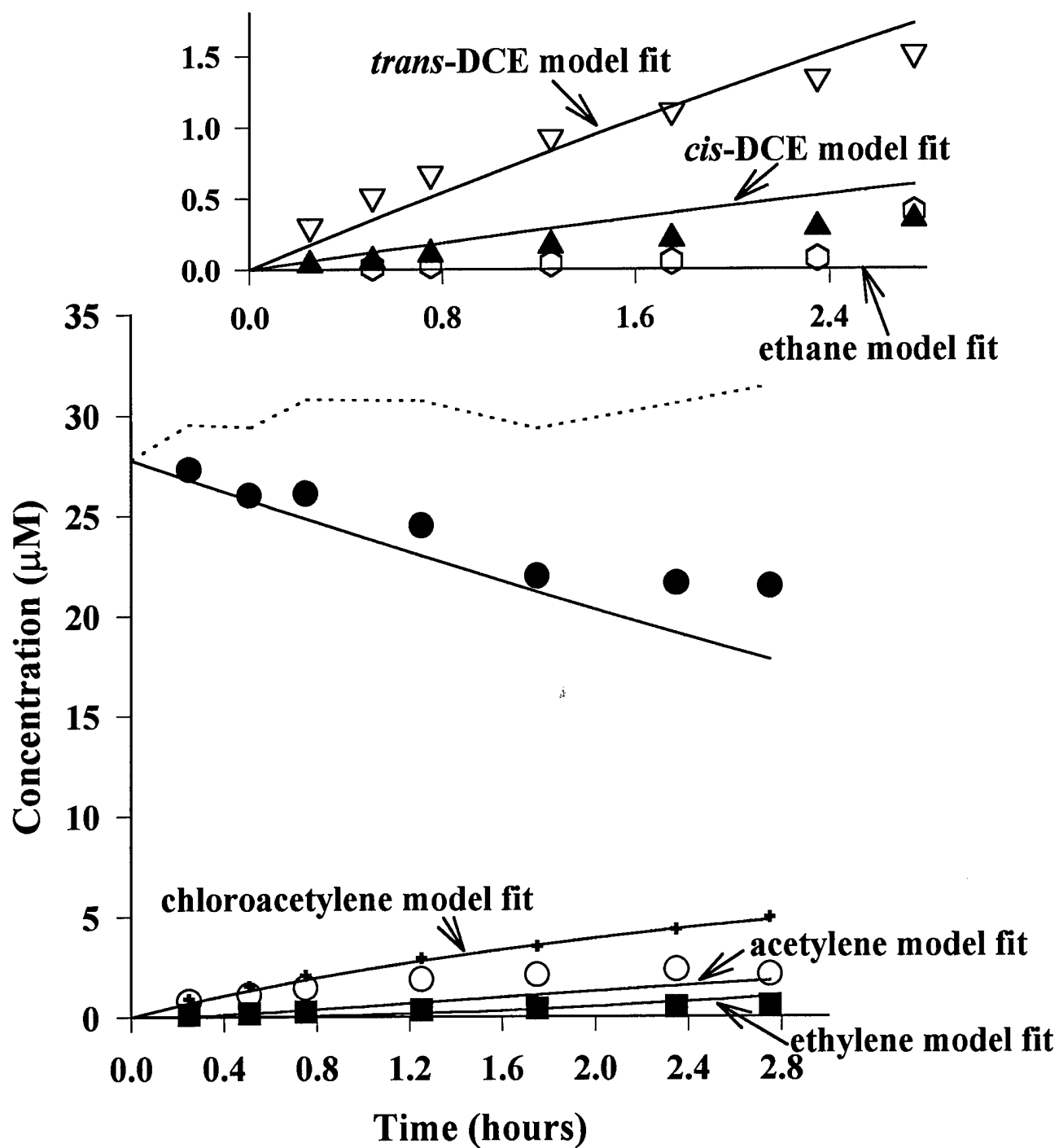


Figure 73 (continued).

c) high initial concentration

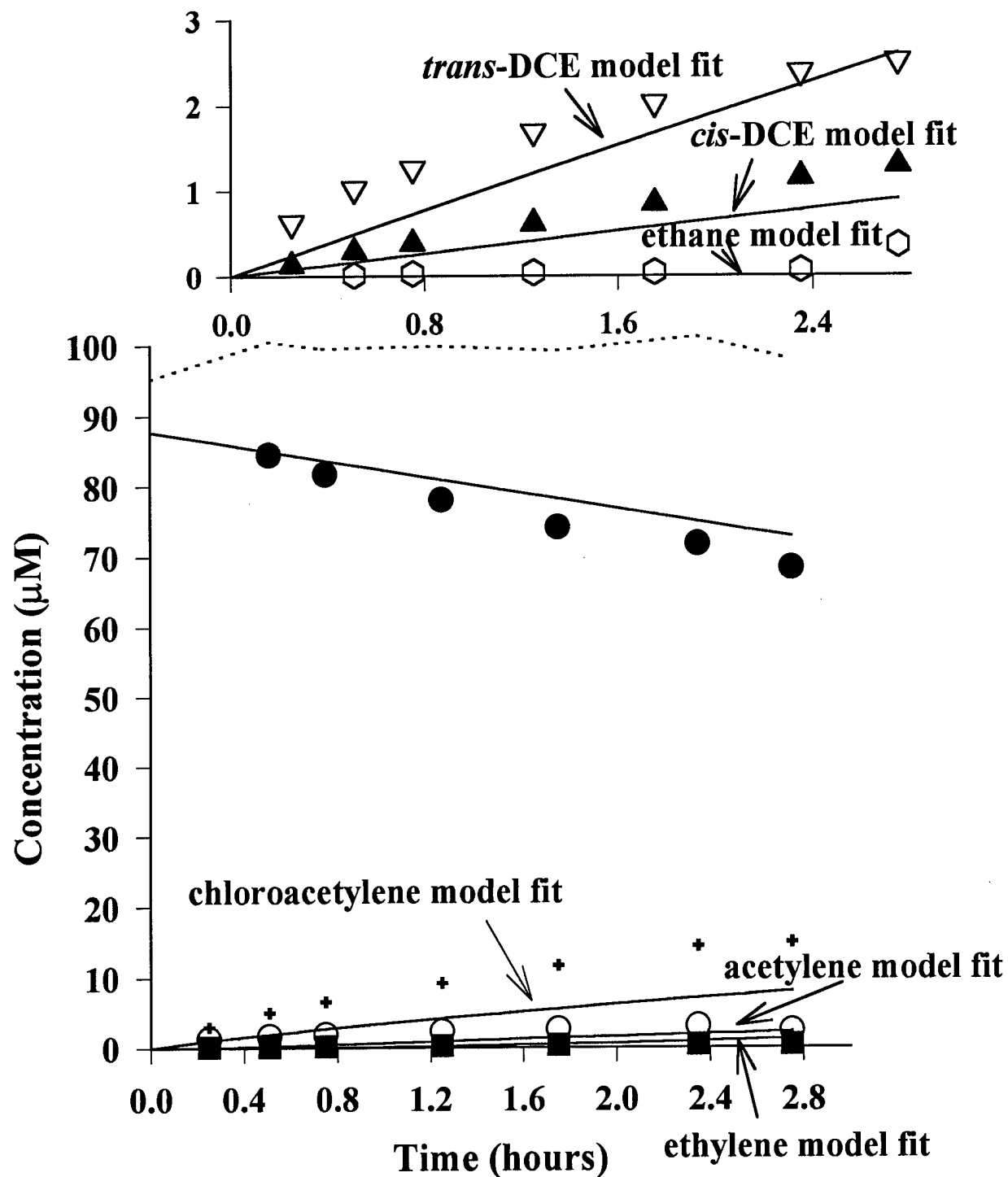
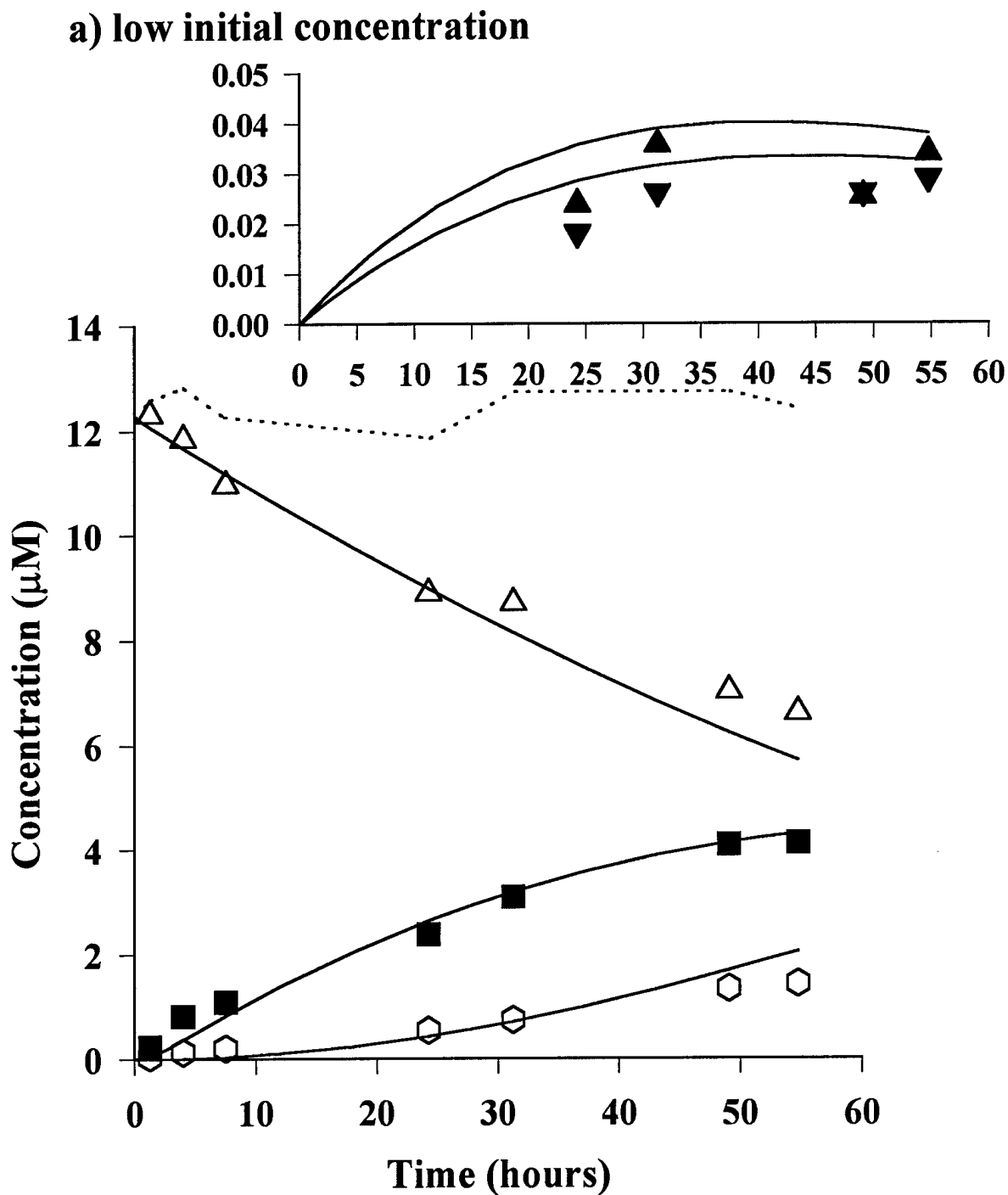


Figure 73 (continued).

#### g. TCE and PCE

As shown in Figure 74, the major products of TCE reduction are ethylene and ethane. Small amounts of *cis*-DCE and 1,1-DCE, and trace amounts of *trans*-DCE (not shown) and C<sub>4</sub> hydrocarbons (not shown) were also observed. The experiments at low TCE concentration displayed substantially more conversion and seemed to bias the fit, even when the data were normalized by initial concentrations. Curves presented in Figure 74 for TCE, therefore, represent predictions based only on a model fit to the appearance of daughter products. The production of ethylene and ethane are predicted quite well via a sequence involving reductive elimination to chloroacetylene, followed by reactions described previously (chloroacetylene → acetylene → ethylene → ethane). As chloroacetylene and acetylene are both extremely reactive, they never accumulated above detection limits; the rate constants previously determined for these species successfully explain the experimental data for ethylene and ethane when substituted into the TCE model.

The distribution of products observed for reduction of PCE was relatively simple. Only ethylene, ethane, and TCE were observed, along with longer carbon chain coupling products (not shown), as seen in Figure 75. At high concentrations, the model seems to underpredict ethane concentration. Because conversions of the parent species were relatively low, kinetic and adsorption parameters for PCE were determined by fitting only the data for the product appearance. Again, reductive elimination of PCE to dichloroacetylene was invoked to explain the observed products. The rapid reduction of the dichloroacetylene and its daughter products leads to the swift conversion to ethylene and ethane. As the DCEs are only minor products of TCE and dichloroacetylene reduction and react quickly relative to PCE and TCE, they do not accumulate to detectable levels.



**Figure 74.** Reduction of TCE (Δ) by 0.25 g Fe(0) in 160 mL of 0.1 M NaCl, 50 mM Tris buffer (pH 7.2) at a) low and b) high initial concentration. Major observed products are ethylene (■) and ethane (◻). Insets show the trace products *cis*-DCE (▲) and 1,1-DCE (▼). Trace amounts of *trans*-DCE and C<sub>4</sub> hydrocarbons were also observed (data not shown). Lines represent model predictions based on parameters presented in Table 10. The dotted lines represent the C<sub>2</sub> mass balance.

**b) high initial concentration**

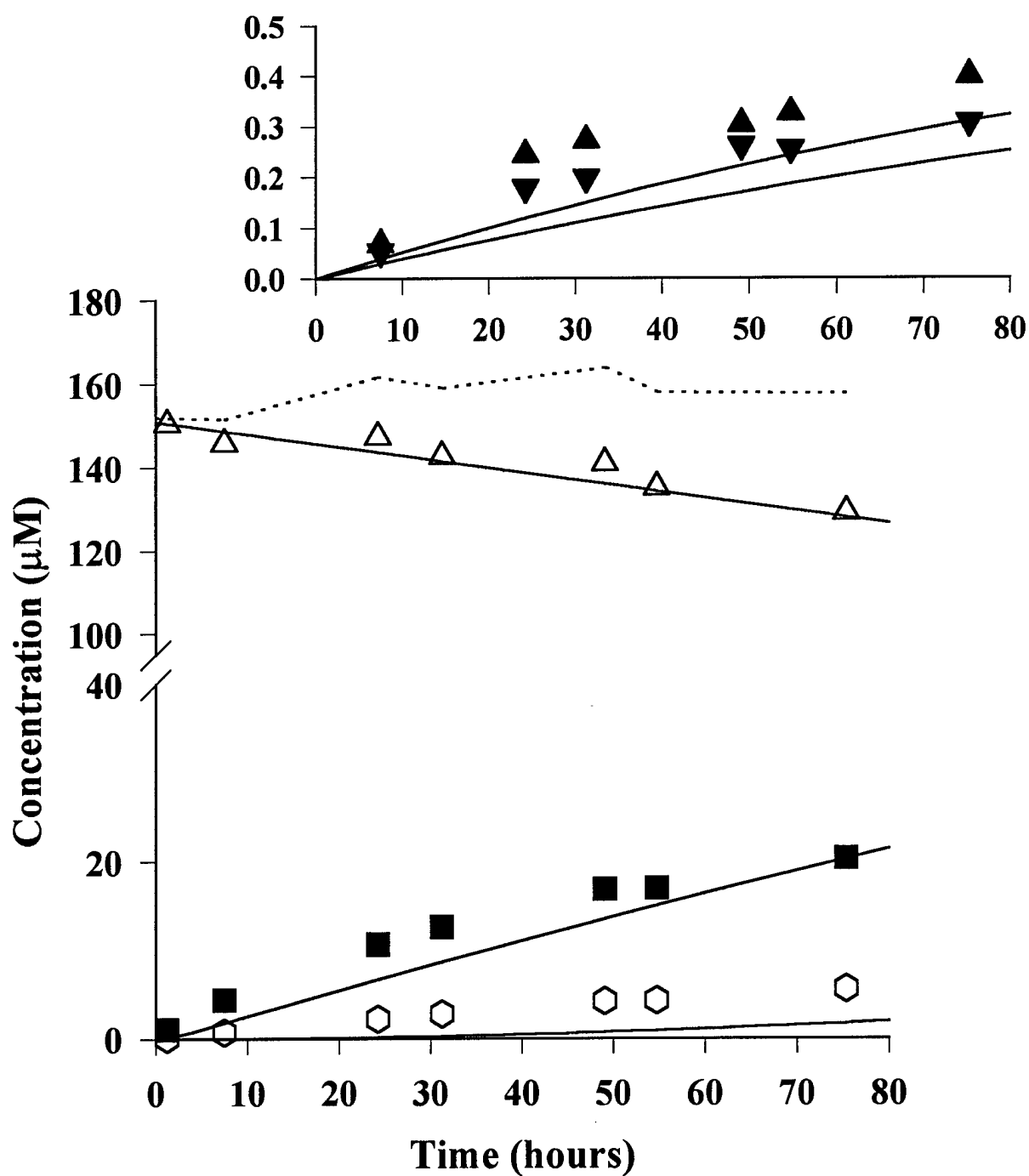
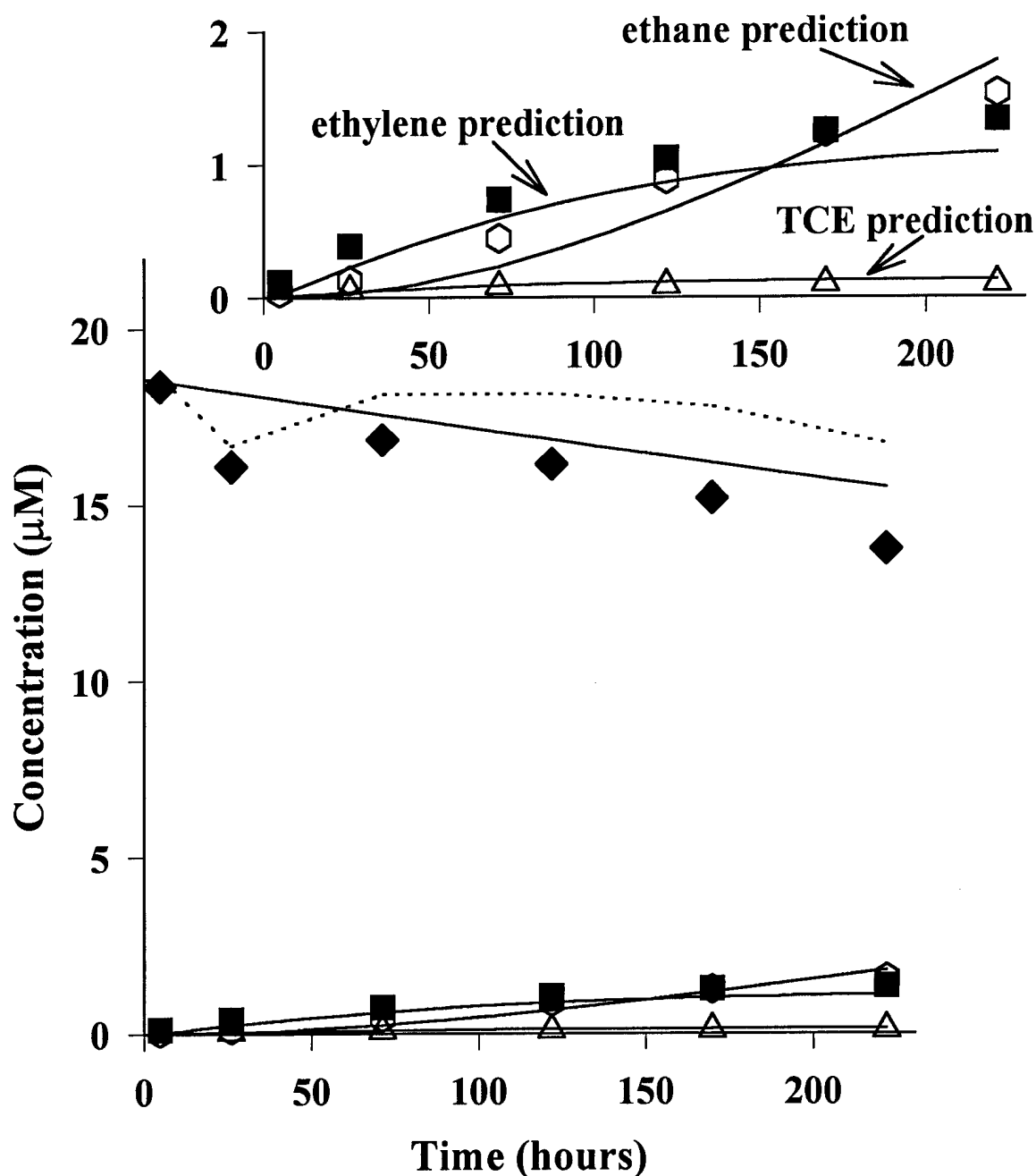


Figure 74 (continued).

a) low initial concentration



**Figure 75.** Reduction of PCE ( $\blacklozenge$ ) by 0.25 g Fe(0) in 160 mL of 0.1 M NaCl, 50 mM Tris buffer (pH 7.2) at a) low and b) high initial concentration. Observed products are ethylene ( $\blacksquare$ ), ethane ( $\hexagon$ ) and TCE ( $\triangle$ ). Insets show the products on an expanded scale. Lines represent model predictions based on the parameters presented in Table 10, but as PCE data were not included in the fitting procedure, the prediction for this species is based on the rate of accumulation of the daughter products. The dotted lines represent the  $\text{C}_2$  mass balance.



**b) high initial concentration**

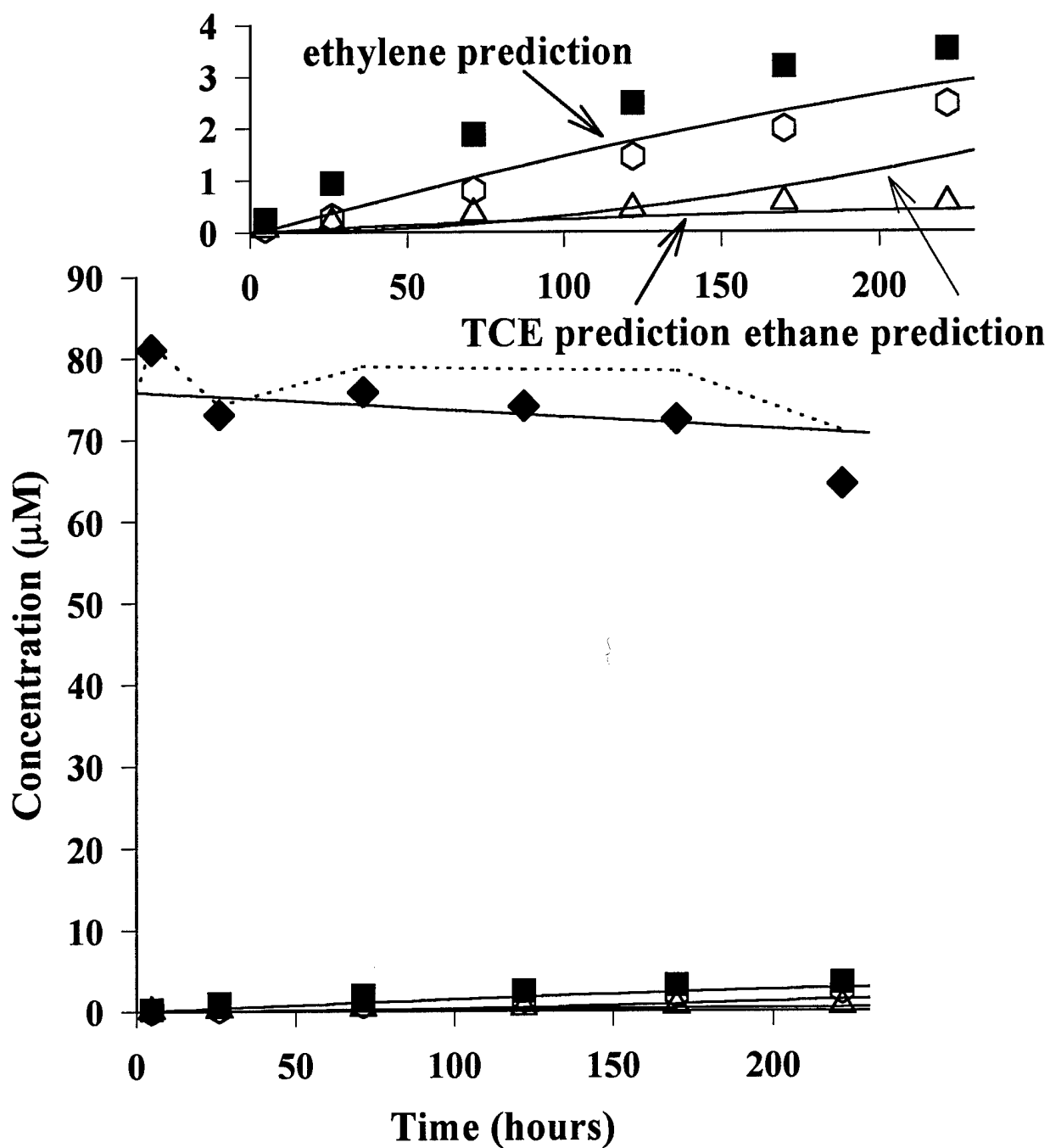


Figure 75 (continued).

#### 4. Competitive Experiments

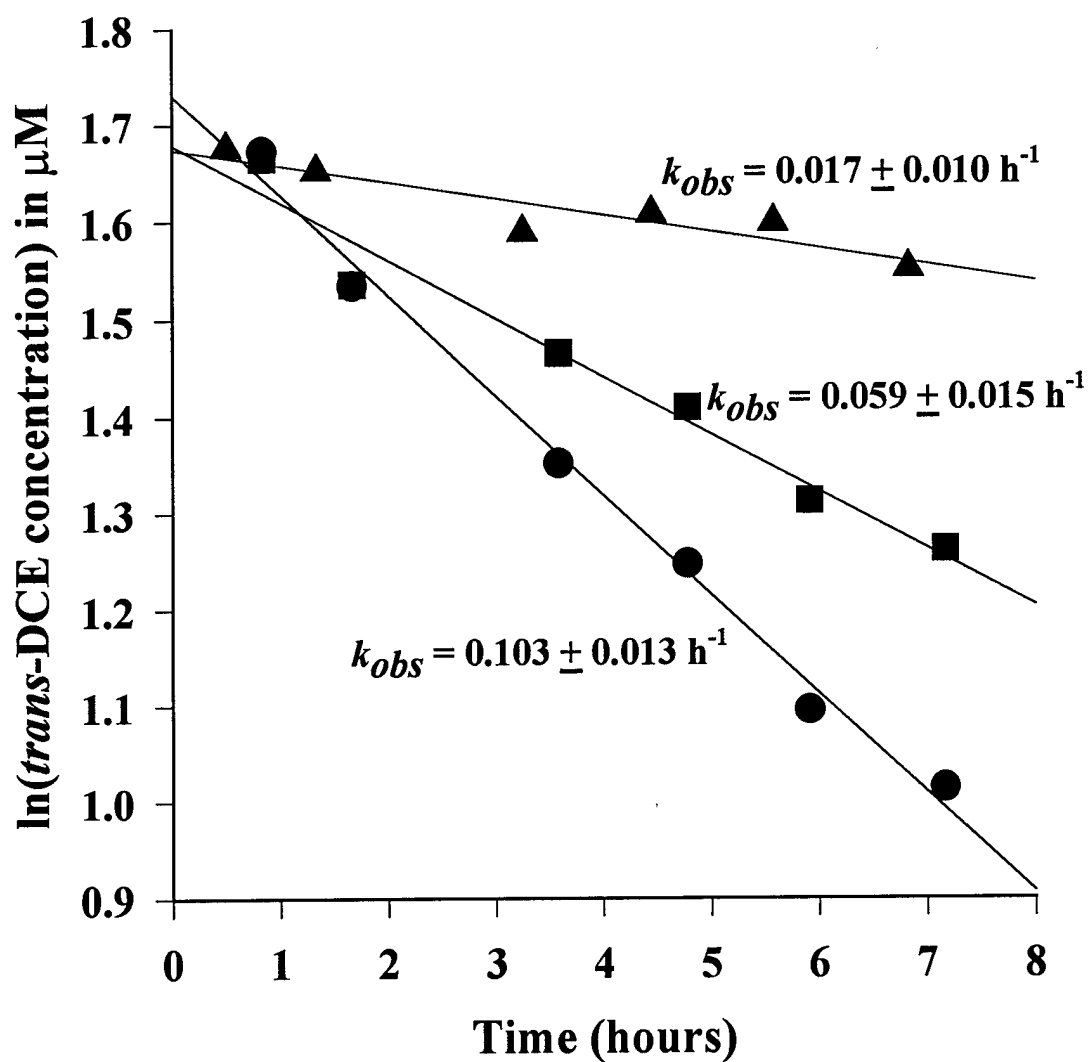
The applicability of the LHHW model to our experimental data implies the existence of intraspecies competition for reactive sites at the metal surface. In order to examine whether interspecies competition also occurs, experiments were conducted in which two species were simultaneously introduced into a reactor and the impact of the second species on the rate of reaction of the first species was determined. In these experiments, the target species was introduced at a concentration of  $\sim 4 \mu\text{M}$  and the potential competitor generally at  $200 \mu\text{M}$ . These experiments were conducted in parallel to those previously described, to allow inclusion of interspecies competition throughout the modeling effort.

Results suggest that substantial interspecies competition for reactive sites can exist. Plots demonstrating the inhibition of *cis*- and *trans*-DCE are given in Figures 76 and 77. Substantial decreases in the observed pseudo-first order rate constant are obtained for the two 1,2-DCE isomers in the presence of a second competing species. The slight differences in initial concentration ( $3.5\text{--}5 \mu\text{M}$ ) for the *cis*- and *trans*-DCE curves shown in Figures 76 and 77 would not be expected to produce the large differences in pseudo-first order rate constant observed.

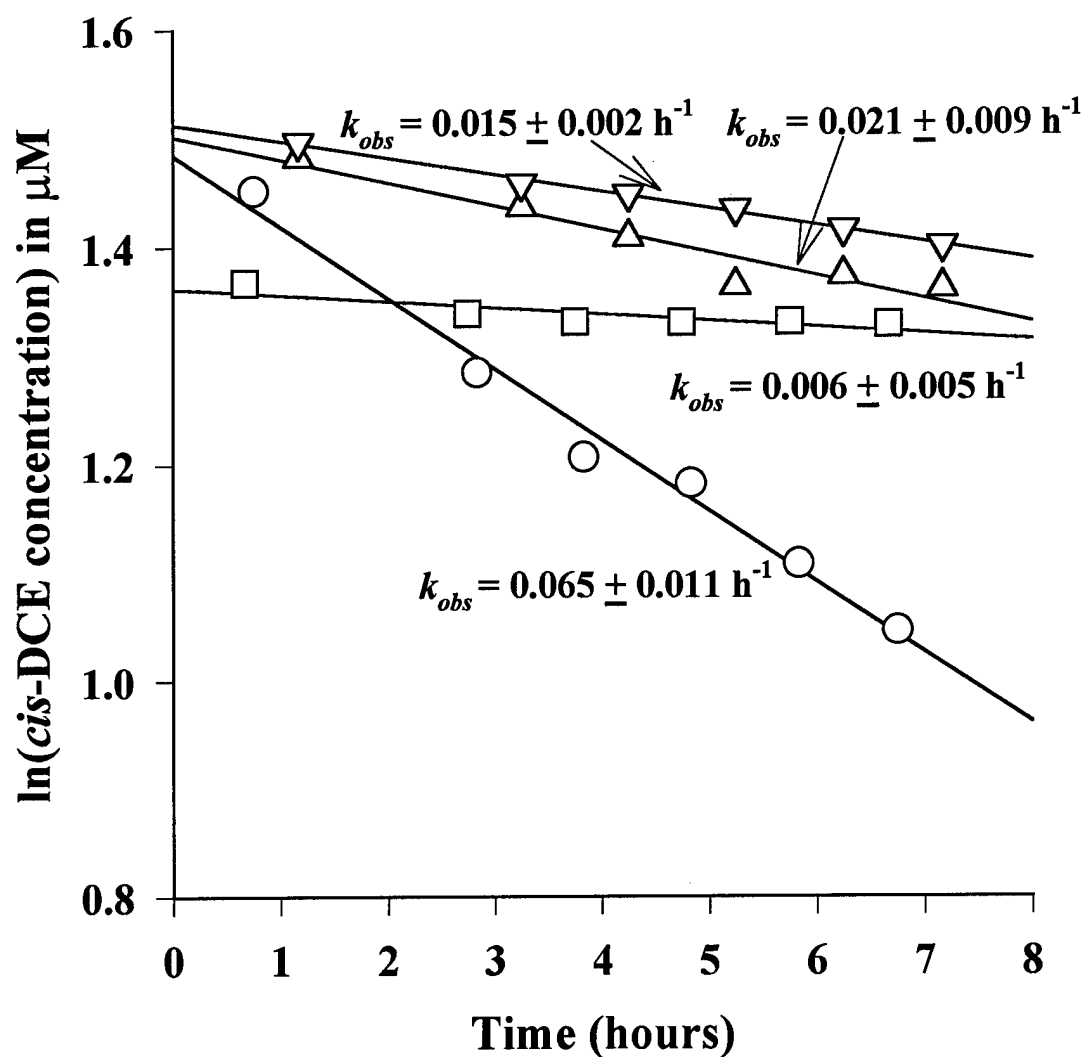
Table 11 lists the adsorption constants determined for the inhibition of the target species by a competitor. In most cases, the calculated value of the interspecies inhibition constant for the competitor (e.g.,  $K_{\text{acetylene}}$  when acetylene was used to inhibit the reaction of vinyl chloride, *cis*- or *trans*-DCE) were within a factor of 2 of those found in Table 10 for self-inhibition of the competitor. The exception seems to be the value of  $K_{\text{cis-DCE}}$  calculated for the inhibition of *trans*-DCE reaction, which was nearly an order of magnitude smaller than the value obtained for self-inhibition.

TABLE 11: INHIBITION CONSTANTS

Competitor	Target Species	$K_{\text{competitor}} (\mu\text{M}^{-1})$
acetylene	<i>cis</i> -DCE	$0.148(\pm 0.063)$
acetylene	vinyl chloride	$0.269(\pm 0.156)$
acetylene	<i>trans</i> -DCE	$0.210(\pm 0.2)$
<i>trans</i> -DCE	<i>cis</i> -DCE	$0.019(\pm 0.003)$
<i>cis</i> -DCE	<i>trans</i> -DCE	$0.004(\pm 0.001)$
1,1-DCE	<i>cis</i> -DCE	$0.011(\pm 0.007)$
1,1-DCE	<i>trans</i> -DCE	$0.019(\pm 0.008)$



**Figure 76.** Reaction of *trans*-DCE in the absence (●) and presence of competitors *cis*-DCE (■), 200  $\mu\text{M}$ ; and acetylene (▲), 100  $\mu\text{M}$ . Experiments were performed in reactors containing 160 mL of 0.1 M NaCl, 50 mM Tris buffer (pH 7.2) and 0.25 g Fe(0). Lines are linear regressions to the data.



**Figure 77.** Reaction of *cis*-DCE in the absence (O) and presence of competitors acetylene (□), 100  $\mu\text{M}$ ; 1,1-DCE ( $\Delta$ ), 200  $\mu\text{M}$ ; and *trans*-DCE ( $\nabla$ ), 200  $\mu\text{M}$ . Experiments were performed in reactors containing 160 mL of 0.1 M NaCl, 50 mM Tris buffer (pH 7.2) and 0.25 g Fe(0). Lines are linear regressions to the data.

Similar experiments were conducted with the chloroacetylenes. Acetylene and the dichloroethylenes did not significantly inhibit the reduction of chloroacetylene or dichloroacetylene, however, as is displayed in Figure 78 for chloroacetylene. As acetylene is produced by the reaction of chloroacetylene, dichloroacetylene, and *cis*- and *trans*-DCE, it is not possible to test whether these species inhibit the reaction of acetylene without recourse to isotopically label acetylene. The assumption was therefore made (as with the other alkynes) that reaction of acetylene was not inhibited by other species.

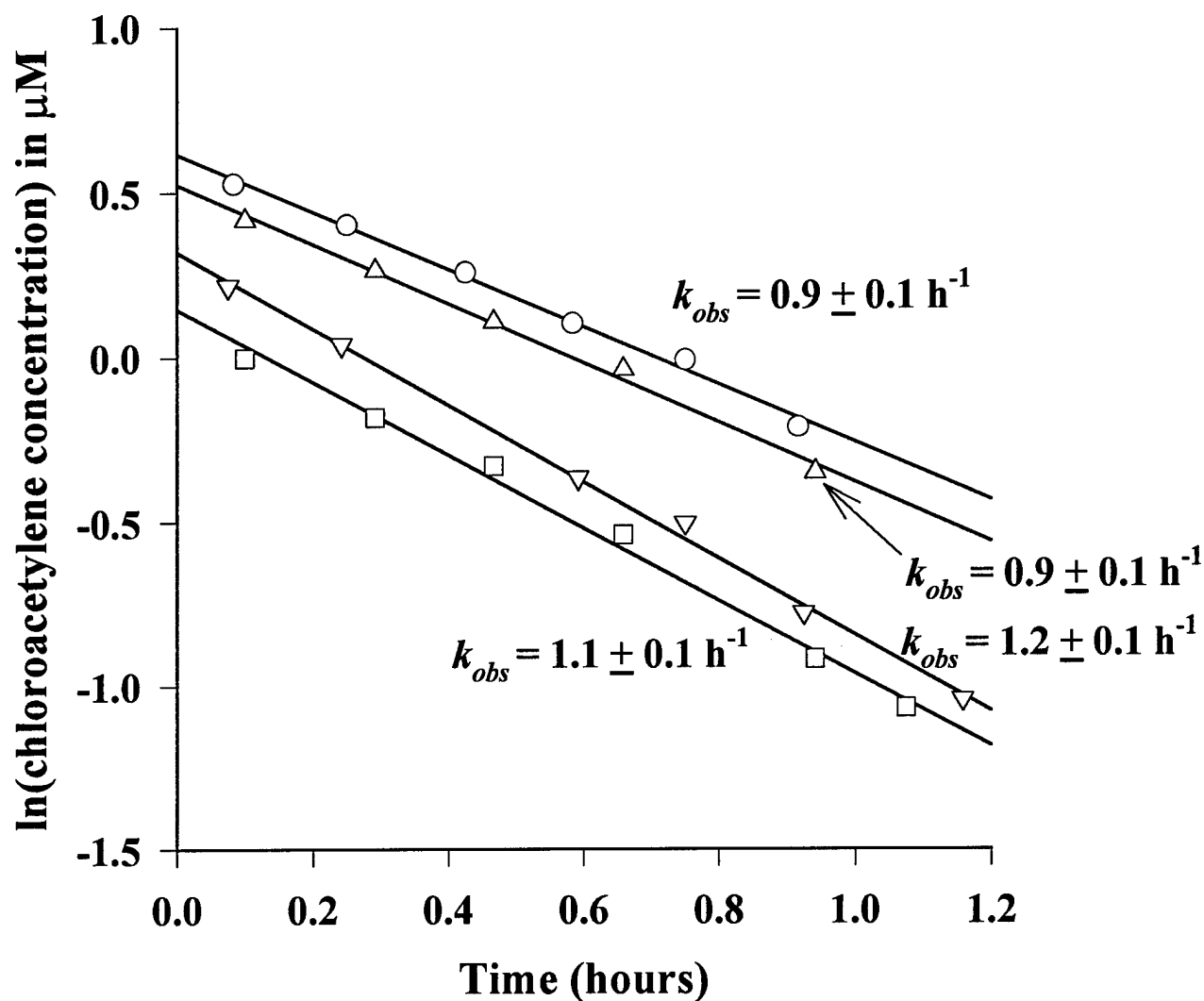


**Figure 78.** Reduction of chloroacetylene in the absence (O) and presence of potential competitors: *trans*-DCE ( $\square$ ), 200  $\mu\text{M}$ ; *cis*-DCE ( $\Delta$ ), 200  $\mu\text{M}$ ; and 1,1-DCE ( $\nabla$ ), 200  $\mu\text{M}$ . Experiments were performed in reactors containing 160 mL of 0.1 M NaCl, 50 mM Tris buffer (pH 7.2) and 0.25 g Fe(0). Lines are linear regressions to the data.

## 5. Comments on the Kinetic Model

The LHHW kinetic model developed in this work describes the experimental data reasonably well. It can be used to model the reaction kinetics of most species over a large range of initial concentrations with only two adjustable parameters (a kinetic parameter and an adsorption constant), even though the pseudo-first order rate "constant" may vary by an order of magnitude over a wide concentration range.

Although the LHHW kinetic model describes the experimental data, it is hindered by experimental limitations. Wherever possible, competition for reactive sites between two species was verified experimentally, but this was not always feasible. Because TCE and PCE react so slowly, any inhibitor introduced would completely disappear before any significant transformation of the PCE or TCE occurred. A second difficulty was that it was not possible to directly determine how a parent compound inhibited its daughter products without using isotopically labeled compounds. If competition could not be verified, it was assumed to occur and the adsorption parameters for intraspecies competition in Table 10 were used. For example, for both reasons listed above, the inhibition of TCE by *trans*-DCE could not be measured, yet the term  $K_{IDCE}C_{IDCE}$  was inserted into the denominator of the equation for TCE disappearance. This assumption may have given rise to underprediction of ethane production. Inhibition of ethylene by other species was included (for an adsorption-limited species, interspecies, but not intraspecies, competition may occur), but such inhibition could not be verified experimentally. The systematic underprediction of ethane suggests that the adsorption parameters in Table 10 may be larger than appropriate for predicting ethylene reaction. Some degree of inhibition does appear necessary, however, for if inhibition is neglected entirely, measured ethane concentrations are consistently overpredicted.

The difficulties in the prediction of acetylenic intermediates from dichloroacetylene reduction, as well as the observation that acetylenic species inhibit chlorinated ethylene reduction, even though chlorinated ethylenes do not inhibit the acetylenes, suggests that more complicated modeling may be required. The LHHW model assumes that all sites possess equal reactivity, but the above observations suggest that a model with different types of reactive sites may be necessary to completely describe the reaction of the highly reactive acetylenic species. Attempts to model the data presented here with a model containing two types of reactive sites did not

provide statistically useful results.

## E. DISCUSSION

### 1. Rate Constant and Initial Rate versus Initial Concentration

Using the parameters in Tables 10, reaction rates and initial pseudo-first order rate constants can be computed as a function of initial concentration. The results are presented as the model curves in Figure 64. These model curves do not represent fits to the  $k_{obs}$  or initial rate versus  $C_0$  data, but rather represent predictions based on the parameters determined from the simultaneous fitting of timecourses obtained at several different  $C_0$  values. The simulations match the data reasonably well in most cases, indicating that the model is internally consistent.

### 2. Factors Affecting Product Distribution

As noted in our work with zinc (Section V), the branching ratios between hydrogenolysis and reductive elimination for the chlorinated ethylenes, and between hydrogenolysis and reduction of the triple bond (hydrogenation) for the chlorinated acetylenes, play crucial roles in determining the product distribution. As this study reveals, reductive  $\beta$ -elimination is the dominant pathway for reaction of iron with chlorinated ethylenes possessing the requisite  $\alpha$ ,  $\beta$  pair of chlorines. Table 12 lists the percentage of reaction occurring via reductive elimination computed as the kinetic parameter ( $k'S_i$ ) for the reductive elimination reaction divided by the overall kinetic constant determined by summing the contributions of reductive elimination and hydrogenolysis.

**TABLE 12: PERCENTAGE OF REACTION OCCURRING VIA REDUCTIVE ELIMINATION**

Species	% Reductive Elimination	$\Delta E_2 = (E_{red. Elim} - E_{hydrogenolysis})$
PCE	87.2	0.049
TCE	97.1	0.066 <sup>a</sup>
<i>cis</i> -DCE	94.0	0.086
<i>trans</i> -DCE	98.8	0.085

<sup>a</sup>Using the value for the reduction of TCE to *cis*-DCE.

The preeminent role played by reductive elimination makes it an important factor in reaction pathway modeling. For *cis*- and *trans*-DCE, the percentage of reaction occurring via reductive elimination is similar for both iron and zinc. For TCE and PCE, however, reductive elimination dominates reaction only when iron serves as the reductant. With zinc, only 15% of PCE and 30% of TCE reaction proceeded through reductive elimination.



For the chlorinated acetylenes, hydrogenolysis dominates over hydrogenation, as shown in Table 13. In the case of dichloroacetylene, these results are substantially different from those observed with Zn(0). When zinc serves as the reductant, 92% of chloroacetylene and only 18% of dichloroacetylene reaction occurs via hydrogenolysis (Section V).

**TABLE 13: FRACTION OF CHLORINATED ACETYLENE REACTION OCCURRING VIA HYDROGENOLYSIS**

Species	% Hydrogenolysis
chloroacetylene	100
dichloroacetylene	76.5

The low degree of hydrogenation of the chlorinated acetylenes (which would produce chlorinated ethylenes) during reaction with Fe(0) makes reductive elimination of PCE and TCE an environmentally desirable reaction. Because virtually none of the chloroacetylene produced from the reductive elimination of TCE is converted to vinyl chloride, reductive elimination of TCE circumvents the production of vinyl chloride. Similarly, most of the dichloroacetylene reacts to chloroacetylene, from which no vinyl chloride is produced. Even the *trans*-DCE and *cis*-DCE formed from the hydrogenation of dichloroacetylene is not overly problematic, for these two species rapidly react predominantly via reductive elimination themselves (see Table 12) to produce acetylene.

### 3. Comparison with Results of Others

It is often assumed that reactivity of the chlorinated ethylenes in reduction reactions should increase with increasing reduction potential. For example, PCE has been found to react more rapidly with transition metal coenzymes than does TCE (Gantzer and Wackett, 1991; Burris *et al.*, 1996; Glod *et al.*, 1997a.) The DCEs have been found to be less reactive with vitamin B<sub>12</sub> than TCE (Glod *et al.*, 1997b; Gantzer and Wackett, 1991), although it has been suggested that this results from a change in reaction mechanism (Glod *et al.*, 1997a, b). In contrast, the overall order of reactivity presented here (VC > DCEs > TCE > PCE) displays the opposite trend. This reversal has also been reported for reduction of chlorinated ethylenes by FeS (Butler and Hayes, 1999), Pd (Lowry and Reinhard, 1999), and a Pd/Fe bimetallic reductant (Kim and Carraway, 1999), although other studies report increasing reaction rates with increasing chlorination for

reaction with Fe(0) (Gillham and O'Hannesin, 1994; Liang *et al.*, 1997; Johnson *et al.*, 1996; Scherer *et al.*, 1998).

One explanation for the disparate results concerning the effect of chlorination on relative reactivity of chloroethylenes with Fe(0) may stem from the neglect by others of the impact of intraspecies competitive effects. The much lower detection limits afforded by GC with electron capture detection (ECD) could have resulted in experiments for PCE and TCE being conducted at much lower aqueous concentrations than is possible for the lesser-chlorinated ethylenes, complicating a direct comparison of rate constants. Another possible explanation is that many prior studies were conducted with iron containing significant levels of carbon impurities which appear to serve as a nonreactive sorptive phase (Burris *et al.*, 1995; Allen-King *et al.*, 1997). The overall rate of organohalide disappearance in such batch systems therefore includes not only reaction, but also losses incurred by sorption. Few studies have carefully differentiated sorption from reaction, with the exception of the work of Burris and co-workers (Burris *et al.*, 1995; Allen-King *et al.*, 1997). Their results demonstrate that sorption (which may easily be mistaken for rapid reaction) is greater for more highly halogenated species; when such sorptive losses were carefully accounted for, PCE was not found to react significantly more rapidly than TCE (Burris *et al.*, 1995).

The reactivity trend in this work also differs sharply from the results presented by Johnson *et al.* (1996) and Scherer *et al.* (1998) in which data were compiled from the literature by normalizing rate constants according to the iron surface area/solution volume. The explanations in the previous paragraph may account for the discrepancy. Other possibilities include bias introduced by (i) normalizing rate constants simply based on iron surface area, when several other factors, including iron type, iron pretreatment, and solution conditions/composition may also affect reaction rate or (ii) lumping data for alkyl with vinyl halides may be inappropriate, due to differences between  $sp^3$  and  $sp^2$  hybridized carbon-halogen bonds.

Product distributions reported herein for TCE compare closely to those reported in column studies conducted by others, potentially signifying similar relative reactivity and branching ratios. For example, our results were virtually identical to the product distribution obtained in column studies (Orth and Gillham, 1996) for which the major products were ethylene and ethane, with <10% chlorinated products. Note that these experiments employed the same Fisher 100

mesh iron, but differed in that a carbonate buffer was used. The difference in buffer composition may explain the ~20 fold higher reactivity observed in the present work when rate constants are normalized to metal loading.

The product distributions observed in this study are also similar to those determined in batch studies (Campbell *et al.*, 1997; Liang *et al.*, 1997). Campbell *et al.* (1997) found that TCE produced mostly ethylene and ethane and traces of *cis*-DCE when reacted with Fisher 40 mesh (cast) iron filings. The observed products of PCE reduction were ethylene and ethane, with traces of TCE. The experiments of Campbell *et al.* (1997) were conducted in the presence of headspace. The detection of volatile intermediates is facilitated by the headspace, but reactions of oxidants are slowed by partitioning into the gas phase away from the reactive metal surface. This could explain why larger concentrations of acetylene were observed, as compared to our zero-headspace systems.

Liang *et al.* (1997) found roughly similar product distributions with Fisher 40 mesh cast iron filings in zero-headspace systems, although these investigators observed larger yields of vinyl chloride than in Campbell *et al.* (1997). This work also provides pseudo-first order rate constants for TCE ( $0.09 \text{ h}^{-1}$ ), *cis*-DCE ( $0.02 \text{ h}^{-1}$ ), *trans*-DCE ( $0.05 \text{ h}^{-1}$ ) and vinyl chloride ( $0.01 \text{ h}^{-1}$ ) from individual experiments all conducted at an initial concentration of ~25  $\mu\text{M}$ . The high rate constant for TCE reaction may reflect sorption to carbon impurities, as described above. Alternatively, the possibility exists that cast iron and electrolytic iron may vary in their reactivity.

Our data are also consistent with field data for PCE and TCE reduction by a commercial grade of iron reported by O'Hannesin and Gillham (1998). As a test to see if the reactivity trends and branching ratios determined in this work could explain the trace amounts of DCE isomers observed, a simulation of the Borden field-site reactive barrier was performed based on the parameters in Table 10. Kinetic parameters obtained herein were scaled to the metal surface area/volume of solution ratio at the field site. In order to fit the field data for the parent compounds (PCE and TCE), the scaled kinetic parameters were then reduced by a factor of 140; the need for this step may arise from differences in the electrolyte composition and the type of iron employed. The accumulation of partially dechlorinated products was then simulated by assuming that the *relative* magnitudes of rate constants for all parent compounds and intermediates (and therefore branching ratios) were identical to those determined in this study.

The adjusted kinetic parameters used in the simulations are given in Table 14. Adsorption constants from Table 10 were used in the model without adjustment.

Using the initial concentration (2040  $\mu\text{M}$  TCE and 350  $\mu\text{M}$  PCE) and groundwater velocity encountered at the Borden test site results in predicted profiles for partially dechlorinated intermediates that were similar to those observed in the field, as shown in Figure 79. The peak concentrations of the DCEs are only predicted to account for ~0.6% of the initial PCE and TCE

**TABLE 14: KINETIC PARAMETERS USED IN THE SIMULATIONS OF THE BORDEN FIELD DATA**

<i>Parent</i>	<i>Product</i>	$(k^s S_d) (\mu\text{M} \cdot \text{h}^{-1})$ <i>all reactions</i>	$(k^s S_d) (\mu\text{M} \cdot \text{h}^{-1})$ <i>hydrogenolysis only</i>
PCE	TCE	0.11	0.85
PCE	dichloroacetylene	0.74	--
TCE	<i>trans</i> -DCE	0.02	0.71
TCE	<i>cis</i> -DCE	0.17	5.40
TCE	1,1-DCE	0.13	4.10
TCE	chloroacetylene	9.89	--
<i>trans</i> -DCE	VC	1.59	133
<i>trans</i> -DCE	acetylene	131	--
<i>cis</i> -DCE	VC	4.07	69.3
<i>cis</i> -DCE	acetylene	65.2	--
1,1-DCE	ethylene	111	111 <sup>a</sup>
acetylene	C <sub>4</sub> 's	2.73	--
acetylene	ethylene	343	--
chloroacetylene	acetylene	192	--
dichloroacetylene	<i>cis</i> -DCE	30.4	--
dichloroacetylene	<i>trans</i> -DCE	88.3	--
dichloroacetylene	chloroacetylene	387	--
<i>Parent</i>	<i>Product</i>	$(k^a S_d) (\text{h}^{-1})$	$(k^a S_d) (\text{h}^{-1})$
VC	ethylene	1.96	1.96
ethylene	ethane	0.66	0.66

<sup>a</sup>In this case, 1,1-DCE reacted to the hydrogenolysis product vinyl chloride.

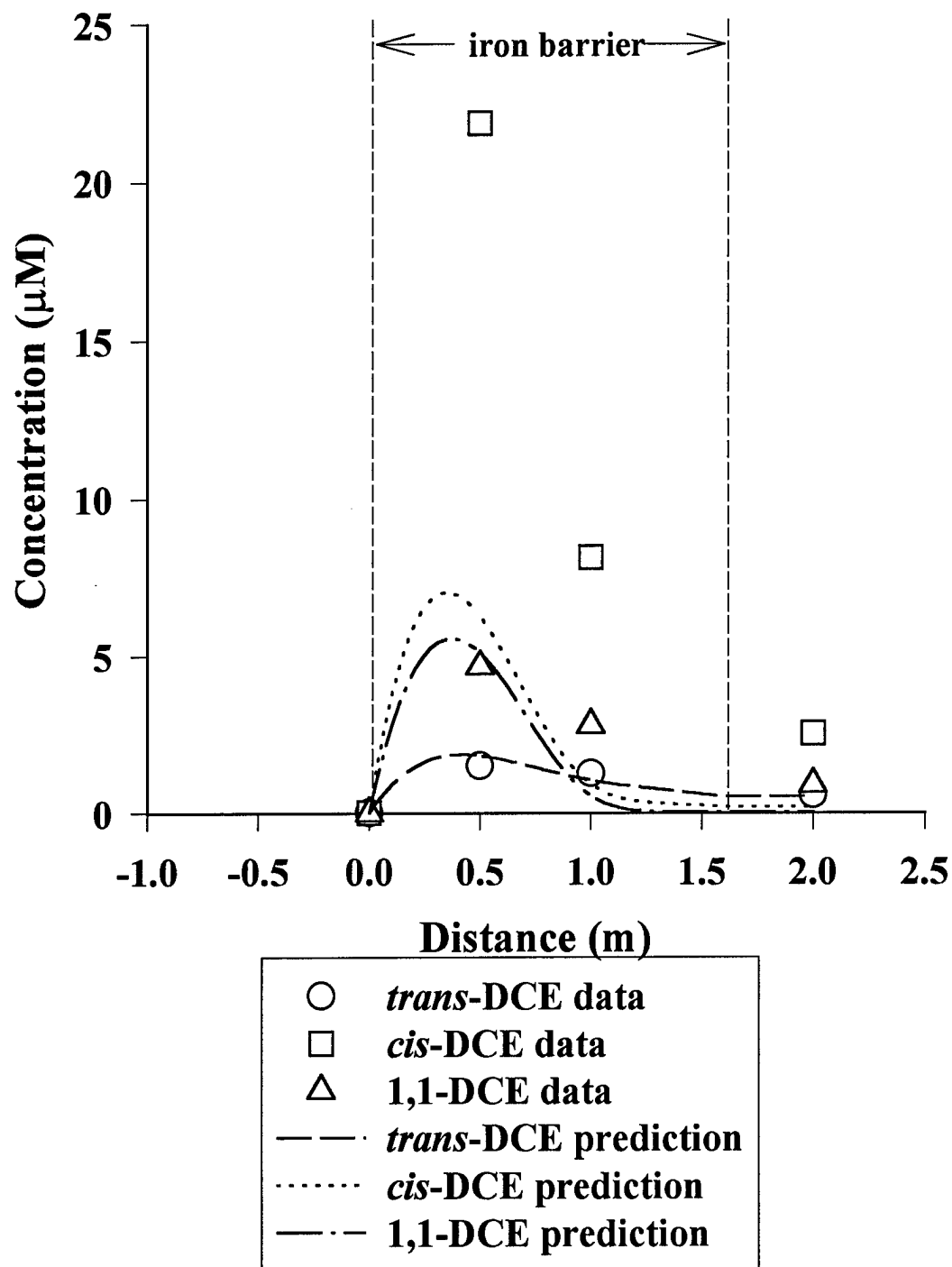


**Figure 79.** Simulation (lines) of intermediates generated in the permeable iron barrier at the Borden test site using a model in which both hydrogenolysis and reductive elimination reactions occur according to the branching ratios determined in this work. The kinetic parameters employed are given in Table 14. Adsorption parameters from Table 10 were employed. Symbols represent the maximum observed concentration of a given species at that sampling point. Influent consists of PCE (350  $\mu\text{M}$ ) and TCE (2040  $\mu\text{M}$ ).

mass (within a factor of 2 of the maximum 1.2% yield observed in the O'Hannesin study). If branching ratios were to favor hydrogenolysis products to the exclusion of reductive elimination products, the peak concentration of the DCE daughter products would be anticipated to comprise > 26% of the influent PCE and TCE concentration, as shown in Figure 80. Moreover, a peak concentration of >200  $\mu\text{M}$  vinyl chloride would be expected, whereas < 1  $\mu\text{M}$  was observed.

If the reactivity sequence in the field experiment for chlorinated ethylenes were the reverse of that trend obtained in our experiments, such that the lesser-chlorinated ethylenes were to react more slowly than PCE or TCE, the branching ratios favoring reductive  $\beta$ -elimination would need to be even higher than those obtained in the present study in order to explain the lack of accumulation of partially dechlorinated ethylenes. A sensitivity analysis on the kinetic parameters of the DCEs demonstrated that the maximum predicted concentration of the DCEs decreased by  $\sim 3$  fold for each order of magnitude increase in the DCE kinetic parameters (adsorption and kinetic parameters of all other species remaining unchanged). Our success in predicting concentrations of intermediates indicates either that reductive  $\beta$ -elimination represents an important pathway under field conditions, or else that the reactivity of the daughter products relative to PCE and TCE is even greater than in our laboratory studies.

Comparison of the product distributions observed in this study in batch systems with column, field, and batch results of other investigators (O'Hannesin and Gillham, 1998; Orth and Gillham, 1996; Campbell *et al.*, 1997; Liang *et al.*, 1997) reveals that even though the reactors, iron types, reaction rates, and solution conditions vary widely, the product distributions change relatively little. Other researchers (Johnson *et al.*, 1996; Scherer *et al.*, 1998) have noted a up to a 3 order of magnitude difference in reported rate constants for a given organohalide, even after corrections are made for differences in metal loading. Nevertheless, even though the absolute *rate* of reaction may be highly dependent upon the iron type and solution conditions, branching ratios appear to be largely independent of these factors.

Devlin *et al.* (1998) also observed that the relative reactivity of nitrobenzenes with Master Builder iron remained constant with time, even though there was an overall loss of reactivity as the iron aged. If confirmed by more detailed measurements, such an invariance of relative reactivity with solution composition or iron type could have practical ramifications. By measuring the rate of reaction for a few compounds with the type of iron to be employed along with the

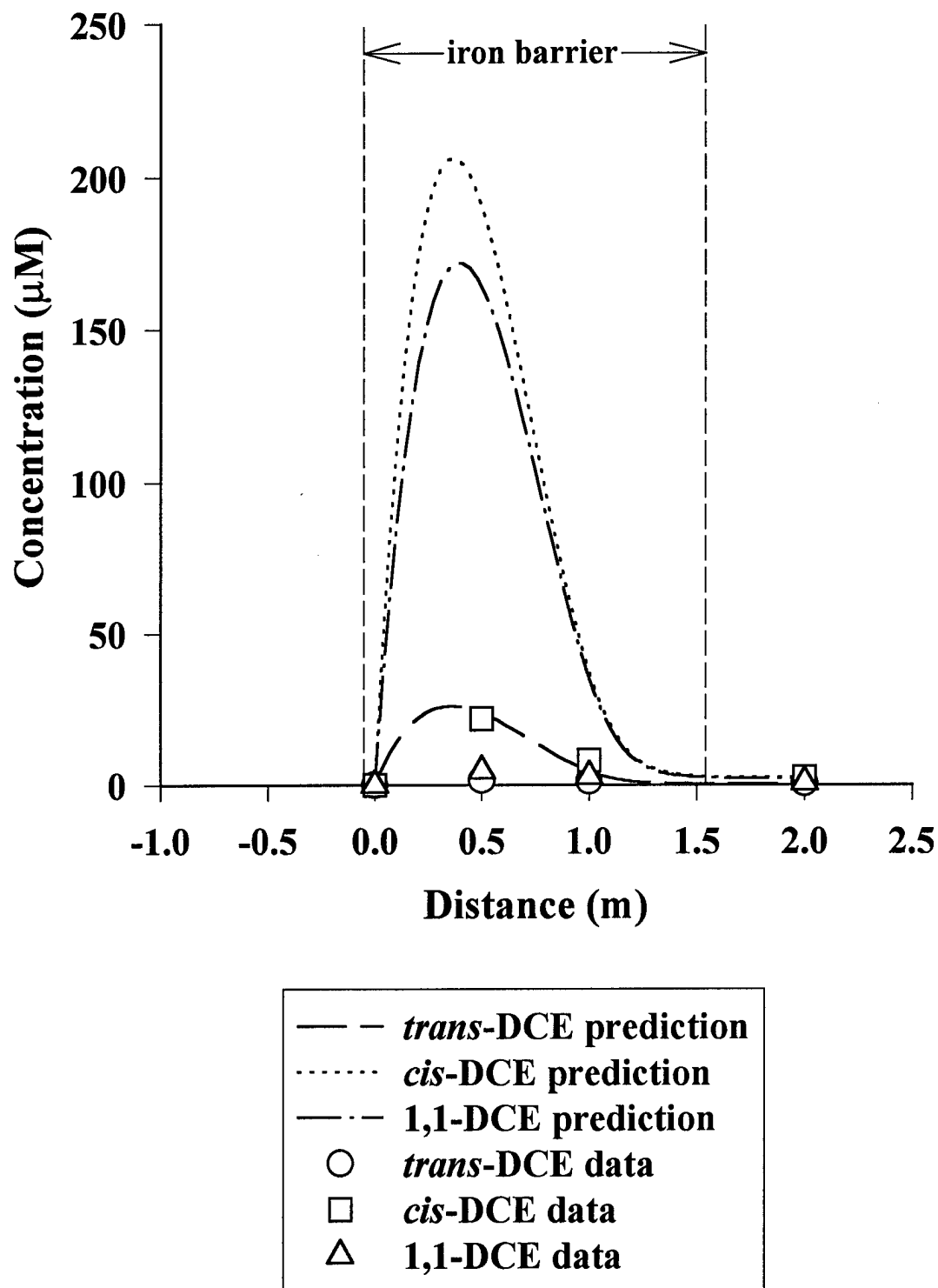


**Figure 80.** Simulation (lines) of intermediates generated in the permeable iron barrier at the Borden test site assuming that reaction only occurs via hydrogenolysis. Symbols represent the maximum observed concentration of a given species at that sampling point. Influent consists of PCE (350  $\mu\text{M}$ ) and TCE (2040  $\mu\text{M}$ ).

groundwater from the contaminated site, reaction rates for other compounds could readily be extrapolated to the system in question, greatly facilitating the design of a permeable barrier.

#### 4. Quantitative Structure-Activity Relationships

In order to develop quantitative structure-activity relationships through which reactivity could be predicted, plots of  $\log(k'S_i)$  (at constant metal loading and therefore  $S_i$ ) were generated for the polychlorinated ethylenes as a function of one- and two-electron reduction potentials. As vinyl chloride displays adsorption-limited kinetics, its kinetic parameter has different units ( $\text{h}^{-1}$  versus  $\mu\text{M/h}$  for reaction-limited species), and is therefore not included in the plots. The data point for 1,1-DCE is also excluded from the correlations with  $E_2$ , for its reduction to ethylene represents a four-electron and not a two-electron reaction.

Correlation with  $E_1$  may represent one approach for predicting overall reactivity of the chlorinated ethylenes, as shown in Figure 81. The regression line [ $\log(k'S_i) = -3.91 (\pm 2.07) \times E_2 - 2.81 (\pm 1.51)$ ;  $R^2(\text{adj.}) = 0.898$ ;  $\text{SE} = 0.293$ ] captures the data for the DCEs, PCE and the dominant TCE pathway (reactions 4+6, which assumes that chloroacetylene is derived from the same radical that forms *cis*-DCE). The uncertainties represent 95% confidence intervals. The minor reactions of TCE to 1,1-DCE and *trans*-DCE (solid points) were excluded from the regression.

As with our prior studies of chlorinated ethylene reduction by zinc (Section V), it would be desirable if QSARs could be developed through which predictions could be made not only of reaction rate, but also of product distributions. Correlation of rate constants for the reductive elimination component of reaction against  $E_2$  (Figure 82a) was reasonable [ $\log(k'S_i) = -30.68 (\pm 29.38) \times E_2 + 17.95 (\pm 17.48)$ ;  $R^2(\text{adj.}) = 0.865$ ;  $\text{SE} = 0.370$ ] despite the small number of data points. A plot of  $\log(k'S_i)$  versus  $E_2$  for the hydrogenolysis reactions is given in Figure 82b. If the point for the reduction of TCE to *trans*-DCE is excluded (solid symbol), the regression equation is  $\log(k'S_i) = -15.05 (\pm 14.62) \times E_2 + 6.04 (\pm 7.67)$ ;  $R^2(\text{adj.}) = 0.709$ ;  $\text{SE} = 0.388$ . Again, uncertainties presented represent 95% confidence limits. Even though correlations with  $E_2$  are not as strong as those obtained earlier with zinc, the relationships presented here for iron are still statistically significant. The hydrogenolysis regression suffers from its dependence on rate constants for reactions which reflect minor pathways; some of these rate constants, therefore, display relatively large uncertainties. For all regressions, the confidence intervals are quite large,



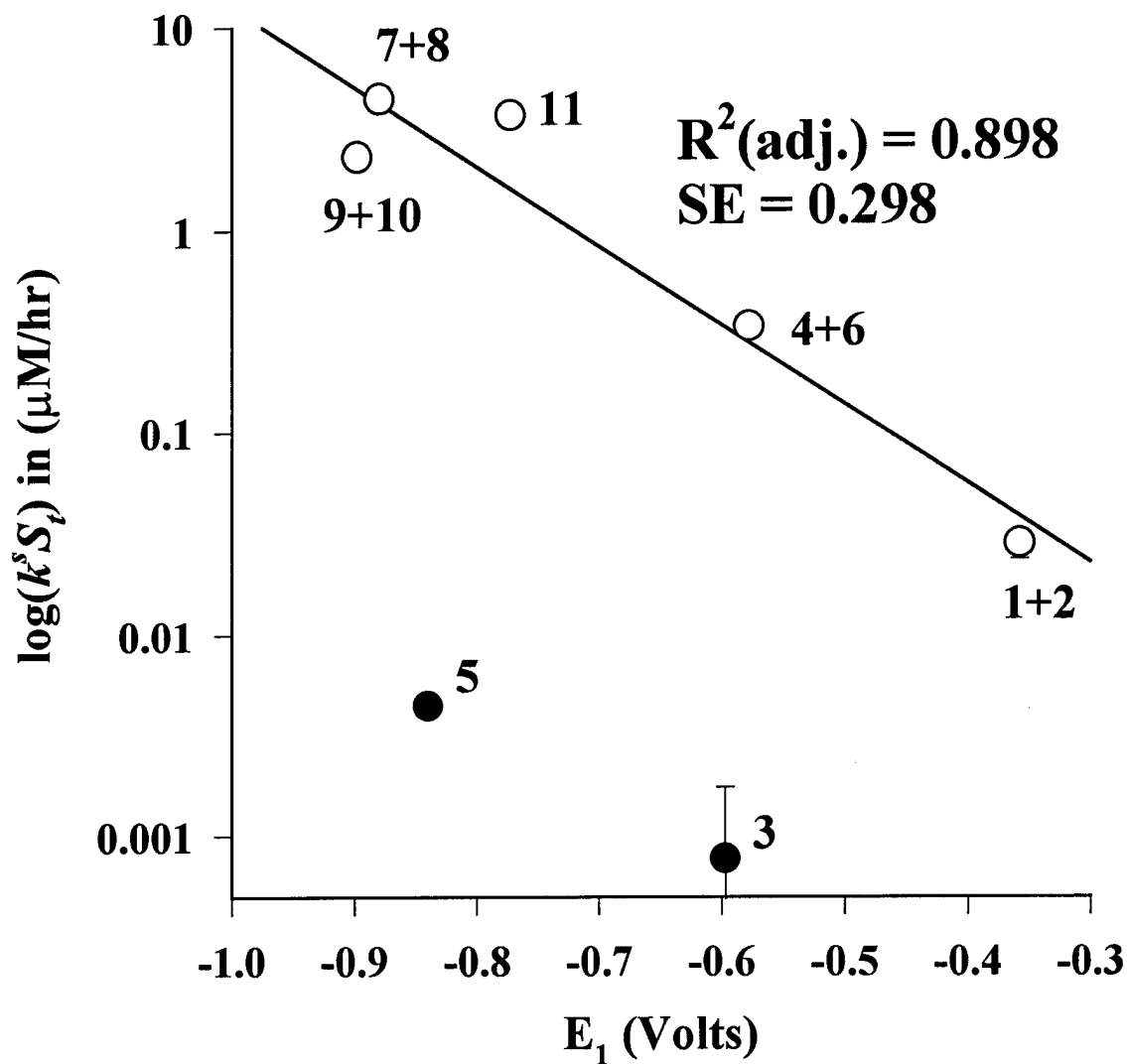


**Figure 81.** Correlation of the kinetic parameter for chlorinated ethylene reduction with one-electron reduction potential ( $E_1$ ). Numbering corresponds to the reactions in Table 10. If no error bar is shown, it is smaller than the symbol. The data points pertaining to reaction of TCE to 1,1-DCE and *trans*-DCE (solid symbols) are excluded from the regression.

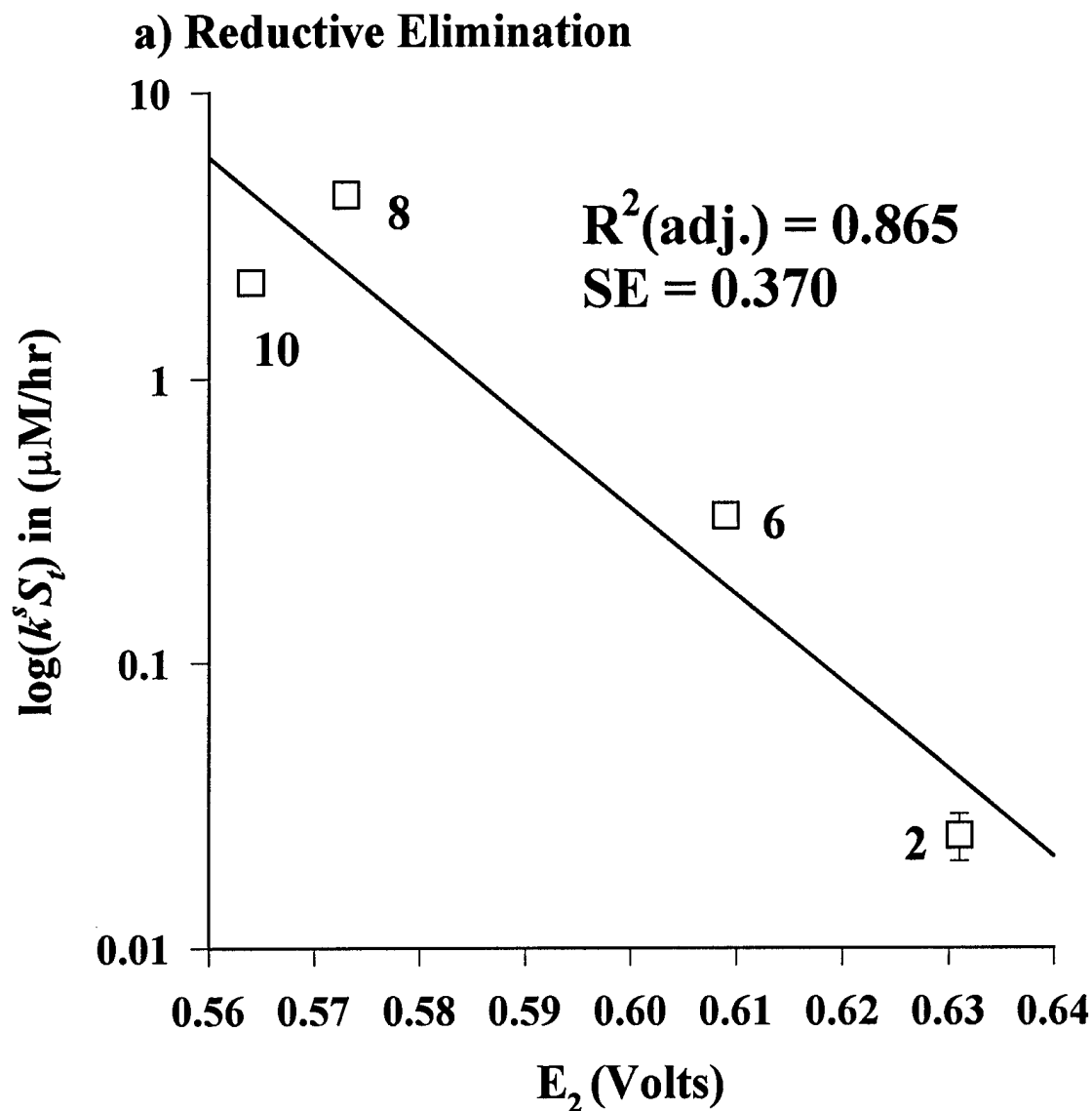


**Figure 82.** Correlation of the kinetic parameter for chlorinated ethylene reduction with two-electron reduction potential for a) reductive elimination and b) hydrogenolysis. Numbering corresponds to the reactions in Table 10. If no error bar (95% confidence limit) is shown, it is smaller than the symbol. The minor reaction of TCE to *trans*-DCE (solid symbol) is excluded from the hydrogenolysis regression.

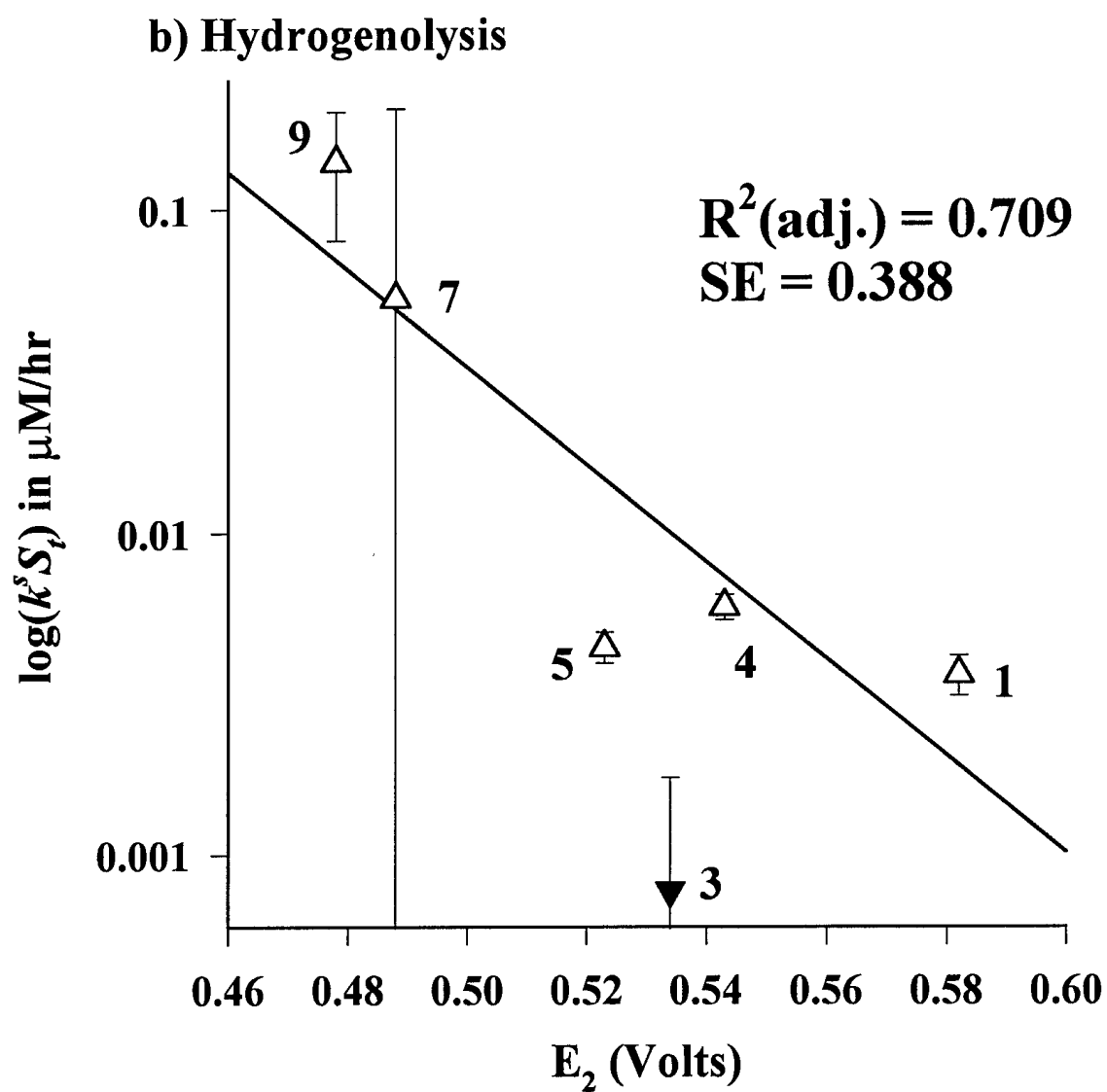


Figure 82 continued.

even though the  $R^2(\text{adj.})$  values are reasonably close to 1. This results from conducting regressions on relatively few, mildly scattered, data points.

Although the correlations found herein are statistically significant, we do not recommend their use for predicting reactivity of untested compounds because the mechanistic significance of the negative slopes is somewhat unclear. The negative slopes mean that as reactions become thermodynamically more favorable, they proceed more slowly. Further experimental investigations will be necessary to more definitively determine the reason for this behavior. One possibility is that unlike zinc, iron will form a passive oxide layer as the applied potential increases (Jones, 1992). Formation of this passive oxide layer decreases the current density on an iron surface by orders of magnitude. The potential at which reaction occurs is a combination of the potentials for iron oxidation, proton reduction, and chlorinated ethylene reduction. The more highly oxidized chlorinated ethylenes (*e.g.*, TCE and PCE) may shift the potential to a region where iron passivates strongly. One factor arguing against this explanation is that the very highly halogenated alkanes appear to react more rapidly with Fe(0) (Johnson *et al.*, 1996; Scherer *et al.*, 1998) than the chlorinated ethylenes, even though their substantially higher reduction potentials might favor greater passivation of the iron. For example, the reactivity of the chlorinated methanes follows the trend  $\text{CCl}_4 > \text{CHCl}_3 \gg \text{CH}_2\text{Cl}_2$  (Matheson and Tratnyek, 1994); the corresponding one-electron reduction potentials are 0.09 and -0.198 volts (substantially more positive than the one-electron reduction potential for PCE). If passivation of the iron were to explain the observed reactivity trend for the chlorinated ethylenes, we would expect a similar trend for the chlorinated methanes, which is not the case.

The negative slopes for the attempted QSARs with iron in this work are contrary to the results presented by Scherer *et al.* (1998) obtained by compiling data from the literature and normalizing rate constants by iron surface area/solution volume. Although it is again difficult to provide a definitive explanation as to why the correlations presented here differ so dramatically from those of Scherer *et al.* (1998), one possibility is that the correlation found in Scherer's work may be biased by normalizing rate constants simply based on iron surface area, when several other factors, including iron type and solution conditions/composition, may also be affecting reaction rate.

There are several other possible sources of bias in the results of Scherer *et al.* (1998).

These include:

- lumping data for both alkyl and vinyl halides in a single correlation. The substantial differences in the electronic environment in the region of the  $sp^3$  hybridized C-Cl bond and the  $sp^2$  hybridized system may render such a treatment inappropriate.
- failure to discriminate between reaction and sorption to nonreactive carbon phases in experimentally-determined disappearance rate constants in batch systems.
- inclusion of rate constants from experiments containing multiple substrates in which competitive effects might have been occurring.
- inclusion of rate constants for intermediates (*e.g.*, DCEs) calculated from their disappearance in the presence of their parent compound (*e.g.*, TCE), biases the rate constant for the intermediate because it is still being produced by the parent.
- The much lower detection limits for highly halogenated compounds afforded by GC with electron capture detection (ECD) could have resulted in experiments for PCE and TCE being conducted at much lower aqueous concentrations than possible for the lesser-chlorinated ethylenes. This complicates a direct comparison of rate constants because intraspecies competitive effects could have been present.

## 5. Model Simulations

As in our previous studies with zinc (Section V), we can demonstrate the difference between the model developed herein (containing both hydrogenolysis and reductive elimination reactions) and a hypothetical model in which reaction proceeds at the same rate but is only allowed to occur via hydrogenolysis. In other words, PCE is assumed to react solely to TCE via a rate constant obtained by summing reactions 1 and 2, TCE is assumed to react solely to a mixture of the three DCE isomers, with an overall rate constant equal to the sum of reactions 3 through 6, and *cis*- and *trans*-DCE react only to vinyl chloride, via a sum of the rate constants for reactions 9 plus 10 or 7 plus 8, respectively.

For PCE or TCE solution in which zinc was the reductant, the production and subsequent decay of *cis*-DCE (the least reactive vinyl chloride progenitor in the system) represented a bottleneck to reaching the drinking water limit for vinyl chloride. With iron metal, however, PCE and TCE are the species which react most slowly. Thus, attaining the drinking water limit for PCE

would be expected to dictate barrier design in the case of a PCE-saturated solution. Required residence times are therefore not greatly influenced by the branching ratios since the daughter species are more reactive than the parent compounds. For a saturated solution of PCE, the model containing only hydrogenolysis reactions requires 8% longer to reach the PCE drinking water limit than the model containing reductive elimination reactions. The model containing only hydrogenolysis reactions takes 10% longer than the model in which reductive elimination is included to reach the TCE limit from a TCE-saturated solution. The increases can be attributed to the larger predicted concentrations of the DCE intermediates, which inhibit the reaction of the PCE and/or TCE.

The major differences between the models lie in the predicted concentrations of intermediates. As previously demonstrated by Figures 79 and 80, even though the products react more quickly than the parent compounds, the peak concentrations of partially dechlorinated intermediates (DCEs, VC) are much higher when all reaction is routed through a hydrogenolysis pathway. Even though the drinking water limits for these species are attained before those for PCE or TCE, the time to reach these limits within the barrier increases 1.1-3 times in the model containing only hydrogenolysis reactions (for PCE or TCE-saturated solutions).

The LHHW kinetic model also has an impact on barrier design, as organohalide concentration and competitive effects will influence reaction rates. For a saturated solution of TCE (8,370  $\mu\text{M}$ ), three different model simulations are given in Figure 83. For all simulations, parameters employed were the same as those used to generate Figures 79 and 80. In the first simulation, a pseudo-first order model was employed, using the adjusted LHHW parameters and an initial TCE concentration of 8,370  $\mu\text{M}$  to calculate a pseudo-first order rate constant (see eqn. 21). This model would give a straight line on a log-linear plot if the initial  $k_{\text{obs}}$  were held constant, but since both axes in Figure 83 are logarithmic, a curve results. In the second simulation, the rate "constant" was allowed to vary according to the LHHW model, including the inhibition of TCE reaction by its daughter products. As can be seen, TCE degradation is substantially more rapid than with the pseudo-first order model, resulting in an order-of-magnitude decrease in the required residence time. In the final simulation, both PCE and TCE are initially present at their aqueous solubility limits. A substantial decrease in the rate of TCE disappearance (relative to the LHHW simulation in which only TCE is present) is seen from the inhibition of the reaction by

PCE, and the residence time needed to reach the drinking water limit for TCE is approximately three times larger than in the absence of PCE.

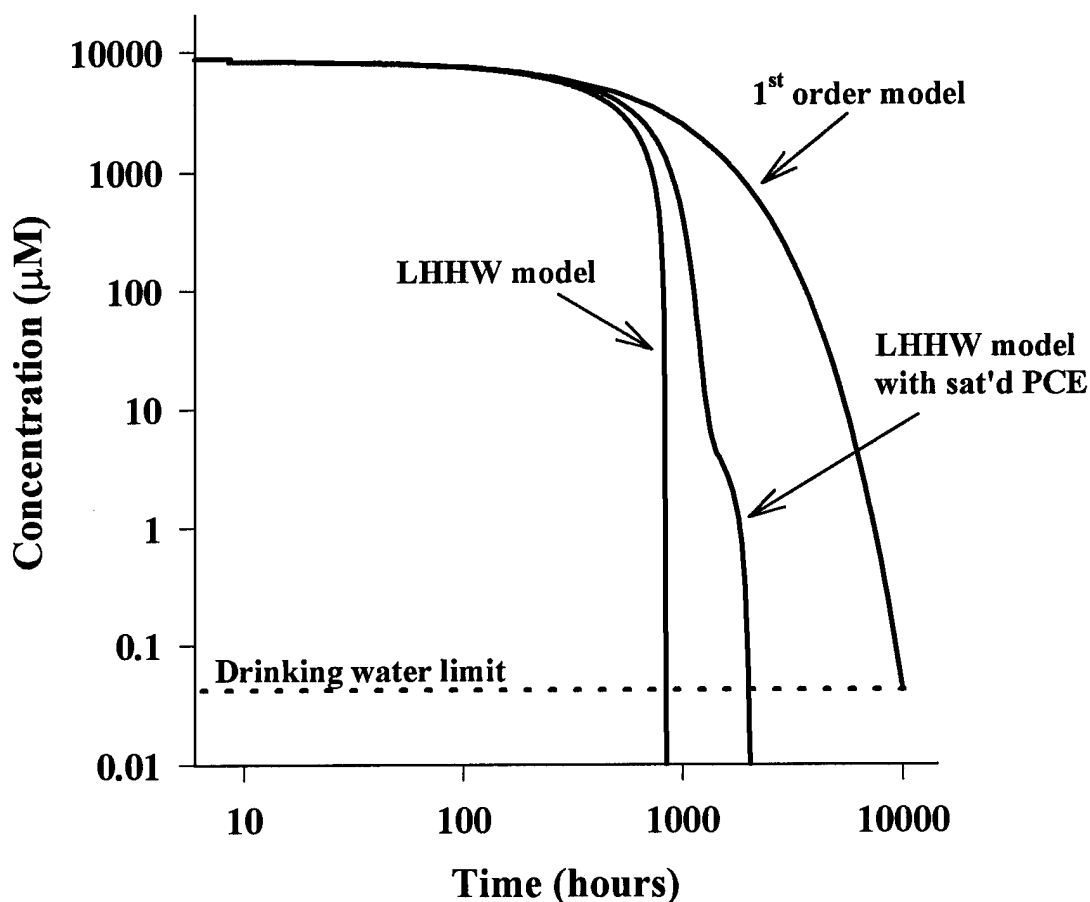


**Figure 83.** Model simulation of TCE degradation starting at saturation using pseudo-first order conditions, the LHHW model, and the LHHW model with PCE also beginning at saturation. The dashed line is the drinking water limit for TCE.

## 6. Mechanistic Insight

The kinetic data reported herein, together with information available in the literature, may shed insight into the mechanism through which chlorinated ethylenes undergo reduction by iron. Any proposed mechanism must accord with our observations that (a) the substantial intra- and interspecies competition for most species indicates that reaction at the surface, rather than adsorption or desorption to/from reactive sites, represents the rate-limiting step; (b) adsorption

constants follow the approximate trend alkynes > PCE, TCE > DCEs >> vinyl chloride, ethylene; (c) the decreasing reactivity for the chlorinated ethylenes with increasing halogenation is opposite to the trend that might be anticipated if electron transfer to a  $\pi^*$  lowest unoccupied molecular orbital (LUMO), accompanied by carbon-halogen bond cleavage, were to limit reaction rates. A proposed mechanism must also be consistent with the observation that even though the *alkyl* halide 1,2-dichloroethane (1,2-DCA) has higher  $E_1$  and  $E_2$  values than *cis*-DCE (Totten, 1999), it is so unreactive with Fe(0) that such treatment is held to be impractical (US EPA, 1998). This inertness contrasts sharply with the high reactivity of the vinyl halide *cis*-1,2-DCE; at many existing installations of Fe(0) barriers, *cis*-DCE actually represents the principal contaminant being treated (RTDF, 1999).

One possible mechanism which appears to be consistent with these observations is provided in Figure 84. In step 1, a  $\pi$ -bonded surface species is formed. The higher adsorption constants for the acetylenes (relative to the ethylenes) is certainly consistent with such a mechanism. In this adsorption step, the alkynes and alkenes are hypothesized to serve as Lewis bases. Although we have no experimental data pertinent to the state of the iron surface in our system (*e.g.*, presence/thickness/uniformity or oxidation state of an iron (hydr)oxide coating), we note that partially or fully oxidized metal ions would represent better Lewis acids.

At first, the increase in  $K$  values with increasing halogenation for the chlorinated ethylenes would seem to counter trends anticipated for  $\pi$ -bonding, assuming that chlorine atoms should withdraw electron density away from the  $\pi$ -system. This trend in adsorption constants is nonetheless consistent with the observed decrease in ionization potentials (inversely related to Lewis basicity; Stair, 1982) for the chlorinated ethylenes with increasing halogenation (Lake and Thompson, 1970) as shown in the correlation between  $\log K$  values and ionization potentials (from Lake and Thompson, 1970) in Figure 85. Although one might assume that PCE should have the highest (rather than the lowest) ionization potential due to the electron-withdrawing effect of the electronegative chlorines, the inductive effects are outweighed by mesomeric (electron-donating) effects of chlorine substituents (Lake and Thompson, 1970). The trend toward increasing adsorption with increasing halogenation for the chlorinated ethylenes is thus entirely consistent with what would be anticipated for  $\pi$ -bonding. We note that the trend towards increasing  $K$  with increasing halogenation could also be explained by nonspecific



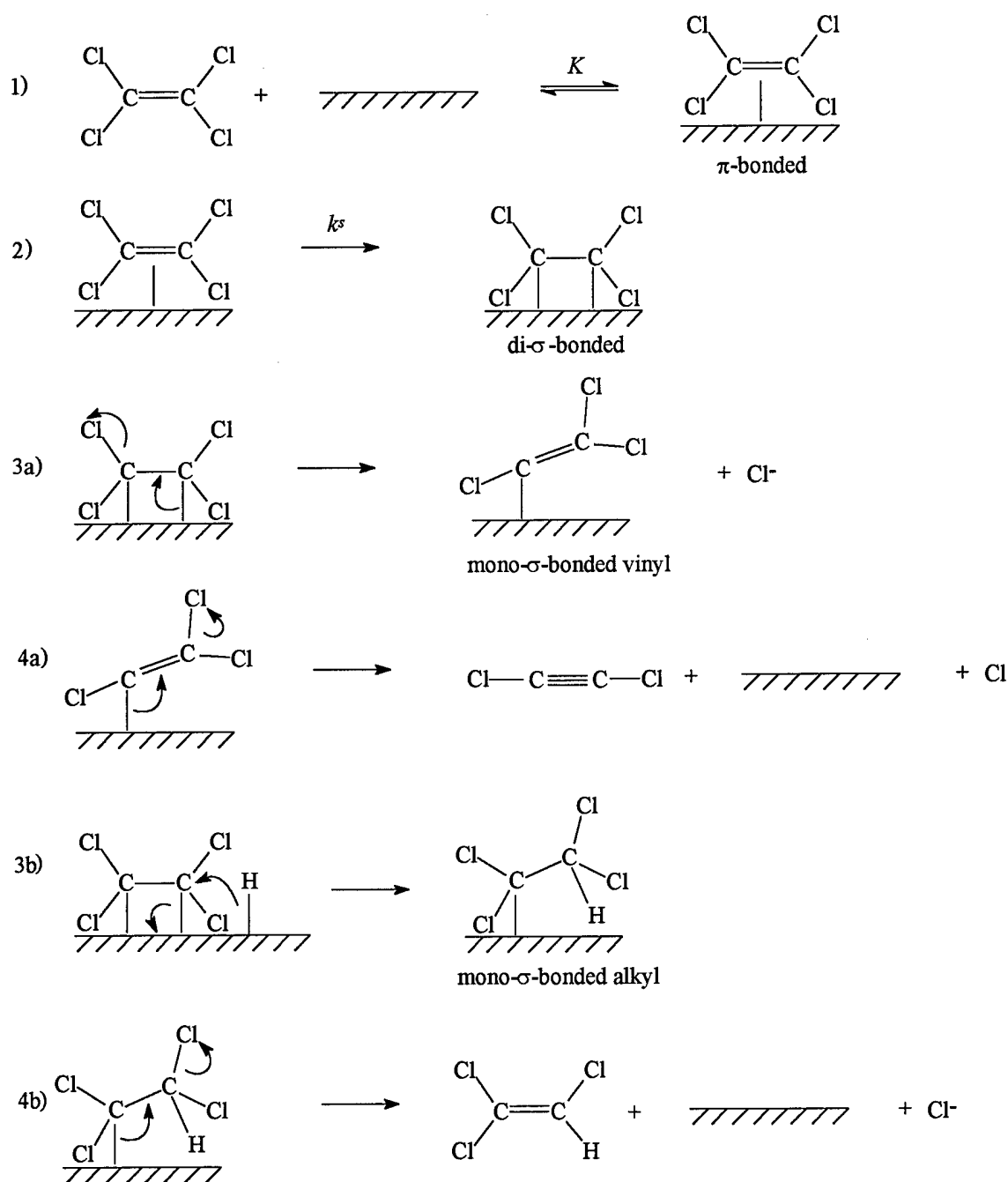


**Figure 84:** Hypothesized mechanism for reaction of PCE with Fe(0). After formation of a di- $\sigma$ -bonded intermediate, reaction may proceed via steps 3a and 4a to give the reductive  $\beta$ -elimination product dichloroacetylene, or via steps 3b and 4b to give the hydrogenolysis product TCE. Although step 3b is depicted as proceeding via hydride transfer, it could also involve hydrogen atom abstraction.

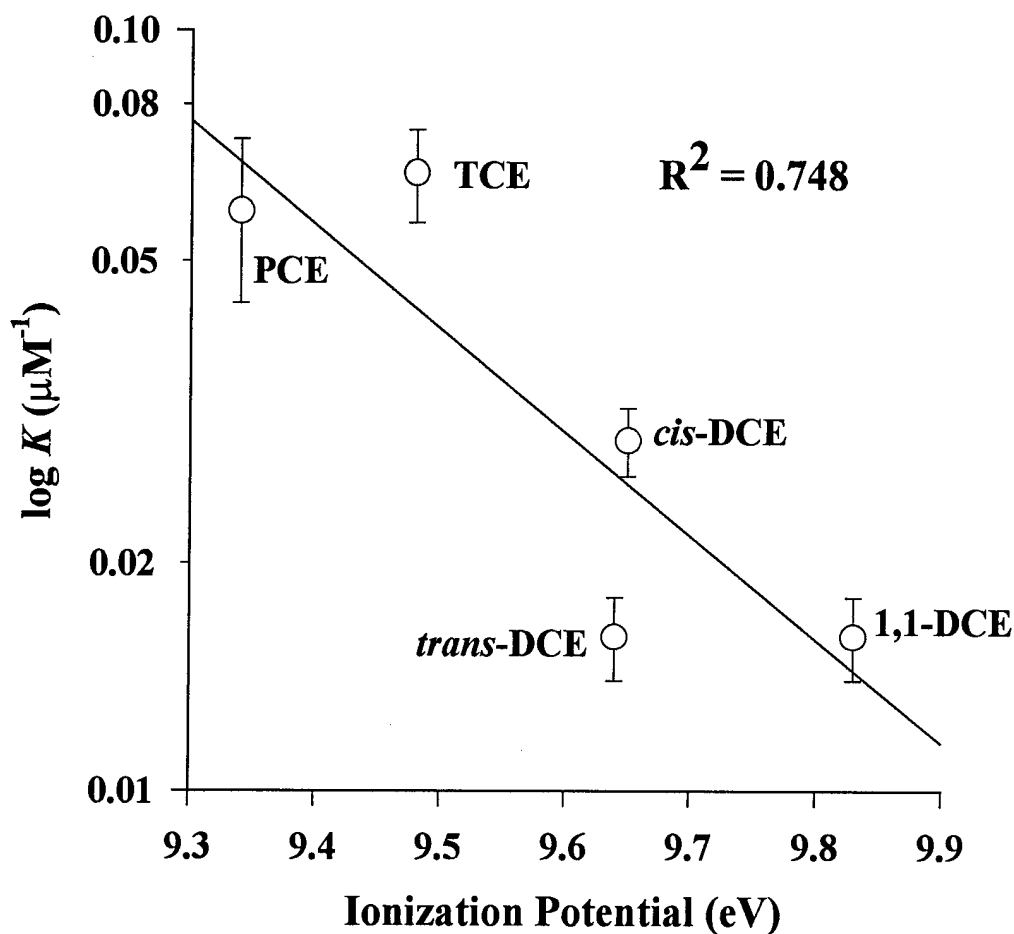


**Figure 85:** Plot of  $\log K$  values versus ionization potential for the chlorinated ethylenes.

(*e.g.*, hydrophobic) interactions; in fact, such nonspecific interactions must be responsible for the adsorption of carbon tetrachloride to reactive sites (Scherer and Tratnyek, 1995; Johnson *et al.*, 1996; Johnson *et al.*, 1998), and may well be at least partially responsible for vinyl halide adsorption. Further studies will be required to evaluate the relative importance of  $\pi$ -bonding and nonspecific interactions in the adsorption of vinyl halides to iron particle surfaces.

In the second step, the  $\pi$ -bonded intermediate forms a di- $\sigma$ -bonded surface-adsorbed species. The di- $\sigma$ -bonded species may undergo two successive fast halide ion elimination steps to form first a mono- $\sigma$ -bonded vinyl surface-adsorbed species and then an acetylene (steps 3a and 4a). Alternatively, rapid reaction with adsorbed hydrogen (involving hydride and/or hydrogen atom transfer) followed by rapid halide ion elimination would give rise to the hydrogenolysis product.

Indirect evidence for formation of the di- $\sigma$ -bonded intermediate (step 2) comes from comparison of the kinetics of chlorinated ethylene reaction with Fe(0) and with ozone ( $O_3$ ). Step 2 in Figure 86 involves conversion of the  $\pi$  system in the ethylenes to a  $\sigma$  bond. Reaction of olefins with ozone also involves destruction of the  $\pi$  system through formation of a primary ozonide via a 1,3-dipolar cycloaddition mechanism. In both the proposed surface reaction and the reaction with ozone, the vinyl halide acts as both electron donor and acceptor. Second-order rate constants for reaction of aqueous ozone (Hoigné and Bader, 1983; Dowideit and von Sonntag, 1998) with chlorinated ethylenes correlate strongly with ( $k'S_r$ ) values obtained in this study, as shown in Figure 86. In both systems, the reactivity trend follows the pattern DCEs>TCE>PCE. For reaction with ozone, this trend has been attributed to the electrophilic character of the reaction. The lesser sensitivity of our kinetic constants to increasing chlorination may have implications for the relative degree of advancement of C=C double bond destruction vs. C-Fe bond formation steps.

Further indirect support for formation of the di- $\sigma$ -bonded intermediate during the rate determining step is provided by kinetic isotope effects on carbon. Recent work by Slater *et al.* (1998) has demonstrated that reaction of TCE with Fe(0) is a strongly fractionating process, with the unreacted TCE (labeled at natural abundance) becoming enriched in  $^{13}C$  as the reaction proceeds. These experiments were conducted by monitoring the reaction of TCE in batch reactors via GC coupled to a combustion-isotope ratio mass spectrometer. Analysis of the data from Slater *et al.* (1998) suggests a composite  $^{13}C$  kinetic isotope effect ( $k_{12C}/k_{13C}$ ) for the two non-identical carbons of 1.015-1.02. This kinetic isotope effect is very similar to that observed (1.017-1.022) in the Diels-Alder reaction of isoprene with maleic anhydride (Singleton and Thomas, 1995), a reaction which also involves conversion of a  $\pi$ -bond to a  $\sigma$ -bond. The maximum primary kinetic

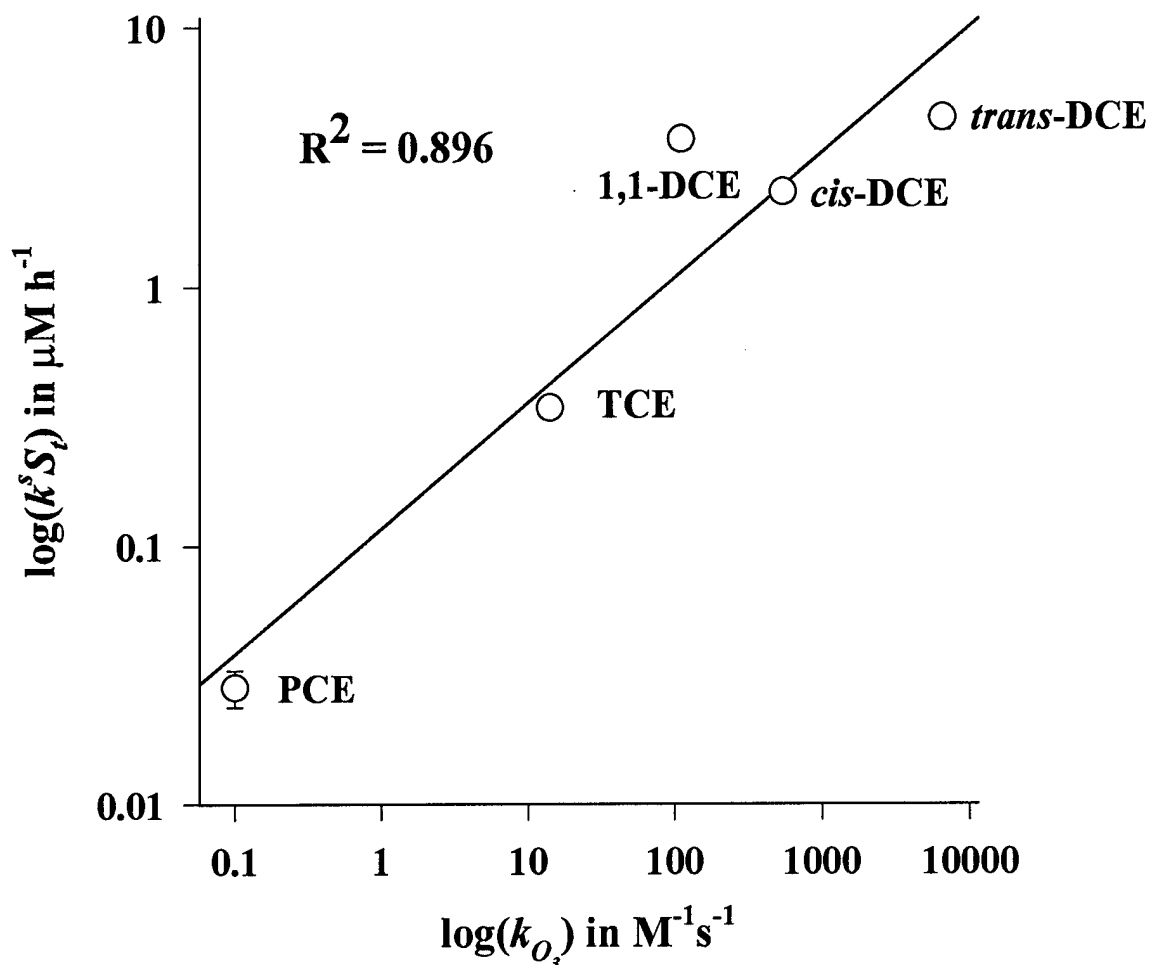


**Figure 86:** Correlation of  $(k^s S_i)$  values for the chlorinated ethylenes (from Table 10) with second order rate constants for reactions with aqueous ozone (Dowideit and von Sonntag, 1998). The rate constant for the reaction of aqueous ozone with PCE is an upper bound.

isotope effect on carbon  $k_{^{12}C}/k_{^{13}C}$  is only 1.04 (Isaacs, 1987), indicating that the observed effect is large enough to reflect a primary, rather than a secondary, kinetic isotope effect. The rate limiting step must therefore involve a change in bonding to carbon.

If the rate limiting step were to involve electron transfer to a  $\pi^*$  LUMO, accompanied by carbon-halogen bond cleavage, we might expect a good inverse correlation between  $(k^s S_i)$  values and bond dissociation energy (BDE). If anything, a weak direct correlation exists between  $\log(k^s S_i)$  and BDE values (calculated from Totten, 1999). Correlation with LUMO values

(Scherer *et al.*, 1998) results in a trend opposite to that anticipated if the rate limiting step were to involve single electron transfer to a  $\pi^*$  LUMO. The kinetic isotope effect and reactivity trends together suggest that the rate limiting step involves formation of the di- $\sigma$ -bonded intermediate (step 2 in Figure 84), as other plausible surface-reaction steps involve cleavage of a C-Cl bond, which should be reflected by increasing reactivity with increasing chlorination.

Although we lack direct evidence for the postulated di- $\sigma$ -bonded intermediate, evidence suggests that olefins will form such species on iron crystal surfaces in the gas phase. The adsorption and reaction of ethylene and acetylene under ultra-high vacuum conditions (UHV) have been studied using Auger electron spectroscopy (AES), thermal desorption spectroscopy (TDS), temperature-programmed reaction spectroscopy (TPRS), low energy electron diffraction (LEED), and high resolution low energy electron loss spectroscopy (HREELS) (Benziger and Madix, 1980; Erley *et al.*, 1982; Seip *et al.*, 1984; Hung and Bernasek, 1995). The results suggest that at temperatures up to  $\sim 240$  K, ethylene adsorbs in a di- $\sigma$ -bonded configuration. Acetylene also displays  $sp^3$  hybridization when adsorbed, indicating substantial bonding to the surfaces. Similar studies also suggest that the chlorinated ethylenes adsorb strongly to iron surfaces. UHV studies by Mason and Textor (1977) and Smentkowski *et al.* (1989) have found results using AES, temperature programmed desorption (TPD), and photoelectron spectroscopy consistent with disassociative adsorption of the chlorinated ethylenes to carbon adatoms and chloride at 300-325 K. Although these results from experiments on iron crystal faces under UHV conditions are not directly comparable to our studies in aqueous solution with iron particles (which may be partially coated by (hydr)oxides), they do suggest chlorinated ethylenes are capable of forming surface-bonded intermediates with at least some iron surfaces.

Experiments were conducted in deuterated water in an attempt to obtain further evidence of a di- $\sigma$ -bonded intermediate. Metals are known to catalyze H/D exchange of ethylene in the gas phase (Ponec and Bond, 1995). The exchange is thought to occur via the interaction of an adsorbed ethylene molecule (probably a di- $\sigma$ -bonded species, although the form of the reactive ethylene is still being debated; Ponec and Bond, 1995) and an adsorbed deuterium atom. The ethylene then desorbs without undergoing reduction to ethane. Similar exchange in the vinyl halides (either parent species or daughter products) would support the existence of the proposed di- $\sigma$ -bonded species.

Fe(0) was observed to catalyze H/D exchange in ethylene; after 48 hours, ethylene- $d_0$  added to D<sub>2</sub>O in the presence of Fe(0) consisted of 24% ethylene- $d_0$ , 46% ethylene- $d_1$ , 22% ethylene- $d_2$ , 7% ethylene- $d_3$ , and <2% ethylene- $d_4$ . No H/D exchange occurred in the absence of iron. If such iron-catalyzed exchange occurs in vinyl halides, it takes place much more slowly: no H/D exchange was observed over a comparable period of time for *cis*-DCE or vinyl chloride, and vinyl chloride formed from *cis*-DCE reduction consisted only of the expected monodeuterated isotopomer. These results therefore neither support nor refute the existence of a di- $\sigma$ -bonded chlorinated intermediate. Note that H/D exchange in acetylene occurs over the course of hours even in the absence of iron.

## **7. Advantages of Fe(0) in Permeable Barriers**

The results presented in this work lend insight into previously unrecognized factors that explain why iron is particularly useful as a reductant for destroying chlorinated ethylenes. Reductive  $\alpha$ - or  $\beta$ -elimination appears to dominate the reactions of polychlorinated ethylenes. In the case of 1,1-DCE, this results in conversion to ethylene as the first closed-shell product. The highly reactive chlorinated acetylene intermediates produced via reductive  $\beta$ -elimination of PCE and TCE undergo hydrogenation to generate chlorinated ethylenes in very limited proportion relative to hydrogenolysis. Branching ratios for reactions with Fe(0) are therefore such that production of lesser chlorinated ethylenes, especially vinyl chloride, is largely circumvented. Finally, the partially dechlorinated daughter products are more reactive than the more highly chlorinated ethylene parent compounds. These factors operate in concert with the result that partially dechlorinated intermediates do not accumulate to high concentrations.

## F. LITERATURE CITED

- Allen-King, R.; Halket, R.M.; Burris, D.R. Reductive transformation and sorption of *cis*- and *trans*-1,2-dichloroethylene in a metallic iron-water system. *Environ. Toxicol. Chem.* **1997**, *16*, 424-429.
- Arnold, W.A.; Ball, W.P.; Roberts, A.L. Polychlorinated ethane reaction with zero-valent zinc: pathways and rate control. *J. Contam. Hydrol.* **1999**, *40*(2), 183-200.
- Benziger, J.B.; Madix, R.J. Reactions and reaction intermediates on iron surfaces. *J. Catal.* **1980**, *65*, 49-58.
- Burris, D.R.; Campbell, T.J.; Manoranjan, V.S. Sorption of trichloroethylene and tetrachloroethylene in a batch reactive zero-valent iron system. *Environ. Sci. Technol.* **1995**, *29*, 2850-2855.
- Burris, D. R.; Delcomyn, C. A.; Smith, M. H.; Roberts, A. L. Reductive dechlorination of tetrachloroethylene and trichloroethylene catalyzed by vitamin B<sub>12</sub> in homogeneous and heterogeneous systems. *Environ. Sci. Technol.* **1996**, *30*, 3047-3052.
- Butler, E. C.; Hayes, K. F. Kinetics of the transformation of trichloroethylene and tetrachloroethylene by iron sulfide. *Environ. Sci. Technol.* **1999**, *33*, 2021-2027.
- Campbell, T.J.; Burris, D.R.; Roberts, A.L.; Wells, J.R. Trichloroethylene and tetrachloroethylene reduction in a batch metallic iron/water/vapor system. *Environ. Toxicol. Chem.* **1997**, *16*, 625-630.
- Carberry, J.J., *Chemical and Catalytic Reactor Engineering*. McGraw-Hill: New York, 1976.
- Cipollone, M.G.; Wolfe, M.L.; Hassan, S.M. Kinetic studies on the use of metallic iron to reduce organic compounds in water under environmental conditions. *Natl. Meet.-Am. Chem. Soc., Div. Environ. Chem.* **1995**, *35*, 812-814 (Abstr.).
- Denis, J.N.; Moyano, A.; Greene, A.E. Practical synthesis of dichloroacetylene. *J. Org. Chem.* **1987**, *52*, 3461-3462.
- Devlin, J.F.; Klausen, J.; Schwarzenbach, R.P. Kinetics of nitroaromatic reduction on granular iron in recirculating batch experiments. *Environ. Sci. Technol.* **1998**, *32*, 1941-1947.

- Dowideit, P.; von Sonntag, C. Reaction of ozone with ethene and its methyl- and chlorine-substituted derivatives in aqueous solution. *Environ. Sci. Technol.* **1998**, *32*, 1112-1119.
- Ebersson, L. Electron transfer reactions in organic chemistry. II. An analysis of alkyl halide reduction by electron transfer reagents on the basis of Marcus theory. *Acta Chem. Scand. B* **1982**, *36*, 533-543.
- Erley, W.; Baro, A.M.; Ibach, H. Vibrational spectra of acetylene and ethylene adsorbed on Fe(100). *Surf. Sci.* **1982**, *120*, 273-290.
- Fennelly, J.P.; Roberts, A.L. Reaction of 1,1,1-trichloroethane with zero-valent metals and bimetallic reductants. *Environ. Sci. Technol.* **1998**, *32*, 1980-88.
- Fogler, S., *Elements of Chemical Reaction Engineering*. 2nd ed. Prentice Hall: Englewood Cliffs, NJ, 1992.
- Froment, G.F.; Bischoff, K.B., *Chemical Reactor Analysis and Design*. 2nd ed. John Wiley & Sons: New York, 1990.
- Gantzer, C. J.; Wackett, L. P. Reductive dechlorination catalyzed by bacterial transition metal coenzymes. *Environ. Sci. Technol.* **1991**, *25*, 715-722.
- Gillham, R.W.; O'Hannesin, S.F. Enhanced degradation of halogenated aliphatics by zero-valent iron. *Ground Water* **1994**, *32*, 958-967.
- Glod, G.; Angst, W.; Hollinger, C.; Schwarzenbach, R. P. Corrinoid-mediated reduction of tetrachloroethene, trichloroethene, and trichlorofluoroethene in homogeneous aqueous solution: reaction kinetics and reaction mechanisms. *Environ. Sci. Technol.* **1997a**, *31*, 253-260.
- Glod, G.; Brodmann, U.; Angst, W.; Hollinger, C.; Schwarzenbach, R.P. Cobalamin-mediated reduction of *cis*- and *trans*-dichloroethene, 1,1-dichloroethene, and vinyl chloride in homogeneous aqueous solution: reaction kinetics and mechanistic considerations. *Environ. Sci. Technol.* **1997b**, *31*, 3154-3160.
- Gotpagar, J.; Grulke, E.; Tsang, T.; Bhattacharyya, D. Reductive dehalogenation of trichloroethylene using zero-valent iron. *Environ. Progr.* **1997**, *16*, 137-143.



- Gotpagar, J.K.; Grulke, E.A.; Bhattacharyya, D. Reductive dehalogenation of trichloroethylene: kinetic models and experimental verification. *J. Haz. Mat.* **1998**, *62*, 243-264.
- Harriott, P. Mass transfer to particles suspended in agitated tanks. *AIChEJ* **1962**, *8*, 93-102.
- Hine, J.; Mookerjee, P.K. The intrinsic hydrophilic character of organic compounds. Correlations in terms of structural contributions. *J. Org. Chem.* **1975**, *40*, 292-297.
- Ho, W.; Yu, Q.; Bozzelli, J.W. Kinetic study on pyrolysis and oxidation of CH<sub>3</sub>Cl in Ar/H<sub>2</sub>/O<sub>2</sub> mixtures. *Combust. Sci. and Tech.* **1992**, *85*, 22-63.
- Hoigné, J.; Bader, H. Rate constants of reaction of ozone with organic and inorganic compounds in water - I. Non-dissociating organic compounds. *Water Res.* **1983**, *17*, 173-183.
- Hung, W.-H.; Bernasek, S.L. Adsorption and decomposition of ethylene and acetylene on Fe(100). *Surf. Sci.* **1995**, *339*, 272-292.
- Isaacs, N. S. *Physical Organic Chemistry*. 1987, New York: John Wiley & Sons, Inc.
- Johnson, T.L.; Scherer, M.M.; Tratnyek, P.G. Kinetics of halogenated organic compound degradation by iron metal. *Environ. Sci. Technol.* **1996**, *30*, 2634-3640.
- Johnson, T.L.; Fish, W.; Gorby, Y.A.; Tratnyek, P.G. Degradation of carbon tetrachloride by iron metal: complexation effects on the oxide surface. *J. Contam. Hydrol.* **1998**, *29*, 379-398.
- Jones, D., *Principles and Prevention of Corrosion*. Macmillan Publishing Company: New York, 1992.
- Kim, Y.H.; Carraway, E.R. Dechlorination of chlorinated ethenes and acetylenes by zero valent bimetals. *Natl. Meet.-Am. Chem. Soc., Div. Environ. Chem.* **1999**, *39*, 351-353.
- Klausen, J.; Trober, S.P.; Haderlein, S.B.; Schwarzenbach, R.P. Reduction of substituted nitrobenzenes by Fe(II) in aqueous mineral suspensions. *Environ. Sci. Technol.* **1995**, *29*, 2396-2404.
- Lake, R.F.; Thompson, H. Photoelectron spectra of halogenated ethylenes. *Proc. Roy. Soc. Lond. A.* **1970**, *315*, 323-338.
- Lesage, S.; Brown, S.; Millar, K. A different mechanism for the reductive dechlorination of chlorinated ethenes: kinetic and spectroscopic evidence. *Environ. Sci. Technol.* **1998**, *32*, 2264-2272.

- Liang, L.; Korte, N.; Goodlaxson, J.D.; Clausen, J.; Fernando, Q.; Muftikian, R. Byproduct formation during the reduction of TCE by zero-valence iron and palladized iron. *Ground Water Monit. Rem.* **1997**, 122-127.
- Lowry, G. V.; Reinhard, M. Hydrodehalogenation of 1- to 3-carbon halogenated organic compounds in water using a palladium catalyst and hydrogen gas. *Environ. Sci. Technol.* **1999**, 33, 1905-1910.
- Mackay, D.; Shiu, W.Y.; Ma, K.C., *Illustrated Handbook of Physical-Chemical Properties and Environmental Fate for Organic Chemicals*, Vol. 3. Lewis Publishers: Boca Raton, FL, 1993.
- Mackenzie, P.D.; Baghel, S.S.; Eykholt, G.R.; Horney, D.P.; Salvo, J.J.; Sivavec, T.M. Pilot-scale demonstration of reductive dechlorination of chlorinated ethenes by iron metal. *Natl. Mtg.-Am. Chem. Soc., Div. Environ. Chem.* **1995**, 35, 796-799 (Abstr.).
- Mason, R.; Textor, M. The chemisorption of simple- and halogeno-substituted unsaturated hydrocarbons on the  $\alpha$ -Fe(111) single crystal surface: photoelectron spectroscopic studies. *Proc. R. Soc. Lond. A.* **1977**, 356, 47-60.
- Matheson, L.J.; Tratnyek, P.G. Reductive dehalogenation of chlorinated methanes by iron metal. *Environ. Sci. Technol.* **1994**, 28, 2045-2053.
- O'Hannesin, S.F.; Gillham, R.W. Long-term performance of an in situ "iron wall" for remediation of VOCs. *Ground Water* **1998**, 36, 164-170.
- Orth, W.S.; Gillham, R.W. Dechlorination of trichloroethene in aqueous solution using  $\text{Fe}^0$ . *Environ. Sci. Technol.* **1996**, 30, 66-71.
- Piganiol, P., *Acetylene Homologs and Derivatives*. Mapleton House: New York, 1950.
- Ponec, V.; Bond, G.C., "Catalysis by Metals and Alloys," In *Studies in Surface Science and Catalysis*, Vol. 95. Eds. B. Dlemon and J.T. Yates. Elsevier: New York, 1995.
- Remediation Technologies Development Forum (RTDF), **1999**. Permeable reactive barrier installation profiles. [Online]. Available: <http://www.rtdf.org/public/permbarr/barrdocs.htm> [April 19, 1999].
- Roberts, A.L.; Totten, L.A.; Arnold, W.A.; Burris, D.R.; Campbell, T.J. Reductive elimination of chlorinated ethylenes by zero-valent metals. *Environ. Sci. Technol.* **1996**, 30, 2654-2659.

- Rutledge, T.F., *Acetylenic Compounds: Preparation and Substitution Reactions*. Reinhold: New York, 1968.
- Scherer, M.M.; Tratnyek, P.G. Dechlorination of carbon tetrachloride by iron metal: effect of reactant concentrations. *Natl. Meet.-Am. Chem. Soc., Div. Environ. Chem.* **1995**, *35*, 805-806(Abstr.).
- Scherer, M.M.; Balko, B.A.; Gallagher, D.A.; Tratnyek, P.G. Correlation analysis of rate constants for dechlorination by zero-valent iron. *Environ. Sci. Technol.* **1998**, *32*, 3026-3033.
- Scherer, M.M.; Balko, B.A.; Tratnyek, P.G., "The Role of Oxides in Reduction Reactions at the Metal-Water Interface", in *Kinetics and Mechanisms of Reactions at the Mineral/Water Interface*, D.L. Sparks and T. Grundl, Editors. 1999, ACS Symposium Series.
- Seip, U.; Tsai, M.-C.; Kuppers, J.; Ertl, G. Interaction of acetylene and ethylene with an Fe(111) surface. *Surf. Sci.* **1984**, *147*, 65-88.
- Semadeni, M.; Chiu, P.; Reinhard, M. Reductive transformation of trichloroethene by cobalamin: reactivities of the intermediates acetylene, chloroacetylene, and the DCE isomers. *Environ. Sci. Technol.* **1998**, *32*, 1207-1213.
- Senzaki, T.; Kumagai, Y. Removal of organochloro compounds in wastewater by reductive treatment: reductive degradation of 1,1,2,2-tetrachloroethane with iron powder. *Kogyo Yosui* **1988**, *357*, 2-7.
- Senzaki, T.; Kumagai, Y. Removal of organic chlorine compounds by use of some reduction processes: processing trichloroethylene with iron powder. *Kogyo Yosui* **1989**, *369*, 19-25.
- Singleton, D.A.; Thomas, A.A. High-precision simultaneous determination of multiple small kinetic isotope effects at natural abundance. *J. Am. Chem. Soc.* **1995**, *117*, 9357-9358.
- Slater, G.F.; Dempster, H.D.; Sherwood-Lollar, B.; Spivack, J.; Brennan, M.; Mackenzie, P. Isotopic tracers of degradation of dissolved chlorinated solvents. *Natural Attenuation: Chlorinated and Recalcitrant Compounds* **1998**, Columbus, OH, May 18-21, 1998, 133-138.
- Smentkowski, V.S.; Cheng, C.C.; Yates, J.T. The interaction of C<sub>2</sub>Cl<sub>4</sub> with Fe(110). *Surf. Sci.* **1989**, *220*, 307-321.

- Stair, P.C. The concept of Lewis acids and bases applied to surfaces. *J. Am. Chem. Soc.* **1982**, *104*, 4044-4052.
- Stang, P.J. Unsaturated carbenes. *Chem. Rev.* **1978**, *78*, 383-405.
- Su, C.; Puls, R.W. Kinetics of trichloroethene reduction by zero valent iron and tin: pretreatment effect, apparent activation energy and intermediate products. *Environ. Sci. Technol.* **1999**, *33*, 163-168.
- Taylor, P.H.; Dellinger, B.; Tirey, D.A. Oxidative pyrolysis of  $\text{CH}_2\text{Cl}_2$ ,  $\text{CHCl}_3$ , and  $\text{CCl}_4$  - I: incineration implications. *Int. J. Chem. Kinetics*, **1991**, *23*, 1051-1074.
- Totten, L.A., *The use of model and probe compounds to investigate the mechanisms of reductive dehalogenation reactions*, in *Department of Geography and Environmental Engineering*. 1999, The Johns Hopkins University: Baltimore.
- Tratnyek, P.G.; Johnson, T.L.; Scherer, M.M.; Eykholt, G.R. Remediating ground water with zero-valent metals: chemical considerations in barrier design. *Ground Water Monit. Rem.* **1997**, 108-114.
- U.S. EPA. *Permeable Reactive Barrier Technologies for Contaminant Remediation*. Office of Solid Waste and Emergency Response, **1998**, EPA/600/R-98/125.
- Vogan, J.L.; Gillham, R.W.; O'Hannesin, S.F.; Matulewicz, W.H.; Rhodes, J.E. Site specific degradation of VOCs in groundwater using zero valent iron. *Natl. Meet.-Am. Chem. Soc., Div. Environ. Chem.* **1995**, *35*, 800-804 (Abstr.).
- Wagman, D. D.; Evans, W. H.; Parker, V. B.; Schumm, R. H.; Halow, I.; Bailey, S. M.; Churney, K. L.; Nuttall, R. L. The NBS tables of chemical thermodynamic properties. Selected values for inorganic and  $\text{C}_1$  and  $\text{C}_2$  organic substances in SI units. *J. Phys. Chem. Ref. Data*, *II*, **1982**, 1-103.
- Wood, W.G., Ed. Surface cleaning, finishing and coating. In *Metals Handbook*; American Society for Metals: Metals Park, OH, 1982; Vol. 5.
- Yamane, C.L.; Warner, S.D.; Gallinatti, J.D.; Szerdy, F.S.; Delfino, T.A. Installation of a subsurface groundwater treatment wall composed of granular zero-valent iron. *Natl. Meet.-Am. Chem. Soc., Div. Environ. Chem.* **1995**, *35*, 792-795 (Abstr.).



## SECTION VII

### REACTION OF 1,1,1-TRICHLOROETHANE WITH ZERO-VALENT METALS AND BIMETALLIC REDUCTANTS

#### A. ABSTRACT

Information concerning the pathways and products of reaction of 1,1,1-trichloroethane (1,1,1-TCA) with zero-valent metals may be critical to the success of *in situ* treatment techniques. Many researchers assume that alkyl polyhalides undergo reduction via stepwise hydrogenolysis (replacement of halogen by hydrogen). Accordingly, 1,1,1-TCA should react to 1,1-dichloroethane (1,1-DCA), thence to chloroethane, and finally to ethane. Experiments conducted in laboratory-scale batch reactors indicate, however, that with zinc, iron and two bimetallic reductants (nickel-plated iron and copper-plated iron), this simplistic stepwise scheme cannot explain observed results. 1,1,1-TCA was found to react rapidly with zinc to form ethane and 1,1-DCA. Independent experiments confirmed that 1,1-DCA reacts too slowly to represent an intermediate in the formation of ethane. In reactions with iron, nickel/iron and copper/iron, *cis*-2-butene, ethylene and 2-butyne were also observed as minor products. Product ratios were dependent on the identity of the metal or bimetallic reductant, with zinc resulting in the lowest yield of chlorinated product. For reactions with iron and bimetallic reductants, a scheme involving successive one-electron reduction steps to form radicals and carbenoids can be invoked to explain the absence of observable intermediates, as well as the formation of products originating from radical or possibly from carbenoid coupling.

#### B. INTRODUCTION

Until its use in applications such as vapor degreasing, cold metal cleaning, printed circuit board manufacture, aerosols, and as a solvent for inks, coatings, and adhesives was curtailed under provisions of the Montreal Protocol (and subsequent amendments), 1,1,1-trichloroethane (1,1,1-TCA) was the single most extensively employed chlorinated solvent, with a U.S. demand in 1989 of 338,000 metric tons (Reed, 1993; Snedecor, 1993). In keeping with its widespread former use, this solvent has been detected at about 20% of the sites on the National Priorities (Superfund) List as identified by the U. S. EPA (1990).

Groundwater contaminated with 1,1,1-TCA (as with other dense chlorinated solvents) is difficult to remediate using conventional pump-and-treat methods, which are inefficient at

extracting organic contaminants from heterogeneous subsurface environments (NRC, 1994). This provides a substantial incentive for development of innovative and cost-effective alternative methods for minimizing the risks associated with contaminants in the subsurface. The possibility of transforming contaminants *in situ* through permeable "barriers" employing zero-valent metals, in particular, has received considerable scrutiny as a replacement for pump-and-treat approaches (Senzaki and Kumagai, 1988; Senzaki and Kumagai, 1989; Gillham and O'Hannesin, 1994; Matheson and Tratnyek, 1994; Agrawal *et al.*, 1995; Boronina *et al.*, 1995; Johnson *et al.*, 1996; Roberts *et al.*, 1996). The success of this technique is, however, contingent on the reaction products being relatively innocuous.

At present, little information is available concerning the pathways through which 1,1,1-TCA reacts with zero-valent metals, including the distribution of the products that result. Many researchers assume that organohalides react with zero-valent metals via hydrogenolysis, involving stepwise replacement of halogen by hydrogen (Gillham and O'Hannesin, 1994; Matheson and Tratnyek, 1994; Schreier and Reinhard, 1994). According to this paradigm, 1,1,1-TCA should react to 1,1-dichloroethane (1,1-DCA), thence to chloroethane, and finally to ethane. The data that do exist concerning products of 1,1,1-TCA reaction with metals are somewhat contradictory, and do not always accord with this sequence.

An early report by Archer (1982) indicated that the reaction of 1,1,1-TCA with Al(0) was complicated by a side reaction of the solvent with AlCl<sub>3</sub> or Al<sub>2</sub>O<sub>3</sub> present at the metal surface, which served as Lewis acids to catalyze dehydrohalogenation to 1,1-dichloroethylene (1,1-DCE). Such a product would be of considerable concern in a zero-valent metal treatment scheme if it were to arise from Fe(0): 1,1-DCE tends to be more persistent in the presence of Fe(0) than is 1,1,1-TCA (Gillham and O'Hannesin, 1994) and drinking water standards for 1,1-DCE are 20 times more stringent (on a molar scale) than for 1,1,1-TCA (Pontius, 1995). Archer further noted that 1,1,1-TCA reacts with Al(0), Sn(0), and Fe(0) to form 2,2,3,3-tetrachlorobutane, which in turn reacts with metals via reductive elimination to *cis* and *trans* 2,3-dichloro-2-butene.

More recently, Gillham and O'Hannesin (1994) studied reactions of Fe(0) with 14 halogenated organic contaminants including 1,1,1-TCA. Products of 1,1,1-TCA reaction were not, however, reported. Schreier and Reinhard (1994) found that 1,1,1-TCA reacts with both Fe(0) and Mn(0) in HEPES buffer. No increase in 1,1-DCA concentration accompanying 1,1,1-

TCA degradation was detected; rather, it was noted that 1,1-DCA (added as a co-substrate) was stable under reaction conditions. Finally, Wilson (1995), citing work conducted by the U.S. EPA National Exposure Research Laboratory, reported that 1,1,1-TCA reacts with Fe(0) to form 1,1-DCA. 1,1-DCA is on the U.S. EPA 1991 Drinking Water Priority List and must be monitored by all drinking water systems (Pontius, 1992), but at this time, no maximum contaminant levels have been established by the EPA for this organohalide. Considerable ambiguity therefore exists concerning the products likely to be encountered in a zero-valent metal based treatment system, leading to uncertainties in the human health risk that might be associated with the presence of partially dehalogenated reaction products in effluent from a subsurface treatment wall.

This study was initiated to better characterize the pathways through which 1,1,1-TCA reacts with two metals (iron and zinc) and two bimetallic reductants (copper-plated iron and nickel-plated iron), with a particular emphasis on the identities of the organic products formed. Additional studies also were carried out with 1,1-DCA and 2-butyne to assess their potential roles as reaction intermediates. Finally, a limited suite of experiments was conducted with isotopically labeled 1,1,1-TCA-2,2,2- $d_3$  in order to provide evidence in support of the hypothesized reaction pathways.

## C. EXPERIMENTAL SECTION

### 1. Reagents

The following chemicals were used as received: 1,1,1-trichloroethane (99%; ChemService); 1,1-dichloroethane (95+%; TCI America); vinylidene chloride (1,1-dichloroethylene, 99%; Aldrich); 2-butyne (99%; Aldrich); chloroethane (in methanol; Supelco); ethane, ethylene, and *cis*-2-butene (Scott Specialty Gases); and 1,1,1-trichloroethane-2,2,2- $d_3$  (98%; Cambridge Isotope Laboratories). Spiking solutions of 1,1,1-TCA, 1,1-DCA, 2-butyne and trideuterated 1,1,1-TCA were prepared in methanol (HPLC grade, J.T. Baker). Samples for additional analyses were extracted into hexane (95% *n*-hexane, ultra-resi analyzed grade, J.T. Baker).

Acid solutions for cleaning metals were prepared within an anaerobic chamber (containing an atmosphere of 10% H<sub>2</sub> and 90% N<sub>2</sub>) using deoxygenated (argon-sparged) deionized water (Milli-Q Plus UV, Millipore). The argon stream was purified using an in-line molecular sieve and



oxygen traps. Copper and nickel solutions for synthesis of bimetallic reductants were prepared by dissolving  $\text{CuCl}_2$  (97%; Aldrich) or  $\text{NiCl}_2$  (98%, Aldrich) in deoxygenated, deionized Milli-Q water under  $\text{N}_2/\text{H}_2$ . Reaction bottles were filled with an Ar-sparged solution consisting of 0.1 M NaCl (99%; J.T. Baker) and 50 mM Tris buffer (tris[hydroxymethyl]aminomethane, reagent grade; Sigma), pH 7.5.

## **2. Metal Preparation**

The surfaces of the zero-valent metals, iron and zinc, used in these experiments were cleaned with acid according to methods recommended by Wood (1982) to remove any surface oxides present. All cleaning steps were carried out within an anaerobic chamber. Zinc metal (Baker, 30 mesh) was washed with 0.4%  $\text{H}_2\text{SO}_4$  for 10 minutes, and iron metal (Fisher, 100 mesh electrolytic) was washed with 1 M HCl for 2 minutes. The acid-washed metals were rinsed 3 times with deoxygenated Milli-Q water, rinsed with acetone, removed from the anaerobic chamber, dried under argon at  $100^\circ\text{C}$  for 30 minutes, and used within 24 hours. Surface area analyses conducted via Kr and  $\text{N}_2$  BET adsorption using a Micromeritics Flowsorb II 2300 device indicated a surface area of  $0.16 \text{ m}^2 \text{ g}^{-1}$  for iron and  $0.035 \text{ m}^2 \text{ g}^{-1}$  for zinc.

## **3. Preparation of Bimetallic Reductants**

Iron was acid-washed and rinsed with deoxygenated water as described above. A dilute solution ( $50 \mu\text{M}$ ) of  $\text{CuCl}_2$  or  $\text{NiCl}_2$  was added slowly (within an anaerobic chamber) to 2 g of iron which was suspended in water by agitation. Once the metal chloride solution had been added, the metal was agitated for an additional minute, rinsed with deoxygenated Milli-Q water, rinsed with acetone, and dried as described above. Assuming all of the catalytic metal was reductively precipitated onto the iron base metal, the content of the Cu or Ni in the bimetallic reductant was calculated as 0.035 mol %.

## **4. Reactions of 1,1,1-TCA and 2-Butyne**

Reactions of 1,1,1-TCA and 2-butyne with metals and bimetallic reductants were carried out in 125 mL (nominal volume; actual volume  $\cong$  150 mL) glass bottles with glass stopcock adapters. The stopcocks were fitted with an NMR septum through which samples could be taken by syringe while maintaining anoxic reaction conditions; the stopcocks served to isolate the rubber septa from the flask contents except during the brief intervals required for sampling. For 1,1,1-

TCA, reactions were run with 0.5 g zinc, 1.0 g iron, 1.0 g nickel/iron, or 1.0 g copper/iron. Metal loadings were the same for 2-butyne (except that reaction with zinc was not investigated). The bottles were filled with deoxygenated Tris/NaCl buffer under an anaerobic atmosphere. Initially, the reaction bottles contained no headspace; less than 2 mL of headspace (presumably resulting from reduction of protons to H<sub>2</sub> by the metal) evolved during the course of a typical experiment. The bottles were spiked with a 0.2 M methanolic solution of 1,1,1-TCA for an initial concentration of approximately 200  $\mu$ M, or with a 0.2 M solution of 2-butyne for an initial concentration of  $\sim$  10  $\mu$ M. The bottles were rotated about their longitudinal axes on a rotator (Cole-Parmer) at 40 rpm throughout the course of the experiments. At regular intervals a 1-mL sample was removed from the bottom of the reaction bottle using a syringe equipped with a long needle while simultaneously adding 1 mL of deoxygenated buffer solution to the top of the bottle with a second syringe. Samples were sealed in 2.6 mL crimp-cap autosampler vials for headspace analysis by gas chromatography (GC) with flame ionization detection (FID), as described below. A 10  $\mu$ L sample aliquot was extracted into 1 mL of hexane for additional analysis of 1,1,1-TCA by GC with electron capture detection (GC/ECD). Efforts were made to follow the reaction of 1,1,1-TCA for at least 3 half-lives.

### **5. Reactions of 1,1-DCA**

Reactions of 1,1-DCA with metals and bimetallic reductants were carried out in 160 mL serum bottles sealed with Teflon<sup>®</sup> septa. Serum bottles were used in preference to the 125 mL reactors employed with 1,1,1-TCA because the pressure buildup caused by hydrogen gas evolution at high metal loadings or over long periods causes the glass stopcock adapters on the reactors to leak. Reactions were run with 2.5 g zinc, 5.0 g iron, 5.0 g nickel/iron, or 5.0 g copper/iron, *i.e.*, at a five-fold higher metal loading than employed with either 1,1,1-TCA or 2-butyne. The bottles were filled with deoxygenated Tris/NaCl buffer and sealed without headspace. Less than  $\sim$  5 mL of headspace evolved during these experiments. The bottles were spiked with 150  $\mu$ L of a 0.2 M 1,1-DCA methanolic solution, and were mixed and sampled as described for 1,1,1-TCA. Because of the dangers posed by the high pressures built up in the serum bottles, timecourses could only be monitored for relatively low conversions (7-15%) of 1,1-DCA.

## 6. Reactions of Deuterated 1,1,1-TCA

In order to confirm hypothesized reaction pathways, additional experiments were conducted using  $\text{Cl}_3\text{C}-\text{CD}_3$  as a starting material. Reactions were carried out in 25 mL serum bottles sealed with Teflon<sup>®</sup> septa. The bottles contained 2 g iron, 2 g nickel/iron or 2 g copper/iron, and were filled with 15 mL of deoxygenated Tris/NaCl buffer leaving approximately 10 mL of headspace in the bottle consisting of 10%  $\text{H}_2$  and 90%  $\text{N}_2$ . The sealed bottles were spiked with 5  $\mu\text{L}$  of a 0.7 M solution of trideuterated 1,1,1-TCA in methanol to give an initial concentration of approximately 200  $\mu\text{M}$ . The bottles were mixed overnight to allow reaction products to accumulate before 50  $\mu\text{L}$  headspace samples were taken directly from the reaction bottle for immediate analysis of reaction products by gas chromatography/mass spectrometry (GC/MS) as described below. Deuterium label retention in the parent compound was verified in separate experiments by monitoring the mass spectrum of the 1,1,1-TCA-2,2,2- $d_3$  over several hours during the course of its reaction with iron.

## 7. Sample Analysis

Headspace samples equilibrated with the 1 mL aqueous reaction aliquots were analyzed on a Carlo Erba GC 8000 gas chromatograph equipped with a Carlo Erba HS850 headspace autosampler, a J&W Scientific GS-Q PLOT column (30 m  $\times$  0.53 mm ID) and an FID. The samples were equilibrated in the autosampler at 60°C for 30 minutes prior to injection of 200  $\mu\text{L}$  of headspace in splitless mode. Data were acquired by a PC-based data acquisition system (*XChrom* v. 2.1; LabSystems, Beverly, MA).

Peak areas were converted to aqueous concentrations by the external standard method, using calibration curves prepared from aqueous standards or gas standards, as appropriate. For 1,1,1-TCA, 1,1-DCA, 1,1-DCE, and 2-butyne, aqueous standards were prepared in 20-mL glass syringes, which were analyzed as described for samples. For ethane, ethylene, and *cis*-2-butene, gas standards (Scott Specialty Gas) were employed. A 2 mL glass syringe with a wetted barrel and 3-way stopcock (one end of which was fitted with a septum) was used to mix and dilute gas standards. A 200  $\mu\text{L}$  aliquot of gas was removed and was manually injected in splitless mode. Results for samples were converted to aqueous concentrations using the appropriate Henry's law

constant. The dimensionless Henry's law constant (expressed as  $\left(\frac{\text{mol} / L_{\text{air}}}{\text{mol} / L_{\text{water}}}\right)$  at 60°C), measured in our laboratory by a modified EPICS method (Gossett, 1987) in Tris/NaCl buffer, is 15.8 for ethane, 8.7 for ethylene, and 5.4 for *cis*-2-butene.

The existence of a small amount of headspace could, in principle, result in a partitioning of the volatile compounds under investigation, thereby influencing reaction mass balances. Based on 25°C Henry's law constants (Mackay *et al.*, 1993) for 1,1,1-TCA ( $0.71 \frac{\text{mol} / L_{\text{air}}}{\text{mol} / L_{\text{water}}}$ ), 1,1-DCA (0.26), and 1,1-DCE (1.1), less than 1.5% of the mass of these halocarbons would have been lost through partitioning to the volumes of headspace that accumulated. For more volatile

hydrocarbon constituents such as ethane ( $K_H' = 20.4 \frac{\text{mol} / L_{\text{air}}}{\text{mol} / L_{\text{water}}}$ ; Hine and Mookerjee, 1975) and ethylene ( $K_H' = 8.7$ ; Hine and Mookerjee, 1975), however, losses could have been more significant, amounting to approximately 20% of the ethane mass and 10% of that of ethylene. Smaller losses would have been anticipated for the other hydrocarbons observed, namely *cis*-2-butene ( $K_H' = 5.8$  at 24°C; determined in our lab according to (McAuliffe, 1971) and 2-butyne ( $K_H'$  est. as 0.44; Meylan and Howard, 1991). Aqueous concentrations reported for all species therefore include a correction for calculated volatilization losses, based on our estimates of the headspace volume that had accumulated at each sampling point.

Detection limits for selected species were calculated from confidence bands around linear calibration curves using the method of Hubaux and Vos (1970). For purposes of assessing detection limits, five-point calibration curves were based on low concentration ranges (generally within a factor of five of the estimated detection limit), rather than on the full concentration range that was used to quantitate the results of the kinetic experiments.

Due to the coelution of 1,1,1-TCA with one possible reaction product, 1-hexene, verification of 1,1,1-TCA concentrations was made by analyzing hexane extracts via cold on-column injection onto an Rtx-1 GC column (30 m  $\times$  0.32 mm ID  $\times$  5.0  $\mu\text{m}$  film thickness; Restek) followed by detection with a Carlo Erba  $^{63}\text{Ni}$  ECD. The GC/ECD results agreed well with results obtained from the headspace GC/FID analysis technique. Identities of all major reaction products observed were confirmed by headspace injections onto a Hewlett-Packard (HP) 5890 GC

equipped with an HP 5970 mass spectrometer detector and a GS-Q PLOT column (30 m  $\times$  0.32 mm ID) or the Rtx-1 column previously described. Products were identified on the basis of retention time (using authentic compounds as standards) and mass spectra. The mass spectra were recorded under electron impact (EI) ionization by conducting scans in the range of  $m/e$  15 to 140; a narrower range ( $m/e$  15 to 40) was used to maximize sensitivity in measuring the spectra of low-molecular weight deuterated products (ethane and ethylene) in the experiment with isotopically labeled 1,1,1-TCA.

## 8. Mass Spectral Modeling

One of the objectives in the experiments conducted with  $\text{Cl}_3\text{C-CD}_3$  was to assess the deuterium content in the reaction products. GC/MS spectra indicated that ethylene and ethane products resulting from reactions of trideuterated 1,1,1-TCA consisted of a mixture of coeluting isotopomers with varying numbers of deuterium atoms. To estimate the retention of the deuterium label among the products, a set of linear programs was developed. Two such programs were developed for ethane, and one for ethylene modeling. For unlabeled compounds, model fits were based on mass spectra of gas standards determined on our instrument, while for deuterated compounds, model fits were based on the eight major peaks reported in the *Eight Peak Index of Mass Spectra* (Mass Spectrometry Data Centre, 1974). In the first ethane fit, the observed mass spectra were assumed to include contributions from: unlabeled ethane; ethane- $d_1$ ; ethane-1,1- $d_2$ ; ethane-1,2- $d_2$ ; and ethane-1,1,1- $d_3$ . We were unable to locate mass spectral information for ethane-1,1,2- $d_3$ , although we expect its mass spectrum is quite similar to that of ethane-1,1,1- $d_3$ ; Ponec and Bond (1995) note that these two isotopomers cannot be differentiated by mass spectrometry. In the second ethane fit, the previous program was supplemented with contributions from ethane-1,1,1,2- $d_4$  and ethane-1,1,2,2- $d_4$ . The following compounds were included in trying to fit observed spectra of ethylene: unlabeled ethylene; ethylene- $d_1$ ; ethylene- $d_2$ ; and ethylene- $d_3$ . Because reported mass spectra for the three dideuterated ethylenes are virtually identical, these isomers were lumped together as a single species in our analysis. For ethylene isotopomers, the most abundant ion is always the parent ion. For ethanes, the molecular ion is not the most abundant ion; relative intensities for the parent ion range from 27% to 42%. The most abundant ions for these species are as follows: unlabeled ethane,  $m/e = 28$ ; ethane- $d_1$ ,  $m/e = 29$ ; ethane-1,1- $d_2$ ,  $m/e = 29$ ; ethane-1,2- $d_2$ ,  $m/e = 30$ ; ethane-1,1,1- $d_3$ ,  $m/e = 30$ ; ethane-1,1,1,2- $d_4$ ,

$m/e = 31$ ; ethane-1,1,2,2- $d_4$ ,  $m/e = 31$ .

A best fit distribution was found by minimizing the objective function:

$$Z = \sum_{i=25}^{36} (U_i + V_i) + L \quad (25)$$

where the index  $i$  denotes the  $m/e$  values, subject to the constraints:

$$\sum_j a_{ij}x_j + U_i - V_i = e_i L \quad \forall i, i=25, \dots, 36 \quad (26)$$

$$\sum_j a_{ij}x_j \leq L \quad \forall i \quad (27)$$

$$\sum_j x_j = 1 \quad (28)$$

$$0 \leq x_j \leq 1 \quad \forall j \quad (29)$$

where the index  $j$  refers to the specific isotopomers considered in the mixture. The constants  $a_{ij}$  represent the theoretical abundance of  $m/e = i$  for isotopomer  $j$ , and  $e_i$  are the experimentally determined abundances for the mixture at each  $m/e$  value. The decision variables  $x_j$  are the fractions of isotopomer  $j$  in the mixture, while  $U_i$  and  $V_i$  are so-called target hitting variables. Their function in the linear program is such that minimizing the objective function is equivalent to minimizing the absolute value of the difference between the experimental and calculated mixtures. Through constraints (27), the decision variable  $L$  equals the largest calculated  $m/e$  abundance and is used to normalize the calculated values to obtain relative intensities.

## D. RESULTS

### 1. Reaction of 1,1,1-TCA and 1,1-DCA with Zn

1,1,1-TCA reacts rapidly with zinc to form ethane and 1,1-DCA (Figure 84). A model fit to the first five data points for 1,1,1-TCA shows a reasonable adherence to exponential decay, with some evidence that the reaction slows down towards the end of the experiment (Figure 84). Pseudo-first order  $k_{\text{obs}}$  values obtained from initial rates, and rate constants normalized to metal surface area loading ( $k_{\text{SA}}$ ; Johnson *et al.*, 1996) are shown in Table 14.

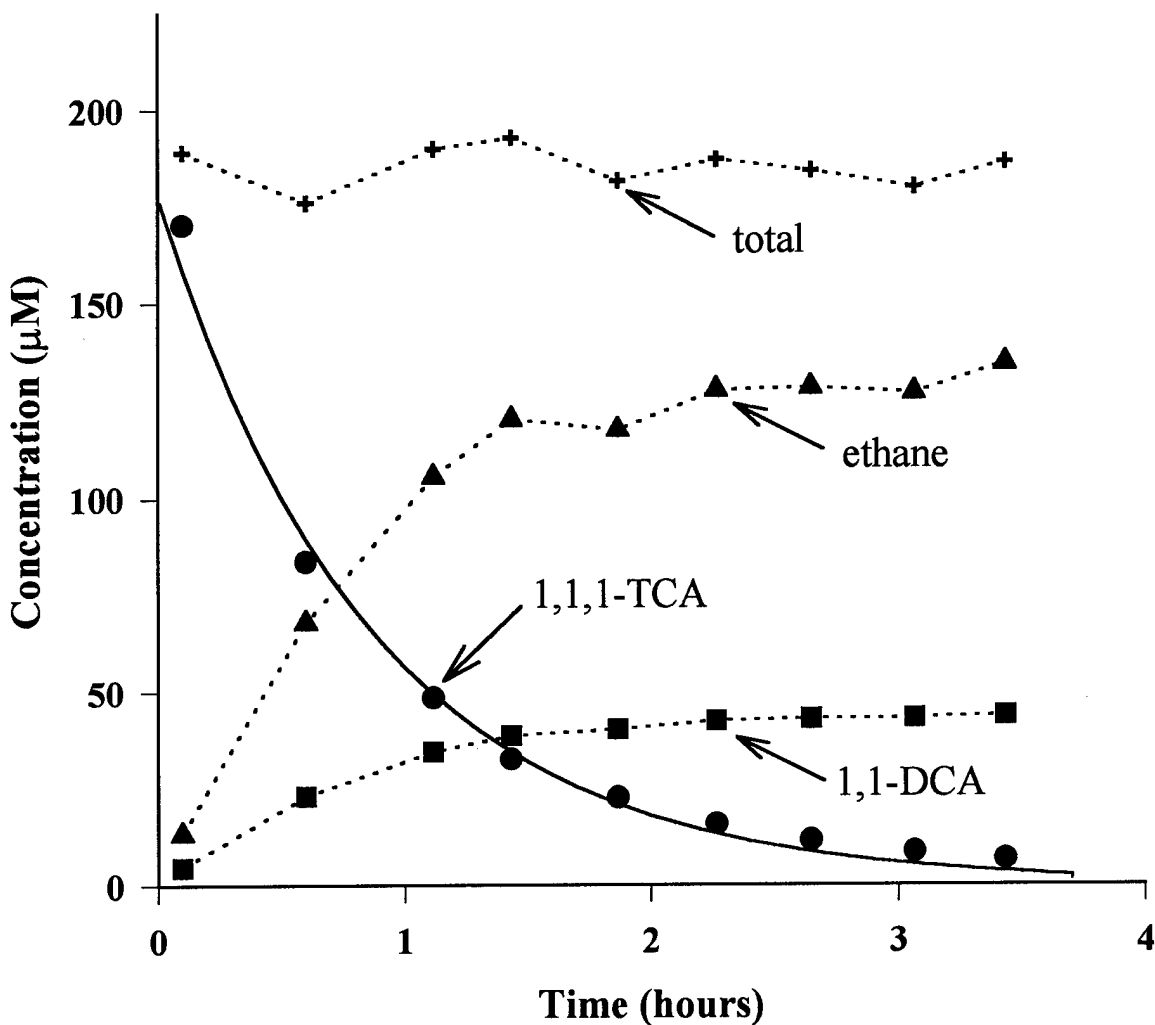


**Figure 87.** Reduction of 1,1,1-TCA in 0.1 M NaCl/0.05 M Tris buffer (pH 7.5) by Zn(0). Solid line reflects exponential decay fit to initial 1,1,1-TCA data.

**TABLE 15. SUMMARY OF REACTION RATE DATA OBTAINED FOR REACTIONS OF 1,1,1-TCA WITH ZERO-VALENT METALS AND BIMETALLIC REDUCTANTS<sup>a</sup>**

reductant	metal mass (g)	$k_{obs}$ (hr <sup>-1</sup> )	$k_{SA}$ (L m <sup>-2</sup> hr <sup>-1</sup> )
zinc	0.5	1.15 ± 0.18	10.0
iron	1.0	0.48 ± 0.06	0.46
nickel/iron	1.0	1.86 ± 0.20	1.77
copper/iron	1.0	1.35 ± 0.04	1.29

<sup>a</sup>In NaCl/Tris buffer, pH 7.5. Metal loading represents mass of metal per 150 ml of buffer solution in reactor. Uncertainties on  $k_{obs}$  values represent 95% confidence limits obtained from an exponential fit to the first five data points.

Ethane is the more abundant product observed, with a lesser amount of 1,1-DCA formed.

The yield of 1,1-DCA was calculated as  $\frac{(1,1\text{-DCA})_t}{(1,1,1\text{-TCA})_0 - (1,1,1\text{-TCA})_t}$ , where the subscript  $t$  denotes concentrations measured at all but the initial timepoint and  $(1,1,1\text{-TCA})_0$  is the model-fit initial TCA concentration. Results indicated a 1,1-DCA yield of  $25.8 \pm 0.5\%$ , where the stated uncertainty reflects 95% confidence limits. Replicate experiments indicated that product distributions determined for reaction of 1,1,1-TCA with zinc (as well as with iron; see below) were reproducible within 5-10%. No organic products were observed in blank experiments conducted with zinc (or iron or the bimetallic reductants employed) plus NaCl/Tris buffer in the absence of 1,1,1-TCA, either in the presence or absence of methanol at the concentration employed as a carrier in the 1,1,1-TCA spike.

The carbon mass balance at the end of the experiment (calculated as the sum of all organic species measured) was approximately 93% of the calculated spiked 1,1,1-TCA concentration (based on the volume of water in the reactor and the concentration of the 1,1,1-TCA in the methanol stock). We suspect that minor losses may have occurred during spiking through the stopcocks, as no other organic products were observed, and mass balances throughout the timecourse agree well with initial 1,1,1-TCA measurements. Lacking authentic standards of 2,2,3,3-tetrachlorobutane, *cis*- and *trans*-2,3-dichloro-2-butene, however, we cannot rule out the possibility that these could have been missed by the analytical techniques employed. Also, the headspace analytical technique is not optimal for products such as acetaldehyde or ethanol, which have low Henry's law constants. The detection limit for acetaldehyde was approximately  $9.2 \mu\text{M}$  (more than an order of magnitude higher than for the volatile organic products reported herein), and that for ethanol was greater than  $200 \mu\text{M}$ . The high detection limit for the latter compound may be in part attributable to the GC column employed, which is not well-suited to quantitative analysis of alcohols.

1,1-DCA represents a two-electron reduction product, and ethane a six electron reduction product. We do not, however, believe that 1,1-DCA is an intermediate in ethane formation. Both reaction products appeared simultaneously, and both persisted throughout the 3.5 hour course of the experiment. Independent experiments demonstrated that 1,1-DCA reacts slowly with zinc to produce ethane, with a half-life of approximately 14 days at a five-fold higher loading of zinc.



This slow rate of reaction precludes 1,1-DCA as an intermediate in the formation of ethane from 1,1,1-TCA.

## **2. Reaction of 1,1,1-TCA and 1,1-DCA with Fe**

Somewhat different products were obtained with iron (Figure 85). With this reductant, 1,1,1-TCA reacted to form mainly 1,1-DCA as a major product ( $67 \pm 2\%$  yield), along with lesser amounts of ethane, *cis*-2-butene, ethylene, and a trace of 2-butyne.

Final mass balances on carbon were approximately 84% relative to the calculated spiked concentration. We do not believe that sorption to the iron metal or impurities therein (as observed by Burris *et al.* (1996) is responsible for the imperfect mass balance. Unlike the cast iron employed by Burris, the Fisher electrolytic iron used in the present study has a very low carbon content (Deng *et al.*, 1997); furthermore, we have not observed any losses in aqueous concentration that could be attributed to sorption of chlorinated ethenes to either Fisher electrolytic iron or to zinc (Sections V and VI). Note that the total mass balance throughout the timecourse coincides closely with the initial 1,1,1-TCA measurement; if reaction to relatively polar products were significant, mass balances would have decayed over time. As with zinc, reactions initially followed pseudo-first order decay with an apparent slowing at later times. Initial rate constants are shown in Table 14.

Complementary experiments with 1,1-DCA again indicate that even though this chlorocarbon reacts to form ethylene and ethane as major products, reaction with iron is too slow (with a half-life of approximately 25 days at a loading of 5.0 g Fe) for 1,1-DCA to represent an intermediate in the formation of ethane or ethylene. Nor is ethylene (a four electron reduction product of 1,1,1-TCA) an intermediate in ethane formation, as independent experiments conducted in our laboratory demonstrate that ethylene reacts too slowly for such a reaction to account for the amount of ethane observed in reduction of 1,1,1-TCA (Section VI). Further evidence that suggests neither 1,1-DCA nor ethylene is an intermediate in ethane formation comes from the observation that yields of 1,1-DCA, ethylene, and ethane were independent of time. These three products must therefore originate from parallel, and not consecutive, reactions.

## **3. Reaction of 1,1,1-TCA and 1,1-DCA with Bimetallic Reductants**

1,1,1-TCA reacted with nickel/iron (Figure 86) at a significantly faster rate than with iron (Table 14). This enhanced reactivity of Ni/Fe accords with observations by other researchers for

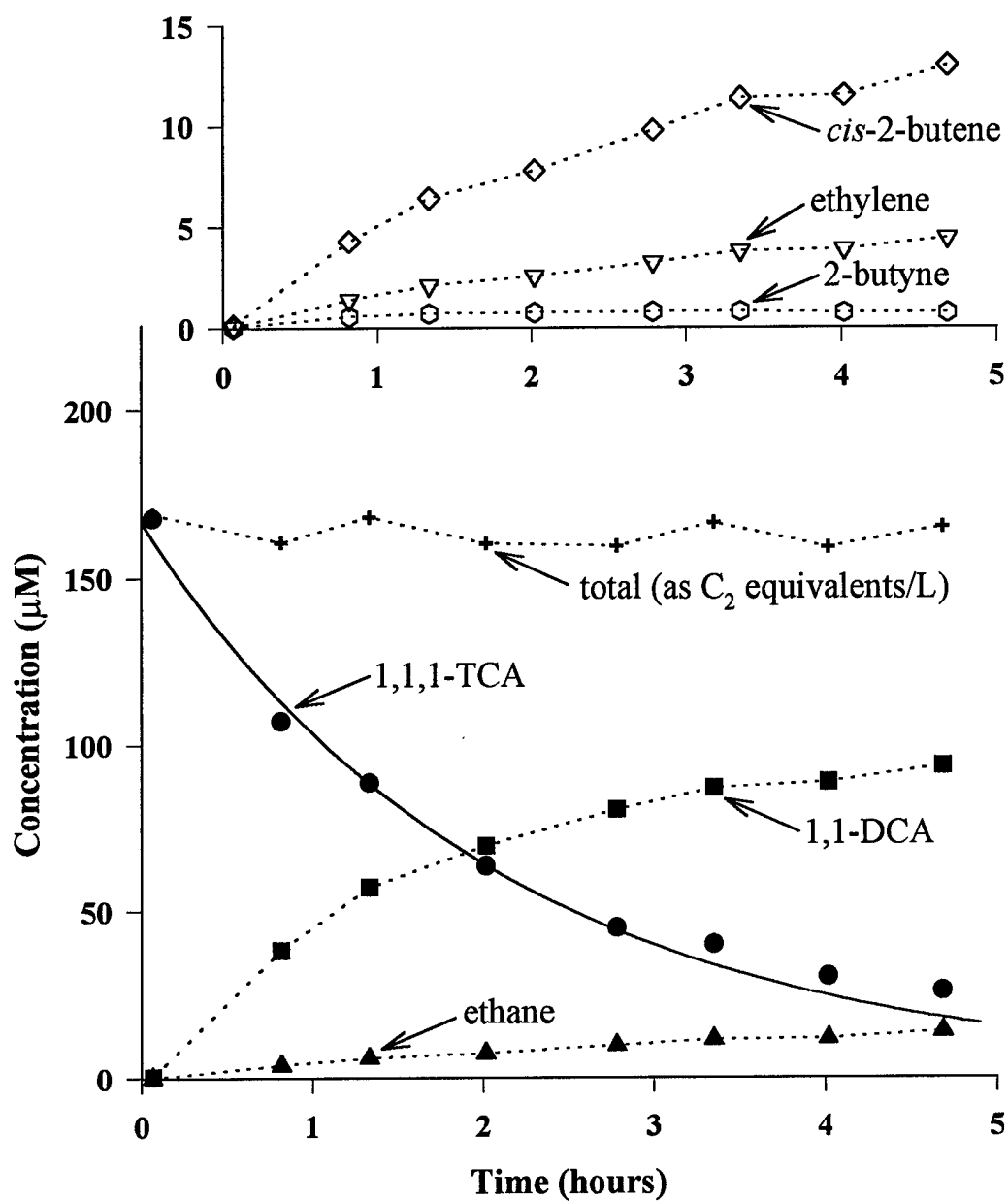


**Figure 88.** Reduction of 1,1,1-TCA in 0.1 M NaCl/0.05 M Tris buffer (pH 7.5) by Fe(0). Solid line reflects exponential decay fit to initial 1,1,1-TCA data. Inset shows minor products not observed in reaction with Zn.

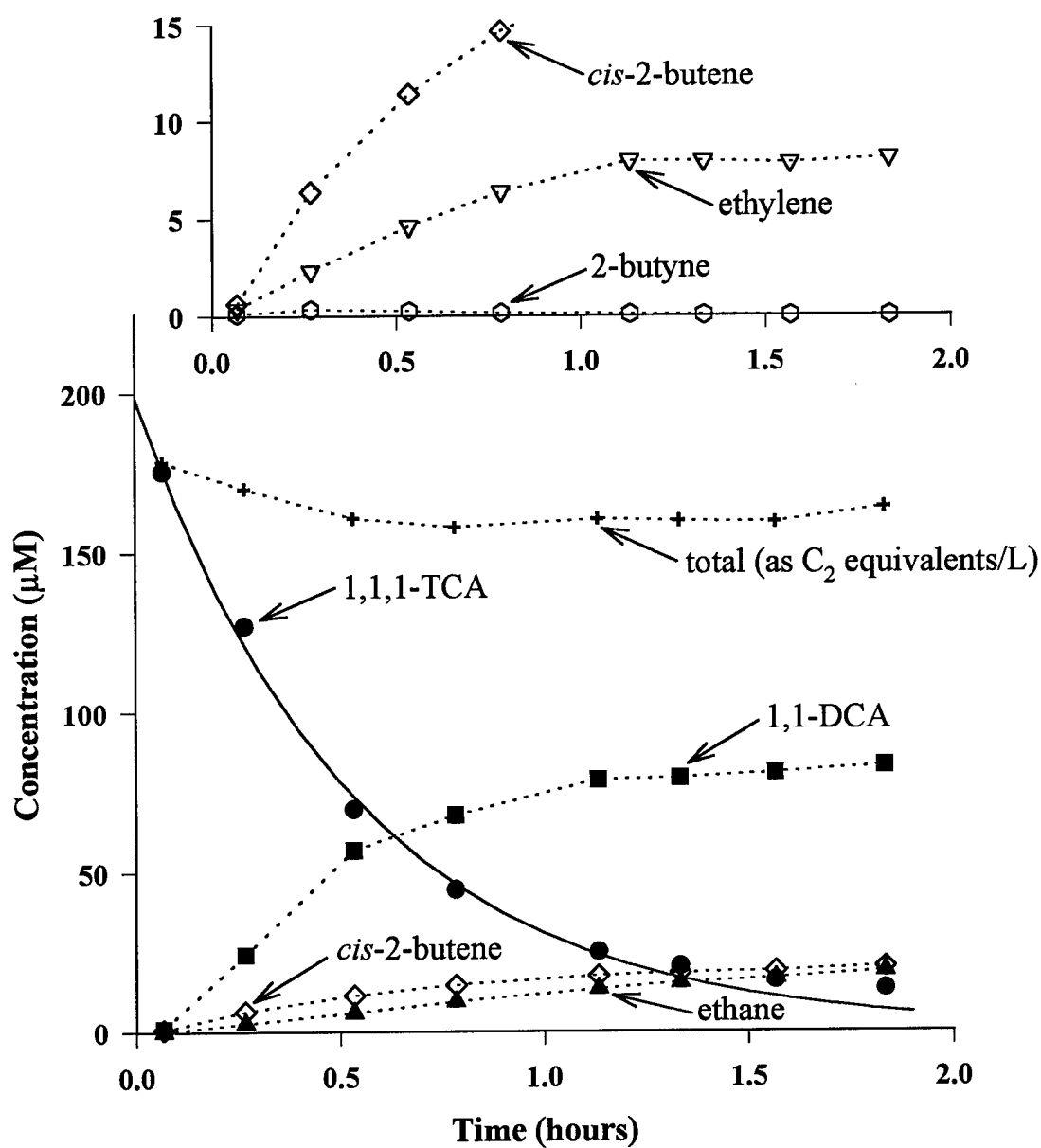


**Figure 89.** Reduction of 1,1,1-TCA by bimetallic (Ni-plated Fe) reductant in 0.1 M NaCl/0.05 M Tris buffer (pH 7.5). Solid line reflects exponential decay fit to initial 1,1,1-TCA data. Inset shows minor products not observed in reaction with Zn.

reactions of chlorinated ethylenes (Appleton, 1996). The increased rate of reaction was accompanied by a small change in the product distribution: a slightly higher yield of *cis*-2-butene and ethylene was obtained, and a lower yield ( $43 \pm 4\%$ ) of 1,1-DCA. As with iron, only a trace of 2-butyne was detected. The carbon mass balance at the end of the experiment was approximately 83% of the calculated spiked concentration. 1,1-DCA again reacts slowly with nickel/iron, with a half life of approximately 9 days at a loading of 5.0 g of Ni/Fe.

A more dramatic change in product distribution was found in the copper/iron system (Figure 87). A substantial increase in yield was observed for ethylene, while a decrease in 1,1-DCA ( $30 \pm 1\%$  yield) and *cis*-2-butene formation was obtained relative to nickel/iron. A significant concentration of 2-butyne was also measured; this product exhibited accumulation and subsequent disappearance indicative of a reaction intermediate. In addition, a trace of 1,1-dichloroethylene (1,1-DCE; detection limit  $0.03 \mu\text{M}$ ) was observed, a product confirmed by GC/MS. Final mass balances on carbon were approximately 76% relative to calculated spiked concentration. Once more, kinetic arguments indicate that 1,1-DCA cannot represent an intermediate in ethane or ethylene formation.

#### **4. Reduction of 2-Butyne**

Reactions of 2-butyne with iron and bimetallic reductants also were examined to assess whether this species could represent an intermediate in *cis*-2-butene formation. With iron and the two bimetallic reductants studied, the major reaction product observed was *cis*-2-butene, with only traces of *trans*-2-butene and 1-butene formed. Preliminary modeling studies based on a simple pseudo-first order approach suggested, however, that the measured rate of 2-butyne reaction was insufficient to account for all of the *cis*-2-butene observed in 1,1,1-TCA experiments. This may indicate limitations of a pseudo-first order approach; alternatively, some additional pathway may be responsible for *cis*-2-butene formation.

In summary, these experiments with 1,1,1-TCA show no evidence that the dehydrohalogenation reported with Al(0) (Archer, 1982) takes place with zero-valent zinc or iron. The expected dehydrohalogenation product, 1,1-DCE, is observed only with copper/iron and only in trace concentrations (less than 2% yield). The major reaction products, 1,1-DCA and

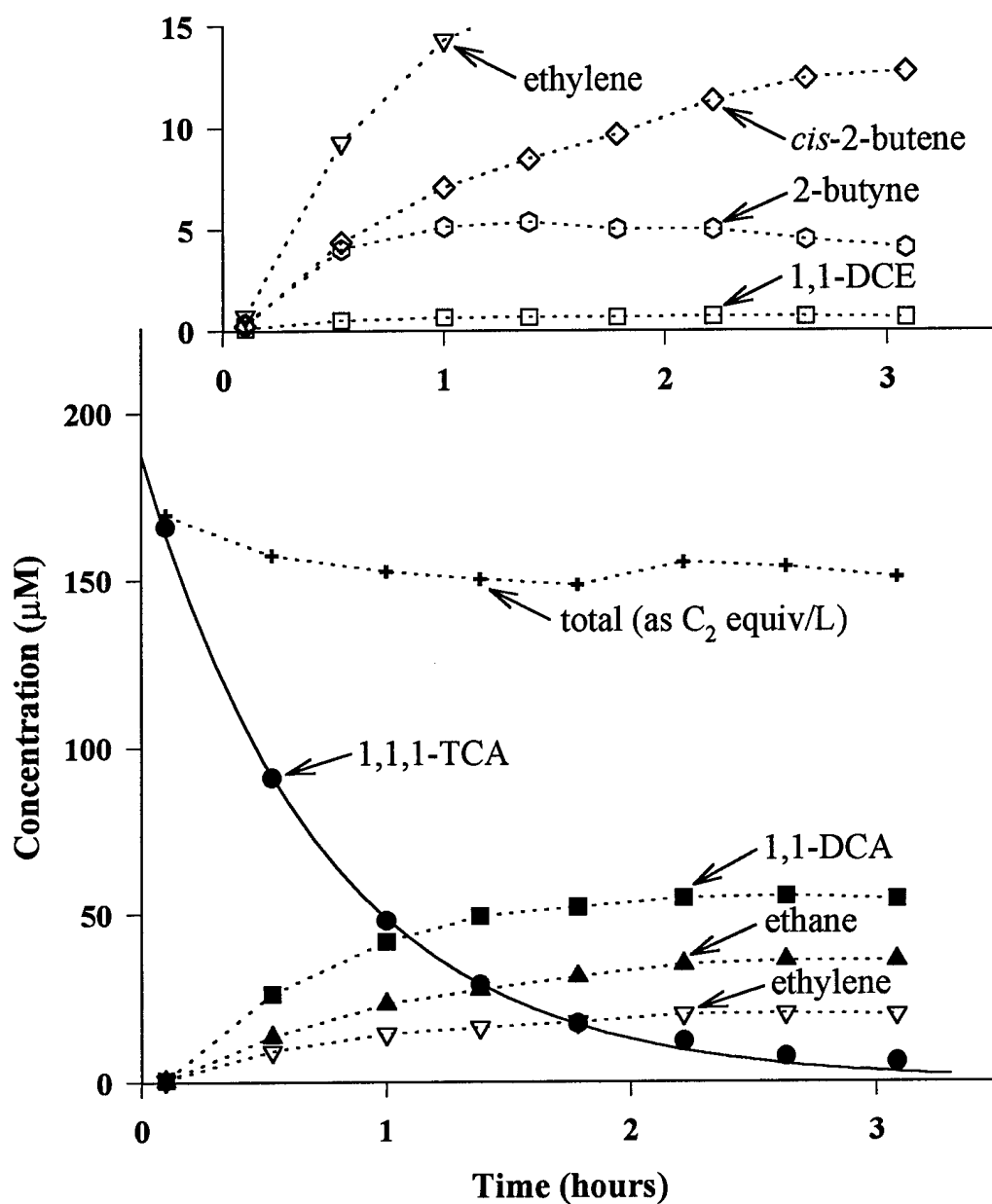


**Figure 90.** Reaction of 1,1,1-TCA with bimetallic (Cu-plated Fe) reductant in 0.1 M NaCl/0.05 M Tris buffer (pH 7.5). Solid line reflects exponential decay fit to initial 1,1,1-TCA data. Inset shows minor products not observed in reaction with Zn.

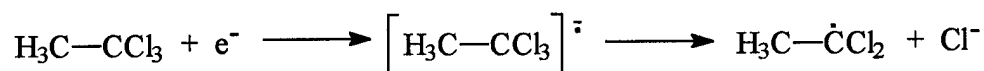
ethane, are consistent with reductive dehalogenation. A simple stepwise reduction from 1,1,1-TCA to 1,1-DCA to chloroethane to ethane does not, however, appear to be involved.

## E. DISCUSSION

### 1. Reaction Pathways

One potential scheme that could account for all of the products observed in our experiments with Fe(0) or reported in the literature is indicated in Figure 88. According to this scheme, ethane is formed via a sequence that involves successive one-electron reduction steps to form radicals and carbenoids, analogous to the pathway involved in reduction of 1,1,1-TCA by Cr(II) in aqueous solution (Castro and W.C. Kray, 1966).

The first step in the sequence involves a one-electron dissociative electron transfer step to result in the 1,1-dichloroethyl radical (Scheme 16):



#### Scheme 16

This radical could couple with other dichloroethyl radicals to form 2,2,3,3-tetrachlorobutane (which could undergo two successive reductive  $\beta$ -elimination reactions to form 2,3-dichloro-2-butenes and thence 2-butyne, which in turn was observed to undergo reduction to *cis*-2-butene). The importance of such coupling reactions would be expected to be dependent on the concentrations of the parent compound, as higher initial 1,1,1-TCA concentrations should give rise to higher steady-state concentrations of radicals.

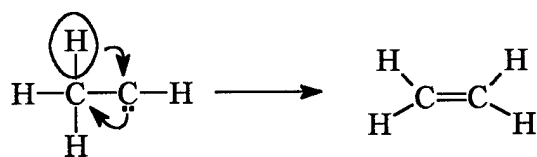
Alternatively, the dichloroethyl radical could undergo a second one-electron reduction to form the dichloroethyl carbanion, either free or complexed as an organometallic species. This carbanion could undergo protonation (to yield 1,1-dichloroethane), or else could undergo  $\alpha$ -elimination to form the  $\text{H}_3\text{C}-\ddot{\text{C}}-\text{Cl}$  carbene (or carbenoid). Carbanions are known to be stabilized by halogen substituents (March, 1985), which could favor the competition between protonation vs.  $\alpha$ -elimination to a carbene; the extra stabilization energy provided by two halogens may explain why 1,1-dichloroethane was observed, but not chloroethane (which would be expected to result from protonation of a chloroethyl carbanion). We note that our detection limit for chloroethane is approximately 0.24  $\mu\text{M}$ . Assuming that (as with 1,1-dichloroethane),



chloroethane is reduced slowly by the zero-valent metals investigated, even a chloroethane yield less than 0.2% should have resulted in detectable accumulation of this product.

We suspect that  $\text{H}_3\text{C}-\ddot{\text{C}}-\text{Cl}$  exists as a carbenoid (*e.g.*, as a carbene-metal complex or  $\alpha$ -haloorganometallic compound; (March, 1985), rather than as a free carbene. A free carbene might be expected to undergo a significant amount of trapping by the solvent, which would be expected to result in formation of acetaldehyde in the case of  $\text{H}_3\text{C}-\ddot{\text{C}}-\text{Cl}$ . There is precedent in the chemical literature for carbenoids as intermediates of polyhaloalkane reduction by zero-valent metals in organic solvents. For example, in the Simmons-Smith synthesis of cyclopropanes through reaction of olefins with  $\text{CH}_2$  (Simmons and Smith, 1959), it is believed that the methylene (generated through the reduction of  $\text{CH}_2\text{I}_2$  by the zinc-copper couple in ether) exists in the form of iodomethylzinc iodide, which is in equilibrium with the dialkylzinc species  $(\text{ICH}_2)_2\text{Zn}\cdot\text{ZnI}_2$  (Blanchard and Simmons, 1964). Although the iodomethylzinc iodide intermediate is sufficiently stable in ether to be isolable (Blanchard and Simmons, 1964), the presence of water could have an enormous impact on the stability of organometallic intermediates, which may only possess only a fleeting existence as reactive intermediates in the present system.

Further reduction of  $\text{H}_3\text{C}-\ddot{\text{C}}-\text{Cl}$ , accompanied by proton transfer, would result in formation of the chloroethyl radical. This radical could undergo reduction to the  $\text{H}_3\text{C}-\ddot{\text{C}}-\text{H}$  carbenoid. One of the characteristic reactions of alkylcarbenes is rearrangement (Kirmse, 1964), with migration of hydrogen (Scheme 17):



**Scheme 17**

Such a rearrangement could explain the ethylene observed. A similar rearrangement of  $\text{H}_3\text{C}-\ddot{\text{C}}-\text{Cl}$  does not appear to be taking place to any significant extent, as no vinyl chloride (detection limit 0.19  $\mu\text{M}$ ) was observed. This may serve as further indication that  $\text{H}_3\text{C}-\ddot{\text{C}}-\text{Cl}$  occurs as a carbenoid rather than as a free carbene.

Finally,  $\text{H}_3\text{C}-\ddot{\text{C}}-\text{H}$  could undergo two successive one-electron reduction steps (accompanied by protonation) to generate the ethyl radical, and finally ethane. The latter product



also results from reduction of ethylene, albeit at rate that is too slow to account for its formation from 1,1,1-TCA reduction (Section VI).

As with the dichloroethyl radical, the chloroethyl radical and the ethyl radical could potentially undergo self-coupling, forming *meso* and *D,L*-2,3-dichlorobutane (in the case of the chloroethyl radical) and *n*-butane (from the ethyl radical). We have previously found that *erythro* and *threo* 2,3-dibromopentane display a high degree of stereospecificity in their reductive elimination by zero-valent metals, reacting almost exclusively to *trans*- and *cis*-2-pentene, respectively (Totten and Roberts, 1995; Section III). Even if reaction of 2,3-dichlorobutanes were to be less stereospecific than reactions of the brominated analogs, we would expect if anything that an excess of *trans*-2-butene (as the more stable isomer) over the *cis* isomer should result from reduction of a racemic mixture of 2,3-dichlorobutanes. Our data indicate that *trans*-2-butene is not formed in appreciable amounts; it did not accumulate above detection limits (0.07  $\mu\text{M}$ ), nor was its likely reduction product, butane, ever observed. Unless the coupling of radicals at the metal surface were to result somehow in a substantial excess of *D,L*-2,3-dichlorobutane over the *meso* isomer, the apparent lack of *trans*-2-butene production would argue against the coupling of chloroethyl radicals. The absence of butane formation is evidence that coupling of ethyl radicals is not a significant process. The lack of apparent coupling by the chloroethyl and ethyl radicals may reflect the decreased stability of these less-highly substituted species (March, 1985), resulting in lower steady-state concentrations and thus diminished probability of encounter with one another.

The possibility that carbenes (or carbenoids) could couple should also be considered. Some authorities (Lowry and Richardson, 1987) have suggested that carbenes can couple to give rise to olefins. Other researchers (March, 1985) argue that because of their very high reactivity, it is unlikely that a free carbene could encounter another before reacting in some other manner, such as by rapid intramolecular rearrangement or reaction with the solvent; alternative explanations should therefore be sought for such apparent "dimerization" reactions. Although coupling of free carbenes in homogeneous solution may indeed be an extremely remote occurrence, the formation of organometallic carbenoids, either as dialkyl species or as monoalkyl species at locally elevated concentrations at the solid-water interface, might increase the probability of coupling. Blanchard and Simmons (1964) have studied the formation of ethylene as a side product of methylene iodide reaction with the zinc-copper couple. Their evidence suggests that ethylene formation occurs

through two simultaneous reactions of an organozinc carbenoid intermediate: (i) reaction of  $(\text{ICH}_2)_2\text{Zn}\cdot\text{ZnI}_2$  with unreacted  $\text{CH}_2\text{I}_2$  to form diiodoethane, which subsequently undergoes reductive elimination to ethylene; (ii) reaction of  $(\text{ICH}_2)_2\text{Zn}\cdot\text{ZnI}_2$  to  $\text{ICH}_2\text{CH}_2\text{ZnI}$ , which in turn reacts to ethylene.

For  $\text{H}_3\text{C}-\ddot{\text{C}}-\text{Cl}$ , the resulting coupling products would be *cis* and *trans* 2,3-dichloro-2-butenes (which could undergo reductive elimination to 2-butyne and then be reduced to *cis*-2-butene); from  $\text{H}_3\text{C}-\ddot{\text{C}}-\text{H}$ , *cis* and/or *trans*-2-butene would be expected. Once again, unless carbenoid coupling occurs in a highly stereospecific manner, the apparent lack of *trans*-2-butene formation would seem to rule out the possibility that  $\text{H}_3\text{C}-\ddot{\text{C}}-\text{H}$  species couple. Further assessment of the likelihood of carbenoid coupling must await a more detailed examination of the natures of these intermediates.

## 2. Experiments with Trideuterated 1,1,1-TCA

Additional evidence concerning reaction pathways was obtained by conducting experiments using trideuterated 1,1,1-TCA. GC/MS studies of products obtained from reaction of this compound with zero-valent iron, nickel/iron and copper/iron showed that ethylene and ethane reaction products are partially deuterated. According to the scheme shown in Figure 88, we would predict that the ethane should consist of ethane-*1,1,1-d*<sub>3</sub>, and that the ethylene should also be trideuterated. The observed spectra did not match library spectra of pure ethane-*1,1,1-d*<sub>3</sub> or trideuterated ethylene (Mass Spectrometry Data Centre, 1974), but rather appeared to represent mixtures of isotopomers exhibiting varying degrees of deuterium label retention. A set of linear programs, described in the experimental section, provided estimates of the distribution of isotopomers in each case.

Experimental and optimized results are shown in Figure 89(a) for ethane and Figure 89(b) for ethylene. The optimal distribution for the first ethane fit (from zero to three deuterium atoms) consisted of 16% unlabeled ethane, 34% ethane-*d*<sub>1</sub>, and 50% ethane-*1,1,1-d*<sub>3</sub>. The calculated spectrum does not match the measured spectra well for the higher molecular weight ions. Improved fit is obtained by allowing ethane-*1,1,1,2-d*<sub>4</sub> and ethane-*1,1,2,2-d*<sub>4</sub> to be present (Figure 89a, fit 2), but the abundance of the  $m/e = 33$  value is still underestimated. The resulting optimized distribution consisted of 6% unlabeled ethane, 32% ethane-*d*<sub>1</sub>, 31% ethane-*1,1,1-d*<sub>3</sub>,

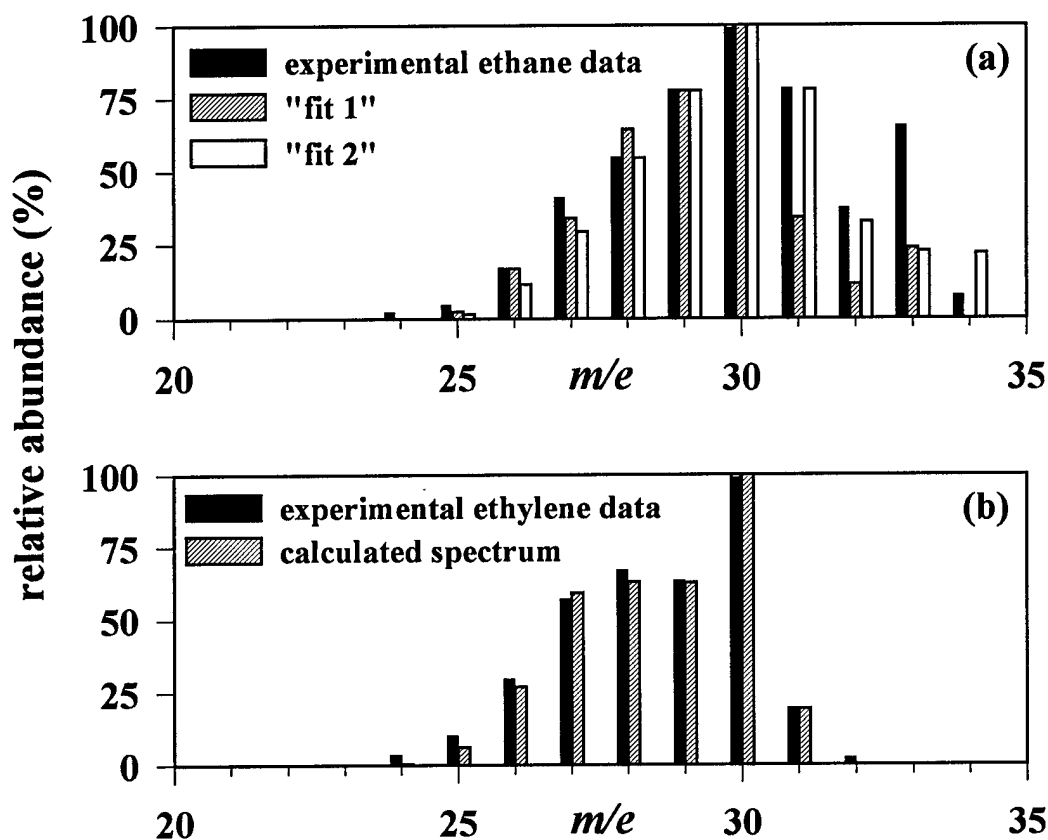


**Figure 92.** Comparison of experimental with calculated GC/MS spectra for reaction of isotopically labeled 1,1,1-TCA-2,2,2- $d_3$  with iron: (a) experimental ethane mixture (solid bars); “best-fit” mass spectrum assuming a mixture of unlabeled, mono-, di-, and trideuterated ethane isotopomers (fit 1, patterned bars); and “best-fit” mass spectrum based on a mixture of unlabeled through tetradeuterated ethanes (fit 2, open bars); (b) experimental ethylene mixture (solid bars) and “best-fit” mass spectrum based on a mixture of unlabeled through trideuterated ethylene isotopomers (patterned bars).

and 31% ethane-1,1,2,2- $d_4$ . Incorporation of higher molecular-weight isotopomers (pentadeuterated or hexadeuterated ethane) into the model did not result in any substantial improvement in fit between predicted and measured spectra.

The imperfect agreement between measured and predicted ethane spectra may reflect limitations of our model and/or the resolution of our mass spectrometric analysis (*e.g.*, limits to

instrumental accuracy; variability in background noise leading to imperfect background corrections; or, perhaps most likely, reliance on published spectra rather than on spectra for partially deuterated ethane isotopomers determined on our instrument). We feel that other possibilities for the imperfect match between predicted and measured spectra, such as that some other product coelutes with the ethane, are unlikely. When experiments were run using unlabeled 1,1,1-TCA, the peak obtained for ethane was readily resolved from all other nearby peaks on the GC column employed, and the mass spectrum was identical to that of an authentic ethane standard. Mass spectrometric analysis of the isotopically labeled 1,1,1-TCA failed to reveal significant levels of impurities (such as 1,1,1-trichloroethane-2,2- $d_2$ ) that might have led to production of dideuterated or lower molecular weight ethane or ethylene isotopomers. No ethane or ethylene accumulation was detected in the absence of 1,1,1-TCA, as previously discussed.

The best-fit distribution of labeled and unlabeled products in the ethylene mixture was: 6% ethylene, 11% ethylene- $d_1$ , 70% ethylene- $d_2$  (mixture of all three possible dideuterated isomers), and 14% ethylene-1,1,2- $d_3$ . In this case, the simulated spectrum matched the experimental spectrum well, as shown in Figure 89(b).

The deviations from the expected deuterium label retention in the ethane and ethylene products suggest that the actual reaction mechanism is more complex than the scheme illustrated in Figure 88. It is possible that H-D exchange could occur either in the reactive intermediates or in the final products ethane or ethylene. Some of the deuterium lost could persist at the surface of the metal, thereby accounting for the variable deuterium retention. Such metal-catalyzed H-D exchange of alkanes and olefins has received intensive scrutiny in the field of metal catalysis (Poniec and Bond, 1995). According to the generally-accepted model, the reaction involves a sequence of steps: (a) adsorption of the hydrocarbon to the metal surface, followed by activation of the C-H (or C-D) bond; (b) dissociation of the carbon-hydrogen bond to yield a metal-bound radical; (c) coupling of the radical with metal-bound atomic H (or D). Most of the prior research, however, pertains to gas-phase reactions, and it is difficult to assess without additional experiments whether such exchange would also occur under the conditions employed in the present study. Certainly no evidence of D-H exchange could be detected in the mass spectrum of 1,1,1-TCA- $d_3$  over several half-lives of reaction with iron. Furthermore, no significant deuterium label loss was apparent in the 2-butyne-1,1,1,4,4,4- $d_6$  or the 1,1-dichloroethane-2,2,2- $d_3$  products

observed (see below). This indicates that H-D exchange, if it occurs under the present reaction conditions, is not invariably a facile process.

The other reaction products, 1,1-dichloroethane, 2-butyne and *cis*-2-butene, were found to consist of 1,1-dichloroethane-2,2,2-*d*<sub>3</sub> (Figure 90a), 2-butyne-1,1,4,4,4-*d*<sub>5</sub> (Figure 90b), and *cis*-2-butene-*d*<sub>6</sub>, shown in Figure 90(c). Note that because of the tendency of hydrocarbons to exhibit a scrambling of hydrogen atoms under electron impact ionization (Meisels *et al.*, 1969, McFadden, 1963), the positions of the deuterium atoms within the *cis*-2-butene cannot be determined from the mass spectrum. The presence of six deuterium atoms in the C<sub>4</sub> products is consistent with their origin via coupling of radicals (or possibly D<sub>3</sub>C- $\ddot{\text{C}}$ -Cl carbenoids) that then undergo reductive elimination and reduction to 2-butyne and *cis*-2-butene. Retention of six deuterium atoms would not have been anticipated if C<sub>4</sub> products were to originate from reduction of aqueous carbonate (Hardy and Gillham, 1996) or from reaction of carbide impurities within the metal (Deng *et al.*, 1997).

### 3. Relevance of Results

In summary, our results confirm Gillham's (1994) and Schreier's (1994) observations that 1,1,1-TCA reacts rapidly with Fe(0). Kinetic analyses and product studies indicate that the reaction does not, however, proceed exclusively through stepwise replacement of halogen by hydrogen, as has been previously proposed as a paradigm for reaction of organohalides with metals. Rather, the data for iron and iron-based bimetallic reductants are consistent with a sequence involving reduction to radicals and carbenoids, resulting in products which reflect reductive  $\alpha$ -elimination and coupling in competition with hydrogenolysis. Whether reaction with zinc also involves free radical intermediates requires additional study. Certainly, none of the coupling products that are often characteristic of free radical reactions, and which were observed for reaction with iron, Ni/Fe, and Cu/Fe, were detected with zinc.

The data reveal interesting differences in the distribution of products obtained with the various reductants employed. A lower yield of 1,1-DCA, for example, was obtained with zinc than with iron or with either of the two bimetallic reductants. In all cases, the reaction of 1,1-DCA was shown by independent experiments to be sufficiently slow as to preclude major differences between the reactivity of the various reductants as an explanation. It seems that the metal serves a role that goes beyond that of a simple source of electrons: specific chemical

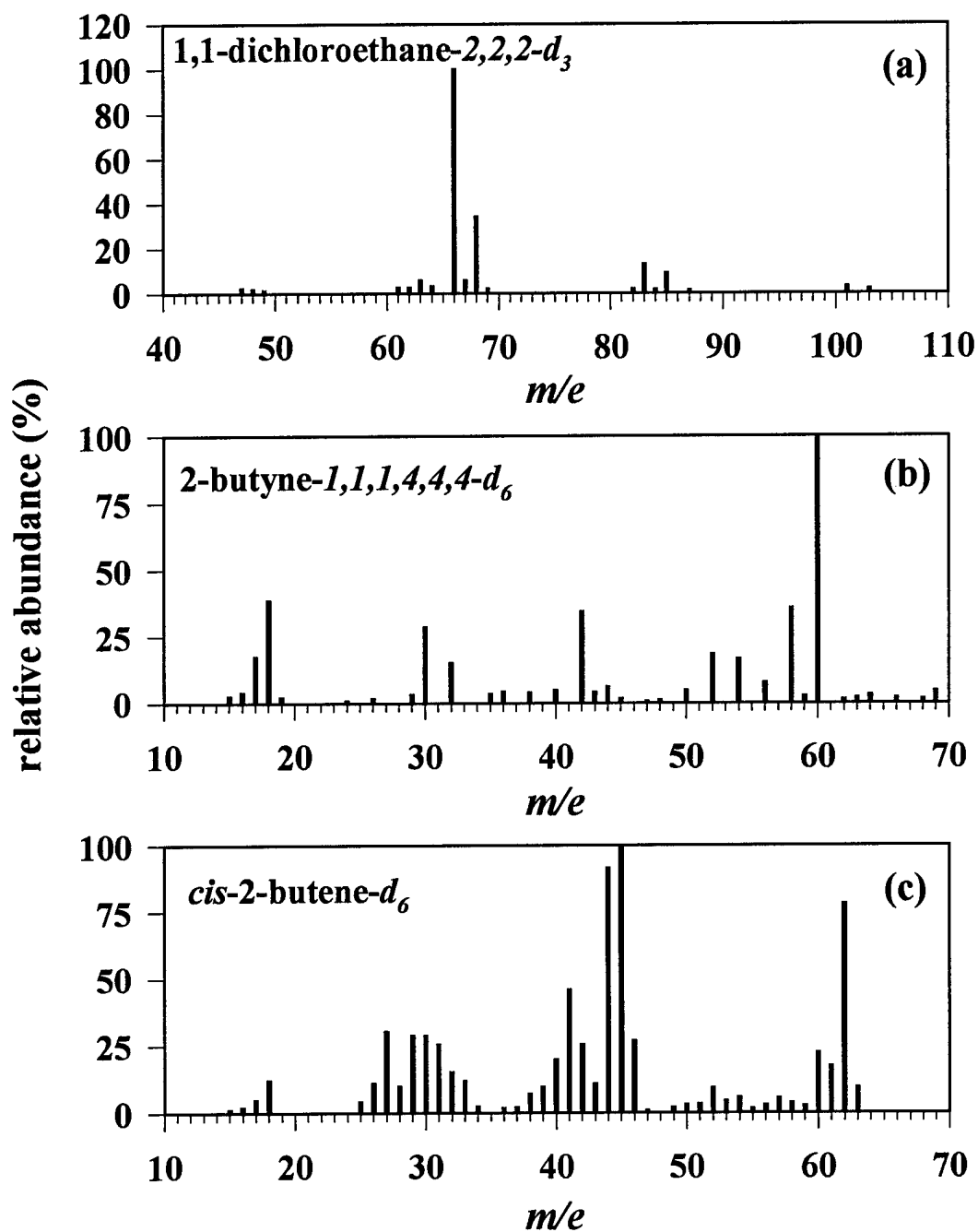


**Figure 93.** GC/MS spectra of (a) 1,1-dichloroethane-2,2,2- $d_3$ ; (b) 2-butyne-1,1,1,4,4,4- $d_6$ ; and (c) *cis*-2-butene- $d_6$  obtained in reaction of 1,1,1-TCA-2,2,2- $d_3$  with iron.

interactions between (potentially partially oxidized) metal species present at the solid-water interface and the organohalide (or reactive intermediates resulting therefrom) are likely to be involved in dictating reactivity and reaction product distribution. Boronina *et al.* (1995) have also found that the identity of the metal plays a part in the distribution of products obtained in the reduction of organohalides: reaction of  $\text{CCl}_4$  with zinc led to dechlorination to methane, while reaction with  $\text{Sn}(0)$  led to  $\text{CO}_2$  and chloroform as major products. A complete explanation for such differences in reactivity and reaction product distributions displayed by various metals and bimetallic reductants is bound to involve a multitude of factors, many of which are still imperfectly understood. Even for reactions as well-studied as metal-promoted H-D exchange in alkanes, Ponec and Bond, (1995) note "It is still quite unclear why adjacent metals can behave so differently as catalysts... Unfortunately the chemical rules governing metals' behaviour have not yet been elucidated... Much work remains to be performed in this field." These statements can be echoed for metal-promoted reductive dehalogenation reactions. Nevertheless, the strong influence that the metal identity exerts on reaction product distribution suggests that it may be feasible to develop a reductant through which the generation of undesirable byproducts could be minimized.

Although the pathways outlined herein for iron are complex, they do make it possible to formulate a reaction scheme which can account for all of the observed reaction products (including the inability of 1,1-DCA and ethylene to represent reaction intermediates). This should facilitate the development of process models which could be used for design of subsurface iron-based treatment walls for 1,1,1-TCA. Additional studies will be required to assess whether reaction with zinc (which does not appear to give rise to coupling products) also proceeds through similar pathways.

## F. LITERATURE CITED

- Agrawal, A.; Tratnyek, P.G.; Stoffyn-Egli, P.; Liang, L. Processes affecting nitro reduction by iron metal: mineralogical consequences of precipitation in aqueous carbonate environments. *Natl. Meet.-Am. Chem. Soc., Div. Environ. Chem.* **1995**, *35*, 720-723 (Abstr.).
- Appleton, E.L. A nickel-iron wall against contaminated groundwater. *Environ. Sci. Technol.* **1996**, *30*, 536A-539A.
- Archer, W.L. Aluminum-1,1,1-trichloroethane. Reactions and inhibition. *Ind. Eng. Chem. Prod. Res. Dev.* **1982**, *21*, 670-672.
- Blanchard, E.P.; Simmons, H.E. Cyclopropane synthesis from methylene iodide, zinc-copper couple, and olefins. II. Nature of the intermediate. *J. Amer. Chem. Soc.* **1964**, *86*, 1337-1347.
- Boronina, T.; Klabunde, K.J.; Sergeev, G. Destruction of organohalides in water using metal particles: carbon tetrachloride/water reactions with magnesium, tin, and zinc. *Environ. Sci. Technol.* **1995**, *29*, 1511-1517.
- Burris, D.R.; Campbell, T.J.; Manoranjan, V.S. Sorption of trichloroethylene and tetrachloroethylene in a batch reactive zero-valent iron system. *Environ. Sci. Technol.* **1996**, *29*, 2850-2855.
- Castro, C.E.; W.C. Kray, J. Carbenoid intermediates from polyhalomethanes and chromium(II). *J. Amer. Chem. Soc.* **1966**, *88*, 4447-4455.
- Deng, B.; Campbell, T.J.; Burris, D.R. Hydrocarbon formation in metallic iron/water systems. *Environ. Sci. Technol.* **1997**, *31*, 1185-1190.
- Gillham, R.W.; O'Hannesin, S.F. Enhanced degradation of halogenated aliphatics by zero-valent iron. *Ground Water* **1994**, *32*, 958-967.
- Gossett, J.M. Measurement of Henry's law constants for C<sub>1</sub> and C<sub>2</sub> chlorinated hydrocarbons. *Environ. Sci. Technol.* **1987**, *21*, 202-208.
- Hardy, L.I.; Gillham, R.W. Formation of hydrocarbons from the reduction of aqueous CO<sub>2</sub> by zero-valent iron. *Environ. Sci. Technol.* **1996**, *30*, 57-65.



- Hine, J.; Mookerjee, P.K. The intrinsic hydrophilic character of organic compounds. Correlations in terms of structural contributions. *J. Org. Chem.* **1975**, *40*, 292-297.
- Hubaux, A.; Vos, G. Decision and detection limits for linear calibration curves. *Analyt. Chem.* **1970**, *42*, 849-855.
- Johnson, T.L.; Scherer, M.M.; Tratnyek, P.G. Kinetics of halogenated organic compound degradation by iron metal. *Environ. Sci. Technol.* **1996**, *30*, 2634-3640.
- Kirmse, W. *Carbene Chemistry*. Academic Press: New York, 1964.
- Lowry, T.H.; Richardson, K.S. *Mechanism and Theory in Organic Chemistry*. 3rd ed. Harper & Row: New York, 1987.
- Mackay, D.; Shiu, W.Y.; Ma, K.C., *Illustrated Handbook of Physical-Chemical Properties and Environmental Fate for Organic Chemicals*. Vol. 3. Lewis Publishers: Boca Raton, FL 1993.
- March, J. *Advanced Organic Chemistry: Reactions, Mechanisms, and Structures*. 3rd ed. John Wiley & Sons: New York, 1985.
- Mass Spectrometry Data Centre, *Eight Peak Index of Mass Spectra*. 2nd ed. Pendragon House: Palo Alto, CA., 1974: Vol. I-1.
- Matheson, L.J.; Tratnyek, P.G. Reductive dehalogenation of chlorinated methanes by iron metal. *Environ. Sci. Technol.* **1994**, *28*, 2045-2053.
- McAuliffe, C. GC Determination of solutes by multiple phase equilibration. *Chem Tech.* **1971**, *1*, 46-51.
- McFadden, W.H. The mass spectra of three deuterated propenes. *J. Phys. Chem.* **1963**, *67*, 1074-1077.
- Meisels, G.G.; Park, J.Y.; Giessner, B.G. Carbon skeletal rearrangement of butene ions. *J. Amer. Chem. Soc.* **1969**, *91*, 1555-1556.
- Meylan, W.M.; Howard, P.H. Bond contribution method for estimating Henry's law constants. *Environ. Toxicol. Chem.* **1991**, *10*, 1283-1293.
- National Research Council. *Alternatives for Ground Water Cleanup*. National Academy Press: Washington, D.C., 1994.

- Ponec, V.; Bond, G.C. *Catalysis by Metals and Alloys*. Studies in Surface Science and Catalysis, Eds. B. Delmon and J.T. Yates. Vol. 95. Elsevier: Amsterdam, 1995.
- Pontius, F.W. A current look at the Federal drinking water regulations. *J. Am. Water Works Assoc.* **1992**, *84*, 36-50.
- Pontius, F.W. An update of the Federal drinking water regulations. *J. Am. Water Works Assoc.* **1995**, *87*, 48-58.
- Reed, D.J., "Chlorocarbons and Chlorohydrocarbons", in *Kirk-Othmer Encyclopedia of Chemical Technology, Fourth Ed.*, J.I. Kroschwitz and M. Howe-Grant, Editors. John Wiley & Sons: New York, 1993, vol 5.
- Roberts, A.L.; Totten, L.A.; Arnold, W.A.; Burris, D.R.; Campbell, T.J. Reductive elimination of chlorinated ethylenes by zero-valent metals. *Environ. Sci. Technol.* **1996**, *30*, 2654-2659.
- Schreier, C.G.; Reinhard, M. Transformation of chlorinated organic compounds by iron and manganese powders in buffered water and in landfill leachate. *Chemosphere* **1994**, *29*, 1743-1753.
- Senzaki, T.; Kumagai, Y. Removal of organochloro compounds in wastewater by reductive treatment: reductive degradation of 1,1,2,2-tetrachloroethane with iron powder. *Kogyo Yousui* **1988**, *357*, 2-7.
- Senzaki, T.; Kumagai, Y. Removal of organic chlorine compounds by use of some reduction processes: processing trichloroethylene with iron powder. *Kogyo Yousui* **1989**, *369*, 19-25.
- Simmons, H.E.; Smith, R.D. A new synthesis of cyclopropanes. *J. Amer. Chem. Soc.* **1959**, *81*, 4256-4264.
- Simmons, H.E.; Blanchard, E.P.; Smith, R.D. Cyclopropane synthesis from methylene iodide, zinc-copper couple, and olefins. III. The methylene-transfer reaction. *J. Amer. Chem. Soc.* **1964**, *86*, 1347-1356.
- Sivavec, T.M.; Mackenzie, P.D.; Horney, D.P. Effect of site groundwater on reactivity of bimetallic media: Deactivation of nickel-plated granular iron. *Natl. Meet.-Am. Chem. Soc., Div. Environ. Chem.* **1997**, *37*, 83-85 (Abstr.).

- Snedecor, G. "Other Chloroethanes", in *Kirk-Othmer Encyclopedia of Chemical Technology*, Fourth Ed., J.I. Kroschwitz and M. Howe-Grant, Editors. Wiley & Sons: New York, 1993.
- Totten, L.A.; Roberts, A.L. Investigating electron transfer pathways during reductive dehalogenation reactions promoted by zero-valent metals. *Natl. Meet.-Am. Chem. Soc., Div. Environ. Chem.* **1995**, 35, 706-710 (Abstr.).
- U.S. Environmental Protection Agency, *1,1,1-Trichloroethane - ATSDR Public Health Statement*, Agency for Toxic Substances and Disease Registry, EPA: Washington, DC, 1990.
- Wilson, E.K. Zero-valent metals provide possible solution to groundwater problems. *C&E News* **1995**, 19-22.
- Wood, W.G., Ed. "Surface cleaning, finishing and coating". In *Metals Handbook*, American Society for Metals: Metals Park, OH, 1982; Vol. 5.

# APPENDIX A: HETEROGENEOUS KINETICS DERIVATION

The derivations given here are very similar to those given in Fogler (1992) and also draw from Carberry (1976) and Froment and Bischoff (1990). First the simplest case of  $A \rightarrow B$  is derived and the experimental data necessary to obtain the required parameters are briefly discussed. Equations that describe more complex systems are subsequently presented.

The sorption of chlorinated ethylenes onto iron measured by Burris *et al.* (1995) and Allen-King *et al.* (1997) has been assumed to reflect sorption to non-reactive sites (most likely carbon impurities in the iron). This sorption is important in the overall mass balance as well as in the overall reaction kinetics in a batch system because it slows the overall rate of reaction by sequestering some of the reactant mass in a non-reactive phase. The adsorption to reactive sites discussed below is considered to be a distinct process from this sorption to non-reactive sites.

## A.1 Definitions

The following table lists the symbols used in the derivation of the model.

**TABLE A-1: EXPLANATION OF SYMBOLS USED IN HETEROGENEOUS KINETIC MODEL**

Symbol	Definition
$C_i$	aqueous concentration of species $i$ [ $M/L^3$ ]
$C_{is}$	adsorbed concentration of species $i$ [ $M/L^3$ ]
$S$	a reactive site
$S_v$	concentration of vacant sites [ $M/L^3$ ]
$S_t$	total concentration of surface sites (vacant and occupied) [ $M/L^3$ ]
$k^a, k^s, k^d$	kinetic rate constants [ $L^3/(M \cdot T)$ , $1/T$ , $1/T$ ] for adsorption limited, surface-reaction limited, and desorption limited cases, respectively
$K$	adsorption equilibrium constants [ $L^3/M$ ]

## A.2 Case 1: $A \rightarrow B$

A reaction of  $A \rightarrow B$  is the simplest transformation that can take place, thus it provides a logical starting point. Once the equations describing this reaction are derived, the more

complicated cases of parallel and sequential reactions can easily be determined by extending/modifying the equations for the simplest case.

### A.2.1 Steps in a Heterogeneous Reaction

Three steps are defined to take place: adsorption of A to the surface, reaction of A to B at the surface, and desorption of B from the surface. Adsorption is assumed to follow a Langmuir isotherm. The reaction steps are usually written:



The rate of adsorption is given by equation A-2 or A-3,

$$r_{ad} = k^a C_A S_v - k^{-a} C_{AS} \tag{A-2}$$

$$r_{ad} = k^a \left( C_A S_v - \frac{C_{AS}}{K_A} \right) \tag{A-3}$$

where  $k^a$  and  $k^{-a}$  are the adsorption and desorption rate constants for the parent compound, A.  $K_A$  is the adsorption equilibrium constant ( $k^a/k^{-a}$ ).

If the surface reaction is assumed to be irreversible, the rate of surface reaction,  $r_s$ , is given by equation (A-4).

$$r_s = k^s C_{AS} \tag{A-4}$$

The rate expression for desorption of the reaction product, B, is similar in form to that for the adsorption of species A. Using  $K_B$ , the adsorption equilibrium constant for species B, the expression for the rate is

$$r_d = k^d (C_{BS} - K_B C_B S_v). \tag{A-5}$$

The final equation necessary is a surface site balance. The total number of sites is the sum of those occupied and unoccupied:

$$S_t = S_v + C_{AS} + C_{BS} \quad (\text{A-6})$$

### A.2.2 Adsorption as the Rate Limiting step

When one step in a sequence is rate limiting, the rate at which the other processes in the sequence take place are dictated by the slow step. Thus, the rate of disappearance of A,  $-r_A$  is:

$$-r_A = r_s = r_{ad} = r_d \quad (\text{A-7})$$

For an adsorption limited reaction,  $k^a$  is small and  $k^s$  and  $k^d$  are large (*i.e.*, the rate constants for reaction and desorption are rapid compared to that of adsorption); therefore, the following assumptions are made:

$$\frac{r_s}{k^s} \approx 0 \quad (\text{A-8})$$

$$\frac{r_d}{k^d} \approx 0 \quad (\text{A-9})$$

Substituting these expressions into equations (A-4) and (A-5), and rearranging:

$$C_{AS} = 0 \text{ and } K_B = \frac{C_{BS}}{C_B S_v} \quad (\text{A-10})$$

These expressions can now be substituted into the site balance:

$$S_t = S_v + K_B C_B S_v \quad (\text{A-11})$$

rearranging:

$$S_v = \frac{S_t}{1 + K_B C_B} \quad (\text{A-12})$$

Now the rate of disappearance of species A is found and expressed in terms of constants and measurable concentrations:

$$-r_A = r_{ad} = k^a C_A S_v \quad (\text{A-13})$$

Substituting for  $S_v$  gives:

$$-r_A = \frac{(k^a S_t) C_A}{1 + K_B C_B} \quad (\text{A-14})$$

For an initial concentration of zero for B, this becomes:

$$r_{ad} = (k^a S_t) C_A \quad (\text{A-15})$$

which is identical to a pseudo-first-order expression. If the experiments show a linear increase in rate with increasing concentration (*i.e.*, the same initial  $k_{obs}$  for different initial concentrations), the system is described as being adsorption limited.

### A.2.3 Surface Reaction as the Rate Limiting Step

For a surface limited reaction,  $k'$  is small and  $k^a$  and  $k^d$  are large. As above, assumptions are made:

$$\frac{r_{ad}}{k^a} \approx 0 \quad (\text{A-17})$$

$$\frac{r_d}{k^d} \approx 0 \quad (\text{A-18})$$

Making these substitutions into equations A-3 and A-5 we find:

$$C_A S_v - \frac{C_{AS}}{K_A} = 0 \text{ or } K_A = \frac{C_{AS}}{C_A S_v} \quad (\text{A-19})$$

$$C_{BS} - K_B C_B S_v = 0 \text{ or } K_B = \frac{C_{BS}}{C_B S_v} \quad (\text{A-20})$$

Using equations (A-19) and (A-20), expressions for  $C_{AS}$  and  $C_{BS}$  are found and substituted into the site balance (equation A-6):

$$S_t = S_v + K_A C_A S_v + K_B C_B S_v \quad (\text{A-21})$$

Rearranging we obtain:

$$S_v = \frac{S_t}{1 + K_A C_A + K_B C_B} \quad (\text{A-22})$$

Now a rate expression for the disappearance of A is found and expressed in terms of constants and measurable concentrations:

$$-r_A = r_s = k^s C_{AS} \quad (\text{A-23})$$

Substituting for  $C_{AS}$  using equation (A-19)

$$-r_A = k^s K_A C_A S_v \quad (\text{A-24})$$

and substituting for  $C_v$  using equation (A-22)

$$-r_A = \frac{(k^s S_t) K_A C_A}{1 + K_A C_A + K_B C_B} \quad (\text{A-25})$$

#### A.2.4 Desorption as the Rate Limiting Step

For a desorption limited reaction, assumptions are made to simplify the expressions for reaction and adsorption

$$\frac{r_s}{k^s} = C_{AS} \approx 0 \quad (\text{A-26})$$

$$\frac{r_{ad}}{k^a} \approx 0 \quad (\text{A-27})$$

Equation A-27 gives rise to the following expression by substituting in (A-3):

$$C_{AS} = K_A C_A S_v$$

From equation A-26,  $C_{AS} = 0$ ; the value of  $S_v$  must also be zero, for the values of  $K_A$  and  $C_A$  are necessarily non-zero. This allows simplification of the site balance:

$$S_t = C_{BS} \quad (\text{A-28})$$

Substituting this into the rate expression for desorption (A-5) and knowing that  $S_v = 0$ , we find that the rate of reaction of species A may be expressed as:



$$-r_A = r_d = (k^d S_t) \quad (\text{A-29})$$

### A.2.5 Determination of the Kinetic and Adsorption Parameters

For the adsorption and desorption limited cases, the determination of the appropriate kinetic parameter,  $(k^a S_t)$  or  $(k^d S_t)$  is relatively straightforward. For the adsorption limited case, a pseudo-first-order model is used. A plot of rate vs. initial concentration will give the kinetic parameter for the desorption limited situation.

When encountering a surface reaction limited case, however, there are two parameters to fit, the kinetic parameter,  $(k^s S_t)$ , and the adsorption parameter,  $K_A$ . Several modeling strategies may be used to find the kinetic and adsorption parameters for a particular species. For simple systems (e.g., in which a parent, A, reacts to a single product, B) and low conversions, the kinetic and adsorption parameters may be determined from a fit of the initial pseudo-first-order rate constant  $k_{obs}$  (determined from the disappearance of the parent) versus initial concentration. A fit of rate versus  $C_0$  may also be used. A linearization of equation (A-25) may also be performed. These strategies, however, are not satisfactory for species that undergo multiple reactions as a second fit must be performed to obtain the contributions to the kinetic parameter. These strategies also require very low conversions to make the assumption that  $C=C_0$ , thus, highly precise analytical methods (capable of measuring very small changes in concentration) are required.

A second option is to simultaneously fit the concentration versus time data for several experiments conducted over a range of initial concentrations (see Appendix B). The use of several sets of data is necessary to define  $(k^s S_t)$  and  $K_A$  with precision. For one individual experiment, many combinations of the two variables may explain the change in concentration over time. As the number of experiments increases, the uncertainty in the model-output parameters diminishes considerably. In addition, if data for both the concentrations of parent species and the daughter products are given as a function of time, the model can calculate the contributions to  $(k^s S_t)$  from parallel reaction pathways.

### A.3 Coupling Reactions

A derivation of the rate expressions for reaction-limited coupling reactions is very similar to that presented in the previous section. The equation used is dependent on the stoichiometry used in the coupling reaction. There are two possibilities:

$$r_s = k^s C_{AS}^2 \quad (\text{A-30})$$

$$r_s = k^s C_{AS} C_A \quad (\text{A-31})$$

Equation (A-30) describes the coupling of two surface bound species. The second equation is for the reaction of one surface bound molecule and one aqueous molecule. Once the substitution for  $C_{AS}$  is made via eqn. (A-19), the differences become more obvious:

$$-r_{Acouple} = \frac{(k^s S_t^2) K_A C_A^2}{(1 + K_A C_A + K_B C_B)^2} \quad (\text{A-32})$$

$$-r_{Acouple} = \frac{(k^s S_t) K_A C_A^2}{(1 + K_A C_A + K_B C_B)} \quad (\text{A-33})$$

For the reaction of two surface-adsorbed molecules, the rate is dependent on the square of the site concentration,  $S_t^2$  (which should be proportional to the square of the metal loading). The inhibition term in the denominator is also raised to the second power. These two possibilities can be distinguished by performing experiments at multiple metal loadings or by using different concentrations of a competitor species, B. The dependence of the kinetic parameter on metal loading will reveal whether equation (A-32) or (A-33) is more appropriate.

### A.4 Case 2: Parallel and Sequential Reactions

The derivation in Section A.2 is easily performed for more complex systems containing parallel and sequential reactions. For a system of parallel reactions  $A \rightarrow B$  and  $A \rightarrow C$  with rate constants  $k_1$  and  $k_2$  respectively (e.g., the reaction of TCE to form *cis*-DCE and *trans*-DCE), the following equation can be derived, assuming all transformations are limited by the rate of the surface reaction.

$$-r_A = \frac{([k_{AB}^s + k_{AC}^s]S_t)K_A C_A}{1 + K_A C_A + K_B C_B + K_C C_C} \quad (\text{A-34})$$

If B also reacts from C, the rate expression for B is:

$$-r_B = \frac{(k_{BC}^s S_t)K_B C_B - (k_{AB}^s S_t)K_A C_A}{1 + K_A C_A + K_B C_B + K_C C_C} \quad (\text{A-35})$$

## A.5 A Complete Model for PCE Reduction

In order to model PCE reduction, the adsorption and rate constants for each species present in the system through the course of the reaction must be found. An example expression is given for *trans*-DCE (produced from TCE and subsequently reacting to other products) in equation (A-36).

$$r_{transDCE} = \frac{dC_{iDCE}}{dt} = \frac{(k_{TCE \rightarrow iDCE}^s S_t)C_{TCE} - ([k_{iDCE \rightarrow j}^s + \dots + k_{iDCE \rightarrow N}^s]S_t)C_{iDCE}}{1 + K_{TCE}C_{TCE} + K_{iDCE}C_{iDCE} + \dots + K_{C_2H_4}C_{C_2H_4} + K_{C_2H_6}C_{C_2H_6}} \quad (\text{A-36})$$

It is possible that some of the terms in the denominator may not be necessary. For example, if the desorption of ethane is rapid, the value of  $K_{C_2H_6}$  would be zero. Using summation notation, the reaction of a parent species,  $i$ , and the appearance and disappearance of all its possible daughter products,  $j$ , may be expressed as:

$$\frac{dC_i}{dt} = - \frac{\left( \sum_{j=1}^{N_j} k_{ij}^s S_t \right) K_i C_i}{1 + \sum_{m=1}^{N_m} K_m C_m} = -k_{obs} C_i \quad (\text{A-37})$$

$$\frac{dC_j}{dt} = \frac{\left( \sum_{i=1}^{N_i} k_{ij}^s S_t \right) K_i C_i}{1 + \sum_{m=1}^{N_m} K_m C_m} - \frac{\left( \sum_{p=1}^{N_p} k_{jp}^s S_t \right) K_j C_j}{1 + \sum_{m=1}^{N_m} K_m C_m} \quad (\text{for all } j) \quad (\text{A-38})$$

## A.6 Effect of the Magnitude of $K$

As discussed previously, the rate-controlling step can be identified experimentally by examining how the initial rate varies as a function of initial concentration. The results may not, however, be entirely unambiguous. Shown in Figure A-1 are three curves and hypothetical data points for a surface reaction limited process. In generating these curves, the value of the kinetic constant,  $k$  is set equal to 5, and the adsorption parameter,  $K$ , was varied according to the values given next to each curve. The curves with  $K=0.05$  and  $0.005$  display obvious curvature. When  $K$  is decreased to  $0.0005$ , however, the curvature is not readily apparent over the concentration range examined. In fact, a linear regression performed on these data results in an  $r^2$  of  $0.996$ . Thus, when  $K$  is very small (resulting in  $KC \ll 1$ ), the surface reaction limited case may be indistinguishable from the adsorption limited case over a concentration range that is experimentally accessible.

## A.7. Comments on the Heterogeneous Kinetic Model

Despite its versatility, the LHHW approach is only a *convenient tool* for modeling heterogeneous reactions and for offering a mathematical interpretation of observed behaviors; it may not represent the physical reality or actual mechanism by which reaction takes place. Because the model is more heavily parameterized than a pseudo-first order kinetic expression, it invariably fits the data better. Other models may also be effective. One such model is of the form  $-r_A = kC_A^n C_B^m$ . In this case, competition for sites is accounted for by the reaction orders,  $n$  and  $m$ , which may be fractional or negative (Froment and Bischoff, 1990). Also, it may not invariably be a simple task to identify the rate controlling step. As discussed above, a surface reaction limited process with a very small adsorption constant is mathematically and experimentally indistinguishable from an adsorption-limited process.

Another possibility is that two steps in the sequence simultaneously control the rate of reaction. Examples of dual rate-controlling steps, *e.g.*, desorption and reaction have for example been observed for the dehydrogenation of *sec*-butyl alcohol (Thaller and Thodos, 1960; Bischoff and Froment, 1962). Mass transfer to or from the surface may also partially control the reaction

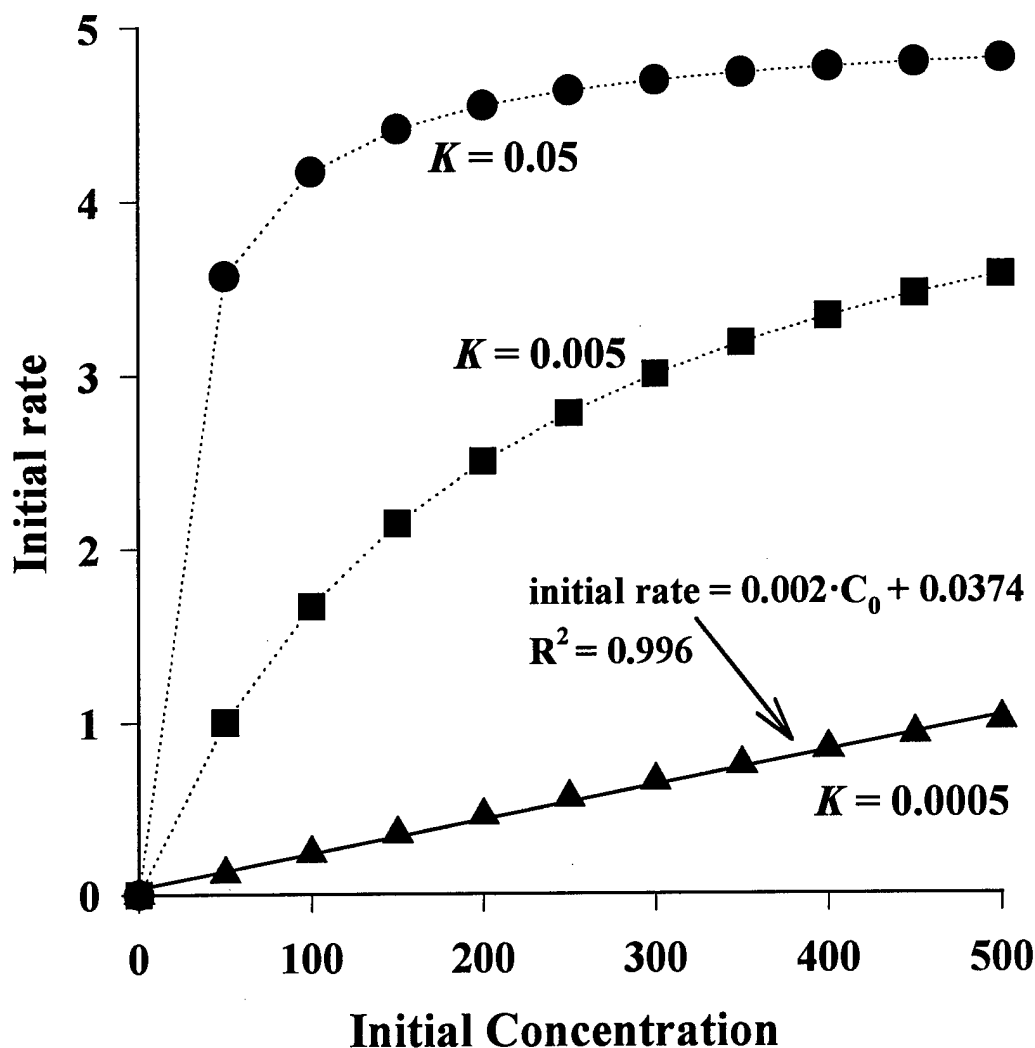


**Figure A-1.** Effect of the adsorption parameter ( $K$ ) on the shape of the initial rate versus initial concentration curve for a surface reaction limited case. Three cases are shown, with  $K=0.05$  (●),  $0.005$  (■) and  $0.0005$  (▲). In the last case, the curve is indistinguishable from the adsorption limited case over this concentration range.

rate (Arnold *et al.*, 1999). Kinetic models for reactions occurring under such conditions can be developed, although the derivations are more complicated than those involving only one ratelimiting step. Simplifying assumptions are therefore commonly invoked. The derivations given here assumes a Langmuir type adsorption (to a single type of site). Other distributions of adsorption energies may also be used [*e.g.*, linear (Temkin) or logarithmic (Freundlich)], although this has been found to exert a minimal effect on the resulting models (Corma *et al.*, 1988).

Other questions also remain. What about surface non-uniformities? Do some species react on one type of site (*e.g.*, edge) and other species on another (*e.g.*, corner)? Surface non-uniformities are often ignored in modeling catalytic reactions. If the coverage of reactive sites is high enough, the non-uniformities may not be "seen" by the reacting species, although cases do exist where it is necessary to account for non-uniformities under certain conditions (Carberry, 1976). A lack of competition between species may indicate that species are reacting on different types of sites. One must be careful with this interpretation, for if a system possesses many more reactive sites than reacting molecules, competition for sites may be muted and difficult to observe (Froment and Bischoff, 1990).

One last difficulty is that LHHW kinetics are most commonly invoked to describe one-step gas phase reactions. The zero-valent metal system employed in this study is an aqueous system in which multiple parallel and sequential reactions occur. In the case of zero-valent metals, LHHW kinetics may be a convenient tool to model the kinetics, but it may represent a simplification of reality. For one thing, zero-valent metal systems are not truly catalytic, for the metal is transformed during the process. Nevertheless, while there is a large excess of metal and the surface is relatively uniform (*e.g.*, it is clean or evenly coated with precipitate), the process can be approximated as one of catalysis.

## **A.8 Literature Cited**

- Allen-King, R.; Halket, R.M.; Burris, D.R. Reductive transformation and sorption of *cis*- and *trans*-1,2-dichloroethylene in a metallic iron-water system. *Environ. Toxicol. Chem.* **1997**, *16*, 424-429.
- Arnold, W.A.; Ball, W.P.; Roberts, A.L. Polychlorinated ethane reaction with zero-valent zinc: pathways and rate control. *J. Contam. Hydrol.* **1999**, *40*(2), 183-200.
- Bischoff, K.B.; Froment, G.F. Rate equations for consecutive heterogeneous processes. *Ind. Eng. Chem. Fund.* **1962**, *1*, 195-200.
- Burris, D.R.; Campbell, T.J.; Manoranjan, V.S. Sorption of trichloroethylene and tetrachloroethylene in a batch reactive zero-valent iron system. *Environ. Sci. Technol.* **1995**, *29*, 2850-2855.
- Carberry, J.J. *Chemical and Catalytic Reactor Engineering*. McGraw-Hill: New York, 1976.
- Corma, A.; Llopis, F.; Monton, J.B.; Weller, S.W. Comparison of models in heterogeneous catalysis for ideal and non-ideal surfaces. *Chem. Eng. Sci.* **1988**, *43*, 785-792.
- Fogler, S. *Elements of Chemical Reaction Engineering*. 2nd ed. Prentice Hall: Englewood Cliffs, NJ, 1992..
- Froment, G.F.; Bischoff, K.B. *Chemical Reactor Analysis and Design*. 2nd ed. John Wiley & Sons: New York, 1990.
- Thaller, L.H.; Thodos, G. The dual nature of a catalytic reaction: the dehydrogenation of *sec*-butyl alcohol to methyl ethyl ketone at elevated pressures. *AIChE J.* **1960**, *6*, 369-373.

## APPENDIX B: MODELING PROCEDURE

The equations developed and used for the modeling of the reactions of the chlorinated ethylenes and other observed intermediates are given below. Both formation and disappearance terms are included for each species where appropriate. Also presented are the *Scientist* models used with the normalized equations. Comments and explanations are given where appropriate.

TABLE B-1: LIST OF ABBREVIATIONS

Species	Abbreviation
Tetrachloroethylene	PCE
Trichloroethylene	TCE
<i>cis</i> -Dichloroethylene	cDCE
<i>trans</i> -Dichloroethylene	tDCE
1,1-Dichloroethylene	1,1DCE
Vinyl Chloride	VC
Ethylene	eth
Ethane	ethane
Acetylene	ace
Chloroacetylene	cace
Dichloroacetylene	dcace
Four carbon species	cfs

### B.1 Inhibition/Competition Term

In the interests of brevity, the term:

$$1 + K_{PCE} C_{PCE} + K_{TCE} C_{TCE} + K_{cDCE} C_{cDCE} + K_{tDCE} C_{tDCE} + K_{1,1DCE} C_{1,1DCE} + K_{ace} C_{ace} + K_{cace} C_{cace} + K_{dcace} C_{dcace}$$

will be abbreviated *inhibit*. This is the competitive/inhibition term that appears in the denominator for most of the species. Vinyl chloride and ethylene are not included, for they do not inhibit themselves: their reaction appears to be adsorption limited (Figure 64), and they do not appear to inhibit the reaction of other species. As reaction of acetylenic species only exhibit self-inhibition, the terms in the rate expressions corresponding to reaction of these compounds do not contain contributions in the denominator from interspecies competition (the *inhibit* term). All kinetic and adsorption parameters correspond to the numbering in Table 10.



## B.2 Equations

PCE

$$\frac{dC_{PCE}}{dt} = \frac{-(k_1+k_2)K_{PCE}C_{PCE}}{inhibit} \quad (B-1)$$

TCE

$$\frac{dC_{TCE}}{dt} = \frac{(k_1)K_{PCE}C_{PCE} - (k_3+k_4+k_5+k_6)K_{TCE}C_{TCE}}{inhibit} \quad (B-2)$$

dichloroacetylene

$$\frac{dC_{dcace}}{dt} = \frac{k_2K_{PCE}C_{PCE}}{inhibit} - \frac{(k_{15}+k_{16}+k_{17})K_{dcace}C_{dcace}}{1+K_{dcace}C_{dcace}} \quad (B-3)$$

chloroacetylene

$$\frac{dC_{cace}}{dt} = \frac{k_6K_{TCE}C_{TCE}}{inhibit} + \frac{k_{17}K_{dcace}C_{dcace}}{1+K_{dcace}C_{dcace}} - \frac{k_{14}K_{cace}C_{cace}}{1+K_{cace}C_{cace}} \quad (B-4)$$

cis-DCE

$$\frac{dC_{cDCE}}{dt} = \frac{k_4K_{TCE}C_{TCE} - (k_9+k_{10})K_{cDCE}C_{cDCE}}{inhibit} + \frac{k_{15}K_{dcace}C_{dcace}}{1+K_{dcace}C_{dcace}} \quad (B-5)$$

trans-DCE

$$\frac{dC_{tDCE}}{dt} = \frac{k_3K_{TCE}C_{TCE} - (k_7+k_8)K_{tDCE}C_{tDCE}}{inhibit} + \frac{k_{16}K_{dcace}C_{dcace}}{1+K_{dcace}C_{dcace}} \quad (B-6)$$

1,1-DCE

$$\frac{dC_{1,1DCE}}{dt} = \frac{k_5K_{TCE}C_{TCE} - k_{11}K_{1,1DCE}C_{1,1DCE}}{inhibit} \quad (B-7)$$

VC

$$\frac{dC_{VC}}{dt} = \frac{k_7K_{tDCE}C_{tDCE} + k_9K_{cDCE}C_{cDCE} - k_{12}C_{VC}}{inhibit} \quad (B-8)$$

acetylene

$$\frac{dC_{ace}}{dt} = \frac{k_{10}K_{cDCE}C_{cDCE} + k_8K_{tDCE}C_{tDCE}}{inhibit} + \frac{k_{14}K_{cace}C_{cace}}{1+K_{cace}C_{cace}} - \frac{k_{13}K_{ace}C_{ace}}{1+K_{ace}C_{ace}} - \frac{k_{18}K_{ace}C_{ace}^2}{1+K_{ace}C_{ace}} \quad (B-9)$$

ethylene

$$\frac{dC_{eth}}{dt} = \frac{k_{13}K_{ace}C_{ace}}{1+K_{ace}C_{ace}} + \frac{k_{11}K_{1,1DCE}C_{1,1DCE} + k_{12}C_{VC} - k_{19}C_{eth}}{inhibit} \quad (B-10)$$

ethane

$$\frac{dC_{ethane}}{dt} = \frac{k_{19}C_{eth}}{inhibit} \quad (B-11)$$

C<sub>4</sub>'s

$$\frac{dC_{cfs}}{dt} = \frac{k_{18}K_{ace}C_{ace}^2}{1+K_{ace}C_{ace}} \quad (B-12)$$

### B.3 Normalization Procedure

The concentration data for all species in each experiment were normalized by the initial concentration determined by performing a pseudo-first order fit to the parent compound decay. The *Scientist* model was provided these normalized data. Equations used for modeling each data set carried out at a variety of different initial concentrations also required normalization. A simplified, normalized equation for PCE is:

$$\frac{d\frac{C_{PCE}}{C_0}}{dt} = \frac{-(k_1+k_2)K_{PCE}\frac{C_{PCE}}{C_0}}{1+K_{PCE}C_{PCE}} \quad \text{or} \quad \frac{dC_{pce}^{norm}}{dt} = \frac{-(k_1+k_2)K_{PCE}C_{PCE}^{norm}}{1+K_{PCE}C_{PCE}} \quad (B-13)$$

The difficulty encountered arises from the presence of  $C_{PCE}$  in the denominator. The data to be fit by the model is normalized, but the extent of inhibition expressed in the denominator is dependent on the actual concentration. The model equations used by *Scientist* had to account for this. Rather than provide the model with both the normalized and the unnormalized data (which would have been computationally prohibitive), the model equations were modified as follows:

$$\frac{dC_{pce}^{norm}}{dt} = \frac{-(k_1+k_2)K_{PCE}C_{PCE}^{norm}}{1+(C_0K_{PCE}C_{PCE}^{norm})} \quad (B-14)$$

The product of  $C_0C_{PCE}^{norm}$  is  $C_{PCE}$ , resulting in the same expression as given in eqn. (B-13). Because the values of  $C_0$  were fixed after the normalization procedure, this strategy did not introduce any extra fitting parameters.

A modification also had to be made to the term corresponding to the coupling reaction of acetylene. The equation is divided by one factor of  $C_0$ , thus only one of the  $C_{ace}$ 's in numerator should be normalized. The second should be the actual concentration. This required the insertion of a factor of  $C_0$  in the numerator of the coupling term as shown in equation (B-15):

$$\frac{dC_{ace}^{norm}}{dt} = \dots - \frac{k_{18} K_{ace} C_{ace}^{norm} (C_{ace}^{norm} C_0)}{1 + (C_0 K_{ace} C_{ace}^{norm})} \quad (B-15)$$

Representative model files for acetylene, *cis*-dichloroethylene, and trichloroethylene are given below (Figures B-1 to B-3). Notice that each model consists of the same set of equations repeated multiple times. One repetition is required for each experimental data set (corresponding to timecourses conducted at different initial concentrations), and the concentrations have different numerical indices in each set. The fitting parameters (*k* and *K* values) inserted in each set of equations are identical. In this manner, one set of parameters was calculated by fitting the data from a set of experiments conducted at different initial concentrations. The comments at the beginning of the models (lines that start with //) clarify the abbreviations used each models.

### B.4 Fitting Procedure

With the set of differential equations described above, the experimental data were fit to determine the appropriate kinetic and adsorption parameters. First, the concentration data for the parent species were fit to a pseudo-first order model for each individual experiment with a given species. This allowed the determination of  $C_0$  and the generation of the  $k_{obs}$  versus  $C_0$  plots.

Using these values for initial concentration, the concentration data for all species from each experiment were divided by  $C_0$  of the parent compound. The data from all the experiments conducted at different initial concentrations were provided to *Scientist*. As shown in the example model files, each experiment was numbered. Before performing the fit, the values of kinetic and adsorption parameters for reaction intermediates determined in independent experiments were set to be equal to the values previously calculated. Once these constraints were in place, a least squares fit was performed to determine the kinetic and adsorption parameters for the parent species. After the values were calculated, they were used to simulate the data (non-normalized) at each initial concentration. In this manner, Figures 65-75 were generated.

```

// MicroMath Scientist Model File for acetylene reaction with Fe(0)
//Include inhibition of ethylene.
//coupling rxn
IndVars: T
DepVars: ace1, ace2, ace3, ace4, ace5, ace6, eth1, eth2, eth3, eth4, eth5, eth6,
ethane1, ethane2, ethane3, ethane4, ethane5, ethane6, cf1, cf2, cf3, cf4, cf5, cf6
Params: k4, k5, k7, Ka1, Ka3, c1, c2, c3, c4, c5, c6,
alpha1=Ka1*ace1/(1+c1*(Ka1*ace1))
beta1=k5*Ka1*ace1*ace1*c1/((1+c1*(Ka1*ace1)))
ace1'=-k4*alpha1-beta1
eth1'=k4*alpha1-k7*eth1/(1+c1*(Ka1*ace1))
ethane1'=k7*eth1/(1+c1*(Ka1*ace1))
cf1'=beta1
alpha2=Ka1*ace2/(1+c2*(Ka1*ace2))
beta2=k5*Ka1*ace2*ace2*c2/((1+c2*(Ka1*ace2)))
ace2'=-k4*alpha2-beta2
eth2'=k4*alpha2-k7*eth2/(1+c2*(Ka1*ace2))
ethane2'=k7*eth2/(1+c2*(Ka1*ace2))
cf2'=beta2
alpha3=Ka1*ace3/(1+c3*(Ka1*ace3))
beta3=k5*ace3*Ka1*ace3*c3/((1+c3*(Ka1*ace3)))
ace3'=-k4*alpha3-beta3
eth3'=k4*alpha3-k7*eth3/(1+c3*(Ka1*ace3))
ethane3'=k7*eth3/(1+c3*(Ka1*ace3))
cf3'=beta3
alpha4=Ka1*ace4/(1+c4*(Ka1*ace4))
beta4=k5*Ka1*ace4*ace4*c4/((1+c4*(Ka1*ace4)))
ace4'=-k4*alpha4-beta4
eth4'=k4*alpha4-k7*eth4/(1+c4*(Ka1*ace4))
ethane4'=k7*eth4/(1+c4*(Ka1*ace4))
cf4'=beta4
alpha5=Ka1*ace5/(1+c5*(Ka1*ace5))
beta5=k5*Ka1*ace5*ace5*c5/((1+c5*(Ka1*ace5)))
ace5'=-k4*alpha5-beta5
eth5'=k4*alpha5-k7*eth5/(1+c5*(Ka1*ace5))
ethane5'=k7*eth5/(1+c5*(Ka1*ace5))
cf5'=beta5
alpha6=Ka1*ace6/(1+c6*(Ka1*ace6))
beta6=k5*Ka1*ace6*ace6*c6/((1+c6*(Ka1*ace6)))
ace6'=-k4*alpha6-beta6
eth6'=k4*alpha6-k7*eth6/(1+c6*(Ka1*ace6))
ethane6'=k7*eth6/(1+c6*(Ka1*ace6))
cf6'=beta6

```

**Figure B-1.** *Scientist* model file for acetylene reaction with Fe(0).

//IC  
T=0  
ace1=1  
ace2=1  
ace3=1  
ace4=1  
ace5=1  
ace6=1  
eth1=0  
eth2=0  
eth3=0  
eth4=0  
eth5=0  
eth6=0  
ethane1=0  
ethane2=0  
ethane3=0  
ethane4=0  
ethane5=0  
ethane6=0  
cf1=0  
cf2=0  
cf3=0  
cf4=0  
cf5=0  
cf6=0

**Figure B-1 (continued).**

**// MicroMath Scientist Model File for *cis*-dichloroethylene reaction with Fe(0)**

IndVars: T

DepVars: cdce1,cdce2,cdce3,cdce4,cdce5, vc1,vc2,vc3,vc4,vc5,ace1,ace2,ace3,ace4,ace5, eth1,eth2,eth3,eth4,eth5,ethane1,ethane2,ethane3,ethane4,ethane5, cf1,cf2,cf3,cf4,cf5

Params: k1, k2, k3, k4, k5, k7, Kace1, Kc,c1,c2,c3,c4,c5

cdce1'=(k1+k2)\*Kc\*cdce1/(1+c1\*(Kace1\*ace1+Kc\*cdce1))

vc1'=k1\*Kc\*cdce1/(1+c1\*(Kace1\*ace1+Kc\*cdce1))-k3\*vc1/(1+c1\*(Kace1\*ace1+Kc\*cdce1))

alpha1=Kace1\*ace1/(1+c1\*(Kace1\*ace1+Kc\*cdce1))

beta1=Kace1\*ace1\*ace1\*c1/((1+c1\*(Kace1\*ace1)))

ace1'=k2\*Kc\*cdce1/(1+c1\*(Kace1\*ace1+Kc\*cdce1))-(k4)\*alpha1-k5\*beta1

eth1'=k4\*alpha1-k7\*eth1/(1+c1\*(Kc\*cdce1))+k3\*vc1/(1+c1\*(Kace1\*ace1+Kc\*cdce1))

ethane1'=k7\*eth1/(1+c1\*(Kc\*cdce1))

cf1'=k5\*beta1

cdce2'=(k1+k2)\*Kc\*cdce2/(1+c2\*(Kace1\*ace2+Kc\*cdce2))

vc2'=k1\*Kc\*cdce2/(1+c2\*(Kace1\*ace2+Kc\*cdce2))-k3\*vc2/(1+c2\*(Kace1\*ace2+Kc\*cdce2))

alpha2=Kace1\*ace2/(1+c2\*(Kace1\*ace2+Kc\*cdce2))

beta2=Kace1\*ace2\*ace2\*c2/((1+c2\*(Kace1\*ace2)))

ace2'=k2\*Kc\*cdce2/(1+c2\*(Kace1\*ace2+Kc\*cdce2))-(k4)\*alpha2-k5\*beta2

eth2'=k4\*alpha2-k7\*eth2/(1+c2\*(Kc\*cdce2))+k3\*vc2/(1+c1\*(Kace1\*ace2+Kc\*cdce2))

ethane2'=k7\*eth2/(1+c2\*(Kc\*cdce2))

cf2'=k5\*beta2

cdce3'=(k1+k2)\*Kc\*cdce3/(1+c3\*(Kace1\*ace3+Kc\*cdce3))

vc3'=k1\*Kc\*cdce3/(1+c3\*(Kace1\*ace3+Kc\*cdce3))-k3\*vc3/(1+c3\*(Kace1\*ace3+Kc\*cdce3))

alpha3=Kace1\*ace3/(1+c3\*(Kace1\*ace3+Kc\*cdce3))

beta3=Kace1\*ace3\*ace3\*c3/((1+c3\*(Kace1\*ace3)))

ace3'=k2\*Kc\*cdce3/(1+c3\*(Kace1\*ace3+Kc\*cdce3))-(k4)\*alpha3-k5\*beta3

eth3'=k4\*alpha3-k7\*eth3/(1+c3\*(Kc\*cdce3))+k3\*vc3/(1+c3\*(Kace1\*ace3+Kc\*cdce3))

ethane3'=k7\*eth3/(1+c3\*(Kc\*cdce3))

cf3'=k5\*beta3

cdce4'=(k1+k2)\*Kc\*cdce4/(1+c4\*(Kace1\*ace4+Kc\*cdce4))

vc4'=k1\*Kc\*cdce4/(1+c4\*(Kace1\*ace4+Kc\*cdce4))-k3\*vc4/(1+c4\*(Kace1\*ace4+Kc\*cdce4))

alpha4=Kace1\*ace4/(1+c4\*(Kace1\*ace4+Kc\*cdce4))

beta4=Kace1\*ace4\*ace4\*c4/((1+c4\*(Kace1\*ace4)))

ace4'=k2\*Kc\*cdce4/(1+c4\*(Kace1\*ace4+Kc\*cdce4))-(k4)\*alpha4-k5\*beta4

eth4'=k4\*alpha4-k7\*eth4/(1+c4\*(Kc\*cdce4))+k3\*vc4/(1+c4\*(Kace1\*ace4+Kc\*cdce4))

ethane4'=k7\*eth4/(1+c4\*(Kc\*cdce4))

cf4'=k5\*beta4

cdce5'=(k1+k2)\*Kc\*cdce5/(1+c5\*(Kace1\*ace5+Kc\*cdce5))

vc5'=k1\*Kc\*cdce5/(1+c5\*(Kace1\*ace5+Kc\*cdce5))-k3\*vc5/(1+c5\*(Kace1\*ace5+Kc\*cdce5))

**Figure B-2.** *Scientist* model file for *cis*-dichloroethylene reaction with Fe(0).

```

alpha5=Kace1*ace5/(1+c5*(Kace1*ace5+Kc*cdce5))
beta5=Kace1*ace5*ace5*c5/((1+c5*(Kace1*ace5)))
ace5'=k2*Kc*cdce5/(1+c5*(Kace1*ace5+Kc*cdce5))-(k4)*alpha5-k5*beta5
eth5'=k4*alpha5-k7*eth5/(1+c5*(Kc*cdce5))+k3*vc5/(1+c5*(Kace1*ace5+Kc*cdce5))
ethane5'=k7*eth5/(1+c5*(Kc*cdce5))
cf5'=k5*beta5
//IC
T=0
cdce1=1
cdce2=1
cdce3=1
cdce4=1
cdce5=1
vc1=0
vc2=0
vc3=0
vc4=0
vc5=0
ace1=0
ace2=0
ace3=0
ace4=0
ace5=0
eth1=0
eth2=0
eth3=0
eth4=0
eth5=0
ethane1=0
ethane2=0
ethane3=0
ethane4=0
ethane5=0
cf1=0
cf2=0
cf3=0
cf4=0
cf5=0

```

**Figure B-2 (continued).**

// MicroMath Scientist Model File for trichloroethylene reaction with Fe(0)

// Acetylene and chloroacetylene are only self inhibited

IndVars: T

DepVars: tc1,tc2,tc3,tc4,tc5,tc6,ca1,ca2,ca3,ca4,ca5,ca6,tdce1,tdce2,tdce3,tdce4,tdce5,tdce6,cdc  
e1,cdce2,cdce3,cdce4,

DepVars: cdce5,cdce6,d1,d2,d3,d4,d5,d6,ace1,ace2,ace3,ace4,ace5,ace6,v1,v2,v3,v4,v5,v6,eth1

DepVars: eth2,eth3,eth4,eth5,eth6,etha1,etha2,etha3,etha4,etha5, etha6

Params: k1,k2,k3,k4,k5,k6,k7,k8,k9,k10,k11,k12,k13,Ktce,Kca,Ktd,Kcd,Kd,c1,c2,c3,c4,c5,c6,  
k14, Kace1

a1=(1+c1\*(Ktce\*tc1+Kca\*ca1+Ktd\*tdce1+Kcd\*cdce1+Kd\*d1+Kace1\*ace1))

b1=(1+c1\*Kca\*ca1)

x1=(1+c1\*Kace1\*ace1)

tc1'=- (k1+k2+k3+k4)\*Ktce\*tc1/a1

ca1'=k1\*Ktce\*tc1/a1-k5\*Kca\*ca1/b1

tdce1'=k2\*Ktce\*tc1/a1-(k6+k7)\*Ktd\*tdce1/a1

cdce1'=k3\*Ktce\*tc1/a1-(k8+k9)\*Kcd\*cdce1/a1

d1'=k4\*Ktce\*tc1/a1-k10\*Kd\*d1/a1

ace1'=k5\*Kca\*ca1/b1+k6\*Ktd\*tdce1/a1+k8\*Kcd\*cdce1/a1-k11\*Kace1\*ace1/x1-

k14\*Kace1\*ace1\*ace1/x1

v1'=k7\*Ktd\*tdce1/a1+k9\*Kcd\*cdce1/a1-k12\*v1/a1

eth1'=k11\*Kace2\*ace1/x1+k12\*v1/a1-k13\*eth1/a1+k10\*Kd\*d1/a1

etha1'=k13\*eth1/a1

a2=(1+c2\*(Ktce\*tc2+Kca\*ca2+Ktd\*tdce2+Kcd\*cdce2+Kd\*d2+Kace1\*ace2))

b2=(1+c2\*Kca\*ca2)

x2=(1+c2\*Kace1\*ace2)

tc2'=- (k1+k2+k3+k4)\*Ktce\*tc2/a2

ca2'=k1\*Ktce\*tc2/a2-k5\*Kca\*ca2/b2

tdce2'=k2\*Ktce\*tc2/a2-(k6+k7)\*Ktd\*tdce2/a2

cdce2'=k3\*Ktce\*tc2/a2-(k8+k9)\*Kcd\*cdce2/a2

d2'=k4\*Ktce\*tc2/a2-k10\*Kd\*d2/a2

ace2'=k5\*Kca\*ca2/b2+k6\*Ktd\*tdce2/a2+k8\*Kcd\*cdce2/a2-k11\*Kace1\*ace2/x2-

k14\*Kace1\*ace2\*ace2/x2

v2'=k7\*Ktd\*tdce2/a2+k9\*Kcd\*cdce2/a2-k12\*v2/a2

eth2'=k11\*Kace2\*ace2/x2+k12\*v2/a2-k13\*eth2/a2+k10\*Kd\*d2/a2

etha2'=k13\*eth2/a2

a3=(1+c3\*(Ktce\*tc3+Kca\*ca3+Ktd\*tdce3+Kcd\*cdce3+Kd\*d3+Kace1\*ace3))

b3=(1+c3\*Kca\*ca3)

x3=(1+c3\*Kace1\*ace3)

tc3'=- (k1+k2+k3+k4)\*Ktce\*tc3/a3

ca3'=k1\*Ktce\*tc3/a3-k5\*Kca\*ca3/b3

tdce3'=k2\*Ktce\*tc3/a3-(k6+k7)\*Ktd\*tdce3/a3

**Figure B-3.** Scientist model file for trichloroethylene reaction with Fe(0).



$$\begin{aligned}
cdce3' &= k3 * Ktce * tc3 / a3 - (k8 + k9) * Kcd * cdce3 / a3 \\
d3' &= k4 * Ktce * tc3 / a3 - k10 * Kd * d3 / a3 \\
ace3' &= k5 * Kca * ca3 / b3 + k6 * Ktd * tdce3 / a3 + k8 * Kcd * cdce3 / a3 - k11 * Kace1 * ace3 / x3 - \\
&k14 * Kace1 * ace3 * ace3 / x3 \\
v3' &= k7 * Ktd * tdce3 / a3 + k9 * Kcd * cdce3 / a3 - k12 * v3 / a3 \\
eth3' &= k11 * Kace2 * ace3 / x3 + k12 * v3 / a3 - k13 * eth3 / a3 + k10 * Kd * d3 / a3 \\
etha3' &= k13 * eth3 / a3 \\
a4 &= (1 + c4 * (Ktce * tc4 + Kca * ca4 + Ktd * tdce4 + Kcd * cdce4 + Kd * d4 + Kace1 * ace4)) \\
b4 &= (1 + c4 * Kca * ca4) \\
x4 &= (1 + c4 * Kace1 * ace4) \\
tc4' &= -(k1 + k2 + k3 + k4) * Ktce * tc4 / a4 \\
ca4' &= k1 * Ktce * tc4 / a4 - k5 * Kca * ca4 / b4 \\
tdce4' &= k2 * Ktce * tc4 / a4 - (k6 + k7) * Ktd * tdce4 / a4 \\
cdce4' &= k3 * Ktce * tc4 / a4 - (k8 + k9) * Kcd * cdce4 / a4 \\
d4' &= k4 * Ktce * tc4 / a4 - k10 * Kd * d4 / a4 \\
ace4' &= k5 * Kca * ca4 / b4 + k6 * Ktd * tdce4 / a4 + k8 * Kcd * cdce4 / a4 - k11 * Kace1 * ace4 / x4 - \\
&k14 * Kace1 * ace4 * ace4 / x4 \\
v4' &= k7 * Ktd * tdce4 / a4 + k9 * Kcd * cdce4 / a4 - k12 * v4 / a4 \\
eth4' &= k11 * Kace2 * ace4 / x4 + k12 * v4 / a4 - k13 * eth4 / a4 + k10 * Kd * d4 / a4 \\
etha4' &= k13 * eth4 / a4 \\
a5 &= (1 + c5 * (Ktce * tc5 + Kca * ca5 + Ktd * tdce5 + Kcd * cdce5 + Kd * d5 + Kace1 * ace5)) \\
b5 &= (1 + c5 * Kca * ca5) \\
x5 &= (1 + c5 * Kace1 * ace5) \\
tc5' &= -(k1 + k2 + k3 + k4) * Ktce * tc5 / a5 \\
ca5' &= k1 * Ktce * tc5 / a5 - k5 * Kca * ca5 / b5 \\
tdce5' &= k2 * Ktce * tc5 / a5 - (k6 + k7) * Ktd * tdce5 / a5 \\
cdce5' &= k3 * Ktce * tc5 / a5 - (k8 + k9) * Kcd * cdce5 / a5 \\
d5' &= k4 * Ktce * tc5 / a5 - k10 * Kd * d5 / a5 \\
ace5' &= k5 * Kca * ca5 / b5 + k6 * Ktd * tdce5 / a5 + k8 * Kcd * cdce5 / a5 - k11 * Kace1 * ace5 / x5 - \\
&k14 * Kace1 * ace5 * ace5 / x5 \\
v5' &= k7 * Ktd * tdce5 / a5 + k9 * Kcd * cdce5 / a5 - k12 * v5 / a5 \\
eth5' &= k11 * Kace2 * ace5 / x5 + k12 * v5 / a5 - k13 * eth5 / a5 + k10 * Kd * d5 / a5 \\
etha5' &= k13 * eth5 / a5 \\
a6 &= (1 + c6 * (Ktce * tc6 + Kca * ca6 + Ktd * tdce6 + Kcd * cdce6 + Kd * d6 + Kace1 * ace6)) \\
b6 &= (1 + c6 * Kca * ca6) \\
x6 &= (1 + c6 * Kace1 * ace6) \\
tc6' &= -(k1 + k2 + k3 + k4) * Ktce * tc6 / a6 \\
ca6' &= k1 * Ktce * tc6 / a6 - k5 * Kca * ca6 / b6 \\
tdce6' &= k2 * Ktce * tc6 / a6 - (k6 + k7) * Ktd * tdce6 / a6 \\
cdce6' &= k3 * Ktce * tc6 / a6 - (k8 + k9) * Kcd * cdce6 / a6 \\
d6' &= k4 * Ktce * tc6 / a6 - k10 * Kd * d6 / a6
\end{aligned}$$

Figure B-3 (continued).

```

ace6'=k5*Kca*ca6/b6+k6*Ktd*tdce6/a6+k8*Kcd*cdce6/a6-k11*Kace1*ace6/x6-
k14*Kace1*ace6*ace6/x6
v6'=k7*Ktd*tdce6/a6+k9*Kcd*cdce6/a6-k12*v6/a6
eth6'=k11*Kace2*ace6/x6+k12*v6/a6-k13*eth6/a6+k10*Kd*d6/a6
etha6'=k13*eth6/a6
//IC
T=0
tc1=1
tc2=1
tc3=1
tc4=1
tc5=1
tc6=1
ca1=0
ca2=0
ca3=0
ca4=0
ca5=0
ca6=0
tdce1=0
tdce2=0
tdce3=0
tdce4=0
tdce5=0
tdce6=0
cdce1=0
cdce2=0
cdce3=0
cdce4=0
cdce5=0
cdce6=0
d1=0
d2=0
d3=0
d4=0
d5=0
d6=0
ace1=0
ace2=0
ace3=0
ace4=0
ace5=0

```

**Figure B-3 (continued).**

ace6=0  
v1=0  
v2=0  
v3=0  
v4=0  
v5=0  
v6=0  
eth1=0  
eth2=0  
eth3=0  
eth4=0  
eth5=0  
eth6=0  
etha1=0  
etha2=0  
etha3=0  
etha4=0  
etha5=0  
etha6=0

**Figure B-3 (continued).**